Jianming Xu
Pan Ming Huang
Editors

Molecular Environmental Soil Science at the Interfaces in the Earth's Critical Zone


ZHEJIANG UNIVERSITY PRESS
浙江大学出版社

Springer

Jianming Xu
Pan Ming Huang

Molecular Environmental Soil Science at the Interfaces in the Earth's Critical Zone

Jianming Xu
Pan Ming Huang

Molecular Environmental Soil Science at the Interfaces in the Earth's Critical Zone

With 132 figures

ZHEJIANG UNIVERSITY PRESS
浙江大学出版社

Springer

Editors
Prof. Jianming Xu
College of Environmental and
Resource Sciences
Zhejiang University
Hangzhou 310029, China
E-mail: jmxu@zju.edu.cn

Prof. Pan Ming Huang †
Department of Soil Science
University of Saskatchewan
Saskatoon SK S7N 5A8
Canada

ISBN 978-7-308-06602-0
Zhejiang University Press, Hangzhou

ISBN 978-3-642-05296-5 e-ISBN 978-3-642-05297-2
Springer Heidelberg Dordrecht London New York

Library of Congress Control Number: 2009937249

Cover design: Frido Steinen-Broo, EStudio Calamar, Spain

Printed on acid-free paper

Springer is a part of Springer Science+Business Media (www.springer.com)

图书在版编目（CIP）数据

地球关键区界面反应:分子水平的环境土壤科学=Molecular Environmental Soil Science at the Interfaces in the Earth's Critical Zone:英文/徐建明,黄盘铭主编.—杭州:浙江大学出版社,2009.10
ISBN 978-7-308-06602-0

Ⅰ.地… Ⅱ.①徐…②黄… Ⅲ.环境土壤学—国际学术会议—文集—英文 Ⅳ.X144—53

中国版本图书馆 CIP 数据核字（2009）第 160469 号

地球关键区界面反应:分子水平的环境土壤科学

徐建明　黄盘铭　主编

责任编辑　黄娟琴
封面设计　Frido Steinen-Broo
出版发行　浙江大学出版社
网址:http://www.zjupress.com
Springer-Verlag GmbH
网址:http://www.springer.com
排　　版　杭州中大图文设计有限公司
印　　刷　杭州富春印务有限公司
开　　本　880mm×1230mm　1/16
印　　张　22.75
字　　数　1021 千
版 印 次　2009 年 10 月第 1 版　2009 年 10 月第 1 次印刷
书　　号　ISBN 978-7-308-06602-0（浙江大学出版社）
ISBN 978-3-642-05296-5（Springer-Verlag GmbH）
定　　价　230.00 元

Editors

Organizing Committee

International Scientific Committee

Shu Tao (China)
Scott X. Chang (Canada)
Udo Schwertmann (Germany)
Ward Chesworth (Canada)
Yongguan Zhu (China)
Yongmin Luo (China)
Zucong Cai (China)
Zhihong Xu (Australia)

National Scientific and Organizing Committee of China

Changqing Song	National Natural Science Foundation of China, Beijing
Changyong Huang	Zhejiang University, Hangzhou
Dongmei Zhou	Institute of Soil Science, CAS, Nanjing
Fan Liu	Huazhong Agricultural University, Wuhan
Gengxin Pan	Nanjing Agricultural University, Nanjing
Haizhen Wang	Zhejiang University, Hangzhou
Hang Li	Southwest University, Chongqing
Jiachun Shi	Zhejiang University, Hangzhou
Jianjun Wu	Zhejiang University, Hangzhou
Jianming Xu	Zhejiang University, Hangzhou
Jizheng He	Research Center for Eco-Environmental Sciences, CAS, Beijing
Lixiang Zhou	Nanjing Agricultural University, Nanjing
Lizhong Zhu	Zhejiang University, Hangzhou
Min Liao	Zhejiang University, Hangzhou
Minggang Xu	The Chinese Academy of Agricultural Sciences, Beijing
Mingkui Zhang	Zhejiang University, Hangzhou
Qiaoyun Huang	Huazhong Agricultural University, Wuhan
Qimei Lin	China Agricultural University, Beijing
Qixing Zhou	Institute of Applied Ecology, CAS, Shenyang
Renkou Xu	Institute of Soil Science, CAS, Nanjing
Sen Dou	Jilin Agricultural University, Changchun
Shenggao Lu	Zhejiang University, Hangzhou
Shiqiang Wei	Southwest University, Chongqing
Xin Jiang	Institute of Soil Science, CAS, Nanjing
Xingmei Liu	Zhejiang University, Hangzhou
Xudong Zhang	Institute of Applied Ecology, CAS, Shenyang
Yahai Lu	China Agricultural University, Beijing
Yan He	Zhejiang University, Hangzhou
Yingxu Chen	Zhejiang University, Hangzhou

Sponsors

International Union of Soil Sciences (IUSS)
The International Union of Pure and Applied Chemistry (IUPAC)
Organisation for the Prohibition of Chemical Weapons (OPCW)
National Natural Science Foundation of China (NSFC)
Soil Science Society of China (SSSC)
Y.C. Tang Disciplinary Development Fund
Zhejiang University
Zhejiang Provincial Natural Science Foundation of China
Zhejiang Provincial Key Laboratory of Subtropical Soil and Plant Nutrition

Preface

Resource depletion and environmental problems are challenging the world for its sustainability. The theme of the International Symposium of Molecular Environmental Soil Science at the Interfaces in the Earth's Critical Zone (ISMESS) is of special significance for understanding environmental pollution and global change processes. The Critical Zone (CZ) is the system of coupled chemical, biological, physical, and geological processes operating together to support life at the Earth's surface. Further advance on the frontiers of knowledge on this subject matter requires scientists to cross disciplines and scales to integrate understanding of processes in the CZ, ranging in scale from the environmental mineral-organism-humus-water-air interfaces to the impact on the globe and humankind. These fundamental interactive processes in the CZ have an enormous impact on ecosystem productivity, services, and integrity, and on human welfare.

Carbon is a major component of soils. Globally, the mass of soil organic carbon is more than that of carbon in living matter and in the atmosphere combined. However, the CO_2 emission from the soil to the atmosphere is the primary mechanism of soil carbon loss. Agricultural practices and land use conversion contribute substantially (approx. 32%) to the total anthropogenic CO_2 emission. Soil organo-mineral-microbe interactions affect carbon turnover and sequestration. Our understanding of the role of mineral colloids in carbon transformation, dynamics, and sequestration in the environment would contribute to developing innovative management strategies to minimize its impact on climate change.

The interfacial interactions at the soil-plant(root)-microbe interface (rhizosphere) profoundly affect the physicochemical and biological processes such as transformation, fate, and toxicity of heavy metals and organic pollutants. Microbial population in the rhizosphere can be 10~100 times larger than the population in the bulk soils. Therefore, the rhizosphere is bathed in root exudates and microbial metabolites and the chemistry and biology at the soil-root interface is governed by biotic (plant roots, microbes) and abiotic (physicochemical reactions) interactions, and thus differs significantly from those in bulk soil. Little is known about the physicochemical and biological interfacial interactions in the rhizosphere, especially at the molecular level. The dynamics, transformations, bioavailability, and toxicity of metal pollutants and anthropogenic organics should be influenced enormously by the chemistry and biology of the rhizosphere.

Nanoparticles are discrete nanometer (10^{-9} m) scale assemblies of atoms. A significant fraction of atoms are exposed on surfaces rather than contained in the particle interior of nanoparticles. The biogeochemical and ecological impacts of nanomaterials are some of the fastest growing areas of research today, with not only vital scientific but also environmental, economic, and societal consequences. Little is known about the distribution, formation, transformation, structural and surface chemistry of environmental nanoparticles and their biogeochemical and ecological impacts.

Material cycling and energy flow processes are affected both by abiotic and biotic factors, which affect ecosystem integrity and the environmental quality. However, there are great knowledge gaps on how and to what extent the processes are affected by the interfacial interactions of environmental nanoparticles, especially at the molecular level. The research on this subject matter should, therefore, be an issue of intense interest on a global scale for years to come.

The objective of this symposium is to provide a forum for the interactions and communication of soil chemists, mineralogists, microbiologists, and physicists with allied scientists including pure chemists, biologists, environmental scientists, ecologists, and ecotoxicologists to address the current state-of-the-art on "Molecular Environmental Soil Science". The main sessions of the symposium were: 1) The Role of Mineral Colloids in Carbon Turnover and Sequestration and the Impact on Climate Change; 2) Biogeochemical Interfacial Reactions and the Transformation, Transport and Fate of Vital and Toxic Elements; 3) Anthropogenic Organics, Crop Protection and Ecotoxicology; 4) Environmental Nanoparticles: Distribution, Formation, Transformation, Structural and Surface Chemistry, and Biogeochemical and Ecological Impacts; and 5) Environmental Processes & Ecosystem Health. Two eminent scientists of the International Union of Pure and Applied Chemistry (IUPAC)

were invited to serve as Plenary Lecturers (IUPAC Lecturers) and 18 world renowned leading scientists were invited to give lectures in the 5 sessions of the symposium.

The symposium was held in Zhejiang University, Hangzhou, China on October 10-14, 2009. Zhejiang University, founded in 1897, is a key comprehensive university whose academic and research endeavors cover eleven disciplines, namely philosophy, literature, history, education, science, economics, law, management, engineering, agriculture and medicine. The University now has 112 specialties for undergraduate studies, and it is entitled to confer masters degrees in 317 programs and doctoral degrees in 283 programs. Under its administration there are 14 National Key Laboratories, 2 National Engineering Research Centers and 3 National Engineering Technology Centers. Besides, it has set up 35 national key specialties and 43 post-doctor stations. Soil Science in Zhejiang University is the National Key Discipline of China.

The participants of this symposium represent five continents: Asian delegates from China, Iran, Pakistan, Vietnam, D.P.R. Korea and R.O. Korea; European scientists from Austria, Belgium, France, Italy, the UK, Russia and Spain; Australasian participants from both Australia and New Zealand; delegates from the USA, Canada and Brazil in the Americas; and representatives from Egypt, Kenya and South Africa on the African continent.

It is the first time to hold such an international symposium in China. The IUPAC Project Committee has contributed to funding the symposium under the program for conferences on New Directions in Chemistry. The Project Committee noted that the Conference identifies, and builds on, the need to view and understand the CZ at the molecular level. It will provide a novel interface that will facilitate the integration of contributions from traditionally separate disciplines. It will add a molecular and nanoparticle dimension to a field of endeavor that has traditionally been viewed on a different scale (dimension). It will identify and focus on emerging challenges for research that will be predominantly cross-discipline in nature. It will help to secure the appreciation of the relevance of chemistry to this field that is of utmost importance to sustain humankind. Therefore, it is hoped that the symposium would lead to identification of gaps in knowledge and as such to provide future research directions and promote research on soil processes at the interfaces at the molecular level in the Earth's Critical Zone. It is expected to advance the frontiers of knowledge on biophysico-chemical processes in soil and related environmental systems and their biogeochemical and ecological impacts and also to promote education in this extremely important and challenging area of science for years to come.

The book of proceedings is composed of extended abstracts that present new ideas, methods, findings, and experiences on the 5 sessions of the symposium. All the extended abstracts have been subject to peer review by external referees, by International Scientific Committee members of the symposium, and by the editors of the proceedings. On behalf of the Organizing Committee, we would like to thank members of the International Scientific Committee and the authors for their invaluable collaboration. Special thanks are extended to our sponsors: The International Union of Soil Sciences, The International Union of Pure and Applied Chemistry, Organization for the Prohibition of Chemical Weapons, National Natural Science Foundation of China, Soil Science Society of China, Y.C. Tang Disciplinary Development Fund, Zhejiang University, Zhejiang Provincial Natural Science Foundation of China, and Zhejiang Provincial Key Laboratory of Subtropical Soil and Plant Nutrition. Valuable personal time of Mr. Jianjun Wu, Dr. Yan He, concerning the careful revising, typesetting and proof-checking of this book is also greatly acknowledged.

Dr. Jianming Xu
Chair of the Organizing Committee
ISMESS 2009

Dr. Pan Ming Huang †
Co-Chair of the Organizing Committee
ISMESS 2009

August 2009

Contents

Session 2 Biogeochemical Interfacial Reactions and the Transformation, Transport and Fate of Vital and Toxic Elements (41)

Plenary Lectures by IUPAC Scientists

Advances in the Use of Synchrotron Radiation to Elucidate Environmental Interfacial Reaction Processes and Mechanisms in the Earth's Critical Zone

Donald Lewis Sparks*

Department of Plant and Soil Sciences, Center for Critical Zone Research,
Delaware Environmental Institute, University of Delaware, Newark, Delaware 19716, USA.
*Corresponding author. Tel. No. (302) 831-0287; Fax No. (302) 831-0605; E-mail: dlsparks@udel.edu.

Abstract: The employment of bright light sources generated at synchrotrons has greatly advanced our understanding of important environmental interfacial (mineral/water, mineral/microbe, plant/soil) reaction processes in the soil, environmental, and geological sciences over the past two decades. This plenary paper will provide background on principles and types of synchrotron radiation techniques with an emphasis on the use of synchrotron-based X-ray absorption spectroscopy (XAS), X-ray fluorescence spectroscopy (XRF), X-ray diffraction (XRD) and microtomography to elucidate speciation of contaminants in heterogeneous soils, surface precipitation phenomena, mechanisms of rapid redox transformations, microbial transformations on mineral surfaces, air and terrestrial emanated particulate reactivity and composition, and metal reactivity and speciation in hyperaccumulator plants.

Keywords: Biogeochemical processes; Environmental interfaces; Molecular scale; Spatial and temporal scales; Surface spectroscopy

Introduction and Discussion

It has become increasingly recognized that to accurately predict and model fate/transport, toxicity, speciation, bioavailability, and risk assessment of plant nutrients, toxic metals, oxyanions, radionuclides, and organic chemicals in the Earth's Critical Zone, we must have fundamental information at multiple spatial and temporal scales, and our research efforts much be multidisciplinary and interdisciplinary. The critical zone is "the heterogeneous, near surface environment in which complex interactions involving rock, soil, water, air and living organisms regulate the natural habitat and determine the availability of life sustaining resources" (NRC, 2001). The critical zone is an interfacial region of mass and energy flux comprising terrestrial, lacustrine, and marine components of the continental crust and is one of two primary loci of life on Earth and for most of human activity. The critical zone is comprised of an array of spatial scales, ranging from the atomic to the global, and temporal scales, ranging from seconds to eons. The physical, chemical, and biological processes within the critical zone mediate exchange of mass and energy which is required for biomass productivity, chemical recycling, and water storage. The critical zone is the most heterogeneous and abstruse portion of the entire Earth (NRC, 2001). If we are going to sustain the planet for human habitation we must understand the physical, chemical, and biological processes and reactions in the critical zone over a range of spatial and temporal scales (NRC, 2001; Hochella, 2002; Sparks, 2002).

With the advent of state-of-the-art, *in-situ*, analytical techniques, some of which are synchrotron-based (e.g., X-ray absorption spectroscopy, XAS) one can elucidate reaction mechanisms at small spatial and

rapid temporal scales. The use of small scale techniques in environmental research has resulted in a multi-disciplinary field of study that environmental and geoscientists are actively involved in-molecular environmental science. Molecular environmental science can be defined as the study of the chemical and physical forms and distribution of contaminants in soils, sediments, waste materials, natural waters, plants, and the atmosphere at the molecular level (Sparks, 2002). Since the first use of XAS in 1987 (Hayes *et al.*, 1987) to study selenate and selenite complexation at the goethite/water interface, there have been a multitude of studies using bulk XAS to determine sorption mechanisms of metal(loids) and radionunclides on mineral surfaces over a range of reaction conditions. With the development of third and fourth generation light sources that afford brighter light and greater spatial resolution, scientists are able to use micro-focused XAS and X-ray fluorescence (XRF) spectroscopy to determine the speciation, distribution, and association of contaminants at the micron scale in heterogeneous soils, biosolids, particulates, and plants. These techniques, along with synchrotron-based X-ray diffraction (XRD), microtomography, and Quick XAS, have opened up research frontiers in a number of areas that will be covered in this plenary talk including speciation of contaminants, which is essential for understanding release mechanisms, spatial resolution, chemical transformations, toxicity, bioavailability, and ultimate impacts on human health; mechanisms of microbial transformations at mineral/metal(loid) interfaces; mechanisms of rapid redox transformations, air and terrestrial emanated particulate reactivity and composition, and metal uptake and speciation in hyperaccumulator plants.

Summary and Conclusions

To successfully address and fund the major research needs in the area of environmental interfacial biogeochemistry, multidisciplinary and interdisciplinary and multifaceted approaches must be carried out. Geochemists, soil scientists, chemists, physicists, biologists, ecologists, and engineers must and will increasingly collaborate. Arguably, one of the major research leitmotifs in the 21st century will be the study of biological effects on geochemical reactions and processes at environmental interfaces in the critical zone. This provides us with a unique opportunity to combine our expertise with that of molecular biologists. We must also employ an array of multiple, molecular scale techniques over a range of temporal scales in combination with macroscopic approaches and computational modeling to solve complex scientific questions related to the Earth's environment.

References

Hayes KF, Roe AL, Brown GE, Jr., Hodgson KO, Leckie JO, Parks GA (1987) In situ X-ray absorption study of surface complexes: Selenium oxyanions on alpha-FeOOH. Science 238:783-786

Hochella MF, Jr. (2002) There's plenty of room at the bottom. Geochim. Cosmochim. Acta. 66:735-743

National Research Council (NRC) (2001) Basic research opportunities in earth science. National Academy Press, Washington DC

Sparks DL (2002) Environmental Soil Chemistry, 2nd Edition. Academic Press, San Diego, CA

Microbial Role in Global Biogeochemical Cycling of Metals and Metalloids at the Interfaces in the Earth's Critical Zone

Geoffrey Michael Gadd*

Division of Molecular Microbiology, College of Life Sciences, University of Dundee, Dundee, DD1 5EH, Scotland, UK.
*Corresponding author. Tel. No. +44 1382 384765; Fax No. +44 1382 388216; E-mail: g.m.gadd@dundee.ac.uk.

Keywords: Microorganisms; Biogeochemical cycling; Metals; Metalloids; Minerals; Geomicrobiology

Microorganisms are intimately involved in many processes of fundamental importance to geology, and these include biotransformations of metals and minerals, as well as related substances like metalloids, and metal radionuclides (Gadd *et al.*, 2005; Gadd, 2007). Such processes are involved in bioweathering, mineral dissolution and formation, and soil formation and development. Integral to all mechanisms are interactions with metals, and microorganisms are intimately involved in metal biogeochemistry with a variety of processes determining mobility, and bioavailability (Gadd, 2005; 2008). The balance between metal mobilization and immobilization varies depending on the organisms involved, their environment, and physico-chemical conditions. Metal mobilization can arise, e.g. from leaching mechanisms, complexation by metabolites, and methylation where this results in volatilization.. Immobilization can result from sorption, transport and intracellular sequestration or precipitation as a variety of "organic" and inorganic biominerals, e.g. oxalates (fungi), carbonates, phosphates and sulfides (Sayer *et al.*, 1999; Burford *et al.*, 2003, 2006). Sorption can be markedly affected by the presence of clay minerals, and clay mineral-biomass aggregates exhibit differing metal binding characteristics (Morley and Gadd, 1995; Gadd, 2009). This may be an important soil process as well as in epi- and endolithic microbial communities that are ubiquitous and associated with a wide variety of rocks and minerals (Burford *et al.*, 2003). In addition, reduction of higher-valency species may effect mobilization, e.g Mn(IV) to Mn(II), or immobilization, e.g. Cr(VI) to Cr(III).

Metal-mineral-microbe interactions can be considered an important topic within the framework of geomicrobiology, which can simply be defined as the roles of microbes in geological processes. Key topics within the geomicrobiology framework include biogeochemical cycling of the elements, mineral formation, mineral degradation (which can include such subjects as bioweathering and biocorrosion, as well as processes leading to soil and sediment formation), and the transformations of metals, metalloids and radionuclides. Apart from being important in natural environments, these processes can have beneficial or detrimental consequences in a human context. Bioremediation refers to the application of biological systems to the clean-up of organic and inorganic pollution with bacteria and fungi being the most important organisms in this context for breakdown, degradation, reclamation or immobilization of pollutants. In contrast, similar microbial activities may result in degradation and spoilage of natural and synthetic materials, rock and mineral-based building materials, acid mine drainage with accompanying metal pollution, biocorrosion of metals, alloys, and related substances, and adverse effects on radionuclide speciation, mobility and containment.

Metals exhibit a range of toxicities towards microorganisms, depending on physico-chemical factors, speciation etc, and while toxic effects can arise from natural processes in the soil, toxic effects on microbial communities are more commonly

associated with anthropogenic contamination or redistribution of toxic metals in aquatic and terrestrial ecosystems. Such contamination can arise from aerial and aquatic sources, as well as agricultural practices, industrial activity, and domestic and industrial wastes. In some cases, microbial activities can result in remobilization of metals from other wastes and transfer into aquatic systems. It is commonly accepted that toxic metals, and their chemical derivatives, metalloids, and organometals can have significant effects on microbial populations and almost every index of microbial activity can be affected. However, metal toxicity is greatly affected by the physico-chemical nature of the environment and the chemical behaviour of the particular metal species in question. Despite apparent toxicity, many microorganisms survive, and flourish in apparently metal-polluted locations and a variety of mechanisms, both active and incidental, contribute to tolerance (Gadd and Griffiths, 1978). All mechanisms depend on some change in metal speciation leading to decreased or increased mobility. Such metal transformations between soluble and insoluble phases are also at the heart of metal biogeochemistry, thus providing a direct link between microbial responses and element cycles. Thus, interactions of microorganisms with metals are extremely important and underpin many aspects of biogeochemistry, geomicrobiology and soil science.

In terrestrial environments, fungi serve as neglected but important geochemical agents (Gadd, 1993; 1999; 2006; 2007). Fungi promote rock weathering and contribute to the dissolution of mineral aggregates in soil through excretion of H^+, organic acids and other ligands, or through redox transformations of mineral constituents. We have found that the main mechanism of metal mobilization from insoluble metal minerals is a combination of acidification and ligand-promoted dissolution: if oxalic acid is produced the production of metal oxalates can occur. Fungi can therefore also play an active or passive role in mineral formation through precipitation of secondary minerals, e.g. oxalates, and through the nucleation of crystalline material onto cell walls that can result in the formation of biogenic micro-fabrics within mineral substrates. Such interactions between fungi and minerals are of importance to biogeochemical cycles including those of C, N, S and P. We have shown that fungi may play an important role in the transformation of micro-fabrics in limestone ($CaCO_3$) and dolomite ($CaMg(CO_3)_2$) and have produced direct evidence of mineralized fungal filaments with secondary carbonates. Experiments have shown that fungi can precipitate calcite ($CaCO_3$) and whewellite (calcium oxalate monohydrate, $CaC_2O_4{\cdot}H_2O$). We have examined elemental profiles of adjacent layers from a sandstone outcrop to find out whether differences in mineralogical composition influenced fungal and bacterial diversity. Culture-independent molecular approaches were used in combination with geochemical analyses, community-level physiological profiling and environmental scanning electron microscopy. A DNA-based community fingerprinting approach (ARISA: automated ribosomal intergenic spacer analysis) combined with construction of fungal and bacterial rRNA gene clone libraries (internal transcribed spacer) was used to assess community structure. Molecular data was combined with X-ray diffraction and X-ray fluorescence to identify those chemical properties that influenced community structure. It was found that sandstone supports a varied microbial diversity and community ribotype profiles differed between mineralogically-distinct sandstones in close proximity to each other (Gleeson *et al.*, 2005; 2006). Canonical correspondence analysis (CCA) illustrated relationships between certain ribotypes and particular chemical elements with Al, Na and Ca appearing to have a considerable impact on microbial community structure. Such molecular and statistical methods provide a powerful tool for resolving rock-inhabiting bacterial and fungal communities, and their relationship to the mineral nature of the substrate.

Other processes that can determine metal bioavailability are important microbially-catalyzed reactions of the natural sulfur cycle. Chemo-lithotrophic leaching by sulfur/sulfide-oxidizing bacteria can result in mobilization from polluted soil matrices, while sulfide production by SRB can result in precipitation of soluble metals as insoluble sulfides, with other redox transformations also being mediated by these organisms, e.g. Cr(VI) to Cr(III) (Smith and Gadd, 2000). We have found metals such as Cd, Co, Cr, Cu, Mn, Ni and Zn can be efficiently leached from contaminated soils, and removed from solution by SRB. In addition, SRB can reduce metalloid oxyanions such as selenite to elemental selenium (Hockin and Gadd, 2003; 2006). We have found that SRB, growing as a biofilm, can mediate formation of elemental sulfur in the presence of selenite. The

indirect, enzymatically-mediated coprecipitation of sulfur and selenium is a generalised ability among SRB, arising from sulfide biogenesis, and can take place under low redox conditions and in the dark (Hockin and Gadd, 2003).

This presentation will detail the above examples of metal-mineral transformations by microorganisms, and discuss their biogeochemical and applied relevance. For bioremediation, solubilization of metal contaminants provides a means of removal from soils, sediments, and solid industrial wastes. Alternatively, immobilization processes may enable metals to be transformed *in situ* and are particularly applicable to removing metals from aqueous solution. Specific highlighted examples in this presentation will include fungal degradation and transformations of copper and lead-containing minerals, depleted uranium and uranium oxides, fungal biodeterioration of concrete (which has implications for storage of radioactive waste), metal sulfide precipitation and reduction of metalloid oxyanions to elemental forms by sulfate-reducing bacteria. The overall aim of the presentation is to emphasise the important diversity of microbial roles in biogeochemical cycling and transformations of metals and related elements in the Earth's critical zone.

References

Burford EP, Fomina M, Gadd G (2003) Fungal involvement in bioweathering and biotransformation of rocks and minerals. Mineral. Mag. 67: 1127-1155

Burford EP, Hillier S, Gadd GM (2006) Biomineralization of fungal hyphae with calcite ($CaCO_3$) and calcium oxalate mono- and dihydrate in carboniferous limestone microcosms. Geomicrobiol. J. 23: 599-611

Gadd GM (1993) Interactions of fungi with toxic metals. New Phytol. 124: 25-60

Gadd GM (1999) Fungal production of citric and oxalic acid: importance in metal speciation, physiology and biogeochemical processes. Advances in Microb. Physiol. 41: 47-92

Gadd GM (2005) Microorganisms in toxic metal polluted soils. In: Buscot F, Varma A (eds.), Microorganisms in Soils: Roles in Genesis and Functions. Springer-Verlag, Berlin, pp. 325-356

Gadd GM (ed.) (2006) Fungi in Biogeochemical Cycles. Cambridge University Press, Cambridge

Gadd GM (2007) Geomycology: biogeochemical transformations of rocks, minerals, metals and radionuclides by fungi, bioweathering and bioremediation. Mycol. Res. 111: 3-49

Gadd GM (2008) Transformation and mobilization of metals by microorganisms. In: Violante A, Huang PM, Gadd GM (eds.), Biophysico-chemical Processes of Heavy Metals and Metalloids in Soil Environments. Wiley, Chichester, pp. 53-96

Gadd GM (2009) Biosorption: critical review of scientific rationale, environmental importance and significance for pollution treatment. J. Chem. Technol. Biot. 84: 13-28

Gadd GM, Griffiths AJ (1978) Microorganisms and heavy metal toxicity. Microbial. Ecol. 4: 303-317

Gadd GM, Semple K, Lappin-Scott H (eds.), (2005) Microorganisms in Earth Systems: Advances in Geomicrobiology. Cambridge University Press, Cambridge

Gleeson DB, Clipson NJW, Melville K, Gadd GM, McDermott FP (2005) Mineralogical control of fungal community structure in a weathered pegmatitic granite. Microbial. Ecol. 50: 360-368

Gleeson DB, Kennedy NM, Clipson NJW, Melville K, Gadd GM, McDermott FP (2006) Mineralogical influences on bacterial community structure on a weathered pegmatitic granite. Microbial. Ecol. 51: 526-534

Hockin S, Gadd GM (2003) Linked redox-precipitation of sulfur and selenium under anaerobic conditions by sulfate-reducing bacterial biofilms. Appl. Environ. Microb. 69: 7063-7072

Hockin S, Gadd GM (2006) Removal of selenate from sulphate-containing media by sulphate-reducing bacterial biofilms. Environ. Microb. 8: 816-826

Morley GF, Gadd GM (1995) Sorption of toxic metals by fungi and clay minerals. Mycol. Res. 99: 1429-1438

Sayer JA, Cotter-Howells JD, Watson C, Hillier S, Gadd GM (1999) Lead mineral transformation by fungi. Curr. Biol. 9: 691-694

Smith WL, Gadd GM (2000) Reduction and precipitation of chromate by mixed culture sulphate-reducing bacterial biofilms. J. Appl. Microb. 88: 983-991

Session 1

The Role of Mineral Colloids in Carbon Turnover and Sequestration and the Impact on Climate Change

Soils as Source and Sink of Environmental Carbon Dioxide

Rattan Lal*

Carbon Management and Sequestration Center, The Ohio State University, Columbus, Ohio 43210 USA.
*Corresponding author. E-mail: lal.1@osu.edu.

World soils contain 2500 Pg C to 1-m depth, comprising of 1500 Pg of soil organic C (SOC) and 950 Pg of soil inorganic C (SIC) (Houghton, 2007; Lal, 2004). Therefore, the soil C pool is 3.1 times more C than the atmospheric pool (800 Pg and increasing at the rate of 4.1 Pg $C \cdot yr^{-1}$) and 4.0 times the biotic pool (620 Pg and decreasing at the rate of 1.6 Pg $C \cdot yr^{-1}$). The current global C budget comprises anthropogenic emissions of 8.0 Pg $C \cdot yr^{-1}$ from fossil fuel combustion and cement manufacture, and 1.6 Pg $C \cdot yr^{-1}$ from deforestation, biomass burning and soil cultivation. Of the total emission of 11.5 Gt C E (including CO_2, CH_4 and N_2O) in 2000, 14% (1.6 Pg) were those due to agricultural activities and 18% (2.1 Pg) from land use conversion. Thus, land use and agriculture contribute about one-third (32%) of total anthropogenic emissions. Confirmed sinks include atmospheric absorption of 4.1 Pg $C \cdot yr^{-1}$, oceanic uptake of 2.3 Pg $C \cdot yr^{-1}$, and a land sink of about 1.5 Pg $C \cdot yr^{-1}$ (WMO, 2008). Thus, there is an unknown terrestrial sink of about 1.7 Pg $C \cdot yr^{-1}$.

Atmospheric concentration of CO_2 has increased from 280 $mg \cdot L^{-1}$ in the pre-industrial era to about 382 $mg \cdot L^{-1}$ by volume, or 582 $mg \cdot L^{-1}$ by mass in 2008. In total, the atmosphere contains approximately 0.01% of the C present in the atmosphere-ocean-upper earth crust system (Oelkers and Cole, 2008). World soils and terrestrial ecosystems have been the source of atmospheric CO_2 ever since the dawn of agriculture about 10,000 years ago, and of CH_4 since the domestication of animals and cultivation of rice paddies about 5,000 years ago (Ruddiman, 2005). Terrestrial ecosystems (soils and vegetation) may have contributed as much as 320 Pg C from pre-historic era to 1850 (Ruddiman, 2005) and about 158 Pg C from 1850 to 2006 (Canadell *et al.*, 2007). Presently, terrestrial ecosystems and agricultural activities contribute about 1.6 Pg C as CO_2 and 3.7 Pg CE (including CO_2, CH_4 and N_2O) (Koonin, 2008). In comparison, fossil fuel combustion have contributed 292 Pg C between 1750 and 2002, and is projected to contribute an additional 200 Pg C between 2003 and 2030 (Holdren, 2008). Therefore, world soils have been historically a major source of atmospheric CO_2. Most agricultural soils have lost 25% to 75% of their SOC pool, and the magnitude of loss is more on severely eroded/degraded than slight or un-degraded soils.

The process of transfer of atmospheric CO_2 into other long-lived pools (geologic, oceanic, terrestrial), called C sequestration, is widely considered an option to mitigated the climate change (Broecker, 2008; Oelkers *et al.*, 2008; Lal, 2008). Sequestration of CO_2 into terrestrial ecosystem (soils, trees) is based on the natural process of photosynthesis. The terrestrial biosphere annually photosynthesizes about 120 Pg C into the biomass. However, almost all of it is returned back to the atmosphere either through plant respiration or soil respiration. Yet, global C budget can be effectively balanced even if merely 8% to 10% of the photosynthesized C is retained in the biosphere.

Conversion to a restorative land use (perennial land use such as forest cover, permanent pastures) and adoption of recommended management practices (RMPs) on agricultural soils can create a positive soil C budget. There is a wide range of RMPs, and no one technology is universally applicable under diverse soils and ecoregional conditions. Some examples of RMPs for cropland include no-till farming with crop residue mulch and cover cropping, use of complex crop rotations including agroforestry, adoption of integrated nutrient management (INM) techniques

including use of biofertilizers (e.g., manure, compost, biological N fixation, mycorrhizae), application of soil amendments (e.g., biochar, soil conditioners), and soil water management (e.g., drip irrigation, water harvesting and recycling). Similarly, RMPs for grazing lands include sowing of improved forage species, controlled grazing with low stocking rate, fire management, water conservation, etc.

The rate of SOC sequestration in agricultural soils is about 0.1 to 1.5 Mg $C \cdot ha^{-1} \cdot yr^{-1}$ depending on climate, soil type, land use and management. The rate is more in cool and humid than in warm and dry regions, and more in heavy-textured than light-textured soils. The potential of C sequestration in terrestrial ecosystems (soils and trees) is about 3 Pg $C \cdot yr^{-1}$ for the next 25 to 50 years. It is equivalent to a total drawdown of about 50 $mg \cdot L^{-1}$ of atmospheric CO_2 (Hansen *et al.*, 2008).

There are numerous co-benefits of C sequestration in soils. Improvement in soil quality increases use-efficiency of input and crop yields. Thus, soil C sequestration is essential to advancing global food security. Other ancillary benefits include increase in biodiversity, improvement in quality of natural waters and decrease in non-point source pollution, and increase in aesthetic value of ecosystems. Soil C sequestration, being a cost-effective (McKinsey and Co., 2008) and a natural process, is a win-win situation. It is a bridge to the future, until non-C or C-neutral fuel sources take effect.

References

Broecker WS (2008) CO_2 capture and storage: possibilities and perspectives. Elements 4: 295-296

Canadell JP, Que're' CL, Raupach MR, Field CB, Buitenhuis ET, Ciais P, Conway TJ, Gillett NP, Houghten RA, Marland G (2007) Contributions to accelerating atmospheric CO_2 growth from economic activity, carbon intensity, and efficiency of natural gas sinks. Available at: http://www.pnas.org/cgi/doi/10.1073/pnas.0702737104

Hansen J, Sato M, Kharecha P, Beerling D, Berner R, Masson-Demotte V, Pagani M, Raymo M, Royer DL, Zachus JC (2008) Target atmospheric CO_2: Where should humanity aim? Safe CO_2, British Columbia, CA

Holdren JP (2008) In proceedings of Climate Challenge. Eighth Annual John P. Chafee Memorial Lecture on Science and the Environment. National Council of Sci. & Env, 17 January 2008, Washington DC

Houghton RA (2007) Balancing the global carbon budget. Ann. Rev. Earth Planet. Sci. Lett. 35: 313-347

Koonin SE (2008) The challenges of CO_2 stabilization. Elements 4: 293-294

Lal R (2004) Soil carbon sequestration impact on global climate change and food security, Science 304: 1623-1627

Lal R (2008) Carbon sequestration. Phil. Trans. Roy. Soc. (B) 363:815-830

McKinsey, Co. (2008) Pathways to Law Carbon Economy. Version 2 of the Global Greenhouse Gas Abatement Cost Curve

Oelkers EH, Cole DR (2008) Carbon dioxide sequestration: A solution to a global problem. Elements 4: 305-310

Ruddiman WF (2005) The anthropogenic greenhouse era began thousands of years ago. Climatic Change 61: 262-292

WMO (2008) Greenhouse Gas Bulletin. World Meteorological Organization, Geneva, Switzerland

Impacts of Mineral Colloids on the Transformation of Biomolecules and Physical and Chemical Protection of Soil Organic Carbon

Pan Ming Huang†

Department of Soil Science, University of Saskatchewan, 51 Campus Drive, Saskatoon, SK S7N 5A8, Canada.

Abstract: Soil mineral colloids, along with enzymes, have the ability to catalyze the transformation of biomolecules, which are from biological residues, root exudates, and biological metabolites, to relatively recalcitrant humic substances (HS). Virtually all HS in a wide range of soils are bound to mineral colloids, especially short-range ordered (SRO) Al and Fe (oxy) hydroxides because of their large specific surface area, high density of reactive sites, and surface reactivity. Soil mineral-HS complexes may anchor unstable plant constituents by various adsorptive forces and/or chemical binding. Highly degradable proteins, for example, may be protected against rapid biodegradation by their neucleophilic addition to mineralcomplexes. Besides chemical protection, mineral colloids have the ability to interact with biomolecules and microorganisms to form microaggregates. Furthermore, organic substances serve as intraicroaggregate binding agents leading to the formation of macroaggregates through biogenic aggregation processes. The vast majority (90%) of soil organic C (SOC) in surface soil is located within aggregates. Undecomposed biological materials have turnover times in terms of years. Turnover times of occluded SOC increase with decreasing aggregate size. SOC in macroaggregates has turnover times in terms of decades and the turnover times are about centennials for SOC in microaggregates. Tounover times of chemically protected SOC through binding to mineral surfaces usually approach millennia. Therefore, mineral colloids play a vital role in governing the transformation and turnover of soil organic matter and the impact on climate change.

Keywords: Mineral colloids; Biomolecules; Humification; Recalcitrance; Occlusion; Aggregation; Complexation; Chemical protection

Introduction

The stocks of organic matter in soils results from the balance between inputs and outputs of SOC within the below-ground environment. Inputs are primarily controlled by net primary productivity; outputs are dominated by the efflux of CO_2 from the soil surface, although methane CH_4 efflux and hydrological leaching of dissolved organic and inorganic and particulate organic C compounds can also be important (Davidson and Janssens, 2006). During the turnover process of organic C, biomolecules are transformedto more recalcitrantHS through enzymatic and mineral catalyzes (Hardie *et al.*, 2009a; Huang and Hardie, 2009). HS and some of the relatively unstable biological residues, root exudates, and microbial metabolites may become physically protected in the interior of soil aggregates. Furthermore, these biologically derived organic components may become sorbed onto surfaces of mineral colloids, especially SRO Al and Fe (oxy) hydroxides, thus chemically protected. Therefore, the pivotal role of mineral colloids in the transformation and turnover of SOC can be addressed in terms of (1) abioticcatalysis of the transformation of biomolecules to HS, (2) physical protection through occlusion of SOC in aggregates, and (3) chemical protection through sorption of SOC on the surface of mineral colloids.

Formation of HS

There is a large volume of work documenting the polycondensation and polymerization of simple biomolecules (e.g., polyphenols, amino acids, and sugars), as catalyzed by soil minerals and enzymes, leading to the formation of HS (Shindo and Huang, 1982; Wang and Huang, 1986; Bollag *et al.*, 1998; Huang and Hardie, 2009). Because these catalysts are ubiquitous in soil environments and the substrate biomolecules are readily available from the continuous decomposition of biological residues, root exudates and microbial metabolite, it is certain that these reactions occur in the natural environment. HS is relatively recalcitrant compared to labile biomolecules (e.g., polysaccharides and protein). There is ample evidence that the biotic community is able to degrade any organic matter of natural origin. Therefore, the recalc-itrance of organic matter is less important in later stages of decomposition. However, the HS formed through abiotic and biotic catalyses would interact with very reactive mineral colloids to form very stable mineral-humic complexes as addressed below. It is well established that HS is largely associated with mineral particles in a wide range of soils (Huang and Hardie, 2009).

Physical Protection

Nearly 90% of SOC in surface soils is located within aggregates (Jastraw *et al.*, 1996) with 20% to 40% of SOC in intra-microaggregates (Carter, 1996). Turnover times of occluded SOC increase with decreasing aggregate size. Turnover times were about 15 to 50 years for SOC stored in macroaggregates and 100 to 300 years for SOC in microaggregates (Puget *et al.*, 2000; Six *et al.*, 2000; John *et al.*, 2005). SOC is stabilized by different aggregate formation processes, biogenic aggregation in macroaggregates and physicoch- emical interactions of mineral colloids with organic substances and microorganisms in microagreegates. Biogenic aggregation is a relatively transient process within the active and intermediate SOC pools and is sensitive to management practices. Occlusion of SOC within microaggregates, especially in the <20 μm is operative over long time scales controlled by pedogenic processes (von Lützow *et al.*, 2006). Mineral colloids, thus, have a vital role in influencing the turnover of SOC through the formation of aggregates.

Chemical Protection

Early experimental evidence such as the work of Allison *et al.* (1949) has led many authors (e.g., Tate and Theng, 1980; Oades *et al.*, 1989) to suggest that the impact of clays on C stabilization will change as a function of clay mineralogy. Soil mineral colloids, especially SRO Al and Fe (oxy)hydroxides have the ability to complex with SOC (Huang and Hardie, 2009) and control the turnover rate and storage of SOC (Torn *et al.*, 1997; Rasmussen *et al.*, 2005). Chemical protection of SOC against decomposition throughass-ociation with mineral surfaces has received increasing attention over the past two decades and has been identified as the most likely mechanism to achieve centennial and millennial protection of SOC (Kögel-Knabner *et al.*, 2008). However, a detailed mechanistic understanding at a molecular level of why sorption of SOC to soil minerals decreases decom-position rates of SOC is lacking. Furthermore, HS, which is formed through mineral and enzymatic catalyses and sub-sequently bound to mineral surfaces to form mineral-humic complexes, may anchor and encapsulate unstable biomolecules by various adsor-ption processes or chemical binding (Bollag *et al.*, 1998; Huang and Hardie, 2009). Any biomolecules intimately associated with HS that cannot be separated effectively by chemical and physical methods may be considered as humic components (Sutton and Sposito, 2005).

Therefore, many unstable biological constituents may survive in mineral-humus complexes in the environment for a significant length of time. Most recently, it has been shown that mineral catalysisnot only promotes the formation of HS from biomolecules but also the genesis of carbonates such as rhodo-chrosite ($MnCO_3$) (Hardie *et al.*, 2009b). This indicates the vital role of mineral catalysis in abiotic carbonate formation from biomolecules, which contributes to C sequestration in natural environments.

Conclusions

Transformations of biomolecules from biological residues, root exudates, and microbial metabolites under enzymatic and mineral catalyses as influenced by climatic factors and anthropogenic activity are important processes contributing to the turnover of SOC. Tissue chemistry, i.e., recalcitrance of biological materials is less important at the late stage of decomposition of SOC. Physical protection by occlusion of SOC in aggregates, which are formed by interactions of mineral colloids with nonliving organic matters and microorganisms, accounts for turnover times of decades and centennials. Chemical protection by bonding of SOC to mineral surfaces to form mineral colloid-humus complexes accounts for the turnover times of millennials. Therefore, pedogenic processes of mineral weathering transformations control the strength of bonding and the amount of SOC stored in the terrestrial ecosystem. It is thus challenging to understand at a molecular level the mechanisms of bonding SOC to mineralsurfaces and how they would govern turnover and stabilization of SOC. This is of fundamental importance in developing innovative land resource management strategies to sequester C in the terrestrial ecosystem.

References

Allison FE, Sherman MS, Pink LA (1949) Maintenance of soil organic matter: I. Inorganic soil colloids as a factor in retention of carbon during formation of humus. Soil Sci. 68: 463-478

Bollag JM, Dec J, Huang PM (1998) Formation mechanisms of complex organic structures in soil habitats. Adv. Agron. 63: 237-266

Carter MR (1996) Analysis of soil organic matter storage in agroecosystems. In: Steward BA (ed.) Structure of Organic Matter Storage in Agricultural Soils. CRC Press, Boca Raton, pp. 3-11

Davidson EA, Janssens IA (2006) Temp-eraturesen-sitivity of soil carbon decomposition and feedbacks to climate change. Nature 440: 165-173

Hardie AG, Dynes JJ, Kozak LM, Huang PM (2009a) The role of glucose in abiotic humif-icationpathways as catalyzed by birnessite. J. Mol. Catalysis A: Chemical (in press)

Hardie AG, Dynes JJ, Kozak LM, Huang PM (2009b) Biomolecule-induced carbonate genesis in abiotic formation of humic substances in nature. Can.J. Soil Sci. (in press)

Huang PM, Hardie AG (2009) Formation mechanisms of humic subst-ances in the environment. In: Senesi N, Xing B, Huang PM (eds.), Biophysico-Chemical Processes of Nonliving Organic Matter in Environmental Systems. Wiley-IUPAC Series, Vol. 2. John Wiley & Sons, Hoboken, NJ (in press)

Jastraw JD, Boutton TW, Miller RM (1996) Carbon dynamics of aggregate-associated organic matter estimated by carbon-13 natural abundance. Soil Sci. Soc. Am. J. 60: 801-807

John B, Yamashita T, Ludwig B, Flessa H (2005) Storage of organic carbon in aggregate and density fractions of silty soils under different types of land use. Geoderma: 128: 63-79

Kögel-Knabner I, Guggenberger G, Kleber M, Kandeler E, Kablitz K, Scheu S, Eusterhues K, Leinweber P (2008) Organo-mineral associations in temperate soils: integrating biology, mineralogy and organic matter chemistry. J. Plant Nut. Soil Sci. 171: 61-82

Oades JM (1989) An introduction to organic matter in mineral soils. In: Dixon JB, Weed SB (eds.) Minerals in Soil Environments. Soil Science Society of America, Madison, WI. pp. 89-159

Puget P, Chenu C, Balesdent J (2000) Dynamics of soil organic matter associated with particle-size fractions of water-stable aggregates. Euro. J. Soil Sci. 51: 595-605

Rasmussen C, Torn MS, Southard RJ (2005) Mineral assemblage and aggregates control carbon dynamics in a California conifer forest. Soil Sci. Soc. Am. J. 69: 1711-1721

Shindo H, Huang PM (1982) Role of Mn(IV) oxide in abiotic formation of humic substances in the environment. Nature 298: 363-365

Six J, Paustian K, Elliot ET, Combrink C (2000) Soil structure and organic matter: I. Distribution of aggregate-size classes and aggregate-associated carbon. Soil Sci. Soc. Am. J. 64: 681-689

Sutton R, Sposito G (2005) Molecular structure in humic substances: The new view. Environ. Sci. Technol. 39: 9009-9015

Tate KG, Theng BKG (1980) Organic matter and its interactions to organic soil constituents. In: Theng BKG (ed.), Soils with Variable Charge. New

Zealand Society of Soil Science, Lower Hutt, pp. 225-249

Torn MS, Trumbore SE, Chadwick OA, Vitousek PM, Hendricks DM (1997) Mineral control of soil organic carbon storage and turnover. Nature 389: 170-173

Von Lützow M, Kögel-Knabner I, Ekschmitt K, Matzner E, Guggenberger G, Marshner B, Flessa H (2006) Stabilization of organic matter in temperate soils: mechanisms and their relevance under different soil conditions – a review . Euro. J. Soil Sci. 57: 426-445

Wang MC, Huang PM (1986) Humic macromolecular interlayering in nontronite through Interaction with phenol monomers. Nature 323: 529-531

Unravelling the Biogeochemical Cycles of Carbon and Nutrients in Forest Ecosystems: Innovative Approaches with Advanced Stable Isotope and NMR Techniques as well as Soil Chemical and Physical Methods

Zhihong Xu*

Centre for Forestry and Horticultural Research and School of Biomolecular and Physical Sciences,
Griffith University, Nathan, Brisbane, Queensland 4111, Australia.
*Corresponding author. Tel. No. +61-7-37353822; Fax No. +61-7-37357773; E-mail: zhihong.xu@griffith.edu.au.

Abstract: Long-term impacts of global climate change (GCC) and local forest management on important biogeochemical cycles of carbon (C) and nutrient cycling in the soil-plant ecosystems are complex and difficult to assess, particularly under gradually and continuously rising atmospheric carbon dixoide concentration [CO_2] and warming in the real world with multiple limiting factors. In this presentation, we highlight the recent developments and applications of advanced stable isotope, nuclear magnetic resonance (NMR) and bio-molecular techniques, in an integrated approach with innovative rhizosphere and tree ring methods, for improving our understanding and management of above- and below-ground C and nutrient cycling processes in forest ecosystems, particularly in response to GCC and local management practices as well as mitigation / adaptation strategies. The opportunities and limitations of these techniques for investigating C and nutrient cycling processes in forest ecosystems are discussed, in the context of both short- and long-term impacts on the above- and below-ground processes. Improved understanding and knowledge of environmental fingerprints of the biogeochemical cycles embedded in tree rings can be effectively used to account for long-term forest productivity and C stocks at local, regional and global scale in response to the future GCC and management options.

Keywords: C and nutrient cycling; Global climate change; Acid deposition; Forest management; Above- and below-ground processes; Integrated approach; Stable isotope; NMR; Bio-molecular technique; Rhizosphere; Tree ring growth

Global Climate Change and Forest Management

Over the last century, atmospheric [CO_2] has increased globally by nearly 30% and temperature by approximately 0.6 ℃, and these trends are projected to continue more rapidly (Xu and Chen, 2006; Xu *et al.*, 2009), particularly with more extreme climatic conditions. The impacts of GCC on future structure, composition, and C and nutrient cycling in forest ecosystems deserve particular attention and further research. Little is known about the impacts of GCC and forest management on plant-soil-microbe interactions. Plant-soil-microbe interactions mainly occur in the rhizosphere, which is defined as the zone of soil that is affected by the root activity of any plant species. The rhizosphere is suggested here as the "hotspot" for plant-soil-microbe interactions the most chemically and biologically active microsite in soil, and represents a complex integrated ecosystem. The ecology in the underworld, particularly below-ground processes and their interactions with above-ground processes, has been highlighted (Science 304, 11 June 2004). There is growing need for improving the understanding and management of important below-ground processes. Understanding rhizosphere C and nutrient cycling processes in relation to rising [CO_2] and temperature is crucial for predicting the response of forest ecosystems to GCC (Xu and Chen, 2006; Xu *et al.*, 2009).

Rhizosphere Study Techniques

The quantitative understanding of rhizosphere processes is poor, since the rhizosphere is a difficult system to physically sample and manipulate (Xu and Chen, 2006). Currently there are two commonly-used methodologies to physically separate rhizosphere soil from bulk soil. One is the hand-shaking method. The second approach involves direct (in situ) sampling of soil adjacent to roots by thin sectioning and/or placement of different sized mesh materials around roots (Xu and Chen, 2006). It is challenging, but necessary to develop sampling techniques and protocols building on the promising hand-shaking method, which takes into account the spatial and temporal variability in the rhizosphere of forest ecosystems. In addition, modelling of rhizosphere will be able to upscale the uptake of nutrients to the whole plant scale.

Microbiological Methods

Soil microbial properties, such as biologically regulated nitrogen (N) transformations, microbial biomass C, N and phosphorus (P), respiration, metabolic quotient and enzyme activity, can be very sensitive to GCC and forest management (Xu and Chen, 2006; Xu *et al.*, 2009). However, information about the impacts of GCC and forest management on soil microbial properties is rather limited. Conventional culture-dependent methods have been used for the measurement of soil microbial composition for more than a hundred years. Nevertheless, only 0.1%~1% of soil microorganisms are accessible by these approaches.

Biomolecular Techniques

Recent advances in bio-molecular techniques make it possible to apply culture-independent and DNA/RNA nuclear acid-based techniques to analyze the targeted sequences of bacterial or fungal DNA directly extracted from soil (Xu and Chen, 2006). The determination of 16S ribosomal RNA (rRNA) genes and 18S rRNA genes has proved most useful for investigating the diversity and composition of bacteria and fungi respectively since these molecules are composed of highly conserved regions and also of regions with considerable sequence variation. The applications of microbial functional genes (e.g., *pmoA* and *amoA*) have greatly improved our understanding of the abundance and composition of specific groups (e.g. methanotrophs and ammonia oxidisers) of microorganisms involving in the biogeochemical cycling.

Stable Isotope and NMR Techniques

Stable isotope techniques are considered as a critical component in the studies of GCC (e.g. elevated [CO_2]) and forest management on soil C and N dynamics (Xu and Chen, 2006). Stable isotope techniques have been found to be a very powerful tool for advancing the understanding of important C and N cycling processes in terrestrial ecosystems. Recent applications of stable isotope techniques to soil biological studies have resulted in significant advances in the understanding of soil microbial processes regulating the C and N cycling in terrestrial ecosystems. It is very exciting to see the combined use of stable isotope and bio-molecular techniques in recent studies (Xu and Chen, 2006; Xu *et al.*, 2009), which have identified specific microorganisms that are actively involved in particular metabolic processes.

NMR techniques have been increasingly used in soil science, geochemistry and environmental science (Xu and Chen, 2006; Xu *et al.*, 2009). In particular, ^{13}C NMR has been widely used to improve the understanding of soil organic matter (SOM) quality and composition in relation to terrestrial C and N cycling processes. Natural abundance ^{15}N cross polarization / magic angle spinning (CP/MAS) NMR spectra of SOM have been obtained by Knicker *et al.* (1993), indicating that almost all signal intensity is in the chemical shift region assigned to peptide/amide N. In the first application of ^{14}N-NMR to soil humic acid (HA) studies, we have discovered the existence of nitrate-N in soil HA (Mao *et al.*, 2002). with the HA nitrate-N closely related to soil N availability and rather responsive to ecosystem management. The advanced NMR techniques need to be assessed for their potential in improving the understanding of rhizosphere C and nutrient cycling, particularly when combined with stable isotope and bio-molecular techniques.

Tree Ring Technique

Most terrestrial ecosystem studies (Xu *et al.*, 2009) on GCC impacts have been undertaken over short periods (<10 years) with one or two factors of contrasting treatments (e.g. with and without N additions) and large step increases (e.g. ambient [CO_2] 350 mg·L^{-1} and elevated [CO_2] 700 mg·L^{-1}). These would be very different from the real world with gradually rising [CO_2] and warming as well as changing rainfall patterns in the context of atmospheric deposition over periods from decades to centuries, particularly for forest ecosystems. Tree ring growth, stable isotope composition and element concentration (over decades or centuries, can provide exciting opportunities to investigate the impacts of GCC and historical episodes (e.g. acid deposition and prescribed burning or wild fires) on important biogeochemical cycles of C and nutrients (Xu and Chen, 2006; Xu *et al.*, 2009), underpinning the long-term tree growth and water use efficiency (WUE) as well as biodiversity of forest ecosystems. However, this type of research approach is not without significant problems, and requires complementary short-term laboratory and field experiments to help tease out the complex interactions among multiple factors of gradual GCC and historical episodes. While rising [CO_2] and atmospheric warming are well recognised GCC phenomena (Xu and Chen, 2006), their long-term impacts on biogeochemical cycles, ecosystem productivity and biodiversity can differ with locations and species / ecosystems (Xu *et al.*, 2009), in the context of local rainfall, temperature, atmospheric deposition/air pollution and soil fertility.

In addition, rising [CO_2] is expected to result in increased plant photosynthesis and reduced stomatal conductance, hence higher plant WUE and $\delta^{13}C$, but this can be counteracted by decreasing plant photosynthesis and $\delta^{13}C$ due to acid deposition and decreasing atmospheric $\delta^{13}C$ from increasing fossil CO_2 emissions respectively. Plant WUE and growth can be increased by elevated [CO_2] and N availability, at least in the short term, but their long-term levels may be counteracted by age-related biologically declining trends and progressive nutrient limitations. The mobility of elements (e.g. N) between adjacent tree rings and differences in stable isotope composition between components of tree ring material (e.g. cellulose against whole tree ring material) can also pose problems in interpreting these ring data, with increasing margins of error. Furthermore, there are limited long-term records of local atmospheric [CO_2], temperature, rainfall and acid deposition for many parts of the world, and either re-constructed or global averages of these parameters would need to be used from ice core and tree ring data for assessing the long-term impact of gradual GCC and historical episodes. These would need to be calibrated and tested by well controlled and focused studies as well as sophisticated mathematical and ecosystem modelling across the diversified regions of the world.

References

Knicker H (2002) The feasibility of using DCPMAS N-15 C-13 NMR spectroscopy for a better characterization of immobilized N-15 during incubation of C-13- and N-15-enriched plant material. Org. Geochem. 33: 237-246

Mao XA, Xu ZH, Luo RS, Mathers NJ, Zhang YH, Saffigna PG (2002) Nitrate in soil humic acids revealed by nitrogen-14 nuclear magnetic resonance spectroscopy. Aust. J. Soil Res. 40: 717-726

Xu ZH, Chen CR (2006) Fingerprinting global climate change and forest management within rhizosphere carbon and nutrient cycling processes. Environ. Sci. Pollut. Res. 13: 293-298

Xu ZH, Chen CR, He J, Liu JX (2009) Trends and challenges in soil research: linking global climate change to local long-term forest productivity. J. Soils Sediments 9: 83-88

Effects of Soil Management from Fallow to Grassland on Soil Microbial and Organic Carbon Dynamics

Yuping Wu[a], Sarah Kemmitt[b,c], Jianming Xu[a], Philip C Brookes[b,*]

[a]Zhejiang Provincial Key Laboratory of Subtropical Soil and Plant Nutrition,
College of Environmental Natural Resource Sciences, Zhejiang University, Hangzhou 310029, China;
[b]Soil Science Department, Rothamsted Research, Harpenden, Herts, AL5 2JQ, UK;
[c]Current address: British Library 96, Euston Road, London NW1 2DB, UK.
[*]Corresponding author. Tel. No. +441582763133; Fax No. +4401582760981; E-mail: philip.brookes@bbsrc.ac.uk.

Abstract: Permanent 60 year fallow, arable and grassland soils from the Highfield Ley-Arable Experiment at Rothamsted Research, UK were used to investigate if extremes in soil management affected soil microbial biomass, microbial activity and microbial diversity. They were incubated under laboratory conditions, with and without amendment with a labile (yeast extract) and recalcitrant substrate (ryegrass). Microbial biomass ATP concentrations were not significantly different between the soils, with or without substrate addition. The biomasses in the three soils also mineralised the two substrates similarly and microbial biosynthesis efficiency (measured as biomass C and ATP) was similar. However, Phospholipid Fatty Acid (PLFA) analysis revealed that microbial community structure, with and without substrates, differed significantly between soils. Therefore substrate type drives soil microbial ecosystem response much more than does soil microbial biodiversity.

Keywords: Biomass; Community structure; Mineralization; Phospholipid fatty acid

Introduction

Currently, links between soil microbial diversity and soil functioning are not well understood. Here we report results where three very contrasting managements: permanent fallow, permanent arable and permanent grassland, have been applied to the same soils for at least 60 years. This represents extreme soil differences where it would be expected that differences in microbial community structure should exist, if anywhere. Our aim was to determine responses of the three different microbial communities to addition of a labile (yeast extract) and a more recalcitrant substrate (ryegrass) and to determine if differences in metabolism of the substrates and efficiencies of microbial biosynthesis was related to differences in initial soil microbial community structure measured by PLFA analysis.

Materials and Methods

Soils

A permanent grassland, permanent arable and permanent fallow from the Highfield Ley-Arable experiment at Rothamsted Research were used. The soil (Aquic Paleudalf (USDA) is a fine silty clay loam (27% clay). Each treatment has been applied for at least 60 years (Johnston, 1994). The fallow and arable soils were sampled 0~23 cm and the grassland soil 0~10 cm depth. The soils were analyzed for total C and N by dry combustion. Soil pH was also measured. The sieved, fresh soils were adjusted to 40% of water holding capacity and then incubated at 25 ℃ for 7 days before use.

Soil Incubations

The moist soil portions, 50 g soil on an oven-dry basis, were amended with yeast extract in solution or

ryegrass (*Lolium perenne* L.), separately, at 5000 μg $C \cdot g^{-1}$ soil. The yeast extract (40.8% total C, 11.45% total N) was added in aqueous solution. The ryegrass (45.7% total C and 3.1% total N) was air-dried and milled (<2 mm). All soils were then adjusted to 50% water holding capacity (WHC). Each replicate was then placed separately into a 1.1 L brown bottle containing 10 mL free water at the base and a vial containing 25 mL 1.0 $mol \cdot L^{-1}$ NaOH. The bottles were stoppered with rubber bungs to exclude air and incubated in the dark at 25 ℃ for up to 112 days in a randomized block design.

Biological Analyses

The CO_2-C evolved from the soils and trapped in the NaOH was determined by autotitration Biomass C was measured by fumigation-extraction (Vance *et al.*, 1987; Wu *et al*., 1990). Soil ATP was measured as described by Jenkinson and Oades (1979) and Tate and Jenkinson (1982). Phospholipid Fatty acids were determined according to Zelles (1997).

Results and Discussion

The initial soil pH was significantly different ($P < 0.05$) between fallow (5.09 ± 0.01), arable (5.80 ± 0.01) and grassland soils (6.05 ± 0.03) after more than 60 years of different land managements (Fig. 1). Total soil C concentrations were 1.21%, 1.70% and 4.02 % and total N concentrations were 0.10%, 0.16% and 0.37% in the fallow, arable and grassland soils respectively. However the three soil C:N ratios were all around 10. The yeast extract and ryegrass were mineralised very similarly and microbial biosynthesis (measured as biomass C and ATP), occurred at about the same efficiency in the three soils. It seems remarkable that the biomass in the amended and unamended soils, incubated with and without two quite different substrates all had comparable biomass ATP concentrations (Fig. 1). The overall mean biomass ATP concentration of 10.8 μmol $ATP \cdot g^{-1}$ biomass C was extremely close to the mean of 10.6 μmol $ATP \cdot g^{-1}$ biomass C obtained from a range of UK and Australian soils reported by Oades and Jenkinson (1978) in the first measurements of ATP ever reported in soil. Later, Jenkinson (1988) and Contin *et al.* (2001) collated all available data in the world literature and obtained highly comparable values of 11.7 and 11.0 μmol $ATP \cdot g^{-1}$ biomass C respectively.

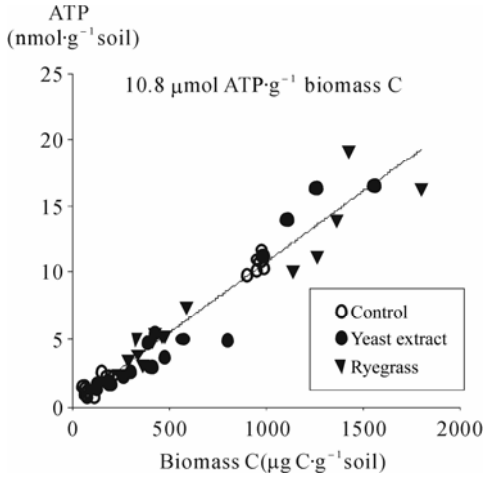

Fig. 1 Biomass ATP concentrations in unamended and mended soils

The community structures, as determined by PLFA analysis, were markedly different in the three unamended soils (Wu *et al.*, 2009). Nearly half of the difference in the data set was represented by differences between fallow, grassland and arable soils (PC1 40.70% for yeast extract added soil, 45.15% for ryegrass added soils). The second dimension accounted for 25.38% (yeast extract) and 21.33% (ryegrass) of the variation, i.e. between control and substrate addition. Thus, overall, more than 65% of the total variation in the data set is accounted for in the two principal components. Considering that the fallow and grassland soils represented the two extremes of management it was surprising that there was comparatively little difference following the addition of this labile substrate in either soil. In contrast there was a shift in the arable soil, which might be considered to occupy a position mid-way between them. With ryegrass there was little change in community structure in the grassland soil. It might be inferred that this is because this ecosystem is best adapted to inputs of ryegrass derived residues so does not need to change to accommodate them. There was a much larger community shift with ryegrass in the arable and fallow soil, with the fallow soil showing the largest response. Unexpectedly, in contrast it shifted least following addition of yeast extract. Reasons for this are not known. It does seem remarkable that a soil fallowed for such a long period showed few if any, significant differences in

responses to substrate inputs compared to soils under permanent arable or grassland management. Thus, soil biodiversity seems not to govern ecosystem response to substrate addition nearly as much as does the nature of the substrate itself.

Acknowledgements

We thank the China Scholarship Council and the Y.C. Tang Disciplinary Development Fund of Zhejiang University for supporting Yuping Wu to study in UK, and PR Hirsh and IM Clark for useful discussion. Rothamsted Research is an Institute of the Biotechnology and Biological Sciences Research Council, UK.

References

Contin A, Todd A, Brookes PC (2001) The ATP concentration in the soil microbial biomass. Soil Biol. Biochem. 33: 701-704

Jenkinson DS (1988) Determination of microbial biomass nitrogen and carbon in soil. In: Wilson JT (ed.), Advances in Nitrogen Cycling in Agricultural Ecosystems. Commonwealth Agricultural Bureau International, Wallingford, pp. 368-386

Jenkinson DS, Oades JM (1979) A method for measuring adenosine triphosphate in soil. Soil Biol. Biochem. 11: 193-199

Johnston AE (1994) The Rothamsted Classical Experiments. In: Leigh RA, and Johnston AE (eds.) Long-term Experiments in Agricultural and Ecological Sciences, CAB International, UK

Oades JN, Jenkinson DS (1979) Adenosine triphosphate content of the soil microbial biomass. Soil Biol. Biochem. 11: 201-204

Tate KR, Jenkinson DS (1982) Adenosine triphosphate measurements in soil: an improved method. Soil Biol. Biochem. 14: 331-335

Vance ED, Brookes PC, Jenkinson DS (1987) An extraction method for measuring soil microbial biomass C. Soil Biol. Biochem. 19: 703-707

Wu J, Joergensen RG, Pommerening B, Chassod R, Brookes PC (1990) Measurement of soil microbial biomass C by fumigation-extraction: an automated procedure. Soil Biol. Biochem. 22: 1167-1169

Wu Y, Kemmitt S, Xu J, Brookes PC (2009) Substrate addition is much more important in driving soil microbial processes than differences in microbial biomass, activity or community structure. Soil Biol. Biochem. (submitted)

Zelles L (1997) Phospholipid fatty acid profiles in selected members of soil microbial communities. Chemosphere 35: 275-294

Effect of Long-term Fertilization on the Sequestration Rate of Physical Fractions of Organic Carbon in Red Soil of Southern China

Minggang Xu[a,*], Xiaogang Tong[a], Xiujun Wang[b]

[a] Institute of Agricultural Resources and Regional Panning, Chinese Academy of Agricultural Sciences/Key Laboratory of Crop Nutrition and Fertilization, Ministry of Agriculture, Beijing 100081 China;
[b] Earth System Science Interdisciplinary Center, University of Maryland Research Park, MD 20740, USA.
[*]Corresponding author. Tel. No. +8610-8210 8661; Fax No. +8610-8210 6225; E-mail: mgxu@caas.ac.cn.

Abstract: Typical red soil samples were collected from 17 years long-term fertilization experiments in Qiyang county of southern China. Physical fractions of the red soil include free particulate organic carbon (fPOC), intra–microaggregate particulate organic carbon (iPOC) and mineral associated organic carbon (MOC), were measured and the effects of fertilization on changes of soil organic carbon (SOC) stocks were analyzed. The results indicated that application of manure and manure-mixed-chemical fertilizer (M, NPKM, 1.5NPKM) significantly enhanced SOC and changed its physical fraction distribution. The highest sequestration rate in fPOC (290.6~408.3 kg·ha^{-1}·yr^{-1}), iPOC (162.0~179.2 kg·ha^{-1}·yr^{-1}) and MOC (322.9~514.5 kg·ha^{-1}·yr^{-1}) were observed in these treatments. However, the content of iPOC and MOC didn't increase in unbalanced chemical fertilizer application treatments (NP, N) in red soil, and they maintained lower SOC sequestration rate. The percentage of SOC sequestration distribution in different physical fractions under balanced fertilization treatments (NPK) followed the order: MOC (45.2%~62.7%) > fPOC (21.9%~35.2%) > iPOC (15.1%~20.0%). The highest percentage of MOC implied that SOC associated silt and clay were the primary mechanism of SOC sequestration in red soil.

Keywords: Long-term fertilization; Soil organic carbon; Physical fractionation; Sequestration rate; Red soil

Introduction

As a nuclear substance in soil, SOC have great functions in cycling plant nutrients, enhancing crop yield and improving the soil physical, chemical and biological properties (Rasool *et al.*, 2008; Manna *et al.*, 2007). Thus, the accurate elucidation and quantification for the dynamic change, capacity, and sequestration of carbon pools under agricultural practices have important significances to validate the potential benefits of SOC sequestration. Most of current SOC models parted the total carbon content of a soil into different fractions by their intrinsic decomposition rate and control factors. Physical fraction is one of the popular methods for SOC fractionation, which was developed by Six *et al.* (2002) and had a very little destroying on SOC fractions. Some researchers reported that fertilization influenced SOC particle-size fractions in a great extent (Wu *et al.*, 2005). However, there has been little research on SOC sequestration rate of different fractions especially in red soils of Southern China. Our aim was to clarify the sequestration rate of different SOC physical fractions to various long-term fertilizations in red soil, typical arable soil of southern China.

Materials and Methods

A long-term fertilization experiment was initiated in 1990 at the experiment station of the Chinese Academy of Agricultural Sciences, Qiyang county (26°45′N, 111°52′E, 120 m altitude), Hunan Province

of southern China. The red soil is classified as Ferralic Cambisol. The experiment consisted of 12 fertilizer treatments, of which eight treatments were chosen for this study, i.e (1) N, (2) NP, (3) NPK, (4) NPK+S(Straw), (5) M (Manure), (6) NPK+M, and (7) 1.5NPK+M, (8) control (CK, unfertilization). The N fertilizer was provided as urea or manure at 300 kg $N{\cdot}ha^{-1}$, P as single superphosphate at 53 kg $P{\cdot}ha^{-1}$, and K as KCl at 100 kg $K{\cdot}ha^{-1}$. The ratio of organic N in NPKM was 30% of total N.

Samples from the top red soil (0~20 cm) were collected in September 2007 and the physical fractions of SOC were extracted by the method described by Six *et al.* (2002). Subsamples of both 1990 and 2007 extracted SOC fractions (fPOC, iPOC and MOC) were ground and analyzed for C and N content using EA 1500 elemental analyzer. All data conformed to assumptions for parametric statistic SPSS package (11.5) was used for statistical tests ($P < 0.05$).

Results and Discussion

Physical Fractions of SOC

Compared with the fPOC content of 1.8 $Mg{\cdot}ha^{-1}$ in control plot, the application of chemical fertilizers (N, NP, NPK) increased fPOC by 0.8~2.7 $Mg{\cdot}ha^{-1}$, while NPKS increased it by 1.8 $Mg{\cdot}ha^{-1}$, and the manure (M) alone, the low rate of manure plus chemical fertilizers (NPKM) and the high rate of manure plus chemical fertilizers (1.5NPKM) by 5.9, 5.6 $Mg{\cdot}ha^{-1}$and 7.6 $Mg{\cdot}ha^{-1}$, respectively. A higher contents of iPOC and MOC were evident in manure (M), manure plus chemical fertilizers(NPKM and 1.5NPKM) and addition of NPK with straw (NPKS), compared with those in other treatments. Maximum values of iPOC (4.8 $Mg{\cdot}ha^{-1}$) and MOC (24.1 $Mg{\cdot}ha^{-1}$) in 1.5NPKM treatments were greater than those in control (1.7 and 15.4 $Mg{\cdot}ha^{-1}$). However, red soil with continuous application of NP and N fertilizer didn't increased the content of MOC and iPOC significantly, while the balanced application fertilizer (NPK) only enhanced iPOC by 0.8 $Mg{\cdot}ha^{-1}$ comparing to the same fraction in control.

Manure (M) and manure plus chemical fertilizers (M, NPKM and 1.5NPKM) showed higher fPOC (290.6~408.3 $kg{\cdot}ha^{-1}{\cdot}yr^{-1}$), iPOC (162.0~179.2 $kg{\cdot}ha^{-1}{\cdot}yr^{-1}$) and MOC (322.9~514.5 $kg{\cdot}ha^{-1}{\cdot}yr^{-1}$) sequestration rates over other treatments (Fig. 1). The organic carbon sequestration rate in iPOC and MOC due to the application of chemical fertilizer plus straw (NPKS) was 45.8 and 127.9 $kg{\cdot}ha^{-1}{\cdot}yr^{-1}$ respectively, followed by NPK, NP and N. However, the sequestration rate of fPOC follow the trend: NPK (124.8 $kg{\cdot}ha^{-1}{\cdot}yr^{-1}$) > NPKS (69.4 $kg{\cdot}ha^{-1}{\cdot}yr^{-1}$) > NP (42.3 $kg{\cdot}ha^{-1}{\cdot}yr^{-1}$) > N (8.9 $kg{\cdot}ha^{-1}{\cdot}yr^{-1}$).

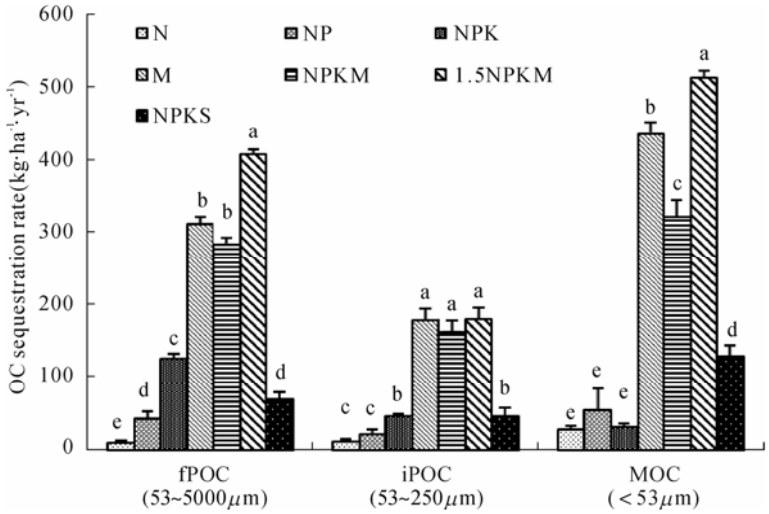

Fig. 1 Organic carbon sequestration rate of different fractions under various fertilization

The distribution of the total organic carbon sequestration in red soil during last 17-year-stocks across the physical fractions was affected by manure and chemical fertilizers significantly. In all treatments, most of the total organic carbon stocks were found in the MOC fraction, which indicated that MOC was the

important pool to sequestrate carbon in red soil. The control and only nitrogen fertilizer (N) had the highest proportion of MOC fraction in 89.0% and 76.6%, and lowest proportion of fPOC. However, the distribution of carbon sequestration into different physical fractions with balanced chemical fertilizer (NPK, NP), chemical fertilizers plus straw, manure alone and manure plus chemical fertilizers was decreased in the order: MOC (45.2%~62.7%) > fPOC (21.9%~35.2%) > iPOC(15.1%~20.0%).

The content of fPOC, iPOC and MOC in initial soil (1990) was 2.4 $Mg \cdot ha^{-1}$, 1.6 $Mg \cdot ha^{-1}$, 14.3 $Mg \cdot ha^{-1}$, 4.0 $Mg \cdot ha^{-1}$, respectively. Values followed by same letter within each fraction between fertilization treatments are not significantly different at 5% level.

Relationship between SOC and Its Fractions

SOC was divided into different physical fractions with different function, composition and lability (Six *et al.*, 2000). For example, the C/N ratio in different physical carbon fractions was in order: fPOC (22.1) > iPOC (17.5) > MOC (7.2) (Fig. 2). The lowest C/N ratio in MOC indicated its higher carbon humification and stability. The intermediate C/N ratio for iPOC fraction reflected the fact that this material was middle production of organic matter. The highest value of C/N in fPOC implied a high content of plant residues in it, considering that plant had a C/N ratio of about 20:1 to 30:1(Diekow *et al.*, 2005). Therefore, the different SOC fractions might have different effect on soil fertility. The regression equations developed between sequestration SOC and its fractions showed that the closest relationship was occurred between iPOC and crop yield. This can be attributed mainly to higher C and N mineralization in microaggregates than that in MOC and POC in sand fraction (Manna *et al.*, 2007), which resulted more nutrition supply during mineralization of organic matter. Thus organic carbon physically protected in microaggregates was not only an important way that sequestrated organic carbon, but also a key pool that supplied nutrition.

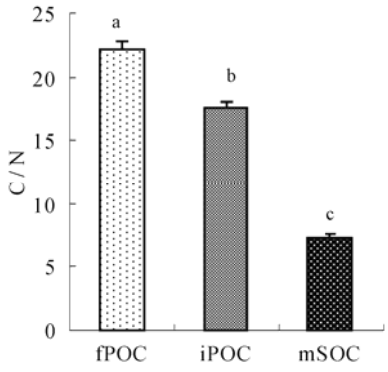

Fig. 2 Ratio of C/N in different physical organic carbon fractions. Values followed by different letters are significantly different at 5% level

References

Diekow J, Mielniczuk J, Knicker H, *et al.* (2005) Carbon and nitrogen stocks in physical fractions of a subtropical Acrisol as influenced by long-term no-till cropping systems and N fertilization. Plant Soil 268: 319-328

Manna MC, Swarup A, Wanjari RH, *et al.* (2007) Long-term fertilization, manure and liming effects on soil organic matter and crop yields. Soil Till. Res. 94: 397-409

Rasool R, Kukal SS, Hira GS (2008) Soil organic carbon and physical properties as affected by long-term application of FYM and inorganic fertilizers in maize–wheat system. Soil Till. Res. 101: 31-36

Six J, Elliott ET, Paustian K (2000) Soil macroaggregate turnover and microaggregate formation: a mechanism for C sequestration under no-tillage agriculture. Soil Biol. Biochem. 32: 2099-2103

Six J, Callewaert P, Lenders S, *et al.* (2002) Measuring and understanding carbon storage in afforested soils by physical fractionation. Soil Sci. Soc. Am. J. 66: 1981-1987

Wu TY, Schoenau JJ, Li FM, *et al.* (2005) Influence of fertilization and organic amendments on organic-carbon fractions in Heilu soil on the Loess Plateau of China. J. Plant Nutri. Soil Sci. 168: 100-107

Abiotic Catalysis of the Maillard and Polyphenol-Maillard Humification Pathways by Soil Clays from Temperate and Tropical Environments

Ailsa Ghillaine Hardie[a,b], James Joseph Dynes[a], Leonard Myrell Kozak[a], Pan Ming Huang†[a]

[a]Department of Soil Science, University of Saskatchewan, 51 Campus Dr., Saskatoon, SK, S7N5A8, Canada;
[b]Department of Soil Science, Stellenbosch University, Private Bag X1, Matieland, 7602, South Africa.

Abstract: The Maillard reaction and integrated polyphenol-Maillard reaction are regarded as important pathways in natural humification. Little is known about the abiotic catalysis of these humification pathways by naturally occurring soils and sediments. Therefore, the objective of this study was to investigate the abiotic catalysis of the Maillard reaction and integrated polyphenol-Maillard reaction by two contrasting soil clays from a temperate (Canadian Prairies) and tropical (Northeastern South Africa) region. Treatments containing an equimolar amount of glucose and glycine (Maillard reaction) or catechol, glucose and glycine (polyphenol-Maillard reaction) in the presence of temperate Mollisol and tropical Oxisol clays, were conducted under environmentally relevant conditions, i.e., pH 7.0 and 45 ℃, for a period of 15 days under sterile conditions. The nature of the humification products were examined through C and Al K-edge, and Fe and Mn L-edge NEXAFS spectroscopy. The Oxisol clay enhanced humification in the Maillard and integrated catechol-Maillard systems to a greater extent than the Mollisol clay, which is attributable to its high content of sesquioxides, particularly poorly-crystalline Mn oxides. The humic substances produced in the Oxisol- and Mollisol-catalyzed polyphenol-Maillard reaction systems were chemically distinct from one another. Changes were observed in the Al coordination and Fe and Mn oxidation states in the soil clays after humification. The Oxisol clay showed a much greater accumulation of organic C compared to the Mollisol clay in the Maillard and catechol-Maillard systems. These results reveal the important role of Fe(III) and Mn(III, IV) oxides present in soils in catalyzing the Maillard reaction and polyphenol-Maillard humification pathways. The findings of this study are of fundamental importance in understanding the role of soil clays from temperate and tropical regions in abiotic humification pathways and C stabilization in natural environments.

Keywords: Abiotic humification; Biomolecules; C, Al, Fe and Mn NEXAFS; Polyphenol-Maillard reaction; Soil clays

Introduction

Abundant research evidence at the molecular level shows that mineral colloids can enhance the humification reactions (oxidative polymerization and polycondensation) of biomolecules such as amino acids, sugars and polyphenols, derived from the breakdown of biological residues and from biological metabolites (Huang, 2000). The polyphenol pathway (polymerzation of polyphenols with/without amino acids) and Maillard reaction (polycondensation of sugars and amino acids) are regarded as important pathways in natural humification (Huang, 2000; Ikan *et al.*, 1996). The significance of linking these two pathways into an integrated polyphenol-Maillard pathway has been shown (Jokic *et al.*, 2004). Little is known about the abiotic catalysis of the Maillard reaction and integrated polyphenol-Maillard reaction by naturally occurring soils and sediments. Therefore, the objective of this study was to investigate the abiotic catalysis of these pathways by two contrasting soil clays from temperate (Canadian Prairies) and

tropical (Northeastern South Africa) regions.

Materials and Methods

The clay fraction was separated from the B horizon of an Oxisol (*Posic Ferrasol*-WRB) from Mpumalanga Province, South Africa, and a B horizon of a Mollisol (*Haplic Chernozem*-WRB) from Saskatchewan, Canada. Selected mineralogical characteristics of the clays are shown in Table 1. Treatments containing an equimolar amount (0.05 mol) of glucose and glycine (Maillard reaction) or catechol, glucose and glycine (polyphenol-Maillard reaction) in the presence of 2.5 g of the Mollisol (temperate) or Oxisol (tropical) clays, and absence (control), were conducted under environmentally relevant conditions, i.e., pH 7.0 and 45 ℃, for a period of 15 days under sterile conditions. At the end of the reaction period the solution and solid phase were separated through ultracentrifugation. The extent of humification in the supernatant was measured with visible absorbance. The humic acid (HA) fraction from the supernatant and organo-mineral solid residue (SR) was isolated and characterized using C and Al K-edge and Fe and Mn L-edge NEXAFS spectroscopy, at the Canadian Light Source (CLS), Saskatoon, SK, Canada. The organic C content of the SR was determined by a combustion method.

Table 1 Mineralogy of the soil clay fractions

Clay	Dominant clay minerals (XRD)	DCB* extractable metals (%)		
		Al	Fe	Mn
Oxisol	gibbsite, hematite, goethite, magnetite	3.44	7.26	6.21
Mollisol	illite, smectite, vermiculite, kaolinite	0.21	0.64	0.06

*Dithionite-citrate bicarbonate extraction

Results and Discussion

The soil clays enhanced browning (humification) in the Maillard and, especially, the catechol-Maillard reaction systems (Table 2-Abs.). The Oxisol clay only lightly enhanced browning in the Maillard reaction system. However, much of the humified products accumulated in the solid phase (Table 2-org. C), which would account for the low visible absorbance. The sesquioxide-rich Oxisol clay (Table 1) was clearly a stronger catalyst of browning in the catechol-Maillard system, and likewise showed a significantly higher C increase in the solid residue (Table 2).

Table 2 Visible absorbances (400 and 600 nm) of the supernatants and net organic C gain in the solid residues (SR) of soil clay-catalyzed Maillard and integrated catechol-Maillard reaction systems

Treatment	Abs. (400 nm)	Abs. (600 nm)	Gain in org. C in SR (mg)
Control Maillard	0.74	0.12	no SR
Control Integrated	2.84	0.42	no SR
Mollisol Maillard	4.65	0.77	+0.21
Mollisol Integrated	21.27	22.62	-1.44
Oxisol Maillard	1.85	1.03	+28.74
Oxisol Integrated	61.87	77.51	+103.94

*Integrated catechol-Maillard system

The humic products produced in the clay-catalyzed catechol-Maillard reaction systems (Fig.1c-e) contained similar functional groups to that of natural HAs (Fig. 1a-b). The HA from the Mollisol-catalyzed catechol-Maillard system (Fig. 1c) was richer in aliphatic carboxylic groups than the HA from the Oxisol-catalyzed catechol-Maillard system (Fig. 1d). However, the SR of the Oxisol-catalyzed catechol Maillard system (Fig. 1e) was richer in aliphatic carboxylic groups compared to that of the HA (Fig. 1d), which is attributed to preferential sorption/ precipitation of polymers possessing COOH groups in the solid residue. This was confirmed by Mn L-edge NEXAFS spectra of the solid residue (Fig. 2c), which indicated that Mn(II) was predominantly bound to humic polymers (Fig. 2d). The Oxisol clay originally contained a mixture of Mn(II), (III) and (IV) (Fig. 2a), which was reduced to Mn(II) during the humification reactions (Fig. 2b-c). The Fe(III) in the Mollisol and Oxisol clays was partially reduced to Fe(II) in the Maillard and polyphenol-Maillard reaction systems (Fe L-edge NEXAFS spectra not shown). An increase in the tetrahedral Al was observed in the Mollisol clay in the Maillard and catechol-Maillard systems (Al K-edge NEXAFS spectra not shown).

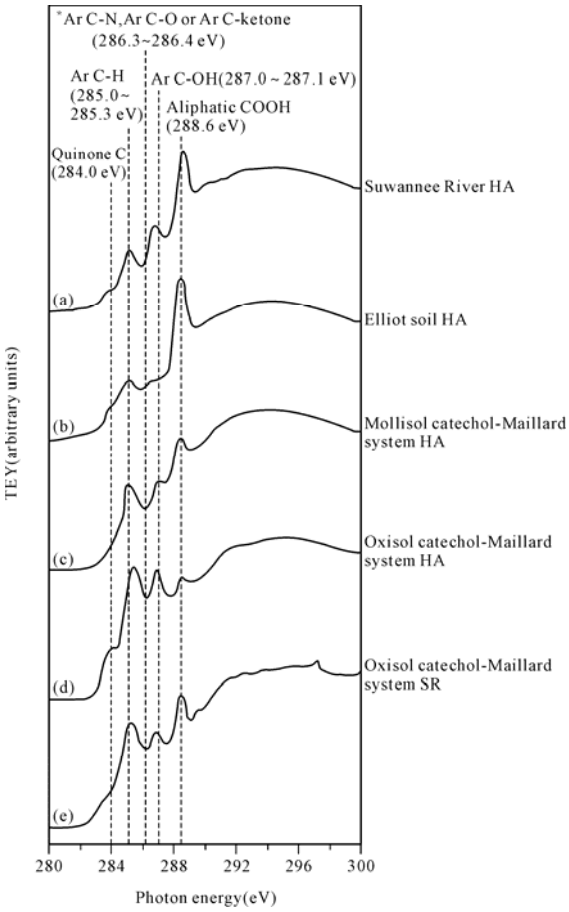

Fig. 1 C K-edge NEXAFS spectra of natural humic acids (HA) (a-b) and HA and solid residues (SR) isolated from the Oxisol and Mollisol-catalyzed catechol-Maillard reaction systems (c-e)

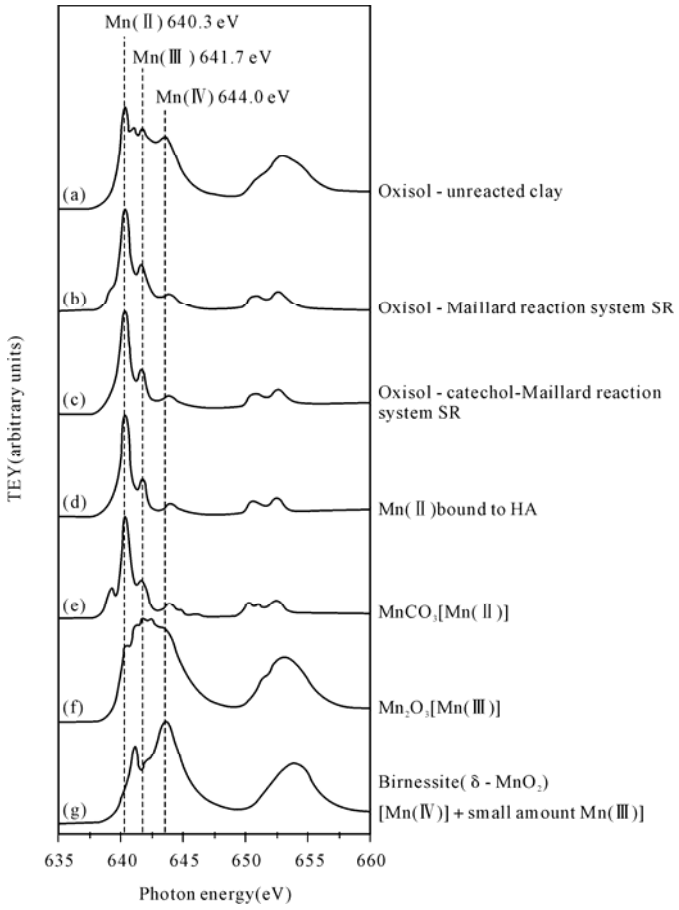

Fig. 2 Mn L-edge NEXAFS spectra of the unreacted Oxisol clay (a), and SR from the Oxisol-catalyzed Maillard (b) and catechol Maillard systems (c), compared to Mn reference compounds (d-g)

Conclusions

The Oxisol clay enhanced humification in the Maillard and integrated catechol-Maillard systems to a much greater extent than the Mollisol clay, which is attributable to its high content of Al and Fe oxides and especially, poorly crystalline Mn oxides. The mineralogy of the clays affected not only the nature of the resultant humic substances, but also the extent of mineral surface alteration and organic C accumulation. The coordination of Al and oxidation state of Fe and Mn was altered in the clays during humification reactions. The Oxisol clay showed a significantly higher accumulation of organic C compared to the Mollisol clay in the Maillard and catechol-Maillard reaction systems. These results reveal the important role of Fe(III) and Mn(III, IV) oxides present in soils in catalyzing the Maillard reaction and polyphenol-Maillard humification pathways. The findings of this study are of fundamental importance in understanding the role of soil clays in abiotic humification pathways and C stabilization in natural environments.

References

Huang PM (2000) Abiotic catalysis. In: Sumner ME (Ed.), Handbook of Soil Science. CRC Press, Boca Raton, pp. B302-B332

Ikan R, Rubinsztain Y, Nissenbaum A, Kaplan IR (1996) Geochemical aspects of the Maillard reaction. In: Ikan R (Ed.), The Maillard Reaction: Consequences for the Chemical and Life Sciences. John Wiley & Sons. Chichester, UK, pp. 1-25

Jokic A, Wang MC, Liu C, Frenkel AI, Huang PM (2004) Integration of the polyphenol and Maillard reactions into a unified abiotic pathway for humification in nature: The role of MnO_2. Org. Geochem. 35: 747-762

Effect of Organic Matter Application on CP-MAS-^{13}C-NMR Spectra of Humic Acids from a Brown Soil

Sen Dou*, Kai Li

College of Resource and Environmental Science, Jilin Agricultural University,
No. 2888. Xincheng Street, Changchun, 130118, Jilin Province, China.
*Corresponding author. Tel. No. +86-431 8453 2851; Fax No. +86-431 8453 2851; E-mail: dousen@tom.com.

Abstract: Organic matter (OM) applications can influence the amount and structural characteristics of humic acid (HA). The objective of this paper was to clarify the effect of long term OM application on the changes of structural characteristics in HAs, which provided new information for improving soil fertility by OM application. The experiment was carried out on a brown soil at Shenyang Agricultural University, Liaoning province, China. The experiment included three treatments: zero-treatment (CK_{br}), and two pig manure (PM) treatments (O_1 and O_2) at the rates of 0.9 t·ha^{-1} and 1.8 t·ha^{-1} of organic carbon, respectively. The samples of the HA fraction were extracted, separated, purified and characterized by elemental composition, differential thermal analysis (DTA), $\Delta \lg K$ value and CP-MAS-^{13}C-NMR. The results indicated that the CP-MAS-^{13}C-NMR spectra of the HA were quite similar to each other. But after OM application, the contents of alkyl C and O-alkyl C increased and the contents of aromatic C and carbonyl C decreased in HAs, indicating that the OM application decreased the content of aromatic C and was simplified the molecular structure in HAs.

Keywords: Organic matter application; CP-MAS-^{13}C-NMR; Humic acids; Brown soil

Introduction

The humified SOM or humic substances (HS) composed of humic acid (HA), fulvic acid (FA) and humin (HM) represent the most microbially recalcitrant and stable reservoir of organic carbon in soil (Piccolo *et al.*, 2004). OM applications can influence the amount and structural characteristics of HS(Dou *et al.*, 2008). During the past few decades, there has been much research on HS, but their chemical structure is still not fully understood.CP-MAS-^{13}C-NMR spectroscopy was considered as an effective method to study structures of HS without dissolving problem compared with liquid ^{13}C-NMR (Conte *et al.*, 1997; Dou *et al.*, 2008). It can directly measure the carbon framework and reflect the nature of HS transformation after OM application (Spaccini *et al.*, 2000). For that reason, this method was applied in the present study. The objective of this paper was to clarify the effect of long term OM application on the changes of structural characteristics in HAs, with the purpose to provide new information for improving soil fertility by OM application.

Materials and Methods

The experiment was carried out on a brown soil (Paleudalf in USDA Soil Taxonomy) at Shenyang Agricultural University, Liaoning province, China (N41°48′; E123°25′). The experiment included three treatments: zero-treatment (CK_{br}), and two pig manure (PM) treatments (O_1 and O_2) at the rates of 0.9 t·ha^{-1} and 1.8 t·ha^{-1} of organic carbon, respectively. The samples of the HA fractions were extracted, separated and purified according to the method described by Dou *et al.* (1991). Elemental composition, differential thermal analysis (DTA), the spectral curve slope $\Delta \lg K$ value, FT-IR and CP-MAS-^{13}C-NMR of HAs were performed.

Results and Discussion

Organic Carbon and Its Composition

The contents of total organic carbon (TOC) were from 8.77 g·kg^{-1} to 12.25 g·kg^{-1}. The relative contents in TOC for water soluble Substances (WSS), HA, and FA were 6.87%, 14.2% and 19.8%, respectively. Comparing the CK_{br}, the contents of WSS, HA and FA for O_1 and O_2 increased, but relative contents of WSS and FA decreased. The content of the HA increased after OM application, which was consistent with other studies (Wang *et al.*, 2001). The content of the WSS increased after the OM application indicating that the increase of labile organic carbon. The C/H mole ratio of the HS could reflect the degree of condensation (Dou *et al.*, 1995).

Chemical and Optical Properties

The chemical and optical properties of HA were listed. The C/H ratio decreased after OM application, from 0.830 (CK_{br}) to 0.754 (O_2). While ΔlgK increased, from 0.623 (CK_{br}) to 0.658 (O_2). The HA structure tended to become simpler. The C/H ratio of the HA decreased after OM application. This indicates that OM application decreased the degree of condensation. The ΔlgK values can be used as the index of HA molecule complexity in the soil. If ΔlgK increased, the molecular structure becomes simpler. After OM application, the increase of ΔlgK indicated that the molecular structure became simpler.

Thermal Properties

It could be seen that HA had exothermic peaks in moderate and high temperature regions. After OM application, heat (H_2) of exothermic peak increased in moderate temperature region, while heat (H_3) of exothermic peak decreased in high temperature region. The heat ratio of exothermic peaks in high temperature region to moderate (H_3/H_2) decreased. From CK_{br} to O_2, H_3/H_2 decreased from 4.31 to 0.86. The HA had moderate and high temperature exothermic peaks. The heat of exothermic peaks in the moderate temperature region might show that aliphatic compounds decomposed and peripheral functional groups decarboxylated. The heat of the exothermic peaks in the high temperature region might show that the HA was oxidized completely and inter-aromatic structures in the molecule decomposed. The heat ratio of the high to moderate temperature exothermic regions (H_3/H_2) decreased significantly after PM application, indicating that the proportion of aromatic structure decreased and the HA molecular structure simplified.

CP-MAS-^{13}C-NMR

The NMR spectra of the HAs were quite similar to each other (Fig. 1a and Fig. 1b).

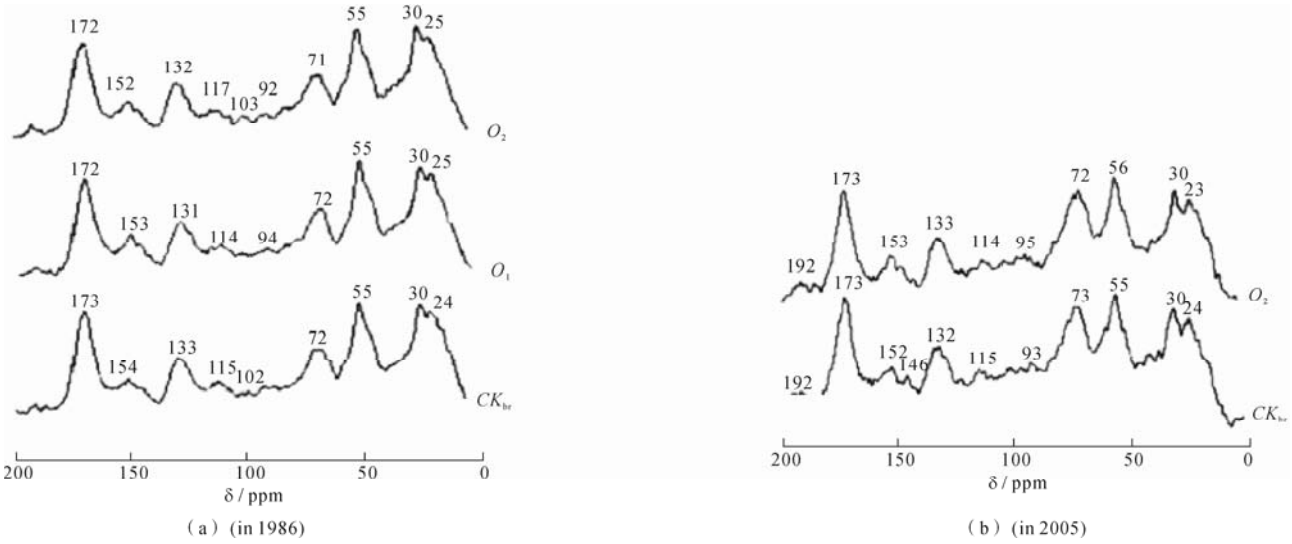

Fig. 1 CP-MAS-^{13}C-NMR spectra of HAs in the field experiment of brown soil collected in 1986(a) and 2005(b). Note: CK_{br}, O_1 and O_2 were treatments with pig manure (*PM*) application into brown soil at annual rates of 0 t·ha^{-1}, 0.9 t·ha^{-1} and 1.8 t·ha^{-1} of organic carbon, respectively

These spectra exhibited signals for alkyl C (0~50 ppm), O-alkyl C (50~110 ppm), aromatic C (110~160 ppm) and carbonyl C (160~200 ppm) regions. The signals in carbonyl C region concentrated between 172 ppm and 173 ppm, and with a small signal occurred in the region of 190~200 ppm, indicating that there was carbonyl C of carboxylic acid, ester and amide, but a little amount carbonyl C of ketonic compounds. In the region of aromatic C, the most obvious peaks were the absorption at 131~133 ppm and 114~117 ppm. The former was mainly the aromatic C substituted by -COOH or -COOMe and the unsubstituted aromatic *meta* to carbons bearing an oxygen or nitrogen atom; the latter was mainly the unsubstituted aromatic C *ortho* and *para* to carbons bearing an oxygen and nitrogen atom. There was a small peak at 152~154 ppm, which was the signal of phenolic OH. The signal at 55~56 ppm was methoxyl C. The signals at 71~73 ppm were due to the -CH(OH)- in carbohydrate. The peak at 102~103 ppm was generally assigned to double oxygen-C in polys-accharide (possibly acetal). The maximum absorption at 30 ppm was the contribution of the polymethylene chain $-(CH_2)_n-$ in saturated hydrocarbons (Wilson, 1981).

After OM application, the contents of alkyl C and O-alkyl C increased and the contents of aromatic C and carbonxyl C decreased except for the samples collected in 1986. Compared with 1986, the contents of O-alkyl C increased and the contents of alkyl C decreased for the same treatment (CK_{br} and O_2). Aromaticity decreased significantly in OM treatments, indicating that the OM decreased the content of aromatic C and was simplified the molecular structure. The increase of relative content of O-alkyl C indicated that OM application increased the content of methoxyl C and -CH(OH)- in carbohydrate. Alkyl C was probably derived from compounds of plants with high resistance to degradation, such as cutin and suberin (Baldock *et al.*, 1992; Preston, 1996), or from newly synthesized products from soil micro-organisms, which are likely to represent the most persistent fraction of stable OM. The alkyl C increased after the OM applications, indicated by the increase of hydrophobic components content and aliphatic character. Compared with the samples collected in 1986, the contents of O-alkyl C increased and the contents of alkyl C decreased for the same treatment (CK_{br} and O_2), indcating that a simplification trend took place in the aliphatic fraction of HA molecular with cultivation time in the tested soil.

We have found that: 1) The contents of HAs increased after OM application; 2) OM application increased the contents of alkyl C and O-alkyl C, and decreased the C/H ratio, aromaticity, and the H_3/H_2 ratio of the HA, which indicated that the HA structure tended to become simpler and more aliphatic; 3) The results obtained by CP-MAS-^{13}C-NMR spectroscopy were mainly corresponding with those obtained by chemical analysis, thermal analysis, optical properties and IR spectroscopy, which indicated that ^{13}C-NMR spectroscopy had a potential in characterizing the structural changes of HA after long-term OM application into soils.

References

Conte P, Piccolo A, van Lagen B, Buurman P, de Jager PA (1997) Quantitative differences in evaluating soil humic substances by liquid and solid-state ^{13}C-NMR spectroscopy. Geoderma 80: 339-352

Dou S, Zhang JJ, Li K (2008) Effect of organic matter applications on ^{13}C-NMR spectra of humic acids of soil. Eur. J. Soil Sci. 59:532-539

Dou S, Chen EF, Xu XC, Zhang JH (1995) Effect of application of organic manures on the structural characteristics of humic acids in soils—the optical properties of HAs. Acta Pedol. Sin. 32: 41-49 (in Chinese)

Dou S, Tan SW, Xu XC, Chen EF (1991) Effect of pig manure application on the structural characteristics of humic acid in brown soil. Pedosphere 1: 345-354

Piccolo A, Spaccini R, Niedwe R, Richter J (2004) Sequestration of a biologically labile organic carong in soil by humified organic matter. Clim. Change 67: 329-349

Spaccuni R, Piccolo A, Haberhauer G, Gerzabek MH (2000) Transformation of organic matter from maize residues into labile and humic fractions of three European soils as revealed by ^{13}C distribution and CPMAS-NMR spectra. Eur. J. Soil Sci. 51: 583-594

Wang, XD, Guan WL, Yin XQ (2001) Dynamic change of chemical composition of corn straw and humic acid during different decomposition period Ⅱ Change of humic acid properties and fractions. Agri. Res. Arid Areas 19: 11-15 (in Chinese)

The Composition and Organic Carbon Distribution of Organo-mineral Complex in a Black Soil as Influenced by Land-use Change and Long-term Fertilization

Xiaozeng Han[a,*], Xueying Hou[a], Haibo Li[b]

[a] Northeast Institute of Geography and Agricultural Ecology, Chinese Academy of Sciences, Harbin 150081, China;
[b]Academy of Jilin Agricultural Technology, Jilin 132101, China.
[*]Corresponding author. Tel. No. +86-451 8660 2940; Fax No. +86-451-8660 3736; E-mail: xzhan@neigaehrb.ac.cn.

Abstract: The aim of this experiment was to examine the impact of natural vegetation restoration and long-term fertilization on the composition and organic carbon distribution of organo-mineral complexes in a black soil. The results showed that the fine sand-size complex was the dominant particle of different size complexes. Contents of silt-size and fine sand-size complexes increased in the NP and NP plus animal manure (NPM) treatments, while the content of clay-size complexes decreased as compare with the non-fertilized treatment (NF). The contents of silt-size and clay-size complexes in the grassland (GL) and the bare land (BL) were the same as that in NF. Land-use change resulted in different dynamics in C sequestration in soil, which made cumulative CO_2 emissions differ significantly among the five treatments during the growing seasons. The content of <20 μm size complex in GL was more than those in NP and NPM. The GL has a potential of sequestering more C than tilled soils due to the stability of SOC stored in the <20 μm size fraction. The cumulative CO_2 emissions increased in the order of NP < GL < NPM. Long-term application of organic manure and vegetation restoration increased the organic carbon content of all sizes of complexes, but increased the cumulative CO_2 emissions. Nevertheless, these soil management practices have substantially increased C sequestration into the soil rather than net C losses.

Keywords: Organo-mineral complex; Land use; SOM; Carbon sequestration; CO_2 emission

Introduction

Land-use change and soil management play a vital role in influencing sequestration and losses of soil carbon (C). The organo-mineral complexes formed the basis of soil fertility and had significant effect on soil C pool. Humus is a by-product of heterogeneous organic compounds produced by microbial metabolisms, and represent the oldest form of organic matter in soils, when it formed, it interacted with inorganic surfaces in soil and often present as organ-mineral complex (Sergey, 1999), indicating its significant resistance to microbial degradation.

Materials and Methods

Soil sampling was performed from the following sites : 1) grassland (GL), fallowed since 1985 with the grass *Leymus chinesis* as the dominant species; 2) bareland (BL), fallowed since 1985, but the grasses were eliminated periodically during the plant growth stage; 3) cropland (CL), three treatments were included since this long-term experiment was established in 1993, in which, no fertilizer applied (NF); nitrogen and phosphorus fertilizer applied (NP), and NP fertilizer together with organic manure (NPM) were selected.

Different size organo-mineral complexes were determined according to Gavinelli *et al.* (1995), involving successive wet sieving procedures of the soil following washing and sedimentation steps. The following fractions were separated: coarse sand-size complex (>200 μm); fine sand-size (20~200 μm); silt-size complexes (2~20 μm) and clay-size complexes (0~2 μm). The soil samples were dispersed by ultrasonication in water: soil 4:1, wet-sieved through 200 μm meshes (extracted through density

fractionation in water), sedimented and decanted to obtain fractions 2~20 μm and 0~2 μm; and centrifuged. All the particle size fractions were dried at 40 °C, weighed and finely ground in an agate mortar, and passed through a 100-mesh sieve for further analysis. One fractionation was carried out for each soil sample. There were 3 replications for each treatment.

Results and Discussion

The content of clay-size complexes had a negative correlation with the content of soil organic carbon (SOC), while positive correlation was observed between contents of fine sand-size complex and SOC. The content of silt-size complex tended to increase with increasing SOC content although it was not significant (Fig. 1). The content of organic carbon (OC) in individual size complexes increased with SOC content. The content of OC in the clay-size, silt-size and fine sand-size complexes highly correlated with SOC content (Fig. 2).

Fig. 3 showed that the cumulative soil resperation negatively correlated with the content of clay-size complex, but positively correlated with the content of fine sand-size complexes. The cumulative soil resperation increased with increasing OC content of individual size complexes (Fig. 4). The results suggest that the capality of a soil to sequester C can be enhanced through an increase in the content of clay-size organo-minetal complexes and OC of silt-size complexes. In this study, SOC were more stable in the bareland, although this kind of soil management was good at increasing C pool in black soils. Long-term application of organic manure and vegetation restoration increased the SOC, but increase the cumulative CO_2 emissions. However, these soil management practices have substantially increased C sequestration into soil rather than net C losses for black soils.

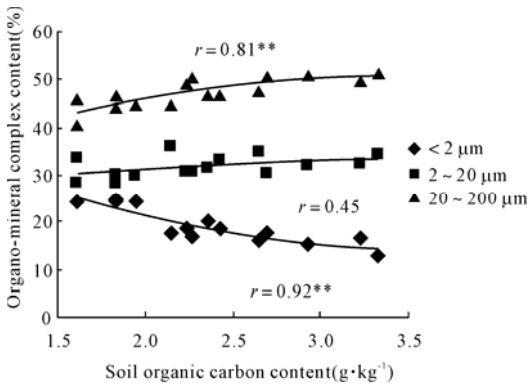

Fig. 1 The relationships between content of soil organic carbon and clay-size, silt-size and fine sand-size complexes

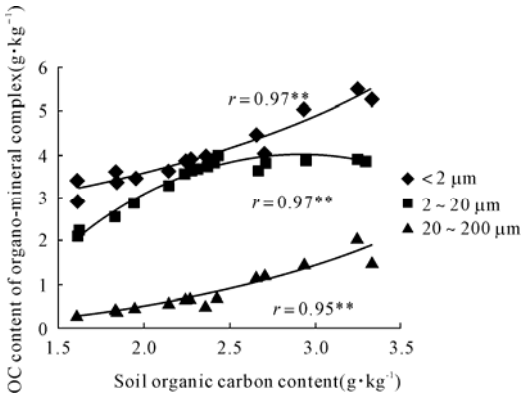

Fig. 2 The relationships between content of soil organic carbon and content of organoc carbon in clay-size, silt-size and fine sand-size complexes

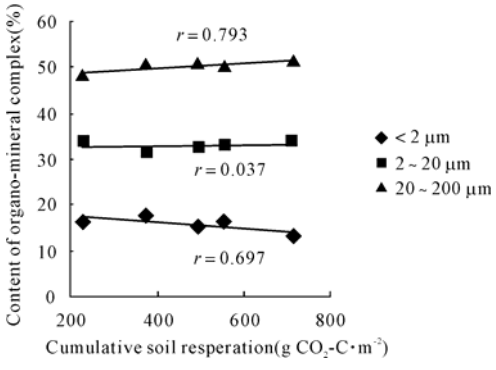

Fig. 3 The relations between cumulative soil respiration and clay-size, silt-size and fine sand-size complexes

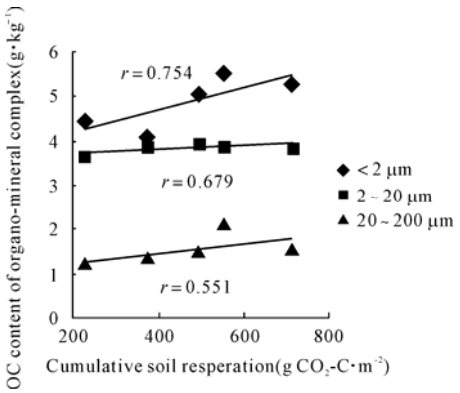

Fig. 4 The relations between cumulative soil resperation and content of organic carbon in clay-size, silt-size and fine sand-size complexes

References

Aurélie M, José AAM, Martial B, *et al.* (2007) Storage and forms of organic carbon in a no-tillage under cover crops system in clayey Oxisol in dryland rice production (Cerrados, Brazil). Soil Till. Res. 94: 122-132

Balesdent J, Besnard E, Arrouays D, *et al.* (1998) The dynamics of carbon in particle-size fraction of soil in a forest-cultivation sequence. Plant Soil 201: 49-57

Christensen BT (1987) Decomposability of organic matter in particle-size fractions from soils with straw incorporation. Soil Boil. Boichem. 19: 425-429

Christensen BT (1992) Physical fraction of soil and organic matter in primary particle size and density separate. Soil Sci. 20: 1-90

Characterization of Dissolved Organic Matter Derived from Rice Straw at Different Decay Stages

Hualin Chen*, Jiangmin Zhou

School of Life and Environmental Sciences, Wenzhou University, Wenzhou 325027, Zhejiang, China.
*Corresponding author. Tel. No. +86-577-88320096; Fax No. +86-577-88373114; E-mail: hualin2100@126.com.

Abstract: This study characterized chemical and structural properties of dissolved organic matter (DOM) derived from different stages of rice straw decay under laboratory conditions. Ten different DOM samples were obtained and characterized using element composition analysis, Fourier-transform infrared spectroscopy, and ^{1}H, ^{13}C-nuclear magnetic resonance spectroscopy. The results showed that at the early stage of straw decay, low-weight-molecular components were dominant, such as carbohydrates, amino acids, and amino sugars. At the second stage, the contents of mono-, oligo-, and polysaccharides increased. At the later stage, aromatic products were dominant because of their strong recalcitrance for microorganisms. As straw decay proceeded, some small molecular chemicals (such as carbohydrates and acid amides) polymerized around the aromatic rings, suggesting that the DOM became more stable with decay time.

Keywords: Dissolved organic carbon; Fourier-transform infrared spectroscopy; ^{1}H,^{13}C-nuclear magnetic resonance spectroscopy

Introduction

Dissolved organic matter (DOM) is ubiquitous in terrestrial and aquatic ecosystems. Returning of rice straw into paddy field is a popular strategy for farming management in many countries, which can increase the soil organic carbon content. However, in addition to soil organic matter, the rice straw also introduces DOM into soil. Many studies have shown the relationships between the decomposition trend of straw in soil and the nutrients cycles (Kumar and Goh, 2003), the changes of soil organic carbon (Kalbitz *et al.*, 2000), and the effects of DOM on microorganisms (Henriksen and Breland, 2002). The objective of this paper was to study the dynamic changes of the structural characteristics of DOM derived from rice straw decay.

Materials and Methods

A total of ten different DOM samples were obtained from the aerobic biodegradation of the rice straw at ten different incubation time. Glass bottles (250 mL) without caps were used as batch reactors, each containing 3 g of rice straw, 30 g of pre-cleaned quartz sand, 5 mL of the inoculum, and 10 mL of distilled water. They were placed in an incubator at 25 ℃. At each time interval of day 0, 3, 7, 14, 21, 35, 49, 63, 91, and 180, five replicate reactors were taken from the incubator, and each was filled with 60 mL of distilled water. The reactors taken from the incubator were capped and shaken for 2 h at 200 r·min^{-1} and 25 ℃. After centrifugation at 12,000 r·min^{-1} for 30 min, the supernatant was withdrawn from each replicate reactor and filtered through a 0.45-μm membrane filter. The filtrates were used for analysis of total DOC content and chemical characterization of the DOM.

Results and Discussion

The DOC content had a minimum value at day 3 (5.4 mg·g^{-1} straw) and a maximum value at day 180

(23.6 $mg \cdot g^{-1}$ straw). From day 0 to day 3, DOC production was negative, suggesting a net consumption of organic carbon by bacteria. From day 3 to day 63, DOC production increased nearly linearly as a function of time, indicating a rapid production and accumulation of DOM due to steady decomposition of rice straw. From day 63 to day 180, the DOM production slowed down and the DOC remained at about 22~24 $mg \cdot g^{-1}$ straw, suggesting DOC production from rice straw decay and biodegradation of DOM approached a quasiequilibrium condition.

The elemental compositions of all DOM samples are summarized in Table 1. The H/C atomic ratio decreasing as a function of decay time might indicate that DOM in the water co-existing with straw became increasingly more aromatic (Bardy *et al.*, 2008). The O/C atomic ratio decreased slightly from day 0 to day 21, then remained almost constant after 35 days, suggesting that the abundance of oxygen-containing functionalities decreased slightly within the early stage.

Table 1 Elemental compositions of DOMs

Straw Decay Time(days)	Elemental Composition (wt%)				Atomic Ratio	
	N	C	H	O	H/C	O/C
0	3.0 (0.08)*	47.4 (1.9)	7.0 (0.09)	42.6 (2.0)	1.77	0.67
3	3.5 (0.03)	50.1 (0.2)	7.0 (0.05)	39.4 (0.3)	1.68	0.59
7	3.9(0.25)	50.2(0.3)	6.5(0.01)	39.4(0.6)	1.56	0.59
14	3.9(0.03)	50.8(0.1)	6.0(0.06)	39.3(0.2)	1.42	0.58
21	3.8 (0.01)	53.3(0.1)	5.9(0.01)	37.0(0.1)	1.33	0.52
35	3.8 (0.06)	52.1 (0.4)	5.7 (0.06)	38.4 (0.6)	1.31	0.55
49	3.5(0.04)	53.2(0.2)	5.6(0.07)	37.7(0.3)	1.27	0.53
63	3.2(0.05)	51.9(0.4)	5.8(0.01)	39.1(0.5)	1.34	0.56
91	3.0 (0.02)	52.9 (0.1)	5.5 (0.02)	38.6 (0.2)	1.24	0.55
180	2.6 (0.25)	53.0 (0.2)	5.4 (0.01)	39.0 (0.5)	1.21	0.55

*Standard deviation ($\pm\sigma$)

The FTIR spectra for the ten DOM samples showed that each spectrum had a very broad absorption peak in high frequencies with a maximum at 3422 cm^{-1} resulting from adsorbed water and –OH stretching of organic functional groups. Additional bands could be assigned to the vibration of carboxyl groups (1723 cm^{-1}). The aliphatic C–H stretching and bending bands could be observed at high (2925 and 2930 cm^{-1}) and low (1383 and 1391 cm^{-1}) frequencies, respectively. Finally, the peaks in the 1088 cm^{-1} and 1050 cm^{-1} range usually resulted from –O– and C–O stretching vibrations, respectively (Poirier *et al.,* 2005).

The ^{1}H-NMR spectra showed that H atoms on the DOMs were predominantly bound to O-containing carbohydrate carbon (2.8~5.5 ppm) and that the abundance of such H atoms decreased rapidly from 61% at day 0 to 35% at day 21, and then increased to 49% at day 91, 42% at day 180. This suggested that the net accumulation of carbohydrates in water decreased in the first stage due to their high biodegradability. After 21 days, the net accumulation of carbohydrates increased likely due to the fast decomposition of cellulose to mono-, oligo-, polysaccharides. The relative abundance of the aromatic-H (6.0~10.0 ppm) apparently increased from 19% at day 0 to 33% at day 14 then leveled off to day 180, indicating that aromatic structures became dominant as a function of straw decay time. These aromatic components mostly derived from the decomposition of lignin, which indicated by the increase of the signals between 3.6 ppm and 3.8 ppm (methyl aryl ethers) with decay time (Said-Pullicino *et al.,* 2007). The aliphatic H peaks within 0.5~2.8 ppm on the DOM did not demonstrate clear trends.

The quantitative results of the solid-state ^{13}C-NMR spectra for the ten DOM samples are presented in Table 2. The peaks within 160~220 ppm are assigned to carboxyl/carbonyl C, which were low for all the

DOMs compared to other three major functional groups. That might be due to the high biodegradability of carboxyl acids, resulting in a low accumulation. The peaks within 110~160 ppm are assigned to aromatic C and the moieties increased as a function of decay time, indicating a net accumulation of DOM fractions with aromatic structures. The peaks within 50~110 ppm are often assigned to O-alkyl C including O-methyl (56 ppm) and carbohydrates (73 ppm). The relatively content of overall O-alkyl C decreased from the initial 46% (day 0) to ≤ 36% for all other DOM. The peak at 56 ppm, being another indicator of lignin-derived compounds, and the peak at 120 ppm became sharper with decay time, showing that the lignin-derived compounds released gradually from rice straw as straw decay proceeded. The alkyl C (0~50 ppm) on DOMs increased from 24% at day 0 to 30% at day 3, then decreased to < 20% (day 91 and day 180), indicating that there were net accumulation of alkyl fractions in DOMs at the early stage of straw decay then these fractions were consumed gradually.

Our results indicated that the DOM derived from rice straw decay were highly heterogeneous in terms of their structural and functional groups, which were likely resulted from the diverse source materials of rice straw. The disposal of rice straw in the field can generate high concentration of DOC in the water of often flooded paddy soil. Such straw-derived DOM may have strong impacts on humification of soil organic carbon, mobility and bioavailability of nutrients, and toxicity of pesticides and heavy metals in paddy soil systems.

Table 2 Results of liquid-state ^{1}H-NMR and solid-state ^{13}C-NMR spectra

Straw Decay Time (d)	H moieties (%)			C moieties (%)			
	O-containing functionalities 2.8~5.5 ppm	Olefinic/ Aromatic 6.0~10 ppm	Aliphatic 0.5~2.8 ppm	carboxyl /carbonyl 160~220 ppm	Aromatic 110~160 ppm	O-alkyl 50~110 ppm	Alkyl 0~50 ppm
0	61	19	20	14	16	46	24
3	47	25	28	15	23	32	30
7	42	28	30	17	25	31	27
14	36	33	31	16	28	29	27
21	35	32	33	15	33	28	24
35	38	32	30	16	31	32	21
49	40	27	33	17	34	29	20
63	46	30	24	12	34	32	22
91	49	31	20	10	39	36	15
180	42	32	26	9	41	34	16

References

Bardy M, Fritsch E, Derenne S, Allard T, do Nascimento NR, Bueno GT (2008) Micromorphology and spectroscopic characteristics of organic matter in waterlogged podzols of the upper Amazon basin. Geoderma 145: 222-230

Henriksen TM, Breland TA (2002) Carbon mineralization, fungal and bacterial growth and wnzyme activities as affected by contact crop residues and soil. Biol. Fert. Soils 35: 41-48

Kalbitz K, Solinger S, Park JH, Michalzik B, Matzner E (2000) Controls on the dynamics of dissolved organic matter in soils: a review. Soil Sci. 165: 277-304

Kumar K, Goh KM (2003) Nitrogen release from crop residues and organic amendments as affected by biochemical composition. Comm. Soil Sci. Plant Anal. 34: 2441-2460

Poirier N, Sohi SP, Gaunt JL, Mahieu N, Randall EW, Powlson DS, Evershed RP (2005) The chemical composition of measurable soil organic matter pools. Org. Geochem. 36: 1174-1189

Said-Pullicino D, Kaiser K, Guggenberger G, Gigliotti G (2007) Changes in the chemical composition of water-extractable organic matter during composting: Distribution between stable and labile organic matter pools. Chemosphere 66: 2166-2176

Organic Fertility of Severely Eroded Soils: Effect of Organic and Inorganic Fertilization and Cropping Patterns

Wiqar Ahmad*, Farmanullah Khan, Muhammad Naeem

Department of Soil and Environmental Sciences, NWFP Agricultural University, Peshawar, Pakistan.
*Corresponding author. Tel. No. 0092 334 8692160; Fax No. 0092 91 9216520; E-mail: wiqar 280 @ yahoo.co.uk.

Abstract: A study was conducted on farmer's field for the restoration of fertility status of severely eroded soils in north west Pakistan during 2006 and 2007. Two factors viz fertilizer treatments included T1 (control), T2 (50% NP also called farmer's practice), T3 (100% NPK) and T4 (20 $t \cdot ha^{-1}$ farmyard manure integrated with 50% N and 100% PK as mineral fertilizers) whereas cropping patterns included C1 (maize-wheat-maize rotation), C2 (maize-lentil-maize rotation) and C3 (maize-wheat+lentil intercrop-maize rotation). Experiment was started in Kharif 2006 and was carried out continuously for four seasons till Rabi 2007. At the end of the experiment, soil samples were collected from the surface (0~20 cm) soil and analyzed for total N, microbial biomass N (MBN), mineralizable N, Organic matter (OM), microbial biomass C (MBC) at day 3, day 6 and day 10 incubation periods. Results suggested that the organic fertility of soil was significantly increased with fertilizer addition and the highest soil organic fertility was found in the treatment that received organic and inorganic fertilizers in integration (T4) which showed 52%, 14%, 17%, 60%, 56%, 57% and 60% increase in total N, mineralizable N, MNB, OM, MBC at day3, day 6 and day 10 over the control treatment respectively. Cropping patterns also affected soil organic fertility where cereal-legume rotation showed 21%, 13%, 6%, 17%, 21%, 22% and 13% increase in the above parameters and time. Fertilizers must be applied in integrated form which carries 50% N from inorganic source and the rest of 50% from organic sources to improve the level of organic fertility of eroded soils on sustained basis. Results further suggested that legumes must be entered into conventional cereal-cereal rotation to improve the N input and organic fertility of severely eroded soils.

Keywords: Cropping patterns; Eroded soils; Farmyard manure; Fertilizers; Organic fertility; Lentils

Introduction

Water erosion has severely affected the natural fertility of agricultural lands in the North-Eastern NWFP, Pakistan. In response to population pressure, the trend of shifting agriculture into high slope lands areas further resulted land disturbance and degradation. These lands require careful handling and land management on scientific lines to make it productive on sustainable basis and to prevent further soil erosion. According to Banning *et al.* (2008), recovery of soil organic matter and mineral nutrient cycling is critical to the success of rehabilitation schemes following major ecosystem disturbance. Integrating organic and mineral fertilizers not only enables the farming system to better adjust to the effects of climate change but also offers a chance for restoring soil fertility on sustained basis. Moreover, inclusion of legumes in crop rotations protect the fragile soil surface and may even counteract erosive forces by restoring the organic matter content and organic fertility of the soil. This study was carried out for two year to investigate for adopting cost effective soil fertility improvement and crop productivity restoration measures on the eroded lands of North-Eastern NWFP, Pakistan. This paper focused on the use of organic and mineral fertilizers and cropping patterns to improve the organic fertility of these eroded lands.

Material and Methods

A field experiment was conducted on farmers field for two years to investigate the cost effective fertility restoration measures for the eroded soils in North-Eastern NWFP, Pakistan. Composite soil samples analysis for 0~20 cm depth revealed that the soil texture was a silty clay loam, free from excess salinity, alkaline in reaction and calcareous in nature. The soil was deficient in organic matter, low in N, P and K contents.

Two factorial split plot design was used for the experiment. Fertilizer treatments included T1 (control), T2 (50% NP also called farmer's practice), T3 (100% NPK) and T4 (20 $t \cdot ha^{-1}$ farmyard manure integrated with 50% N and 100% PK as mineral fertilizers). Cropping patterns included C1 (maize-wheat-maize rotation), C2 (maize-lentil-maize rotation) and C3 (maize-wheat+lentil intercrop-maize rotation). Well rotten FYM was obtained from NWFP Agricultural University Dairy Farm well before each season application and applied one month before field cultivation. At end of the experiment, soil samples from 0~20 cm depth were collected from each treatment plot and were analyzed for soil microbial properties.

Microbial biomass C and N were determined as Biomass C = (Fc-Ufc)/Kc where Fc =CO_2 produced from fumigated soil, Ufc =CO_2 produced from un-fumigated soil, Kc = 0.45 (Jenkinson and Ladd, 1981). Biomass N = (Fn-Ufn)/Kn where Fn = The NH_4-N mineralized during 10 days from fumigated soil, Ufn = The NH_4-N mineralized during 10 days from un-fumigated soil, Kn=0.54 (Jenkinson, 1988). Mineralizable N estimated as the difference of mineral N determined at day and at day 10. Total N in soil was determined by the Kjeldhal method. Organic matter in soil samples was determined by the Walkely-Black procedure.

Results and Discussion

Microbial biomass C was significantly increased with fertilizers (Fig. 1a). Highest microbial biomass C was observed in the plots treated with combined organic and mineral soil amendments. These observation might be due to the increase of soil organic matter as a result of farmyard manure application and the increase of plant biomass production (Rabary *et al.*, 2008). The content of microbial biomass C in the cropping patterns containing legume as sole crop or intercrop with cereals increased (Fig. 1b). This might be the N rich leguminous organic matter (Giller, 2001).

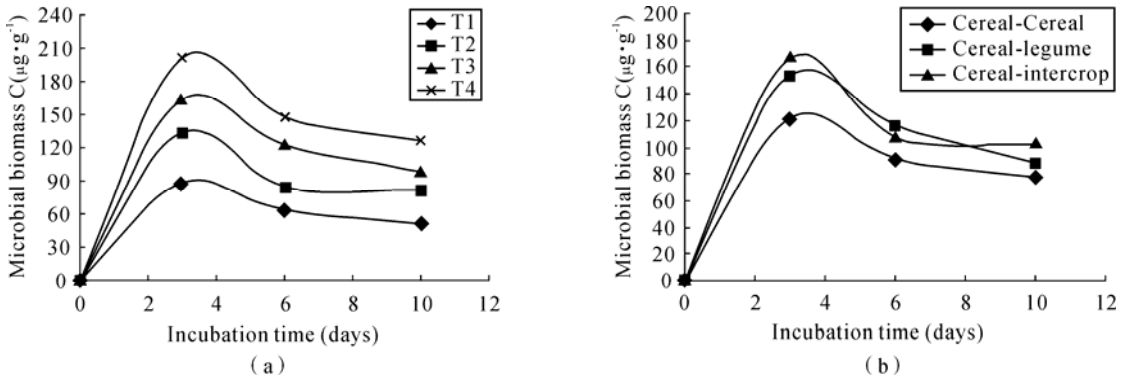

Fig. 1 Effect of (a) fertilizer treatments (b) cropping patterns on soil microbial biomass C in severely eroded soils

Fertilizers improved soil organic matter and total N content and their respective highest values were found in the plots receiving mixed farmyard manure and mineral fertilizers (Shafi *et al.*, 2006) followed by mineral fertilizers alone compared to the control plot (Goyal *et al.*, 2006). Increase in soil OM in the cropping patterns containing legumes might be due to falling leaf letters on the surface (Giller, 2003) and the nitrogen rich residues left in soil after the above ground parts were got harvested (Ussiri *et al.*, 2006). Increased microbial biomass N, and mineralizable N with fertilizer application and maximum biomass N

was recorded in mixed application of farmyard manure and mineral fertilizers. This might be due to increased soil organic matter that alter soil biochemical properties by providing source of nutrients to both plants and microbes (Monaco *et al.*, 2008). Microbial biomass N found in the cropping pattern having legumes in rotation were maximum and the values were in line with the published data. This might be due to N_2 fixation and N released from organic matter decomposition and subsequently incorporated into microbial biomass (Jensen, 1994). The nodulated roots and above ground residues, after the crop harvest, represent a valuable source of N (Giller, 2001) and soil organic matter (Campbell *et al.*, 1991) the decomposition of which provide a meaningful contribution to the N economy of soil (Glasener *et al.*, 2002). Legume based cropping pattern generally support higher contents of soil microbial parameters including microbial activity, microbial biomass carbon and N and microbial number (Kirchner *et al.*, 1993).

Conclusion

The integrated use of 20 $t \cdot ha^{-1}$ FYM and 50% mineral N along with 100% PK for four consecutive seasons significantly improved soil organic fertility over the mineral fertilizer treatments alone. Moreover, cereal-legume crop rotation also showed improvement in the studied parameters of organic soil fertility of these eroded soil. Our results suggested that the present recommended dose of mineral fertilizers are not adequate for the restoration of soil fertility and crop productivity of severely eroded soils. Fertilizers must be applied in integrated form which may carry 50% N from inorganic source and the rest of 50% from organic sources to improve the level of organic fertility of eroded soils on sustained basis. Results further suggested that legumes must be entered into conventional cereal-cereal rotation to improve the N input and organic fertility of severely eroded soils.

References

Banning NC, Grant CD, Jones DL, Murphy DV (2008) Recovery of soil organic matter, organic matter turnover and nitrogen cycling in a post-mining forest rehabilitation chronosequence. Soil Biol. Biochem. 40 (8): 2021-2031

Campbell CA, Beiderbecke VO, Center RP, Lafond GP (1991) Effect of crop rotations and cultural practices on soil organic matter, microbial biomass and respiration in a thin black chernozem. Can. J. Soil Sci. 71: 363-376

Giller KE (2001) Nitrogen Fixation in Tropical Cropping Systems. CAB International, Wallingford, UK, pp. 423

Glasener KM, Wagger MG, MacKown CT, Volk RJ (2002) Contributions of shoot and root N15 labelled legume nitro gen sources to a sequence of three cereal crops. Soil Sci. Soc. Am. J. 66: 523-530

Goyal S, Sakamoto K, Inubushi L, Kamaewada K (2006) Long-term effects of inorganic fertilization and organic amendments on soil organic matter and soil microbial properties in Andisols. Archives of Agron. Soil Sci. 52 (6): 617-625

Kirchner MJ, Wollum AG, King LD (1993) Soil microbial populations and activities in reduced chemical input agro ecosystems. Soil Sci. Soc. Am. J. 57: 1289-1295

Monaco S, Hatch DJ, Sacco D, Bertora C, Grignani C (2008) Changes in chemical and biochemical soil properties induced by 11-yr repeated additions of different organic materials in maize-based forage systems. Soil Biol. Biochem. 40(3): 608-615

Rabary B, Sall S, Letourmy P, Husson O, Ralambofetra E, Moussa N, Chotte JL (2008) Effects of living mulches or residue amendments on soil microbial properties in direct seeded cropping systems of Madagascar. Appl. Soil Ecol. 39(2): 236-243

Shafi M, Bakht J, Tariq Jan M, shah Z (2006) Soil C and N dynamics and maize yield as affected by cropping systems and residue management in North-western Pakistan. Soil Till. Res. 94: 520-529

Giller K (2003) Kick-starting legumes. AGRIS record NL2004716213, LEISA Magazine 19(4): 19-20

Ussiri DA, Lal R, Jacinthe PA (2006) Post-reclamation land use effects on properties and carbon sequestration in minesoils of southeastern Ohio. Soil Sci. 171: 261-271

Session 2

Biogeochemical Interfacial Reactions and the Transformation, Transport and Fate of Vital and Toxic Elements

Role of Biomolecules in Influencing Transformation Mechanisms of Metals and Metalloids in Soil Environments

Antonio Violante*

Dipartimento di Scienze del Suolo, della Pianta e dell'Ambiente,
Università di Napoli Federico II, 80055 Portici (Napoli), Italy.
*Corresponding author. Tel. No. +39 0812539175; Fax No. +39 081 2539186; E-mail: violante@unina.it.

Abstract: Characterizing the factors which affect the mobility, bioavailability, leaching and toxicity of metals and metalloids in soil environments is of paramount importance. Special attention is devoted to the influence of biomolecules, mainly roots exudates, as well as pH, nature of the sorbents, redox reactions on the transformation mechanisms of trace elements in cationic and anionic forms in soils. Time of reaction and the surface coverage have a great influence on the sorption/desorption processes of trace elements in the presence of organic ligands. Leaching and extraction tests are widely used for assessing trace element phytoavailability.

Keywords: Heavy metals and metalloids; Soil components; Adsorption/desorption processes; Biomolecules; Phytoavailability

Introduction

The aim of this presentation is to provide information on the factors which affect the mobility of trace elements. Special attention is devoted to the influence of biomolecules, mainly root exudates, on the transformation mechanisms of metals and metalloids in soil environments. Because soils are heterogeneous, heavy metals and metalloids can be involved in a series of complex chemical and biological interactions including sorption-desorption reactions, precipitation and dissolution, oxidation-reduction and solution and surface phase complexation.

Sorption-desorption processes of elements in cationic form differ greatly from those in anionic form. These reactions are affected by many factors, such as pH, nature of the sorbents, presence and concentration of organic and inorganic ligands, including humic and fulvic acid, root exudates and nutrients. The soil components responsible for trace element sorption include, soil organic matter, phyllosilicates, carbonates, microorganisms and variable charge minerals (constituents such as Fe, Al, Mn and Ti oxides, short-range ordered aluminosilicates as well as phyllosilicates coated by OH-Al or OH-Fe species) whose charge varies with the pH of the soil solution. Soil components differ greatly in their sorption capacities, their cation and anion exchange capacities, and the binding energies of their sorption sites. However, in soil environments, organic matter, phyllosilicates and OH-Fe and OH-Al species are constantly in close association with each other, forming organo mineral complexes having different shape, size, charge and reactivity towards nutrients, xenobiotics and bipolymers (Violante *et al.*, 2002).

Except for some noncrystalline minerals, humic substances appear to have the greatest capacity for sorption of trace elements in cationic form. A body of evidence has demonstrated that humic matter and metal oxides are much more effective scavengers of trace elements in cationic form, than even the most efficient sorbent among phyllosilicates, indicating that specific sorption and other complexation processes are the dominant binding mechanisms (Jackson, 1998; Huang and Germida, 2002; Spark, 2003).

Trace elements in cationic form are probably not dominantly sorbed on 001 faces of phyllosilicates because they are always vastly outnumbered by other

cations with which they compete (Jackson, 1998). They may be strongly sorbed only on the edges of the phyllosilicates. However, clay minerals have also an important role as carriers of associated oxides and humic substances forming organo-mineral complexes.

Free-living bacteria and their extra-cellular macromolecular products (e.g. fibrils) can accumulate trace elements and may have mineral coatings with bound metals on their surfaces (Beveridge, 1989). All microorganisms contain biopolymers such as proteins, nucleic acids, and polysaccharides which provide reactive sites for binding metal ions. The cell surfaces of all bacteria are negatively charged containing different types of negatively charged functional groups, such as carboxyl, hydroxyl and phosphoryl that can adsorb metal cations, and retain them by mineral nucleation. Bacteria therefore play an important role in the speciation, fate and transport of metals, metalloids and radionuclides in soil and associated environments. The ability of bacteria to accumulate toxic metals also varies with cell age.

Variable charge minerals selectively sorb polyvalent cations even when their surfaces are positively charged (solution pH values lower than the point of zero charge [PZC] of the sorbent). Most transition cations (Pb, Cu, Cr, Ni, Co, Zn, Al, Fe, Mn) are often sorbed more strongly than alkaline earth cations. Spectroscopic techniques such as electron spin resonance (ESR) and Extended X-ray Absorption Fine Structure Spectroscopy (EXAFS) have been used for the identification of metal complexes at the surfaces of Al, Fe or Mn oxides, silicate clays and soil organic matter. pH affects sorption of trace elements, either by changing the number of sites available for sorption (sorption increases by increasing pH) or by changing the concentration of cation species (Me^{2+}, $MeOH^{+}$, $Me(OH)_2$).

In the last decade extensive research has been carried out on the heterogeneous precipitation of trace elements on the surfaces of minerals, using modern spectroscopy techniques such as synchrotron-based X-ray absorption spectroscopy (Sparks, 2003). Sorption of metals, such as Ni, on an array of phyllosilicates and Al-oxide, could result in formation of mixed metal-Al hydroxide surface precipitates which appear to be coprecipitates. These neo-formed phase shares structural features common to the hydrotalcite group of minerals and the LDHs, also known as anionic clays.

Trace elements which exist in anionic form are sorbed primarily by chemisorption at reactive sites of metal oxides and allophanes and at the edges of phyllosilicates (Violante *et al.*, 2002). Usually, they are not sorbed on soil organic matter, but certain elements (e.g. borate, arsenate, arsenite) are found to be bound to humic acids (Violante *et al.*, 2008). Arsenate and arsenite have maximum adsorption on humic acids at pH 5.5 and 8.0, respectively. Arsenate adsorbs onto solid phase humic acids more extensively than arsenite, with amine (NH_2) groups suspected as the primary functional group responsible for arsenic retention. Some anions may bond indirectly to organic groups through a bridging hydrolytic species of Al, Fe and Mn.

Sorption of anions onto variable charge minerals and soils varies with pH. Anions may be specifically or nonspecifically sorbed, forming *inner-sphere* or *outer-sphere* complexes. Ligands which are specifically sorbed replace OH^- or OH_2 groups from the surfaces of variable charge minerals, which involve direct coordination to the surface metal atom. Trace elements, which form inner-sphere complexes, are arsenate, arsenite, molybdate, and selenite, which may form different surface complexes on inorganic soil components: monodentate, bidentate-binuclear and bidentate-mononuclear complex in different proportions depending on pH and surface coverage (Violante *et al.*, 2008).

The presence of biomolecules as well as pH, surface properties of the sorbents, the number of sites available for sorption, the nature and charge of Me-L species in solution influence trace element sorption onto soil inorganic components. Organic ligands (e.g., organic acids) which form strong complexes with trace element cation usually prevent or reverse their association with negatively charged sorbents, as clay minerals, by forming stable dissolved or dispersed negatively charged complexes with the cations (Violante *et al.*, 2008). In contrast, the presence of certain foreign ligands, occurring naturally in the rhizosphere, such as siderophores produced by microorganisms and phytosiderophores exuded by plants, may promote the formation of positive complexes and, consequently, the sorption of trace elements onto phyllosilicates. The processes, which affect the sorption of trace element cations onto variable charge minerals in the presence of complexing agents, are particularly complex and are different from those onto phyllosilicates (Violante *et al.*, 2008). Usually, high concentrations of low

molecular weight organic acids may promote the formation of negative complexes with metal ions and favour their sorption onto variable charge minerals, whereas siderophores may promote the formation of positive complexes, preventing sorption. In conclusion, biological ligands play a very important role on the mobility and then the phytoavailability of trace elements at soil-root interface (Huang and Germida, 2002).

The presence of organic ligands also affects the sorption of trace elements in anionic form by competing for available sorption sites and/or reducing the surface charge of the variable charge minerals and soils (Violante *et al.*, 2002; 2008). The competition depends on the affinity of the anions for the surfaces of the sorbents as well as the nature and surface properties of the minerals and soils. It has been demonstrated that competition in sorption between selected organic ligands and arsenate may vary greatly on different soil minerals and on soils characterized by different mineralogy and chemical properties. Time of reaction and the surface coverage have also a great influence on the competitive sorption between trace elements and organic ligands (Violante and Pigna, 2002).

Trace elements in anionic form may be easily sorbed by "anionic clays" (double layered hydroxides) which are present in soils. For example, "green rusts" are green-blue Fe(II)/Fe(III) hydroxides which are formed by a number of abiotic and biotic processes under circumneutral to alkaline conditions in suboxic environments and are postulated to be intermediate phases in the formation of iro(oxyhydro)oxides (Violante *et al.*, 2002). They may be important for trace metal mobility because of their high reactive surface area (Violante *et al.*, 2009). Furthermore, redox reactions, both biotic and abiotic, are of great importance in controlling the oxidation state and thus, the mobility, the phytoavailability and the toxicity of many elements, such as Cr, Se, Co, Pb, As, Ni and Cu (Huang and Germida, 2002; Sparks, 2003; Violante *et al.*, 2008).

In contrast to sorption studies relatively little information is available on the desorption of metals and metalloids from soils or soil components. Presence of biomolecules has a significant impact on the desorption of trace elements. Usually, desorption studies have biphasic reaction processes; a fast reaction followed by a slow reaction. A number of factors, such as the type, mineralogy and crystallinity of the sorbents, the pH, the pe, the surface coverage, the residence time of metals and metalloids on the surfaces of soil components may affect the desorption of trace elements. Some studies on the effect of residence time on the desorption of some heavy metals and metalloids have been carried out. Usually, the longer the residence time, the greater the decrease in trace element desorption, because of a rearrangement of surface complexes and/or a conversion of surface complexes into surface precipitates (Sparks, 2003; Pigna *et al.*, 2006). In soil environments trace elements may be not only sorbed on but also coprecipitated in metal oxides. Their partial removal by organic ligands from coprecipitates has received some attention (Violante *et al.*, 2008).

Organic ligands are important in the formation and transformation of metal precipitates. They have an important effect on the nature, morphology and surface properties of aluminum and iron hydroxides and oxyhydroxides. Organic complexing anions delay or inhibit, at certain critical concentrations, the crystallization of aluminum and iron oxides, favoring the formation of short-range ordered precipitates. Organic anions adsorbed or coprecipitated with aluminum and iron have a great influence on the adsorption of heavy metals and metalloids as well as nutrients, organic pollutants and biopolymers (Violante *et al.*, 2002).

Excessive levels of many toxic elements can result in soil quality degradation, crop yield reduction, and poor quality of agricultural products, consequently posing significant hazards to human, animal, and ecosystem health. Therefore, the bioavailability of essential and non-essential metals and metalloids is a crucial problem in agricultural and environmental studies. There has been a steady increase in the number of investigations related to both understanding the processes involved in the uptake of an element by plants, and to finding the most reliable methods for the prediction of availability of a given element to plants.

References

Beveridge TJ (1989) Metal ions and bacteria. In: Beveridge TJ, and Doyle RJ (eds.), Metal Ions and Bacteria. Wiley, New York, pp.1-29

Huang PM, Germida JJ (2002) Chemical and Biochemical Processes in the Rhizosphere: Metal

Pollutants. In: Huang PM, Bollag JM, Senesi N (eds.), Interactions between Soil Particles and Microorganisms: Impact on the Terrestrial Ecosystem, John Wiley & Sons, New York, 381-438

Jackson TA (1998) The Biogeochemical and Ecological Significance of Interactions between Colloidal Minerals and Trace Elements. In: Parker A, Rae JE (eds.), Environmental Interactions of Clays, Springer-Verlag, Berlin, pp.93-205

Pigna M, Krishnamurti GSR, Violante A (2006) Kinetics of arsenate sorption-desorption from metal oxides: Effect of residence time. Soil Sci. Soc. Am. J. 70: 2017-2027

Sparks DL (2003) Environmental Soil Chemistry. 2nd Edition. Academic Press, San Diego

Violante A, Huang PM, Gadd G (2008) Biophysico-Chemical Processes of Metals and Metalloids in Soil Environments. John Wiley & Sons

Violante A, Pigna M (2002) Competitive sorption of arsenate and phosphate on different clay minerals and soils. Soil Sci. Soc. Am. J. 66: 1788-1796

Violante A, Pucci M, Cozzolino V, Zhu J, Pigna M (2009) Sorption/desorption of arsenate on/from Mg-Al layered double hydroxides: Influence of phosphate. J. Colloid Interface Sci. 333: 63-70

Violante A, Krishnamurti GSR, Huang PM (2002) Impact of organic substances on the formation of metal oxides in soil environments. In: Huang PM, Bollag JM, Senesi N (eds.), Interactions between Soil Particles and Microorganisms: Impact on the Terrestrial Ecosystem. John Wiley & Sons, New York, pp.381-438

Biogeochemical Processes of Arsenic in Paddy Soils

Yongguan Zhu*, Wenju Liu, Guilan Duan, Paul Williams, Guoxin Sun

Sate Key Lab of Urban and Regional Ecology, Research Center for Eco-environmental Sciences,
Chinese Academy of Sciences, Beijing 100085, China.
*Corresponding author. Tel. No. + (86)10-62936940; Fax No. + (86)10-62936940; E-mail: ygzhu@rcees.ac.cn.

Abstract: Arsenic (As) is ubiquitous in the environment, and is regarded as class I carcinogen. For populations taking rice as the stable food, rice is the major pathway for human exposure to As. As dynamics in the soil-rice system is therefore critical in risk assessment and reduction for Southeast Asia, where As contamination widely distributes. The aim of this paper is to give an overview of biogeochemical processes in the soil-rice system, with strong focus on how molecular tools (physical, chemical and biological) can be used to unravel the mechanisms of arsenic transport, uptake and metabolism in this system.

Keywords: Arsenic; Biogeochemistry; Health risk; Molecular environmental science; Rice

Introduction

Inorganic As is classified as a non-threshold carcinogen with a linear dose response for chronic low level exposure. Rice is the staple food for nearly half of the population globally, and arsenic (As) elevation in rice has recently been reported to add cancer risks to populations in many regions (Zhu *et al.*, 2008; Meharg *et al.*, 2009). This is in part due to rice being particularly efficient at taking up As from soil (Williams *et al.*, 2007) and exacerbated in major rice growing regions of the world with elevated As in paddy soil due to anthropogenic contamination, such as mining activities and irrigation with As-tainted groundwater (Williams *et al.*, 2006, 2007; Zhu *et al.*, 2007). This paper aims to provide an overview of As dynamics in the soil-rice system, with an emphasis on how molecular tools (physical, chemical and biological) can be used to unravel the mechanisms of As transport, uptake and metabolism in this system.

Arsenic in Paddy Soils-the Role of Redox Potential

Arsenic enters paddy soils from anthropogenic (mining activities) and geogenic (As in groundwater used for irrigation) sources. Under anaerobic conditions, arsenic exists mainly in the form of arsenite, and its concentration usually increases quickly after flooding. Managing soil water regime can have significant effect on both the mobility and speciation of arsenic in paddy soils, therefore As accumulation in rice plants (Li *et al.*, 2009).

Rhizosphere Processes

Rhizosphere processes, among many others are crucial in determining the mobility and bioavailability of As in soil-rice systems. Several studies have pointed to the role of iron plaque on rice root surface in modulating the dynamics of As in soil-rice systems (Liu *et al.*, 2004; 2006). It is well known that microbes are heavily involved in the oxidation and reduction of iron, but their role in iron plaque formation/dissolution, and thus As bioavailability is not clear. In the past five years or so, our group has been investigating whether nitrate-dependent iron oxidizing bacteria and iron reducing bacteria are involved in As sequestration and release in paddy soils, and rhizosphere soils in particular.

Uptake and Metabolism

Arsenic in the environment mainly exists in two

inorganic oxidation states, arsenate (As(V)) and arsenite (As(III)). As (V) and As (III) enter plant cells via phosphate transporters and aquaglyceroporins, respectively, as was reviewed in Bhattacharjee *et al.* (2008). Once taken up, As (V) is reduced to As (III), catalyzed largely by arsenate reductases, members of the superfamily of protein tyrosine phosphatase (PTPase). As (III) can then be complexed with glutathione (GSH) or phytochelatins (PCs), Raab *et al.* (2005) identified up to 14 different species of arsenic complexes in sunflower plants. As (III) or complexed As(III) is then transported across the tonoplast and sequestered in the vacuole. Most data support the idea that arsenic is translocated from the roots to the tissues above ground, mostly in the form of As (III) (Xu *et al.*, 2007; Su *et al.*, 2008). As(III) can be methylated to form monomethylarsenate (MMAs(V)), dimethylarsenate (DMAs(V)) and trimethylarsine oxide (TMAO(V)) in *planta* (Wu *et al.*, 2002; Zhao *et al.*, 2009).

Conclusion

Arsenic dynamics in the soil-rice system is complex, and molecular tools are important in providing insights into the mechanisms that regulate As accumulation in rice grain.

Acknowledgements

This paper is based on many studies conducted in China and the UK, and I would like to appreciate my sincere thanks to collaborators at home and abroad.

References

Bhattacharjee H, Mukhopadhyay R, Thiyagarajan S, Rosen BP (2008) Aquaglyceroporins: ancient channels for metalloids. J. Biol. 7: 33

Liu WJ, Zhu YG, Hu Y, Williams PN, Gault AG, Meharg AA, Charnock JM, Smith FA (2006) Arsenic sequestration in iron plaque, its accumulation and speciation in mature rice plants (Oryza sativa L.). Environ. Sci. Technol. 40: 5730-5736

Liu WJ, Zhu YG, Smith FA, Smith SE (2004) Do phosphorus nutrition and iron plaque alter arsenate (As) uptake by rice seedlings in hydroponic culture? New Phytol. 162: 481-488

Meharg AA, Williams PN, Adomako E, Lawgali YY, Deacon C, Villada A, Cambell R CJ, Sun G, Zhu YG, Feldmann J, Raab A, Zhao FJ, Islam R, Hossain S, Yanai J (2009) Geographical Variation in Total and Inorganic Arsenic Content of Polished (White) Rice. Environ. Sci. Technol. 43: 1612-1617

Raab A, Schat H, Meharg AA, Feldmann J (2005) Uptake, translocation and transformation of arsenate and arsenite in sunflower (Heliannthus annuus): formation of arsenic-phytochelatin compexes during exposure to high arsenic concentrations. New Phytol. 168: 551-558

Su YH, McGrath SP, Zhu YG, Zhao FJ (2008) Highly efficient xylem transport of arsenite in the arsenic hyperaccumulator Pteris vittata. New Phytol. 180: 434-441

Williams PN, Islam MR, Adomako EE, Raab A, Hossain SA, Zhu YG, Feldmann J, Meharg AA (2006) Increase in rice grain arsenic for regions of Bangladesh irrigating paddies with elevated arsenic in groundwaters. Environ. Sci. Technol. 40: 4903-4908

Williams PN, Villada A, Deacon C, Raab A, Figuerola J, Green AJ, Feldmann J, Meharg AA (2007) Greatly enhanced arsenic shoot assimilation in rice leads to elevated grain levels compared to wheat and barley. Environ. Sci. Technol. 41: 6854-6859

Wu JH, Zhang R, Lilley RM (2002) Methylation of arsenic in vitro by cell extracts from the bentgrass (Agrostis tenuis): effct of acute exposure of plants to arsenate. Funct. Plant Biol. 29: 73-80

Xu XY, McGrath SP, Zhao FJ (2007) Rapid reduction of arsenate in the medium mediated by plant roots. New Phytol. 176: 590-599

Zhao FJ, Ma JF, Meharg AA, McGrath SP (2009) Arsenic uptake and metabolism in plants. New Phytol. doi: 10.111/j.1469-8137.2008.02716.x.

Zhu YG, Sun GX, Lei M, Teng M, Liu YX, Chen NC, Wang LH, Carey AM, Deacon C, Raab A, Meharg AA, Williams PN (2008a) High percentage inorganic arsenic content of mining impacted and nonimpacted Chinese rice. Environ. Sci. Technol. 42: 5008-5013

Zhu YG, Williams PN, Meharg AA (2008b) Exposure to inorganic arsenic from rice: A global health issue? Environ. Pollut. 154: 169-171

Soil Microorganism-mineral-organic Matter Interactions and the Impact on Metal Mobility

Jacques Berthelin*

Laboratoire des Interactions Micro-organismes-Minéraux-Matières Organiques dans les Sols (LIMOS), UMR 7137 CNRS-Nancy-Université, Université Henry Poincaré - Nancy I, Faculté des Sciences, BP239, 54506 Vandoeuvre lès Nancy Cedex, France.
*Corresponding author. E-mail: jacques.berthelin@limos.uhp-nancy.fr.

Soils are huge reservoirs of micro-organisms. They contain all the main groups of microorganisms with a very large diversity of bacteria, fungi, algae, protozoa. In the upper layers of soils, bacteria can have a biomass of 1,000 to 4,000 $kg \cdot ha^{-1}$ and an average number of 106 to 109 g^{-1} of dry soil. Fungi have approximately the same to slightly higher biomass. Both bacteria and fungi are now well recognized as key agents of biogeochemical cycling of major and trace elements and as main actors of soil functioning. Other microorganisms as algae (photo-synthetic organisms), present at the soil surface, are not so well known in soils and play a minor role, but are considered as endolithic pioner organisms involved in rock weathering particularly in cold and warm deserts. Lichens, a symbiotic association between algae and fungi, are also interesting as colonizing organisms and weathering agents.

Soil fungi and the larger part of soil bacteria are chemoorganotroph, living at the expense of organic compounds, but different strategic groups of bacteria are chemolithotroph, living at the expense of inorganic compounds (sulfur oxidizers, iron oxidizers, ammonium oxidizers, … and CO_2 fixing organisms). In order to generate energy for their growth microorganisms oxidize organic or inorganic materials (electron donors) and reduce for their aerobic or anaerobic respiration and for fermentation processes, inorganic (O_2, NO_3^-, Mn^{4+}, Fe^{3+}, SO_4^{2-}, CO_2) and organic compounds. They also form and release metabolic (acid, complexing, alkaline) compounds. All these energetic, nutritional strategies and metabolic pathways can be directly or indirecly involved in the solubilisation or insolubilisation of mineral elements, the weathering of minerals, the formation and deposit of minerals and of organo-mineral compounds.

The main microbial processes involved in solubilisation of metals are briefly summarized here after (1) production of acid and/or chelating or complexing compounds able to dissolve and weather silicates, phosphates, carbonates, oxides, sulfides, (2) reduction of iron and manganese involving dissolution of oxides and oxyhydroxides and of associated elements (Al, Ni, Co, Cr, …), (3) oxydation of sulfides and metal polysulfides bearing metals (Cu, Pb, Ni…), (4) biosorption and bioaccumulation of many metals (uptake from solutions or from solid phases), (5) direct or indirect oxydation (e.g. U, Cr, Hg) or reduction (e.g. Ra) of different elements.

Microbial insolubilisation of metals can involve different types of reactions (1) biodegradation of organic ligands releasing a chelated or complexed metals, (2) formation of hydroxides and oxyhydroxides of iron and manganese acting as sinks for metals, (3) sulfate reduction and deposit of metal sulfides (e.g. Ni, Pb, Cu,…), (4) bioaccumulation, biosorption processes independently and in excess of the nutrient requirements (many metals are concerned).

Some general mechanisms concern processes involving changes in speciation of metals by dissolution of parent materials, by reduction or oxydation or acidification of their environments. At the opposite specific mechanisms occured such as methylation processes and volatiliztion of elements

(Pb, Sn, Sb).

All these processes depend on biological, physical and chemical environmental parameters: availability of organic and inorganic energy sources (electron donors and acceptors) and nutrient conditions (e.g. deficiency in nutriments such as iron, nitrogen…) for the microorganisms, adaptability and activity of microbial communities, cristallochemistry and surface properties of minerals, particle size of minerals, humidity, temperature… They occur in all the types of soils, both in rhizosphere and non rhizosphere soils. Depending on the processes involved, the interactions at the surface of the minerals e.g. contact or not contact with the mineral surfaces are of great importance in particular for the oxidation or reduction processes.

To illustrate more accurately the impact of microorganism-mineral-organic matter interactions on the metal mobility, examples are well provided by the biogeochemical cycle of iron and some associated major (Al, Mn) and trace elements (Ni , Co , Cr ,…).

Iron, 4th element of the earth crust and essential micronutrient, occurs in soils, mainly as primary and secondary minerals, originating either from parent material or from their weathering (oxides, silicates, carbonates, sulfides, phosphates), but also as organo-mineral compounds. It is present at low solubility, excepted in acid and or reducing conditions. Iron is consequently more often not or slightly bioavailable. But it has a high reactivity due to its ability to be reduced or oxidized or to form organo-mineral soluble complexes. Its mobility is determined by acid-base and redox conditions and by the presence of organic ligands. Such parameters are not strictly chemically and physico-chemically mediated, but are controlled by microbial activities involving different chemoorganotroph and chemolithotroph communities which permanently determined and modify the biotic and abiotic factors. In fact, soils contain bacterial and fungal communities which by different strategies are involved in iron and metal dissolution and accumulation processes.

In acid and neutral environmental conditions, aerobic or micro-aerophilic autotrophic or mixotrophic bacterial communities oxidize ferrous to ferric iron for their energetic requirements. Iron oxidation is often associated to sulfur and directly or indirectly to metal and non metals dissolution. Surface, cristallochemical, electrochemical properties of sulfides are of major interest. Such processes are at the origin of dissolution of metals (Cu, Ni, U,…) and they end in the formation of ferric deposits as hydroxides or oxyhydroxides associated to other elements excepted in acid or complexing conditions. In strong acid conditions, bioleaching (solubilization, extraction) of metals is dominant.

Other bacterial communities, aero-anaerobic or anaerobic, use ferric iron as electron acceptor in anaerobic respiration or in complement of fermentation. Iron is mobilized (solubilized) as ferrous iron accompanied by other metals present in oxides and oxyhydroxides and can stay in solution in reducing or acidic conditions. Such processes occur not only in waterlogged conditions but also in temporarily hydromorphic soils. They concern soluble forms (ferric chloride, ferric citrate, …) and insoluble forms of iron (lepidocrocite, goethithe, hematite, limonite). The IRB regulation depends on crystallinity, particle size (surface area) substitution in the mineral structure, presence of ligands increasing dissolution, presence of suttle promoting electron transfer (e.g. quinonic compounds such as ADQS), contact between bacteria and mineral… Very significant correlations are observed between IRB activity and soil organic matter (OM) mineralization but with different rates and yields, depending on the availability of organic compounds and of iron and of the biodegradability of OM. These processes are largely spread in different environments. They modify the distribution of iron and of their associated elements (e.g. heavy metals) in the different compartments of the solid phase. They increase their availability ad coefficient transfer to the plants.

These iron reducing bacterial (IRB) communities present a very large diversity of bacterial populations as recently observed using molecular biology tools. They have also a large adaptability associated to their diversity. They are strongly involved in the functioning and evolution of soils in temperate, tropical, cold countries and can have beneficial or harmful effects.

Fungi (mycorrhizal and saprophytic) and bacteria synthesize and release complexing agents (e.g. polycar-boxylic, hydroxy-carboxylic, phenolic, hydroxamic … acids) of iron. The rhizospheric bacteria producing such compounds are involved in mineral weathering and the solubilisation of iron and other metals and so promote their transfer to the plant. Some of these complexing agents, the siderophores, having 3 acid hydroxamic functional groups or 3

di-ortho-phenol (catechol) functional groups form very stable organo-metallic complexes involved in dissolution and transfer of ferric iron. Other metals are concerned less specifically. They are very efficient in dissolution of ferric oxides.

All these processes, more or less specifically involved in solubilization and/or deposit of metals, end in the cycling of metals, weathering of minerals, functioning of soils, increase of metals availability in both rhizospheric and non rhizospheric soil sites. They occur in the weathering of different minerals and the behaviour of many elements (iron, aluminium, trace metals, phosphorus, non metal trace elements, sulphur, arsenic…) and can have beneficial but also harmful effects in the plant - soil systems (e.g. beneficial or toxical effect on rice in paddy fields). The knowledge of the structure and functions of microbial communities involved is in progress but with the parameters controlling their dynamic and activities they need to be better well defined (e.g. availability of organic matter and iron). Basis for models and for environmental biotechnologies are also well progressing.

Rhizosphere Processes and Management for Improving Nutrient Use Efficiency and Crop Productivity

Fusuo Zhang*, Jianbo Shen, Jingying Jing, Long Li, Xinping Chen

College of Resource and Environmental Sciences, China Agricultural University, Beijing 100193, China.
*Corresponding author. Tel. No. +86-10-62732499; Fax No. +86-10-62731016; E-mail: zhangfs@cau.edu.cn.

Abstract: High input, high output, low nutrient resource use efficiency and deteriorating environmental problems reflect the typical characteristics of intensive farming system in China. How to achieve synchronously high nutrient use efficiency as well as high crop productivity has become a great challenge in the intensive agriculture of China. In the past two decades, crop production has not proportionally been increased with increasing input of chemical fertilizers, leading to low nutrient use efficiency and increasing environmental problems. Traditional nutrient management strategy was highly dependent on external chemical fertilizer input, but ignored exploring biological potential of efficient acquisition and use of soil nutrient resources by plants intrinsically. Rhizosphere is the key centre of interactions among plants, soils and microorganisms; the chemical and biological processes occurring in the rhizosphere not only determine mobilization and acquisition of soil nutrients, but also control nutrient use efficiency by crops. The rhizosphere management strategy lays emphasis on maximizing the efficiency of root and rhizosphere processes in nutrient acquisition towards high-yield and high-efficiency sustainable crop production by optimizing nutrient supply in root zone, regulating root morphological and physiological traits, and manipulating rhizosphere processes and interactions. The strategies of rhizosphere management are proved to be an effective approach to increasing nutrient use efficiency and crop productivity towards sustainable crop production for main crops in China.

Keywords: Rhizosphere management; Soil nutrients; Nutrient use efficiency; Crop productivity; Root exudation; Rhizosphere processes

Introduction

Significant advances have been made in soil improvement and enhancing crop yields in China over the last two decades. Increasing soil fertility by inputs of fertilizers to increase crop production has been one of the important strategies in Chinese agriculture since 1980. During the 1980s, not only did the total grain yield show a positive relationship with the total consumption of fertilizers, but 50% of the increased food production was also attributed to the use of fertilizers. However, although the total consumption of fertilizers continued to increase rapidly nationwide, the total food production eventually ceased to increase proportionately. High rates of fertilizer application had resulted in both the accumulation of large amounts of N and P in soils and a decline in the effectiveness of fertilizers. Moreover, the environment became more problematical. The main reason has been that too much effort has been made to increase fertilizer inputs while ignoring the potential benefits of biological processes through exploitation of soil nutrient resources by crops.

Rhizosphere processes are the linkage between plant processes and soil processes, to some extent, determine the bioavailability of soil nutrients and nutrient use efficiency, and thus affect crop productivity and environmental effects (Zhang *et al*., 2002, 2004). The rhizosphere management strategies lay emphasis on maximizing the efficiency of root and rhizosphere processes in nutrient acquisition towards high-yield and high-efficiency sustainable crop production by optimizing nutrient input in the rooting zone, regulating root growth and manipulating rhizosphere interactions (Fig. 1). Therefore, managing the rhizosphere ecosystem and rhizosphere processes can be one of the most important approaches to enhancing nutrient-resource use efficiency and crop productivity in main cropping systems in China.

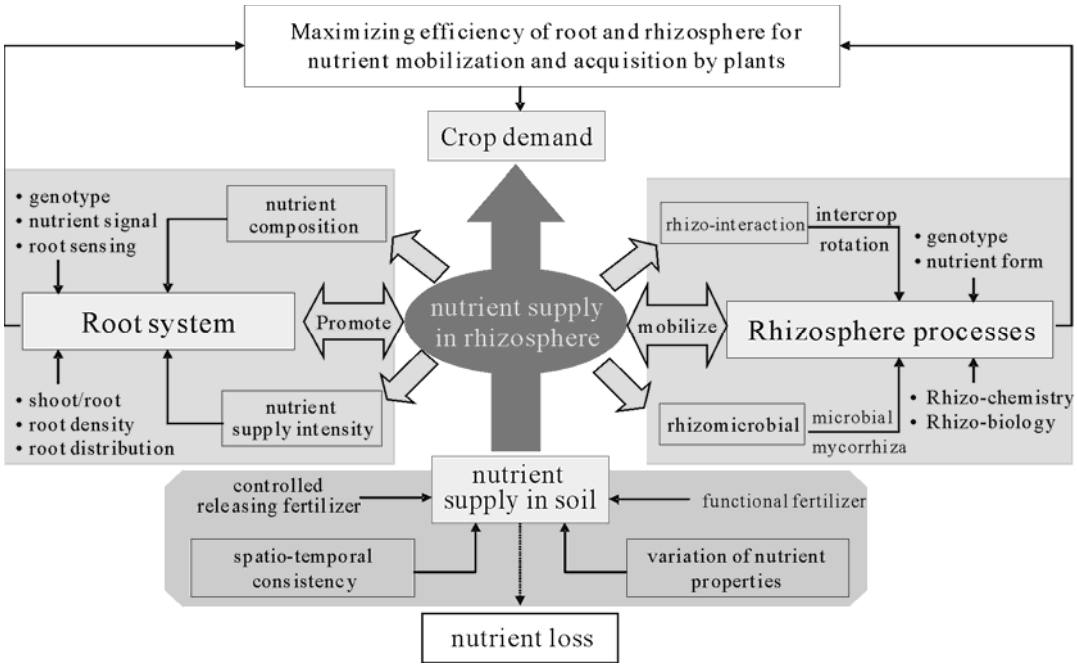

Fig. 1 Strategies for rhizosphere management

Managing Root Zone Nutrients in Plant-soil Systems for Efficient Nutrient use by Crops

Nutrient dynamics in the rooting zone of plant-soil systems reflect the ability of nutrient supply and nutrient availability, and thus influence crop production in agricultural ecosystems. The strategies of root zone nutrient management for efficient nutrient resource use of main crops have been established in China. In the traditional fertilization, people have been concerned with increasing nutrient concentrations in the soil solution by excessive fertilizer application but have neglected the nutrient activation by crop roots. The new method requires dynamic monitoring of nutrient concentration in root zone for establishing suitable nutrient supply intensity at different growth stages of crops in order to realize the synchronization of crop nutrient uptake, soil nutrient supply and fertilizer input. The establishment of root zone nutrient management strategy provides an effective approach to solving the huge conflict among high-yielding crops, efficient nutrient use and environmental protection.

Regulating Root Growth and Development for Improving Crop Nutrition and Yield

The root growth or proliferation can be effectively stimulated by changing nutrient supply intensity and composition, which significantly enhances the absorption area of soil nutrients. Severe nutrient deficiency in root zone causes stunt of root growth; excessive nutrient supply to plant roots results in inhibition of root growth. The healthy root system of crops can be effectively established when soil nutrient supply intensity is kept at an optimum level. The critical level of soil nutrient supply intensity is varied at different growth stages. In north or northeast China, a relatively high soil nutrient supply intensity can be achieved by application of N and P as starter fertilizer, which is needed for early root system establishment due to low temperature and low nutrient supply at the early seedling stage. At late stage, much more nutrients from soil can be mobilized and utilized by the powerful root system, leading to decreased dependency of crops on fertilizer supply. As for the intensive vegetable cropping system in which excessive nutrients are applied, it is important for efficient nutrient use to match root growth with nutrient distribution in soil profiles because large amount of nutrients could be washed away from active root zone under excess irrigation. The main approaches of root system management include quantifying and monitoring the root-zone nutrient concentration required by crops at different growth stages, controlling the root-zone nutrient concentration at a suitable range through accurate fertilizer supply and matching spatial-temporal

relationship between soil nutrient supply and root growth as well as distribution.

On the other hand, localized application of nutrients can significantly stimulate root proliferation (Shen *et al*., 2005). Our field experimental results demonstrated that localized application of N and P significantly enhanced the maize growth, including increased biomass of shoots and roots, leaf area, chlorophyll content and nutrient uptake because large number of lateral roots were induced at the local root zone at seedling stage. Root growth and root system establishment are important for resource capture and acquisition such as water and nutrients, and thus determine nutrient use efficiency by crops.

Improvement of Crop Nutrition and Yield by Manipulation of Rhizosphere Processes

Rhizosphere is not only an interface between roots and soils, but also the centre of interactions among plants, soils and microorganisms. The chemical and biological processes occurring in the rhizosphere determine mobilization and acquisition of soil nutrients, and even control nutrient use efficiency by crops (Zhang, 2006). Our studies showed that localized application of super-phosphates combined with NH_4^+-N significantly improved crop growth because NH_4^+-N supply induced an evident rhizosphere acidification, leading to increased availability of soil phosphates. Proton release and carboxylate exudation from cluster roots of white lupin can effectively mobilize sparingly soluble phosphorus in soil through altering rhizosphere processes. Nutrition of N and P in maize can be significantly improved by fababean intercropped with maize through rhizosphere interactions due to strong rhizosphere acidification of fababean (Li *et al*., 2008). Interspecific belowground interactions and rhizosphere effects between intercropped species play an important role in yield advantage of intercropping. Using crop genotypes with efficient nutrient utilization that can mobilize soil nutrients in the root zone may be an effective approach to increasing nutrient use efficiency and crop productivity. An alternative strategy for rhizosphere management is to employ beneficial symbiotic association between rhizosphere microorganism and plant roots, particularly mycorrhiza. Mycorrhiza has great potential in assisting the host plants to take up scarce and immobile nutrients, particularly P. However, how to explore the biological potential of mycorrhiza in intensive farming system will be a challenge for rhizosphere management. To develop the method for dual inoculation with mycorrhiza fungi and rhizobia is promising for improving nutrient use efficiency and crop productivity.

In conclusion, the strategies of rhizosphere management may improve nutrient use efficiency and crop production via exploitation of biological potential for nutritional enhancement and regulation of rhizosphere processes by crops through technological innovation and applications. The strategies are proved to be an effective approach to achieving sustainable agriculture production for main crops in China.

Acknowledgements

This study was supported by NSFC (30890131, 30871591) and MST (2006BAD25B02).

References

Li L, Li SM, Sun JH, Zhou LL, Bao XG, Zhang HG, Zhang FS (2007) Diversity enhances agricultural productivity via rhizosphere phosphorus facilitation on phosphorus-deficient soils. PNAS 104: 11192-11196

Shen J, Li H, Neumann G, Zhang F (2005) Nutrient uptake, cluster root formation and exudation of protons and citrate in *Lupinus albus* as affected by localized supply of phosphorus in a split-root system. Plant Sci. 168: 837-845

Zhang FS (2006) Biological processes in the rhizosphere: a frontier in the future of soil science. In: Alfred E. Hartemink (ed.), The Future of Soil Science, Wageningen: IUSS International Union of Soil Sciences, pp.155-157

Zhang FS, Shen JB, Li L, Liu XJ (2004) An overview of rhizosphere processes related with plant nutrition in major cropping systems in China. Plant Soil 260: 89-99

Zhang F, Shen J, Zhu Y (2002) Nutrient interactions in soil-plant systems. In: Lal R (ed.), Encyclopedia of soil science Marcel Dekker, New York, pp. 885-887

Effect of Soil Hg Stress on Expression of Heat Shock Protein Gene in Springtail *Folsomia Candida*

Yurong Liu, Yuanming Zheng, Yu Da, Jizheng He*

State Key Laboratory of Urban and Regional Ecology, Research Centre for Eco-Environmental Sciences, Chinese Academy of Sciences, Beijing 100085, China.
*Corresponding author. Tel. No. +86-10-62849788; Fax No. 86-10-62923563; E-mail: jzhe@rcees.ac.cn.

Abstract: Transcriptional responses of hsp70 gene of the *Folsomia candida* were detected by relative real-time PCR assay when the springtail was exposed to a vegetable soil with different Hg concentrations or different exposure time. Results showed that the hsp70 gene expression level was significantly up-regulated when soil Hg was ≥ 0.25 mg·kg^{-1}. The responses of this gene expression were strongly induced after 48 hours exposure under 1 mg·kg^{-1} of soil Hg, which was probably due to the fast and sensitive response of the gene transcription to the Hg stress. Thus, the results suggested that the gene could be used as a biomarker to monitor the Hg pollution in soil and help early and fast environmental diagnostics or ecological risk assessment of Hg contaminated soils.

Keywords: *Folsomia candida*; Hsp70 gene; Soil; Hg; Risk assessment

Introduction

Soil mercury (Hg) pollution is a worldwide problem that could threaten the sustainability of essential soil functions, and the safety of human health (Nriagu and Pacyna, 1988). The evaluation on Hg toxicity and bioavailability has been widely concerned (Tsui and Wang, 2006; Golding *et al.*, 2007). Springtail *Folsomia candida* is one of the important model organism, which has been used in ecotoxicological tests of pollutant(s). Biomarkers are early and predictive responses to sublethal toxicant stress which provide measures of several rather than single effects of toxicants (Nota *et al.*, 2008). Heat shock protein (hsp) gene, as a potential biomarker in despite of debates and limitation, has been greatly concerned in other organisms (Adams, 2001; Brulle *et al.*, 2006), such as earthworms, among which the stress-inducible hsp70 is the most highly concerned and largest in all of the hsp families. We hypothesized that the Hg stress would impact the expression of hsp70 in the springtail *Folsomia candida* with the different soil Hg concentration and exposure time.

Materials and Methods

The soil used in the study was collected from a vegetable field in the suburb of Beijing city, China. It was a typical fluvo-aquic sandy loam. The strain of *Folsomia candida* was provided by the Institute of Plant Physiology and Ecology, Chinese Academy of Sciences (Shanghai, China). Chronic toxicity tests were conducted following the ISO 11267 method. Five replicates were used for each exposure. The test vessels were kept at 20±1 °C with a 12:12 h light/dark cycle for 28 d. At the end of exposure, juveniles and adults were counted after extraction by water floating. The test of hsp 70 gene expression was investigated by an exposed experiment. The soil was spiked with Hg concentrations ranging from 0.25 to 8 mg·kg^{-1} (i.e., 0.25, 0.5, 1, 2, 4, 8 mg·kg^{-1}). Four replicates were designed for both control and the spiked soils. Exposure time was 4 days. For the dynamic assay of hsp 70 gene expression, soil was spiked with a final concentration of 1 mg·kg^{-1} of soil Hg, and springtails were collected after the different exposure time, i.e., 6, 12, 24, 48, 96, 240 h. All the test vessels were kept at 20±1 °C with a 12:12 h light/dark cycle. When the

exposure was ended, the springtails were extracted from the spiked soil by water floating, and carefully moved to Petri dishes containing a mixture of charcoal/plaster-of-Paris to remove surplus water. Then they were put into sterile tubes in which they were snap frozen in liquid nitrogen and kept in -80 °C for RNA extraction. All expression analyses were conducted on total RNA extracted from the exposed springtails, using Trizol reagent according to the manufacturer's instruction. Real-time PCR assays were performed on iCycler iQ 5 thermocycler (bio-Rad) for both target and internal control gene.

Results and Discussion

The effects of Hg contaminated soil on the reproduction of springtails are given in Fig. 1. There was a decreasing trend with the increase of soil Hg concentration. The EC_{50} value of soil Hg stress based on reproduction was 9.86 $mg \cdot kg^{-1}$. A significant decrease of reproduction was found at the concentration of 10 $mg \cdot kg^{-1}$ compared with the control soil, and no juvenile was found at the concentration of 20 $mg \cdot kg^{-1}$. These data suggested that the reproduction of *Folsomia candida* was sensitive to soil Hg stress. Mercury exposure had significant effects on the relative expression of hsp70 gene compared with the control (Fig. 1). Significantly higher expression level of hsp70 gene was found when the concentration of soil Hg was ≥ 0.25 $mg \cdot kg^{-1}$, which indicated that the hsp70 gene could be induced at the very low soil Hg concentration. This could be explained by that Hg stress transiently increased the expression of hsp70 gene as a protection against harmful injury. There was a increasing trend of expression with the rise of soil Hg concentration and the highest expression level of hsp70 gene was observed at 8 $mg \cdot kg^{-1}$ soil Hg. No significantly different expression level of hsp70 gene was observed from 0 to 24 h exposure of soil Hg (Fig. 2).

Afterwards the hsp70 gene expression increased significantly, being about three times as high as that of control, and this finding suggested that the gene in *Folsomia candida* coding hsp70 protein was strongly induced after 48 h (Fig. 3). Then there was some fluctuation in the expression levels, which were still higher than that in the control. Totally, the relative expression levels of the 2 d, 4 d and 10 d exposure times were significantly higher than the gene expression level of any other treatments. Those variations at the individual level following Hg exposure depended, at least in part, on those genes responsible for the adaptive mechanisms being regulated or differentially expressed. Therefore, specific relationships of dose-response and time-response to the pollutant(s) of interest should be established to better understanding these phenomena.

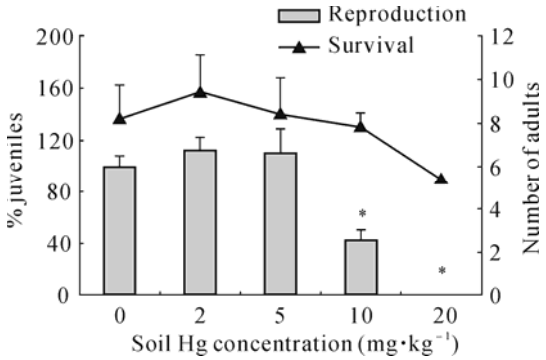

Fig. 1 Population development (bar; left Y-axis) and adult survival (curve; right Y-axis) of the springtail *Folsomia candida* exposed for 28 days to the Hg-contaminated soils (P<0.05)

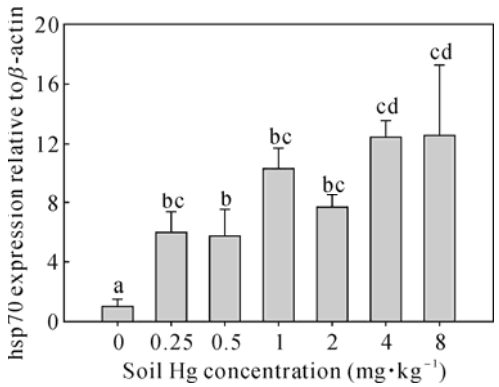

Fig. 2 Expression of hsp70 gene in *Folsomia candida* exposed to a control and a series of concentration of soil Hg. Bars are the mean of 4 expression relative ± SE. Columns within each concentration not sharing the same letter are significantly different (P<0.05)

In summary, these results further confirmed the sensitivity of the springtail *Folsomia candida* to Hg contaminated soils as far as reproduction was concerned. The relative quantification of hsp70 gene expression indicated that the expression of hsp70 gene was more sensitive to Hg contaminated soils compared with the responses at individual level. The hsp70 gene was strongly induced after 48 h when the *Folsomia candida* was exposed to 1 $mg \cdot kg^{-1}$ of soil Hg. These results indicated that the response of hsp70

gene expression of *Folsomia candida* to soil Hg contamination was most sensitive among the three bioassays, which suggested that hsp70 gene expression could be used as a promising tool for early environmental diagnostics and risk assessment. However, because of limited study of functional gene of *Folsomia candida* exposed to contaminated soils, further work is necessary to investigate the effects of different pollutants on gene expression of springtail *Folsomia candida*.

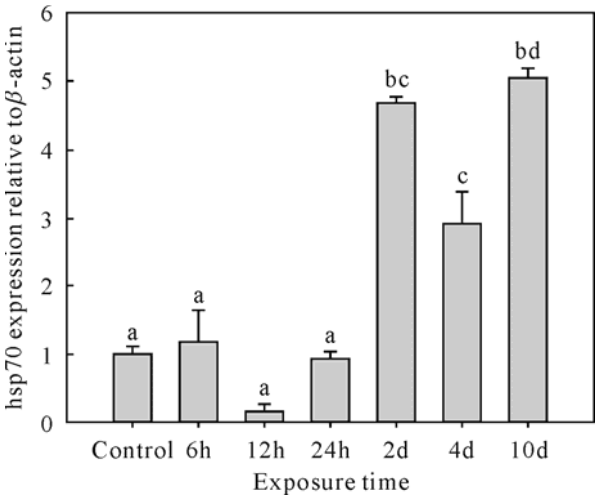

Fig. 3 Expression of hsp70 gene in *Folsomia candida* at series of time following 1 mg·kg^{-1} of soil Hg exposure. Bars are the mean of 4 expression relative ± SE. Columns within each time not sharing the same letter are significantly different (P<0.05)

References

Adams SM (2001) Biomarker/bioindicator response profiles of organisms can help differentiate between sources of anthropogenic stressors in aquatic ecosystems. Biomarkers 6: 33-44

Brulle F, Mitta G, Cocquerelle C, Vieau D, Lemiere S, Lepretre A, vandenBulcke F (2006) Cloning and real-time PCR testing of 14 potential biomarkers in Eisenia fetida following cadmium exposure. Environ. Sci. Technol. 40: 2844-2850

Golding GR, Kelly CA, SparlingR, Loewen PC, Barkay T (2007) Evaluation of mercury toxicity as a predictor of mercury Bioavailability. Environ. Sci. Technol. 41: 5685-5692

Nota B, Timmermans MJTN, Franken O, Montagne-Wajer K, Marien J, de Boer ME, de Boer TE, Ylstra B, Van Straalen NM, Roelofs D (2008) Gene Expression Analysis of Collembola in Cadmium Containing Soil. Environ. Sci. Technol. 42: 8152-8157

Nriagu JO, Pacyna JM (1988) Quantitative assessment of worldwide contamination of air, water, and soils by trace-metals. Nature 333: 134-139

Tsui MTK, Wang WX (2006) Acute toxicity of mercury to Daphnia magna under different conditions. Environ. Sci. Technol. 40: 4025-4030

Antimony, Arsenic and Other Toxic Elements in the Topsoil of an Antimony Mine Area

Xiangqin Wang[a], Mengchang He[a,*], Jianhong Xi[a], Xiaofei Lu[a], Jun Xie[b]

[a] State Key Laboratory of Water Environment Simulation, School of Environment, Beijing Normal University, No. 19, Xinjiekouwai Street, Beijing 100875, China;
[b] Environmental Mornitoring Station of Lenshuijiang City, Lenshuijiang 417500, Hunan, China.
[*]Corresponding author. Tel. No. +8610-58807172; Fax No. +8610-58807172; E-mail: hemc@bnu.edu.cn.

Abstract: Twenty nine topsoil samples were collected from the Xikuangshan antimony mine and analyzed by ICP-MS, ICP-OES and HG-AFS for the following elements: As, Cd, Cr, Cu, Co, Ni, Hg, Pb, Sb and Zn. The objective of this study was to assess the level of topsoil contamination of Xikuangshan's agricultural land. The concentration ranges ($mg \cdot kg^{-1}$) of the elements are: As 13~267, Cd 0.7~96.8, Cr 81~315, Cu 23~261, Ni 29~86, Pb 27~423, Sb 10~2159 and Zn 68~4217. Average concentrations of As, Cd, Sb and Zn exceeded the limits of agricultural production and human health. The accumulation of Cr, Cu, Ni and Pb in the topsoil of Xikuangshan area were minor than the other four heavy metals; these elements did not exceeded the threshold. Except for the background effect of the soils, anthropogenic factors are the major contributor to the the increased concentrations of heavy metals in soil. Combined with the principal component analysis, it was found that smelters and mining activities were the main sources of soil heavy metals while the lithology background of this area and agricultural practices play important roles in the accumulation of heavy metals.

Keywords: Distribution; Heavy metals; Topsoil; Xikuangshan antimony mine

Introduction

Heavy metals reaching the soil remain present in the pedosphere for many years even after removing the pollution sources (Chen *et al.*, 1997; Imperto *et al.*, 2003). Variations caused by differences in soil texture, geological origin and anthropogenic sources of heavy metals result in spatial variability (Bak *et al.*, 1997). Synergistic effects among metallic pollutants may deteriorate the situation. Therefore, to define hazards and to propose treatments, and eventually new and more appropriate utilization of soils in mining areas, the studies on speciation, geochemistry and behaviour of heavy metals in mine soils are required. The Xikuangshan antimony mine, located at the west of Hunan province, China, is one of the largest antimony mines in the world. Antimony (Sb) and other heavy metals pollution from this mining and smelting area is very severe in general, and has caused significant environmental problems in China (He, 2007). The main objective of this study was to identify the main sources of heavy metals in Xikuangshan agricultural topsoil at the antimony mining and smelting area by conducting multivariate statistical analysis. The results will contribute to the assessment of soil quality of mining and smelting areas and the management of regional environment.

Materials and Methods

Twenty nine environmental samples (all of them are tilled soils) were collected from Xikuangshan antimony mining and smelting areas. The soils were collected in the year 2008 with the help of GPS by holes dug which has a motor-driven excavator on

different farmlands with depths ranging from 10~20 cm. At each site, 3~4 cores were taken randomly, then mixed thoroughly and stored in clean polypropylene bags. On returning to laboratory, the soils were air-dried and sieved to <2 mm and ground using an agate mortar (grain size <50 μm) to obtain consistent physical properties and reproducibility of chemical analyses between the individual samples. The sample pH was measured in a MilliQ+ deionised water suspension (1:2.5 v/v) after 1-h agitation using a Schott Handylab 1 pH meter. The total organic carbon (TOC) content was determined using an elemental analysis (Vario EL, Elementar, Germany) after soils were treated with 1 mol·L^{-1} HCl to remove carbonates. The cation exchange capacity (CEC) was determined as the sum of the basic cations. The concentrations of Co, Cu, Ni, Pb and Zn were determined by ICP-MS. Concentrations of As, Sb and Hg were determined with HG-AFS. Concentrations of Cr, P, Al and Fe were determined by ICP-OES. The principal component analysis (PCA) and partial correlation analysis were used for the data processing.

Results and Discussion

Table 1 shows the concentrations of 8 heavy metals in the topsoil of Xikuangshan. Geometric means were calculated and used to describe the central trend according to the log-normal distribution type of 6 heavy metals except As and Sb (Chen *et al.*, 1999). Compared with their respective natural background values, all of them exhibited much higher concentrations than the natural background, especially Sb. The Sb concentrations in some samples were a thousand times higher than the background values. Average concentrations of As, Cd, Sb and Zn exceeded the soil criteria of these heavy metals for agricultural production and human health. Much attention should be paid on the accumulation of these four heavy metals. The accumulation of Cr, Cu, Ni and Pb in the topsoil was minor; these elements did not exceed the soil criteria of these heavy metals for agricultural production and human health. Although there existed some areas with high concentrations caused by human activities, the concentration of these four elements was still under control.

Table 1 Concentrations of heavy metals in Xikuangshan agricultural topsoil

	Concentrations (n=29) (mg·kg^{-1})				Environmental standard	
	mean	min	max	Geometric means	class1	class2
As	69	13	267	47	15	25
Cd	8.6	0.68	96.8	3495	0.2	1.0
Cr	169	81	315	155	90	250
Cu	54	23	261	45	35	100
Ni	45	29	85	43	40	60
Pb	106	27	423	74	35	350
Sb	659	10	2158	373	0.2	370
Zn	453	68	4217	250	100	300
pH	7.43	5.59	8.22	7.38	None	None
CEC (cmol·kg^{-1})	17.2	9.15	30.65	16.31	None	None
TOC (%)	4.65	1.97	11.73	3.98	None	None

SEPA 1995. Class1 is the natural background level; class 2 is for the need of agricultural production and human health

According to the results of PCA (Table 2), the original variables could be reduced to 5 factors (F1~F5), which accounted for 83% of the total variances. Zn, Pb, Cu and Cd had the main loadings in F1, As, Cr, Hg were mainly distributed in F2, Co and Ni were mainly distributed in F3, Sb was in F4.

However, not all heavy metals could be distributed in one factor, for example, As and Cr partially in F4, Cu partially in F3 and F4, Pb partially in F4 and F5. These suggested that As, Cr, Cu and Pb might be controlled by more than one factor. The high positive loading of Mn in F5 indicates the presence of manganese oxides-hydroxides in the study area.

Table 2 Total variance explained

Component	Rotation Sums of Squared Loadings		
	Total	% of Variance	Cumulative (%)
1	3.1	22.4	22.4
2	2.5	18.2	40.6
3	2.5	17.9	58.5
4	2.0	14.1	72.6
5	1.4	10.1	82.7

Zinc Cd, Cu and Pb are sulfophilic element. They belong to the same main group (Table 3). Therefore, grouping of these elements in F1 reflects the sulfide mineralization paragenesis in Xikuangshan area. F2 is a factor with high positive loading for P and Hg, and median positive loading for As and Cr. According to Kabata Pendias *et al.* (1992), P is associated with phosphate fertilizers, so grouping these variables in F2 could be related to agricultural practices. F3 shows high positive scores of Co and Ni, and the significant correlations, indicating that Co and Ni have the similar sources. The main source of of these two elements should be pedogenic materials. As and Sb are known to form complexes in the environment, and have similar geochemical behaviours in the environment (Wilson *et al.*, 2004), so grouping of the two elements in F4 indicates their similar geochemical behavior in the environment and also reflects the lithology of the area. And there is a natural Sb contamination of topsoil due to the mining and smelting activities of this area. F5 shows positive loadings of Mn and partial contribution of Pb. The variability of the elements in this factor can easily be attributed to the known manganese oxides-hydroxides.

Relationships between heavy metal concentrations and Al_2O_3 and Fe_2O_3 were analyzed. Ni and Fe_2O_3 were not significantly correlated with As and Sb. The same phenomena were observed between Ni and Cd, Cu and Sb, Co and Sb, Ni and Pb, Zn and Sb, Sb and Fe_2O_3. No significant correlations were found between Cr and the other metals or compounds. But Cr had a significant correlation with TOC with the coefficient of 0.517, much higher than the correlation coefficients between TOC and the other heavy metals. Except for the correlations listed above, negative correlations existed between Co and Cr, Ni and Sb, Cr and Fe_2O_3, Sb and Fe_2O_3, Sb and Al_2O_3.

Table 3 Component matrixes for soil heavy metals in Xikuangshan mine area

Components	Rotated Component Matrix				
	1	2	3	4	5
Zn	0.965	0.112	0.088	0.069	0.018
Cd	0.950	0.155	-0.011	-0.026	0.012
Pb	0.672	-0.075	0.089	0.345	0.383
Cu	0.568	0.020	0.418	0.525	0.261
Hg	-0.038	0.838	0.049	0.184	0.120
Al_2O_3	0.244	0.776	0.280	-0.151	0.159
P	0.516	0.697	0.046	-0.004	-0.096
Cr	-0.093	0.540	-0.094	0.438	-0.413
Co	0.189	-0.013	0.915	0.266	0.061
Ni	-0.186	0.171	0.884	-0.117	-0.129
Fe_2O_3	0.255	0.155	0.757	-0.198	0.353
As	0.210	0.589	0.157	0.615	0.288
Sb	0.083	-0.041	-0.085	0.906	-0.039
Mn	0.069	0.128	0.055	0.048	0.866

Rotation Method: Varimax with Kaiser Normalization

Acknowledgments

This work was supported by National Natural Science Foundation of China (40873077, 20777009)

References

Bak J, Jensen J, Larsen MM, Pritzl G, Scott-Fordsmand J (1997) A heavy metal monitoring-programme in Denmark. Sci. Total Environ. 207: 179-186

Chen M, Ma LQ, Harris WG (1999) Baseline concentrations of 15 trace elements in Florida surface soils. J. Environ. Qual. 28: 1173-1181

Chen TB, Wong JWC, Zhou HY, Wong MH (1997) Assessment of trace metal distribution and contamination in surface soils of Hong Kong. Environ. Pollut. 96: 61-68

He MC (2007) Distribution and phytoavailability of antimony at an antimony mining and smelting area, Hunan, China. Environ. Geochem. Health 29: 209-219

Imperato M, Adamo P, Naimo D, Arienzo M, Stanzione D, Violante P (2003) Spatial distribution of heavy metals in urban soils of Naples city (Italy). Environ. Pollut. 124: 247-256

Kabata-Pendias A, Pendias H (1992) Trace elements in soils and Plants. CRC Press, Boca Raton, FL

Wilson NJ, Craw D, Hunter K (2004) Antimony distribution and environmental mobility at an historic antimony smelter site, New Zealand. Environ. Pollut. 129: 257-266

Microcalorimetric and Potentiometric Titration Studies on the Adsorption of Copper by *P. putida* and *B. thuringiensis* and Their Composites with Minerals

Linchuan Fang, Peng Cai, Pengxiang Li, Wei Liang, Qiaoyun Huang*

State Key Laboratory of Agricultural Microbiology, Huazhong Agricultural University, Wuhan 430070, China.
*Corresponding author. Tel. No. +86 27 87671033; Fax No. +86 27 87280670; E-mail: qyhuang@mail.hzau.edu.cn.

Abstract: In order to have a better understanding on the interactions of heavy metals with bacteria and minerals in soil and associated environments, isothermal titration calorimetry (ITC), potentiometric titration and equilibrium sorption experiments were conducted to investigate the adsorption behavior of Cu^{2+} by *Bacillus thuringiensis*, *Escherichia coli* and their composites with minerals. The adsorption capacity of Cu(II) by bacteria-montmorillonite composite was higher than that by their individual components, whereas bacteria-goethite composite adsorbed less Cu(II) than their individual components. Potentiometric titration revealed that some new adsorption sites were created in bacteria-montmorillonite systems and some adsorption sites were masked in bacteria-goethite systems. The thermodynamic parameters were obtained from the ITC experiments. The negative ΔG values indicated that the adsorptions of Cu(II) by bacteria, minerals and their composites were spontaneous processes. The ΔH values revealed that the reactive sites on bacterial surfaces were more important than those on minerals in binding heavy metals. The positive ΔS values suggested the dominant inner-sphere complexes of Cu(II) on the surface of bacteria, minerals and their composites.

Keywords: Adsorption; Bacteria-mineral composite; Copper; Isothermal titration calorimetry; Potentiometric titration

Introduction

The fate of toxic metallic cations in the soil environment depends largely on their interactions with inorganic and organic surfaces, principally minerals and microorganisms, respectively. Most of the previous studies regarding metallic ion adsorption focused mainly on clays or organic matter such as microorganisms as individual components rather than their mixtures. The present study was conducted to investigate the adsorption behavior of Cu^{2+} by two bacteria and their composites with minerals.

Materials and Methods

Two bacteria, i.e., *Bacillus thuringiensis* (Gram-positive) and *Pseudomonas putida CZ1* (Gram-negative), three minerals, i.e., goethite, montmorillonite and kaolinite were used. Adsorption was conducted in batch experiments with the nonliving cells, minerals or their composites (1:1 ratio of bacteria to mineral) in a 10 mL plastic tube containing 0.01 mol·L^{-1} KNO_3 to maintain constant ionic strength. Potentiometric titration was performed according to the procedures described by Yee *et al.* (2004). The cells were kept at 30.0±0.1 °C using a water bath. Equipment and data acquisition were under PC control. The weighted nonliving cells, minerals or their composites (1:1 ratio of bacteria to mineral) and 4 mL of 1 mol·L^{-1} KNO_3 solution, DD water (CO_2-free) were put into the titration cell. After introduction of electrodes, burette tips, and the N_2 source, the cell was closed. The titration experiments were conducted in a N_2 atmosphere and ion strength was 0.1 mol·L^{-1}. The suspension was titrated using 0.4865 mol·L^{-1}

NaOH and 0.5270 mol·L^{-1} HCl solutions. The pH was adjusted to approximately 2.5 in the beginning of the experiment by the addition of HCl. The cell suspension was equilibrated for 40 min and titrated to pH 10 with NaOH. At each titration step a stability of 0.1 mV·s^{-1} was attained before the next aliquot of titrant was added. The adsorption heat of Cu(II) on the surface of cells, minerals and their composites was recorded by an isothermal microcalorimeter TAM III. A total volume of 180 μL Cu(II) (10 mmol·L^{-1}) suspensions was titrated into the ampoule for nine injections at a rate of 1 μL·s^{-1}. Control experiments for the measurements of background heats were performed by titrating Cu(II) suspension into deionized distilled water in the absence of bacterial cells, minerals or their composites.

Results and Discussions

Table 1 shows the determined and the predicted values for the metal-binding capacities of the bacteria-mineral composites at a mineral/bacteria ratio of 1:1. The *B. thuringiensis*– and *P. putida*–montmorillonite mixture bound 30.6% and 16.4% larger amount of Cu(II) than those predicted by their individual components. However, goethite– and kaolinite–*B. thuringiensis* composites decreased by 18.0%~19.6%, and goethite–and kaolinite–*P. putida* mixtures decreased by 6.5%~10% in their adsorption for Cu(II) than their individual constituents.

Table 1 Comparison for the binding capacities of Cu(II) by bacteria–minerals mixtures with predicted values at the bacteria/inerals ratio of 1:1

Bacteria, minerals and their composites	Amount of Cu(II) bound (mg·g^{-1})		
	Calculated[a]	observed[b]	difference
B. thuringiensis	-	28.15	-
Montmorillonite + *B. thuringiensis*	21.22	27.72	6.50
Goethite + *B. thuringiensis*	18.79	15.10	-3.69
Kaolinite + *B. thuringiensis*	15.97	13.10	-2.87
P. putida	-	13.16	-
Montmorillonite + *P. putida*	17.50	20.38	2.88
Goethite + *P. putida*	15.07	14.09	-0.98
Kaolinite + *P. putida*	12.24	11.02	-1.22

The potentiometric titration of nonliving cells, minerals and their composites with 0.01 mol·L^{-1} KNO_3 at 30 ℃ indicated that all samples provided substantial buffering capacity over a wide pH range (Fig. 1). As for pure mineral systems, the order of buffering capacity was goethite > montmorillonite > kaolinite and the sequence for bacteria was *B. thuringiensis* > *P. putida*. The concentrations of the binding sites for bacteria-mineral composites were quite different from the pure bacterial or mineral surfaces. The concentration of reactive sites increased for bacteria-montmorillonite systems and decreased for bacteria-goethite systems. The results implied that the interactions between minerals and bacteria may mask or extend the adsorption sites on the surfaces of the composites.

A typical power-time curve derived from the ITC experiments was shown in Fig. 2. The adsorption heat of Cu(II) on the surface of bacteria, minerals and bacteria-mineral composites was corrected by subtracting the dilution heat of Cu(II) from the total heat. Nine peaks were observed in the curve and each one stood for the heat evolved from each titration of Cu(II) into the bacteria, minerals or their composites suspensions. The positive heat power values indicated that adsorption of Cu(II) was an exothermic process and the negative heat power values indicated that the process was an endothermic process. Nine positive signals were observed in the power–time curves from injection one to nine for the sorption of Cu(II) on minerals. For bacterial systems, the negative signals were detected from injection one to four or five and

the positive signals were recorded afterwards. Similar signal changes were found for the adsorption of Cu(II) on mineral–bacteria mixtures. However, the net heat of each injection in mineral–bacteria mixtures was much lower than that in the pure bacterial systems, indicating that the presence of minerals weakened the net heat of bacterial systems.

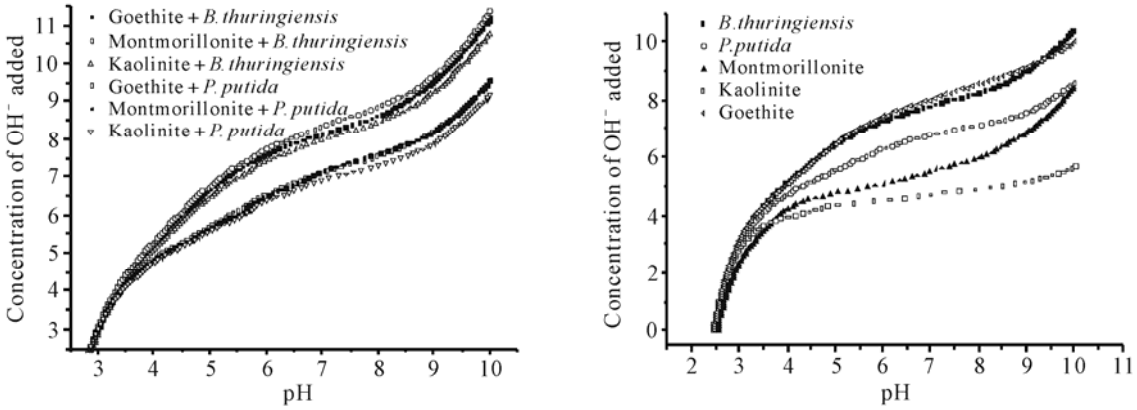

Fig. 1 Potentiometric titration curves for bacteria, minerals and their composites

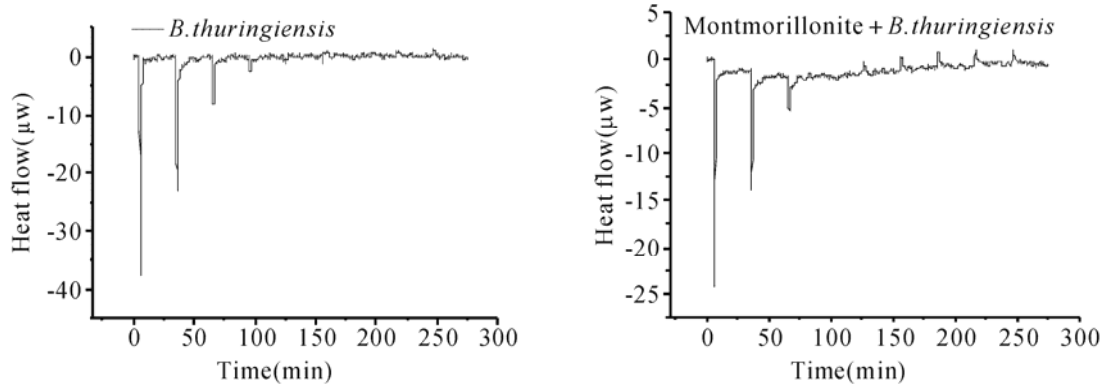

Fig. 2 The power–time curves for the titration of Cu(II) into *B. thuringiensis* and Montmorillonite+*B. thuringiensis* suspensions in the presence of 0.01 mol·L^{-1} KNO_3 at pH 5.0 and 30 °C

The negative ΔG values indicated that Cu(II) adsorption by bacteria, minerals and their composites were spontaneous processes. The ΔH values of Cu(II) adsorption on all adsorbents were from −1.71 to 7.32 kJ·mol^{-1}, among which they were obviously higher for bacteria than for minerals. The enthalpy changes for Cu(II) adsorption by bacteria were similar to the data expected for Cu(II) complexation by anionic oxygen ligands. Furthermore, the ΔH values of Cu(II) adsorption on bacteria were decreased considerably in the absence of the minerals. The entropy changes (ΔS) for Cu(II) adsorption on all adsorbents were positive, suggesting that the inner-sphere complexes were dominant for Cu(II) on the surface of bacteria, minerals and bacteria-mineral composites (Gorman-lewis *et al.*, 2006).

References

Chen XC, Hu SP, Shen CF, Dou CM, Shi JY, Chen YX (2009) Interaction of Pseudomonas putida CZ1 with clays and ability of the composite to immobilize copper and zinc from solution. Bioresource Technol. 100 (1): 330-337

Gorman-Lewis D, Fein JB, Jensen MP (2006) Enthalpies and entropies of proton and cadmium adsorption onto Bacillus subtilis bacterial cells from calorimetric measurements Geochim. Cosmochim. Ac. 70: 4862-4873

Templeton AS, Trainor TP, Spormann AM, Traina SJ, Brown Jr GE (2001) Pb(II) distributions at

biofilm–metal oxide interfaces. Proc. Natl. Acad. Sci. USA 98: 11897-11902

Walker SG, Flemming CA, Ferris FG, Beveridge TJ, Bailey GW (1989) Physicochemical interaction of Escherichia coli cell envelopes and Bacillus subtilis cell walls with two clays and ability of the composite to immobilize heavy metals from solution. Appl. Environ. Microbiol. 55: 2976-2984

Yee N, Benning LG, Phoenix VR, Ferris FG (2004) Characterization of metal–cyanobacteria sorption reactions: a combined macroscopic and infrared spectroscopic investigation. Environ. Sci. Technol. 38: 775-782

Sorption, Transformation and Migration of Zn in Some Soils with Percolated Water Regime

Galina Vasilievna Motuzova*, Natalia Jurievna Barsova

Department of Soil Chemistry, Faculty of Soil Science, Moscow State University after M.V. Lomonosov, Leninskie Gory, Moscow, 119991, Russia.
* Corresponding author. Fax No. (495) 939-29-47; E-mail: motuzova@mail.ru.

Abstract: There were determined the parameters of applied Zn sorption by two taiga soils with different properties, composition of their formed species and the migration of their available ones. The laboratory and field experiments were used in this work. Laboratory experiments have identified the great potential absorption capacity of soils (especially of the upper organic horizons) towards applied zinc and ability to retain it relatively firmly. But this ability is not fully realized in artificial pollution under field conditions. This proves that the upper soil horizons are indeed a "critical area" of the crust even in the soils with percolated water regime.

Keywords: Heavy metals; Migration; Pollution; Protective ability of soil; Soil; Sorption

Introduction

One of the main ecological function of soil is to serve as the main communication between chemicals that input on the soil surface from the outside (pollutants from anthropogenic sources) and their redistribution to other natural media (plants, ground water). Three groups of processes provide this function of soil: 1) the uptake of various contaminants (heavy metals are more important, 2) their incorporation into the soil compounds, 3) the migration of mobile species of heavy metals from soils to the neighboring media (Goldberg, 1998; Parker, van Genuchten, 1984). Increasing of the chemicals emissions demonstrates the relevance of the development of a methodological basis for an adequate assessment of the consequences the environmental pollution with heavy metals.

Materials and Methods

The objects of investigation are two soils: 1) podzolic light loam soil (forest biogeocenoze) with the litter A0 (h=3~5 cm, pH(H_2O)=5.4), horizons AE, E (h=10~15 cm, pH(H_2O)=4.3~4.8, Corg= 1.0% ~6.2%), and deeper horizons EB, EBD,BD; 2) soddy loamy sand soil (meadow biogeocenoze) occurring on the second terrace of the Volga river; it has the litter (h=0.5 cm), soddy horizon (h=5 cm, pH 6.7~6.9, Corg 3.1%), horizon A (h= 23 cm), sandy alluvium (C). The experiments of Zn sorption – desorption were determined in the static laboratory conditions with water solution of Zn $(NO_3)_2$ (C_{Zn} 0~250 (500) mg·L^{-1}); for podzolic soil in the presence and absence of 0.01 mol·L^{-1} $CaCl_2$, under different pH levels (2.5~5.3) The parameters of Zn sorption (Q max and K) were calculated on the base of Zn isotherms according to Langmuir equation. The strength of Zn fixation was determined by the desorption of adsorbed Zn ions using different reagents (0. 01 mol·L^{-1} $CaCl_2$, 1 mol·L^{-1} NH_4 $(CH_3COO)_2$ for extraction of exchangeable species). In the field experiment some plots of the investigated soils (700~2500 cm^2) were poured with solutions of Zn nitrates with the various concentrations of 0~62 mg·L^{-1} Some plots were not contaminated and considered as reference (background) ones. The

annual volume of precipitation of 500 $mL \cdot cm^{-2}$ was added during 2 weeks (1~2 times a day). The treatments have been repeated during three years on the soddy soil and two years on the podzolic soil. The percolated water was collected in the lyzimeters, installed under plots that were put on two depths, 27 and 55 cm. After the completion of the experiments the soil samples were taken by individual horizons from all the reference and experimental plots. Soil samples were ground and passed through 1 mm sieve. The content of Zn species in soil samples was determined by using some extragents (H_2O, 0.01 $mol \cdot L^{-1}$. $CaCl_2$, AAB pH 4.8, 1 $mol \cdot L^{-1}$ HNO_3, 1 $mol \cdot L^{-1}$ $MgCl_2$, 1% EDTA, H_2O_2, hydroxylamine in CH_3COOH). Extraction by the solution of 1 $mol \cdot L^{-1}$ HNO_3 was used to divide firmly and non firmly tied Zn species. Zn content in the lyzimetric water, in soils and extracts was determined by AAS and ICP methods.

Results and Discussions

Soddy Soil

High levels of pH (6.7~6.9), high buffer ability of the soddy soil are favorable for the active Zn sorption (from the solution of Zn salts with pH near 7.0) in the laboratory experiment in static conditions. Soddy horizon A was the most active (Table 1). It takes place because of Zn specific sorption by organic material and formation of hardly soluble organic and mineral Zn salts.

Table 1 Maximum levels of Zn sorption by different horizons of soddy soil ($mg \cdot kg^{-1}$)

Soil	A0	A soddy+A	C
Soddy	>13080	1900	1600

The ability of the lying below soil horizons to sorb Zn is almost an order of magnitude less than of the upper horizon, but their strength of Zn fixation is not equal. The field experiment has shown that in spite of intensive pouring of the plots lyzimetric water reached only depth 27 cm, and they did not penetrate to 55 cm. Zn concentration in the lyzimetric water has not exceeded 17% from the initials its concentration during the first year of the experiment and it was account of near 1% on the next years. The initial Zn concentration in the lyzimentric water was not reached during two weeks of experiment.

The total Zn content increased to 20~80 times in the upper 5 cm of soddy soil, that has been polluted in the field conditions during their pouring by Zn containing solutions. The added Zn has augmented the supply of those Zn species, that were not firmly bound with solid soil substances (they can be soluble in 1 $mol \cdot L^{-1}$ HNO_3) and half of them were presented by exchangeable species.

Podzolic Soil

The ability of A0 horizon of the acid podzolic soil to sorb Zn in static laboratory experiment from the solution of Zn salts (pH 4.5) is rather high (Table 2), it exceeds the ability of humus-accumulative horizon almost two times. It depends sufficiently on the presence of plant residues and living organisms in litter horizon.

Table 2 Maximum levels of Zn sorption by different horizons of the podzolic soil ($mg \cdot kg^{-1}$)

Soil	A0	AE	E
Podzolic	3000	1690	250

Acidification of the solution interacting with soil decreases Zn sorption in podzolic soil in different degree, depending on chemical properties of the horizon, and initial metal concentration. This decrease is greatest for E horizon, which has lower acid-base buffer capacity than other horizons.

The acid-base buffer ability of the litter is high, that is way the changing the pH of the original salt solution (with low Zn concentration) from 5.3 to 3.0 did not lead to reduction in Zn sorption: the declining was marked only at pH 2.5. Nevertheless the adding in the soil of Zn salt solution with high Zn concentration (~150 $mg \cdot L^{-1}$) provides some declining of pH level in the equilibrium solution. The ability of AE horizon to retain Zn ions is less, than in litter horizon, but most part of metal is in the available form. Eluvial horizon, as usually, sorbed less Zn, but retains it more strongly.

Field experiment has shown that water has appeared in the lyzimeters after some days of plots pouring. But Zn concentration in the lyzimetric water was high and has closed to the original level to 15-th day of pouring. The more was the quantity of Zn - the less part of it was sorbed.

Comparison of sorbed metal quantity under

different conditions, was possible only for the litter horizons because the load of metal was known only for these horizons. The load is unknown for the different horizons.

Table 3 Quantity of Zn sorbed by litter (mg·kg^{-1})

Initial* concentration Zn, mg·L^{-1}	Laboratory (batch equilibrium) Experiment			Field Experiment	
	∑c**	Q	Qmax	∑c**	Q
		Podzolic soil			
12	1505	1310	5755	12100	980
42	4055	3205		44470	1864
		Soddy soil			
25	5232	4760	>13080	152000	5680
62	n.d..			328000	12500

*for batch experiment - equilibrium concentration; **∑c –total Zn load

One can see from the Table 3 that potential capacity of the litter horizons is high, especially for soddy soil. But only half of it is observed in litter horizons podzolic soil under field conditions, although the load there is greater than in laboratory by an order of magnitude.

Table 4 Distribution of Zn in the soils, polluted in the field experiment

Zn concentration in lyzimetric water (% from the initial concentration)	Zn removal with lyzimetric water from litter horizon (% Zn added)	Zn accumulation in the polluted soils of the experimental plot (% of load)
	Soddy soil	
0.1~17	0.01~0.15	50~65
	Podzolic soil	
65~95	1.5~3.0	30~37

The calculation of Zn balance in these soils artificially contaminated by Zn-containing solution shows that the dozen of Zn percolating to the lyzimeters at 30 cm depth did not exceed 3% of the load. The remaining 97% was distributed in soil volume of experimental plots as follows: 30%~37% in podzolic and 50%~65 % in soddy soil, the rest part of Zn migrates horizontally and was taken by plants (Table 4).

Conclusions

The processes of sorption, transformation of chemicals (heavy metals) in the upper layers of soil and the migration of their mobile components are the most important for the ecosystem. This is clear evidence that the part of the Earth's surface, where these processes take place, presents the "critical zone", which is understood as the "decisive, turning point, particularly important" zone of the Earth's crust. The methods for determining the parameters of the processes occurring in the "critical zone" are very important. The laboratory techniques allow determining the potential absorption capacity of metal and the strength of their retention, to identify the influence on the adsorption of the inherent soil properties and various related factors. But the potential sorption capacity of soils in the environment is not fully realized. The field experiments that simulate soil pollution, or full-scale monitoring of contaminated soils, however, indicate a real protective ability of soil and the state of ecosystem. But in this case the identification of the functional dependence of buffer capacity of soils from different factors is difficult. The best option to receive the adequate information about the situation in the "critical zone" is the use the combination of laboratory and field methods for the characteristic processes of absorption, transformation and migration of heavy metals. The experiment with two soils with different properties has showed that low litter of soils serves as a powerful barrier to heavy metals in the area with percolated water regime. The upper part of soil is able to absorb and retain heavy metals, limiting their migration, and protecting groundwater from contamination.

References

Goldberg S (1998) Ion adsorption at the Soil Particle-Solution Interface: Modeling and Mechanisms. In Structure and Surface Reactions of Soil Particles. Huang PM, Senesi N and Buffle J, Willey J & Sons. NY, USA. pp. 375-412

Parker JC, van Genuchten MTh (1984) Determination transport parameters from laboratory and field tracer experiments. Bulletin 84-3, Virginia Agricultural Experimental Station, Blacksburg

Speciation and Biochemical Transformations of Sulfur and Copper in Rice Rhizosphere and Bulk Soil—XANES Evidence of Sulfur and Copper Associations

Huirong Lin[a,b], Jiyan Shi[a,b,*], Bei Wu[a,b], Jianjun Yang[a,b], Yingxu Chen[a,b], Yidong Zhao[c], Tiandou Hu[c]

[a]Ministry of Agriculture Key Laboratory of Non-point Source Pollution Control, Hangzhou 310029, China;
[b]Institute of Environmental Science and Technology, Zhejiang University, Hangzhou 310029, China;
[c]Institute of High Energy Physics, Chinese Academy of Science, Beijing Synchrotron Radiation Facility, Beijing, 100049, China.
[*]Corresponding author. Tel. No. +86-571-86971424; Fax No. +86-571-86971898; E-mail: shijiyan@zju.edu.cn.

Abstract: The speciation of sulfur and copper in rice rhizosphere and bulk soil was investigated using integrated approach including sequential extraction and X-ray absorption near edge spectroscopy (XANES). Our results showed that Cu speciation exhibited a difference in rhizosphere and bulk soil of rice. In a flooded paddy soil, most Cu in the rhizosphere existed as Cu (II), whereas part of Cu transformed to Cu (I) in the bulk soil. Sulfur XANES showed the presence of multiple both oxidized and reduced states of sulfur in studied soil samples, with more oxidized sulfur in the rhizosphere than in the bulk soil. Copper and sulfur speciation changed depending on redox conditions. Changes in redox potential and microbial action shifted the sulfur oxidation and reduction reaction and affected the Cu speciation. Sulfur transformation played an important role on Cu speciation.

Keywords: XANES; Copper; Sulfur; Speciation; Rice rhizosphere; Bulk soil

Introduction

In paddy soils, it is suggested that sulfur cycling takes place. Changes of redox conditions in rice rhizosphere and bulk soil led to microbially mediated sulfur transformation, thus affecting heavy metal behavior as the sulfur function groups play an important role in heavy metal geochemical transformations (Karlsson *et al.*, 2007; Martinez *et al.*, 2002). The objective of this work was to investigate how sulfur transformation in a paddy soil affected Cu biogeochemical processes.

Materials and Methods

Soil samples were collected from a rice field in Shaoxing, Zhejiang Province, China. Some properties of the soil are as following: organic matter content, 2.26%; pH, 5.63; total P, 0.542 $g \cdot kg^{-1}$; total K, 13.0 $g \cdot kg^{-1}$; total S, 0.247 $g \cdot kg^{-1}$. A glasshouse study using the soil treated with 500 $mg \cdot kg^{-1}$ copper and 1 $g \cdot kg^{-1}$ sulfur was conducted. After 3 months of soil aging, rice seedlings were transplanted. Tap water was added to keep flooded. After 45 days, Eh measurements were carried out in situ by inserting the electrodes into the rhizosphere and bulk soil and using The Orion Epoxy Sure-Flow Combination Rdeox/ORP (9678BN) following the manufacturer's instruction. Rhizosphere and bulk soil was collected and freeze-dried before further analysis. The speciation of Cu in the soil was determined by a sequential extraction procedure which divided heavy metals into five binding forms, namely, exchangeable, carbonate-bound, Fe/Mn oxide-bound, sulfide/organic matter-bound and residual. The determination of operational S fractions involved the sequential extraction of water-soluble sulfur, absorbed sulfur and HCl-soluble sulfur. Inductively coupled plasma atomic emission spectrometry (ICP-AES, IRIS/AP) was used to determine S and Cu contents in different extractions. Sulfur and copper species in soil samples were analyzed by sequential extraction and

X-Ray absorption Spectroscopy at Beijing Synchrotron Radiation Facility, Institute of High Energy Physics of China.

Results and Discussion

Redox potential (Eh) in the rhizosphere were higher than those in the bulk soil (Table 1). We presented an in situ X-ray absorption spectroscopy (XAS) study on Cu and sulfur to provide insights into how rice responded to Cu pollution under the action of sulfur. Sulfur XANES showed the presence of multiple, both oxidized and reduced, states of sulfur in the studied soil samples, with more oxidized sulfur in the rhizosphere than the bulk soil (Fig. 2). Most sulfur transformations are fundamentally controlled by biosphere processes, especially by the specialized metabolisms of microorganisms. The presence of reduced and oxidized states of sulfur might correlate to the presence of sulfur oxidizing bacteria (SOB) oxidized reduced sulfur and sulfate reducing bacteria (SRB) contributing to sulfate reduction, respectively (Engel *et al.*, 2007).

Table 1 Eh variation in rhizosphere and bulk soil of rice

Samples	Before planting (mV)	15 days (mV)	45 days (mV)
Rhizosphere soil	-	393 ± 16	264 ± 60
Bulk soil	299 ± 72	396 ± 130	196 ± 19

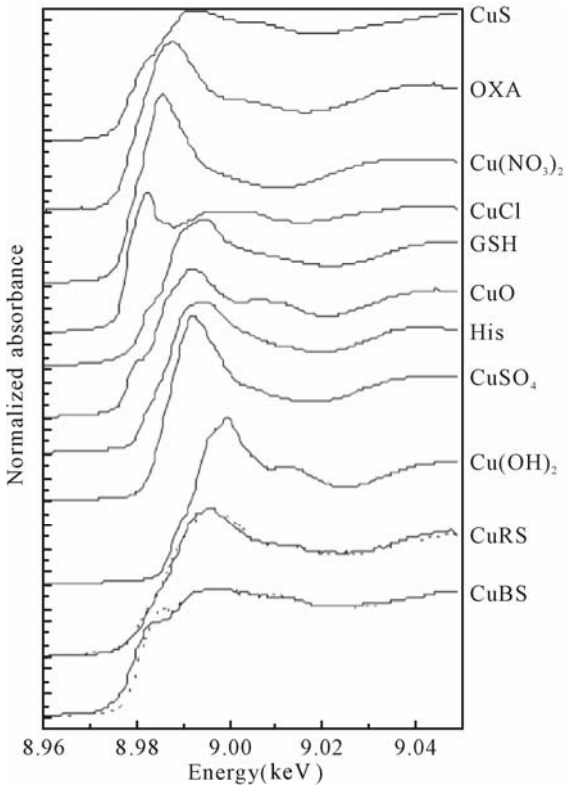

Fig. 1 Comparison of copper K-edge XANES spectra of reference compounds and rice rhizosphere soil samples

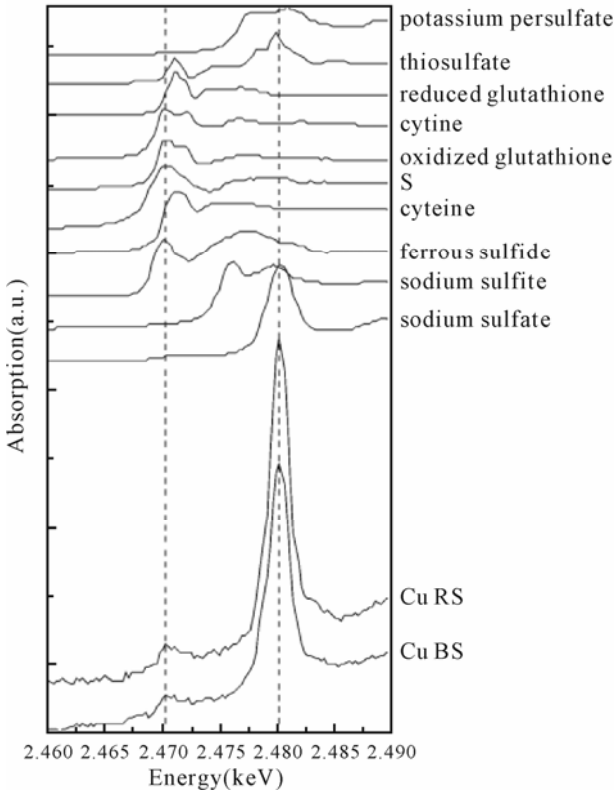

Fig. 2 Comparison of sulfur K-edge XANES spectra of reference compounds and samples

The edge for Cu(I) occurs at a lower energy than the edges for Cu(II) (Fig. 1). The spectra of Cu K-edge positions of the rhizosphere samples were around that of aqueous Cu, indicating that Cu(II) was predominant in the samples. Copper in the rhizosphere existed as Cu(II) under anoxic conditions, whereas about 44% of Cu transformed to Cu(I) in anaerobic bulk soil (Table 2). Copper and sulfur speciation changed depending on redox conditions. Changes of redox and microbial action shifted the sulfur oxidation-reduction reactions and affected the Cu speciation. Sulfur functional groups played an important role on

Cu transformations. The combined action of SOB and SRB led to the oxidation and reduction of metal sulfide which played a crucial role in transformation and mobility of heavy metals in soil (Templeton *et al.*, 2009).

Table 2 The results of fitting the XANES spectra with a linear combination of the measured data sets of representative model compounds. Copper oxidation states were assigned according to the similarity of the absorption edge energies of reference compounds. Rss: Residual sum of squares

Samples	Cu-His	CuS	$CuSO_4$	$Cu(NO_3)_2$	CuO	Cu-OXA	CuCl	Rss
Cu-Rhizosphere soil	0.038	0.366	0.339	0.192	0.066	-	-	0.11
Cu-Bulk soil	-	0.360	-	-	0.153	0.047	0.440	0.36

References

Engel AS, Lichtenberg H, Prange A, Hormes J (2007) Speciation of sulfur from filamentous microbial mats from sulfidic cave springs using X-ray absorption near-edge spectroscopy. FEMS Microbiol. Lett. 269: 54-62

Karlsson T, Skyllberg U (2007) Complexation of zinc in organic soils-EXAFS evidence for sulfur associations. Environ. Sci. Technol. 41: 119-124

Martinez CE, McBride MB, Kandianis MT, Duxbury JM, Yoon SJ, Bleam WF (2002) Zinc-sulfur and cadmium-sulfur association in metalliferous pleats evidence from spectroscopy, distribution coefficients, and phytoavailability. Environ. Sci. Technol. 36: 3683-3689

Templeton A, Knowles E (2009) Microbial Transformations of Minerals and Metals: Recent advances in geomicrobiology derived from synchrotron-based X-ray spectroscopy and X-ray microscopy. Annu. Rev. Earth. Planet. Sci. 37: 21-25

Population Dynamics of Ammonia Oxidizing Bacteria and Archaea and Relationships with Nitrification Rate in New Zealand Grazed Grassland Soils

Hong Jie Di[a,*], Keith C. Cameron[a], Jupei Shen[b], Jizheng He[b],
Chris S. Winefield[c], Maureen O'Callaghan[d], Saman Bowatte[e]

[a] Centre for Soil and Environmental Quality, PO Box 84, Lincoln University, Lincoln 7647, Canterbury, New Zealand;
[b] Research Centre for Eco-Environmental Sciences, Chinese Academy of Sciences, 18 Shuangqing Road, Beijing 100085, China;
[c] Faculty of Agriculture and Life Sciences, PO Box 84, Lincoln University, Lincoln 7647, Canterbury, New Zealand;
[d] AgResearch Ltd, Agriculture and Science Centre, PO Box 60, Lincoln, Canterbury, New Zealand;
[e] AgResearch Ltd, Palmerston North, New Zealand.
[*] Corresponding author. E-mail: Hong.Di@lincoln.ac.nz.

Abstract: The oxidation of ammonia (NH_3) to nitrate (NO_3^-) in different ecosystems is a key process in the global nitrogen (N) cycle which has major ecological and environmental implications both in influencing nitrous oxide (N_2O) emissions and nitrate leaching. We investigated the population dynamics of ammonia oxidising bacteria (AOB) and ammonia oxidising archaea (AOA) under controlled laboratory conditions using quantitative polymerase chain reaction (qPCR or real-time PCR) in six different intensively managed dairy grassland soils sampled from across New Zealand. The AOA *amoA* gene copy numbers varied from 1.27×10^7 to 3.85×10^6. The AOA to AOB ratio varied from 10.7 to 0.2. While the AOB population grew by 3.2 to 10.4 fold in response to the addition of a urine-N substrate and were significantly inhibited by a nitrification inhibitor, dicyandiamide (DCD), the AOA population remained largely unchanged irrespective of the urine-N and DCD treatments. A significant exponential quantitative relationship was found between the AOB population and the nitrification rate, whereas no such relationship was found with AOA. These findings suggest that nitrification rate is more closely related to the dynamics of AOB than to that of AOA in these grassland soils with high nitrogen loads.

Keywords: Ammonia oxidizing bacteria; Ammonia oxidizing archaea; Nitrification; Grazed grassland soil; Nitrification inhibitor

Introduction

Nitrification is a key biogeochemical process of the nitrogen (N) cycle which results in the oxidation of ammonia (NH_3) to nitrite (NO_2^-) and then to nitrate (NO_3^-). This process has major environmental and ecological consequences, because it releases nitrous oxide (N_2O) which is a potent greenhouse gas and NO_3^- which can be leached from soil and thus contaminate groundwater and surface waters. Until recently, the first, rate-limiting, step of nitrification, the oxidisation of NH_3 to NO_2^-, was thought to be carried out mainly by autotrophic ammonia-oxidizing bacteria (AOB). Recently, however, the AMO genes have also been found in the domain Archaea, suggesting the possible presence of ammonia oxidising archaea (AOA) (Prosser and Nicol, 2008). However, the role of AOB and AOA in ammonia oxidization is not well understood and the relationships between the populations of AOB and AOA and nitrification rate are unknown. The objectives of this research were to study AOB and AOA populations in a range of intensively grazed grassland soils from across New Zealand and to determine their relationships with nitrification rate.

Materials and Methods

We collected soil samples from six locations

representing high fertility grazed grassland soils from major dairy farming regions across New Zealand. These samples were taken from sites where long-term research had been conducted on nitrogen cycling, nitrate leaching, and nitrous oxide emissions. These soils receive high nitrogen inputs annually in the forms of fertilizers and biological N fixation by white clover plants (*Trifolium repens.).* We quantified the *amoA* gene copy numbers using real-time polymerase chain reaction with two different primer sets to target the AOA and AOB populations (Rotthauwe *et al.*, 1997; Francis *et al.*, 2005). In a three-month laboratory incubation study, the six soils were amended with a dairy cow urine-N substrate at a rate equivalent to 1000 kg N·ha^{-1} to simulate the N loading rate under a typical dairy cow urine patch in grazed grassland (Di and Cameron, 2002). Animal urine-N is predominantly urea which, upon hydrolysis in the soil, produces ammonium (NH_4^+) as a substrate for ammonia oxidizers. A nitrification inhibitor (DCD) was applied to a separate urine-amended treatment. The AOA and AOB population dynamics and nitrification rate were determined.

Results and Discussion

Both AOA and AOB *amoA* genes were detected in large numbers but they varied widely in the six different soils. The AOA population size was greater than that of the AOB in three soils, was similar to the AOB in two soils but was much greater than that of AOA in one soil. The AOA to AOB ratio in this study varied from 10.7 to 0.2. All the AOB clones recovered were closely related to the *Nitrosospira* species and no clones were closely aligned with the *Nitrosomonas* species. Most of the AOA clones are closely aligned with the soil clade but 14 AOA clones are aligned with a thermophilic cluster.

The AOB population increased by 3.2 to 10.4 folds following the application of the urine-N substrate but was significantly inhibited when the nitrification inhibitor, DCD, was applied (Fig. 1a). The AOA populations remained largely unaffected by either the addition of the urine-N substrate, or the nitrification inhibitor treatment in all the soils (Fig. 1b). In all six soils, the addition of the urine-N substrate significantly increased the nitrification rate, as indicated by the rising NO_3^--concentrations, but the nitrification rates were reduced by the nitrification inhibitor treatment (Fig. 1c).

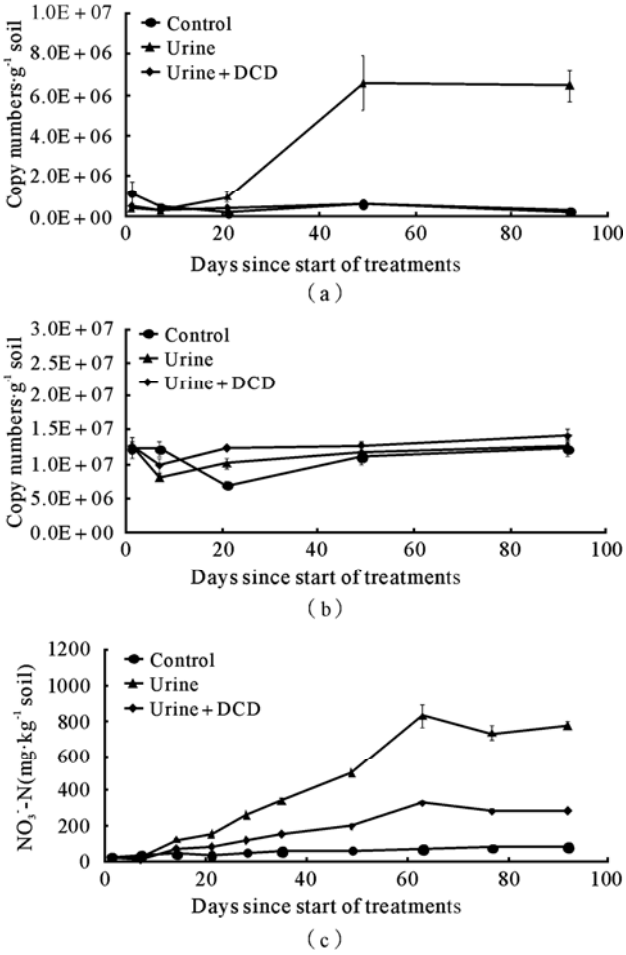

Fig. 1 (a) AOB *amoA* gene copy numbers (± SE); (b) AOA *amoA* gene copy numbers (± SE); (c) Nitrate-N concentration (± SE) in the Waikato soil, as affected by applications of cow urine-N and DCD. Similar trends were found in the other five soils

The following significant exponential relationship was found between the NO_3^--N concentration and the AOB population:

$$y = 847.9 - 739.6\ \mathrm{EXP}\ (-0.018x)$$
$$R^2 = 0.56,\ P < 0.001$$

where y is the amount of NO_3^--N produced (mg N·kg^{-1} soil) and x is the AOB *amoA* gene copy numbers (million copies g·soil^{-1}) after 49 days of incubation. However, no quantitative relationship was found between the NO_3^--N concentration and the AOA populations.

Therefore, this study shows that although both AOA and AOB were detected in large numbers in all six soils, it was only the AOB populations that grew in response to the supply of the large dose of ammonia-N substrate, were inhibited by the

nitrification inhibitor, and were quantitatively related to nitrification rates. These results clearly demonstrate the ability of the AOB populations to grow and to influence nitrification in the high-N loading soils under animal urine patches in grazed grassland. AOA may be particularly adapted to unfavourable environmental conditions, e.g. low nutrient environments, and the high ammonia concentrations in the intensively grazed grassland soils might have provided an unfavourable condition for the AOA populations and might have inhibited their growth.

Acknowledgments

We would like to thank the New Zealand Foundation for Research, Science and Technology (FRST) for funding; Drs Ross Monaghan, Stewart Ledgard and Mark Sheppard of AgResearch and Dr Bruce Thorrold and Deanne Waugh of Dairy NZ for assistance with soil sampling, Emily Gerard and Shona Brock of AgResearch and Jie Lei, Steve Moore, Carole Barlow, and Trevor Hendry of Lincoln University, for technical support.

References

Di HJ, Cameron KC (2002) The use of a nitrification inhibitor, dicyandiamide (DCD), to reduce nitrate leaching from cow urine patches in a grazed dairy pasture under irrigation. Soil Use Manage 18: 395-403

Francis CA, Roberts KJ, Beman JM, Santoro AE, Oakley BB (2005) Ubiquity and diversity of ammonia-oxidizing archaea in water columns and sediments of the ocean. Proceed Nation Acad Sci, USA 102: 14683-14688

Prosser JI, Nicol GW (2008) Relative contributions of archaea and bacteria to aerobic ammonia oxidation in the environment. Environ Microbiol. 10: 2931-2941

Rotthauwe JH, Witzel KP, Liesack W (1997) The ammonia monooxygenase structural gene amoA as a functional marker: Molecular fine-scale analysis of natural ammonia-oxidizing populations. Appl Environ. Microbiol. 63: 4704-4712

Plant Clonal Systems as a Strategy for Nitrate Pollution Removal in Cold Latitudes

Derong Lin[a,b], Lijiang Hu[a,b], Hong You[a], Dipayn Sarkar[c], Baoshan Xing[d], Kalidas Shetty[a,c,*]

[a] State Key Laboratory of Urban Water Resource and Environment, Harbin Institute of Technology, Harbin 150090, China;
[b] Chemistry Department, Harbin Institute of Technology, Harbin 150001, China;
[c] Department of Food Science, University of Massachusetts, Amherst, MA 01003, USA;
[d] Department of Plant, Soil and Insect Sciences, Science, University of Massachusetts, Amherst, MA 01003, USA.
[*] Corresponding author. Tel. No. +1-413-545-1022; Fax No. +1-413-545-1262; E-mail: kalidas@foodsci.umass.edu.

Abstract: Nitrate removal is a major challenge in drinking water systems of major cities of the world and these are more acute in colder latitudes where metabolic conversion rates of biological species in the winter are slower. In order to achieve rapid nitrate removal we need multiple strategies including use of constructed wetlands in localized controlled greenhouse environments. In such localized controlled micro-environments higher temperatures can be managed for plant growth in hydroponics system through which nitrate contaminated water is fed for denitrification. Denitrification is a process that converts nitrate to gaseous nitrogen. This process is also referred to as "removal of nutrients". The advantage of denitrification is that less oxygen is needed for the digestion of organic compounds in the aeration basin and specifically selected plants are needed for effective strategy. In the overall strategy to develop effective plant systems for controlled environment removal of nitrate pollution we have developed plant tissue culture technologies to isolate cold tolerant plant species that can be grown in aquatic and hydroponic environments. The use of innovative tissue culture technologies allows isolation of plant clonal lines of single seed phenotype origin that can be screened for cold tolerance and nitrate removal in aquatic zones. Such single seed plant clonal isolations are being evaluated for nitrate removal in the range of 25~50 $mg \cdot L^{-1}$ in hydroponic environments. The results of optimal removal of nitrate in greenhouse hydroponic studies will be presented. One group of plant species that hold promise for use in controlled greenhouse environments are species of aquatic mints. Strategy for specific clonal screening and use in cold latitude wetlands and greenhouse system for temperature control in the winter will be presented.

Keywords: Nitrogen pollution; Plant clonal systems; Greenhouse microenvironments; Denitrification; Cold latitudes; Metabolic conversion; Hydroponic systems

Introduction

Water plays a very important role in every aspect of biological life and their interrelationships. With the need for rapid economic development, people exploit natural resource and pay little attention to protect water resources, which leads to serious water pollution challenges. Significant amounts of NH_3-N increase gradually every year. Obviously, research and technology for treatment to remove NH_3-N and nitrate in water is necessary and urgently needed.

Among the above strategies a very robust man-made marsh system with an effective constucted wetlands with right choice of robust plants and controlled temperature microenvironments holds much promise. This can help nitrogen removal efficiently when combined with other physical (filteration), chemical (POSS materials) and biologically combined enzyme technology and microbial immbolization methods. Many studies have indicated that planted wetlands exhibited greater nitrate, and in general high nitrogen pollution removal than unplanted wetlands (Tanner 1996; Lin *et al.*, 2002). Planting macrophytes such as *Penniserum* (Lin *et al.*, 2002) and *Glyceria* (Tanner,

1996) indicated higher rates of nitrate removal. Therefore choice of right kind of plant macrophyte species can enhance strategies for nitrogen removal in constructed wetlands.

Despite the above progress nitrogen pollution removal in cold latitudes is a challenge and also design of appropriate constructed wetland system for cold latitudes is even a bigger challenge. However many of these plant species selections can be enhanced by screening the right variety of robust plants that can withstand high nitrate removal loads in constructed wetlands in cold latitudes. This can be achieved by novel tissue culture-based micropropagation technologies to screen the right robust plants with cold tolerance and robust rooting and shooting characteristics.

Our proposal is to use novel tissue culture-based micropropagation technologies developed in our laboratory (Zheng *et al.*, 2001) to advance efficient nitrogen pollution removal in cold latitudes. In this approach we will have 3 innovations: 1) screening right combinations of robust clonal phenotypes of plant macrophytes for ammonia and nitrate removal in cold latitudes; 2) improving robustness of plant macrophyte clonal system for nitrate removal using microbial interactions based on previous technologies developed in our laboratory (Strycharz *et al.*, 2002); 3) integrating plant macrophyte combination in greenhouse controlled environment microclimate to enhance localized nitrate removal in hydroponic systems. Such as multi-faceted plant macrophyte system can than be integrated with other methods for efficiency of nitrogen pollution removal.

Materials and Methods

Plant Clonal Systems

Cold tolerant perennials that have excellent over wintering dormancy of seeds will be targeted for screening robust clonal phenotypes from a mixture of heterogeneous seed sources from local microclimates and cold tolerant ecotypes of similar range of latitude. The clonal phenotypes will be specifically targeted for cold tolerance, excellent shoot/root ratio and adaptability hydroponic or aquatic environment. Based on tolerance response those seeds that proliferate with excellent shooting and rooting characteristics will be further multiplied clonally and rapidly under *in vitro* conditions.

Nitrate and Ammonia Uptake Studies

Nitrate and Ammonia uptake studies of various clonal lines that are screened will be investigated in hypdroponic greenhouse systems. Ratios of nitrate and ammonia will be varied and uptake and growth characteristics will be determined. Specific pilot hydroponic studies will evaluate specific conditions of high nitrogen pollution and also mixture of plant clonal phenotype and species. Temperature conditions will also be optimized and uptake under reduced light and autumn temperatures will be determined. Deep and shallow root combinations of plant macrophyte combinations will also be explored.

Beneficial Bacterial Interactions

Many plant growth promoting and root associated beneficial bacterial systems will be co-cultivated with plant clonal phenotypes and those that survive the hydroponic conditions best will be screened. Particular interest will be on root associated bacterial systems and combinations that survive well under high nitrogen hydroponic conditions and enhance the overall robustness and cold stress adaptation of the plant macrophytes.

Integration of Plant-Bacterial Combinations in Greenhouse Microenvironments

Greenhouse microenvironments can be targeted for development close to water treatment plants. Before high nitrogen polluted water enters the water treatment systems that uses combination filters or physico-chemical methods for nitrogen pollution removal, it can be passed through hydroponic greenhouse systems with controlled micro-climates in the winter.

Results and Discussion

In many constructed wetland systems the choice of plant macrophyte systems is poor. We have developed very innovative plant tissue culture-based micropropagation technologies that help to screen specific clonal phenotypes from heterogeneous seed sources of plant macrophytes that can be adapted to high nitrate controlled aquatic systems. Further we can rapidly screen the clonal phenotypes for not only robust adaptation to cold conditions but also those that can root and shoot optimally under high water

conditions. Once robust rooting and shooting clonally phen-otypes are selected for aquatic greenhouse microen-vironments appropriate plant root associated bacterial systems can be screened for enhancing the plant adaptation. Role root associated rhizosphere bacteria in nitrogen metabolism is well established. If such beneficial bacteria for strong root biofilms can be developed they can enhance the nitrogen removal efficiency of plant clonal macrophytes. In previous studies in our laboratory we have extensively used bacterial combinations to enhance the function of plant clonal phenotypes. Such an approach is very novel and such an innovation has potential for success in this project. Bacterial systems also withstand cold stress better and have the potential to enhance the cold stress tolerance of plant macrophytes as well.

The combination of right cold tolerant plant clonal phenotype with beneficial bacterial combinations can be integrated into greenhouse microenvironments with hydroponic/aquatic growing system. The intake water flow can be nitrogen contaminated water stream with controlled flow. The plant-bacterial combinations can be in complete hydroponic system with continuous flow of water or plant-microbe combinations can be grow in artificial solid medium airborne over water flow with roots growing into the contaminated water flow. The flow rate control will be important and per hour nitrate conversion rate will be important depending on the nitrogen load. The temperature control for optimum nitrogen removal can be optimized. Another interesting aspect of this study is whether higher value greens, food herbs and medicinal plants can be adapted for high value production. This will depend on overall quality of the contaminated water. Such a strategy could also include use of waste biomass and carbon for energy requirements for plant growth and therefore integrate photosynthesis with nitrate removal into high value plant and even fresh food productivity.

Conclusions

Therefore a novel system can be an integrated food, health and energy integrated solution while removing unwanted and unhealthy nitrates from the environments. Such integrated innovations are urgently needed as all bioresource challenges are integrated challenges where one defect affects other levels. Such an integrated approach can be foundations of new global and sustainable economies based on environmental and energy balance.

References

Lin YF, Jing SR, Wang TW, Lee DY (2002) Effects of macrophytes and external carbon sources on nitrate removal from groundwater in constructed wetlands. Environ. Pollut. 119: 413-420

Strycharz S, Shetty K (2002) Peroxidase activity and phenolic content in elite clonal lines of Mentha pulegium in respense to polymeric dye R-478 and Agrobacterium rhizogenes. Proc. Biochem. 37: 805-812

Tanner C (1996) Plants for constructed wetland treatment systems-A comparison of the growth and nutrient uptake of eight emergent species. Ecol. Eng. 7: 59-83

Zheng Z, Sheth U, Nadiga M, Pinkham JL, Shetty K (2001) A model for the role of proline-linked phenolic synthesis and peroxidase activity associated with polymeric dye tolerance in oregano. Proc. Biochem. 36: 941-946

Effect of Ionic Strength on Specific Adsorption of Ions by Variable Charge Soils: Experimental Testification on the Adsorption Model of Bowden *et al.*

Renkou Xu*, Jun Jiang, Cheng Cheng

State Key Laboratory of Soil and Sustainable Agriculture, Institute of Soil Science,
Chinese Academy of Sciences, P.O. Box 821, Nanjing, China.
*Corresponding author. Tel. No. +86 25 86881183; Fax No. +86 25 86881000; E-mail: rkxu@issas.ac.cn.

Abstract: The intersection of adsorption-pH curves for phosphate and arsenate by variable charge soils were observed at different ionic strengths (a characteristic pH). Above this pH, the adsorption of the two anions increased with increasing ionic strength, whereas below it the reverse trend occurred. Under the acidic conditions, Cu(II) adsorption by goethite and γ-Al_2O_3 also increased with the increasing ionic strength. The change of the adsorption plane potential on variable-charge soils and Fe/Al oxides with ionic strength was responsible for the variation of specific adsorption of the anions and Cu(II). The zeta potential of soil colloids and Fe/Al oxides changed with ionic strength as an opposite trend to their surface charges. This gave an experimental proof to support the interpretation.

Keywords: Variable-charge soils; Specific adsorption; Ionic strength; Diffuse double layers; Zeta potential

Introduction

It has been observed that a characteristic pH usually occurs above which adsorption of phosphate by goethite and variable charge soils increases with the increase in ionic strength and below this a reverse trend occurs (Barrow *et al.*, 1980; Bolan *et al.*, 1986). An adsorption model has been developed by Bowden *et al.* (1980) to describe the adsorption mechanism of anions by goethite. This model is applied to explain the effect of ionic strength and pH on the adsorption of phosphate on goethite and soils (Barrow *et al.*, 1980; Bolan *et al.*, 1986). According to the model, the effect of ionic strength on the adsorption operates through its effect on electrostatic potential in the plane of adsorption (Barrow *et al.*, 1980). However, applications of such a complex model are generally not subject to direct experimental confirmation because they employed several fitting parameters that can not be analytically measured (McBride, 1997). In this article, the adsorption model is used to interpret the effect of ionic strength on the adsorption of phosphate and arsenate by variable- charge soils and the Cu(II) adsorption by Fe/Al oxides, and the key hypothesis of the adsorption model was testified with zeta potential measurements.

Effect of Ionic Strength on Phosphate Adsorption

Experimental results indicated that the intersection of phosphate adsorption-pH curves, obtained at different ionic strengths (a characteristic pH), was observed for the three variable-charge soils. Above this pH, the adsorption of phosphate increased with increasing ionic strength, whereas below it the reverse trend occurred (Fig. 1). The intersect pH was 3.75 for the Ultisol from Guangxi, which was lower than the value of PZSE (point of zero salt effect, 4.05) of the soil. A similar changing trend of arsenate adsorption with ionic strength in these variable-charge soils was also observed. The effects of ionic strength and pH on the adsorption of phosphate and arsenate by these soils were interpreted with the help of adsorption model developed earlier.

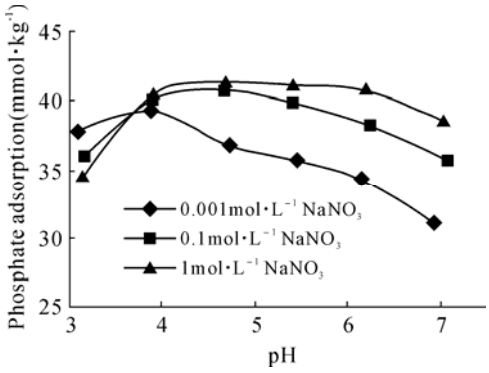

Fig. 1 Effect of ionic strength on phosphate adsorption by an Ultisol from Guangxi. Bars are ±SE

According to the model, the specific adsorption of anions on the surfaces of variable-charge soils occurred in a separate plane. Because these anions had a high binding constant, they coordinated to the surface and nearer the surface than electrolyte ions. When pH was higher than the PZNC (Point of Zero Net Charge) of the Oxisols, the soils possessed net negative charge, and the surface potential and the potential in the adsorption plane were negative. The surface charge became more negative with the increase of ionic strength ($NaNO_3$ as supporting electrolyte) (Wang *et al.*, 2009). Under this condition, the counter-ion in the diffuse layer was a cation (Na^+) and the number of cations per unit area increased with increasing electrolyte concentration. Therefore, the increase in the number of cations in the diffuse layer made the potential at the adsorption plane less negative, thus allowing increases in the adsorption of phosphate and arsenate by the soils. The increased adsorption of phosphate and arsenate by variable-charge soils with increasing concentration of $NaNO_3$ was attributed to the change of the potential in the adsorption plane induced by the change of ionic strength.

Confirmation of Effect Mechanism of Ionic Strength

The zeta potential is an electrical potential at the shear plane of the electric double layer on colloidal particles. The shear plane is near the adsorption plane in the model. Hence, the changing trends of zeta potential with pH at different ionic strengths should be similar to that on the adsorption plane for these soil samples. The results of zeta potential suggested that the potential in adsorption plane became less negative with increasing ionic strength above the soil PZNC and decreased with increasing ionic strength below the soil PZNC (Fig. 2). These results support the hypothesis of the adsorption model that potential in the adsorption plane changes with ionic strength with an opposite trend to the surface charge of these soils.

The phosphate adsorption by these soils was related not only to the ionic strength but also to the types of electrolytes present. K^+ increased phosphate adsorption more than Na^+ due to the greater hydrated radius of Na^+ than K^+ (Wang *et al.*, 2009). The results showed that the zeta potential of the colloid of the Oxisol in 0.01 mol·L^{-1} KNO_3 system was less negative than that in 0.01 mol·L^{-1} $NaNO_3$ system. This suggests that more K^+ entered the shear plane of the electric double layer on colloid particles of the soil than Na^+, which made the zeta potential and the potential on adsorption plane less negative.

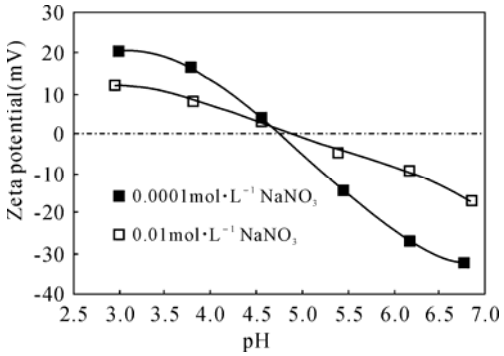

Fig. 2 Effect of ionic strength on zeta potential of colloids of the Ultisol from Guangxi at different pH values

When water and 0.1 mol·L^{-1} $NaNO_3$ were used to desorb the phosphate adsorbed on variable-charge soils, it was found that the amount of phosphate desorbed by water was greater than that by 0.1 mol·L^{-1} $NaNO_3$ at higher pH, and the difference of phosphate desorption between water and 0.1 mol·L^{-1} $NaNO_3$ increased with increasing the system pH. These results suggest that ionic strength affects the adsorption and desor-ption of phosphate in variable-charge soils through a similar mechanism.

Effect of Ionic Strength on Cu(II) Adsorption

It was reported that the adsorption of Cu(II) by goethite under acidic conditions was increased with increasing ionic strength, and the effect of ionic

strength on Cu(II) adsorption was ascribed to the depression of diffuse layer and OH^- release with the increase of ionic strength (Zhou *et al.*, 1996). However, we consider that the hypothesis of the model developed by Bowden *et al.* (1980) can also be used to interpret the effect of ionic strength on Cu(II) adsorption by Fe/Al oxides. When pH was lower than the PZNC of Fe/Al oxides, the oxides carried positive charges on their surfaces, and the surface potential and the potential in the adsorption plane were positive. The surface charge on Fe/Al oxides became more positive with increases in ionic strength ($NaNO_3$ as supporting electrolyte). Under this condition, the counter-ion in the diffuse layer was an anion (NO_3^-) and the number of anions per unit area increased with an increase in electrolyte concentration. Therefore, the increase in the number of anions in the diffuse layer decreased the potential at the adsorption plane, and thus increased the adsorption of Cu(II) by Fe/Al oxides. Our results indicate that the zeta potential of goethite decreases with the increasing ionic strength when pH is lower than PZSE, which is opposite to the effect of ionic strength on surface charge (Fig. 3). Therefore, the potential on the adsorption plane was also decreased with the increasing ionic strength and thus increased Cu(II) adsorption on the oxides.

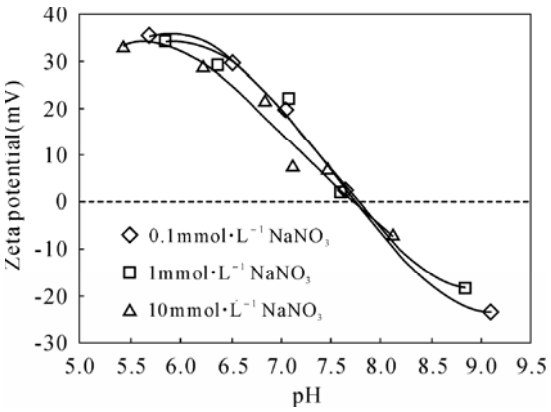

Fig. 3 Effect of ionic strength on zeta potential of goethite at different pH values

Conclusions

The change of the adsorption plane potential on variable-charge soils and Fe/Al oxides with ionic strength was responsible for the increase in the adsorption of anions when pH was greater than the PZNC of the adsorbents and in the adsorption of heavy metal cations when pH was lower than the PZNC of the adsorbents. The zeta potential of soil colloids and Fe/Al oxides changed with ionic strength as an opposite trend to their surface charges. This gave experimental evidence for the interpretation.

Acknowledgement

This research was supported by the National Natural Science Foundation of China (No. 40701079).

References

Barrow NJ, Bowden JW, Posner AM, Quirk JP (1980) Describing the effects of electrolyte on adsorption of phosphate by a variable charge surface. Aust. J. Soil Res.18: 395-404

Bolan NS, Syers JK, Tillman RW (1986) Ionic strength effects on surface charge and adsorption of phosphate and sulphate by soils. J. Soil Sci. 37:379-388

Bowden JW, Nagarajah S, Barrow NJ, Posner AM, Qurirk JP (1980) Describing the adsorption of phosphate, citrate and selenite on a variable-charge mineral surface. Aust. J. Soil Res. 18: 49-60

McBride MB (1997) A critique of diffuse double layer models applied to colloid and surface chemistry. Clay Clay Miner. 45: 598-608

Wang Y, Jiang J, Xu RK, Tiwari D (2009) Phosphate adsorption at variable charge soil/water interfaces as influenced by ionic strength. Aust. J. Soil Res. 47: 529-536

Zhou DH, Xu FL, Dong YY, Li XY (1996) Some problems relating to characterizing specific adsorption of heavy-metal ions on surface of oxide–Effect of accompanying anions. Chinese Sci. Bull. 47: 1483-1487

Estimation of the Electrostatic Repulsive Force among Charged Clay Particles in Aqueous Systems

Hang Li*, Jie Hou, Xinmin Liu

College of Resources and Environment, Southwest University, Chongqing, 400716, China.
*Corresponding author. Tel. No. +86-023 6825 0674; Fax No. +86-023 6825 0444; E-mail: hli22002@yahoo.com.cn.

Abstract: Electrostatic force of charged particles is crucial for some important physical processes in a wide range of scientific fields, such as the bio-molecular assemblies in modern biophysics, diffusion-controlled chemical kinetics and ion transport in soils, as well as soil particle aggregation and dispersion, which may be closely relevant to soil erosion and water eutrophication in environment. In this report, an approach for theoretical estimation of the electrostatic repulsive force among clay particles in aqueous solutions was suggested. The results showed that: 1) the suggested theory for the electrostatic force calculation was well verified by our experiment; 2) the accurate surface potential value is the key in obtaining an accurate calculation of the electrostatic force; 3) the electrostatic repulsive force among clay particles in aqueous solution will sharply increase with the decrease of electrolyte concentration in bulk solution of soil. The suggested approach may be important in the studies of soil particle interaction and charged particle transportation.

Keywords: Charged clay particles; Surface potential; Electrostatic repulsive force

Introduction

Even though soil is electrically neutral macroscopically, the potential gradient in the diffuse double layer (DDL) adjacent to the solid/liquid interface is not zero. It is well known that, soil is charged with net negative charges in normal conditions. Therefore, the negative charges on soil particle surface together with counter-ions in DDL will form an electrostatic field in the soil solution adjacent to the soil particle surface. For a clay/aqueous system, if the surface potential is known in advance, the strength of the electrostatic field can be easily calculated with the classic double layer theory (Sposito, 1984; Sparks, 1986). For example, if supposing the surface potential of soil particle is -300 mV, and supposing the electrolyte concentration of 1:1 type in bulk solution is 10^{-4} mol·L^{-1} and the temperature would be 298 K, the calculated electric field strength on clay surface would be -2.88×10^{8} V·m^{-1}. At the distances away from particle surface of 30Å, 100 Å and 300 Å, the calculated electric field strength would decrease to -1.61×10^{7} V·m^{-1}, -3.44×10^{6} V·m^{-1} and -1.80×10^{6} V·m^{-1} respectively; and even at a distance of 1000 Å away from particle surface, the electric field strength would be not yet zero but -1.30×10^{5} V·m^{-1}. Therefore, it will be of no question that the electric field origin from charged clay surface could extend into deep soil solution.

Actually, for any type of colloidal nano-particles in the nature, the electrostatic force is universally existed. At present, researches have shown that, the electrostatic field from particle surface plays a major role in the DNA condensation, aggregation, stretching, packaging and diffusion (Schwinefus and Bloomfield, 2000; Kohlstedt *et al.*, 2007). For bacteria, the bacterial-bacteria interaction and the bacteria- surface interaction are also influenced by the electrostatic field origin from the bacteria and solid surface (Soni and Balasubramanian, 2008). Undoubtedly, electrostatic force of charged clay particles is crucial for

some important physical and chemical processes in soils, such as diffusion-controlled chemical kinetics, ion transport, clay particles aggregation and dispersion as well as soil erosion.

In the estimation of the electrostatic force, the key parameter is the surface potential. Along with the establishment of the universally applicable method for the surface potential determination (Li *et al.*, 2004; Hou *et al.*, 2008; Li *et al.*, 2008), the theoretical estimation of the electrostatic repulsive force among clay particles in aqueous solutions could be carried out.

Theory

According to the classic DLVO theory and its recent development (Liang *et al.*, 2007), as the average distance between two adjacent particle surfaces is λ (dm), the total repulsive force among clay particles in aqueous system is:

$$P_T(\lambda)=P_{EDL}(\lambda)+P_H(\lambda) \tag{1}$$

where $P_T(\lambda)$ is the total repulsive pressure (atm) of clay in aqueous system, $P_{EDL}(\lambda)$ is the pressure (atm) comes from the electric repulsive force, and the $P_H(\lambda)$ is the pressure (atm) comes from the hydration force of clay particles in aqueous solution.

However, the hydration force was observed only at a distance shorter than 15 Å between surfaces of two adjacent particles (Pashley, 1981; Pashley and Israel-achvili, 1984; Ducker and Pashley, 1992). Therefore, as the distance between surfaces of two particles is larger than 15 Å, the electrostatic repulsive force is the sole source of the total repulsive force:

$$P_T(\lambda)= P_{EDL}(\lambda) \tag{2}$$

According to the Langmuir equation, for symmetric electrolytes, the electrostatic repulsive force could be estimated through the following equation:

$$P_{EDL}(\lambda)=\frac{2}{101}RTc_0\left\{\cosh\left[\frac{ZF\varphi(\lambda/2)}{RT}\right]-1\right\} \tag{3}$$

where $\varphi(\lambda/2)$ is the potential at the overlapping position of two DDLs ($\lambda/2$) for adjacent two particles with unit V; c_0 is the concentration of electrolyte in bulk solution with unit mol·L^{-1}; R is the gas constant with unit J·mol^{-1}·K^{-1}; T is the absolute temperature with unit K; F is the Faraday constant with unit C·mol^{-1}, and the unit of $P_{EDL}(\lambda)$ is atm in Eq. (3).

From Eq. (3), the key in the calculation of the electrostatic force is how to obtain the values of $\varphi(\lambda/2)$. Li *et al.* obtained an equation to calculate the value of $\varphi(\lambda/2)$ from the value of surface potential $\varphi(0)$ (Li *et al.,* 2003), and later a more accurate equation was also obtained for calculating $\varphi(\lambda/2)$, and for symmetric electrolyte, it can be expressed as (Hou *et al.*, 2009; Li *et al.*, 2009):

$$\frac{\pi}{2}\left[1+\left(\frac{1}{2}\right)^2 e^{\frac{2ZF\varphi(\lambda/2)}{RT}}+\left(\frac{3}{8}\right)^2 e^{\frac{4ZF\varphi(\lambda/2)_d}{RT}}\right] - \arcsin e^{\frac{ZF\varphi(0)-ZF\varphi(\lambda/2)_d}{2RT}} = \frac{1}{4}\lambda\kappa e^{-\frac{ZF\varphi(\lambda/2)}{2RT}} \tag{4}$$

where κ is the Debye-Hückel parameter with unit 1·dm^{-1}, and:

$$\kappa=\sqrt{\frac{8\pi F^2 c_0}{\varepsilon RT}}$$

From Eq. (4), if the surface potential on clay surface was known in advance, the $\varphi(\lambda/2)$ value could be calculated, and introducing the $\varphi(\lambda/2)$ value into Eq. (3), the electrostatic repulsive force could be estimated. Showing that, the surface potential is the key parameter in the calculation of the electrostatic repulsive force among clay particles in aqueous solutions. A universally applicable method for the determination of surface potential was established by Li *et al.* (Li *et al.*, 2004; Hou *et al.*, 2008; Li *et al.*, 2009), it makes us possible to calculate the electrostatic repulsive force theoretically.

Verification of the Theory

By using the combined universally applicable method for the surface properties determination, we simultaneously determined the surface potential, surface charge density and the specific surface area of montmorillonite in one experiment. The obtained specific surface area was 573 m^2·g^{-1}, the charge density was -8.9×10^{-4} mmol$_C$·m^{-2}; the surface potential in 10^{-4} mol·L^{-1} 1:1 type of electrolyte was

-257 mV. Therefore, based on the above suggested theories, the electro-static repulsive pressures at different distances between two adjacent particle surfaces can be calculated.

On the other hand, the attractive pressure comes from the long range van der waals attractive force could be estimated with the following equation:

$$P_{vdw}(\lambda) = \frac{10^{-3} \times A_{eff}}{0.6\pi} \lambda^{-3} \quad (5)$$

where A_{eff} is the effective Hamaker constant in aqueous system, here it was taken 2.25×10^{-20} J (Helmy, 1998), P_{vdw} is the attractive pressure (atm).

The calculated electric repulsive pressure and the van der waals attractive pressure are shown in Fig. 1. From Fig. 1, we can see: 1) the electrostatic repulsive force was so strong that, as the λ was lees than 50 Å, the repulsive pressure was much higher than 1 atm; and as the λ value decrease to 25 Å, the repulsive pressure sharply increase to 8 atm. As λ=25 Å in average, the corresponding water content will be 85% in mass ratio for the montomorillonite. 2) As λ>25 Å, the van der waals attractive force is much lower than the electrostatic repulsive force.

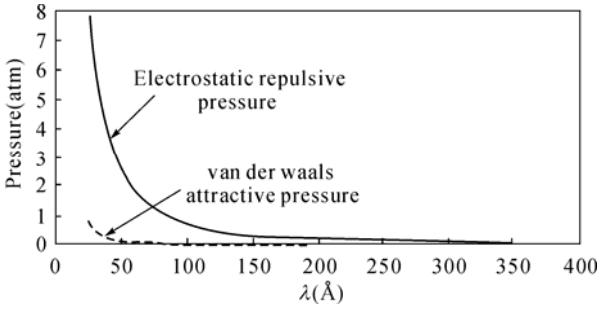

Fig. 1 The theoretical curves of P_{EDL} vs. λ (line) and P_{vdw} vs. λ (dashed line)

Therefore the net repulsive force (P_{net}) of montmorillonite could be calculated through the following equation as λ>15 Å:

$$P_{net}(\lambda) = P_{EDL}(\lambda) - P_{vdw}(\lambda) \quad (6)$$

Low experimentally determined the net repulsive pressure of 36 different montmorillonites as λ>25Å under the same conditions (Low, 1980; 1981). The comparison of the net repulsive pressures between the theoretical calculations and the experimental results at different λ values are shown in Fig. 2. Fig. 2 shows that, the results of the theoretical calculation of our theory and the experimental measuring of Low is in good agreement with each other. However, as the zeta potential to be used as the surrogate of the surface potential, the theoretical results of the electrostatic repulsive force deviated from the experimental data absolutely (Low, 1981). Therefore, the correct surface potential value is the key in obtaining an accurate theoretical calculation of the electrostatic repulsive force of the charged clay particles.

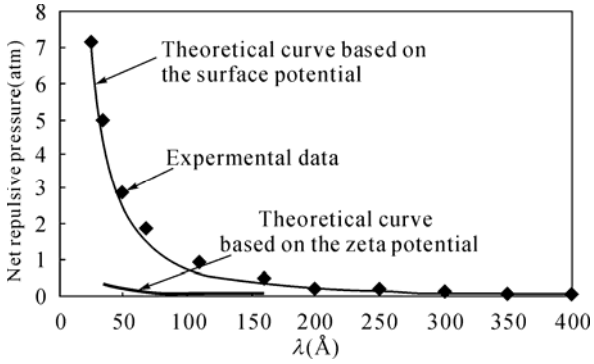

Fig. 2 Comparison of net repulsive pressures between the theoretical calculations and the experimental measurements. The experimental data and the theoretical curve based on the zeta potential were cited from Low's experiment (Low, 1980; 1981)

Electrolyte Concentration Dependence of the Electrostatic Repulsive Force

According to the determined results of surface charge density and the specific surface area of the montmorillonite, using the theory developed by Li *et al.* (2004), the surface potential of the montmorillonite in different electrolyte concentrations could be obtained. By using those obtained surface potential, the electrostatic repulsive pressure could be calculated by adopting the theories discussed above. The calculated electrostatic repulsive pressure under concentrations of 10^{-4} mol·L^{-1}, 5×10^{-4} mol·L^{-1}, 10^{-3} mol·L^{-1} and 5×10^{-3} mol·L^{-1} are respectively shown in Fig. 3. Fig. 3 clearly shows that, the electrostatic repulsive force among clay particles sharply increase with the decrease of electrolyte concentration in bulk solution of soil.

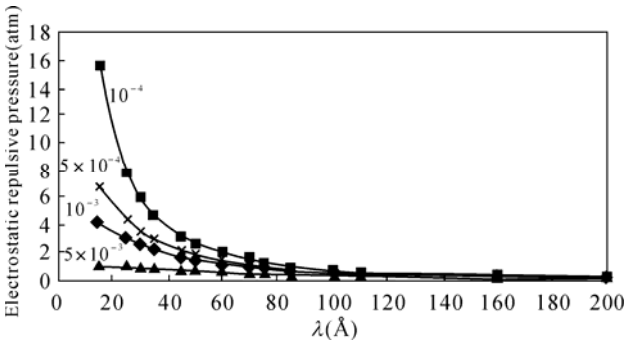

Fig. 3 The electrostatic repulsive pressures of montmorillonite in different electrolyte concentrations (the number on curves are concentration value)

For natural soil, the total quantities of electrolytes will be constant approximately, so the water content will determine the electrolyte concentration. Obviously, both precipitation and irrigation may decrease the electrolyte concentration, which will lead to the increase of the electrostatic repulsive force sharply. So the electrostatic repulsive force may be a key inner force in aggregates destroying in soil.

References

Ducker WA, Pashley RM (1992) Forces between mica surface in the presence of rod-shaped divalent counter-ions. Langmuir 8: 109-112

Helmy AK (1998) The limited swelling of montmorillonite. J. Colloid Interface Sci. 207: 128-129

Hou J, Li H, L Wu (2009) Determination of Clay Surface Potential: a More Reliable Approach. Soil Sci. Soc. Am. J. 73(4)

Kohlstedt KL, Solis FJ, Vernizzi G, de la Cruz MO (2007) Spontaneous Chirality via Long-Range Electrostatic Forces. Phys. Rev. Lett. 99

Li H, Wei SQ, Qin CL, *et al.* (2003) Discussion on position of shear plane. J. Colloid Interface Sci. 258: 40-44

Li H, Qin, CL, Wei SQ, *et al.* (2004) An approach to the method for determination of surface potential on solid/liquid interface: theory. J. Colloid Interface Sci. 275: 172-176

Li H, Peng XH, Wu L, *et al.* (2009) Surface potential dependence of the Hamaker constant. J. Phys. Chem. C 113: 4419-4425

Li H, Hou J, Liu XM, *et al.* (2009) A Combined Determination Method for Surface Potential, Surface Charge Density and Specific Surface Ares of Charged Particles: Theory and Application. In submission consideration

Liang Y, Hilal N, Langston P, Starov V (2007) Interaction forces between colloidal particles in liquid: Theory and experiment. Adv. Colloid Interfac. 134-135, 151-166

Low PF (1980) The swelling of clay: II. Montmorillonites. Soil Sci. Soc. Am. J. 44: 667-676

Low PF (1981) The swelling of clay: III. Dissociation of exchangeable cations. Soil Sci. Soc. Am. J. 45: 1074-1078

Pashley RM (1981) DLVO and hydration forces between mica surfaces in Li^+, Na^+, K^+, and Cs^+ electrolyte solutions: a correlation of double-layer and hydration forces with surface cation exchange properties. J. Colloid Interface Sci. 83: 531-546

Pashley RM, Israelachvili JN (1984) Molecular layering of water in thin films between mica surfaces and its relation to hydration forces. J. Colloid Interface Sci. 101: 511-523

Schwinefus JJ, Bloomfield VA (2000) The Greater Negative Charge Density of DNA in Tris-Borate Buffers Does Not Enhance DNA Cond-ensation by Multivalent Cations. Biopolymers 54: 572-577

Soni KA, Balasubramanian AK (2008) Zeta Potential of Selected Bacteria in Drinking Water WhenDead, Starved, or Exposed to Minimal and Rich Culture Media. Curr. Microbiol. 56: 93-97

Sparks DL (1999) Soil Physical Chemistry, 2nd ed. CRC Press, New York

Sposito G (1984) The Surface Chemistry of Soils. Oxford University press, New York, Clarendon Press, Oxford

Kinetics of As(III) and Cr(III) Oxidation by OH-birnessites with Various Average Oxidation States (AOSs)

Xionghan Feng*, Jiali Xu, Fan Liu, Wenfeng Tan

Key Laboratory of Subtropical Agriculture and Environment, Ministry of Agriculture,
Huazhong Agricultural University, Wuhan, 430070, China.
*Corresponding author. Tel. No. +86-27 8728 0271; Fax No. +86-27 8728 8618; E-mail: fxh73@mail.hzau.edu.cn.

Abstract: A series of alkaline birnessites (OH-birnessites), termed as Bir-OH1, Bir-OH2 and Bir-OH3, with average oxidation states (AOSs) of 4.02, 3.85 and 3.70 were synthesized. The PZCs of the OH-birnessites, around 1~2, decreased with the increase of AOS. Oxidation of Cr(III) and As(III) by OH-birnessites in the initial reaction stage complied with the pseudo first order kinetics. The apparent reaction rate constants (K_{obs}) in the initial reaction stage increased with the increase of AOS. The K_{obs} of Cr(III) oxidation by the tested samples in order were: Bir-OH1 (0.0342 min^{-1}) > Bir-OH2 (0.0178 min^{-1}) > Bir-OH3 (0.0148 min^{-1}). Those of As(III) oxidation were: Bir-OH1 (0.0951 min^{-1}) > Bir-OH2 (0.0396 min^{-1}) > Bir-OH3 (0.0071 min^{-1}). The K_{obs} also increased with increase of AOS. It was indicated that Mn(IV) and Mn(III) in birnessite had different reactivities, the AOS of OH-birnessites which was determined by the ratio of Mn(IV) and Mn(III) played an important role in affecting oxidation kinetics. In the initial stage of Cr(III) oxidation, Mn(II) release lagged behind Cr(VI) release. More and more Mn(II) were released to the solution as the reaction went on, and the ratios of released Mn(II) to Cr(VI) gradually approached the theoretical value of the reaction stoichiometry. While for As(III) oxidation, nearly no Mn(II) was detected in the whole oxidation process, the produced Mn(II) adsorbed to the surface of OH-birnessites and then formed precipitate, preventing the reaction from going on. It was implied that Cr(III) and As(III) oxidation had different kinetic behaviors on the surface of OH-birnessites.

Keywords: Adsorption/desorption; Oxide; Electrolyte; Birnessite

Introduction

As/Cr are naturally occurring toxic elements, widely known for their toxicity even at low concentrations. Developing efficient treatments for controlling As/Cr pollution and understanding As/Cr behavior in the environment are major public health issues gaining increasing attention in recent years. Manganese oxide is known to oxidize elements with variable valences to impact and determine their soil environmental behaviors, such as As and Cr.

Birnessite, the most common family among manganese oxides in soils, mainly comprises of $Mn(IV)O_6$ and $Mn(III)O_6$ octahedra. Different proportion of Mn(IV) to Mn(III) in birnessites results in various AOSs. The rate of Cr(III) oxidation was greater for todorokite and birnessite containing the most Mn(IV) and least for lithiophorite containing a greater proportion of Mn(III) (Kim *et al.*, 2002). However it was found that Mn oxides that exhibited the greatest Cr(III) oxidizing ability among seven Mn oxides were those containing Mn(III), and particular those containing Mn(III) and Mn(II) (Weaver and Hochella, 2003). Mn(III) availability may be an important factor in the oxidation of Cr(III) to Cr(VI) (Nico and Zasoski, 2000). Therefore, how AOSs in Mn oxides influence their reactivity is still in dabate and behaviors of As(III) and Cr(III) oxidation on the surface of birnessite are not fully understood. In this paper, scanning electron microscope (SEM), X-ray diffraction (XRD), X-ray Photoelectron Spectroscopy (XPS) and Batch kinetic method were used to

determine the surface properties and kinetics of Cr(III)/As(III) oxidation by synthesized birnessites with various Mn average oxidation states (AOSs).

Materials and Methods

Birnessite Syntheses

OH-birnessites were prepared in alkaline media by modification of the method of Villalobos *et al.* (2003). 125-mL aliquots of 12.475, 7.458, 4.992 g $MnCl_2 \cdot 4H_2O$ were mixed with 44 g NaOH in 250 mL distilled deionized water to prepare a pink gel precipitate of $Mn(OH)_2$. A 250-mL aliquot of $KMnO_4$ solution was added drop by drop to $Mn(OH)_2$ precipitates to control the molar ratios of Mn(II) to Mn(VII) to be 1.5, 2.5 and 3 respectively, and stired vigorously to form dark gray precipitates. After further stirring for 30 min, the products were aged for 12 h at 60 ℃. All of the synthetic birnessites were purified by electrical dialysis at a voltage of 150~220 V until the supernatant conductivities were below 20 $\mu S \cdot cm^{-1}$ and then dried at 40 ℃.

Characterization

XRD, TEM and XPS were used to characterize OH-birnessites before and after reaction. The Mn average oxidation state (AOS) was measured using the oxalic acid-permanganate backtitration method. A Quantachrome Autosorb-1 instrument was used to measure the surface areas.

Batch Kinetics Experiments

Oxidations of Cr(III)/As(III) were begun by adding 100 mL of $Cr(NO_3)_3/NaAsO_2$ and 0.1 $mol \cdot L^{-1}$ $NaNO_3$ solution to the birnessite suspension at ambient room temperature, 20±2 ℃. The pH was adjusted by 0.1 $mol \cdot L^{-1}$ HNO_3 and 0.1 $mol \cdot L^{-1}$ NaOH solution. The resulting initial concentration and pH for Cr(III) oxidation were 1 $mmol \cdot L^{-1}$ and 4 ± 0.03 $mmol \cdot L^{-1}$. Those for As(III) oxidation were 0.2 $mmol \cdot L^{-1}$ and 7 ± 0.03 $mmol \cdot L^{-1}$. At designated interval times, 1~2 mL aliquots were removed from reaction solution, filtered through 0.45 μm Millipore membrane. Final pH values were within 0.5 pH units of initial values. The control experiments indicated the dissolved O_2 had almost no effects on the oxidation reaction under experimental conditions. The concentrations of Cr(VI) in the filtrates were determined using the diphenylcarbazide chromagen method (Bartlett and James, 1979). Those of As(V) was determined using the colorimetric method described by Oscarson *et al.* (1980). Each run was made in triplicate.

Results and discussion

The synthesized OH^-birnessites, termed as Bir-OH1, Bir-OH2 and Bir-OH3, were XRD pure phase with AOSs of 4.02, 3.85 and 3.70. As shown in Fig.1, oxidation rate of Cr(III)/As(III) increased with increase of AOS. OH-birnessites with higher AOSs also possessed greater equilibrium oxidation of Cr(III)/As(III).

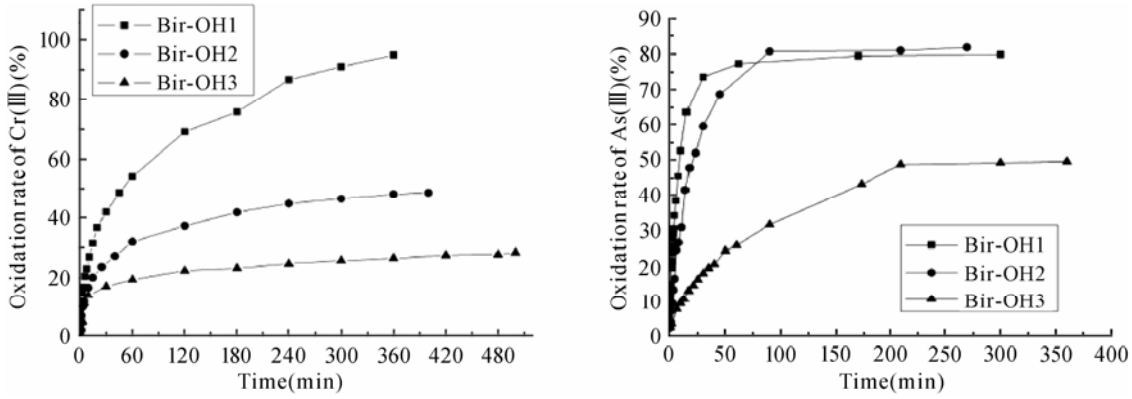

Fig. 1 Relationship between AOSs and Cr(III) (left) / As(III) (rigt) oxidation rates for OH-birnessites

The linear relationship between $\ln(C/C_0)$ and time during Cr(III)/As(III) oxidation(Fig. 2) indicated that the oxidation of Cr(III)/As(III) by all OH-birnessites was a first-order reaction within the initial 20 min

reaction period. The reaction rate constants (Kobs) of As(III) oxidation by Bir-OH1, Bir-OH2 and Bir-OH3 were 0.0342 min^{-1}, 0.0178 min^{-1} and 0.0148 min^{-1}, respectively. Those of Cr(III) oxidation were 0.0951 min^{-1}, 0.0396 min^{-1} and 0.0071 min^{-1}, respectively. Therefore, ratio of Mn(IV) and Mn(III) in birnessites played an important role in determining oxidation kinetics.

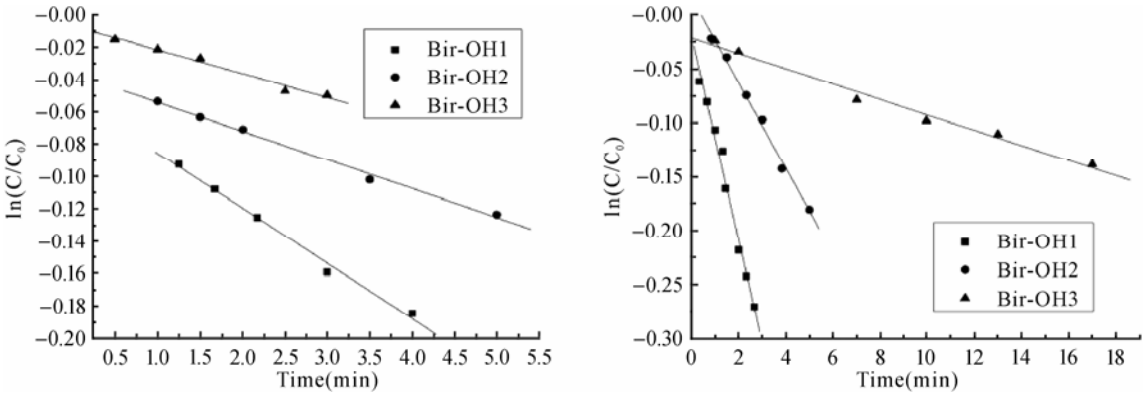

Fig. 2 Pseudo first-order fitting of Cr(III) (left) / As(III) (rigt) oxidation kinetics within the initial reaction period

Fig. 3 showed that the release of Mn^{2+} during Cr (III) and As(III) oxidation was different. For Cr (III) oxidation, the molar ratios of Mn(II) to Cr (VI) gradually approached the theoretical value (line in the left panel of Fig. 3) of the reaction stoichiometry. However, nearly no Mn(II) was detected in the whole process of As(III) oxidation by OH-birnessites, except that little amount of Mn(II) released for Bir-OH3 in the late stage of the reaction. During As (III) oxidation most of produced Mn^{2+} retained on the surface to form precipitate. The TEM analyses also supported such conclusion. In addition, the rate constants for As (III) oxidation decreased much more sharply than those for Cr (III) oxidation during the whole oxidation processes. Thus, Cr (III) and As (III) oxidation had different kinetic behaviors on the surface of OH-birnessites.

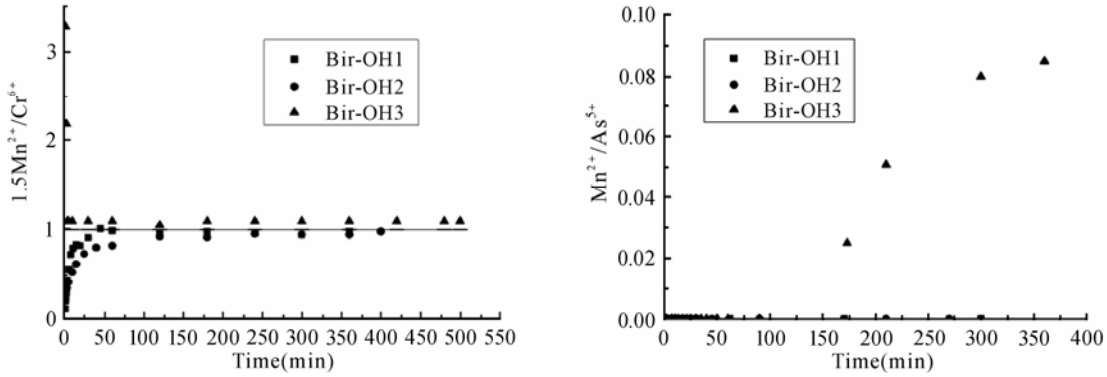

Fig. 3 Relationship between amount of Released Mn^{2+} and reaction time during Cr(III) (left) / As(III) (right) oxidation

References

Kim JB, Dixon JB, Chusuei CC, *et al.* (2002) Oxidation of Chromium(III) to (VI) by Manganese Oxides. Soil Sci. Soc Am. J. 66: 306-315

Nico PS, Zssoski RJ (2000) Importance of Mn(III) availablity on the rate of Cr(III) oxidation on δ-MnO_2. Environ. Sci. Technol. 34: 3363-3367

Weaver RM, Hochella MF Jr (2003) The reactivity of seven Mn-oxides with Cr^{3+}aq: A comparative analysis of a complex, environ-mentally important redox reaction. Am. Mineral. 88: 2016-2027

Adsorption/Desorption Kinetics of Zn in Soils: Influence of Phosphate

H. Magdi Selim[a,*], Keli Zhao[a,b], Lixia Liao[a], Jianming Xu[b]

[a] School of Plant, Environmental and Soil Sciences, Louisiana State University AgCenter, Baton Rouge, LA 70803, USA;
[b] Zhejiang Provincial Key Laboratory of Subtropical Soil and Plant Nutrition,
College of Environmental and Natural Resource Sciences, Zhejiang University, Hangzhou 310029, China.
[*]Corresponding author. Tel. No. +1 225-578-1332; Fax No. +1 225-578-1403; E-mail: mselim@agctr.lsu.edu.

Abstract: Transport of heavy metals such as zinc in soils may be affected by several rate limiting processes including kinetic sorption and release. Batch kinetic experiments were carried out to evaluate sorption and desorption of Zn for soils having distinctly different properties. A second objective was to test the hypothesis that phosphate additions to soils increases zinc adsorption. Sorption isotherms exhibited strong nonlinearity as well as kinetic behavior. Distinct differences in the amount of Zn sorbed among the different soils where highest sorption was observed for the neutral Webster soil. In contrast Windsor and Olivier (acidic) soils exhibited lower sorption capacities where Windsor soil showed least sorption. The influence of P on increased Zn sorption was clearly manifested in the isotherms where similar trends were observed for the two acidic and neutral soils. Distinct discrepancies between adsorption and successive desorption isotherms indicate considerable hysteresis for Zn release the extent of which varied among the three soils. For the two acidic soils Zn released ranged from 50%~60% of that sorbed whereas for the neutral soil only10%~15% of sorbed Zn was released over time.

Keywords: Heavy metals and soil; Hysteresis; Isotherms; Kinetics; Phosphorus; Release; Zinc

Introduction

Heavy metals are considered as potential pollutants to the soil and groundwater environment. Primary sources of heavy metal contamination include mining, smelting, plating, alloy production, and other industrial as well as anthropogenic factors. A secondary source is contaminated industrial waste and sewage sludge disposal on land. Zinc is among heavy metals which may be present at elevated levels in contaminated soils concentrations. Zinc is also an essential micronutrient for plants and animals. Zinc availability and mobility in soils is controlled by several interactions with the soil-water environment. Thus, understanding of the complex interactions of Zn in the environment is a prerequisite in the effort to predict their behavior in the vadose zone.

In this study, the main objective was to evaluate the sorption and desorption of Zn for soils having distinctly different properties. Time-dependent Zn release from soils was measured and efforts to quantify release or desorption kinetics based on multi-site and multireaction nonlinear modeling were carried out. A second objective was to test the hypothesis that phosphate additions to soils increases zinc adsorption. Therefore, zinc adsorption isotherms were constructed for three soils in the presence of different concentrations of phosphate solutions. The influence of phosphate on Zn hysteretic desorption was also quantified.

Materials and Methods

Three surface soils from the Ap horizon (0~10 cm) of Olivier loam (fine-silty, mixed, thermic Aquic Fragiudalf), Windsor sand (mixed, mesic Typic Dipsamment), and Webster loam (fine loamy, mixed, mesic Typic Haplaquoll) were used in this study . The pH values for Olivier, Windsor, and Webster soils

were 5.80, 6.11, and 6.92, respectively, and the respective CEC value were 2.0, 8.6 and 27.0 cmol·kg^{-1}. Additional soil properties for these soils have been reported by Buchter *et al.* (1989).

Adsorption of Zn was studied using the batch methods. According to the procedure, triplicate 3-g samples of each soil were placed in polypropylene tubes and mixed with 30-mL solutions of known Zn concentrations. Six initial Zn concentrations (C_o) were used, namely 20, 40, 60, 80, and 100, and 150 mg·L^{-1}. Reagent-grade $Zn(NO_3)_2$ was prepared in 0.01 mol·L^{-1} KNO_3 background solution in order to maintain somewhat constant ionic strength. The samples were shaken at 150 rpm on a reciprocal shaker for 24 h and subsequently centrifuged for 10 minutes at 4000 rpm. A 3-mL aliquot was sampled from the supernatant and the collected samples were analyzed for total Zn concentration using ICP-AES (Spectro Citros CCD).

Release or desorption commenced immediately following the 24 hours adsorption step using sequential or successive dilutions of the slurries to induce Zn release. Each desorption step was carried out by replacing the supernatant with 0.01 mol·L^{-1} KNO_3 background solution and shaking for 1 or 3 d durations. Ten desorption steps were carried out; the first desorption step was 1 d and was followed by 3 d intervals for a total desorption reaction of 28 d. The fraction of Zn desorbed from the soils was calculated based on the change in concentration in solution (before and after desorption). Moreover, during adsorption as well as desorption experiments, the pH and Eh of the mixed solution were measured following each reaction time.

To study the influence of P on Zn adsorption as well as release, the above Zn batch experiments were also carried out where different levels of P were added in the solution. Three levels of P were used; namely 25, 50 and 100 mg·L^{-1}. The form P used KH_2PO_4 in 0.01 mol·L^{-1} KNO_3 as background solution.

Results and Discussion

Zinc adsorption isotherms describing the distribution between aqueous and sorbed phases for the three soils are presented in Fig. 1 for 24 h of reaction time. For each soil a family of isotherms are represented where different initial P concentrations were added (from 0 to 150 mg·L^{-1}). Distinct differences of the extent of the amount of Zn sorbed among the different soils where highest sorption was observed for the neutral Webster soil. This was expected since Webster soil is a fine loamy Haplaquoll with 3.7% calcium carbonates. The two acidic soils exhibited lower sorption capacities where Windsor soil showed least sorption. Similar behavior was observed by Hinz and Selim (1994) who stated that stronger retention for Zn by Olivier compare to Windsor may be due to the relatively high CEC caused by predominately smectitic clays. In contrast, Windsor is an Entisol and contains parent material that has not been completely weathered to secondary minerals and hence lower sorption capacity for Zn.

The influence of P on increased Zn sorption was clearly manifested in the isotherms shown in Fig. 1 where similar trends were observed for acidic and neutral soils. Saeed and Fox (1979) showed that P fertilization increased Zn adsorption by soils from

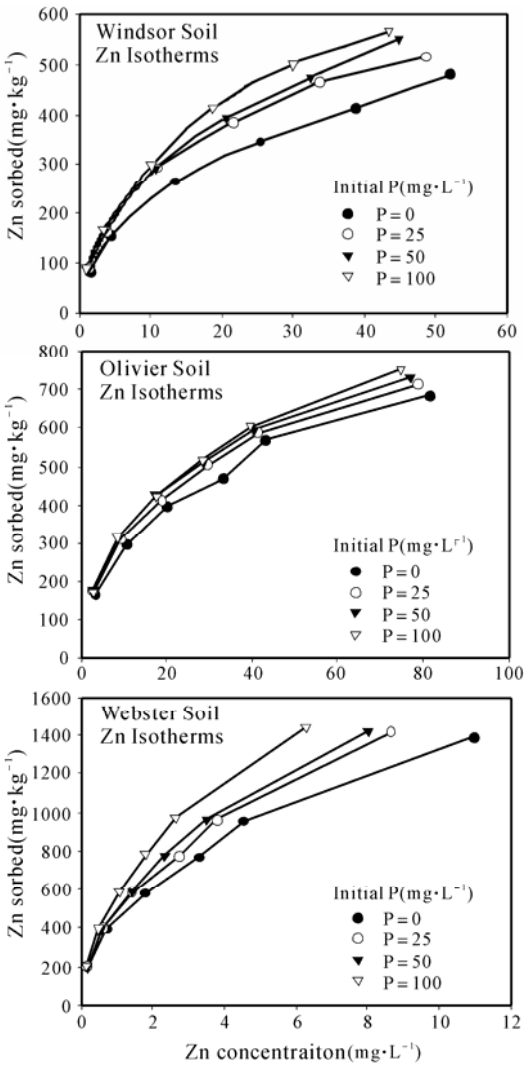

Fig. 1 Zinc adsorption isotherms after 24 h sorption in the presence of different P concentrations

Hawaii that contained colloids predominantly of the variable charge type. Their results support the hypothesis that phosphate additions to soils increase Zinc adsorption by increasing the negative charge on iron and aluminum oxide systems. Wang and Harrell (2005) reported that Zinc sorption was enhanced by $H_2PO_4^-$ as opposed to Cl^- or NO_3^- in acid soils.

Desorption Hysteresis: Desorption or release results which followed adsorption, are presented as isotherms in the traditional manner in Fig. 2. Distinct discrepancies between adsorption and successive

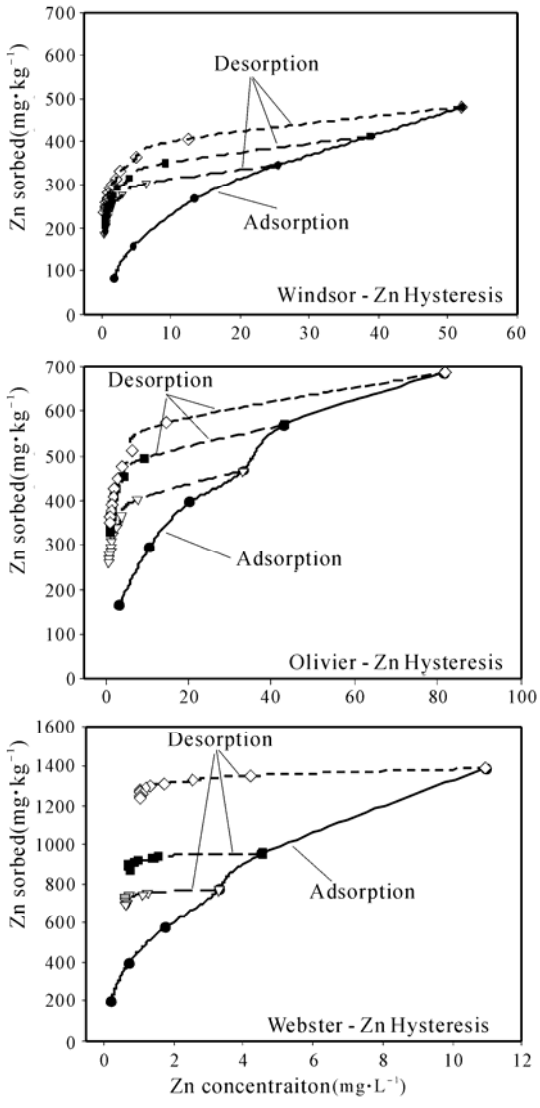

Fig. 2 Adsorption and desorption isotherms for three soils without added P

desorption isotherms clearly indicate considerable hysteresis for Zn release the extent of which varied among the three soils. This observed hysteresis was not surprising and is indicative of non-equilibrium behavior of Zn retention. Since significant irreversibility of Zn sorbed on mineral surfaces and soils has been extensively reported, this observed desorption hysteresis might be due to kinetic retention behavior, such as slow diffusion as well as irreversible retention.

Desorption results illustrate the extent of kinetic during release of Zn in the three soils. Webster soil exhibited limited kinetics or very slow release where desorption isotherms exhibited little release over time for all initial concentrations studied. In contrast, for the two acidic soils Zn release during sorption exhibited release kinetics where the amount of Zn released or desorbed over 28 d ranged from 50%~60% of that sorbed. For the neutral Webster, only 10%~15% of the sorbed Zn was released following 28 d of desorption. Although higher Zn amounts were sorbed as a result of the presence of P, similar patters of the release curves were obtained for all P concentrations. Thus, the kinetics of Zn retention was not altered by the presence of increased amounts of P.

References

Buchter B, Davidoff BY, Amacher MC, Hinz H, Iskandar IK, Selim HM (1989) Correlation between Freundlich Kd and n retention parameters with soils and elements. Soil Sci. 148: 370-379

Hinz C, Selim HM (1994) Transport of Zn and Cd in Soils: Experimental Evidence and Modeling Approaches. Soil Sci. Soc. Am. J. 58: 1316-1327

Saeed M, Fox RL (1979) Influence of phosphate fertilization on zinc adsorption by tropical soils. Soil Sci. Soc. Am. J. 43: 683-686

Wang JJ, Harrell DL (2005) Effect of ammonium, potassium, and sodium cations and phosphate, nitrate, and chloride anions on Zinc sorption and lability in selected acid and calcareous soils. Soil Sci. Soc. Am. J. 69: 1036-1046

Bioavailability and Redistribution of Trace Metals in Soil Washed with a Sulfosuccinamate Formulation

Maria del Carmen Hernández-Soriano[b], Aránzazu Pea[a], Maria Dolores Mingorance[a,*]

[a] Estación Experimental del Zaidín, CSIC, Granada 18008, Spain;
[b] Division of Soil and Water Management, KU Leuven, Heverlee 3001, Belgium.
[*]Corresponding author. Tel. No. +34-958 181600; Fax No. +34-958 129600; E-mail: mdmingor@eez.csic.es.

Abstract: Leaching tests using single and sequential extraction procedures were conducted in four contaminated soils to evaluate changes in metal partitioning before and after washing with the anionic sulfosuccinamate surfactant Aerosol 22 (A22). Evaluation of metal redistribution is of major importance to understand trace metals behaviour and reduce environmental risks. For the four soils, differing in the level of contamination, the distribution of metals in the four fractions was altered after washing with A22, which may be due to the strong extraction and complexation potential of the carboxylate function in the sulfosuccinamate surfactant. Besides, results from sequential extraction showed that, in general, surfactant largely extracted the metals bound to the carbonates and organic matter, while only a minority percentage of extraction corresponded with the oxyhydroxides fraction. Single extractions confirmed that the presence of the sulfosuccinamate compound in soil increases metal bioavailavility and therefore comprises a risk for the environment.

Keywords: Trace metals; Anionic surfactant; Sequential extraction; Single extraction

Introduction

Trace metals are highly persistent in soil and may have long-term effects on soil properties and environmental quality. Mobility of metals, which largely depends on metal speciation and distribution in the soil, may be altered by the presence of co-solutes in the soil solution as being sulfo-carboxylic compounds like the anionic surfactant Aerosol 22. These compounds constitute the largest group of synthetic surfactants, accounting for approximately 50% of the world's production (Rosen, 2004). Their presence on disposing wastes and wastewater, commonly used as organic amendments or for irrigation purposes, can accelerate to some extent the release of metals, constituting a threatening for the environment. Therefore, the objective of this work was to evaluate the changes in Cd, Cu, Pb and Zn distribution in contaminated soils after treatment with an anionic surfactant, and to provide useful information for the environmental risk assessment of metal contamination.

Materials and Methods

An artificially contaminated soil (CS), a sludge amended (SWS) and two naturally contaminated soils (MT and SS) were used, comprising a wide range of metal contents. Pseudo-total metal analysis was performed with *aqua regia* under microwave digester (Milestone 1200 Mega, Italy). Samples of 10 g of each soil were mixed with 500 mL of A22 solution at 26 $mg \cdot L^{-1}$ (16 CMC) and placed on an end-over-end shaker at 25 ºC during 24 h. Later, samples were centrifuged at 3000 $r \cdot min^{-1}$ and the supernatant was acidified with HNO_3 until analysis of Cd, Cu, Pb, and Zn contents by AAS. The solid (CS+A22) was

washed with two portions of MQ water and air-dried.

Bioavailable metal fractions were determined by single extractants and fractionation of metal in the soil samples was evaluated using sequential extraction scheme following the 3-steps procedure from Standard Measurements and Testing (SM&T-SES). Details on the experimental conditions are available elsewhere (Rauret *et al.* 2000; López-Sánchez *et al.*, 2002). SES was carried out into centrifuge tube. After each SES step, the suspensions were centrifuged at 3000 $r \cdot min^{-1}$. The supernatants were carefully removed and metals content analyzed by AAS.

Results and Discussion

Batch assays under static equilibrium were performed to simulate irrigation practices. Sequential extractions provide useful information to estimate metal partitioning and distribution in the geochemical phases. In those sequential schemes, extractants are applied in order of increasing reactivity and the consecutive fractions obtained correspond with metals forms of lower mobility (Rauret, 1998). The three steps of SES are associated with the exchangeable +water- and acid-soluble phases (F1), the reducible phase (bound to iron and manganese oxides, F2) and the oxidizable phase (bound to organic matter or sulphides, F3). Residual fraction (F4) represents the least available metal, fixed in the soil solid phase. Fig. 1 summarizes the metal distribution for the four soils assayed, according to these fractions and the redistribution of metals after treatment with the anionic surfactant A22. In general, a clear decreasing was observed for the metals associated to F1 with an overall increasing in the ratio of metal bounded to Fe and Mn oxy-hydroxides. Cadmium appeared generally associated to phases F1 and F2 and washing with A22 soils mobilized Cd mostly from F1 for all soils. Besides, for soils SS and SWS migration of Cd to F2 and F3 was induced. Copper is mainly associated to organic matter and oxides and results indicated that A22 may mobilize Cu mostly from the organic matter fraction, inducing a diffusion of Cu from F2 to F3 in soil SS and even from F4 to F3 in SWS. Lead is mainly located in the reducible (F2, 49%) and in the oxidizable or residual fractions, depending on the soil, and only the Pb associated with organic matter may be readily mobilized. Redistribution of Pb shown in Fig. 1 indicates that Pb in F1 was extracted with A22 and metal was mobilized from the solid mineral phase to organic matter fraction (SS and SWS) or F2 (MT). Finally, Zn was mostly present in F1 and F2 and metal release after A22 washing corresponded to these fractions. Therefore, treatment of CS with A22 solutions induced in general metal release from the most labile soil fractions for Cd, Pb and Zn and also from the reducible fraction for Cu. Zinc and Cd are the metals most easily extracted as metals corresponding to the first fraction are more prone to mobilization. In this fraction are included weakly-bounded metals, retained on soil surface by electrostatic interactions, which can be released by changes in ionic composition, modifications of adsorption/desorption of metals on soil constituents or affected by production or consumption of protons.

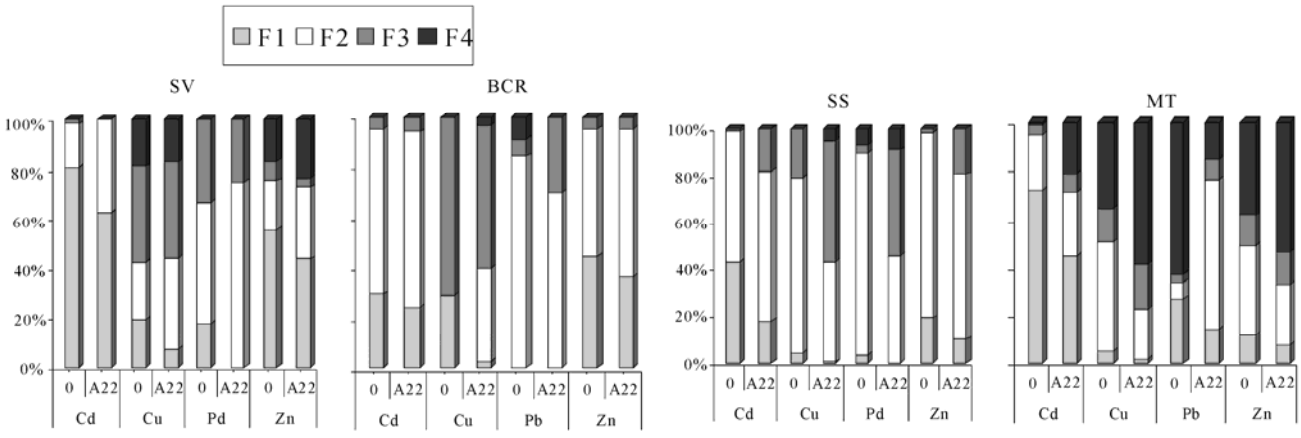

Fig. 1 Fractionation patterns of metals in four soils before and after washing with Aerosol 22 solutions. F1: adsorbed-exchangeable carbonate fraction, F2: reducible fraction, F3: oxidizable fraction, F4: residual fraction. 0: Fractionation in non-treated soil, A22: Fractionation after washing with A22

After soil washing with A22 metal species remaining in soil may be those of lowest availability and major content of metals is located in the reducible fraction. The observed reducible fraction sorption trend was Pb>Cu ≈ Zn and therefore, these metals, and particularly Pb, may be released from contaminated soil under reducing conditions, as previously reported (Pérez *et al.*, 2008).

Environmental risk assessment of metal contamination comprises the estimation of metal toxicity for living organisms, which directly depends on the chemical forms present in the soil (Kestern and Föstner, 1989). Thus, single extractants with an increasing ability for metal extraction as follows: $CaCl_2$<AcOH<NaOAc<EDTA, were tested and results are summarized in Fig. 2. The strongest one, EDTA, extracts metal from several soil compartments through a fast, competitive complexation reaction. Aerosol 22 exhibited a similar behaviour for the extraction of Cd, Cu and Zn, differing for Pb. In this case, A22 effect is comparable to the readily and available fraction extracted by sodium acetate.

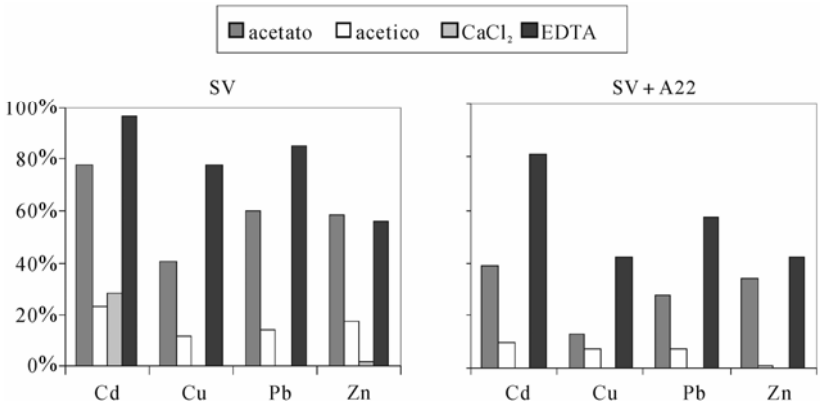

Fig. 2 Percentage of metal extracted by different extractants in non-treated soil (SV) and soil previously washed with A22

References

Kestern M, Forstner U (1989) Speciation of trace elements in sediments. In: Batley GE (ed.), Trace Element Speciation. Analytical Methods and Problems. CRC Press, Boca Raton, pp. 245-318

López-Sánchez JF, Sahuquillo A, Rauret G, Lachica M, Barahona E, Gómez A, Ure AM, Muntau H, Quevauviller Ph (2002) Extraction procedures for soil analysis. In: Quevauviller Ph (ed.), Methodology in Soil and Sediment Fraction Studies, Simple and Sequential Extraction Procedures. The Royal Society of Chemistry, Cambridge, UK.

Pérez G, López-Mesas M, Valiente M (2008) Assessment of Heavy Metals Remobilization by Fractionation: Comparison of Leaching Tests Applied to Roadside Sediments. Environ. Sci. Technol. 42: 2309-2315

Rauret G (1998) Extraction procedures for the determination of heavy metals in contaminated soil and sediment. Talanta. 46: 449-455

Rauret G, López-Sánchez JF, Sahuquillo A, Barahona E, Lachica M, Ure AM, Davidson CM, Gomez A, Lück D, Bacon J, Yli-Halla M, Muntau H, Quevauviller Ph (2000) Application of a modified BCR sequential extraction (three-step) procedure for the determination of extractable trace metal contents in a sewage sludge amended soil reference material (CRM 483), complemented by a three-year stability study of acetic and EDTA extractable metal content. J. Environ. Monit. 2: 228-233

Rosen MJ (2004) Surfactant and interfacial phenomena. John Wiley & Sons. New York, USA

Fractions of Cd, Zn and Their Correlation with Soil Black Carbon in Contaminated Soils Affected by a Smelting Furnace

Ling Liu[a], Na Li[a], Longhua Wu[a,*], Zhu Li[a], Jinping Jiang[a], Yugen Jiang[b], Xiya Qiu[b], Yongming Luo[a]

[a] Key Laboratory of Soil Environment and Pollution Remediation, Institute of Soil Science, Chinese Academy of Sciences, Nanjing 210008, China;
[b] Faculty of Soil and Fertilizers, Fuyang Bureau of Agriculture, Fuyang 311400, China.
[*]Corresponding author. E-mail: lhwu@issas.ac.cn.

Abstract: Investigation and analysis of soils in the heavily polluted farm field nearby a smelting furnace showed that heavy metal concentrations and organic carbon content in the soil decreased with increasing distance from the smelting furnace. Zinc (Zn) and cadmium (Ca) concentrations in surface soil decreased from 27107 $mg \cdot kg^{-1}$ to 892 $mg \cdot kg^{-1}$ and from 18.7 $mg \cdot kg^{-1}$ to 1.04 $mg \cdot kg^{-1}$, respectively. It was found that soil organic carbon and black carbon had significantly positive relationship with the concentrations of total Zn and Cd in surface soils. BCR sequential extraction procedure was used to determine the concentration of Zn and Cd speciation forms in the contaminated soil. It was shown that Cd and Zn were predominant in exchangeable and reducible fractions. Heavy metal concentrations in soil size fractions tended to increase as particle size decreased.

Keywords: Contaminated soil; Cd; Zn; Soil organic carbon; Black carbon

Introduction

Smelting activity was a chief source of heavy metals into the agricultural soil (Madrid *et al.*, 2008). Numerous studies have demonstrated that soil organic matter plays an important role in the fate of heavy metals in soil systems (Lee *et al.*, 1996; Yin *et al.*, 2002). In addition to the higher risk associated with finer soil particles because of the possibility of ingestion or inhalation (Yamamoto *et al.*, 2006), many pollutants are present in finer soil particles at a higher concentration than in larger size particles (Ajmone-Marsan *et al.*, 2007). Therefore, heavy metals present in the finest fractions of contaminated agricultural soils are another point to be considered with respect to heavy metal transfers to humans.

Materials and Methods

The experimental area was in the suburb of Hangzhou, Zhejiang Province. The site was associated in the past (from 1980 to 1998) to a factory smelting copper. The smelting furnace used pyro-metallurgic, and had no equipment for dust removal or safe work practices, resulted in large quantities of metals emitted to the atmosphere in the form of dust and then deposited on to soils. Samples were collected in May 2007. Eleven sampling sites were in four parallel lines. The first three sampling sites were selected 50 m from a smelting furnace and each site was 4 m away from each other (I-1, I-2, and I-3). Samples II-1, II-2, and II-3 were collected 22 m from the first three sites. Samples III-1, III-2, and III-3 were collected 61 m from the first three sites. Samples IV-1, IV-2, and IV-3 were collected 131 m from the first three sites. At each sampling site, 0~15 cm surface soil, 15~30 cm, 30~45 cm and 80~100 cm soils were collected (Fig. 1).

Results

The metal concentrations in the soil decreased with increasing distance from the smelting furnace.

Heavy metal concentrations were relatively high at the surface soil layer (0~15 cm), and decreased with increasing soil depth. In general, at IV-(1,2) site, concentrations of Cd and Zn were low. At the other three sites, the mean concentrations of Cd and Zn decreased in the order: I-(1,2,3) > II-(1,2,3) > III-(1,2,3).

Organic carbon content of the soils decreased in the order: I-(1, 2, 3) > II-(1, 2, 3) > IV-(1, 2) > III-(1, 2, 3). The C content in black carbon ranged from 18.4 $g \cdot kg^{-1}$ to 36.7 $g \cdot kg^{-1}$. The C content in soil black carbon decreased with the increasing distance from the smelting furnace.

BCR sequential extraction results showed that Cd concentrations in the exchangeable, water and acid soluble fractions and reducible fraction were predominant (>40% of the total Cd concentration). Cadmium concentration in the residual fraction did not exceed 50% of the total Cd concentration. In these sites, Zn enrichment in the exchangeable, water and acid soluble fractions and reducible fraction were especially noticeable. Of the four forms, Zn gave the lowest proportion in the oxidisable fraction, which usually comprised < 20%.

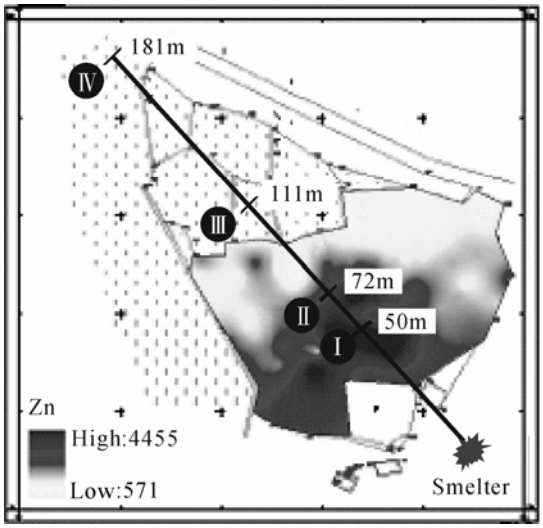

Fig. 1 Sketch map of the sampling site

The soil surface samples of I-2 (High) and III-2 (Low) were separated into five fractions: fine sand, 50~250 μm; silt, 5~50 μm; fine silt, 1~5 μm; colloid fraction, 0.1~1 μm; nanocolloid fraction, <0.1 μm (Tang *et al.*, 2009). The first three (fine sand, silt and fine silt) of the five fractions were predominant. Fig. 2 and Fig. 3 showed that the concentrations of Cd and Zn in the five fractions increased with decreasing particle size.

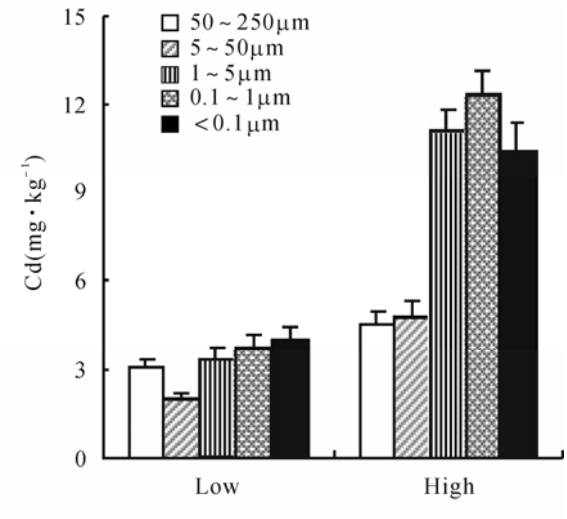

Fig. 2 Cd concentrations in size fractions

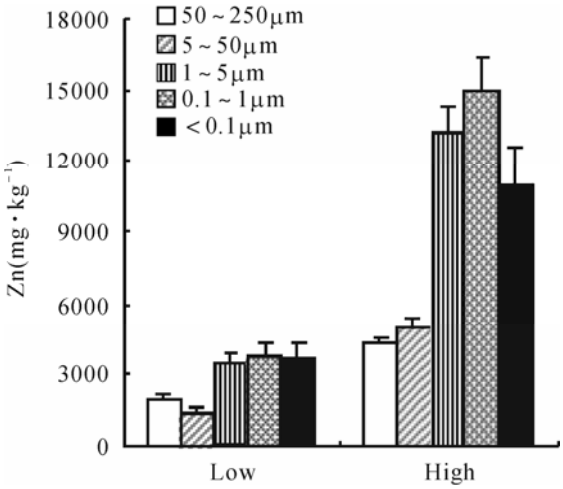

Fig. 3 Zn concentrations in size fractions

References

Ajmone-Marsan F, Biasioli M, Kralj T, Grcman H, Davidson CM, Hursthouse AS, Madrid L, Rodrigues S (2007) Metals in particle-size fractions of the soils of five European cities. Environ. Pollut. 152: 73-81

Lee SZ, Allen HE, Huang CP, Sparks DL, Sanders PE, Peijnenberg WJGM (1996) Predicting soil-water partition coefficient for cadmium. Environ. Sci. Technol. 30: 3418-3424

Madrid F, Diaz-Barrients E, Madrid L (2008) Availability and bio-accessibility of metals in the clay fraction of urban soils of Sevilla. Environ. Pollut. 156: 605-610

Tang ZY, Wu LH, Luo YM, Christie P (2009) Size fraction and characterization of nanocolloidal perticles in soils. Environ. Geochem. Hlth 31: 1-10

Yamamoto N, Takahashi Y, Yoshinaga J, Tanaka A, Shibata Y (2006) Size distribution of soil particles adhered to children's hands. Archives of Environ. Contam. Tox. 51: 157-163

Yin Y, Impellitteri CA, You S, Allen HE (2002) The importance of organic matter distribution and extract soil: solution ratio on the desorption of heavy metals from soils. Sci. Total Environ. 287: 107-119

Formation of the Metal Complexes between Protoporphyrin IX and Divalent Metal Cations in the Environment

Chi-In Jung[a], Jeong-Im Yang[a], Chul-Ho Park[b], Jee-Bum Lee[c], Hyoung-Ryun Park[a,*]

[a] Department of Chemistry and Research Institute of Basic Science, Chonnam National University, Gwangju, R.O. Korea 500-757;
[b] Department of Cosmetic Science, Nambu University, Gwangju, R.O. Korea 506-706;
[c] Department of Dermatology,Chonnam National University Medical School, Gwangju, R.O. Korea, 501-757.
[*]Corresponding author. Tel. No. +82-62 530 3376; Fax No. +82-62 530 3389; E-mail: hrpark@chonnam.ac.kr.

Abstract: Protoporphyrin IX is very slightly soluble in water whereas it is soluble in acidic as well as in basic aqueous solution. The UV-vis absorption spectrum of the protoporphyrin IX shows a very sharp and strong maximum absorption peak at 400 nm in acetonitrile-water mixture solution (1:1 v/v). The maximum absorption peaks reacted with divalent transition metal ions such as Cu^{2+}, Zn^{2+}, Fe^{2+} were shifted to a longer wavelength and the absorbance of the maximum peak decreased as the contents of metal ions increased. However, the absorbance of the maximum absorption peak combined with representative divalent metal ion, Mg^{2+} has nearly same value and the peak did not shifted. The formation constant (K_f) of the metal protoporphyrin IX complexes reacted with Cu^{2+}, Zn^{2+}, Fe^{2+} in acetonitrile-water mixture solution (1:1 v/v) were found to be 370, 418 and 24, respectively.

Keywords: Protoporphyrin IX; Metal complex; Uv-vis spectrum; Formation constants; Divalent metal ions

Introduction

Metal porphyrins such as chlorophyll, cytochrome c and hemoglobin are one of the most important compounds in an organism, because they have multiple chemical and biological action, including antioxidants, photosensitizer, chelating, anticarcinogenic, bacteriostatic and secretory activities (Miessler and Tarr, 2004). They are released large quantities into soil, when vegetations as well as animals are died and decomposed. The metal complexes have an effect on the soil environment (Zheng *et al.*, 2008). Plants absorb metals that are essential for growth (i.e., Cu, Fe, Zn, Mn) (Liphadzi *et al.*, 2003). It is, therefore, interesting to investigate the properties on the metal porphyrin complexes. The aim of this work was to examine the formation of metal complex between protoporphyrin IX as a model substance with several divalent metal cations such as Cu^{2+}, Zn^{2+}, Fe^{2+} and Mg^{2+}. Particularly, the formation constant (K_f) of metal porphyrin complexes give us some useful information for their decomposition into metal and porphyrin derivatives in soil.

Materials and methods

Protoporphyrin IX was purchased from Sigma Chemical Co. (St. Louis, MO) and used without further purification. The Chemicals used as metal cations [$CuCl_2$, $ZnCl_2$, $FeCl_2$, $MgCl_2$] were obtained from Aldrich Chemical Co. (ACS reagent grade). Acetonitrile was purchased from Fluka Chemical Co (HPLC grade) and used as received. Because porphyrin derivatives are very slightly soluble in water, we prepared two kinds of solutions to form the metal protoporphyrin IX complexes; protoporphyrin IX was dissolved in acetonitrile and divalent metal cations were dissolved in distilled water. Each of the solutions was mixed in a test tube and metal protoporphyrin IX complexes were prepared using ultrasonic cleaner. The solutions prepared were then taken their UV/vis absorption spectra using a UV/vis Spectrophotometer (Uvikon, model 943, Italy). The formation constant (K_f) of the metal complexes was obtained using the equation proposed by Sanchez *et al*. (Sanchez *et al.*, 1977).

Results and discussion

The UV-vis absorption spectrum of the 2.4 μmol·L^{-1} protoporphyrin IX in acetonitrile-water mixture solution (1:1 v/v) was measured by UV-vis spectrophotometer to investigate the formation of metal complex. The spectrum shows a very sharp and strong absorption maximum peak at 400 nm in the solution. Its molar extinction coefficient was found to be 82600 L·mol^{-1}·cm^{-1} in acetonitrile. To prepare the protoporphyrin IX metal complex, protoporphyrin IX dissolving in acetonitrile and divalent metal cations dissolving in distilled water were mixed in a test tube. The absorbance of the protoporphyrin IX at the absorption maximum peak is changed at the initial stage of the reaction after mixing the two kinds of mixture solutions. It is no more changed after shaking the two kinds of mixture solution for 100 hours (Fig. 1). It implies that the formation rate of the metal protoporphyrin IX complexes is relatively slow and it needs about 100 hours to complete the formation of metal protoporphyrin IX complexes under these experimental conditions. It corresponds to 4 hours reaction time using ultrasonic cleaner. The UV-vis absorption spectra of the 2.4 μmol·L^{-1} protoporphyrin IX in acetonitrile-water mixture solution treated with ultrasonic cleaner for 4 hours were shown nearly same shape of absorption peak and same absorbance treated with shaking the two kinds of mixture solution for 100 hours. The result indicates that porphyrin derivatives are relatively stable substances and it is difficult to coordinate surrounding the hydrated metal ions.

The absorbance at the absorption maximum peak of the protoporphyrin IX decreased and shifted to a longer wavelength as the contents of metal ions (Cu^{2+}, Zn^{2+}, Fe^{2+}) increased (Fig. 2). However, in the case of Mg^{2+} ion, the absorbance at the absorption maximum peak of the protoporphyrin IX was found to be nearly same value and the peak did not shifted. The result supports that metal complexes were produced by the combination of protoporphyrin IX with the divalent transition metal cations, although metal complex was hardly produced by Mg^{2+} ion. When the metal ions are contained in soil, they could react with porphyrin derivates such as protoporphyrin IX.

Because the porphyrin derivatives are good photo-sensitizer, the substances could be easily excited by the absorption of the sunlight on the surface in soil and might be performed some chemical reaction with substances in soil. As a result, some bacterium presented in soil might be killed by the chemical reaction. It might be related to the formation of metal complexes, because these are generally known as a better photosensitizer than prophyrin derivatives themselves (Wrighton, 1977). Moreover, there are some metal ions in soil and the metal ions which are essential substances to grow up some plants. In the case of formation of metal complexes, the concentration of metal in soil will be decreased and affected to the growth of plants. It is, therefore, the formation of metal complexes have an effect on the soil environment. The formation constant (K_f) of the metal protopor-phyrin IX complexes reacted with Cu^{2+}, Zn^{2+}, Fe^{2+} in acetonitrile-water mixture solution (1:1 v/v) were found to be 370, 418 and 24, respectively.

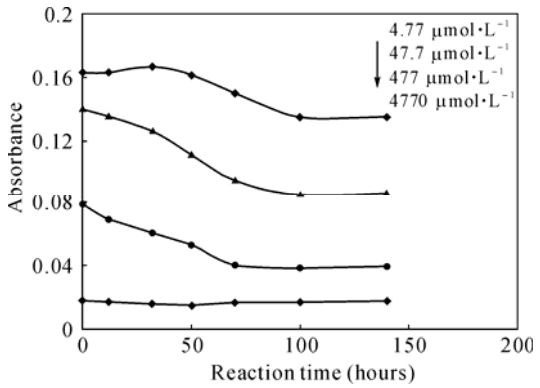

Fig. 1 Changes of the absorbance at the absorption maximum peak of the 2.4 μmol·L^{-1} protoporphyrin IX after mixing the protoporphyrin IX in acetonitrile and Zn^{2+} ion in distilled water (1:1 v/v)

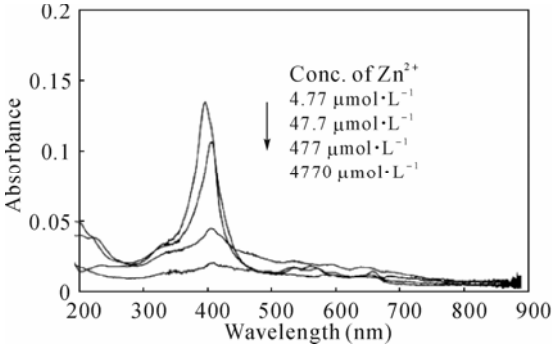

Fig. 2 UV-vis absorption spectra of the 2.4 μmol·L^{-1} protoporphyrin IX reacted with various concentration of Zn^{2+} ion in acetonitrile-water mixture solution (1:1 v/v)

This study took a further step toward describing

special effects of the photodegradation for the chemicals and organisms contained in soils, because it is very important to predict the soil environment.

References

Liphadzi M, Kirkham K, Mankin K, Paulsen G (2003) EDTA-assisted heavy-metal uptake by poplar and sunflower grown at a long-term sewage-sludge farm. Plant Soil 257: 171-182

Miessler GL, Tarr DA (2004) Inorganic Chemistry. Pearson Education Inc., Upper Saddle River, USA

Sanchez JC, Leyva JA, Ceba MR (1977) A New Method for Determining the Composition and Stability Constant of Complexes of the Form A_mB_n. Anal. Chim. Acta. 90: 223-231

Wrighton MS (1977) Inorganic and Organometallic Photochemistry. American Chemical Society, Washington DC, USA

Zheng YM, Chen TB, He JZ (2008) Relationship between Heavy metals and soil minerals. J. Soils Sediments 8: 51-58

The Impact of Urban Activities on Heavy Metal Distribution and Bioavailability Index in Selected Tropical Urban Soils

John Onam Onyatta[a,*], Charles Kibii Chepkwony[b], Peter Olengo Ongoma[b]

[a] National Council for Science and Technology, P. O. Box 30623-00100 Nairobi, Kenya;
[b]Egerton University, P. O. Box 536, Njoro, Kenya.
[*]Corresponding author. Tel. No. +254-722652159; E-mail: joonyatta@yahoo.com.

Abstract: The distribution and bioavailability of heavy metals in the environment is of particular concern because of their potential toxicity to the ecosystem. A study was conducted to investigate the impact of informal industries (commonly known in Kenya as *Jua kali* industries) on the heavy metal distribution and bioavailability indices in selected tropical urban soil samples from Nakuru town, Kenya. The study revealed that both the total metal contents and the bioavailability indices varied with the soil site and depended upon the intensity of industrial activities (painting, oil spills from engine overhauls, deposited wastes) on the sites. The informal industrial sites had higher levels of heavy metal content than the non-industrial sites, indicating that the informal industrial activities in these areas contributed to the elevated amounts of heavy metals. The mean heavy metal content in the informal industrial sites was highest for Zn followed by Fe, Pb, Mn and Cu. In the non-industrial sites, the trend was the same; however, lower values were obtained. The amounts of heavy metal extracted varied with the nature of the extractant. AAAc-EDTA extracted the highest amounts of the metals both from the industrial and non-industrial sites. The AAAc-EDTA extractable metal could be taken as the bioavailability index of the metals for the soils studied. The study is of significance in developing regulations for setting up informal industrial sheds in relation to micro-urban farming.

Keywords: Heavy metal distribution; Informal industrial site; Non-industrial; Bioavailability index; Tropical urban soil; Micro-urban farming

Introduction

Rapid urbanization and growing unemployment has led people in urban centres to grow crops in hazardous areas such as scrap yards, roadsides and dumpsites for solid and liquid wastes. The low income-producers' groups are utilizing these open spaces to grow various crops. Municipal wastes contain toxic metals from different anthropogenic sources. The wastes from the informal industries may contain a variety of metallic substances including batteries, consumer electronics, ceramics, electric light bulbs, paint chips, used motor oil, and plastics. Crops grown in metal contaminated soils have higher concentrations of metals than those grown on uncontaminated soil (Nabulo, 2006). There is concern in Kenya over the establishment of informal industries (*Jua Kali*) in the open spaces on the public land within the urban centres that are used for motor vehicle repairs, paint sprays, welding etc. The low-income micro-urban farmers use such abandoned spaces to grow crops to enhance urban food security, income and environmental management. The heavy metal deposition in such open spaces could seep into the groundwater system and could also be taken up by the crops. Plants growing in polluted environments can accumulate trace elements at high concentrations causing serious risks to consumers (Alloway, 1991). Anthropogenic substances, either organic or inorganic in nature, upon entering the soil may not only adversely affect its productivity potential, but may also compromise the quality of the food chain and

groundwater (Bollag *et al.*, 2005). The objective of this study was therefore to investigate the impact of informal industrial activities on the heavy metal content of the urban soils and their bioavailability indices.

Materials and Methods

Five *Jua Kali* and two non-*Jua Kali* soils with different physic-chemical properties were used in this study. The soils were obtained from 0~30 cm depth and the sites were selected on the basis of the extent of *jua kali* activities (car repair, painting, welding etc). The 0~30 cm depth was chosen to include both the plough layer and the region for the heavy metal migration in the soil profile (Onyatta and Huang, 1999; Biddappa *et al.*, 1982). The distance between the pits was 50 m to give representative area coverage during the sampling. The soil samples were then mixed to form a composite sample representing each sampling site. These soils are classified as phaeozems (FAO/UNESCO, 1985). The soil samples were air dried, and ground with a wooden roller to pass through a <2 mm sieve for subsequent analysis. The pH of the soil in water (1: 2.5) was determined using a pH-meter (Model 80, Griffin and George, Britain). The organic carbon content of the soils was determined according to the procedure of Black and Walkley (1965). Pertinent soil properties are presented in Table 1. The total metal content of the soil samples was determined using the HF-$HClO_4$ digestion technique while the bioavailability index was determined using various extractants (ammonium acetate-acetic acid-ethylene diamine tetraacetic acid (AAAc-EDTA), 0.01 mol·L^{-1} HCl; 0.01 mol·L^{-1} $CaCl_2$; 0.01 mol·L^{-1} $MgSO_4$).

Table 1 The pH, carbon and the content of heavy metals in Jua kali (Informal industrial) and non-jua kali (non-industrial) sites in Nakuru town, Kenya

Site	pH	C	Total metal content				
			Zn	Cu	Pb	Fe	Mn
Non-jua kali		%			μg·g^{-1}		
Nakuru Athletics club	6.45	2.75	62.50	1.30	16.05	49.54	12.58
Nyayo Gardens	5.50	4.56	125.00	5.15	55.40	83.88	43.42
Jua kali							
Hotel Waterbuck	7.02	4.19	157.50	19.20	101.85	105.69	7.98
Shabab	7.20	2.89	165.00	29.95	112.90	110.72	88.49
Nakuru Bus stage	7.01	2.31	177.50	4.65	32.70	119.11	25.63
General Hospital	6.75	3.90	107.50	3.50	33.65	72.14	26.37
Nakuru Nursing Home	6.72	3.40	192.50	24.93	55.60	129.18	43.58
$LSD_{0.05}$	0.34	0.03	0.34	0.06	0.03	1.03	0.24
$LSD_{0.01}$	0.52	0.05	0.53	0.09	0.05	1.61	0.37

Results and Discussion

The results show that in both *Jua kali* and *non jua kali* sites, the total metal content followed the same trend, however, the levels were higher in *Jua Kali* sites. (Order: Zn (160.00 μg·g^{-1} soil) > Fe (107.37 μg·g^{-1} soil) > Pb (67.34 μg·g^{-1} soil >Mn (38.41 μg·g^{-1} soil) > Cu (16.44 μg·g^{-1} soil). In non *Jua Kali* site, the order was: Zn (93.75 μg·g^{-1} soil)> Fe (66.71 μg·g^{-1} soil) >Pb (35.73 μg·g^{-1} soil)> Mn (28.00 μg·g^{-1} soil > Cu (3.32 μg·g^{-1} soil). The high levels observed in the *Jua kali* sites could be attributed to the industrial activities in these sites. The levels of the heavy metals varied with the intensity of the industrial activities in the sites studied. A statistical (Least Significance Difference) analysis of the metal content values for the soils of the *Jua kali* sites and the non-*jua kali* sites at 90% and 95% confidence levels using a computer programme (StatView SE + Graphics programme) showed that there was a significant difference between the metal contents of the soils obtained from *jua kali* and non *jua kali* sites (Table 1). The

bioavailability index which was taken as the amount of the metal extracted by the reagents varied with the nature of the extractant and with the soil site. The study showed that the AAAc-EDTA extracted the highest amount of the metals both from the *Jua Kali* and *non-jua kali* sites. The order of extraction was as follows: AAAc-ETDA>HCl>$CaCl_2$>$MgSO_4$.

The informal industrial activities (*Jua-Kali activities*) are responsible for the high metal contents observed in the urban soils studied and is influenced by the activities on the site. AAAc-EDTA extractant could be used to assess the heavy metal bioavailability of these soils at a buffered pH. This study is of significance in assessing the impact of *Jua-Kali* activities in relation to the heavy metal content of the urban soils and in developing regulations for setting up informal industrial sheds with reference to micro-urban farming in Kenya.

References

Alloway BJ (1990) Soil processes and the behaviour of metals. In: Alloway BJ (ed.) Heavy metals in soils. Blackie and Sons. N.Y. pp. 7-27

Biddappa CC, Mitsuo C, Kikuo K (1982) Migration of heavy metals in two Japanese soils. Plant Soil 66: 299-316

Black IA, Walkley A (1965) Methods of soil analysis, Part 2. Agronomy 9. Am. Soc. Agron., Incl., Madison, Wis

Bollag JM, Berthelin J, Adriano DC, Huang PM (2005) Impact of soil mineral-organic component-microorganism interactions on restoration of terrestrial ecosystems. In Soil Abiotic and Biotic Interactions and Impact of on the Ecosystem and Human Welfare. Huang PM, Violante A, Bollaand JM, Vityakon P(eds). Science Publishers, Inc., Enfield, USA. pp.51-70

FAO/UNESCO (1985) Soil map of the world. Legend. Rome

Nabulo G (2006) Assessment of heavy metal contamination of food crops and vegetables grown in and around Kampala City, Uganda. PhD. Thesis, Makarere, University Uganda

Onyatta JO, Huang PM (1999) Chemical speciation and bioavailability index of Cadmium for selected tropical soils in Kenya. Geoderma 91: 87-101

Nitrate Accumulation as Affected by Nitrogen Fertilization and Foliar Application of Micronutrients in Rocket Plant

Ayman Mohamed El-Ghamry*

Soils Dept., Faculty of Agriculture, Mansoura University, Egypt
*Corresponding author. E-mail: aymanelghamry@mans.edu.eg

Abstract: Field experiment was carried out in season 2007/2008 in a special farm near El-Mansoura City Dakahlya Governorate, Egypt to estimate the effect of N fertilization levels (0, 70, 105 and 140 kg N·ha^{-1}) in the form of NH_4NO_3 33.5% N as soil application and foliar application of Fe-EDTA at the rate of 300 mg·kg^{-1}, Mo as sodium molybdate at the rate of 50 mg·L^{-1} and their mixture (Fe + Mo) at the same used rates, each treatment was replicated three times. The results can be summarized as follow: Increasing N levels from 70, 105 and 140 kg N·ha^{-1} significantly increased all growth parameters i.e. plant height (cm), fresh and dry weight (g·plant^{-1}) for rocket plant at marketing stage as compared to the control treatment. Foliar spraying of Fe or Mo either as a solely addition or in combination together on plants fertilized by N rates (70, 105 and 140 kg N·ha^{-1}) significantly increased plant height, fresh and dry weight of rocket as compared to the untreated one. The average values of all growth parameters under study with foliar spraying of micronutrients were higher than that obtained without spraying under any level of N fertilization. Nitrate and nitrite concentrations in the fresh leaves of rocket plant were gradually and significantly increased due to increasing N level from 0 up to 140 kg N·ha^{-1}. On the contrary of this trend, the activity of nitrate reductase enzyme (μm NO_2·min^{-1}·g^{-1} FW) was sharply and significantly decreased as the level of N fertilization was increased. Foliar application of Fe or Mo either in a single form or combined together in the presence of N levels under investigation significantly decreased the mean values of NO_3-N and NO_2-N mg·kg^{-1} in the leaves of rocket plant than those obtained for the plants treated with the same N levels only. As for the activity of nitrate reductase enzyme, foliar spraying of (Fe+Mo) was superior for increasing the mean values of this parameter at any level of N fertilization. Applying nitrogen at the rates of 70, 105 and 140 kg N·ha^{-1} resulted in significantly increase the values of N% over the control treatment. Foliar spraying of Fe or Mo in single form combined with the same N rates under study led to an increase in the average values of N% rocket leaves compared with those obtained from the same N rates without Fe or Mo in foliar way. Such effect of Fe or Mo spraying was realized when (Fe+Mo) were foliarly applied tell the rate of 105 kg N·ha^{-1}. Increasing the rate of N addition from 105 to 140 kg·ha^{-1} in the presence of (Fe+Mo) had no significant effect on the values of N% in rocket leaves. The mean values of Fe and Mo in rocket leaves significantly decrease as the level of N fertilization was increased. The mean values of Fe and Mo in rocket leaves significantly decrease as the level of N fertilization was increased. An adversely effect was realized due to spraying of (Fe+Mo) combined with the investigated N rates, whereas the mean values of Fe and Mo in rocket leaves significantly increased as the level of N fertilizer was increased. The calculate values of N/Fe and N/Mo ratios did not increase due to an increase of N rates in the presence of (Fe+Mo) foliar addition, but it tended to be constant around (18×10^{-2}) and (19×10^{-3}) for N/Fe and N/Mo, respectively.

Keywords: N fertilization; Nitrate and nitrite accumulation; Micronutrients spraying; Rocket plant

Introduction

Considerable attention has been focused recently on the factors affecting nitrate accumulation in vegetables. Several plant species accumulate NO_3^- as a result of increasing nitrogen fertilizer supply.

Two main grievances have been advanced against dietary nitrate, the risk of methomoglobinaemia in infants and the possibility of an increase in the incidence of cancers in adults.

It is currently accepted that intake of nitrate implies a risk of methaemoglobinaemia (blue baby syndrome) for young infants. The haemoglobin molecule in the red blood cells has the important function of transporting oxygen. Methaemoglobin is an oxidized form of haemoglobin that is oxidized, from the Fe^{2+} to Fe^{3+} state. If the methaemoglobin level is abnormally high, the condition is known as methaemoglobinaemia (Sulotto *et al.*, 1994).

Avery (1999) define methaemoglobinaemia as the condition in which more than 1% of haemoglobin is oxidized to methaemoglobin. Nitrate itself in contrast to nitrite does not have the ability to transform haemoglobin into methaemoglobin. Nitrite oxidation of oxyhaemoglobin is reported according to the equation of Kosaka *et al.* (1979) as follows:

$$4HbO_2 + 4NO_2^- + 4H^+ \longrightarrow 4Hb^+ + 4NO_3^- + O_2 + 2H_2O$$

(HbO_2; Oxyhaemoglobin; Hb^+; Methaemoglobin)

The occurrence of nitrate in food (notably in vegetables), whatever its origin, enters the blood, is secreted with saliva; and part of nitrate is then reduced to nitrite by bacteria in the mouth. The saliva is swallowed, hence the nitrite enters the normally acidic stomach. Nitrite is reactive under acidic conditions. It can decompose to form nitric oxide, and it can react with a variety of organic compounds in food and in gastric secretions to form nitrose compounds (NOC_5). Most NOC_5 is likely to be responsible for a significant proportion of several cancers. This indicated the still angoing depate on a possible link between nitrate, nitrite, nitrosamins and cancer, based on the proposed sequence involving nitrosation reactions as follows:

Nitrate $\longrightarrow$ Nitrite $\longrightarrow$ Nitrosomines reactive metabolites that interfere with DNA $\longrightarrow$ Cancer (Williams, 1988).

Other claims have been advanced against dietary nitrate such as: an increased risk of fetal mortality risk of genotoxicity, an increased risk of congenital male formation, a tendency towards enlargement of the thyroid gland, an early onset of hypertension and enhanced incidence of childhood diabetes (Hirondel and Hirondel, 2001).

Official bodies recommended limits to human exposure to nitrate. These limits are set in order to avoid any impairment of health, even for exposure over a whole life time. Burdon (1961) indicated that the fatal adult dose in human being in the order of 15 to 70 mg of NO_3-N per kilogram of body weight.

Reinink *et al.* (1988) announced that the world health organization has tentatively fixed acceptable daily intake of nitrate at 3.65 $mg \cdot kg^{-1}$ body weight, and for nitrite at 0.13 $mg \cdot kg^{-1}$ body weight.

Markiewicz *et al.* (1995) found that the respective maximum limits for NO_3-N and NO_2-N in fresh vegetables to be safe for the human consumption are, 167 $mg \cdot kg^{-1}$ for nitrate and 0.67 $mg \cdot kg^{-1}$ for nitrite. Hanafy *et al.* (1997) investigated that several European countries have passed legislation regarding permissible levels of NO_3-N in vegetables per kg to be used for processing of foods for babies and children 64 mg (Switzerland), 89 mg (UK), 98 mg (France) and 36 mg in Germany as a fresh product.

The current acceptable daily intake of nitrate for man according to the European scientific committee is set at 3.7 mg $NO_3^- \cdot kg^{-1}$ body weight$\cdot day^{-1}$ while the same limit of NO_2^- was recommended as 0.06 mg $NO_2^- \cdot kg^{-1}$ body weight$\cdot day^{-1}$ Hirondel and Herondel (2001).

The aims of this investigation are to determine the effect of Iron and molybdenum as foliar application in the presence of N rates on reducing the accumulation of nitrate and nitrite in rocket plant due to its effect on the formation and activity of nitrate reductase enzymes.

Materials and Methods

Field experiment was carried out in season 2007/ 2008 in a special farm near El-Mansoura City Dakahlya Governorate to estimate the effect of N fertilization levels and foliar application of some micronutrients on plant growth and chemical composition of rocket plant.

16 treatments were arranged in complete randomized block design, which were the simple possible combination between; 4 levels of N fertilizers and 4 treatments of micronutrient addition in foliar application.

The soil experimental field was clayey in texture and fertile soil, chemical analysis of the experimental soil before sowing was presented in Table 1 as determined according to Jackson (1976) and Chapman and Prott (1961).

Table 1 Chemical properties of the used soil

mg·kg^{-1}					EC* dS·m^{-1}	pH**
N	P	K	Fe***	Mo***		
68.5	5.1	425	13.5	0.73	0.37	7.6

* soil extraction 1:5 (soil : water)
** soil suspension 1:2.5 (soil : water)
*** extracted by DTPA

Plots of 6 m^2 were buildup. Each plot consisted of five rows; 3 m long and 40 cm wide; rocket seeds c.v. Balady planted on 26 October, 2006; in hills, 15 cm apart on both side of rows. Two weeks later, plants were thinning to the most suitable uniform plants per hill. Thus the plant population could be estimated as about 950,000 plant·ha^{-1}.

Four levels of N fertilizer (0, 70, 105 and 140 kg N·ha^{-1}) in the form of NH_4NO_3 33.5% N as soil application were splited to two equal portions and applied as sid-dressing at 20 and 27 days after planting. And four treatments as foliar application of some micronutrients as follow:

1-Tap water as a control treatment.

2-Fe-EDTA at the rate of 300 mg·L^{-1}.

3-Mo as sodium molybdate at the rate of 50 mg·L^{-1}.

4-Mixture of micronutrients (iron, and molybdenum) at the same used rates, each treatment was replicated three times.

At marketing stage, 60 day from sowing, three plants (foliage) were randomly taken from each plot and carried immediately to the laboratory. These samples were weighed and NO_3-N, NO_2-N and the activity of NO_3-reductase enzyme were determined in the fresh materials of rocket plant. Also, plant height and fresh weight were recorded. Leaf samples were washed 3 times with 0.05 mol·L^{-1} HCl solution followed by washing 3 times with redistilled water, then oven dried at 70 ℃ till constant weight. The dry matter was calculated in expression of g·plant^{-1} and thoroughly ground for chemical analysis.

Nitrate and nitrite were determined according to the method described by Singh (1988), nitrate reductase (NR) activity measured by colorimetric determination of nitrite according to (Hageman and Reed, 1980). Chemical composition of plant leaves including Total nitrogen (%) using micro-Kjeldahl, Total phosphorus (%) was estimated colourimetrically using the chlorostannus reduce molybdo phosphoric blue colour method in sulphoric system, Potassium (%) using a flame photometer as described by Jackson (1967). Total iron and molybdenum were measured in the digested plant samples using an Atomic Absorption Spectrophotometer according to Chapman and Pratt (1961).

All obtained data were subjected to statistical analysis according to Gomez and Gomez (1984). Means of treatments were compared using new least significant differences (NLSD) as described by Waller and Duncan (1969).

Results and Discussion

Plant Growth Parameters

Data presented in Table 2 illustrated the effect of N levels as soil fertilization, Fe, Mo, (Fe + Mo) and their interaction on plant height (cm), fresh and dry weight (g·plant^{-1}) for rocket plant at marketing stage.

As for the effect of N fertilization levels data at Table 2 show that, increasing N levels from 70, 105 and 140 kg N·ha^{-1} significantly increased all growth parameters of rocket plant as compared to the control treatment. The average increases over the control treatment were 9%, 11% and 12% for plant height, 8%, 15% and 17 % for fresh weight and 13%, 17% and 14% for dry weight for the treatments of 70, 105 and 140 kg N·ha^{-1}, respectively. On the other hand, increasing the level of N fertilizer from 105 to 140 kg·ha^{-1} had no significant effect between the values of plant height and fresh weight of rocket plant while such effect significantly decreased the mean values of dry weight (g·plant^{-1}).

These results stated that such increments may be due to the physiological effect of N nutrition on vegetative growth and plant development. The favourable effect of N application at the high rates on plant fresh weight can be caused to the increase in moisture content of plant foliage rather than any increase in dry matter content.

These results are in harmony with those obtained by Mahmoud (1993); Gawish (1997) and Abd Allah (2001) who indicated that raising N level from 70 to 105, 140 and 175 kg·ha^{-1}. Significantly increased fresh and dry weight of spinach plant increasing N levels from 140 to 175 kg·ha^{-1} significantly increased fresh and dry weight of spinach plant increasing N level from 140 to 175 kg·ha^{-1} significantly decreased the dry matter content (g·plant^{-1}).

Table 2 Effect of N fertilization and foliar application of micronutrients on rocket plant growth

N levels (kg·ha^{-1})	Micro-nutrients	P. Height (cm)	F. W. (g·plant^{-1})	D. W. (g·plant^{-1})
0	0	14.55	8.74	0.94
	Fe	15.23	9.32	1.00
	Mo	14.70	8.95	0.96
	Mix	15.53	9.35	1.02
70	0	15.90	9.41	1.06
	Fe	17.85	9.97	1.21
	Mo	16.73	10.54	1.12
	Mix	18.08	11.84	1.24
105	0	16.20	10.08	1.10
	Fe	18.83	12.61	1.31
	Mo	17.03	10.95	1.14
	Mix	19.13	13.45	1.38
140	0	16.28	10.21	1.07
	Fe	18.90	12.72	1.34
	Mo	17.15	11.00	1.17
	Mix	19.28	13.61	1.42
LSD 5%		0.12	0.15	0.02

Regarding with the effect of micronutrients, data of Table 2 indicate that the foliar spraying of Fe or Mo either as a solely addition or in combination together on plants fertilized by N rates (70, 105 and 140 kg N·ha^{-1}) significantly increased plant height, fresh and dry weight of rocket as compared to the untreated one. The average values of all growth parameters under study under the foliar spraying of micronutrients are higher than that obtained without spraying under any level of N fertilization. In addition, foliar application of Fe+Mo as a mixture was most effective than the solely addition of Fe or Mo. Moreover, foliar application of (Fe +Mo) was more pronounced in increasing plant height, fresh and dry weight for rocket plant under the lowest N levels (70 and 105 kg·ha^{-1}) than that of the highest level of N (140 kg·ha^{-1}). In the presence of (Fe+Mo) foliar application, increasing N level from 0 to 70 kg·ha^{-1} led to increase plant height, fresh and dry weight, respectively by 16%, 27% and 23%. Raising the level of N from 70 to 105 kg·ha^{-1} resulted in an increase by 6%, 14% and 11%, respectively. The increase percent due to raising the level of N from 105 to 140 kg·ha^{-1} were 0.7%, 1% and 3% for plant height, fresh and dry weight, respectively.

The favorable role of iron and molybdenum on stimulating vegetative growth of rocket plant may be referred to the role played by these nutrients on plant bioactivities, the enzymatic system responsible of biosynthesis of amino acids, protein, chlorophyll as well as through out improvement of the nutrient status.

These results are confirmed with those of Mhamoud (1993), Kheir *et al.* (1991), and El-Agrodi *et al.* (2001) who investigated that, foliar application of (Fe+Mo) combined with N rates (70, 105, 140 and 175 kg N·ha^{-1}) significantly increased fresh and dry weight of lettuce plant compared with those obtained due to applying the same N rates only.

NO_3-N, NO_2-N and Nitrate Reductase Activity

Data illustrated in Table 3 show the effect of N fertilization levels, foliar spraying of Fe or/and Mo as well as their interactions on nitrate and nitrite accumulation as well as nitrate reductase (NR) activity in rocket plant at marketing stage.

Table 3 Effect of N fertilization and foliar application of micronutrients on NO_3^-, NO_2^- and NR

N levels kg·ha^{-1}	Micro-nutrients	NO_3^- (mg·kg^{-1})	NO_2^- (mg·kg^{-1})	NR (μmNO_2^-· min^{-1}·g^{-1} FW)
0	0	323	2.77	136
	Fe	311	2.55	151
	Mo	303	2.58	158
	Mix	292	2.43	163
70	0	410	3.42	75
	Fe	389	3.29	89
	Mo	358	3.04	113
	Mix	333	2.79	126
105	0	458	3.78	51
	Fe	420	3.56	72
	Mo	369	3.12	108
	Mix	340	2.82	123
140	0	491	4.06	36
	Fe	435	3.65	66
	Mo	379	3.20	97
	Mix	348	2.88	121
LSD 5%		17.5	0.09	6.5

Concerning with the effect of N fertilization data at Table 3 reveal that nitrate and nitrite concentrations in the fresh leaves of rocket plant were gradually and significantly increased due to increasing N level from 0 up to 140 kg·ha^{-1}. The highest values (491 and 4.06 mg·kg^{-1}) for NO_3-N and NO_2-N, respectively were recorded from the plants received 140 kg N·ha^{-1}., whereas the lowest one (323 and 2.77 mg·kg^{-1}) were obtained from the untreated plants. On the contrary of this trend, the activity of nitrate reductase enzyme (μm NO_2^-·min^{-1}·g^{-1} FW) was sharply and significantly decreased as the level of N fertilization was increased. The rates of decreasing % less than the control treatment were accounted to be 81%, 167% and 278% from the treatments of 70, 105 and 140 kg N·ha^{-1}, respectively.

It can be concluded that under heavy nitrogen application leafy vegetables (rocket) may absorb great quantity of NO_3^- than its assimilation capacity, the different between N absorption and assimilation may be great and the unutilized nitrogen will be stored as nitrate in plant tissues.

Data at Table 3 also indicate that foliar application of Fe or Mo either in a single form or combined together in the presence of N levels under investigation significantly decreased the mean values of NO_3-N and NO_2-N (mg·kg^{-1}) in the leaves of rocket plant than those obtained for the plants treated with the same N levels only. Such effect was more pronounced for the treatment of Fe+Mo. Moreover, increasing the level of N fertilization from 105 to 140 kg·ha^{-1} with foliarly applied of Fe or/and Mo had no significant effect between the mean values of these parameters. As for the activity of nitrate reductase enzyme, foliar spraying of (Fe+Mo) was superior for increasing the mean values of this parameter at any level of N fertilization as shown in Fig. 1.

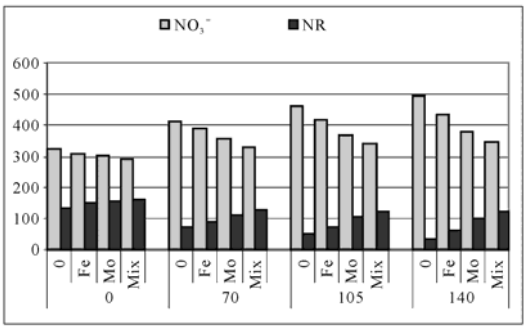

Fig. 1 Interrelation between nitrate accumulation and nitrate reductase activity as affected by N fertilization and foliar application of micronutrients

The mean values gain to be approximately constant around the level of 123±3 under all treatments of N fertilization 70, 105 and 140 kgN·ha^{-1}. On the other hand, solely spraying of Fe or Mo under the same levels of N fertilization led to a moderately effect on the activity of (NR) tell the rate of 105 kgN·ha^{-1}. Increasing the level of N fertilizer from 105 to 140 kg·ha^{-1}, sharply decrease the activity of nitrate reductase in the leaves of rocket plant.

In respect to the effect of Fe and Mo spraying on decreasing the content of nitrate and nitrite in rocket plant, such finding could be explained on the basis of the beneficial and stimulation effect of iron and molybdenum on the activity of nitrate reductase enzymes.

These results were confirmed with those of Crawford and CamPbell (1990); Kheir *et al.* (1991) and Hanafy *et al.* (1997) who indicate that micronutrient solution containing Fe and Mo decreased NO_3-N and NO_2-N in leafy vegetables.

***N%, Fe and Mo* (mg·kg^{-1})**

Data at Table 4 indicate the effect of N fertilization, Fe and Mo foliar application and their interactions on N, Fe and Mo contents in the dry matter of rocket leaves at marketing stage.

Regarding the effect of N fertilization data show that applying nitrogen at the rates of 70, 105 and 140 kg N·ha^{-1} resulted in significantly increase the values of N% which accounted to be 20.5%, 34.5% and 64.6% over the control treatment, respectively. Foliar spraying of Fe or Mo in a single form combined with the same N rates under study led to an increase in the average values of N% rocket leaves compared with those obtained from the same N rates without Fe or Mo in foliar way. Such effect of Fe or Mo spraying was realized when (Fe+Mo) were foliarly applied tell the rate of 105 kg N·ha^{-1}. Increasing the rate of N addition from 105 to 140 kg·ha^{-1} in the presence of (Fe+Mo) had no significant effect on the values of N% in rocket leaves.

As shown from Table 4, in spite of foliar application of Fe or/and Mo coupled with N rates under study led to sharp decreases in insoluble nitrogen forms (NO_3^- and NO_2^-) compared with an addition of N rates only, it resulted in increases the total nitrogen content in rocket leaves.

It can be concluded that (Fe+Mo) foliar spraying led to an increase in the activity of nitrate reductase enzymes, consequently more reduction of NO_3-N and

NO_2-N were happened resulted in producing nitrogen compound like protein.

Such results were reported by Shafshak and Abo-Sedra (1990), Mahmoud (1995) and Abd-Allah (2001).

Data at Table 4 indicate that, increasing the level of N fertilization from 70, 105 and 140 kg N·ha^{-1} significantly decreased the mean value of Fe and Mo contents in rocket leaves as compared to the control treatment. Foliar application of Fe or Mo in a single form under any rates of N fertilization studied significantly increased the mean values of Fe and Mo contents than those obtained for the plants received N rates only, but the mean values of Fe and Mo in rocket leaves were significantly decreased as the level of N fertilization was increased. An adversely effect was realized due to spraying of (Fe+Mo) combined with the investigated N rates, whereas the mean values of Fe and Mo in rocket leaves significantly increased as the level of N fertilizer was increased. The increases percentage over the untreated plants were 12.7%, 24.0% and 30.5% for Fe contents and 20.8%, 37.6% and 48.8% for Mo contents for the treatments of 70, 105 and 140 kg N·ha^{-1}, respectively.

Table 4 Effect of N fertilization and foliar application of micronutrients on N%, Fe and Mo (mg·kg^{-1})

N levels (kg·ha^{-1})	Micro-nutrients	N%	Fe (mg·kg^{-1})	Mo (mg·kg^{-1})
0	0	2.29	12.54	0.28
	Fe	2.36	25.46	0.58
	Mo	2.3	17.63	1.67
	Mix	2.57	14.28	1.25
70	0	2.76	11.86	0.25
	Fe	3.00	22.89	0.45
	Mo	2.85	14.89	0.94
	Mix	2.87	16.10	1.51
105	0	3.08	11.75	0.24
	Fe	3.51	20.93	0.43
	Mo	3.22	13.26	0.66
	Mix	3.24	17.71	1.72
140	0	3.77	10.9	0.22
	Fe	4.3	20.38	0.33
	Mo	3.92	11.99	0.54
	Mix	3.34	18.63	1.86
LSD 5%		0.14	0.08	0.02

To understand the results mentioned previously, N/Fe and N/Mo ratios as affected by N rates Fe and Mo addition were calculated as shown at Table 5. Data reflected that, the calculated values of N/Fe and N/Mo were gradually increased as the level of N fertilization was increased in the presence and absence of Fe or Mo spraying as solely addition. On the contrary of this trend, the average values of N/Fe and N/Mo ratios did not increase due to an increase of N rates in the presence of (Fe + Mo) foliar addition, but it tended to be constant around (18×10^{-2}) and (19×10^{-3}) for N/Fe and N/Mo, respectively.

Table 5 Effect of N fertilization and foliar application of micronutrients on N/Fe and N/Mo ratios

N/Fe ratio ×10^{-2}

Micronutrients / N level	0	Fe	Mo	Mix (Fe+Mo)
0	18.3	9.3	13	18
70	23.3	13.1	19.1	17.8
105	26.2	16.8	24.3	18.3
140	34.6	21.1	32.7	17.9

N/Mo ratio ×10^{-3}

Micronutrients / N level	0	Fe	Mo	Mix (Fe+Mo)
0	81.8	40.7	13.8	20.6
70	110.4	66.7	30.3	19
105	128.3	81.6	48.8	18.8
140	171.4	130.3	72.6	18

It can be concluded that N fertilization to rocket plant at the rates of this study induced imbalance between N, Fe and Mo in rocket leaves which can be corrected by foliar application of (Fe+Mo). Which parallel with the lowest values of NO_3^- and NO_2^- accumulation in rocket leaves.

Conclusion

Under the same condition of this experiment it can be concluded that N fertilization to rocket plant at the rates of this study induced imbalance between N, Fe and Mo in rocket leaves which can be corrected by foliar application of (Fe +Mo). Which parallel with the lowest values of NO_3^- and NO_2^- accumulation in rocket leaves.

References

Abd Allah GEA (2001) Effect of heavy nitrogen application on yield and chemical composition of some vegetable crops. Ph.D. Thesis, Fac. Agric. Mansoura Univ. Egypt

Avery AA (1999) Infantile methemoglobinemia: reexamining the role of drinking water nitrates. Environ. Health Persp. 107: 583-586

Burdon EH (1961) The toxicology of nitrates and nitrites with part reference to the protability of water supplies. Analyst 86: 429-433

Chapman HD, Pratt (1961) Methods of soil analysis, Part 2 A. S. S. Madison Wisconsin

Crawford NM, CamPbell WH (1990) Fertile fields. Plant Cell 2: 829-835

El-Agrodi W, El-Sirafi ZM, Ahmed AR, Baddour GA (2001) Effect of heavy nitrogen application on nitrate contamination in lettuce plant at marketing stages. J. Agric. Sci. 26: 8263-8275

Gawish AR (1997) Trails to reduce nitrate and oxalate contents in some leafy vegetables. 1- Interactive effect of different nitrogen fertilization regimes and nitrification inhibitor on growth and yield of both spinach and lettuce. Zagazig J. Agric. Res. 24 (1)

Gomes KA, Gomes AA (1984) Statistical procedures for agricultural research 2nd ed. John Willey and sons Pub, pp. 139-153

Hageman RH, Reed AJ (1980) In: Pietro AS (ed.), Methods in Enzymology. Vol. 69, Part C, Academic Press New York pp. 270

Hanafy AH, Kheir NF, Talaat NB (1997) Physiological studies on reducing the accumulation of nitrate in Jew's mallow and radish plants. Bull. Fac. Agri., Univ. Cairo. 48: 158-164

Hirondel JI, I'Hirondel JL (2001) Nitrate and man, Toxic, Harmless or beneficial. Centre Hospitalier Universitaire de Caen, France

Jakson ML (1967) Soil chemical analysis advanced course. Dept. of soils, Univ. of Wise., Madison 6, Wishensin, USA

Kheir NF, Hanafy AAH, Abou El-Hassan EA, Harb EMZ (1991) Physiological studies on the harardaus nitrate accumulation in some vegetables. Bull. Cac. of Agric. Univ., Cairo 42: 557-576

Kosaka H, Imaizumi K, Imai K, Tyuma I (1979) Stoichiometry of the reaction oxyhemoglobin with nitrate. Biochim. Biophy. Acta 581: 184-188

Mahmoud S (1995) Effect of planting date and fertilization level on yield and quality of lettuce. M. Sc. Thesis Fac. Agric. Moshtohor. Zagazig Univ.

Mahmoud HAF (1993) Response of some lettuce cultivars. To foliar nutrition. Egypt J. Applied Sci. 8: 238-251

Markiewicz R, Omietsanuik N, Pawlowska I, Wskaa A, Wska MB (1995) Concentration of nitrates in frozen vegetables. Bromatologia I. Chemia. Toksykologicznd 28: 199-121

Reinink K, Groenwold R, Bootsma A (1988) Genotypical differences in nitrate content in lactuca sativa, L. related species and correlation with dry matter content. Euphytica 36: 11-18

Shafshak, Nadia S, Abo-Sedera FA (1990) Effect of different nitrogen sources and levels on growth, yield and nitrate accumulation in some lettuce varieties. Annual of Agri. Moshtohor 28: 619-623

Singh JP (1988) A rapid method for fertermination of nitrate in soil and plant extracts. Plant Soil 110: 137-139

Sulotto F, Romano C, Insana A, Arrubba Cacciola, Erutti A (1994) Valori normali di carbossiemoglobinemia e di metemoglobinemia in un campione di militari di leva. La Medicina del Lavoro 85: 289-298

Waller RA, Duncan DB (1969) Abays rule for symmetric multiple cimposition problem. Amer. State. Assoc. J. pp.1485-1503

Williams DLH (1988) Nitrosation. Cambridge University Press, Cambridge, UK

Fractions of Heave Metals in Paddy Fields and Their Spatial Relationship to Rice Plant

Keli Zhao, Xingmei Liu, Jiachun Shi, Jianming Xu*

Zhejiang Provincial Key Laboratory of Subtropical Soil and Plant Nutrition, College of Environmental and Natural Resource Sciences, Zhejiang University, Hangzhou 310029, China.
*Corresponding author. Tel. No. +86-571 8697 1955; Fax No. +86-571 8697 1955; E-mail: jmxu@zju.edu.cn.

Abstract: To access the distribution in fractions of heavy metals in paddy fields in Wenling city in Zhejiang Province, China, extensive sampling was carried out to identify spatial correlation and bioavailability to rice grown on these soils at the regional scale. The results showed that Cd in soil were predominantly association with exchangeable and Fe-Mn oxide fraction; while Cu, Ni, Pb and Zn with residual fraction. Most heavy metals studied in rice were significantly (P<0.01) correlated with exchangeable fraction, which is considered as readily bioavailability to rice.

Keywords: Cross-correlogram; Heavy metals; Paddy fields; Soil-rice system; Spatial correlation

Introduction

Heavy metal contamination in agriculture lands poses a potential threat to safe crop production in China and worldwide. Rice is the dominant agricultural product in China and ranks second by quantity in the world. Therefore heavy metals contamination in agriculture soils and their transfer in a soil-rice system have been of increasing concern. Many previous studies were often concerned with total heavy metal concentration. It can provide information on the degree and extent of contamination, however, limited information on mobility and bioavailability of heavy metals in soil. Thus, more and more studies focused on the chemical fractions, which play an influential role in mobility and potential bioavailability of heavy metals in soil. The overall goals of this study were to quantify heavy metals concentrations and determine the distribution in fractions of heavy metals in present paddy fields as well as their bioavailability to rice plants grown on these soils.

Materials and Methods

This research was carried out in the city of Wenling, which is located in the southeast Zhejiang province, China. It is not only representative rice-production areas but also a highly industrialized area in Zhejiang and southeast China. At rice harvest time (October, 2006), 96 pairs of rice and soil samples with same location were collected from Wenling, by means of a completely randomized design, on the basis of a land use map at 1:50000 scale. Rice in this study was focused on the rice grain.

Soil samples were prepared in the laboratory at ambient temperature. Soil pH, organic matter, electronic conductivity and particle size distribution were analyzed according to the national standard methods in China (Agricultural Chemistry Committee of China，1983). Total concentrations of Cd, Cu, Ni, Pb and Zn in soil and rice were digested using HF-HNO_3-$HClO_4$ and HNO_3-H_2O_2, respectively. Frac-tions of heavy metals in soil were analyzed using the modified method of sequential extraction initially proposed by Tessier *et al.* (1979), in which heavy metals were participated in five fractions, including exchangeable, carbonate bound specifically adsorbed, Fe-Mn oxide bound, organic/sulphide bound and residual fraction.

The cross-correlogram was used to determine spatial correlation between heavy metals in rice and fractions of heavy metals in soil.

Results and Discussion

In this study, the carbonate bound specifically adsorbed fraction was not detected because of the acidic paddy soil. In Fig. 1, Cd was largely associated with exchangeable fraction, followed by Fe-Mn oxide fraction. The percentage of Cd in fractions decreased in the order of exchangeable > Fe-Mn oxide bound> residual >organic/sulphide bound fraction. In contrast, the fractions of Ni, Pb and Zn showed a similar

distribution and followed the order as residual>Fe-Mn oxide bound > organic/sulphide bound >exchangeable fraction; for Cu, it presented different and decreased in the order of residual > organic/sulphide bound > Fe-Mn oxide bound fraction.

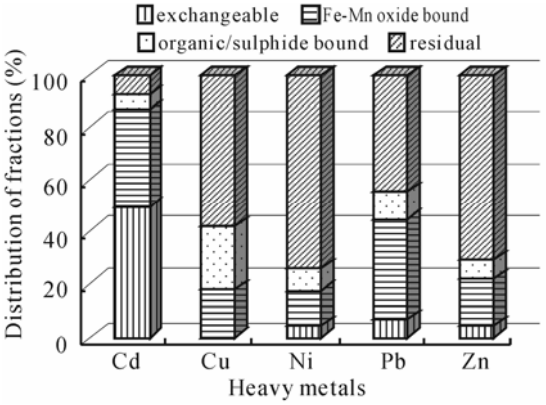

Fig. 1 Distribution of heavy metals in fractions as percentages of the total in paddy fields

Cross-correlograms were constructed to quantitatively determine the spatial relationship for each heavy metal between concentration in rice and fraction concentrations in soil. It can be observed (Fig. 2) that heavy metal concentrations in rice were positively correlated with each heavy metal fraction in soil, except that Zn in rice was negatively correlated with Zn residual fraction. Most of heavy metals in rice were strongest spatial correlated with exchangeable fraction in soil, secondly with organic/sulphide bound fraction. Cd concentration in rice was significantly (P<0.01) spatial correlated with exchangeable, organic bound and Fe-Mn oxide bound fraction, and the correlation was stronger than those of other heavy metals as r coefficients for Cd showed higher values. The cross-correlogram of Zn was similar to that of Cd. Ni in rice was significantly (P<0.01) spatial correlated with exchangeable fraction and weak correlation with organic bound fraction. No significant correlation exhibited between Ni in rice and, Fe-Mn oxide bound and residual fraction. However, Cu in rice was signi-ficantly (P<0.01) spatial correlated with organic bound fraction, while weaker with Fe-Mn oxide fraction.

It is well known that exchangeable fraction is considered as readily and potentially bioavailability so that most studied heavy metals in rice were strong correlated with this fraction (Fig. 2); residual fraction is entrapped within the crystal structure of the minerals and represents the liable fraction, thus, the correlation between heavy metals in rice and residual fraction were poor (Fig. 2). The Fe-Mn oxide fraction are commonly stable under natural condition, however, they would transfer depend on the conditions.

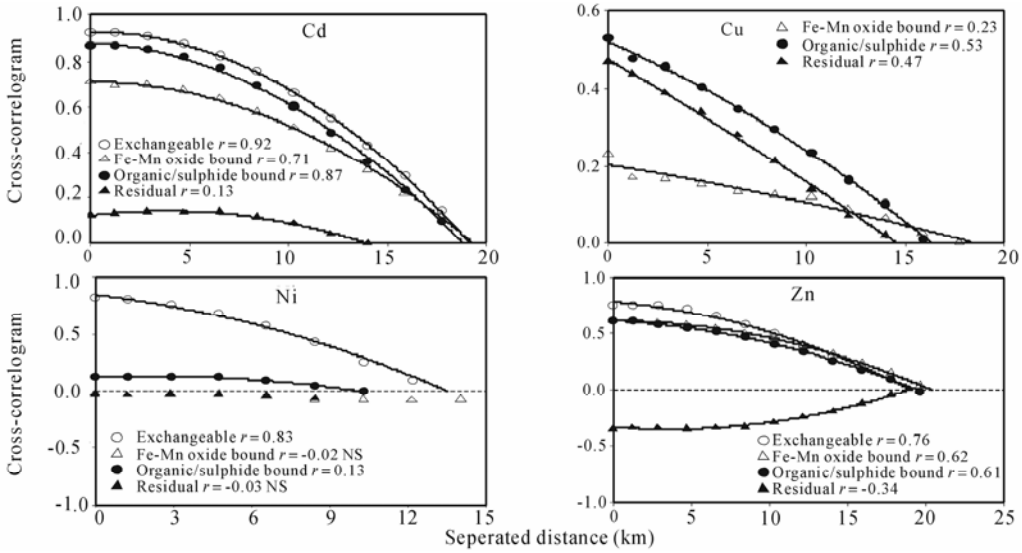

Fig. 2 Cross-correlogram between heavy metal in rice and fractions in soil. The Pearson's coefficients (r) were significant at the 0.01 level; NS means not significant

Acknowledgements

This work was supported by the National Natural Science Foundation of China (40601051), and the National Basic Research Program of China (2005CB121104).

References

Agricultural Chemistry Committee of China (1983) Conventional methods of soil and agricultural chemistry analysis. Science Press, Beijing

Tessier A, Campbell PGC, Bisson M (1979) Sequential extraction procedure for the speciation of particulate trace metals. Analy. Chem. 51: 844-851

Competitive Sorption of Nickel and Cadmium in Soils

Lixia Liao[a], Amitava Roy[b], Gregory Merchan[b], H. Magdi Selim[a,*]

[a] School of Plant, Environmental and Soil Science, Louisiana State University AgCenter, Baton Rouge, LA 70803;
[b] Center for Advanced Microstructures and Devices, Louisiana State University Baton Rouge, LA 70803.
[*]Corresponding author. Tel. No. +1 225-578-1332; Fax No. +1 225-578-1403; E-mail: mselim@agctr.lsu.edu.

Abstract: Competing ions strongly affect heavy metal retention and release in soils. In this study, we evaluated the sorption of Ni and Cd in single and binary Ni-Cd systems in three different soils; Windsor sand, Olivier loam and Webster loam. Nickel and Cadmium sorption isotherms were obtained after 24 hours of reaction and exhibited L-type patterns. Cd adsorption on the two acidic soils (Windsor and Olivier) was larger than Ni. In contrast, for Webster soil with a neutral pH, Ni sorption was larger than Cd. The Freundlich model was utilized to describe Ni and Cd adsorption isotherms. The estimates for K_f indicated that Ni sorption by the soils was significantly inhibited by the presence of Cd. Similarly, the sorption of Cd was suppressed by the presence of Ni ions. It was also found that when the added metal concentration increased in Ni-Cd system, the suppressed effect of the metal ion competition increased. Moreover, kinetic batch experiments were carried out to study Ni retention behavior. Ni sorption increased with increasing reaction time for all soils and the rate of sorption varied among soils. Desorption of Ni was hysteretic in nature, which indicated a lack of equilibrium retention and/or irreversible or slowly reversible processes. Soil samples with highest Ni concentrations were analyzed through EXAFS. The EXAFS results provided evidence of irreversible reaction for Webster soil which exhibited strongest affinity for Ni.

Keywords: Competitive sorption; Heavy metals; Kinetic sorption and XAFS

Introduction

Heavy metals are recognized as significant pollutants in soils and groundwater where they are released due to different industrial and anthropogenic activities. Since in most cases soil contamination involves several heavy metals, multi-ion sorption studies need to be investigated.

Few studies suggested that Ni may be considered as weakly bonded heavy metal when compared to others such as Pb, Cu and Hg. Specifically, Ni was observed to have low affinity in acidic soils and was thus considered mobile and susceptible to transport in soils. Under neutral to alkaline conditions, Ni was found to form multinuclear complexes on several mineral phases. Moreover, several studies indicated that Ni sorption by natural solids is time-dependent ranging from a few days to several months for quasi equilibrium to be attained (Scheidegger *et al.*, 1998). A number of sorption mechanisms are proposed to account for Ni kinetic behavior including heterogeneity of sorption sites. In this present study, two acidic soils (Olivier, Windsor) and one non-acidic soil (Webste) were selected. The main objective was to evaluate the sorption of Ni and Cd in single and binary Ni-Cd systems of different soils. Ni kinetic retention and release behavior were also quantified. Te predictive capability of a multireaction model (MRM) for describing kinetic sorption of Ni was also examined.

Material and Methods

Surface samples of two acidic soils (Windsor and Olivier) and one neutral soil (Webster) were selected in the competitive study. The pH values for Windsor, Olivier, and Webster soils were 6.11, 5.80 and 6.92,

respectively, and the respective CEC value were 2.0, 8.6 and 27.0 cmol·kg^{-1}. Additional soil properties for these soils have been reported by Buchter *et al.* (1989). Batch equilibration technique was conducted to study Ni and/or Cd adsorption in all soils. Kinetic retention by the batch method was utilized to quantify adsorption and desorption isotherms for Nickel by the three soils. The high concentration samples were then analyzed by X-ray absorption of fine structure spectra (XAFS). The XAS measurements were conducted at the Double Crystal Monochromator beamline of the Center for Advanced Microstructures and Devices (CAMD), Louisiana State University, Baton Rouge, Louisiana. CAMD operates a synchrotron at 1.3 GeV. Typical current in the ring varies from 200 to 100 mA.

Results and Discussion

Cd adsorption on the two acidic soils (Windsor and Olivier) was larger than Ni. In contrast, for Webster soil with a neutral pH, Ni sorption was larger than Cd. The Freundlich model was utilized to describe Ni and Cd adsorption isotherms through nonlinear least-square optimization. The isotherms for both Ni(II) and Cd(II) are regarded as highly nonlinear and are characterized by Freundlich $n < 1$. The value for the dimensionless reaction order n for Windsor, Olivier and Webster soil were 0.64, 0.57 and 0.55 for Cd and 0.50, 0.56 and 0.52 for Ni, respectively. These n values were within a narrow range (0.50~0.64) for all three soils and reflected the observed similarities of the overall shape of both Ni and Cd sorption isotherms. The estimated K_f indicated that Ni sorption by the soils was significantly inhibited by the presence of Cd. Similarly, the sorption of Cd was suppressed by the presence of Ni ions. It was also found that when the added metal concentration increased in Ni-Cd system, the suppressed effect of the metal ion competition increased.

For both Windsor and Olivier soil, Cd adsorption was much higher than that for Ni. This was expected because of the common view that reactions of heavy metal cations with soil minerals are related to metal-ion hydrolysis. Similar conclusion would be made if based on the hard-soft acid-base principle (HSAB). In contrast, Webster soil exhibited higher affinity of Ni than Cd. Similar adsorption preference of Ni over Cd was reported by Antoniadis and Tsadilas (2007). They considered that specific metal sorption (inner sphere complexion) was the dominant reaction for Ni sorption in their soils. A kinetic sorption study described that the adsorption of Ni was larger than Cd on hematite (Jeon *et al.*, 2003). Recently, based on new XAFS and HRTEM technique, Ni-Al layered double hydroxide (LDH) was considered to be responsible for the sorption behavior above pH 6.5 on pyrophyllite and kaolinite surface (Scheidegger *et al.*, 1996; Eric *et al.*, 2001). The EXAFS results provided evidence of irreversible reaction for Webster soil which exhibited strongest affinity for Ni. Fig. 1 reveals the presence of distinctive beat pattern at about 8.0 Å in the Webster-Ni samples. The Fourier-transforms of XAFS spectra (not showed here) showed a peak at about R≈1.8 Å which represents the first coordination shell of Ni. A second peak representing the second Ni coordination shell can be observed at R≈2.8 Å in the spectra of Ni Webster sample and moreover, the intensity of second shell peaks increased with time progressed. Evidence from fitting those data will be provided in the future.

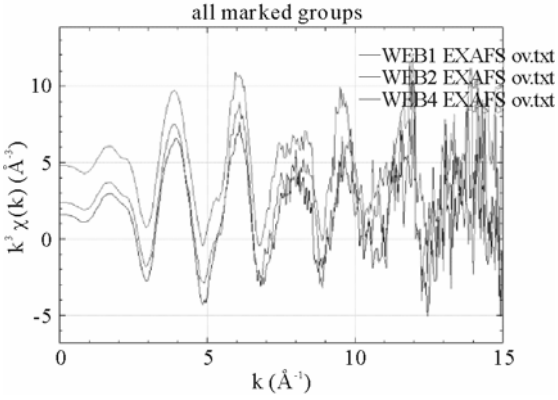

Fig. 1 EXAFS K-edge χk^3 spectra of Ni sorbed on Webster samples

The time dependence of Ni sorption and release for all concentration was illustrated in Fig. 2. For all soils, the sorption rate of Ni decreased as input concentration increased. An initial rapid uptake occurred for any input concentration, which was presented by the rapid decrease of Ni concentration. However, the rate of sorption varied for different soils. At the highest input concentration, 31% of initial Ni was sorbed in 2 hours, and this value increased to 46% after reaction of 504 h for Windsor soil. Although this is a relative large increase, the total sorption amount is small compared to the sorption for Olivier. For Olivier, Ni sorption was initially rapid

with 67% of Ni sorbed in 2 h, followed by a more gradual sorption period in which 80% of Ni was sorbed within 504 h. The kinetics for Webster were characterized by an extremely rapid initial step with nearly 91% of Ni sorbed in 2 hours, followed by a much slower sorption region where about 95% of the Ni was sorbed from the solution after reaction of 672 h. Such two-stage reaction is a characteristic of several heavy metal sorptions on clays, oxide surfaces and soils as suggested by Eric *et al.* (2001), Voegelin *et al.* (2001). Although the sorption of divalent metal ions onto oxides has been reported to be completed within few seconds (Voegelin *et al.*, 2001), slow kinetics have also been observed when sorption continued for several days or months.

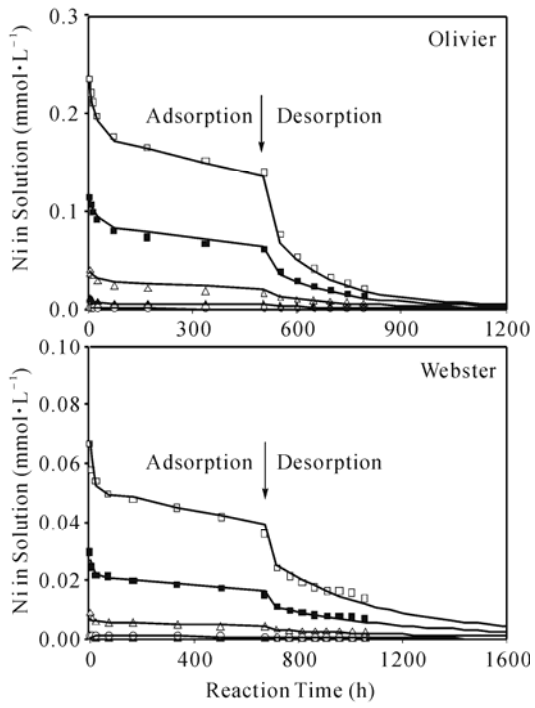

Fig. 2 Nickel concentration in solution versus reaction time for two soils. Solid lines are MRM simulations by utilizing parameters optimized from experimental adsorption data sets listed in

References

Antoniadis V, Tsadilas CD (2007) Sorption of Cadmium, Nickel and Zinc in mono- and multimetal systems. Appl. Geochem. 22: 2375-2380

Buchter B, Davidoff B, Amacher C, Hinz C, Iskandar IK, Selim HM (1989) Correlation of freundlich Kd and n retention parameters with soils and elements. Soil Sci. 148: 370-379

Eric MJ, Naprstek BR, Brady PV (2001) Kinetics of Ni(II) sorption and desorption on Kaolinite: Residence time effects. Soil Sci. 166: 11-17

Jeon B, Dempsey BA, Burgos WD (2003) Sorption kinetics of Fe(II), Zn(II), Co(II), Ni(II), Cd(II), and Fe(II)/Me(II) onto hematite. Water Res. 37: 4135-4142

Scheidegger AM, Lamble GM, Sparks DL (1996) Investigation of Ni sorption on Pyrophyllite: An XAFS study. Environ. Sci. Technol. 30: 548-554

Scheidegger AM, Strawn DG, Lamble GM, Sparks DL (1998) The kinetics of Mixed Ni-Al hydroxide formation on clay and aluminum oxide minerals: A time-resolved XAFS study. Geochimica et Cosmochimica Acta 62: 2233-2245

Voegelin A, Vulava VM, Kretzschmar R (2001) Reaction-based model describing competitive sorption and transport of Cd, Zn, and Ni in an acidic soil. Environ. Sci. Technol. 35: 1651-1657

Interaction Effect between P and K Fertilization on Faba Bean Plant (*Vicia* faba L.) Grown under Salt Affected Soils

Mohamed Rida Abd EL-Hady Mohamed Ebrahem[a,b,c,*], Adel Mohamed Abd EL-Hameed Abd EL-Mohsen[a,b,c]

[a] Plant Nutrition Dep., Soil, Water & Environment Res.Ins., Agric., Res. Center , Giza, Egypt;
[b] Cairo Univ. Street, Giza, Egypt Tel: 002025720608 – 002025725549 Fax : 002025725549 Post code : 12619 Giza, Egypt;
[c] Mansoura Lab.
[*]Corresponding author. Tel. No. 0020507498154 ; Mobile: 0020166054084; E-mail: prof.dr.mohamedrida9@gmail.com.

Abstract: Two field experiment were carried in the winter seasons of 2006/2007 and 2007/2008. To study the interaction effect of P and K fertilization on growth, yield, nodules formation, proteins%, phytic acid% and nutrients uptake of faba bean plants grown under salt affected soils. The experimental soils used represent nonsaline (2.36 $dS \cdot m^{-1}$ EC) and saline (5.6 $dS \cdot m^{-1}$ EC). The effect of three P levels (0%, 50%, 75%, 100% from recommended dose as superphosphate 15.5% P_2O_5), the foliar K levels (0%, 1%, 2% from recommended dose in the form of potassium sulphate 48% K_2O) and seeds (Skha1 cultivar) before sown inoculated by ryzobium. A split-split plot design with four replicates were used. The main findings could be summarized as follows: 1) Saline conditions decreased the plant height, No of branches/plant, seed weight/plant, 100-seed weight, seed yield (ardab/fed.), straw yield (ton/fed.) No. of nodules/plant, protein % and nutrients uptake (N, P, K $Kg \cdot fed^{-1}$) in both seasons. And the heights results were obtained from normal soils, while saline conditions increased significantly phytic acid%. 2) Adding 2% K(foliar) significantly increased all studied factors under study in both seasons except phytic acid%, where adding 1%K(foliar) casing rising values of phytic acid in both seasons. 3) 100% P treatment gave the highly significant increase in all factors in both seasons. 4) The interaction between all studied treatments on faba bean characteristics under study had a significant effect , which , the best results were obtained from the interactions of normal soils with 2% K and 100% P treatment at all studied factors except the interaction of saline soils with 0% K and 100% P gave the highest results for phytic acid%. 5) It can be noticed that , ryzobium can not act their roles well in nodules formation under saline conditions.

Keywords: Nonsaline soil; Ndulations; Phosphorus; Potassium saline soil

Introduction

It well known that soil salinity and sodicity have a detrimental effect on many plant growth and their yields. Rietz and Haynes (2003) concluded that agriculture-induced salinity and sodicity not only influences the chemical and physical characteristics of soils but also greatly affects soil microbial and biochemical properties. The aim of this work is to study the interactions effect of P and K fertilizations with inoculat-ion by ryzobium on some faba bean plant growth characteristics and yield under salt affected soils.

Materials and Methods

Two field experiments were established to fulfill the objective of present work. Two soils, represent, nonsaline (2.36 $dS \cdot m^{-1}$ EC) and saline (5.67 $dS \cdot m^{-1}$ EC) soils and pH were 7.6 and 8.1, respectively. Both soils were clayey, nonsaline containing 51.48% clay, 29.18% silt and 19.34% sand ,while, the saline soil have 55.31% clay, 26.56% silt and 18.13% sand. Available nutrients of N, P, K were: 43.12, 10.5 and 378 $mg \cdot kg^{-1}$ respectively for nonsaline soil and 31.41, 8.86 and 268 $mg \cdot kg^{-1}$, respectively, for saline soil. All analysis were determined according to Black (1965)

and Page (1982). Studied crop was faba bean plant (*Vicia Faba L.*) "Skha 1 cultivar" sown after inoculated by rayzobium at 23rd and 29th of November in the two seasons 2006/2007 and 2007/2008 in winter, respectively. The experimental plots were designed in split-split plot in complete randomized blocks. The main plots were nonsaline and saline soils. The sub plots were K fertilizer rates (0%, 1%, 2% as foliar in the form of potassium sulphate 48% K_2O), while, the sub-sub plots were P fertilization levels (0%, 50%, 75%, 100% as P_2O_5 from recommended dose in the form of superphosphate 15.5% P_2O_5). Most plant characteristics were measured after 90 days from sowing (peak of flowering). The uprooted plant in 1st and 2nd seasons were taken and dried at 70 ℃, ground in porcelain mortar, so taken for N, P, K analysis and calculated as uptake (kg·fed^{-1}). Straw yield (ton·fed^{-1}) and grain (Ardab·fed^{-1}) measured after harvesting. Proteins and phytic acids were determined in seeds. All collected data were statistically analyzed according to Gomes and Gomes (1984).

Results and Discussion

Data in Table 1 showed that, the saline conditions

Table 1 The interactions effect soil kinds with K and P fertilization on seed yield, straw yield, No of nodules, protein% and N, P, K uptake on faba bean plants in both seasons

Treatment		Seed yield ardab·fed^{-1}		Straw yield ton·fed^{-1}		No. of nodules		Protein %		N Uptake kg·fed^{-1}		P Uptake kg·fed^{-1}		K Uptake kg·fed^{-1}	
		2006/07	2007/08	2006/07	2007/08	2006/07	2007/08	2006/07	2007/08	2006/07	2007/08	2006/07	2007/08	2006/07	2007/08
A: Main(Soil)															
Salty		3.19	2.92	1.14	1.07	44.15	44.86	11.3	11.27	13.63	13.74	4.88	5.36	13.37	11.27
Nonsaline		7.04	7.25	1.89	2.12	110.08	110.93	14.74	14.63	36.79	38.17	9.57	9.99	37.65	14.63
L.S.D 5%		0.0055	0.0083	0.012	0.0041	0.039	0.0166	0.0055	0.0207	0.0166	1.2956	2.55	0.0124	0.0041	0.0207
B: Sub K															
0%		3.85	4.22	1.17	1.46	65.24	70.72	12.85	12.76	24.59	25.09	6.75	7.14	24.95	12.76
1%		5.39	5.29	1.61	1.54	79.31	79.43	13.03	13	25.11	26.21	7.27	7.62	25.65	13
2%		6.11	5.73	1.78	1.8	86.79	83.54	13.18	13.11	25.92	26.56	7.64	8.27	25.93	13.11
L.S.D 5%		0.0112	0.0054	0.0076	0.0072	0.022	0.0054	0.0059	0.0072	0.0086	0.8541	0.009	0.0061	0.0027	0.0072
C: Sub-Sub P															
0%		3.79	3.52	0.68	0.79	62.31	65.3	11.56	11.45	19.27	19.41	5.62	5.95	19.53	11.45
50%		4.7	4.63	1.25	1.37	73.65	75.02	12.57	12.6	24.54	25.09	6.7	7.33	25.22	12.6
75%		5.55	5.76	1.87	1.89	82.8	82.21	13.8	13.56	27.22	28.47	7.9	8.28	27.38	13.56
100%		6.42	6.42	2.28	2.34	89.7	89.05	14.15	14.2	29.81	30.84	8.68	9.15	29.9	14.2
L.S.D 5%		0.0084	0.0068	0.0062	0.0069	0.027	0.0088	0.0069	0.0062	0.0055	0.8668	0.006	0.0069	0.007	0.0062
A*B*C : Interactions															
salty soil	0%	0%	1.5	1.3	0.25	0.35	25.5	29.66	10.12	10.23	11.21	10.88	3.89	4.01	10.33	10.23
		50%	2.33	2.1	0.4	0.44	33.66	37.31	10.78	10.87	13.1	13.55	4.01	4.46	12.89	10.87
		75%	2.9	3.44	0.88	0.86	45.7	43.54	11.63	11.34	14.66	14.34	4.66	4.8	14.21	11.34
		100%	3.25	3.67	1.15	1.01	49.33	51.12	11.88	11.78	14.8	14.94	4.93	5.22	15.22	11.78
	1%	0%	2.76	1.88	0.55	0.46	30.35	32.47	10.35	10.31	11.37	11.23	4.21	4.08	10.88	10.31
		50%	3.1	2.25	0.87	0.89	37.18	41.21	10.91	11.1	13.54	13.66	4.78	5.21	13.09	11.1
		75%	3.83	3.15	1.73	1.1	46.81	46.56	11.73	11.91	14.11	15.34	5.11	5.66	14.87	11.91
		100%	4.1	4	2.12	1.83	56.65	52.12	12.12	12.01	14.88	16	5.33	6.01	15.44	12.01
	2%	0%	2.89	2.1	0.67	0.76	44.00	40.65	10.41	10.31	11.89	11.88	4.66	5.1	11	10.31
		50%	3.35	3.1	1.15	1.05	48.18	48.12	11.41	11.21	14.01	14.02	5.15	5.91	12.93	11.21
		75%	3.98	3.88	1.87	1.93	53.25	55.22	12	11.91	14.66	15.93	5.77	6.66	14.05	11.91
		100%	4.2	4.15	2.1	2.21	59.12	60.32	12.15	12.31	15.33	16.76	6.01	7.22	15.52	12.31

Treatment			Seed yield ardab·fed^{-1}		Straw yield ton·fed^{-1}		No. of nodules		Protein %		N Uptake kg·fed^{-1}		P Uptake kg·fed^{-1}		K Uptake kg·fed^{-1}	
			2006/07	2007/08	2006/07	2007/08	2006 /07	2007 /08	2006/07	2007 /08	2006/07	2007 /08	2006/07	2007 /08	2006/07	2007 /08
Nonsaline soil	0%	0%	3.55	4.48	0.66	0.88	79.79	88.90	12.63	12.73	26.7	26.6	6.31	6.76	26.83	12.73
		50%	4.87	5.89	1.55	2.1	85.12	97.77	13.78	13.33	33.81	34.73	8.02	8.93	35.88	13.33
		75%	5.9	6.13	2.17	2.93	96.37	105.33	15.66	15.45	39.32	40.54	10.35	10.93	40.09	15.45
		100%	6.44	6.78	2.3	3.1	106.47	112.1	16.23	16.34	43.14	45.12	11.83	12.01	44.12	16.34
	1%	0%	5.34	5.5	0.83	1.12	93.12	100.10	12.98	12.63	27.12	29.42	7.12	7.66	28.83	12.63
		50%	6.87	7.1	1.66	1.87	115.33	112.35	14.1	14.45	35.41	36.36	9.12	9.91	37.12	15.45
		75%	7.33	8.78	2.25	2.13	125.33	121.31	15.86	15.67	40.12	42.23	10.66	10.55	40.44	15.67
		100%	9.78	9.64	2.87	2.89	129.74	129.32	16.22	16.77	44.34	45.46	11.83	11.88	44.54	16.77
	2%	0%	6.67	5.88	1.1	1.18	101.12	100.00	12.8	12.5	27.33	30.1	7.52	8.1	29.3	12.5
		50%	7.66	7.36	1.88	1.87	122.32	113.35	14.44	14.63	37.38	38.23	9.09	9.55	39.4	14.63
		75%	9.33	9.15	2.33	2.36	129.34	121.32	15.91	15.1	40.44	42.46	10.83	11.05	40.64	15.1
		100%	10.77	10.25	3.13	3	136.87	0129.3	16.3	16.01	46.34	46.74	12.12	12.55	44.56	16.01
L.S.D 5%					0.0264	0.0295	0.1149	0.0287	0.0293	0.0262	0.0234	3.6777	0.0253	0.0295	0.0295	0.0262

causing significant decrease in all studied factors under study in both seasons. Soil salinity decreased seed yield , straw yield, No. of nodules and protein by 54.69%, 39.68%, 59.88% and 23.34% and by 59.72%, 49.53%, 59.56% and 22.97% in both seasons respectively. Also the uptake of N, P and K were decreased significantly with salt conditions.

In respect of adding K and P fertilizers. It is clear that adding 2% K and the treatment of 100% P gave the highest values for all studied factors in both seasons.

The interactions effect between all studied treatments on faba bean plants characteristics under study had significant decreasing effect comparing with saline soils and nonsaline soils. And the best results were obtained from the interactions of nonsaline soils with 2% K and 100% P treatment in both seasons.

It can be conclude that, ryzobium can not act their roles well in formation of nodules under saline conditions.

References

Black CA (1982) Methods of soil analysis. Part 2. American society of Agronomy, Inc. Publisher, Madison, Wisconsin, USA

Gomez KA, Gomez AA (1984) Statistical Procedures for Agriculture Research". John Willy and Sons Inc., New York, USA

Page AL, Miller H, Keeny DR (1982) Methods of Soil Analysis, part 2: Chemical and Microbiological properties. Am. Soc. Agron. Madison, Wisconsin, USA

Rietz DN, Haynes RJ (2003) Effect of irrigation-induced salinity and sodicity on soil microbial activity. Soil Biol. Biochem. 35(6): 845-854

Design of a POSS-modified Zeolite Structure and the Study of the Enhancement of Ammonia-nitrogen Removal from Drinking Water

Derong Lin[a,b], Lijiang Hu[b,*], Qun Zhang[b], Hong You[a]

[a] State Key Laboratory of Urban Water Resource and Environment, Harbin Institute of Technology, Harbin 150090, China;
[b] Chemistry Department, Harbin Institute of Technology, Harbin 150001, China.
[*]Corresponding author. Tel. No. +861-451-86412679; Fax No. +86-451-86221048; E-mail: hulijiang2008@126.com.

Abstract: In this work, the mesoporous zeolite molecular sieve (ZMS) surface was modified using polyhedral ologomeric silsesquioxane (POSS) with carboxyl sodium terminal groups ($POSS^{-COONa}$) as ion-exchange active groups. The characterization of the $POSS^{-COONa}$ structure by standard techniques (such as SEM, TEM, XRD, etc.) was investigated and discussed. With this approach, the exchange capacity of ammonia-nitrogen (NH_3-N) in water would be greatly increased. The diffusion behavior of NH_3-N in the pores of POSS-modified ZMS was calculated using a molecular dynamic simulation (MDS) program of the Materials Stutio (MS) software which facilitate to study the effect of POSS modification on pore structure and exchange capacity. The interface binding energy between $POSS^{-COONa}$ and ZMS was calculated using MDS, facilitating the study of a simple regeneration method for exchanged active groups. It was estimated that the weight of the POSS-modified ZMS could be reduced by 25% for the same 90% of NH_3-N removal rate of the normal ZMS under the same conditions. If the removal rate of the normal ZMS for a higher concentration of NH_3-N in water was 60%~70%, the removal rate of the POSS-modified ZMS could be up to 80%~90%.

Keywords: Zeolite molecular sieves (ZMS); Polyhedral ologomeric silsesquioxane (POSS); Modification; NH_3-N removal

Introduction

Water plays a very important role in every aspect of biological life and its interrelationships. With the need for rapid economic development, natural resources are exploited, and little attention is paid to the protection of water resources, leading to serious water pollution problems. The amount of NH_3-N in water body increases gradually every year. Obviously, research and technology for the NH_3-N removal and nitrate in water is urgently needed (Jorgensen *et al.*, 2003).

There are many kinds of NH_3-N wastewater treatment techniques. The most important techniques mainly include air stripping, chemical precipitation, membrane absorption, biological techniques, advanced oxidation, break-point chlorination, man-made marsh sewage disposal, catalytic-wet oxidation (Seigrist, 1996; Boardman and McVeigh, 1998; Ruiz, 2003; Zdybiewska and Kula, 1991; Soares and Silvas, 1996). There are two disadvantages in the traditional methods using ZMS to remove NH_3-N in water. First, a certain aperture diameter (AD) for ZMS or a certain zeolite microstructure must be selected due to the AD (2.86 Å) of ammonium or to protect ZMS from the interference of other particles. For example, the clinotilolite molecular sieves (CMS) AD (3~5 Å) is usually selected to remove NH_3-N from water. Second, the specific surface area of ZMS is very large (around 500~1000 $m^2 \cdot g^{-1}$), but at present the maximum adsorption can reach only 20 $mg \cdot g^{-1}$ (Wang *et al.*, 2007), which means that the adsorption efficiency of a normal ZMS is very low. A similar conclusion was also drawn from a calculated result: only a single ammonia ion can be adsorbed on each 100 $(Å)^2$ surface area by 10 Si (Al) atoms on an average

surface. The natural ZMS AD has a wide distribution, especially the most mesoporous ZMS AD (2~50 nm) which cannot be used for the treatment of NH_3-N in water and is a waste of resource.

In this paper, polyhedral ologomeric silsesquioxane (POSS) with carboxyl sodium terminal groups ($POSS^{-COONa}$) as ion-exchange active groups was selected to modify the mesoporous ZMS surface for NH_3-N removal in water. The aim of this work was to determine the enhancement scale of the NH_3-N ion-exchange in water and the regeneration using the $POSS^{-COONa}$ modified ZMS. In addition, this work also focused on the influence of the modification, the pore structure and ion-exchange treatment mechanism on the enhancement scale of the NH_3-N ion-exchange and the regeneration of the modified ZMS using a molecular dynamic simulation (MDS) program of the Materials Stutio (MS) software.

Materials and Methods

$POSS^{-COOH}$ was prepared using rice hull ash (RHA) (utilization of a waste resource) and octatetramethyl-ammonia-POSS (OTMA-POSS) as a precursor, then the $POSS^{-COOH}$ was reacted with NaOH to produce the modifier, $POSS^{-COONa}$. The structure of the $POSS^{-COONa}$ modifier was characterized with standard spectroscopic techniques: FTIR (Avatar 360), NMR (^1H, ^{13}C and ^{29}Si) (Bruker AV 400) and UV-MALDI-TOF MS (Bruker, Billerica) (Zhang *et al.*, 2008).

$POSS^{-COONa}$-modified ZMS was a result of the condensation of Si-OH in $POSS^{-COONa}$ and Si-OH in ZMS to form a relatively stable Si-O-Si bond and to produce a number of active groups (-COONa) in the surface for exchange of ions. The components of the modified ZMS were identified by an element analyzer, XRD and XPS spectrometry; the groups and the group location in the structure were determined by FTIR and NMR; the surface characterization of modified structure was characterized using SEM and TEM.

Experiments to determine the removal of NH_3-N with ZMS and the modified ZMS through static and dynamic ion-exchange methods (Wang *et al.*, 2007) were performed to determine the maximum static and dynamic saturation exchange capacity and its kinetic equation and to analyze the influences of temperature, NH_3-N concentration in the water, flow speed and other factors on the removal of NH_3-N by the modified ZMS. For the regeneration experiment, the exchange-saturated $POSS^{-COONa}$-modified ZMS was washed repeatedly using a low-concentration NaOH solution or a mixed solution containing NaOH to exchange for the NH_3-N; the regenerated modified ZMS was then dried.

The MS software used for the following three parts was reported in this work: 1) Research on ion-exchange treatment mechanism for the modified ZMS. Models of the ZMS and the modified ZMS were generated using Build Crystals and Build Surface models and were optimized using the Discover module. The adsorption process on the modified ZMS surface was simulated using the Density Functional Theory (DFT); then the adsorption mechanism was determined based on the changes in energy. 2) Influence of the $POSS^{-COONa}$ modification on the pore structure of the ZMS. Models of the ZMS pore structure before and after the modification were generated using the Amorphous Cell model and were optimized with the Discover module. The diffusion process of the NH_3-N in the pores was simulated using molecular dynamics. The diffusion coefficients were calculated from the mean-square displacement (MSD) versus the time of the NH_3-N in the pores by using the Einstein Equation. The influence of the modification on the pore structure of the ZMS was analyzed according to a change in the diffusion coefficients (Wang *et al.*, 2009) 3) Influence of the modification on a regeneration of the zeolite. The regeneration efficiency was validated by the $DMol^3$ and LST/QST modules.

Results and Discussion

$POSS^{-COONa}$ Modifier Structure

A simplified formulation of the POSS structure is $(RSiO_{1.5})_n$ (Lichtenhan, 2003). Generally, the R group linked to an Si atom is an organic active group (OH, alkylene, epoxy ring, vinyl, etc.). If R contains a carboxyl sodium group in the POSS as the active groups, the sodium ion can easily be exchanged with NH_3-N in water, and the sodium ion will not impact on the water quality when it enters into the water. Usually POSS is an oligomer containing 6~12 Si atoms, i.e., each POSS contains 6~12 active groups (assuming that each R contains only one carboxyl sodium salt group). Therefore, the activity of these POSS oligomers can be enhanced 6~12 times for the NH_3-N exchange when the mesoporous ZMS surface

is modified with POSS, and each POSS occupies at the most 100 $(Å)^2$. This process will not reduce the AD more than 20% (assuming that the ZMS AD is 10 nm) and will not affect the diffusion, adsorption and ion exchange of ammonia in the ZMS. The characterization of the $POSS^{-COONa}$ structure by some standard techniques (such as SEM, TEM, XRD, etc.) will be provided and discussed in the full paper.

NH_3-N Removal Capacity

The assumptions: 1) In the modified natural ZMS 1g with a pore diameter of 10 nm and a specific surface area of 500 $m^2 \cdot g^{-1}$, the NH_3-N removal capacity is 10 $mg \cdot g^{-1}$; 2) After modification, the ZMS weight increases to 1.4g, and the pore diameter decreases to 8 nm; 3) The specific surface area decreases to 64% with a decrease in the pore diameter. Therefore, the NH_3-N removal capacity using the modified ZMS was estimated to be $10 \times 0.34 \times 8/1.4 = 36$ $mg \cdot g^{-1}$, which was much higher than the current capacity (20 $mg \cdot g^{-1}$). The ultimate effect of the modified ZMS could increase to 27 $mg \cdot g^{-1}$, if considering the interference from other ions, water temperature, pH, etc. The weight of the POSS-modified ZMS could be reduced by 25% for the same 90% of the NH_3-N removal rate of the normal ZMS and under the same conditions. If the removal rate of the normal ZMS for a higher concentration of NH_3-N in water was 60%~70%, the removal rate of the POSS modified ZMS could be up to 80%~90% (Fig. 1).

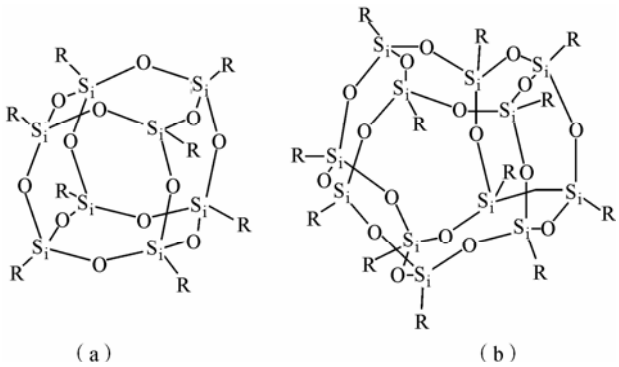

Fig. 1 POSS structures: (a) $(RSiO_{1.5})_8$ and (b) $(RSiO_{1.5})_{12}$

Conclusions

The mesoporous zeolite molecular sieve (ZMS) can be modified using polyhedral ologomeric silsesquioxane (POSS) with carboxyl sodium terminal groups ($POSS^{-COONa}$) as ion-exchange active groups. Comparing with the removal rate (60%~70%) of the normal ZMS for a higher concentration of NH_3-N in water, the removal rate of the POSS-modified ZMS can be up to 80%~90%, which seems impossible to be achieved by the current available methods.

References

Boardman GD, McVeigh PJ (1998) Use of air stripping technology to remove ammonia from biologically treated blue crab processing waste-water. J. Aquat. Food Prod. Tech. 7(4): 81-97

Jorgensen TC, Weatherley LR (2003) Ammonia removal from wastewater by ion exchange in the presence of organic contaminants. Wat. Res. 37: 1723-1728

Lichtenhan JD (2003) Economic and Commercialization of Nanostructured Hybrid Chemicals. In Organic/Inorganic Hybrid Materials. Blum FD and Laine RM (eds.), Division of Polymer Chemistry, Inc., ACS. USA, pp.17-41

Ruiz G (2003) Nitrification with hight nitrite acculnulation for the treatment of wastewater with high ammo nia concentration. Water. Res. 37(6): 1371-1377

Seigrist H (1996) Nitrogen removal from digester supernatant–Comparison of chemical and biological methods. Wat. Sci. Tech. 34(7): 399-406

Soares J, Silvas A (1996) Amonia removal in a pilot-scale wsp complex in Northeast Brazil. Water Sci. Technol. 33(7): 165-171

Wang D, Chen X, Zhang X, Liu Y, Hu L (2009) Enhancement corrosion resistance of hybrid films and its validation by gas-molecule diffusion coefficients using MD simulation. J. Sol-Gel Sci. Tech. 49(3): 293-300

Wang YF, Lin F, Pang WQ (2007) Ammonium exchange in aqueous solution using Chinese natural clinoptilolite and modified zeolite. J. Hazar. Mater 142: 160-164

Zdybiewska MW, Kula B (1991) Removal of ammonia Nitroge by the precipitation method on the example of some slected waste waters. Water Sci. Techno1. 23: 229-234

Zhang X, Hu L, Sun D, Zhao W (2008) Study of three-dimensional configurations of organic/ inorganic hybrid nanostructural blocks: A quantum chemical investigation for cage structure of (glycidoxypropyl) silsesquioxanes. J. Mol. Struc. 872: 197-204

Study on Immobilizing Soil Exogenous Lead Using Phosphate Rock

Guanjie Jiang, Hongqing Hu*, Yonghong Liu, Chang Yang, Haizheng Yang

College of Resources and Environment, Huazhong Agricultural University, Wuhan 430070, China.
*Corresponding author. Tel. No. +86-27 6205 8679; Fax No. +86-27 8728 8618; E-mail: hqhu@mail.hzau.edu.cn.

Abstract: The effect of phosphate rock (PR) on exogenous Pb fractions in yellow cinnamon soil (S1) and latosol soil (S2) were studied by Tessier's sequential extraction procedures after PR was applied into the two soils at four levels of 0, 50, 500 and 2000 mg·kg^{-1}. The results indicated that the content of exchangeable Pb in two soils decreased significantly with the rising of PR amount, which reached the minimum of 2.95 mg·kg^{-1} for yellow cinnamon soil and 3.57 mg·kg^{-1} for latosol soil under the treatment of 2000 mg P·kg^{-1} soil (PR3). Both of the residual fractions of Pb in the two soils reached the maximum under the treatment of 2000 mg P·kg^{-1} soil, 38.5 mg·kg^{-1} for yellow cinnamon soil and 66.1 mg·kg^{-1} for latosol soil. To sum up, the content of exogenous exchangeable Pb decreased and the residual fraction augmented conversely for both soils after the two soils being applied with testing PR. In conclusion, the result reflected that Pb had been immobilized effectively by PR in two tested soils.

Keywords: Immobilization; Lead (Pb) fraction; Phosphate rock; Soil

Introduction

Lead (Pb) is a highly toxic heavy metal, which can be released into the environment via numerous paths (Fisher *et al.*, 2006). The bioavailability of Pb ions can be decreased by complexation with various materials in order to decrease their toxicity (Miretzky and Fernandez-Cirelli, 2008). Pb chemical immobilization using phosphate addition is a widely accepted technique to immobilize Pb from aqueous solution and contaminated soils (Cao *et al.*, 2002). The purpose of this research was to use the low-grade phosphate rock to immobilize exogenous Pb in yellow cinnamon soil and latosol soil, providing the scientific basis for the comprehensive utilization of middle and low grade-phosphate rock.

Materials and Methods

Soil samples, collected from Zaoyang city of Hubei province and Chengmai county of Hainan province, were the top-layer (0~20 cm) of yellow cinnamon soil and latosol soil, respectively. The pH, OM, CEC, total P, available P, Pb were 5.31, 18.4 g·kg^{-1}, 21.0 cmol·kg^{-1}, 0.533 g·kg^{-1}, 20.5 mg·kg^{-1}, 28.7 mg·kg^{-1} for yellow cinnamon soil, and 4.30, 20.5 g·kg^{-1}, 9.0 cmol·kg^{-1}, 0.679 g·kg^{-1}, 3.81 mg·kg^{-1}, 27.2 mg·kg^{-1} for latosol soil, respectively. The tested PR was purchased from Huji, Jinxiang industry district in Zhongxiang city of Hubei province. The soil samples were sieved through a stainless steel screen with 0.149-mm mesh. The contents of total P, calcium, citric acid-soluble P, Pb of PR were 23.2% (P_2O_5), 38.1% (CaO), 2.6% (P_2O_5), 18.9 mg·kg^{-1}, respectively. Both yellow cinnamon soil and latosol soil were defined as Pb-contaminated soils after being treated with 200 mg·kg^{-1} Pb by adding analytically-pure $Pb(NO_3)_2$, then the two soils were adjusted to reach 20% weight water content and aged 30 d at room temperature. After 0, 50, 500 or 2000 mg·kg^{-1} PR (CK, PR1, PR2, and PR3) was applied to the two aged soils and kept for 2d, the soils were air-dried and grounded. The soils were digested with HNO_3-HCl-$HClO_4$ and the total content of Pb were determined by flame atomic absorption spectrometry (FAAS-240). The

forms of Pb were classified by Tessier's sequential extraction procedures. The determination of basic physical and chemical properties of soil was resorted to Analysis of Agricultural Soil. Total P of PR was dissolved with heated nitric acid at a ratio of 1:1, the soluble P was extracted by 2% citric acid and determined by vanadium-molybdate-yellow colorimetry. All experimental data was analyzed using Excel and SAS software.

Table 1 The content of soil exchangeable Pb ($mg \cdot kg^{-1}$) treated by phosphate rocks in two soils

Soil	Concentration of PR (mg $P \cdot kg^{-1}$)			
	0 (CK)	50 (PR1)	500 (PR2)	2000 (PR3)
S1	21.2a±0.25 (9.2%)	16.1b±0.32 (7.0%)	9.11c±0.15 (4.0%)	2.95d±0.36 (1.3%)
S2	36.5a±1.04 (16.1%)	28.9b±0.05 (12.7%)	16.4c±0.88 (7.2%)	3.57d±0.06 (1.6%)

Note: Different letters mean significant difference at 5% level. The rates of the exchangeable Pb accounted for the total content are present in the brackets

Table 2 Content of soil residual Pb ($mg \cdot kg^{-1}$) treated by phosphate rock in two soils

Soil	Concentration of PR (mg $P \cdot kg^{-1}$)			
	0 (CK)	50 (PR1)	500 (PR2)	2000 (PR3)
S1	0.44c±0.08 (0.2%)	28.3b±0.10 (12.4%)	28.3b±0.43 (12.4%)	38.5a±1.86 (16.8%)
S2	51.3b±0.69 (22.6%)	9.22c±0.52 (4.1%)	49.1b±1.05 (21.6%)	66.1a±2.86 (29.1%)

Note: Different letters mean significant difference at 5% level. The rates of the residual Pb accounted for the total content are present in the brackets

Results and Discussion

As shown in Table 1, for the CK treatment, the exchangeable Pb content in yellow cinnamon soil was 21.2 $mg \cdot kg^{-1}$, while under the PR1, PR2 and PR3 treatments they were 16.1, 9.11 and 2.95 $mg \cdot kg^{-1}$ which were 24.1%, 57.0% and 86.1% lower than that of CK, respectively. For the CK treatment of latosol soil, the content of exchangeable Pb was 36.5 $mg \cdot kg^{-1}$, while it was 28.9, 16.4 and 3.57 $mg \cdot kg^{-1}$ for the treatments of PR1, PR2 and PR3, respectively. After application of PR, on the whole, the change trend of exchangeable Pb content in the latosol soil resembled yellow cinnamon soil. However, the exchangeable Pb content in latosol soil declined much more than that in yellow cinnamon soil possibly because of the disparity of soil CEC which was higher in yellow cinnamon soil than in latosol soil. Meanwhile, the sharp difference of negative charges between the two soils owing to the distinct components of soil colloids caused difference of Pb^{2+} adsorption capacity, thereby resulting in the disparate quantities of the exchangeable Pb for two soils. This manifestation was in line with the widely accepted notion that the adsorption capacity of heavy metals in soil increased with the enhancement of soil pH, organic matter and CEC (Ma and Gade, 1999).

As shown in Table 2, the content of soil residual Pb at the treatment of CK was 0.44 $mg \cdot kg^{-1}$ in yellow cinnamon soil, and 28.3, 28.3 and 38.5 $mg \cdot kg^{-1}$ at the treatments of PR1, PR2 and PR3 respectively. After application of PR, the contents of residual Pb were 64.3 to 87.5 times that of CK for the treatments of PR1, PR2, PR3 and increased significantly in the soil. The content of residual Pb under treatments of CK, PR1, PR2 and PR3 were 51.3, 9.2, 49.1 and 66.1 $mg \cdot kg^{-1}$ in latosol soil, showing that it was lower for treatment of PR1 than that of any other treatments and there was no significant difference between the treatments of CK and PR2. The content of residual Pb reached the maximum under the treatment of PR3, which was 1.29 times that of CK. After the application of PR, the residual Pb content reached the largest amount under the treatment of PR3, in this way, the lead was effectively retained in two soils. An increasing trend for the residual Pb content was emerged in yellow cinnamon soil since the increase of PR. However, the variation trend of residual Pb in yellow cinnamon soil was different from that in latosol soil, possibly for the reason of that the

available P was extremely low in latosol soil (3.81 $mg \cdot kg^{-1}$), and there existed a competitive adsorption between Pb^{2+} and other cations in soils for treatment PR1. With regard to the pH, which in two soils increased with the amount of PR (the pH of yellow cinnamon soil were 5.07, 5.12, 5.20, 6.39 and the pH of latosol soil were 4.16, 4.24, 4.74, 5.59, for relevant treatments, respectively). Previous studies had shown that as long as hydroxyapatite was applied to soil as a major source of phosphorus, it not only provided Ca to the soils, but also enhanced soil pH (Garrido *et al.*, 2006). The dissolution of PR, whose total calcium content accounted for 38.1%, consumed H^+ for the great volume of it existed as $CaCO_3$, contributing to the increase of pH for the two soils afterwards. The higher pH was in favor of the existence of PO_4^{3-} , thereby increased residual Pb with addition of PR in two soils. The residual Pb content of CK was significantly higher than that of PR1 treatment in latosol soil. And for all the treatments except PR1, the residual Pb contents in latosol soil were higher than those in yellow cinnamon soil likely in virtue of the specific adsorption of iron, aluminum, manganese oxides and their hydrates to Pb^{2+}, the mechanism needed research in depth.

Conclusions

The content of exchangeable Pb in yellow cinnamon soil and latosol soil decreased significantly with the increase of PR applied. After application of PR, the residual Pb in yellow cinnamon soil rose markedly, and the residual Pb in the two soils reached the maximum under the treatment of 2000 mg $P \cdot kg^{-1}$ soil. To sum up, after the two soils being applied with PR, the content of exogenous Pb had been immobilized effectively in yellow cinnamon soil and latosol soil.

References

Cao XD, Ma LQ, Chen M, Singh SP, Harris WG (2002) Impacts of phosphate amendments on lead biogeochemistry at a contaminated site. Environ. Sci. Technol. 36(24): 5296-5304

Fisher IJ, Pain DJ, Thomas VG (2006) A review of lead poisoning from ammunition sources in terrestrial birds. Biol. Conserv. 131: 421-432

Garrido F, Illera V, Campbell CG, García-González MT (2006) Regulating the mobility of Cd, Cu and Pb in an acid soil with amendments of phosphogypsum, sugar foam, and phosphoric rock. Eur. J. Soil Sci. 57(2): 95-105

Ma LQ, Gade NR (1999) Aqueous Pb reduction in Pb-contaminated soils by Florida phosphate rocks. Water Air Soil Poll. 110: 1-16

Miretzky P, Fernandez-Cirelli A (2008) Phosphates for Pb immobilization in soils: a review. Environ. Chem. Lett. 6: 121-133

Long-term Fertilizer Application Alters the Balance and Vertical Distribution of Phosphorus in a Calcarosol

Dang Thanh Vu[a,c], Caixian Tang[a,*], Roger Armstrong[b]

[a]Department of Agricultural Sciences, La Trobe University, Victoria 3086, Australia;
[b]Department of Primary Industries, Victoria 3401, Australia;
[c]Institute for Soils and Fertilizers, Hanoi, Vietnam.
[*]Corresponding author. Tel. No. +61 3 9479 2184; Fax No. +61 3 9471 0224; E-mail: C.Tang@latrobe.edu.au.

Abstract: The information on the distribution of P fertiliser in soil profile would be beneficial for better P management in farming systems. The aim of this study is to investigate how the long-term application of fertiliser P affects the vertical distribution of P in the soil and P balance. Soil samples were collected from a long-term permanent P fertiliser trial and were sequentially extracted for P fractions. There was a net negative P balance over the 66 years in the nil-P and low P (3 kg P·ha^{-1}) treatments. In contrast, applying 12 kg P·ha^{-1} to each wheat crop led to a highly positive P balance of 106 kg P·ha^{-1} in this soil, resulting in P accumulation in the top 10 cm. Nil and low P application rates resulted in lower soil Pi content at 5~20 cm depth. The transformation of the residual P fertiliser into all Pi fractions suggests that the applied P had transferred into different P forms which are either readily available or sparingly available to subsequent crops.

Keywords: Calcarosol; P balance; P history; Phosphorus fractionation; Phosphorus transformation

Introduction

The low efficiency of utilization of P derived from fertiliser by grain crops contributes to most of this P being transformed into sparingly available forms that are unavailable to plants (Bertrand *et al.*, 2003; Vu *et al.*, 2008). The vertical distribution of soil P is important in P management, particularly in environments where plant production is limited by soil water deficits. Rapid drying of the soil surface resulting from high temperatures and low humidity during the growing season, prevents crops from accessing P located in the topsoil. Furthermore, subsoil P can significantly contribute to plant growth when the topsoil P has been severely depleted (Wang *et al.*, 2007). Information on the distribution of P fertiliser in soil profile would assist in the development of better P management strategies in farming systems, particularly in Mediterranean regions. This study aimed to investigate how the long-term application of fertiliser P affects the vertical distribution of P in the soil and P balance.

Materials and Methods

Soil samples were collected from a long-term permanent P fertiliser trial established in 1940 at Mallee Research Station at Walpeup in Victoria, Australia (35°07'S, 141°59'E; annual rainfall 325 mm). Soil samples were collected from the 0~5, 5~10, 10~20, 20~30 and 30~40 cm depths in 2006 using a hydraulic soil sampler. Soil samples were air-dried and sieved through a 2-mm sieve. Sub-samples were ground to pass through 0.5 mm and retained for P fractionation. Soil P fractions were sequentially extracted using a modified method of Hedley *et al.* (1982). Briefly, P was extracted by shaking 0.5 g of air-dried soil for 17 h in 30 mL of each of the following solutions: 1) H_2O; 2) 0.5 mol·L^{-1} $NaHCO_3$; 3) 0.1 mol·L^{-1} NaOH; and 4) 0.5 mol·L^{-1} H_2SO_4. The residue was digested using H_2SO_4+H_2O_2 for the

measurement of residual P fraction (Tiessen and Moir 1993). Inorganic P (Pi) in extracts was determined using the phospho-molypdate method of Murphy and Riley (1962).

Table 1 Phosphorus balance and Olsen P content of the soil after 66 years of P application. Numbers in brackets are the standard deviation of the mean

P treatment	P input ($kg \cdot ha^{-1}$)	Grain P removal ($kg \cdot ha^{-1}$)	P balance* ($kg \cdot ha^{-1}$)	Olsen P ($mg \cdot kg^{-1}$)
0 P	0	73	-73	5.1 (1.5)
3 kg $P \cdot ha^{-1}$	66	126	-64	8.7 (2.1)
12 kg $P \cdot ha^{-1}$	264	158	106	24.5 (3.4)

*P balance was calculated as the difference between the total P input and P removal by grains. All the crop residues were returned to the soils

Results and Discussion

A total of 66 and 264 kg $P \cdot ha^{-1}$ was applied to treatments with 3 and 12 kg $P \cdot ha^{-1}$ over 66 years, respectively (Table 1). The continuous depletion of P during 66 years in the nil-P plot and low P rate (3 kg $P \cdot ha^{-1}$) resulted in negative P balance. In contrast, the applying 12 kg $P \cdot ha^{-1}$ to each wheat crop led to a highly positive P balance at 106 kg $P \cdot ha^{-1}$ in this soil. The negative P balance associated with P removal by crop resulted in lower available P (Olsen P; 3.1~4.7 $mg \cdot kg^{-1}$) in plots receiving zero or 3 kg $P \cdot ha^{-1}$. In contrast, plots receiving more P than removed in grain had higher Olsen P concentrations (24.5 $mg \cdot kg^{-1}$).

Applying 12 kg $P \cdot ha^{-1}$ significantly increased all Pi fractions in the soil depth of 0~15 cm (Fig. 1). The labile P fractions (water- and bicarbonate-extractable Pi) of the soil with positive P balance increased by 3 to 5 times compared to soils with negative P balances. Similarly, P from the P fertiliser that was not utilised by the crop was transformed into less labile Pi fractions such as NaOH-Pi and H_2SO_4-Pi at concentrations 2 to 3 times greater than the treatments receiving zero or 3 kg $P \cdot ha^{-1}$. There were significantly lower concentrations of Pi in the soil layer 5~20 cm compared to the surface 0~5 cm and 20~40 cm, indicating that the crop utilized soil P in the subsurface layers when the soil was P deficient.

Similarly, Pi content was lower in the depth 5~20 cm of the soils received zero and 3 kg $P \cdot ha^{-1}$ than in the other soil depths, further indicating that where there was a negative P balance, subsoil P was depleted by plants (Fig. 1).

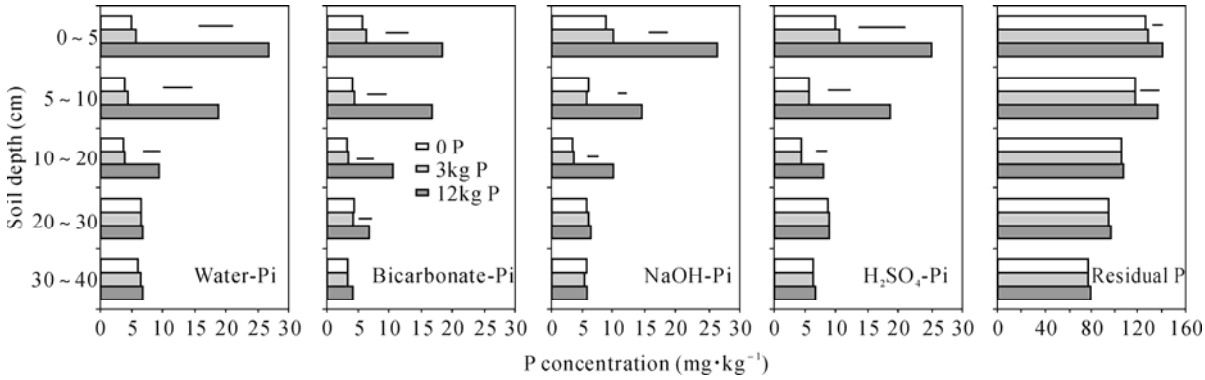

Fig. 1 The vertical distribution of inorganic (Pi) fractions of a Calcarosol following long-term (66 years) of P application. Bars represent least significant difference (LSD values at P=0.05) where the effect of P treatment is significant

The depletion of subsoil P has important implications to the contribution of subsoil P. It is evident from our study that during 66 years of crop rotations, the native P continuously contributed P to the wheat even with high grain yields in some years (data not shown). This is associated with a decrease of

all Pi fractions in the soil depth of 5~20 cm, confirming that the subsoil P is of great importance in contributing P for wheat growth in this Calcarosol soil in the semi-arid environment. It has been reported that fertiliser P rarely contribute more than 15% to 20% of P in the crop with the balance coming from the soil (Mclaughlin *et al.*, 1988).

Increases in range of Pi fractions suggests that residues from the P fertilizer eventually transform into different P forms which are either readily available or sparingly available to subsequent crops. This was consistent with previous findings that the changes of P fractions following long-term P application mainly occurred in Pi fractions such as resin-Pi, bicarbonate-Pi, NaOH-Pi and H_2SO_4-Pi (Blake *et al.*, 2003). The transformation of the applied P into the acid P pool (H_2SO_4-Pi) was due to the reactions of the applied P with the high Ca content of the Calcarosol (Bertrand *et al.*, 2003). The contribution of subsoil P to plant P uptake is probably due to the low P content in the topsoil (Richards *et al.*, 1995). However, there is evidence that the subsoil P is depleted even when P supply was sufficient in the topsoil of a black Vertosol (Wang *et al.*, 2007).

The utilization of subsoil P may also result from the greater level of moisture in deeper soil layers (compared to the soil surface) under the semi-arid conditions that characterise the Mallee. This may be further supported by the higher root length density in the subsoil compared to the surface soil in the dry growing seasons.

Conclusions

There was evidence of the accumulation of applied P in the top 10 cm and also the depletion of subsoil P by wheat grown in this soil, depending on P balance. The residual P fertiliser was transformed into all Pi fractions and residual P pool, and was in the forms that are both readily available and sparingly available to subsequent crops.

References

Bertrand I, Holloway RE, Armstrong RD, McLaughlin MJ (2003) Chemical characteristics of phosphorus in alkaline soils from southern Australia. Aust J. Soil Res. 41: 61-76

Blake L, Johnston AE, Poulton P, Goulding KWT (2003) Changes in soil phosphorus fractions following positive and negative phosphorus balances for long periods. Plant Soil 254: 245-261

Hedley MJ, Stewart JWB, Chauhan BS (1982) Changes in the inorganic and organic phosphorus fractions induced by cultivation practices and by laboratory incubation. Soil Sci. Soc. Am. J. 46: 970-976

McLaughlin MJ, Alston AM, Martin JK (1988) Phosphorus cycling in wheat/pasture rotations. I. The source of phosphorus taken up by wheat. Aust J. Soil Res. 26: 323-331

Murphy J, Riley JP (1962) A modified single solution method for the determination of phosphate in natural waters. Analyt. Chim. Acta 27: 31-36

Richards JE, Bates TE, Sheppard SC (1995) Changes in the forms and distribution of soil phosphorus due to long-term corn production. Can. J. Soil Sci. 75: 311-318

Tiessen H, Moir JO (1993) Characterisation of available P by sequential extraction. In: Carter MR (ed.) Soil Sampling and Methods of Analysis. Lewis Publishers, London pp. 75-86

Vu DT, Tang C, Armstrong RD (2008) Changes and availability of P fractions following 65 years of P application to a calcareous soil in a Mediterranean climate. Plant Soil 304: 21-33

Wang X, Lester DW, Guppy CN, Lockwood PV, Tang C (2007) Changes in phosphorus fractions at various soil depths following long-term P fertiliser application on a Black Vertosol from south-eastern Queensland. Aust. J. Soil Res. 45: 524-532

Nitrate Nutrition But Not Rhizosphere pH Enhances Zinc Hyperaccumulation in *Thlaspi caerulescens* (Prayon)

Alison C Monsant[a], Gaelle Ng Kam Chuen[a], Yaodong Wang[b], Caixian Tang[a,*]

[a]Department of Agricultural Science, La Trobe University, Bundoora, Australia;
[b]School of Botany, University of Melbourne, Australia.
[*]Corresponding author. Tel. No. +61 3 9479 2184; Fax No. +61 3 9471 0224; E-mail: C.Tang@latrobe.edu.au.

Abstract: The Zn phytoremediation potential can be improved by applying nitrate fertilizers to increase the biomass and Zn content of shoots. However, it is uncertain whether this is due to assimilation of the nitrate specifically or as a consequence of a pH increase in the rhizosphere induced by nitrate uptake. A solution culture experiment was conducted to understand the effect of nitrogen form and solution pH on Zn phytoextraction and element composition in roots and shoots of *Thlaspi caerulescens* (Prayon). The plants were grown with basal nutrients including 300 μmol·L^{-1} Zn and supplied with $(NH_4)_2SO_4$, NH_4NO_3 or $Ca(NO_3)_2$. The solutions were maintained at pH 4.5 or 6.5. The provision of NO_3^- rather than NH_4^+ was more effective at either pH 4.5 or 6.5 in maximizing Zn accumulation in the shoots. The effect of N form on Zn and Ca accumulation was confirmed to be similar. The lower concentration of N in NO_3^--fed shoots suggests that it is the N compounds within the plant, and not the quantity of N, which increased Zn tolerance and promoted hyperaccumulation in *T. caerulescens*.

Keywords: Ammonium (NH_4^+); Nitrate (NO_3^-); Phytoextraction; Solution pH; *Thlaspi caerulescens*; Zinc (Zn)

Introduction

Nitrate is more effective than ammonium for increasing Zn phytoextraction in *T. caerulescens* (Monsant *et al.*, 2008; Xie *et al.*, 2009). However, it is difficult to determine whether the N form or the pH change is responsible for enhanced Zn phytoextraction, given that a pH increase in the rhizosphere occurs in response to NO_3^- uptake (Hinsinger *et al.*, 2003). A solution culture experiment enables separation of these variables by maintaining a constant solution pH. Nitrogen uptake and metabolism are considered fundamental to the ability of plants to take up and accumulate Zn (Smirnoff and Stewart, 1987; Sharma and Dietz, 2006) although the mechanism by which N form affects Zn accumulation is uncertain. Therefore, a detailed examination of Zn and nutrient elements in response to N form and pH will contribute to our understanding of the mechanism of Zn hyperaccumu-lation in *T. caerulescens*.

Materials and Methods

A solution-culture experiment was conducted in a controlled-environment cabinet. Seedlings of *Thlaspi caerulescens* J. & C. Presl (Prayon) were grown in 5-L pots which were aerated with decarboxylated air. The experiment consisted of 6 treatments: 3 N forms (500 μmol·L^{-1} N) [NH_4^+ as $(NH_4)_2SO_4$, NH_4^+ and NO_3^- as NH_4NO_3, NO_3^- as $Ca(NO_3)_2$] and 2 pH [4.5 and 6.5] with 3 replicates. Treatments were applied from day 18 to 31 from sowing. The basal nutrients (μmol·L^{-1}) in solution were: 300 $ZnSO_4{\cdot}7H_2O$; 20 KH_2PO_4; 600 K_2SO_4; 200 $MgSO_4{\cdot}7H_2O$; 100 $CaCl_2{\cdot}2H_2O$; 1000 MES-TES; 10 FeEDDHA; 10 FeEDTA; 5 H_3BO_3; 1 $MnSO_4{\cdot}H_2O$; 0.2 $CuSO_4{\cdot}5H_2O$; 0.03 $Na_2MoO_4{\cdot}2H_2O$. The solution pH was adjusted daily and solutions replaced every second day. The average pH did not differ from the target pH by more than 0.25 units. The Ca and K concentrations were kept equivalent in all treatments by additions of $CaSO_4$ and K_2SO_4. Shoots and roots were oven-dried

at 70 °C for 48 h, finely ground and then digested in nitric and perchloric acids. The solutions were analyzed for Zn, Ca, and Mg by ICP-AES. Concentrations of N were determined with an Elementar Analyzer®. A desorption experiment was performed to determine the concentration of Zn in the root apoplasm. The roots of intact plants were washed and then submerged in ice-cold 5 mmol·L^{-1} $Pb(NO_3)_2$ for 1 h. The $Pb(NO_3)_2$ solutions were analyzed for Zn by ICP-AES. To examine the cellular localization of Zn and nutrient elements, fresh leaves were cryo-fixed, freeze-dried and then hand-sectioned to 50 µm. MicroPIXE analysis was conducted at ANSTO using a High Energy (3 MeV) Heavy Ion Microprobe with a 3-µm spot size and 0.5 ~ 1 nA beam current. A high-purity Ge detector was used. Data analyses and images were obtained with GeoPIXE software. Sample means and comparison of means were made with SPSS using one-way ANOVA post hoc multiple comparisons with the Tukey HSD test, and were performed separately for roots and shoots. Results were considered significant at the $P \leq 0.05$ level.

Table 1 Effects of N form and solution pH on a) growth and element composition and b) Zn shoot/root ratio and Zn desorption from roots. Treatments assigned different letters indicate a significant difference between the means ($P \leq 0.05$)

(a)	N treatment	Solution pH	Dry weight (mg·plant^{-1})		Zn oncentration (mg·g^{-1})		Zn content (mg·plant^{-1})		Ca concentration (mg·g^{-1})		N concentration (mg·g^{-1})	
Shoots	NO_3^-	4.5	24.56	a	12.3	b	0.30	b	15.7	bc	61.2	b
		6.5	22.03	a	17.6	a	0.39	a	23.3	a	58.7	b
	NH_4NO_3	4.5	23.53	a	5.8	d	0.14	c	7.5	d	69.3	a
		6.5	24.21	a	11.3	c	0.27	b	14.5	c	68.2	a
	NH_4^+	4.5	14.80	c	2.3	e	0.03	d	4.9	e	48.0	c
		6.5	17.28	bc	5.7	d	0.10	c	6.9	d	69.9	a
Roots	NO_3^-	4.5	7.02	a	4.0	c	0.02	d	3.2	a	51.8	b
		6.5	6.88	a	12.5	a	0.09	a	4.3	a	47.7	c
	NH_4NO_3	4.5	6.13	a	3.0	c	0.02	d	3.1	a	51.9	b
		6.5	5.37	a	9.4	b	0.07	b	3.8	a	54.5	a
	NH_4^+	4.5	2.21	b	3.1	c	0.01	d	3.5	a	not measured	
		6.5	5.36	a	8.5	b	0.05	c	3.6	a	53.7	ab

(b)	N treatment	Solution pH	Zn concentration Shoot/root ratio		Desorbed Zn(mg·g^{-1})	
	NO_3^-	4.5	3.10	a	1.4	bc
		6.5	1.42	c	3.6	a
	NH_4NO_3	4.5	1.95	b	0.7	c
		6.5	1.20	c	3.0	ab
	NH_4^+	4.5	0.76	d	0.0	c
		6.5	0.68	d	3.3	ab

Results and Discussion

Shoot dry weights of the NO_3^- and NH_4NO_3 treatments were equally higher than the NH_4^+ treatment by up to 40% and 29% at pH 4.5 and 6.5, respectively, whereas solution pH did not significantly affect shoot dry weight (Table 1a). In contrast, root dry weights were equivalent for all other treatments except for NH_4^+ at pH 4.5, probably due to ammonium toxicity. The Zn concentration in shoots which received the NO_3^- treatment was higher than shoots supplied with NH_4^+ by up to 68% at pH 6.5, and 81% at pH 4.5. Furthermore, irrespective of pH, the Zn concentration in shoots of the NO_3^- treatment was higher than NH_4NO_3 or NH_4^+. The ratio of shoot/root Zn concentrations was highest for the NO_3^--fed plants, indicating that NO_3^- increased Zn translocation while a higher proportion of Zn was retained in the roots for the NH_4^+ treatment (Table 1b). The improved phytoextraction potential of NO_3^- was evident by the Zn content for this treatment being higher than the NH_4^+ treatment by up to 75% at pH 6.5 and 89% at pH 4.5. The higher Zn concentration in roots of the NO_3^--fed plants was not a result of adsorbed Zn on the root apoplasm, since Zn desorption was similar between N forms although it was always higher at pH 6.5 than at pH 4.5. Therefore, NO_3^- enhanced Zn uptake into the root symplasm. The concentrations of Ca and Mg in the shoots and the shoot/root Ca concentration ratios (data not shown) followed the same trend as the effect of N form on Zn,

suggesting that the translocation and accumulation mechanisms of Zn, Ca and Mg are similar. Interestingly, the N concentration in shoots and roots were lower for the NO_3^- treatments, whereas solution pH had no effect on N concentration in shoots. The μ-PIXE maps indicate a strong spatial correlation between Zn and Ca in the upper and lower epidermal cells in the leaf (Fig. 1). To a lesser extent, Cl and S also spatially correlated with Zn in epidermal cells, whereas Fe and P did not.

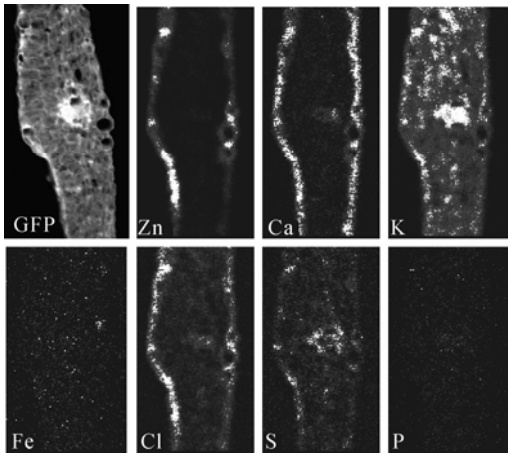

Fig. 1 Micro PIXE mapping of nutrient elements in leaves of *T. caerulescens* grown with 300 μmol·L^{-1} Zn and NO_3^- treatment

Understanding the mechanism of Zn accumulation in shoots in the model species *T. caerulescens* is important for advancing the science of phytoremediation. Shoot biomass and thus plant growth was enhanced by NO_3^- directly, and not by a preference for pH 4.5 or 6.5. This suggests that plant growth is more sensitive to N form and less sensitive to varying solution pH within the experimental range. In addition, NO_3^- resulted in higher Zn, Ca and Mg uptake into roots, translocation to shoots and accumulation in shoots. These results clearly indicate the important role of NO_3^- in Zn hyperaccumulation. The N concentration in shoots and roots were lower in the NO_3^- relative to the NH_4^+ treatment, suggesting that it is the N compounds formed within the plant, rather than the quantity of N that explain an increase in Zn tolerance and promote hyperaccumulation. These findings refocus phytoextraction research onto the mechanism of NO_3^- metabolism and its effect on Zn uptake in *T. caerulescens*. The form of N taken up, the plant species and the concentration of available N determine the assimilation within the plant, and also affect pH stat mechanisms (Raven and Smith, 1976; Hinsinger *et al.*, 2003). Thus, the potential of these N assimilatory products to complex with Zn, decrease its toxicity and increase its accumulation remains unanswered. Localisation of Zn in epidermal vacuoles is well established (Broadley *et al.*, 2006), although the μ-PIXE results presented here confirm the relationship between Zn and other element distribution in NO_3^--fed *T. caerulescens*. The interaction between Zn and Ca accumulation in response to NO_3^- should be considered together.

Acknowledgement

Helpful discussions were kindly provided by Professor A.J.M. Baker, School of Botany, University of Melbourne.

References

Broadley MR, White PJ, Hammond JP, Zelko I, Lux A (2006) Zinc in Plants. New Phytol. 173: 677-702

Hinsinger P, Plassard C, Tang C, Jaillard B (2003) Origins of root-mediated pH changes in the rhizosphere and their responses to environmental constraints: A review. Plant Soil 248: 43-59

Monsant AC, Tang C, Baker AJM (2008) The effect of nitrogen form on rhizosphere soil pH and zinc phytoextraction by Thlaspi caerulescens. Chemosphere 73: 635-642

Raven JA, Smith FA (1976) Nitrogen Assimilation and Transport in Vascular Land Plants in Relation to Intracellular pH Regulation New Phytol. 76: 415-431

Sharma SS, Dietz KJ (2006) The significance of amino acids and amino acid-derived molecules in plant responses and adaptation to heavy metal stress. J. Exp. Bot. 57: 711-726

Smirnoff N, Stewart GR (1987) Nitrogen assimilation and zinc toxicity to zinc-tolerant and non-tolerant clones of Deschampsia cespitosa (L.) Beauv. New Phytol. 107: 671-680

Xie Y, Jiang RF, Zhang FS, McGrath S, Zhao F (2009) Effect of nitrogen form on the rhizosphere dynamics and uptake of cadmium and zinc by the hyperaccumulator Thlaspi caerulescens. Plant Soil 318: 205-215

Adsorption of Phosphate and Arsenate on New Al_{13}-Oxalate Precipitate: Spectroscopic and Macroscopic Competitive Adsorption Investigations

Jing Liu[a,b,*], Fenghua Zhao[c]

[a] Department of Environment & Resource, Southwest University of Science and Technology, Mianyang 621010, China;
[b] The Key State Laboratory of Coal Resource & Mining Safety, China University of Mining and Technology, Beijing 100083, China;
[c] Department of Resource and Earth Science, China University of Mining and Technology, Beijing 100083, China.
[*]Corresponding author. E-mail: Jingliu@swust.edu.cn.

Abstract: Coprecipitates of aluminum-organics play important roles in the transport of phosphate and arsenate in soil environment. A new polynuclear aluminum organomineral precipitate (Al_{13}-Oxalate precipitate) was prepared to investigate the adsorption behavior of phosphate and arsenate on a noncrystalline aluminum precipitate. Important thermodynamic parameters of adsorption reactions were evaluated using macroscopic adsorption data and the macroscopic competitive adsorption of two oxyanions also was investigated. The result shows that the adsorption reactions basically are a diffusion process, and that phosphate has a stronger chemical interaction with substrate than arsenate. FTIR spectroscopic studies have provided evidence for the formation of two different types of phosphate complexes in substrate, protonated bidentate and deprotonated bidentate complexes at pH 4 and pH ≥6, respectively. The XPS studies indicate that the precipitate substrate can acts as Lewis acid when adsorbing two oxyanions, and that more electron transfer relative to O in the substrate occurs during adsorption of phosphate compared to that of arsenate, meanwhile surface carboxylic carbon (COO-) is involved in the complexation reaction.

Keywords: Spectroscopic study; Adsorption; Al_{13}; Complexes

Introduction

$[AlO_4Al_{12}(OH)_{24}(H_2O)_{12}]^{7+}$($Al_{13}$ for short) has been the subject of a large number of studies reviewed thoroughly in environmental, geochemical and mineralogical monographs and the literature of the past five decades (e.g. Johansson, 1960; Bersch, 1986; Hsu, 1986; Sposito, 1996; Casey, 2006). Low-molecular-mass organic acids (LMMOA), ubiquitously present in soil, sediment and water, can be secreted by plant roots and released by microogrganisms (Huang and Violante, 1986; Cristofaro *et al.*, 2000). These organic acids can format short-range ordered polynuclear aluminum organomineral precipitates with Al_{13}. They are ubiquitous in nature and are an important sink for oxyanions such as phosphate and arsenate. The study of the adsorption behavior of inorganic oxyanions on them has particular relevance to the water-solid interface process controlling transport, fate and bioavailability of oxyanions in soils and surface water system.

Materials and Methods

A. Preparation of Al_{13}-Oxalate Precipitate

Solutions mainly containing Al_{13} species were prepared by hydrolyzing 25 mL 0.25 mol·L^{-1} $AlCl_3$ with 60 mL 0.25 mol·L^{-1} NaOH, of which the base injection rate was accurately kept at 4 mL NaOH·min^{-1} by means of a peristaltic pump. When the basicity ($R=OH/Al_T$) of solution reached 2.4, the solution was stored for one day at room temperature. Al_{13}-Oxalate precipitate was synthesized by rapid addition of 70 mL 0.1 mol·L^{-1} ammonium oxalate into a conical flask containing 85 mL of 6.25×10^{-2} mol·L^{-1} total

aluminum. The gel-solution system was aged for one day, with the system pH of 7.77, and filtrated through 0.25 μm filter, and the precipitate was then washed with deionized water until the conductivity of the filtrate was less than 20 $\mu s \cdot cm^{-1}$ and free of Cl^- (by 0.1 $mol \cdot L^{-1}$ $AgNO_3$). The precipitate was air-dried and finally ground with an agate mortar and pestle.

Al_{13} sulfate crystals were synthesized by injecting 62.5 mL 0.1 $mol \cdot L^{-1}$ Na_2SO_4 solution into the above mother Al_{13} solution with a basicity of 2.4, to SO_4^{2-} Al_T^{-1} mole ratio of 1:1, the crystals were allowed to form at room temperature for two weeks.

The Al_{13}-Oxalate precipitate was digested by 1:1 HCl, and the amounts of oxalate and total Al were determined using ion chromatography (Metrohm IC792) and Ferron spectrophotometry (UNIC UV2802) at 370 nm, respectively. The specific surface of Al_{13}-Oxalate precipitates was determined by a multiple point Bruanuer-Emmet-Teller (BET). Nitrogen adsorption isotherm obtained with an AS-1C-VP Surface Area Analyzer (QUANTA Corporation, USA).

The XRD patterns of precipitates and crystals were collected using Norelco X-ray diffractometer with graphite monochromated Cu $K_{\alpha 1}$ radiation, λ=1.5418 Å, step 0.1° and 2Θ from 5 and 80°.

Infrared spectra of all samples (precipitates and absorbent) were collected by Vector 22 with a DTGS detector (Bruker Company). Pellets for IR analysis were prepared by mixing 0.5% samples with KBr. Spectra were obtained at a resolution of 0.5 cm^{-1}, and the wavenumbers were collected from 400 to 4000 cm^{-1}.

Solid-state ^{27}Al MAS NMR spectra of Al_{13}-Oxalate precipitates were acquired at 78.2 MHz on a Bruker AV-300 spectrometer with complete solid state accessories using a Doty MAS (magic angle) high spinning probe, a spinning rate of 10 kHz with single-pulse excitation, a pulse width of 0.5 s, a relaxation delay of 0.5 s. The dried precipitate sample were placed in sealed rotors (4-mm outside diameter) and spun at about 10 kHz.

The XPS studies were carried out with ESCALAB 250 photoelectron spectrometer (ThermoFisher), using an aluminum anode, operating at 90 W, and spot size was 500 μm.

B. Adsorption Experiments

Competitive adsorption experiments were conducted under three conditions, i.e. simultaneous addition and two kinds of sequential additions (either phosphate or arsenate added first). Prior to addition of phosphate and arsenate, aliquots of Al_{13}-Oxalate precipitate suspensions (2 $g \cdot L^{-1}$) were ultrasonicated for 15 min to ensure particle separation. The initial ion of both phosphate and arsenate was 40 $mmol \cdot L^{-1}$. The pH of suspensions was adjusted at 4.0 (I=0) using 0.01~1 $mol \cdot L^{-1}$ HCl solutions and the suspension was then left to reach equilibrium in a temperature-controlled water bath shaker. The pH was measured with a PHSJ-4 pH meter after the electrodes were calibrated using potassium biphthalate buffer of pH=4 and sodium and potassium phosphate buffer of pH=6.86. At appropriate times, aliquots were removed and filtered using 0.25 μm filters. The concentrations of residual anions in the supernatants were determined by hydride generation atomic fluorescence spectrometry.

Results and Discussion

A. FTIR

The IR spectra of PO_4^{3-} adsorbed on the Al_{13}-Oxalate precipitate at different pH values are shown in Fig. 1. The IR spectra of absorbed samples vary with pH. Bands occurring between 1000 and 1200 cm^{-1} are attributed to the vibration of phosphate absorbed. The adsorption band at 1151 cm^{-1} should be assigned to ν (P=O) vibration of $\equiv Al_2HPO_4$, and the intensity of this band decreases with pH increasing, which caused by variation of surface phosphate quantity. The band occurring at 1132 cm^{-1} is assigned as the asymmetric vibration ν_a(P-OAl). With increasing pH, the new shoulder occurs in 1096 cm^{-1}, which was assigned by Tejedor-Tejedor and Anderson (1990) as the ν (P-O) vibration of $\equiv Al_2PO_4$. Based on these bands, it can be proposed that upon increasing pH from 4 to 10, the predominant surface adsorption species of phosphate probably vary from protonated bidentate complex to deprotonated bidentate complex, which results in the overall symmetry of phosphate absorbed increasing (C_1 sysmmetry at pH 4; C_{2v} or C_{3v} symmetry at pH≥6), and causes the presence of band at 1096 cm^{-1}. Tejedor-Tejedor and Anderson (1990) reported that two bands at 1096 and 1044 cm^{-1} appear in IR spectra of surface iron-phosphate complexes on α-FeOOH. Rose *et al.* (1997) also reported that ν_3 vibration of monodentate mononuclear complex of Fe-PO4 occurs in 1034 and 1095 cm^{-1}. Arai and Sparks (2001)

adopted ATR-FTIR to study adsorption of phosphate on ferrihydrite (a poorly crystalline ferric mineral), and showed that inner-sphere surface complexes format during adsorption process, and the surface complexes at pH≥7.5 are nonprotonated bidentate binuclear species (Fe_2PO_4).

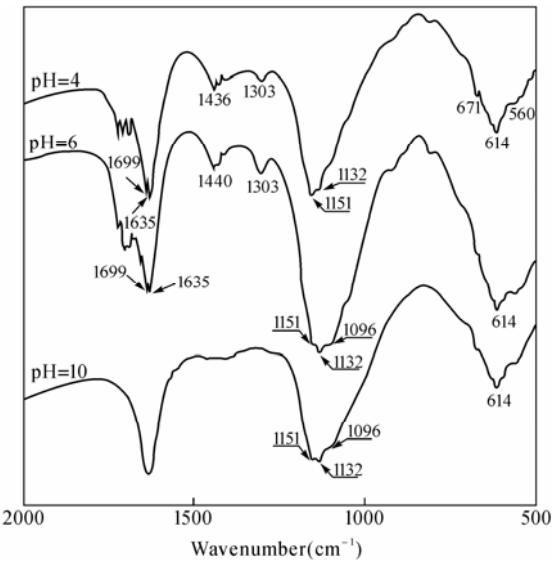

Fig. 1 FTIR spectra of phosphate (PO_4^{3-}) adsorbed on Al_{13}-Oxalate precipitate at different pH value

B. XPS

The surface adsorption of phosphate and arsenate at pH values of 4 and 10 was revealed by spectrophotometry (Fig. 2). Between pH 4 and 10 the P(2p), signals from surface decreases dramatically, the surface atomic concentration ratio of P/Al reduces from 0.65% to 0.48%; the ratio of As/Al reduces from 1.02% to 0.38%.

The oxygen charge of the original precipitate and its variation on adsorptive substrate can be calculated according to de Jong *et al.* (1994). The result indicates the obvious electron transfer occurs from original preci-pitate to adsorptive substrate during the chemisorption of phosphate and arsenate on Al_{13}-Oxalate precipitate. It can be considered that the surface oxygen of the substrate acts as Lewis acid, an electron acceptor to phosphate and arsenate admolecules.

For C(1s) core level, two peaks are identified at ≈289 and 284 eV, as illustrated in Fig. 2. Consulting the literature data (Han *et al.*, 2000; Tanner *et al.*, 2002), they can be attributed to the The peak at ≈289 eV shifts to a lower value by 1 eV after adsorption

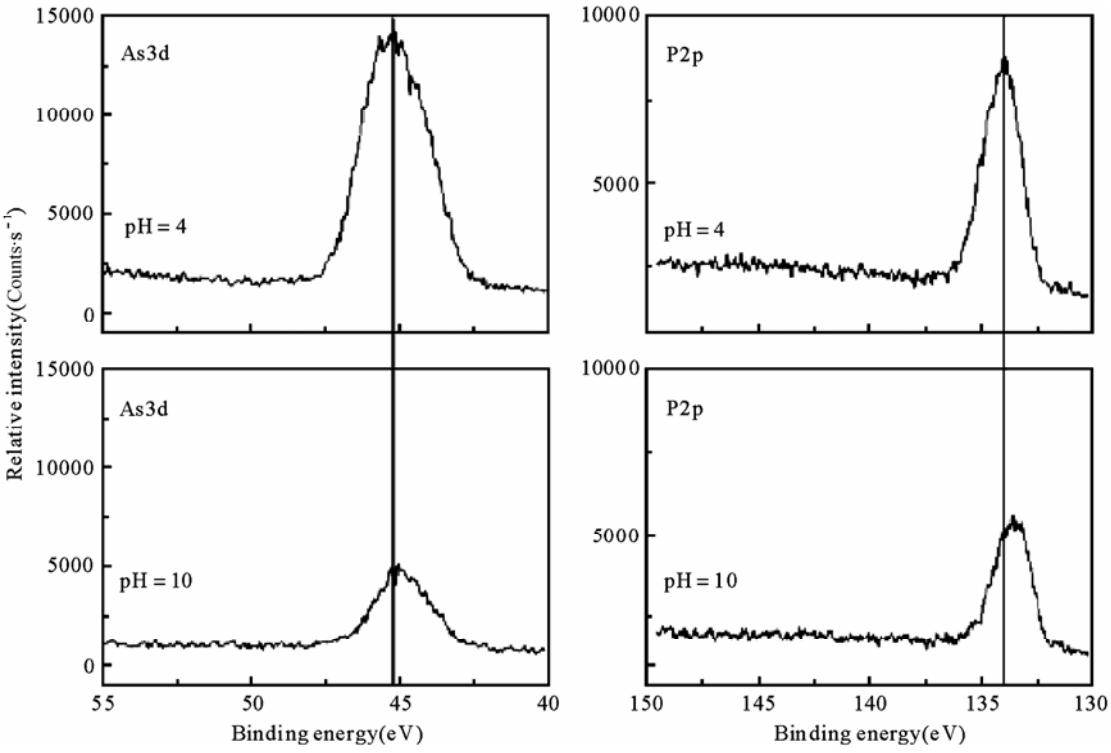

Fig. 2 As(3d) and P(2p) core level photoelectron spectra of anions adsorbed on Al_{13}-Oxalate precipitate

which implies that the formation of aromatic carbon (C-C) and carboxylic carbon (COO^-). inner-sphere complexes or chemical bonds between phosphate and surface carboxylic carbon. In contrast, the peak at 284 eV that is associated with the binding energy of the C atoms in the C-C group does not shift, indicating that the aromatic carbon (C-C) is not involved in the complexation reaction.

References

Arai Y, Sparks DL (2001) ATR-FTIR spectroscopic investigation on phosphate adsorption mechanisms at the ferrihydrite-water interface. J. Colloid Interface Sci. 241: 317-326

De Jong BHWS, Ellerbroek D, Spek AL (1994) Low-temperature structure of lithium nesosilicate, Li4SiO4, and its Li1S and O1S X-ray photoelectron spectrum. Acta Cryst. B 50: 511-518

Huang PM, Schnitzer M (1986) Interactions of Soil Minerals with Natural Organics and Microbes. Soil Science Society of America, Inc., Madisn, Wisconsin USA

Rose JM, Flank AM, Bottero JY, Masion A, Garcia F (1997) Nucleation and growth mechanisms of Fe oxohydrides in the presence of PO43- ions. Langmuir 13: 1827-1834

Sparks DL (1998) Soil physical chemistry 2nd ed. CRC press, Boca Raton, Fla

Spositio G (1996) Environmental chemistry of aluminum 2nd ed. CRC Press Inc., Florida in America

Tejedor-Tejedor MI, Anderson MA (1990) Protonation of phosphate on the surface of goethite as studied by CIR-FTIR and electrophoretic mobility. Langmuir 6: 602-611

Short-term Changes of pH Values and Aluminium Activity in Acid Soils after the Application of Nitrogen Fertilizers

Hejie Pi, Qingru Zeng*, Zhaohui Jiang, Jianyu Liao, Xiaoyou Feng, Yulin Sun

College of Resources and Environment, Hunan Agricultural University, Changsha 410128, China.
*Corresponding author. Tel. No. 86-0731-4673620; Fax No. 86-0731-4519180; E-mail: qrzeng@163.com.

Abstract: Laboratory experiments were conducted to investigate the effects of nitrogen fertilizers on the soil pH, Al activity and Al phytotoxicity in 3 acidic soils. The results showed that application of urea and ammonium carbonate caused a significant increase in soil pH, and enhanced with the raising concentrations. However, application of ammonium sulfate induced a distinct decrease in soil pH. Moreover, application of urea and ammonium carbonate caused a profound decline in soil' exchangeable Al. In contrast, application of ammonium sulfate induced a noticeable increase in soil' exchangeable Al, and reinforced with the enhanced concentrations when compared with the no-fertilizer control. In our study, urea and ammonium carbonate significantly decreased exchangeable Al in acid soils, therefore reduced Al toxicity to maize seedlings. On the contrary, ammonium sulfate enhanced Al toxicity to maize seedlings and inhibited their growth.

Keywords: Al toxicity; Exchangeable Al; Nitrogen fertilizers; Soil pH

Introduction

Red-yellow soils of south China have a soil-forming process with disilication and high Al, and in this region, pH ranges from 4.5 to 6.0, while soil's exchangeable Al accounts for 20%~80% of total exchangeable cations. In this circumstance, crop yield and quality can be greatly affected. Assuming that soil pH values are under a certain threshold, free Al ions are easily detected and they can influent growth process of plants at the organ, tissue and molecular levels (Ryan *et al.*, 1993). The objective of this study was to investigate the effects of nitrogen fertilizers on soil pH, contents of exchangeable Al, and growth of maize seedlings.

Materials and Methods

Three different soils were collected form A horizons of red soils in Hunan province, southern China, with soil pH of 4.64, 5.00 and 4.54, respectively. Twenty grams of air-dried soil was placed into 250-mL flasks. Three nitrogen fertilizers (urea, ammonium sulfate, ammonium carbonate) were incorporated at the application rates of 0, 5, 10, 20 and 40 $mmol \cdot kg^{-1}$. Flasks were incubated at 80% water-holding capacity and at 25 ℃ for 7 days. Following incubation, three replicated samples were allowed to determine the pH, while the other three replicated samples were extracted by 100 mL of 1 $mol \cdot L^{-1}$ KCl solution for exchangeable Al analysis.

Twenty grams of soil 3 had been previously treated with fertilizers (urea, ammonium sulfate, ammonium carbonate) at 20 $mmol \cdot kg^{-1}$ for a week and subsequently extracted with 1 $mol \cdot L^{-1}$ KCl solution at a 1:5 soil:water ratio. 10 mL of the KCl-extractions was mixed with 190 mL of aerated nutrient solutions which consisted of 4 $mmol \cdot L^{-1}$ KNO_3, 1 $mmol \cdot L^{-1}$ KH_2PO_4, 1 $mmol \cdot L^{-1}$ $MgSO_4$, and 1 $mmol \cdot L^{-1}$ $CaCl_2$. Controls were maintained by using 10 mL of the KCl solution mixed with 190 mL of aerated nutrient solutions. Forty uniform maize seeds (*Zea mays* L. cv. Jing 8) were placed on each tray and incubated with a 9-h day length, 25 ℃ temperature and 80% relative humidity. After 3 days of sowing, the root length and weight, shoot height and weight of each seedling were measured.

Table 1 Changes in soil pH induced by application of different nitrogen fertilizers at application rates of 0, 5, 10, 20 and 40 mmol·kg^{-1} for one week

Fertilizer types	Soil types	Fertilizer concentration (mmol·kg^{-1} soil)				
		0	5	10	20	40
Urea	Soil 1	4.64a ± 0.21	5.15b ± 0.14	5.63c ± 0.17	5.79c ± 0.11	6.88d ± 0.15
	Soil 2	5.00a ± 0.17	5.13a ± 0.09	5.39b ± 0.23	6.27c± 0.13	7.18d ± 0.22
	Soil 3	4.54a ± 0.11	4.82a ± 0.16	5.14b ± 0.14	5.82c ± 0.16	7.06d ± 0.14
Ammonium sulfate	Soil 1	4.64a ± 0.19	4.38b ± 0.07	4.29b± 0.11	4.20b± 0.14	4.11b± 0.15
	Soil 2	5.00a ± 0.12	4.26b ± 0.14	4.16b ± 0.18	4.06b ± 0.08	3.95c ± 0.09
	Soil 3	4.54a ± 0.13	4.40a ± 0.16	4.36a ± 0.09	4.25a ± 0.12	4.15b ± 0.16
Ammonium carbonate	Soil 1	4.64a ± 0.18	4.96b ± 0.23	5.24c ± 0.16	6.09d ± 0.21	7.92e ± 0.31
	Soil 2	5.00a ± 0.11	5.08a ± 0.15	5.18a ± 0.12	5.94b ± 0.24	7.77c ± 0.22
	Soil 3	4.54a ± 0.14	4.57a ± 0.17	5.03b ± 0.20	6.06c ± 0.15	7.89d ± 0.18

Means with the same letter are not significantly different at the 5% level using Duncan's multiple range test

Results and Discussion

Changes in soil pH induced by application of different nitrogen fertilizers are presented in Table 1. In all soils, pH raised with application of urea and ammonium catbonate, but declined with application of ammonium sulfate as compared with the controls. Given that urea and ammonium carbonate consume hydrogen ions (H^+) during hydrolysis, which in turn increase soil pH (Kissel *et al.*, 1988). However, ammonium sulfate is reported to be an acidifying fertilizer and release hydrogen ions during nitrification (Zhang *et al.*, 2002), therefore, a decrease in soil pH occurred. In addition, it seems that pH changes correlated highly with fertilizer concentrations. Generally, pH increased with increasing concentrations of urea and ammonium catbonate, but reduced with raising concentrations of ammonium sulfate application in all soils.

Changes in soil exchangeable Al are presented in Table 2. It is clear that exchangeable Al decreased in the urea and ammonium catbonate treatments, while increased in the ammonium sulfate treatment as compared with the controls. The concentration of exchangeable Al correlated closely with fertilizer concentrations. The negative relationship between soil pH and exchangeable Al demonstrated that exchangeable Al can be effectively controlled through altering soil pH by application of urea and ammonium carbonate. In addition, the hydrolisis of urea and ammonium carbonate can raised soil pH, thus most of the exchangeable Al in soils precipitated as insoluble gibbsite. Furthermore, when the soil pH exceeds 8.2, exchangeable Al in soil solutions will precipitate carbonate ions (CO_3^{2-}).

The effects of different nitrogen fertilizers on the growth of maize seedlings are presented in Fig. 1. Root and shoot length were expressed as seedlings elongation growth. Root weight and shoot weight were expressed as seedlings biomass accumulation. It is obvious that in the urea and ammonium carbonate treatments the growth indexes of maize seedlings obtained were higher than in the control. On the contrary, the growth indexes were lower in the ammonium sulfate treatment than in the control. Pronounced symptoms of Al toxicity detected in the maize seedlings in ammonium sulfate treatment. Many studies have implied that the inhibition of root apical elongation and division is the most visible symptom of Al toxicity in plants (Kinraide *et al.*, 1992), which was further supported by our experiment.

Table 2 Changes in soil exchangeable Al (μg·g^{-1} dry soil) induced by application of different nitrogen fertilizers at application rates of 0, 5, 10, 20, and 40 mmol·kg^{-1} for one week

Fertilizer types	Soil types	Fertilizer concentration (mmol·kg^{-1} soil)				
	types	0	5	10	20	40
Urea	Soil 1	293a ± 20.5	244b ± 16.3	182c ± 9.86	158d ± 10.2	86e ± 6.64
	Soil 2	387a ± 13.7	301b ± 19.1	267c ± 13.2	131d ± 7.53	20e ± 3.41
	Soil 3	341a ± 11.4	325a ± 24.7	203c ± 15.5	82d ± 6.31	31e ± 2.26
Ammonium sulfate	Soil 1	293a ± 18.1	350b ± 21.4	378b ± 24.1	386b ± 18.5	488e ± 31.7
	Soil 2	387a ± 15.6	389a ± 18.5	462c ± 20.8	508d ± 26.7	589e ± 36.2
	Soil 3	341a ± 24.1	367a ± 13.6	446c ± 27.3	448c ± 21.9	454c ± 24.9
Ammonium carbonate	Soil 1	293a ± 12.8	270a ± 17.7	160c ± 14.7	49d ± 5.11	43d ± 3.87
	Soil 2	387a ± 28.9	370a ± 27.2	215c ± 16.2	113d ± 7.32	79e ± 5.26
	Soil 3	341a ± 18.2	276b ± 16.8	172c ± 12.4	46d ± 4.05	16e ± 2.02

Means with the same letter are not significantly different at the 5% level using Duncan's multiple range test

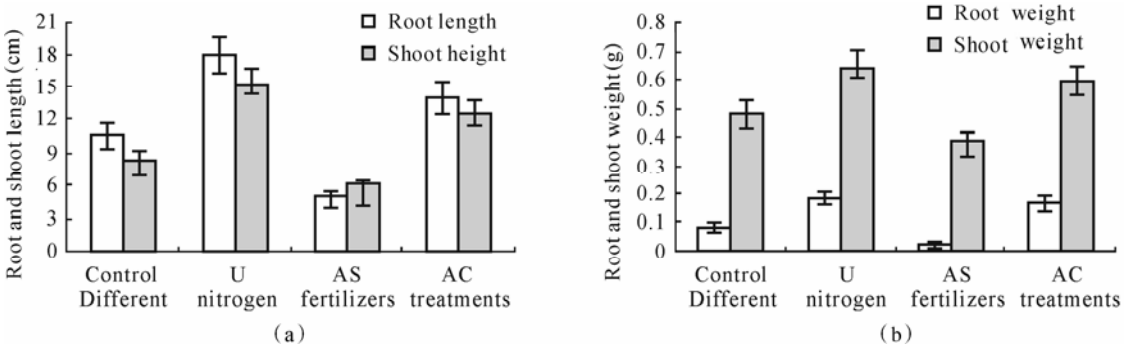

Fig.1 The growth of maize plants with changes of Al toxicity induced by application of different nitrogen fertilizers (U=Urea, AS=Ammonium sulfate AC=Ammonium catbonate)

Acknowledgements

We thank the National Natural Science Foundation of China (Grant No. 30770389) for funding this research.

References

Kinraide TB, Ryan PR, Kochian LV (1992) Interactive effects of Al^{3+}, H^+ and other cations on root elongation considered in terms of cell-surface electrical potential. Plant Physiol. 99: 1461-1468

Kissel DE, Cabrera ML, Ferguson RB (1988) Reactions of ammonia and urea-hydrolysis products with soil. Soil Sci. Soc. Am. 52: 1793-1796

Ryan PR, Ditomaso JM, Kochina LV (1993) Aluminum toxicity in roots: An investigation of spatial sensitivity and the role of the root cap. J. Exp. Bot. 44: 437-446

Zhang SL, Yang XY, Lu DQ, Tong YA (2002) Effect of soil moisture, temperature and different nitrogen fertilizers on nitrification. Acta Ecol. Sin. 22: 2147-215

Transformation of Nitrogen and Its Effects on Metal Elements by Coated Urea Application in Soils from South China

Zhaohui Jiang[a,b], Qingru Zeng[a,*],Hejie Pi[a], Bohan Liao[a], Xiaoyou Feng[a], Yulin Sun[a]

[a] College of Resources and Environment, Hunan Agricultural University, Changsha 410128, China;
[b] College of Chemical and Biological Engineering, Changsha University of Science and Technology，Changsha 410004, China.
[*]Corresponding author. Tel. No. 86-0731-4673620; Fax No. 86-0731-4519180; E-mail: qrzeng@163.com.

Abstract: This paper studied the transformation of N and its effects on metal elements under supply of two types of urea. The results showed that hydrolysis rate of coated urea was lower than common urea. After 48 days incubation, the concentrations of NH_4^+ and NO_3^- in soil were greater by coated urea application than that by common urea application. Urea application decreased in the first week, and then increased the concentrations of Al, Mn and Ca while the effect of treatment on soil pH followed the opposite pattern. In pH 4~8, concentrations of these elements were negatively correlated with soil pH.

Keywords: Coated urea; pH; Peak value; Metal element

Introduction

Urea is the most common fertilizer used in agriculture. However, it has been estimated that loss of fertilizer N ranges from 20% to 80% of the applied N (Hargrove and Kissel, 1979). Controlled release fertilizers have been shown to reduce N loss, thereby increase fertilizers efficiency, and decrease environmental pollution (Martin, 1997). Up to date, controlled release fertilizers have been studied intensively worldwide. Whereas research has focused on the development and application effects of new controlled release fertilizers, the environmental impacts have been neglected (Shoji and Kanno, 1994; Shaviv and Mikkelsen, 1993). Following urea hydrolysis, hydrogen ions are consumed and successively soil pH increases. On the contrary, hydrogen ions are produced and consequently soil pH decreases during the follow-up process of nitrification. These changes of soil pH might cause changes in bioavailabilty of soil elements. The information on quantitative relationships between soil pH and contents of exchangeable elements during a short-term of fertilizer application is limited. Moreover, environmental effects of N losses focused on soils with rice, wheat and maize growth in the literature, while studies on horticultural soils are largely ignored. Nitrogen leaching is closely linked to N form. Therefore, in this incubation experiment, we studied the transformations of common urea and coated urea in two different types of soils, and how the N transformation affected the bioavailability of three majore elements.

Materials and Methods

Two different soils were used. One was collected in vegetable garden alluvial soil (Soil 1), and the other was vegetable garden red soil (Soil 2). They were collected from A horizon of vegetable gardenl in Hunan Province, southern China. The physical-chemical properties of soils tested are listed in Table 1. Fertilizers used were common urea (46.0% N content) and coated urea (25.5% N content). 20 g air-dried soil was added into a series of 250-mL flasks. Each received the amount of urea equivalent to 0.30 g $N \cdot kg^{-1}$ soil, thoroughly mixed, and then moistened to 200 g

water·kg^{-1}, which represents the moisture levels under field conditions. Soils treated with urea were incubated at room temperature (25 ℃) At 0, 1, 2, 3, 4, 5, 6, 7, 8, 9, 14, 23, 33 and 48 days after urea application, three replicated soils were sampled for pH measurement and the other three samples were extracted by 1 mol·L^{-1} KCl solutions. The extracts were then filtered and analyzed for urea residues, NH_4^+, NO_3^-, and exchangeable Al, Mn and Ca.

Results and Discussion

The common urea was quickly hydrolyzed in both soils, approximately finished 5 days after application. However, the coated urea was hydrolyzed slowly, which took up to 14 days to complete. Urea hydrolysis can induce high soil pH (Table 2). The

Table 1 The basic physical - chemical properties of sample soils

Soil types	pH	OM (g·kg^{-1})	CEC (cmol·kg^{-1})	Available N (mg·kg^{-1})	Urease activity (mg·kg^{-1}·h^{-1})
Soil 1	5.78	24.30	8.92	112	45.92
Soil 2	5.50	18.69	11.03	91	30.72

Table 2 The changes in soil pH after urea application to an alluvial soil (Soil 1) and a red soil (Soil 2)

Soil types	Fertilizers types	Time after treatment(days)								
		0	3	5	7	9	14	23	33	48
Soil 1	Common urea	5.78a±0.12	7.25a±0.08	7.99a±0.16	7.83a±0.10	7.69a±0.23	7.51a±0.13	6.76a±0.12	5.8a±0.16	4.65a±0.07
	Coated urea	5.78a±0.15	6.11c±0.13	6.76c±0.12	7.24b±0.14	7.44a±0.16	7.25a±0.15	6.43a±0.15	4.94b±0.13	4.2b±0.05
Soil 2	Common urea	5.5a±0.14	6.72b±0.21	6.88b±0.11	6.76c±0.20	6.54b±0.14	6.14b±0.21	4.68b±0.09	4.34c±0.07	4.2b±0.07
	Coated urea	5.5a±0.11	5.82c±0.15	6.1c±0.22	6.45c±0.15	6.62b±0.22	6.28b±0.13	4.78b±0.06	4.37c±0.06	4.12b±0.06

Each value is the mean of three replicates ±s.d, Means followed by a common letter, at the same time after application, are not significantly different at the 5% level by Duncan's multiple range test

results showed that in both soils, the pH peak occurred on the 5th day after common urea application, and this coincided with the urea hydrolysis. In comparison, the pH peak appeared on the 9th day following coated urea used, and this did not correspond to urea hydrolysis. This might be that the nitrification started to occur in the coated urea treatments after 9 days, which counteracted pH increase and thus pH peak was lower than that in the common urea treatment. In Fig. 1, ammonium concentration increased to maximum at Day 6~8 for common urea, and then declined. By day 48, ammonium content was higher than the initial value, but the differences was not significant. On the other hand, ammonium increased slowly with coated urea treatments, reached the maximum at Day 14, and the peak value was lower than in the common urea treatments. In this case ammonia volatilization was inhibited. As respect to day 48, ammonium content in the coated urea treatments were higher than in the common urea treatments. Nitrate concentration increased slowly in the original phase. In the alluvial soil, nitrate increased quickly over 23 days and by day 48, the amount of nitrate in soil reached 70% of the applied nitrogen. In the red soil, nitrate increased quickly over 14 days and by day 48, 80% of the applied nitrogen was converted to nitrate. These data corresponded to soil pH change: the soil pH decreased

slowly during the initial 23 days after fertilizers applied in the alluvial soil. In contrast, the soil pH decreased faster in the red soil. However, irrespective of soil types, during the initial 33 days after fertilizer application, the nitrification rate in the coated urea treatments was lower than that in the common urea treatments. This resulted in more ammonium present in the coated urea treatments and hence reduced the risk of nitrate leaching. After 33 days, the nitrification rate in thr coated urea treatments increased quickly. By 48 day, the amount of nitrate in the coated treatments were greater than in the common urea treatments, and the total amount of nitrate and ammonium in the coated treatments was recovered over 90%, more than that in the common urea treatments which was measured approximately 80%. Table 3 showed that the effects of urea application on exchangeable Al, Mn and Ca followed the same trend. The exchangeable fraction of each element initially decreased as the pH value increased, and then increased with pH decrease. The contents of exchangeable Al, Mn and Ca correlated negatively with pH. Aluminium was the most affected element by the pH. When the pH increased to over 7.0, there was just a little exchangeable Al in soil. Calcium was least affected. However, the concentrations of exchangeable Mn were generally lower in the common urea treatments than those in the coated urea because the peak pH of the common urea treatment was greater.

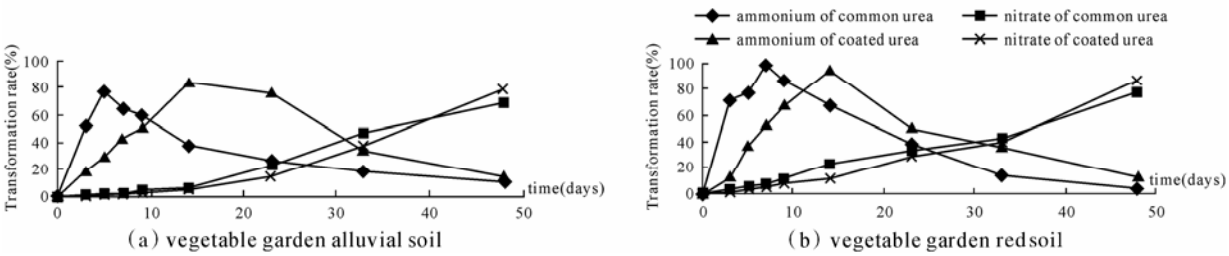

Fig. 1 The concentrations of ammonium and nitrate in soils after two types of urea was applied at 0.30 g N·kg^{-1} soil

Table 3 Contents of extractable Al, Mn and Ca (mg·kg^{-1} soil) in the vegetable garden alluvial soil after two types of urea was applied at 0.30 g N·kg^{-1} soil

Elements	Fertilizers types	Time after treatment (days)								
		0	3	5	7	9	14	23	33	48
Al	Common urea	8.54b±0.18	2.78d±0.10	0.00g±0.00	0.77f±0.06	0.93f±0.08	1.86e±0.12	4.55c±0.36	8.2b±0.24	18.74a±0.71
	Coated urea	8.92c±0.46	7.42c±0.51	2.50d±0.21	1.31df±0.12	0.00f±0.00	0.41f±0.03	6.62c±0.26	29.3b±0.96	36.2a±0.86
Mn	Common urea	23.1b±0.45	7.3df±0.12	0.5g±0.06	1.5g±0.08	5.6f±0.21	6.7f±0.32	8.9d±0.25	13.3c±0.61	30.6a±0.83
	Coated urea	23.9b±0.38	21.3c±0.56	17.3d±0.27	13.9f±0.18	11.8f±0.26	11.9f±0.35	12.7f±0.24	25.8b±0.55	32.2a±0.76
Ca	Common urea	1111a±50.3	1058bc±41.2	977c±33.5	985bc±41.2	1028b±46.7	1051b±51.2	1077ab±36.2	1102ab±42.7	1198a±60.1
	Coated urea	1046ab±33.8	1009ab±38.1	996ab±34.2	962bc±26.1	950bc±22.5	911c±28.6	1001abc±27.6	1089a±33.9	1102a±40.5

Each value is the mean of three replicates ±s.d, Means followed by a common letter, at the same time after application, are not significantly different at the 5% level by Duncan's multiple range test

Acknowledgements

We thank the National Natural Science Foundation of China (Grant No. 30770389) for funding this research.

References

Hargrove WL, Kissel DE (1979) Ammonia volatilization from surface applications of urea in the field and laboratory. Sci Soc. Am. J. 43: 359-363

Martin ET (1997) Controlled-release and stabilized fertilizers in agriculture. Paris: The International Fertilizer Industry Association, pp.47-53

Shoji S, Kanno H (1994) Use of polyolefin-coated fertilizers for increasing fertilizer efficience and reducing nitrate leaching and nitrous oxide emissions. Fert. Res. 39: 147-152

Shaviv A, Mikkelsen RL (1993) Slow release fertilizers to increase efficiency of nutrient use and minimize environmental degradation. A review. Fert. Res. 35: 1-12

Impacts of Copper on Rice Growth and Yield as Affected by Pig Manure

Jianjun Wu*, Xiuling Yu, Zaffar Malik, Hao Chen, Jianming Xu*

Zhejiang Provincial Key Laboratory of Subtropical Soil and Plant Nutrition, Hangzhou 310029,
College of Environment and Natural Resource Sciences, Zhejiang University, Hangzhou 310029, China.
*Corresponding author. Tel. No. +86-571 8697 1955; Fax No. +86-571 8697 1955;
E-mail: wujianjun@zju.edu.cn and jmxu@zju.edu.cn.

A**bstract:** A pot experiment was conducted to investigate the impacts of copper (Cu) on rice growth and yield grown in artificially Cu-contaminated paddy soil amended with 0%, 1% and 3% manure. Results showed that low level of Cu (i.e. 200 mg·kg^{-1}) at 0% and 1% manure increased number of tillers significantly, while high levels of Cu (i.e. 600 and 800 mg·kg^{-1}) caused significant reduction. Addition of 3% manure significantly decreased number of tillers at 100 and 800 mg·kg^{-1} of Cu but increased obviously at 200 and 400 mg·kg^{-1}. The average grain yield decreased along with increasing Cu levels at 0% manure and 30%~72% reduction was observed at 400~800 mg·kg^{-1}. Grain yield was increased by 1% manure at 100, 200 and 400 mg·kg^{-1} but decreased by 38% and 41% at 600 and 800 mg·kg^{-1} compared to the control. In contrast to 0% and 1% manure, average grain yield for 3% manure was lowest at 100 and 200 mg·kg^{-1}, while it was highest at 600 mg·kg^{-1} compared to the corresponding control. Concentrations of Cu in rice grains increased with the increase of soil Cu levels at 0% manure, whereas application of 1% and 3% manure substantially decreased Cu contents in the grains and the effect of 3% manure was more remarkable. The results also showed that manure application decreased the amount of DTPA-extractable Cu and reduced Cu bioavailability, which resulted in the reduction of Cu uptake by rice.

Keywords: Paddy rice; Copper; Pig manure; DTPA-extractable Cu

Introduction

Copper is an essential micronutrient for plants but can be toxic at higher concentrations. High levels of Cu were found to inhibit the normal growth and development of plants. The uptake of Cu by plants and its translocation to upper parts especially to grains in several major crops are directly related to human health. Application of manure serves as a means of nutrients in the form of N, P, and K and organic matter, resulting in increased crop growth and production. Manure also decreases heavy metal bioavailability by transforming them into fractions associated with organic ligands (Walker *et al.*, 2004). The objective of this study was to investigate the phytotoxic effect of Cu on rice growth and yield when applied to the soil with different rates of Cu and pig manure. Moreover, interactions between copper and pig manure were also assessed for their impacts on rice growth and yield.

Materials and Method

To study the effect of Cu on rice growth and yield as affected by manure, a pot experiment was conducted. Soil was collected from uncontaminated paddy rice-growing area in Jiaxing, and pig manure was collected from Huzhou, Zhejiang Province, China. The pH of the soil was 5.71, whereas pH and EC of the manure were 7.54 and 2.85 dS·m^{-1}, respectively. Soil contained 40.9 mg·kg^{-1} of Cu, 2.59 g·kg^{-1} total N, 31.3 g·kg^{-1} of OM, and 16.6 cmol·kg^{-1} of CEC with available P and K of 21.9 and 141.9 mg·kg^{-1}, respectively. The sand, silt and clay contents of the soil were 24.7%, 53.1% and 22.2%, respectively.

Manure had Cu content of 376 mg·kg^{-1}, OC 346 g·kg^{-1}, and total N, P, and K of 27.3, 9.99, and 9.08 g·kg^{-1}, respectively. Copper in the form of $CuSO_4 \cdot 5H_2O$ salt solution was added to obtain a series of soil Cu levels of 100, 200, 400, 600 and 800 mg·kg^{-1} (dry weight) along with three levels (0%, 1% and 3%) of pig manure, respectively. Total Cu concentration in the control soils was 41 mg·kg^{-1} (CK_0), 60 mg·kg^{-1} (CK_1) and 98 mg·kg^{-1} (CK_3) for 0%, 1% and 3% manure, respectively. The pots, each containing five kg of soil, were submerged for two weeks before transplanting.

Six rice seedlings were transplanted to each pot which was maintained under submerged conditions during the whole growing period. Tillers were counted weekly and grain yield and yield components were determined at harvest. Grain Cu contents were determined after digestion with HNO_3 and H_2O_2 (30%). Extractable Cu contents in the soil were measured with diethylenetriamine-pentaacetic acid (DTPA) as described by Lindsay and Norvell (1978). Grain Cu contents in digestion mixture and extractable Cu contents in solution were determined by atomic absorption spectrophotometer (Analytikjena, nov AA 300, Germany).

Results and Discussion

The number of tillers at the control was considered as standard (100%) and the % number of tillers under all other Cu levels were compared with the control to study the effect of Cu on tillering at three levels of manure. The % number of tillers at July 11 showed the initial number transplanted (Fig. 1). The % number of tillers decreased at high doses of Cu but increased at low levels i.e. 200 mg·kg^{-1} of Cu at 0% manure. At 1% manure, % number of tillers also decreased at high doses but the decrease was not pronounced compared to 0% manure, also tillers increased significantly at 200 mg·kg^{-1} of Cu. Similarly, significant increase was noted for % number of tillers at 200 and 400 mg·kg^{-1} at 3% manure, except for 100 and 800 mg·kg^{-1} of Cu where significant reduction was observed. Rice grain yield decreased with increase in concentrations of Cu. At 0% manure a reduction of 30%, 64% and 72% was recorded at 400, 600 and 800 mg·kg^{-1} of Cu, respectively (Table 1). These findings concur with that of Xu *et al.* (2006), who found a reduction of 10% by soil Cu level of 100 mg·kg^{-1} and about 50% by soil Cu levels of 300~500 mg·kg^{-1} and grain yield was reduced by 90% when Cu concentration reached to 1000 mg·kg^{-1}.

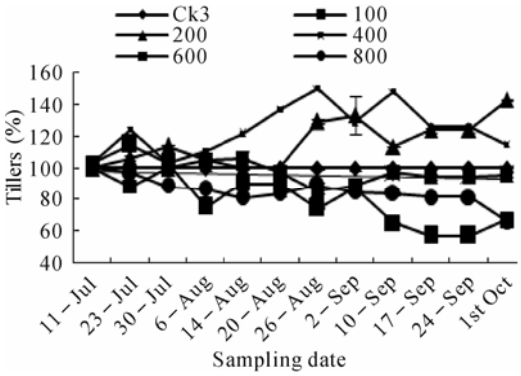

Fig. 1 Effect of Cu level in soil on number of tillers at 3% level of manure at different growth stages. Values are % of the control (Ck3). Bars represent means ± SD

Table 1 Effect of Cu levels in soil on average grain yield and Cu in grains at 0%, 1% and 3% manure

Manure	Cu levels	Average grain yield (g·pot^{-1}, dry wt)	Total Cu in Grains (mg·kg^{-1})
0%	CK_0	12.22 abc	5.94 hi
	100	13.72 ab	8.56 def
	200	10.50 abcd	10.52 bc
	400	8.53 bcde	12.35 ab
	600	4.36 ef	13.84 a
	800	3.35 ef	13.22 a
1%	CK_1	8.82 bcde	7.15 efgh
	100	12.82 ab	6.58 ghi
	200	14.53 a	7.93 efg
	400	12.36 abc	10.15 cd
	600	5.44 def	8.52 def
	800	5.17 def	8.63 cde
3%	CK_3	7.07 cdef	5.68 hi
	100	3.93 f	3.27 j
	200	3.41 ef	4.77 ij
	400	6.01 def	6.02 ghi
	600	8.67 bcde	6.71 fgh
	800	5.91 def	5.66 hi
F test			
Manure		**	**
Cu		*	**
Manure x Cu		**	**

Note: same letter after the data within a column means no significant differences at p=0.05; * and ** indicates significant at the p<0.05 and p<0.01 level, respectively

Addition of 1% manure increased the grain yield at low Cu levels but decresed the yield by 38% and 41% at 600 and 800 mg·kg^{-1} of Cu, respectively. In contrast, the yield at 3% manure decreased by 62% and 52% at 100 and 200 mg·kg^{-1} of Cu, respectively but only by 16% at 800 mg·kg^{-1} of Cu, while grain yield increased at 600 mg·kg^{-1} of Cu compared to Ck3. Addition of manure seemed to reduce the toxicity of Cu but the reduction of yield at 100 and 200 mg·kg^{-1} of Cu needed to be further investigated. Manure compost showed the promotive effect on the grain yield of wheat grown in Cd-polluted soils (Liu *et al.*, 2009).

Soil extractable Cu increased with increasing levels of Cu but decreased with growth stages (Fig. 2), and there was a similar trend for 0%, 1% and 3% manure. Whereas the extractable Cu tended to decrease from planting to harvest, the decrease was more pronounced at the tillering stage. Reductions of 8.06, 5.12, 1.90, 1.18 and 1.25 fold were found from planting to harvest at 0% manure for 100, 200, 400, 600 and 800 mg·kg^{-1} of Cu, respectively.

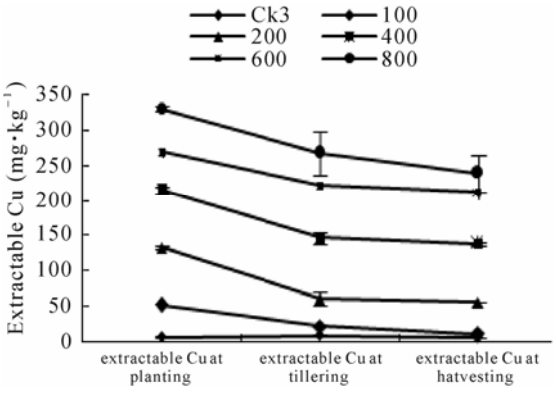

Fig. 2 Dynamic behavior of DTPA-extractable Cu at 3% manure at different growth stages. Bars represent means ±SD

For low levels of Cu at 1% and 3% manure, extractable Cu was decreased significantly, with reductions of 4.25, 2.77 and 1.54 folds at 1% manure and 4.41, 2.38 and 1.56 folds at 3% manure for 100, 200 and 400 mg·kg^{-1} of Cu, respectively, from planting to harvest. Significant decreases in extractable Cu and increases in Cu contents in grains at 0% manure as compared with 1% and 3% manure suggest that more Cu was absorbed by plants at 0% manure, and addition of manure significantly reduced Cu uptake by plants. Copper concentrations in grains were increased consistently with the elevated Cu levels at 0% manure. A significant and positive effect of manure was found for reduced Cu uptake into the grains (Table 1). Cu accumulation in grains was much lower at 1% and 3% manure even at higher levels of Cu as compared to 0% manure. This restricted supply of Cu to the grains was probably due to manure decreased the bioavailability of Cu and then alleviated Cu toxicity to rice growth (Li *et al.*, 2008).

Acknowledgements

This work was supported by the National Basic Research Program of China (973 Program, Grant No. 2005 CB121104), and the Project of China Association for Science and Technology (2009ZCYJ17).

References

Li P, Wang XX, Zhang TL, Zhou DM, He YQ (2008) Effects of several amendments on rice growth and uptake of copper and cadmium from a contaminated soil. J. Environ. Sci., 20: 449-455

Lindsay WL, Norvell WA (1978) Development of a DTPA soil test for Zn, Fe, Mn and Cu. Soil Sci. Soc. Am. J. 42: 421-428

Liu L, Chen H, Cai P, Liang W, Huang Q (2009) Immobilization and phytotoxicity of Cd in contaminated soil amended with chicken manure compost. J. Hazard. Mater. 163: 563-567

Xu J, Yang L, Wang Z, Dong G, Huang J, Wang Y (2006) Toxicity of copper on rice growth and accumulation of copper in rice grain in copper contaminated soil. Chemosphere 62: 602-607

Walker DJ, Clemente R, Bernal MP (2004) Contrasting effects of manure and compost on soil pH, heavy metals availability and growth of Chenopodium album L. in a soil contaminated by pyritic mine waste. Chemosphere 57: 215-224

The Effects of Several Amendments on Forms of Lead and Its Uptake by Two Cultivars of *Brassica Chinensis* in an Acid Red Soil

Xia Li, Jiachun Shi*, Jianming Xu*, Jianjun Wu

Zhejiang Provincial Key Laboratory of Subtropical Soil and Plant Nutrition,
College of Environmental and Natural Resource Sciences, Zhejiang University, Hangzhou 310029, China.
*Corresponding author. Tel. No. +86-517 8697 1955; Fax No. +86-571 8697 1955; E-mail: jcshi@zju.edu.cn and jmxu@zju.edu.cn.

Abstract: We conducted a greenhouse study to examine the effects of various amendments on forms and bioavailability of Pb in red soils, and the differences in responses of two cultivars of *Brassica Chinensis* with contrasting resistance to Pb. The results showed that red soils with Pb contamination could be remedied by the amendments, and the uptake of Pb in plants could be decreased. The growth of plants was affected by the bioavailable forms of Pb and soil pH. The two cultivars differed in responses to the treatments. The best treatment was calcium magnesium phosphate which immobilized Pb to more residual forms, and significantly reduced the uptake of Pb in plants.

Keywords: Red soil; Forms of lead; Uptake; Phosphate amendment; Organic matter; Bioavailability

Introduction

Acid soils with Pb contamination have more damage to plants growth than other soils, while Pb contamination threatens to food safety and human health. Most studies on the Pb remediation were performed using various phosphate amendments. Different phosphate amendments have different effects on the form of Pb in soil, in which phosphate fertilizers have the best effect. Organic materials with abundant organic matter play an important role in reducing soil Pb bioavailability and improving soil environment. A number of other soil amendments have been tested to immobilize Pb in soils, such as fly ash, lime and zeolites (Jurate *et al.*, 2008). The aim of this study was to compare the effects of various amendments on forms and bioavailability of Pb in an acid red soil, and the responses of the two cultivars of vegetables.

Materials and Methods

A paddy soil on quaternary red clay was used in this study. The soil was a typical red soil containing 22.5% clay, 49.7% silt and 24.5% sand. The organic matter, pH and total Pb were 1.36%, 4.72 and 53 $mg \cdot kg^{-1}$, respectively. Soil amendments used in this study include organic and inorganic, and these were (1) peat (PE), (2) pig manure (PM), (3) straw manure (SM), (4) single superphosphate (SSP), (5) calcium magnesium phosphate(CM), and (6) phosphate rock (RP). Two cultivars of *Brassica Chinensis* (Huangguan qingjiang and Sijiqing) with contrasting resistance were chosen for the greenhouse pot experiments. The soil was given a concentration of 600 mg $Pb \cdot kg^{-1}$ as $Pb(NO_3)$, and mixed thoroughly. Each amendment was applied at two levels of phosphate amendments 350 and 1050 mg $P_2O_5 \cdot kg^{-1}$ soil, and of organic matter amendments 10 and 30 $g \cdot kg^{-1}$ soil, respectively. The experiment had thirteen treatments (including the control) with three replicates per treatment. Each treatment was also applied with chemical fertilizers. And then 1.4 kg of soil was placed in each plastic pot (20 cm × 20 cm). The amendments were mixed with the soil thoroughly. After a two-week incubation period, 15 seeds were planted in each pot. One week later uniformly emerged seedlings were thinned to three per pot. The

experiment was performed for two months in a greenhouse at 18~25 ℃, and watered as required. At harvest, plants were removed from pots and the shoots separated from the roots. Two parts were washed rapidly and thoroughly in de-ionized water, and then dried at 70 ℃ for 24 h, and weighed. About 100 g soil sample of each treatment was collected for the following analyses. Soil pH was determined by a pH meter, in 1:5 soil:water suspension. The plants samples were digested with 1:4 HNO_3-$HClO_4$; the forms of Pb in soils were determined by sequential extraction according to the method of Tessier *et al.* (1979), into water-soluble, exchangeable, carbonate-bound, Fe/Mn oxide-bound, organic-bound and residual fractions. Concentrations of Pd in extracts were measured by AAS.

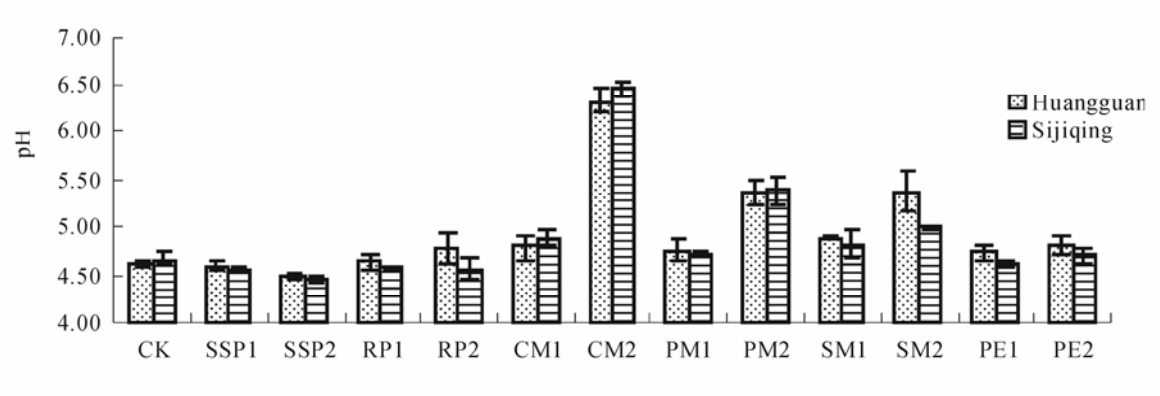

Fig. 1 Change of soil pH after growing plants of *Brassica Chinensis* cv. Huangguan qingjiang and Sijiqing with various amendments for two months. Bars are ± standard error of the mean

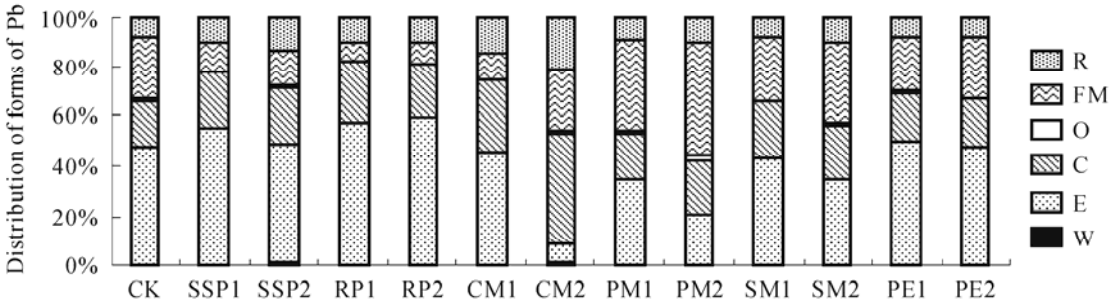

Fig. 2 Distribution of different forms of Pb in soils after growing Sijiqing plants for two months with various soil amendments (W, water-soluble; E, exchangeable; C, carbonate-bound; FM, Fe/Mn oxide-bound; O, organic-bound; R, residual Pb)

Results and Discussion

The pH values of the soils are shown in Fig. 1. The results showed that soil pH was significantly affected by the application of various amendments, and two cultivars responded to treatments similarly. The calcium magnesium phosphate treatments were the most efficient at increasing soil pH due to its strong alkalinity. The soil pH in these treatments increased with increasing level of application with the pH increased by about 2.5 units at the higher level. All organic amendments raised the soil pH, of which the higher application rate of pig manure and straw manure also had significant effect. The peat treatments increased pH at two levels. Due to its acidity, the treatment of single superphosphate decreased the soil pH while phosphate rock had little effect on soil pH. Distribution of different forms of Pb in soils after growing plants is shown in Fig. 2. Pb occurred primarily in exchangeable, carbonate-bound, Fe/Mn oxide-bound and residual forms. The water-soluble and organic-bound fractions were very low for

all treatments, and only a small proportion of Pb was observed in the organic-bound fraction for the pig manure treatment. It suggests that the exchangeable fraction is bioavailable for plants (Zhu *et al.*, 2004). Application of single superphosphate and phosphate rock at two levels increased the exchangeable fraction whereas calcium magnesium phosphate, pig manure and straw manure treatments at the higher level decreased the exchangeable fraction. Application of peat had a slight increase in the exchangeable fraction. The proportion of the residual Pb was increased with calcium magnesium phosphate application.

Amendments had significant effects on Pb uptake by the two vegetable cultivars (Table 1). The accumulation of Pb in shoots and roots showed similar trends for both cultivars. Pb concentrations were lower in shoots than in roots. Huangguan generally had higher Pb uptake in shoots than Sijiqing, while the opposite was true in roots, indicating that Sijiqing can immobilize Pb in roots more effectively and transported less Pb to shoots. For both cultivars, the lowest accumulation of Pb was found in the treatments of calcium magnesium phosphate at high level, followed by pig manure treatment at high level and calcium magnesium phosphate at low level. The decreased Pb accumulation in these treatments might be attributed to their increase of soil pH. Single super phosphate treatments decreased Pb concentrations in plants tissues, which might be attributed to the decreased Pb mobility via ionic exchange and precipitation of pyromorphite-type minerals with a lower soil pH (Zhu *et al.*, 2004). Four treatments of phosphate rock and straw manure had no significant effects on the accumulation of Pb in plants. The application of peat decreased the uptake of Pb for plants. A previous study showed that Huangguan and Sijiqing were Pb-sensitive and Pb-resistant, respectively.

Table 1 Concentration of Pb in plants grown in Pb contaminated soil with various soil amendments

Treatment	Huangguan ($mg \cdot kg^{-1}$)		Sijiqing ($mg \cdot kg^{-1}$)	
	Shoot	Root	Shoot	Root
CK	13.71ab	55.40a	12.53a	68.34ab
SSP1	5.19de	25.90de	3.91c	26.70f
SSP2	2.89ef	19.57ef	2.87c	24.44f
RP1	13.54ab	49.80ab	12.66a	51.24cd
RP2	14.26ab	36.06bcd	12.85a	62.39bc
CM1	4.75def	19.29ef	3.46c	26.95f
CM2	1.33f	3.00g	1.23c	4.23g
PM1	8.02cd	30.67cde	8.05b	46.98d
PM2	3.46ef	6.92fg	3.42c	9.03g
SM1	14.65a	34.26cd	13.14a	79.45a
SM2	9.92c	30.20cde	8.92b	31.79ef
PE1	11.16bc	41.70abc	11.06ab	42.32de
PE2	5.10de	27.56cde	4.38c	27.92ef

(Mean values denoted by the same letter in a column do not differ significantly according to the LSD test at $P<0.05$)

Table 2 showed that the amendments generally increased the biomass of shoots for both cultivars, and had slight effects on roots biomass. Biomass of shoots responded the treatments similarly although Sijiqing produced higher shoot biomass than Huangguan. Of all the treatments, calcium magnesium phosphate treatments significantly increased shoots biomass. Various amendments altered the forms of Pb in soil. Application of calcium magnesium phosphate immobilized Pb to more residual forms, and significantly reduced the uptake of Pb in plants. It has been determined that organic matter absorbs Pb in soil and reduces the bioavailability of soil Pb (Pichtel *et al.*, 2008). It is observed that exchangeable and residual forms of Pb in soil significantly affect the Pb concentrations in plants (Table 3). Soil pH is an

important factor that may also affect bioavailability of Pb in soils, and thus the Pb uptake of plants effectively. The correlations between pH and various fractions are shown in Table 3. These results indicate that the growth of two cultivars was affected by the bioavailable forms of Pb. Both soil pH and forms of Pb are important in remediation of acid soils with Pb contamination.

Acknowledgements

This work was jointly supported by the Project of China Association for Science and Technology (2009ZCYJ17) and the National Natural Science Foundation of China (40701069).

Table 2 Biomass of plants grown for two months Pb contaminated soil with various soil amendments

Treatment	Huangguan (g·pot^{-1})		Sijiqing (g·pot^{-1})	
	Shoot	Root	Shoot	Root
CK	0.77gh	0.1180ab	1.09f	0.1258abc
SSP1	1.09ef	0.1330a	1.37de	0.1584a
SSP2	1.28de	0.1396a	1.43cd	0.1425a
RP1	0.91fgh	0.0870bcd	0.98fg	0.0896de
RP2	0.89fgh	0.0860cd	0.97fg	0.1075bcd
CM1	1.86b	0.1183a	1.91b	0.1321ab
CM2	2.52a	0.1092abc	2.61a	0.1433a
PM1	1.39cd	0.0778d	1.42cd	0.0971d
PM2	1.60c	0.0717d	1.64c	0.1015bcd
SM1	0.71h	0.0577d	0.78g	0.0996cd
SM2	0.83gh	0.0560d	1.15ef	0.0627e
PE1	1.01fg	0.0766d	1.05f	0.0793de
PE2	1.50cd	0.0795cd	1.56cd	0.0870de

(Mean values denoted by the same letter in a column do not differ significantly according to the LSD test at $P<0.05$)

Table 3 Correlation coefficients (r) between Pb concentrations in plants and soil pH and forms of Pb in soils (n=13)

	pH	W	E	C	O	FM	R
Shoot	-0.38*	-0.23	0.61*	-0.39	-0.46	-0.09	-0.61*
Root	-0.52**	-0.35	0.56*	-0.59*	-0.59*	-0.23	-0.68**
Shoot	-0.44**	-0.46	0.49	-0.53	-0.52	-0.15	-0.71**
Root	-0.61**	-0.19	0.78**	-0.55*	-0.62*	-0.2	-0.69**

*,** Significant at $p<0.05$ and 0.001,respectively

References

Jurate K, Anders L, Christian M (2008) Stabilization of As, Cr, Cu, Pb and Zn in soil using amendments –A review. Waste Manag. 28: 219-220

Pichtel J, Bradway DJ (2008) Conventional crops and organic amendments for Pb, Cd and Zn treatment at a severely contaminated site. Biol. Technol. 99: 1242-1251

Tessier A, Campbell PGC, Bisson M (1979) Sequential extraction procedure for the speciation of particulate trace metals. Anal. Chem. 51: 844-851

Zhu YG, Chen SB, Yang JC (2004) Effects of soil amendments on lead uptake by two vegetable crops from a lead-contaminated soil from Anhui, China. Environ. Int. 30: 355-356

Does Iron Plaque Improve the Uptake and Translocation of Lead by Broad-leaf Cattail in Lead-contaminated Soils

Shunqin Zhong[a,b], Jianming Xu[a,*], Jiachun Shi[a,*], Jianjun Wu[a]

[a] Zhejiang Provincial Key Laboratory of Subtropical Soil and Plant Nutrition, College of Environmental and Natural Resource Sciences, Zhejiang University, Hangzhou 310029, China;
[b] Department of Resource Environment and Tourism Management, Hengyang Normal University, Hengyang, 421008, China.
[*]Corresponding author. Tel. No. +86571-86971955; Fax No. +86571-86971955; E-mail: jcshi@zju.edu.cn and jmxu@zju.edu.cn.

Abstract: The inhibited or enhanced uptake of heavy metals by iron plaque has been observed. The relationship between amounts of adsorption and accumulation of heavy metals and iron plaque on roots of wetland plant is still unclear. This study examined the effects of iron plaque on lead (Pb) absorption and translocation between underground and above-ground parts of a wetland plant species. Broad-leaf cattail (*Typha latifolia* L.) was grown in soil for four weeks under waterlogged conditions in a greenhouse. The soils were treated by Pb as lead nitrate at four levels (0, 100, 500 and 1000 mg Pb·kg^{-1}) and waterlogged for two weeks. The results showed that the amount of iron plaque in the treatment with addition of 500 mg Fe·kg^{-1} was general higher than that of the treatment with addition of 100 mg Fe·kg^{-1}, Lead concentrations in both shoots and roots treated by 500 mg Fe·kg^{-1} was more than that of the treatment with 100 mg Fe·kg^{-1}. When the ratio of added Fe and Pb was 1, the accumulation of Pb in plants was higher than that of other treatments at the same Pd level. Appropriate amount of iron supplied will benefit lead accumulation in plant, which help the removal or stabilization of lead in constructed wetland.

Keywords: Broad-leaf cattail; Iron plaque; Lead; Waterlogged soil

Introduction

Constructed wetland was widely built for removal of heavy metals in treating waste water. Sediment-ation, sorption, co-precipitation, cation exchange, phytoaccumulation are the main processes of heavy metal removal (Sheoran *et al.*, 2006). Iron-oxide coating (iron plaque) has been found on the roots of many wetland plants (Hansel *et al.* 2001). Iron (hydr) oxide precipitates, or plaque, occurring on the surface of roots, consists of mainly ferrihydrite, goethite and siderite (Hansel *et al.*, 2001). The high capacity of functional groups on iron hydroxides to sequester metals by adsorption and/or co-precipitation has attracted research interests (Liu *et al.*, 2004). However, the relationship between the amount of absorption and accumulation of heavy metals and iron plaque on roots of wetland plant is still unclear. The present study aimed to examine the effects of addition of iron in Pd-contaminated soil on the formation of iron plaque and Pb absorption and translocation in wetland species *Typha latifolia* L.

Materials and Methods

Materials

Clayey illitic thermic typic epiaqualfs was collected from 0~30 cm in an abandoned paddy field in Jiaxing of Zhejiang province, China. The soil was sieved through a 2-mm sieve after air-dried. It had a pH of 5.61 (soil: water =1: 2.5) and organic matter content of 3.62%, and its total Fe and Pb were 2.95% and 45.6 mg·kg^{-1}, respectively.

Experiment Conducted

The experiment was conducted in a greenhouse. The uniform seedlings were selected and transplanted

into plastic pots filled with 1.5 kg soil, which had been treated with four levels of Pd [0, 100, 500 and 1000 mg Pb·kg^{-1} as $Pb(NO_3)_2$], two levels of iron (100 and 500 mg Fe·kg^{-1} as $FeSO_4$). The soil was waterlogged for two weeks, and then kept about 0.5 cm thickness of water above soil surface for four weeks. Each treatment was replicated three times.

Analytical Methods

At harvest, plant samples were separated into shoots and roots. Fresh roots were washed with tap water, then rinsed in deionized water, and dried by filter paper. The iron plaque was then extracted using the cold DCB technique (Taylor *et al.* 1983). The plant parts were rinsed with tap water and then with deionized water twice, dried at 105 ℃ for 30 minutes, and then kept at 80 ℃ for 24 h and dry weights recorded. Ground samples (about 0.2~0.5 g weight) were digested in 10 mL concentrated nitric acid by the microwave digestion. The concentrations of Fe and Pb were determined by an atomic spectrophotometer (NovAA300, Germany).

Results and Discussions

The dry weight of roots was significantly affected by both Pb addition (F=21.4, p<0.01) and Fe supply (F=15.3, p<0.01), and the interaction of Pb and Fe was significant (F=5.6, p<0.01). The root weight increased initially and then decreased with increasing Pb dose, and its dry weight was more at the 100 mg Fe·kg^{-1} level than that of at 500 mg·kg^{-1} Fe level except the treatment of 500 mg Pb·kg^{-1}. However, the dry weight of shoots was not significantly affected by either Fe or Pb addition. The Pb concentration in DCB extracts was significantly affected by Fe (F=4.93, p<0.05) and Pb (F=21.4, p<0.01) supply levels, but the interaction of Fe and Pb was not significant (F =0.92, p>0.05). Lead concentrations in roots ranged from 68 to 1497 mg·kg^{-1}, and that in shoots ranged from 29 to 105 mg·kg^{-1}. Lead content in both shoots and roots treated with 500 mg Fe·kg^{-1} was higher than that with 100 mg Fe·kg^{-1}. The amount of Pb accumulated per plant ranged from 0.5 to 2.6 mg, and more lead was accumulated in shoots. When the ratio of added Fe to Pb was 1, the accumulation of Pb was higher than that of other treatments at a given lead level (Fig. 1).

The results showed that broad-leaf cattail could endure high concentrations of Pb and Fe, in agreement with the findings by Ye *et al.* (1997). The pH value in rhizosphere was decreased because of the oxidation of ferrous around the root of plant, and the value of pH in the treatment with 500 mg Fe·kg^{-1} was lower than that of the treatment of 500 mg Fe·kg^{-1}. The change in pH value induced by Fe addition enhanced the availability of Pb, favouring Pb adsorption. Both excessive Fe and Pb had a great influence on root metabolism, and high Pb concentrations inhibited photosynthesis (Parys *et al.*, 1998), which resulted in poor plant growth.

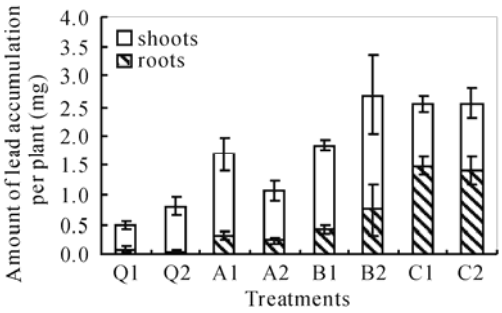

Fig. 1 The accumulation of Pb in shoots and roots of the plants exposed to various Pb levels. 1 and 2 indicate treatments with 100 and 500 mg Fe·kg^{-1}, respectively. Bars are means±s.d., Q: control (no lead addition), A: 100 mg Pb·kg^{-1}, B: 500 mg Pb·kg^{-1}, C: 1000 mg Pb·kg^{-1}

The accumulation of Pb in the shoot was higher than that of the root at 0, 100 and 500 mg·kg^{-1} Pb levels, even though the Pb concentration was higher in the roots than in shoots. More iron plaque was formed on the roots when more Fe was added. Physical chemistry feature in the rhizoshphere was changed because of iron plaque formed. Thus Pb uptake was enhanced by iron plaque on the roots. Similar results were obtained by Liu *et al.* (2007) who found that iron plaque enhanced Pb adsorption on the root surface, and benefited Pb to translate from root surface into root in rice (Oryza sativa L.). Ye *et al.* (1998) also found that iron plaque was not a primary barrier to Pb absorption and translocation in *Typha latifolia.* So the amount of Pb accumulated in plant depended on the amount of iron plaque formed and any factors influencing plant growth.

Conclusions

Iron supply enhanced the formation of iron plaque,

improved Pb absorption and translocation from roots to shoots. When the ratio of added Fe and Pb was 1, Pb accumulation was higher than that of other treatments at a given Pd level. We suggest that consideration of Fe content was necessary for broad-leaf cattail uptake and translocation of Pb in Pb-contaminated wetland.

Acknowledgements

This work was jointly supported by the Project of China Association for Science and Technology (2009ZCYJ17), the National Natural Science Foundation of China (40701069), and the Science and Technology Projects of Zhejiang Province (2007C 22015).

References

Hansel CM, Fendorf S, Sutton S, Newville M (2001) Characterization of Fe plaque and associated metals on the roots of mine-waste impacted aquatic plants. Environ. Sci. Technol. 35: 3863-3868

Liu WJ, Zhu YG, Smith FA, Smith SE (2004) Do iron plaque and genotypes affect arsenate uptake and translocation by rice seedlings (Oryza sativa L.) grown in solution culture? J. Exp. Bot. 55: 1707-1713

Liu YJ, Zhu YG, Ding H, Guo W, Chen Z, Liu WJ (2007) The effect of root surface iron plaque on Pb uptake by rice (Oryza sativa L.) roots (in Chinese). Environ. Chem. 26: 328-331

Parys E, Romanowska E, Siedlecka M, Poskuta JW (1998) The effect of lead on photosynthesis and respiration in detached leaves and in mesophyll protoplasts of Pisum sativum. Acta Physiol. Plant 20: 313-322

Sheoran AS, Sheoran V (2006) Heavy metal removal mechanism of acid mine drainage in wetlands: A critical review. Miner. Eng. 19: 105-116

Taylor GJ, Crowder AA (1983) Use of the DCB technique for extraction of hydrous iron oxides from roots of wetland plants. Am. J. Bot. 70: 1254-1257

Ye ZH, Baker AJM, Wong MH, Willis AJ (1997) Zinc, lead and cadmium tolerance, uptake and accumulation by Typha latifolia L. New Phytol. 136: 469-480

The Influence of Zn^{2+} and Mn^{2+} on Pb^{2+} Adsorption Behaviors of Birnessite

Fan Liu*, Wei Zhao, Wenfeng Tan, Xionghan Feng

Key Laboratory of Subtropical Agriculture and Environment, Ministry of Agriculture,
Huazhong Agricultural University, Wuhan, 430070, China.
*Corresponding author. Tel. No. +86-27 8728 0271; Fax No. +86-27 8728 8618; E-mail: liufan@mail.hzau.edu.cn.

Abstract: The present study comparatively investigated Pb^{2+} adsorption behaviors of the birnessite with high Mn average oxidation state (AOS) before and after treatment of preadsorption with Zn^{2+} and Mn^{2+}, respectively. The association of vacant Mn octahedral sites with Pb^{2+} adsorption was further understood from the variances of birnessite AOS, d(110)-interplanar spacing, maximum Pb^{2+} adsorption, maximum Zn^{2+} and Mn^{2+} release during the Pb^{2+} adsorption before and after treatments. The birnessite AOS and d(110)-interplanar spacing were almost unchanged as the concentration of Zn^{2+} increased, indicative of the unchanged vacant Mn octahedral sites, whereas the maximum Pb^{2+} adsorption decreased from 3190 to 2030 mmol·kg^{-1} due to occupancy of the treating Zn^{2+} in adsorption sites. However, the AOS of the Mn^{2+}-treated birnessites decreased and most of the treating Mn^{2+} were oxidized to Mn^{3+} and located below or above vacant Mn octahedral sites or migrated into vacant Mn octahedral sites. Increasing Mn^{2+} concentration from 1 to 2.4 mmol·L^{-1} increased the d(110)-interplanar spacing of the treated birnessites from 0.1416 to 0.14196 nm but decreased the maximum Pb^{2+} adsorption of the treated birnessites from 3190 to 1332 mmol·kg^{-1}, indicating the decrease in the amount of vacant Mn octahedral sites, mainly due to the increase of the produced Mn^{3+} migrating into vacant Mn octahedral sites. Therefore, birnesstie Pb^{2+} adsorption capacity was largely determined by the number of Mn site vacancies.

Keywords: Zn^{2+} adsorption; Birnessite; Pb^{2+} adsorption; Mn site vacancies

Introduction

Lead (Pb) contamination is ubiquitous and has received more and more attention. Manganese oxides, highly active in various chemical reactions, are widely distributed in soils, sediments and ocean manganese nodules. Understanding the reactivity of manganese oxides with Pb is necessary to predict the fate and transport of Pb in the environment and to optimize the remediation efforts. The phyllomanganate birnessite is the most common family among manganese oxides in soils.

The synthesis of birnessite can be achieved by the reduction of potassium permanganate in a strong acidic medium. The resulting birnessite has hexagonal layer symmetry with layers comprising edge-sharing $Mn(IV)O_6$ octahedra, $Mn(III)O_6$ octahedra and vacant Mn octahedral sites (Villalobos *et al.*, 2006). Some Mn^{2+} and Mn^{3+} are located above or below vacant Mn octahedral sites in birnessit. Studies have indicated that birnessite structural vacancies account for a negative layer charge and are associated with adsorption of Pb, Zn, Cu, Cd, and Ni, and oxidation of Co^{2+}, Cr^{3+} and transformation of minerals. Feng *et al.* (2007) found birnessite possessed the greatest adsorption affinity and amount for Pb^{2+} among heavy metal ions. Lanson *et al.* (2002) noted that surface-adsorbed Pb on birnessite was octahedrally coordinated and around 75% of the Pb was located either above or below vacant Mn sites.

The aims of this study were to investigate the variances of birnessite structure, maximum Pb^{2+} adsorption and maximum Mn^{2+}, Zn^{2+} release and thereby to understand the relation between vacant Mn octahedral sites and maximum Pb^{2+} adsorption.

Materials and Methods

The birnessite was synthesized by the reduction of potassium permanganate in a strong acidic medium. X-ray diffraction (XRD) and transmission electron microscopic (TEM) were used to characterize the product. The Mn average oxidation state (AOS) was measured using the oxalic acid-permanganate back-titration method.

Treatment of Birnessite

5.0 g samples of HB0 were added respectively to 3 L aliquots of 1, 1.5, 1.8, 2, 2.2 and 2.4 mmol·L^{-1} $Mn(NO_3)_2$ with pH adjusted to 5.0. The reaction was continued for 24 h with vigorous stirring. The pH of the reaction system was maintained at pH 5.0. The obtained samples were designated as M1, M2, M3, M4, M5 and M6, respectively. Treatment with Zn^{2+} of birnessite was similar to that of Mn^{2+}, except for Zn^{2+} concentrations of 1, 1.5, 1.8, 2 and 2.4 mmol·L^{-1}, respectively. The obtained samples were designated as Z1, Z2, Z3, Z4 and Z5, respectively.

Adsorption Experiments

Isothermal Pb^{2+} adsorption to all samples, including HB0, M(1-6) and Z(1-5), was measured using 5 g·L^{-1} sample suspensions at pH 5.00 using a series of Pb^{2+} solutions at concentrations from 0 to 15 mmol Pb·L^{-1}. The ionic strength was adjusted to 0.15 mol·L^{-1} using $NaNO_3$. The pH of the 5 g·L^{-1} birnessite suspensions was maintained at 5.00 by the addition of 0.1 mol·L^{-1} HNO_3 or 0.1 mol·L^{-1} NaOH until the pH value was stabilized to pH 5.00 ± 0.05. Then, 5 mL aliquots of the birnessite sample suspensions were mixed with 10 mL of Pb^{2+} solutions with a range of initial concentrations in 50-mL polyethylene centrifuge tubes. A solid to liquid ratio of approximately 1.67 g·$L^{-1}$was obtained and the Pb^{2+} concentrations ranged from 0 to 10 mmol·L^{-1} with an ionic strength of 0.1 during the reaction. The amount of H^+ released was determined from the recorded additions of standard HNO_3/NaOH solutions. All measurements were performed in triplicate and averaged.

Results and Discussion

Based on the XRD and TEM analyses, the structural type of the minerals was unchanged before and after the treatments. The (110)-interlayer spacing for the Z series of birnessites after the treatment of the HB0 was hardly changed as the concentration of Zn^{2+} increased (Fig. 1). However, the (110)-interlayer spacing for the M series of birnessites after the treatment of the HB0 increased from 0.14161 nm to 0.14196 nm as the concentration of Mn^{2+} increased from 1 to 2.4 mmol·L^{-1}, indicative of the migration of treating Mn^{2+} into the MnO_6 layer of birnessites. The AOSs of the M series samples ranged from 3.75 to 3.85 and decreased as increasing addition of Mn^{2+}. In comparison, those of the Z series samples AOS ranged from 3.94 to 3.96 but was almost unchanged as addition of Zn^{2+} increased (Table 1).

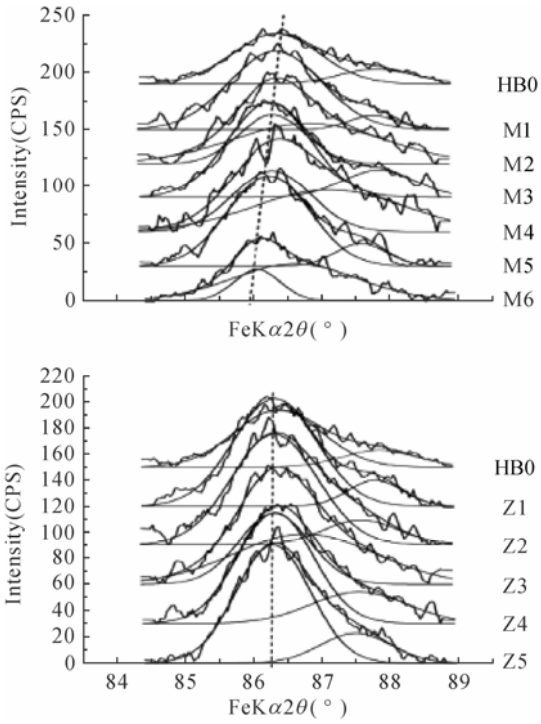

Fig. 1 (110) crystal plane diffraction peaks of the samples. (top) M series, (bottom) Z series

All the adsorption isotherms were fitted using Langmuir non-linear model and the fitting parameters are listed in Table 1. Maximum Pb^{2+} adsorption decreased from 3190 to 1332 mmol·kg^{-1} as the treating Mn^{2+} increased. Though the AOSs of the Z series of birnessites were very similar, maximum Pb^{2+} adsorption decreased from 3190 to 2030 mmol·kg^{-1}. The results showed that maximum Pb^{2+} adsorption on the M and Z series of birnessites were significantly less than that of the HB0 sample, and maximum Pb^{2+} adsorption on the M series of samples was far less

than that of the Z series samples (Fig. 2). Almost no Mn^{2+} was released during Pb^{2+} adsorption on the HB0. Maximum Mn^{2+} release from the M series of birnessites increased from 86 to 281 mmol·kg^{-1}. Almost no Mn^{2+} was released from the Z series of birnessites, yet maximum Zn^{2+} release from the Z series of birnessites increased from 155 to 560 mmol·kg^{-1}. Therefore, the treating Mn^{2+} either is adsorbed above or below vacant sites or is oxidized to Mn^{3+} adsorbed above or below vacant sites or migrated into vacant sites. While the treating Zn^{2+} is only adsorbed above or below vacant sites. Consequently, Pb^{2+} adsorption capacity of birnessites was largely determined by the number of vacant Mn sites.

Table 1 Mn^{2+} or Zn^{2+} adsorbed on the HB0 during the treatment and Langmuir fitting for adsorption of Pb^{2+} on the samples

sample	*AOS*	Mn^{2+} adsorbed (mmol·kg^{-1})	Pb^{2+} A_{max} (mmol·kg^{-1})	Maximum Mn^{2+} release (mmol·kg^{-1})	sample	*AOS*	Zn^{2+} adsorbed (mmol·kg^{-1})	Pb^{2+} A_{max} (mmol·kg^{-1})	Maximum Zn^{2+} release (mmol·kg^{-1})
HB0	3.96		3190	7					
M1	3.85	560	1785	86	Z1	3.95	600	2670	155
M2	3.85	880	1710	100	Z2	3.94	870	2160	249
M3	3.82	1060	1607	172	Z3	3.96	1060	2110	285
M4	3.78	1170	1692	157	Z4	3.96	1170	2290	312
M5	3.77	1310	1581	270	—	—	—	—	—
M6	3.75	1440	1332	281	Z5	3.96	1410	2030	560

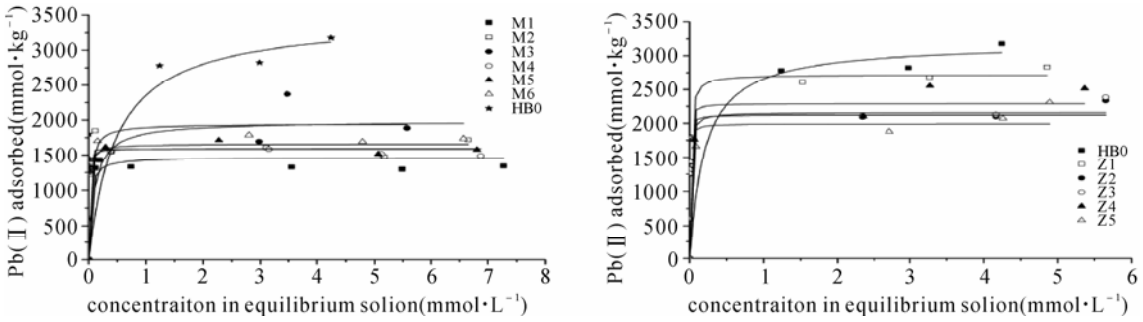

Fig. 2 Isotherms of Pb^{2+} adsorption. (left) M series. (right) Z series

References

Feng XH, Zhai LM, Tan WF, Liu F, He JZ (2007) Adsorption and redox reactions of heavy metals on synthesized Mn oxide minerals. Environ. Pollut. 147(2): 366-373

Lanson B, Drits VB, Feng Q, Manceau A (2002) Structure of synthetic Na-birnessite: Evidence for a triclinic one-layer unit cell. Am. Mineral 87(11-12): 1662-1671

Villalobos M, Lanson B, Manceau A, Toner B, Sposito G (2006) Structural model for the biogenic Mn oxide produced by Pseudomonas putida. Am. Mineral 91(4): 489-502

Removal of Arsenite in Water Using Biogenic Schwertmannite as Adsorbent

Yuehua Liao, Jianru Liang, Lixiang Zhou*

College of Resources and Environmental Sciences, Nanjing Agricultural University, Nanjing 210095, China.
*Corresponding author. Tel. No. +86-25-84395160; Fax No. +86-25-84395160; E-mail: lxzhou@njau.edu.cn.

Abstract: Synthesis of schwertmannite through oxidation of ferrous sulfate by *Acidithiobacillus ferrooxidan*s cells and adsorption of arsenite [As(III)] from water were investigated in the present study. Furthermore, the stability of As(III)-sorbed biogenic schwertmannite was studied. Results showed that hedge-hog like schwertmannite formed after reaction for 72 h were spheroid particles with a diameter of approximately 2.5 μm and its chemical formula could be expressed as $Fe_8O_8(OH)_{4.42}(SO_4)_{1.79}$. As(III) in water could be effectively removed by biogenic schwertmannite with a maximum adsorption capacity of 113.9 mg As(III) per g of adsorbent and the optimum pH for As(III) adsorption was in the range of 7~10. The As(III) removal was unaffected by the competing monovalent anions such as Cl^- and NO_3^-, whereas PO_4^{3-} and SO_4^{2-} greatly decreased the As (III) removal efficiency only when the molar ratio of P to As and S to As in solution reached 75:1 and 750:1, respectively. Furthermore, As(III)-sorbed biogenic schwertmannite exhibited no mineralogy phase change after ageing at pH 6.0 and 8.5 for 90 d. And As(III) could be effectively immobilized in biogenic schwertmannite, indicating that the transformation of metastable schwertmannite to goethite was significantly inhibited by sorption of As(III). The study shows that synthetic biogenic schwertmannite can be a very efficient innovative adsorbent for removing As(III) from water.

Keywords: Arsenite (As) removal; Biogenic schwertmannite; Adsorption; Adsorbent; Water

Introduction

Naturally occurring schwertmannite has been found to be an efficient scavenger of arsenic (As) from water bodies in acid mine drainage (AMD) streams (Fukushi *et al.*, 2003). However, little information on biosynthesis of schwertmannite and further applying it in As removal from water is available. The objectives of the present study were to prepare schwertmannite adsorbent through oxidation of ferrous sulfate by A. ferrooxidans cells and to investigate As(III) removal from water by biogenic schwertmannite adsorption.

Materials and Methods

Preparation of Biogenic Schwertmannite Adsorbent

Ten milliliter of freshly-prepared A. ferrooxidans LX5 cell suspensions were introduced into 500-mL Erlenmeyer flask containing 240 mL of ferrous sulfate solution with Fe^{2+} initial concentration of 0.144 $mol \cdot L^{-1}$. The flasks were incubated at 180 rpm and 28 °C and the precipitates formed in the flasks were harvested by filtering through a Whatman No.4 filter paper. The dried precipitate was identified to be schwertmannite by X–ray diffraction (XRD) and FE-SEM etc.

Arsenite Adsorption Isotherms

The adsorption isotherms were constructed by adding 10 mg of biogenic schwertmannite adsorbent to a 100-mL conical flask containing 40 mL of As(III) solutions in 0.01 $mol \cdot L^{-1}$ NaCl at pH of 7.5. Initial arsenic concentrations were varied from 1.0 to 60.0 $mg \cdot L^{-1}$. The pH 7.5 was controlled by adding 0.1 $mol \cdot L^{-1}$ NaOH or HCl solutions. All flasks were shaken for 4 h in a reciprocating shaker at 180 $r \cdot min^{-1}$ and 15, 25, and 35±0.2 ℃ respectively. After 4 h, the supernatant was filtered through a 0.45-μm membrane

and determined for As(III) concentration. A control without the addition of schwertmannite was also carried out in the study.

pH Effect on As(III) Adsorption

Ten milligram of schwertmannite adsorbent was added to a 100-mL conical flask containing 40 mL of As(III) solutions. The initial As(III) concentration was 1 mg·L^{-1}, and the solution pH was adjusted to desired values in the range of 3~12. As described above, the As(III) adsorption under different pH was determined.

Competing Anion Effects on As(III) Adsorption

Ten milligram of schwertmannite adsorbent was added to 100-mL conical flasks containing 40 mL of arsenite solution in the absence and presence of Cl^-, NO_3^-, SO_4^{2-} and PO_4^{3-}. The initial As(III) concentration was 1 mg·L^{-1} and the competing anions from sodium salt were set to 0, 0.001, 0.01 and 0.1 mol·L^{-1}. The pH of the suspension was adjusted to 7.5. Subsequent procedures were similar to those mentioned above.

Results and Discussion

XRD patterns of the prepared precipitate displayed a poor crystallinity with eight broad peaks (Fig. 1), which was the same as schwertmannite particles. However, SEM images showed that schwertmannite particles formed after reaction at different time varied greatly in size and in morphology (photoes not shown). Moreover, the characteristic "hedge-hog" appearance for schwertmannite was observed to occur in the products after reaction for 72 h. And after reaction for 168 h, the schwertmannite particles were balls with a diameter of 4 μm and aggregate to form much large particles.

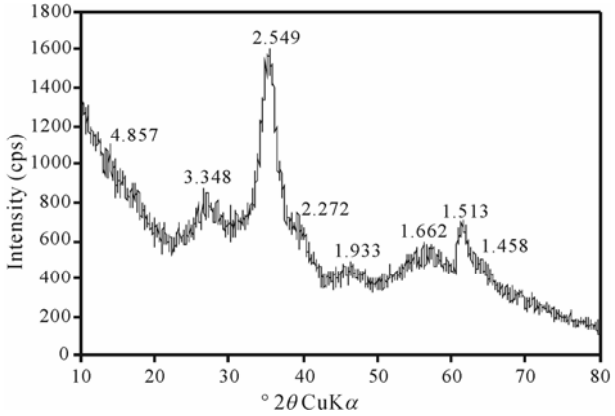

Fig. 1 XRD patterns for the precipitates formed through oxidation of $FeSO_4$ by *Acidithiobacillus ferrooxidan*s cells

As(III) adsorption isotherms at different temperature are given in Fig. 2. Calculated from the Langmuir equation, the maximum adsorption capacity of the biogenic schwertmannite for As(III) was found to be 113.9 mg·g^{-1} at pH 7.5 and 25 ℃, which was much greater than that of activated alumina (Singh and Pant, 2004) and even recently reported iron based adsorbents (Mohan and Pittman Jr., 2007).

As(III) adsorption on schwertmannite increased with the increase of solution pH in the range of 3~10 to a maximum adsorption around pH 7~10. The features of As(III) removal on schwertmannite responding to various pH levels had great potential significance in engineering application. Because the pH of natural water is often in the range of 6~8.5, therefore the pH pre-adjustment is not needed for the contaminated water when schwertmannite is applied in the removal of As(III).

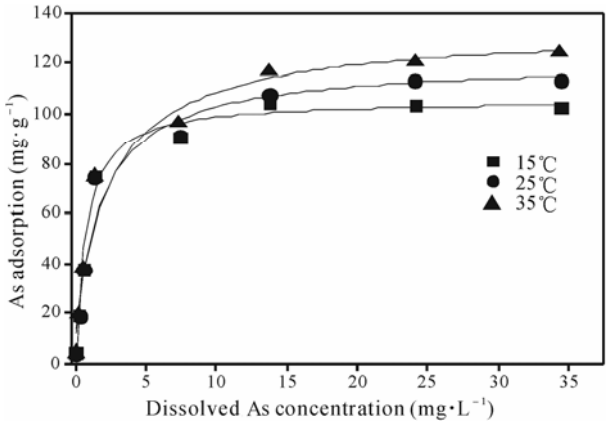

Fig. 2 As(III) adsorption isotherms on schwertmannite under different temperature conditions

The presence of monovalent nitrate or chloride at various concentrations (i.e. 0~0.1 mol·L^{-1}) showed hardly any impact on the As(III) adsorption on schwertmannite, as indicated that the As(III) removal efficiency remained above 98% (Fig. 3). However, the As(III) uptake was observed to decrease slightly to 95.4 % when the bivalent sulfate concentration was as high as 0.01 mol·L^{-1}, whereas it decreased to 89.6 % when the sulfate concentration increased to 0.1 mol·L^{-1} in which molar ratio of S to As was 750:1. Unlike nitrate and sulfate, the presence of trivalent phosphate significantly decreased the As(III) removal efficiency from 90.1% to 80.4% when the concentration of phosphate increased from 0.001 to 0.01 mol·L^{-1} in which molar ratio of P to As was from 750:1 to 75:1, while it reduced to 46.2% when phosphate

concentration reached 0.1 mol·L^{-1}.

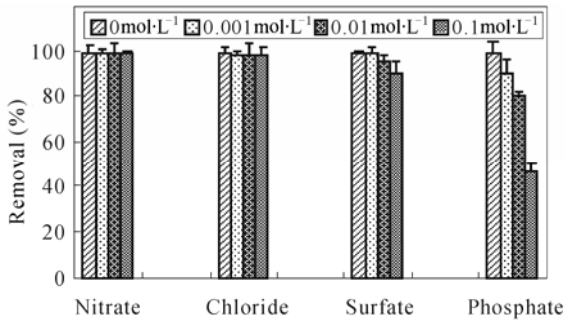

Fig. 3 Effect of competing anions on As(III) removal by schwertmannite. (Schwertmannite 0.25g·L^{-1}, As(III) 1 mg·L^{-1}, pH 7.5, 180 r·min^{-1} and 25 ± 0.2 ℃, equilibrium time 4 h)

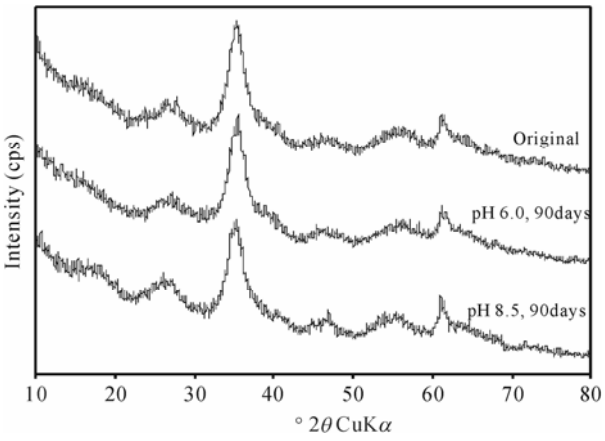

Fig. 4 XRD patterns for the As(III)-sorbed schwertmannite aged at pH 6.0 and 8.5 for 90 days

As shown in Fig. 4, the mineral phase of As(III)-sorbed biogenic schwertmannite with an As(III) content of 9.24 wt % was very stable at 25±1 ℃ and at pH 6.0 and 8.5 for 90 d, as had been shown that there were no changes of XRD patterns for schwertmannite after 90 days and XRD patterns of all samples showing 8 line peaks that were typical for schwertmannite. Furthermore, the arsenic released from As(III)-sorbed schwertmannite under such a condition was negligible.

To conclude, schwertmannite synthesized through oxidation of $FeSO_4$ by *Acidithiobacillus ferrooxidan*s cells can be a very efficient adsorbent for arsenite removal from water.

References

Fukushi K, Sasaki M, Sato T, Yanase N, Amano H, Ikeda H (2003) A natural attenuation of arsenic in drainage from an abandoned arsenic mine dump. Appl. Geochem. 18: 1267-1278

Mohana D, Pittman Jr CU (2007) Arsenic removal from water/wastewater using adsorbents–A critical review. J. Hazard. Mater. 142: 1-53

Singh TS, Pant KK (2004) Equilibrium, kinetics and thermodynamic studies for adsorption of As(III) on activated alumina. Sep. Purif. Technol. 36: 139-147

Wien Effect Measurements in Soil Colloidal Suspensions: A Novel Method for Characterizing the Interactions between Charged Particles and Counter Ions

Yujun Wang, Dongmei Zhou*, Chengbao Li, Haowen Zhu, Wei Wang, Jun Zhou

State Key Laboratory of Soil and Sustainable Agriculture, Institute of Soil Science,
Chinese Academy of Sciences, Nanjing 210008, China.
*Corresponding author. Tel. No. +86-25-86881180; Fax No. +86-25-86881000; E-mail: dmzhou@issas.ac.cn.

Abstract: Adsorption is one of the most important chemical processes at the interface between soil particles and water. It determines the quantity of plant nutrients and pollutants which are retained on the surfaces of soil particles, and therefore, is one of the primary processes that affect transport of nutrients and contaminants in soils. The Wien effect, i.e., the dependence of the electrical conductivity of soil suspensions on electrical field strength, was proposed as the basis of a new method to characterize energy relationships between cations and soil particles. The results showed that the mean Gibbs free binding energies of the heavy metal ions with yellow-brown, black and brown soil particles decreased in the order of $Pb^{2+} > Zn^{2+} > Cu^{2+} > Cd^{2+}$, $Pb^{2+} > Cu^{2+} > Zn^{2+} > Cd^{2+}$ and $Pb^{2+} > Cd^{2+} > Cu^{2+} > Zn^{2+}$, respectively, where the range of binding energies for yellow-brown soil (7.16~8.54 $kJ \cdot mol^{-1}$) was less than that for black soil (9.05~9.88 $kJ \cdot mol^{-1}$). The electrical field-dependent mean Gibbs free adsorption energies of these heavy metal ions for yellow-brown, black and brown soils descended in the order of $Cu^{2+} > Cd^{2+} > Pb^{2+} > Zn^{2+}$, $Cu^{2+} > Zn^{2+} > Pb^{2+} > Cd^{2+}$, and $Cu^{2+} > Pb^{2+} > Cd^{2+} > Zn^{2+}$, respectively. The mean Gibbs free adsorption energies of Cu^{2+}, Zn^{2+}, Cd^{2+} and Pb^{2+} at a field strength of 150 $kV \cdot cm^{-1}$, for example, were in the range of 1.23 to 2.15 $kJ \cdot mol^{-1}$ for the three soils.

Keywords: Wien effect; Mean Gibbs free adsorption energy; Mean Gibbs free binding energy; Heavy metal; Soil

Introduction

The interactions of heavy metal cations with soil particles have been studied extensively and reported in the literatures of soil and environmental sciences. Most evaluations of these cation-soil particle interactions have relied on the inference from adsorption isotherms, whose determination is laborious and time consuming. Recently, Critter and Airoldi (2003) experimentally determined the ion-exchange equilibrium on the interface between cationic latosol soils and aqueous solutions, and calculated the Gibbs free energy, ΔG by linearization of the Langmuir equation. The negative ΔG values that they determined represented spontaneous ion exchange with the hydrogenated soils, which indicated high affinities of these soils for calcium and lead. To summarize, the investigation of energy relationships between cations and soil particles in the second half of the 20th century was based on the indirect deduction, rather than the direct measurement. Since there is no practical and simple method to determine the binding energy of cations to soil particles, this attribute was not studied or reported extensively.

Recently, a new method for evaluating the interactions of ions with charged colloidal particles, based on measurements of the Wien effect in suspensions, has been developed. In a previous article (Li *et al.*, 2005), a new method to determine the binding (or bonding) energy and the adsorption energies of cations with soil particles, in terms of mean Gibbs free energy, ΔG, was presented; it was based on measurement of the Wien effect in soil suspensions. In the present study we used the new method to evaluate the mean Gibbs free binding and

adsorption energies of four heavy metal ions (Cu^{2+}, Zn^{2+}, Cd^{2+}, and Pb^{2+}) on yellow-brown, black and brown soil particles.

Materials and Methods

Preparations of Homoionic Soil Samples and Suspensions

A yellow-brown soil (Alfisol, Nanjing, Jiangsu), a brown soil (Alfisol, Weihai, Shandong) and a black soil (Mollisol, Haerbin, Heilongjiang), which were expected to carry only negative charge, were collected from a depth of about 1 m. Some properties of the tested soils were listed in Table 1. The clay fraction, comprising particles less than 2 μm in diameter, was separated by sedimentation, dried, and ground. The clay fractions of the three soils were saturated with the four different heavy metal cations by three sequential equilibrations with 1 $mol \cdot L^{-1}$ solutions of the chlorides of these heavy metals. The clay samples were then washed until the concentrated chloride supernatants were discarded.

Table 1 Properties of the tested soils

Soil	Depth (cm)	Clay content (<2μm)(%)	O.M. ($g \cdot kg^{-1}$)	Fe_2O_3 ($g \cdot kg^{-1}$)	pH (H_2O)
Yellow-brown soil	50~100	15.9	5.4	16.9	6.46
Brown soil	40~70	23.0	7.0	24.0	6.40
Black soil	80~100	19.6	13.6	11.4	6.86

Suspensions were prepared by adding deionized water to soil colloid samples in 50-mL plastic bottles to a solid concentration of 10 $g \cdot L^{-1}$. The plastic bottles were sealed and shaken for 30 min, and the suspensions were dispersed ultrasonically for 45 min. The homoionic suspensions were allowed to stand for about 7~10 days in order to achieve sufficient equilibration of ion reactions in the suspensions, prior to the measurements in strong electrical fields. The electrical conductivities under weak electrical fields (EC_0) were measured.

Wien Effect Measurement Procedure

The weak-field EC of the suspensions was determined with a regular conductivity bridge, to ensure that it was well within the measurement range of 500 Ω to 20 kΩ of the SHP-2 apparatus. The test suspension was poured into the electrode cell, which was connected to the apparatus via regular copper wires and crocodile clips, and the resistance of the variable resistor was set to about the expected resistance of the test sample. An initial, relatively low voltage of about 1.5 kV was selected, and the spark gap button was pressed to initiate a short pulse. The needle of the galvanometer jumped to the right or left, depending on the direction of the current in the comparison circuit, which, in turn, depended on whether the variable resistance was higher or lower than that of the electrode cell. The variable resistor was adjusted and the procedure was repeated, usually for three to five pulses, until a minimal needle jump was achieved, indicating that the resistances of the variable resistor and the test sample were equal. The resistance of the variable resistor was then determined with a regular meter. It was necessary to wait for a few seconds between successive pulses, to allow full charging of the high-voltage capacitor, and to allow the suspension in the electrode cell to cool down to its initial temperature of 25 ℃. The suspension was stirred with a thin Plexiglas rod between pulses, in order to ensure homogeneity. After the resistance had been determined for a given applied voltage, the voltage was raised to the next required level, and the above procedure was repeated. The measurements were terminated when the voltage had been raised to a level at which sparking (dielectric breakdown) through the suspension occurred. Then, the measurements were repeated in the reverse order using the same suspensions, proceeding from high to low voltages, to eliminate the effects of possible long-term heating and other irreversible phenomena. The data presented in Fig. 1 are the means of these two sets of measurements; the standard errors were usually smaller than the symbols on the graphs. All the reported measurements were made at a constant temperature of 25 ℃.

All the theoretical derivation of mean Gibbs free adsorption energy and mean Gibbs free binding energy of heavy metal on soil by Wien effect of soil suspension were listed in paper (Li *et al.*, 2005; Wang *et al.*, 2008).

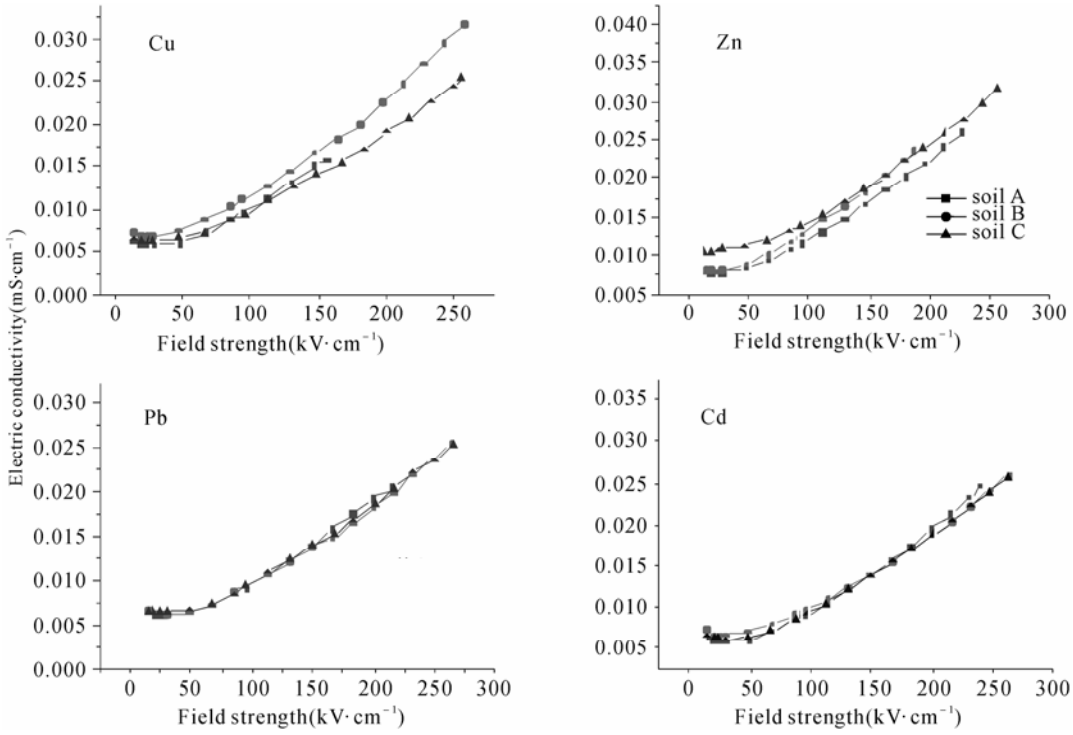

Fig. 1 Electrical conductivity of suspensions (10 g·kg^{-1}) of yellow-brown (A) and black (B) and brown (C) soil particles saturated with various heavy metal ions in deionized water depended on field strength

Results and Discussion

Mean Gibbs Free Binding Energy

The parameters required for calculating the mean Gibbs free binding energy (ΔG_{bi}) from the EC_0 measurements and mean free binding energies are presented in Table 2. The ΔG_{bi} values, were calculated from the EC_0 measurements. The results showed that the mean Gibbs free binding energies of the heavy metal ions with yellow-brown, black and brown soil particles decreased in the order of $Pb^{2+} > Zn^{2+} \geq Cu^{2+} > Cd^{2+}$, $Pb^{2+} > Cu^{2+} > Zn^{2+} > Cd^{2+}$ and $Pb^{2+} > Cd^{2+} > Cu^{2+} > Zn^{2+}$, respectively, where the range of binding energies for yellow-brown soil (7.16~8.54 kJ·mol^{-1}) is less than that for black soil (9.05~9.88 kJ·mol^{-1}). It may be due to its higher organic matter contained in.

EC-Field Strength Relationships

The effects of field strength on the electrical conductivities of the suspensions in deionized water of yellow-brown soil, black soil and brown soil particles saturated with various heavy metal ions, are shown in Fig. 1. With weak electrical fields (about 15 kV·cm^{-1}), the EC values of the suspensions ranged from 0.006 to 0.01 mS·cm^{-1}, and were closely related to the nature of the saturating heavy metal ions. Negative Wien effects (EC(E) smaller than EC_0) appeared at applied fields in the range of about 15 to 50 kV·cm^{-1}. It was suggested previously that the negative second Wien effect arised from a double-layer polarization that caused a temporary re-adsorption of ions on the soil particle dipoles (within the finite pulse duration of 10^{-6} to 10^{-5} s), which led to a decrease in the measured transient electrical conductivity (Schelly and Astumian, 1984). Beyond the concave segments of the EC vs. E curves, the EC increased more steeply. The electrical field-dependent mean Gibbs free adsorption energies of these heavy metal ions for yellow-brown, black and brown soils were calculated and shown in Table 3. The magnitude of adsorption energy of heavy metal on the soil descended in the order of $Cu^{2+} > Cd^{2+} > Pb^{2+} > Zn^{2+}$, $Cu^{2+} > Zn^{2+} > Pb^{2+} > Cd^{2+}$, and $Cu^{2+} > Pb^{2+} > Cd^{2+} > Zn^{2+}$, respectively. The mean Gibbs free adsorption energies of Cu^{2+}, Zn^{2+}, Cd^{2+} and Pb^{2+} at a field

strength of 150 kV·cm^{-1}, for example, were in the range of 1.23 to 2.15 kJ·mol^{-1} for the three soils. This difference may stem from the higher content of organic matter in black soil than in the yellow-brown soil (13.6 and 5.4 g·kg^{-1}, respectively).

Table 2 The electrical conductivity under weak electrical fields (EC_0, mS·cm^{-1}) and pH of the various tested soil suspensions of solids concentration (c_p) of 10 g·L^{-1}, cation exchange capacity at prescribed pH (*CEC*), equivalent ionic conductivity (λ), fraction of ionized ions under weak electrical fields (f_0), Gibbs mean free binding energy (ΔG_{bi}) as determined by EC_0 measurements

Suspension	Yellow-Brown soil (A)				Black soil (B)				Brown soil (C)			
	Cu^{2+}	Zn^{2+}	Pb^{2+}	Cd^{2+}	Cu^{2+}	Zn^{2+}	Pb^{2+}	Cd^{2+}	Cu^{2+}	Zn^{2+}	Pb^{2+}	Cd^{2+}
pH	4.78	5.52	5.03	4.60	5.31	6.06	5.49	5.38	5.17	6.38	5.71	5.59
CEC (mol·kg^{-1})	0.127	0.214	0.158	0.103	0.278	0.326	0.291	0.286	0.170	0.220	0.213	0.205
λ (mS·cm^{-1}·mol^{-1}·L)	53.6	52.8	69.5	54.0	53.6	52.8	69.5	54.0	53.6	52.8	69.5	54.0
Ec_0 (mS·cm^{-1})	0.007	0.010	0.007	0.006	0.008	0.009	0.008	0.008	0.007	0.012	0.007	0.007
f_0	0.048	0.043	0.032	0.065	0.025	0.025	0.019	0.026	0.037	0.051	0.023	0.033
ΔG_{bi} (KJ·mol^{-1})	7.50	7.80	8.54	7.16	9.12	9.11	9.88	9.05	8.18	7.36	9.35	8.49

Table 3 Mean Gibbs free adsorption energies (kJ·mol^{-1}) of various heavy metal ions adsorbed on the surfaces of yellow-brown soil and black soil particles at several field strengths

Cation	Yellow-Brown Soil			Black Soil			Brown Soil		
	100	150	200	100	150	200	100	150	200
	kV·cm^{-1}								
Cu^{2+}	1.26	2.15	3.03	1.21	2.11	2.73	1.01	1.71	2.56
Zn^{2+}	0.91	1.56	2.21	1.13	1.91	/	0.68	1.23	1.79
Pb^{2+}	0.95	1.75	2.51	0.86	1.52	2.32	0.92	1.64	2.49
Cd^{2+}	1.18	1.93	2.92	0.75	1.41	2.26	0.97	1.67	2.53

Acknowledgements

We acknowledge the support of the Knowledge Innovation Program of the Chinese Academy of Sciences (ISSASIP 0718) and the National Natural Science Foundation of China under projects No. 40401030, 40871114.

References

Critter SAM, Airoldi C (2003) Adsorption and desorption processes on red Latosol soil surface. Geoderma 111:57-74

Li CB, Zhao AZ, Friedman SP (2005) A new method to evaluate adsorption energies between cations and soil particles via Wien effect measurements in dilute suspensions. Environ. Sci. Technol. 39: 6757-6764

Schelly ZA, Astumian RD (1984) A theory for the apparent 'negative second Wien effect" observed in electric-field jump studies of suspensions. J. Phys. Chem. 88: 1152-1156

Wang YJ, Li CB, Wang W, *et al.* (2008) Wien Effect Determination of Adsorption Energies between Heavy Metal Ions and Soil Particles. Soil Sci. Soc. Am. J.72: 56-62

Can Zn, Ca and Sulfate Amendments Affect Cadmium Uptake in Rice (*Oryza sativa* L.)

Linfei Hu[a,b], Jianming Xu[a], Jianjun Wu[a], Murray B. McBride[b,*]

[a] Zhejiang Provincial Key Laboratory of Subtropical Soil and Plant Nutrition, College of Environmental and Natural Resource Sciences, Zhejiang University, Hangzhou 310029, China;
[b] Department of Crop and Soil Sciences, Bradfield Hall, Cornell University, Ithaca, NY 14853 USA.
[*]Corresponding author. Tel. No. +1 -607 255 1728; Fax No. +1 -607 255 3207; E-mail: mbm7@cornell.edu.

Abstract: To investigate the effect of Ca, Zn and sulfate on Cd uptake and cultivar differences, a greenhouse experiment was carried out using two cultivars (*indica* type Teqing and *japonica* type Jefferson) of paddy rice with different levels of Zn sulfate and gypsum amendments. Total concentrations of Cd, Ca, Zn and S were measured in rice shoots and grain. Cd uptake by rice plants was affected significantly by Cd-amendment ($p< 0.001$). No difference in Cd uptake was measured between the treatments with and without Zn-amendment. However, the experiment exhibited a difference in Cd uptake as affected by rice cultivar. At the high Cd loading, there appeared to be the same uptake tendency in the Teqing cultivar for Cd, Zn and Ca. Reduction of plant Cd followed that of S during the maturation of the Teqing cultivar, whereas plant Ca decreased as the Zn concentration increased with maturation in the Jefferson cultivar.

Keywords: Cadmium uptake; Rice cultivars; Heavy metal

Introduction

Cadmium (Cd), a potentially toxic heavy metal with no known biological function, occurs widely in small amounts in nature associated with the Zn ore sphalerite and is therefore a waste product of Zn mining (Lindsay, 1979). Paddy rice soils in several regions of southeastern China have been contaminated by heavy metals, especially by Cd as a result of mining, industrial waste disposal, fertilizer applications and sewage sludge disposal on land (Alloway, 1990; Naidu *et al.*, 1997), which has eventually increased Cd concentrat-ions in food crops. The impact of Cd contamination on soil quality and crop growth therefore has become a public concern worldwide (Obata and Umebayashi, 1997). Considering the potential physiological competitive relationship between Cd and Zn and the importance of Ca in plant structure and cell signaling, this study was initiated to investigate the potential for reducing Cd uptake by paddy rice by using Zn sulfate and gypsum soil amendments. Sulfates added to paddy rice soils could have the benefit of immobilizing Cd into insoluble sulfide minerals under anoxic conditions.

Materials and Methods

Two different rice cultivars, Teqing (photo-insensitive *indica* type) from China and Jefferson (a tolerant tropical *japonica* type) from USA, were used in this experiment. Calcareous soil (pH=7.1) used in this experiment was collected in Cortland, New York, USA. The experiment was performed in 9 treatments with 6 replicates per treatment. NPK (10-10-10) fertilizer blend was incorporated into the air-dried soil at the rate of 120 kg $N{\cdot}ha^{-1}$. 170 kg of this soil mixture was placed in each of 9 plastic-lined treatment boxes with the dimensions of 90.7 cm×70.7 cm×20.3 cm (width × length × height). After application of chemical fertilizers, different Cd, Zn and Ca concentrations (Table 1) were added in the

form of $CdSO_4$, $ZnSO_4$ and $CaSO_4$ to each treatment and mixed well. The soil in each treatment box was then flooded with 5 cm water above the soil surface for 10 days, and thereafter 6 seedlings of each rice cultivar were transplanted into each box as 6 replicates of each treatment on September 25, 2008. The boxes were kept in the greenhouse with a natural day/night regime and watered as required. Three of the six rice shoot were sampled and analyzed at the tillering stage on Nov 12, 2008; the remaining rice shoots were harvested and analyzed at the ripening stage on Feb 4, 2009.

Table 1 Experiment design for the treatments of pot experiment

Treatment	Cd ($mg \cdot kg^{-1}$)	Zn ($mg \cdot kg^{-1}$)	Ca ($mg \cdot kg^{-1}$)
T1	0	0	0
T2	2	0	0
T3	2	20	0
T4	2	0	60
T5	2	20	60
T6	10	0	0
T7	10	20	0
T8	10	0	60
T9	10	20	60

Soil pH and total contents of heavy metals in the soil were measured before rice transplanting started. The soil pH was measured using a glass pH electrode with a water-soil ratio of 2:1.

Initial rice sampling at the tillering stage involved collection and analysis of the entire rice shoot (cut at water level). Subsequent sampling at the ripening stage involved shoot and grain tissues of both rice cultivars with leaves and grain being analysed for total Cd, Ca, S, and Zn. Rice tissue samples for elemental analysis were oven-dried at 70 ℃, ground, and finally acid-digested using a microwave digester (CEM MarsXpress). The concentrations of Cd, Zn, Ca and S were then measured by axial-view ICP emission. Soil samples were collected before rice seedlings were transplanted, air-dried and acid-digested using microwave digester. Total Cd, Zn and S in the soils were then measured by axial-view ICP emission.

Results and Discussion

Uptake coefficients for Cd transfer into whole plant, foliar and grain tissues were quite low at both levels of added Cd (about 2.26±0.3 and 9.09±0.6 $mg \cdot kg^{-1}$ total soil Cd) for both rice cultivars tested. However, the high Cd loading resulted in higher Cd concentrations of foliar and whole-plant than the low loading, with both Cd loadings leading to plant Cd concentrations higher than that in rice plants grown on the uncontaminated control soil. Cd concentrations in rice shoots at tillering stage were higher than that at the ripening stage, especially in the Teqing treatments and high Cd loading Jefferson treatments.

Concentrations of Ca, S and Zn in rice shoots showed no significant difference between treatments at either the tillering stage or the ripening stage despite the Zn sulfate and gypsum amendments. It is likely that the Ca uptake largely depends on plant physiological control, and furthermore the Ca added to the soil is a small amount comparing to the Ca already presented in the soil. The high pH and calcareous nature of the soil explains the low plant availability of the added Zn.

However, plant S concentrations did show a reduction at the ripening stage concomitant with a decline of Cd concentrations, especially in the Teqing treatments (Fig. 1(A)). Conversely, a significant increase in Ca concentration occurred at the ripening stage in the Jefferson cultivar while Zn concentration displayed a decrease (Fig. 1 (B)). Fig. 2 suggests a similar uptake tendency in the Teqing variety for Cd, Zn and Ca, especially at high Cd loading treatments.

Rice grain Cd concentrations, measured in Teqing, although higher than in grain from the control treatment (mean value, 0.02 $mg \cdot kg^{-1}$), were not significantly different for the low (mean value, 0.21 $mg \cdot kg^{-1}$) and high soil Cd (mean value, 0.20 $mg \cdot kg^{-1}$) loadings. This relatively low uptake efficiency into rice grain, as well as in rice shoots, can probably be attributed to the high pH and calcareous nature of the soil used in this study, which can be expected to control Cd at very low solubility in soil solution. The lack of effectiveness of the gypsum and Zn amendments is possibly a consequence of the already low phytoavailability of Cd added to this soil type.

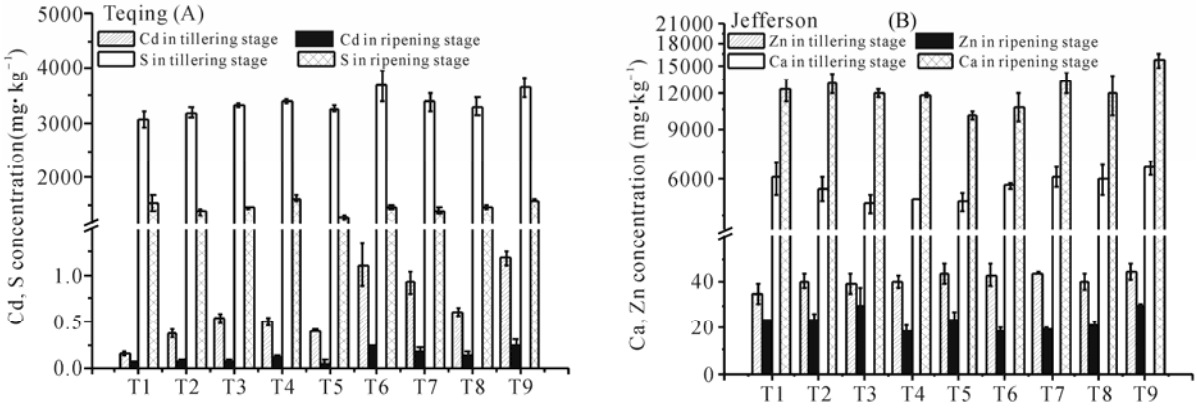

Fig. 1 Concentration of Cd and S in rice shoots of Teqing cultivar(A), Ca and Zn in rice shoots of Jefferson cultivar (B) at both tillering and ripening stage; Bars are the standard error of means of three replicates

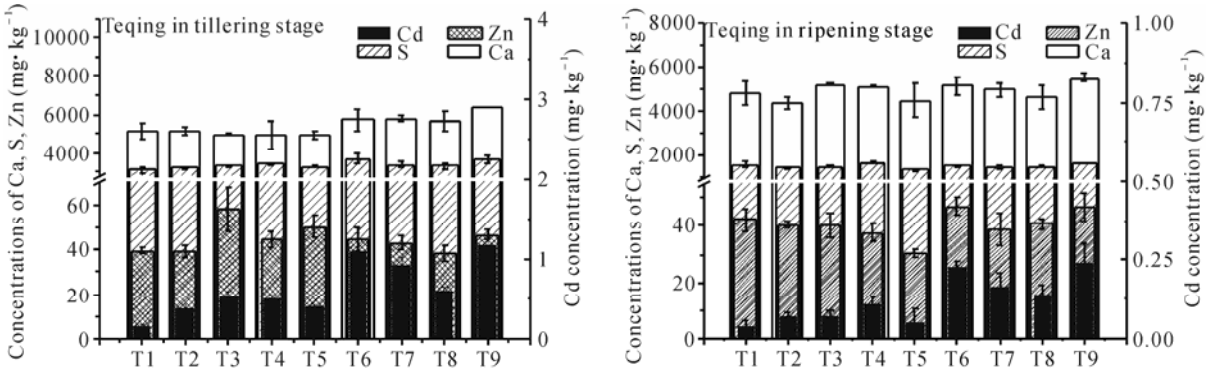

Fig. 2 Concentrations of Ca, S, Zn and Cd in shoots of Teqing cultivar at tillering stage (left graph) and ripening stage (right gragh); Bars are the standard error of means of three replicates

References

Alloway BJ (1990) Cadmium. In Heavy Metals in Soils. B.J. Alloway (Ed.). Wiley, New York, USA. pp. 100-124

Lindsay WL (1979) Chemical Equilibria in Soils. Wiley, New York, USA

Naidu R, Kookana RS, Sumner ME, Harter RD, Tiller KG (1997) Cadmium sorption and transport in variable charge soils: a review. J. Environ. Qual. 26: 602-617

Obata H, Umebayashi M (1997) Effects of cadmium on mineral nutrient concentrations in plants differing in tolerance for cadmium. J. Plant Nutri. 20: 97-105

Dynamics of As Species in the Interface of Soil and Rice Roots under Three Water Regimes

Wenju Liu*, Lina Chen, Ying Wang

College of Resources and Environmental Sciences, Hebei Agricultural University, Baoding 071000, Hebei Province, China.
*Corresponding author. Tel. No. (86)312-7528228; Fax No. + (86)312-7528208; E-mail: liuwj@hebau.edu.cn.

Abstract: Arsenic (As) is an ubiquitous metalloid, widely distributed in the environment through both natural and anthropogenic pathways. A compartmented soil-sand culture system with rhizo-bag was used to investigate the dynamics of As and Fe species in the soil solution of rhizosphere under three water regimes in whole growing stages of rice plants. The results showed that flooded regime increased significantly concentrations of arsenite and arsenate at booting stage and grain-filling stage (p<0.001, the highest concentration: 2.67 mg·L^{-1}) comparing with other two water regimes, unflooded and flooded-unflooded. There were significantly positive correlations between As and Fe species in soil solution of rhizosphere, between As concentrations in iron plaque and amounts of iron plaque formed as well.

Keywords: Rice; Flooded; Flooded-unflooded; Unflooded; Iron plaque; Arsenite and arsenate in soil solution

Introduction

Arsenic (As) exposure from consumption of rice can be substantial, particularly for the population on subsistence rice diet in South Asia for whom rice is the staple food. Paddy rice has a much enhanced As accumulation compared with other cereal crops for flooded condition of rice (Williams *et al*., 2007). Xu *et al.* (2008) investigated the dynamics of As speciation under flooded and aerobic conditions through adding As in normal soil. Rice grown on As-contaminated paddy soils can accumulate high levels of As in grains (Zhu *et al*., 2008). Therefore, development of manag-ement practices to reduce As concentrations in rice requires a better understanding of behaviors of arsenic species in rhizosphere soil from As-contaminated area in whole growing stages. We investigated the dynamics of As and Fe species related to Eh in the soil solution of rhizosphere under three water regimes using a soil-sand combined culture system.

Materials and Methods

A compartmented soil-sand culture system was set up. Rice seedlings were grown in the rhizo-bag (made of 35 μm nylon mesh, 5 cm radii and 80 cm height, one plant per bag) with quartz sand, and the 4 rhizo-bags was placed into a bigger PVC pot (outer compartment, 20 cm radii and 40 cm height) filled with 10 kg As-contaminated soil. The previous experiment using transparent rhizo-box showed that the length of most rice roots was about 40 cm, so the rhizo-bag and PVC pot of 40 cm height were used in this experiment. As-contaminated soil was collected from Shangyu, Zhejiang province where the soil was contaminated for mining activities. The principal soil properties were measured following standard procedures, and were as follows. The total C, CEC, pH were 9.82 g·kg^{-1}, 7.45 cmol(+)·kg^{-1} and 7.72, respectively. Texture: loam; Fe_2O_3: 1.77%; Total Fe: 2.69%; available P: 12.9 mg·kg^{-1}; total As: 383 mg·kg^{-1}. The rhizo-sampler (Rhizosphere Research Products, Wageningen, The Netherlands) was buried

along each mesh bag and kept always adjacent to the rice root for the real-time collection of soil solution in the rhizosphere. As species in soil solution was separated by the cartridges (Metalsoft centre, USA) (Fig. 1).

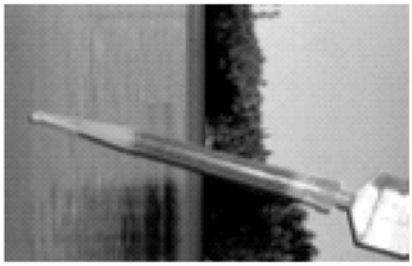

Fig.1 The cartridge for As species separation

The concentrations of Fe and As were measured by an inductively coupled plasma-optical emission spectrometer (ICPOES, Optima 2000 DV, Perkin Elmer, USA) and atomic fluorescence spectrometry (AF-610A, Beijing Ruili Analytical Instrument Co., Beijing, China) respectively.

Results and Discussion

The concentrations of As^{3+} and As^{5+} in soil solution under flooded condition were markedly higher than those under unflooded and flooded-unflooded conditions except for tillering stage (P<0.001, Table 1) for the growth of rice seedlings requiring flooded-unflooded condition at this stage according to the property of rice cultivar from local research centre. After tillering stage, flooded regime increased arsenite and arsenate significantly, being 500~1000 and 20~60 folds, respectively at booting and grain-filling stages (the highest concentration: 2.67 $mg \cdot L^{-1}$), as compared with other two water regimes. The predominant species of arsenic was arsenate under unflooded and flooded-unflooded conditions, which was in consistent with previous results. However, 46%~58% of As was arsenite and 40%~54% of As was arsenate in the soil solution. These were not in consistent with the results of Xu *et al*. (2008).

Table 2 showed the correlations in soil solution of rhizosphere between concentrations of Fe^{2+} and As^{3+}, Fe^{3+} and As^{5+}. The details were as follow: the concentrations of As^{3+} and Fe^{2+} got their max-correlative coefficients under flooded and flooded-unflooded conditions respectively (r_a=0.56, P<0.001; r_b=0.76, P<0.001), However, there was no correlation between As and Fe concentrations under unflooded of water regime. Moreover, there was only positive correlation between Fe^{3+} and As^{5+} concentration under flooded condition.

Table 1 Dynamics of As^{3+} and As^{5+} concentrations and percentage of As^{3+} and As^{5+} in the soil solution of rhizosphere under three water regimes during the whole growing stages of rice (means±SE, n=4)

Water regimes	Growing stages	As^{3+} ($\mu g \cdot L^{-1}$)	As^{5+} ($\mu g \cdot L^{-1}$)	As^{3+} (%)	As^{5+} (%)
Unflooded	I*	7.06±0.84	27.5±2.26	14.3	85.7
	II	0.31±0.15	27.9±5.35	4.30	95.7
	III	4.02±0.69	23.4±263	12.1	87.9
	IV	23.4±7.71	28.9±5.06	26.4	73.6
Flooded and Unflooded	I	7.06±0.84	27.5±2.26	14.3	85.7
	II	0.15±0.04	38.1±6.67	0.37	99.6
	III	59.1±12.1	81.3±6.38	35.8	64.3
	IV	0.34±0.05	27.6±6.84	1.11	98.9
Flooded	I	7.06±0.84	27.5±2.26	14.3	85.7
	II	1399±163	998±309	60.2	39.8
	III	2665±593	1729±368	46.4	53.6
	IV	13.9±3.90	58.0±7.10	58.4	41.6

*I: Tillering stage, II: Booting stage, III: Grain-filling stage, IV: Maturity stage

Table 2 The correlationship of As-Fe in the soil solution under three water regimes

	Fe^{2+}-As^{3+}			Fe^{3+}-As^{5+}		
	a*	b	c	a	b	c
r	0.56	0.76	0.09	0.42	0.11	-0.21
P	<0.001	<0.001	0.36	<0.001	0.29	0.41

a: Flooded，b: Flooded-unflooded, c: Unflooded

Iron plaque is commonly formed on the surfaces of rice roots as a result of release of oxygen and oxidants into the rhizosphere and had a high affinity to Arsenate. The results showed that amount of iron plaque formed at flooded was markedly higher than those at unflooded and flooded-unflooded (P<0.001). It was very clear that there were significant differences in amounts of iron plaque among 4 growth stages (P<0.001) and followed the rank of I<III<<II

and IV. Finally, there were significantly positive correlations between As concentrations in iron plaque and amounts of iron plaque (P<0.001, Table 3) despite different growing stages or three water regimes.

Table 3 The correlationship of As-Fe in the root plaque of rice under different water regimes

Water regimes	Flooded	Flooded-unflooded	Unflooded
r	0.788**	0.695**	0.733**
P	<0.001	<0.001	<0.001

Acknowledgements

This study was financially supported by the Natural Science Foundation of China and the Natural Science Foundation of Hebei Province (40673060, D2007000553)

References

Williams PN, Villada A, Deacon C, Raab A, Figuerola J, Green AJ, Feldmann J, Meharg AA (2007) Greatly enhanced arsenic shoot assimilation in rice leads to elevated grain export; comparison with wheat & barley. Environ. Sci. Technol. 41, 6854-6859

Xu XY, McGrath SP, Meharg A, Zhao FJ. Growing rice aerobically markedly decreases arsenic accumulation (2008) Environ. Sci. Technol. 42, 5574-5579

Zhu YG, Sun GX, Lei M, Teng M, Liu YX, Chen NC, Wang LH, Carey AM, Deacon C, Raab A, Meharg AA, Williams PN (2008) High percentage inorganic arsenic content of mining impacted and non-impacted Chinese rice. Environ. Sci. Technol. 42, 5008-5013

Extra Supply of Calcium Is Not Required for Maximal Root Growth in the Nitrate and Phosphorus-rich Patch in an Acid Soil

Chandrakumara Weligama[a], Caixian Tang[a,*], Peter W.G. Sale[a], Mark K. Conyers[b], De Li Liu[b]

[a]Department of Agricultural Sciences, La Trobe University, Melbourne, Victoria 3086, Australia;
[b] NSW Department of Primary Industries (EH Graham Centre for Agricultural Innovation), Wagga Wagga Agricultural Institute, PMB, Wagga Wagga, New South Wales 2650, Australia.
[*]Corresponding author. Tel. No. +61 3 94792184; Fax No. +61 3 94710224; E-mail: C.Tang@latrobe.edu.au.

Abstract: Subsurface acidity is a major concern in agricultural soils. Surface application of lime is not effective and therefore alternative approaches are being tested to combat subsurface acidity. The supply of NO_3^- increases excess anion uptake and results in rhizosphere alkalisation which can use as a method of biological amelioration. A glasshouse study was conducted with wheat to examine the effect of localised supply of P and Ca alone or combination with NO_3^- on subsurface root proliferation and rhizosphere alkalisation in an acid soil. The results show that localised supply of NO_3^- plus P in the subsurface maximises root proliferation without extra Ca supply.

Keywords: Nutrient banding; Heterogeneity; Soil management; *Triticum aestivum*; N uptake

Introduction

Subsurface acidity is a key limiting factor in some agricultural soils. The application of lime to the surface is ineffective in combating subsurface acidity due to the immobility of lime (Conyers *et al*., 2003). An alternative approach for combating subsurface acidity is to supply of NO_3^--N to the subsoil which results in excess anion uptake and increases rhizosphere pH (Weligama *et al*., 2008). However, there needs to be sufficient root growth in the subsurface in order to capture NO_3^- ions.

Roots have been shown to proliferate in soils where there are locally available N and P (Robinson 1994). However, there is increasing evidence that root response to localised nutrients depends on the nutritional status of the plant (Zhang and Forde, 1998), and that the plant roots need an adequate supply of all nutrients to achieve maximal growth (Weligama *et al*., 2008; Officer *et al*., 2009). In addition, acid or alkaline soil conditions may alter root response to nutrient-rich soil patches (Weligama *et al*., 2008; Officer *et al*., 2009).

Our previous study showed that localised application of N as $Ca(NO_3)_2$ had a marked effect on root proliferation in a strongly acid soil (Weligama *et al*., 2008). However, the addition of P with N in the nutrient-enriched soil layer maximised root growth. Although, Ca was supplied as a basal nutrient in the whole soil column, N banded layer had "a luxury level" of calcium supply which suggests that extra Ca provided in nutrient-rich layer of the acid soil may contribute to improved root response to the localised nutrient supply. The purpose of this study was to investigate whether the supply of P and Ca alone or in combination with N, contributes to the root proliferation in the nutrient-rich soil layer in an acid soil.

Material and Methods

The experiment was carried out using 50-cm soil columns in the naturally lit glasshouse conditions in La Trobe University farm, Victoria (37º42'S, 145º02'E). The columns contained a sandy soil with low pH (3.6 in 0.01 $mol \cdot L^{-1}$ $CaCl_2$) and pH buffering capacity (0.81 $cmol \cdot pH^{-1} \cdot kg^{-1}$). The column preparation and soil compaction were detailed in

Weligama *et al*. (2008). Aluminium tolerant (ET8) wheat (*Triticum aestivum* L.) genotype was grown for 42 days. Treatments included the supply of NO_3^-, P and Ca alone or in combination to the subsurface 10~15 cm soil layer. This involved addition of KNO_3, KH_2PO_4 and $CaCl_2$ (extra) at rates of 340, 176 and 173 mg, respectively. The control treatment received the same amount of N, P and Ca supplied to the whole soil column. Basal nutrients were supplied uniformly to the whole soil column as detailed in Weligama *et al*. (2008) except for K which was adjusted for the K content in KNO_3 and KH_2PO_4. At harvest, the soil was sampled by dividing into the 0~10, 10~15, 15~25 and 25~50 cm layers. Roots were recovered, the rhizosphere and bulk soil collected. Measurements included the shoot and root dry matter, the rhizosphere pH for all soil layers and the concentrations of N, P, Ca, Mg, K and Na in shoots.

Results and Discussion

The localised supply of NP and NPCa resulted in significant increase in shoot and root dry weights, and root length compared to the control (Table 1). There was no treatment effect on ion concentrations in shoots except for N and P (data not presented). The localised supply of P with N or/and Ca significantly increased total uptake of N, P and Ca by shoots (Table 1). Maximum root proliferation in the nutrient-enriched soil layer (10~15 cm) occurred with the NPCa and NP treatments (Fig. 1A) where there was significantly more root mass that all other treatments apart from the NCa treatment. In contrast, the supply of P and Ca alone or in combination in the enriched layer did not increase root mass in that layer, compared to the control. Therefore, the key factor for root growth stimulation in the nutrient-enriched soil layer appeared to be the presence of NO_3^- and P. It has been shown that localised NO_3^- can signal to the lateral root tips to increase elongation (Zhang and Forde, 1998). Further, the enrichment of N and P together in the same soil layer had "a compounding effect" on root proliferation compared to the localised supply of N alone. This occurred even with a sufficient background supply of phosphorus distributed throughout the column.

Another key feature of this study was the maximum rhizosphere alkalisation occurred in the N-enriched soil layer irrespective of whether P or/and extra Ca were present (Fig. 1B). This can be attributed to the excess uptake of anions in NO_3^- form over cations from the enriched layer. In our previous study, the maximum alkalisation in nutrient-enriched soil layer occurred when N and P supplied together compared to the N alone treatment (Weligama *et al*., 2008). However, in that study, there was no background P supplied to the soil column with the N-enriched soil layer. The increased availability of P is known to increase NO_3^- uptake by plants (Schjørring, 1986) which explains the discrepancy between the two experiments.

Table 1 Shoot & root dry matter, root lengths and total uptake of N, P & Ca by shoots of wheat grown for 42 days with various combinations of localised supply of NO_3^-, P and Ca in acid soil columns (* and *** represent probability of ≤0.05 and ≤ 0.001, respectively)

Treatments	Shoot DM ($g \cdot column^{-1}$)	Root DM ($g \cdot column^{-1}$)	Root length ($m \cdot column^{-1}$)	Total uptake by shoots ($mg \cdot column^{-1}$)		
				N	P	Ca
NPCa 0~50 cm	1.24	0.70	36.0	34.6	2.6	4.3
N 10~15 cm	1.33	0.58	34.9	40.3	3.3	4.6
P 10~15 cm	1.67	0.73	44.7	52.9	5.2	5.8
Ca 10~15 cm	1.30	0.69	32.6	32.8	2.8	5.2
NP 10~15 cm	1.83	0.78	46.2	64.5	6.6	7.1
NCa 10~15 cm	1.51	0.68	41.4	50.2	4.0	6.3
PCa 10~15 cm	1.72	0.68	41.8	65.0	6.0	7.1
NPCa 10~15 cm	2.07	0.80	51.9	67.0	8.4	7.6
LSD (P=0.05)	0.51	0.10	6.5	20.4	2.4	2.1
Levels of significance	*	*	***	*	***	*

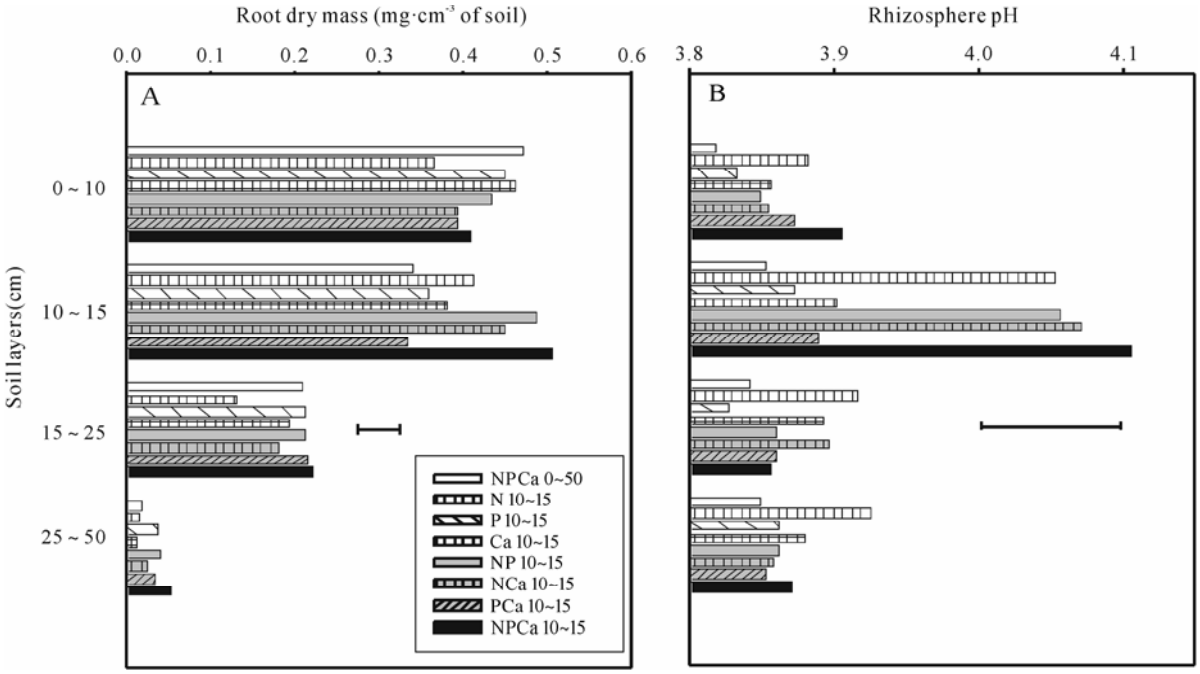

Fig. 1 Changes of root dry mass (A) and rhizosphere pH (B) after growing wheat plants for 42 days in 50-cm soil columns with different combination of N, P and Ca placements in 10~15 cm(shaded in grey). Values are means of threeeplicates. Horizontal bars are LSD(*P*=0.05) for comparing any two treatments

This study confirms that the supply of P with N in the nutrient-rich patch maximises root proliferation in this acid soil. The supply of extra Ca is not required in acid soils to achieve maximum root growth when there is sufficient background Ca in the soil profile. On the other hand, maximum rhizosphere alkalisation was achieved with the supply of N alone in the nutrient-enriched layer, when sufficient background P was available.

Acknowledgement

We thank the Australian Research Council for financial support.

References

Conyers MK, Mullen CL, Scott BJ, Poile GJ, Braysher BD (2003) Long-term benefits of limestone applications to soil properties and to cereal crop yields in southern and central New South Wales. Aust. J. Exp. Agric. 43: 71-78

Officer SJ, Dunbabin VM, Armstrong RD, Norton RM (2009) Wheat roots proliferate in response to nitrogen and phosphorus fertilisers in Sodosol and Vertosol soils of south-eastern Australia. Aust. J. Soil Res. 47: 91-102

Robinson D (1994) The response of plants to non-uniform supplies of nutrients. New Phytol 127: 635-674

Schjørring JK (1986) Nitrate and ammonium absorption by plants growing at sufficient or insufficient level of phosphorus in nutrient solutions. Plant Soil 91: 313-318

Weligama C, Tang C, Sale P, Conyers M, Liu D (2008) Localised nitrate and phosphate application enhances root proliferation by wheat and maximises rhizosphere alkalisation in acid subsoil. Plant Soil 312: 101-115

Zhang H, Forde BG (1998) An Arabidopsis MADS box gene that controls nutrient-induced changes in root architecture. Science 279: 407-409

Effect of Natural Acid Peat Application on the Phytoextraction of Cadmium from Contaminated Soils

Iksong Ham[a,b], Jianming Xu[a,*], Linfei Hu[a], Pan Ming Huang†[a,c]

[a] Zhejiang Provincial Key Laboratory of Subtropical Soil and Plant Nutrition, College of Environmental and Natural Resource Sciences, Zhejiang University, Hangzhou 310029, China;
[b] Institute of Agricultural Chemistry Science, Sariwon Kyeungsang Agriculture University, Sariwon, Huanghae north province, D.P.R of Korea;
[c] Department of Soil Science, University of Saskatchewan, Saskatoon, SK S7N 5A8, Canada.
[*]Corresponding author. Tel. No. +86-571 86971955; Fax No. +86-571 8697 1955; E-mail: jmxu@zju.edu.cn.

Abstract: Cadmium（Cd） poses a major environmental and human health threat because of its constant release to the environment through anthropogenic activities. Therefore, cost-effective remediation procedures for Cd contamination should be developed to restore ecosystem heath. Phytoremediation, the use of plants to extract contaminants from soils and groundwater has revealed great potential. However, it is limited by the fact that plants need time, nutrient supply and, moreover, have a limited metal uptake capacity. To increase Cd uptake by plants, the effects of the application of natural acid peat and the resulting decrease in soil pH on the amount of Cd taken up by plants were investigated in a pot experiment using two paddy soils contaminated artificially with Cd. An experiment was conducted using a root-bag technique，and four treatments of peat were applied : control(no peat treatment) and peat application（2.5, 5.0, 10.0 g·kg^{-1} ）. The peat was applied to the soil at two Cd dosages(2.5 and 5.0 mg Cd·kg^{-1} soil). The uptake of Cd by plant *Brassica campestris ssp. Chinesis L* was determined and its relation to the amounts of total and bioavailable Cd in the soil was investigated. It was found that the amount of bioavailabile Cd of the soils, as determined by diethylenetriaminepentaacetic acid (DTPA) extraction, was little affected by applications of the peat ,but plant uptake of Cd was enhanced, in some cases up to 114.6%~123.6%. At the contamination level of 2.5 mg Cd·kg^{-1} soil, the peat added at a rate of 5.0 g·kg^{-1} soil increased the Cd concentration in the shoot from 9.7 to 11.6 mg·kg^{-1} in the blue clayed paddy soil and from 13.1 to 16.1 mg·kg^{-1} in the yellow mettled paddy soil. At the contamination level of 5.0 mg Cd·kg^{-1} soil, the peat added at a rate of 10.0 g·kg^{-1} soil increased the Cd concentration in the shoot from 25.3 to 29.8 mg·kg^{-1} and from 29.1 to 33.4 mg·kg^{-1} in the blue clayed paddy soil and the yellow mettled paddy soil, respectively. The amount of Cd in shoots (mg·plant^{-1}) was also significantly increased by the application of 5.0 and 10.0 g peat·kg^{-1} soil. The enhancement is attributable to the decrease in pH and chelate-assisted phytoextraction, resulting in higher Cd availability.

Keywords: Phytoremediation; Cadmium; Natural acid peat

Introduction

A large number of paddy fields were contaminated with cadmium (Cd) by mining wastewater (Yamane, 1981), resulting in serious human health problems such as "itai-itai" disease. Most soils contaminated with Cd have been restored by soil topdressing. However, brown rice containing Cd concentrations higher than the acceptable limit of 0.1 mg·kg^{-1} is still sometimes produced and large areas of paddy fields produce brown rice containing more than 0.4 mg Cd· kg^{-1} rice. Remediation of such large areas by top dressing

is impractical because of the high cost. Therefore, other remediation methods for removing Cd from soil need to be developed.

Phytoremediation is defined as the use of green plants in removing pollutants from the environment, or in rendering them harmless (Raskin *et al*., 1997). In contrast to other remediation technologies, such as land filling, fixation and leaching, phytoremediation is relatively cost-effective, aesthetically pleasing and requires smaller disposal facilities (Glass, 1999). Moreover, phytoremediation offers the great advantage of causing only minimal environmental disturbance, since it does not adversely alter the soil matrix. Thus after successful phytoremediation, the soil can directly be used for agricultural purposes. Toxic heavy metals and organic pollutants are both targets for phytoreme-diation. Salt *et al*. (1998) summarized the following phytoremediation sub-groups: (1) phytoextraction−the use of pollutant-accumulating plants to remove metals or organic pollutants from soil by concentrating them in harvestable parts, (2) phytodegradation−the process whereby plants and associated microorganisms are used to degrade organic pollutants, (3) rhizofiltration-whereby plant roots are used to absorb pollutants, mainly metals, from water and aqueous waste streams, (4) phytostabilisation−whereby plants reduce the bioavailability of pollutants in the environment, and (5) phytovolatilisation−the use of plants to volatilise certain pollutants and remove them from air.

The concept of phytoextraction was first put forward by Chaney(1997) based on the previous literature. Phytoextraction can be divided into two approaches, namely, continuous phytoextractoin and chelate-assisted phytoextractoin. Furthermore Salt (1998), among others reported that heavy metal uptake by plants from contaminated soils were increased by using fertilizer. All plants have the potential to extract metals from soils, but some plants have shown the ability to extract, accumulate and tolerate high levels of heavy metals; such plants are termed hyperaccumu-lators. According to Brown *et al*. (1995), hyperaccumu-lator species are those plants whose leaves may contain >100 mg $Cd \cdot kg^{-1}$. *Thlaspi caerulescens* is a well-known hyperaccumulator of Cd (McGrath, 1998). However, it grows slowly and displays low biomass production (Ebbs *et al*., 1997). Because biomass production in most hyperaccumulator species is low, heavy metal removal from soil is limited (Kayser *et al*., 2000). The amount of Cd taken up by a plant is calculated as the product of the Cd concentration and the biomass of the plant. Therefore, for efficient phytoremediation of Cd-contaminated soil, plants that can accumulate high Cd concentrations and also have a high biomass must be used. *Brassica campestris ssp. Chinesis L* plants exhibit a relatively high Cd concentration and biomass (Sun *et al*., 2005).

Plant uptake of Cd is generally limited by metal solubility. Increasing the bioavailability of heavy metal concentration in the soil enhances the uptake of heavy metals in plants. The bioavailability of metals in soil is affected by numerous factors, such as cation exchange capacity, pH values of the soil, excess amounts of fertilizers, and chelators.These may all be manipulated to improve Cd phytoextraction. Chelators, such as EDTA increase the solubility of metal cations, and thus their bioavailability to plants. The positive effects of EDTA on the phytoextraction of metals are, however, accompanied by negative effects on the soil. Its non-selective nature in extracting metals is a disadvantage, since this agent extracts a wide variety of metals, including alkaline earth cations, such as Ca and Mg, which are necessary for plant growth (Barona *et al*., 2001). Moreover, EDTA is not easily biode-gradable, and may remain adsorbed to soil particles even after soil cleaning (Wasay *et al*., 1998). EDTA has also the effect of decreasing severely the plant growth (Chen and Cutright, 2001).

The success of phytoextraction depends on appropriate soil management practices to make metals more available to plants. Therefore, successful phy-toremediation must include the mobilization of heavy metals into the soil that is in direct contact with the roots (Begonia *et al*., 2003). In particular, soil pH is the single most important soil property that determines Cd bioavailability to plants (Adriano 2001). Hattori *et al*. (2006) investigated the effects of soil application of chloride and of a decrease in soil pH on Cd uptake by sunflower, kenaf and sorghum plants. Among the diverse strategies to enhance phytoextraction, pH adjustment has received the most attention, because bioavailability of Cd is largely controlled by soil pH. Although reducing soil pH appears to be an effective strategy to enhance Cd and Zn phytoextraction, precaution is needed because low pH and elevated metal concentrations may cause negative impacts to already vulnerable soil ecological systems.

Therefore, the application of natural acid peat to contaminated soils could be a promising method for

phytoextractoin of Cd, because of its acidity and complexation ability to release soil Cd.

The objective of this research was, thus, Cd to investigate the ability of natural acid peat in enhancing the phytoextraction of Cd from the soils by the use of *Brassica campestris ssp. Chinesis L* plants under well controlled laboratory conditions.

Materials and methods

Soil and Peat Characterization

The two soils were collected from Jiaxing, Zhejiang Province, China: soil 1 Yellow mottled paddy soil; soil 2 Blue clayed paddy soil). Peat was from "SUNSHINE"brand of Canada, which was supplied from Zhejiang Hongyue company. It was dried, ground and sieved. Peat particles of less than 2 mm in diameter was used in this study. The soil was air-dried at room temperature and then passed through a 2-mm mesh sieve. The general properties of soils and peat are shown in Table 1.

Total heavy metal concentrations of the soils were determined with atomic absorption spectroscopy (AAS) using flame mode following HF-HNO_3-$HClO_4$ digestion procedures (Wei, 1992). Soil pH was measured in a soil water suspension (10 g soil to 25 ml deionized water) after shaking for 2 min at 180 rpm and standing for 30min. The peat pH was measured in a peat water suspension (1:5).

Table 1 Properties of the soils and peat studied

sample	Total								Bio-Cd[b] mg·kg^{-1}
	pH	CEC[a]	C	N	Zn	Cu	P+b	Cd	
	(H_2O)	cmol(+)·kg^{-1}	%	g·kg^{-1}	mg·kg^{-1}	mg·kg^{-1}	mg·kg^{-1}	mg·kg^{-1}	
peat	3.03	58.3	33.8	14.9	265.3	27.6	108.4	1.71	-
soil 1	4.45	8.7	1.37	1.27	96.46	35.43	22.72	0.173	0.058
soil 2	6.69	17.2	2.41	2.28	147.4	45.03	31.12	0.313	0.137

CEC[a]: cation exchange capacity, Bio- Cd[b]: 0.005 mol·L^{-1} DTPA extracting bioavailable Cd

The bioavailable Cd of the soil was determined by the DTPA method((Risser, 1990). The suspension was then filtered through blue ribbon analytical filter paper. One litre of the DTPA extracting solution contained 14.9 g tetraethanolamine (TEA), 1.97 g of DTPA, and 1.47 g of $CaCl_2·2H_2O$ and the pH was adjusted to 7.3 with 1 mol·L^{-1} HCl. The resulting solution contained 0.005 mol·L^{-1} DTPA, 0.01 mol·L^{-1} $CaCl_2$, and 0.1 mol·L^{-1} TEA. In a 125 mL flask, 20 mL of the DTPA solution were added to 10 g of air-dried soil.The flask was covered with a plastic stopper and shaken for 1 h. Cadmium analysis in the filtrate was performed by flame AAS. Standards for the AAS calibration were prepared in the extraction solution by the addition of appropriate quantities of Cd.

Pot Experiment

The pot experiments were conducted in a greenhouse from May to June 2007. Two kilograms of air-dried and sieved soils were filled into respective 2.0 L plastic pots. Two levels of Cd (2.5 and 5.0 mg Cd·kg^{-1} soil) were applied by adding $CdCl_2·5H_2O$ to each of the soil samples. To each pot the following amounts of fertilizers were applied: 0.3 g $CO(NH_2)_2$, 0.2 g KH_2PO_4 and 0.15 g KCl. A root-bag technique was used to separate the rhizosphere and bulk soil.A root bag (10 cm in diameter,10 cm in depth), made of 300-mesh nylon screen, was filled with 500 g soil, and then buried in the center of a plastic pot (19 cm in diameter,14 cm in depth) containing 2.0 kg soil. 30 days after the application of Cd and the fertilizers, the peat was applied in a dry form at the three rates: 0 (CK treatment), 2.5 (P1), 5.0 (P2) and 10.0 (P3) g peat·kg^{-1} soil . Each treatment was conducted in triplicates.

The pots was subsequently incubated in the greenhouse for 7 weeks. *Brassica campestris ssp. Chinesis L* plant was used as the phytoextracting plant for the pot experiments. This selection was based on the plant's ability to produce a great biomass in a very short time. Seeds of *Brassica campestris ssp. Chinesis L* plant were germinated in a quartzite and seedlings

with similar biomass were transferred into the pots which contained the soil spiked with Cd and peat. Six seedlings were planted into each pot and were thinned to three plants after 3 week. Thereafter, the experiment was initiated and plants were harvested after 4 weeks of growth.

Plant and Soil Analysis

At harvest, plants above ground were cut. Plant samples were rinsed with deionised water, dried between Kleenex tissues to avoid surface contamination, and oven driedat 70 ℃ for 48 h to a constant weight. The dry weight was determined and the samples were homogenised in particle size by grinding in a mill. After milling, 0.5 g±2 mg of each dried plant tissue sample was digested with HNO_3 and H_2O_2 in a microwave digester. The Cd concentration of the digested plant sample was analyzed using atomic absorption spectroscopy (AAS).

The bioavailable Cd of the bulk and rhizosphere soils treated with different levels of Cd at the method (Risser and Baker, 1990) as described in section 2.1 was determined by the DTPA.

Statistical Analysis

Each pot experiment was conducted in triplicate (n = 3). Statistical analysis of the data was performed by using SPSS 11.5. The statistical significance of the differences between the experimental data was then evaluated.

Results

Plant Biomass

The effect of natural acid peat on the dry matter yields of plants are shown in Fig. 1. The dry biomass of the shoots from the two soils shows almost no variation among the various peat treatments and various Cd concentrations of soil. The dry biomass of shoots in soil 2 was higher than that in soil 1, which may be attributable to the differences in soil properties. The application of natural acid peat to two Cd contaminated soils did not adversely affect dry matter production of plant.

Cadmium Concentration in Plants

As presented in Fig. 2, Cd concentrations in the shoots of plant markedly increased with rising Cd concentration in the soils. In addition, the increase of natural acid peat levels increased the Cd uptake in shoots at all Cd concentration of soils. The Cd concentration of shoots in soil 1 has a tendency to be higher than that of soil 2.

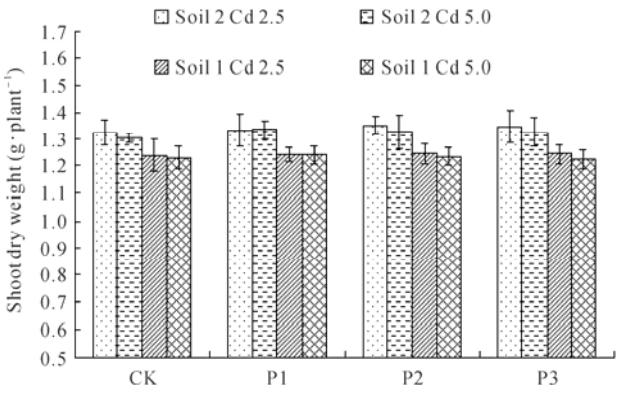

Fig. 1 Effect of the application of natural acid peat to two soils on the shoot dry weight of the plant. CK, P1, P2 and P3 stand for the control (no peat treatment) and peat treatments at 2.5, 5.0 and 10.0 g peat·kg^{-1} soil, respectively. Bars represent standard error

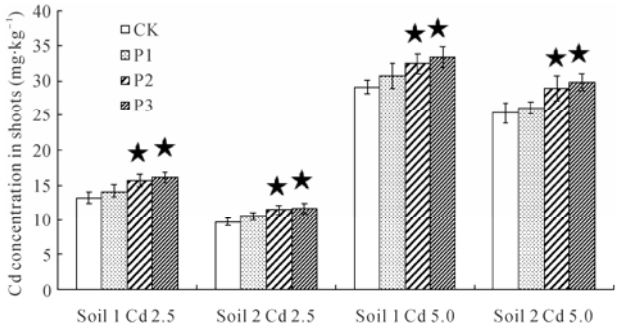

Fig. 2 Effect of Cd and peat applications to soil on Cd concentration in shoots of plant. CK, P1, P2 and P3 stand for the control (no peat treatment) and peat treatments at 2.5, 5.0 and 10.0 g peat·kg^{-1} soil, respectively. Error bars represent standard error of triplicates （n =3） Bars marked with(★) are statistically different form the control($p < 0.05$)

The peat treatment at 2.5 g peat·kg^{-1} soil shows the tend of increasing the Cd concentration in shoots, however, the increase is not statistically different with the control. The Cd concentration in shoots with the treatment at 5.0 g peat·kg^{-1} soil caused a higher concentration of Cd in the shoots compared with 2.5 g peat·kg^{-1} soil. However, that at the treatment with 10.0 g peat·kg^{-1} soil had no observable further increase in the Cd concentration in shoots compared with the 5.0 g peat·kg^{-1} soil treatment. Nevertheless, the applicat-ion of the natural acid peat at the 5 g or 10 g peat·kg^{-1} soil significantly increased the Cd

concentration in the shoot compared with the no peat treatment (Fig. 2).

Amount of Cadmium Absorbed by Plant

The amount of Cd absorbed by the plant was commonly related to the concentration of Cd in the shoot and dry matter yield of the shoots. The dry biomass of the shoots did not vary considerably with the peat treatment (Fig. 1), whereas the Cd concentrations in shoots of the plant increased with rising peat levels (Fig. 2). As a result, the increase of amount of Cd absorbed by the plant with the application of natural acid peat (Fig. 3) is consistent with the tend of the increase of Cd concentration in the shoots with increasing the amount of the peat applied (Fig. 2).

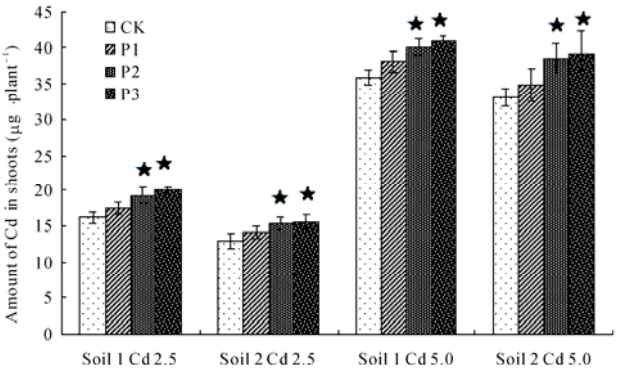

Fig. 3 Amount of Cd accumulated in shoots of plant on application of natural acid peat. CK, P1, P2 and P3 stand for the control (no peat treatment) and peat treatments at 2.5, 5.0 and 10.0 g peat·kg^{-1} soil, respectively. Error bars represent standard error of triplicates （n = 3）. Bars marked with(★) are statistically different from the control($p < 0.05$)

As presented in Fig. 3, the amounts of Cd absorbed in shoots were markedly increased with rising Cd concentration in the soils. The rising peat levels increased the amount of Cd in shoots at all Cd concentrations of soils. The treatment with 2.5 g peat·kg^{-1} soil tended to be higher compared with the no peat treatment. Furthermore, the amount of Cd in shoots with the treatment at 5.0 and 10.0 g peat·kg^{-1} soil was significantly higer then that in the no peat treatment.

Concentrations of Bioavailable Cadmium in the Rhizosphere and Bulk Soil after Harvesting

The potentially bioavailable Cd concentrations, as determined by DTPA extraction, are shown in Table 2. Irrespective of the Cd concentration of the soil, the bioavailable Cd concentrations of the bulk soil increased with the increase of the level of natural acid peat treatment. The difference of the bioavailable Cd concentrations in the control treatment (CK) between the rhizosphere and bulk soil was not pronounced, whereas the bioavaible Cd concentration in the rhizosphere soil where at peat was added, tended to be higher than that of the bulk soil.

For the treatment with 5 g peat·kg^{-1} soil, the content of bioavailable Cd concentrations of soil 1 at the contamination levels of 2.5 and 5.0 mg Cd·kg^{-1} soil were 2.07 and 3.91 mg Cd·kg^{-1} soil, respectively, in the rhizosphere and 2.24 and 4.19 mg Cd·kg^{-1} soil in the bulk soil, and those in soil 2 was 1.74 and 2.79 mg Cd·kg^{-1} soil in the rhizosphere and 1.89 and 3.05 mg Cd·kg^{-1} soil in the bulk soil, respectively. The

Table 2 Concentrations of bioavailable cadmium in the rhizosphere and bulk soils

Peat treatment dosage	Soil 1						Soil 2					
	2.5 mg Cd·kg^{-1}			5.0 mg Cd·kg^{-1}			2.5 mg Cd·kg^{-1}			5.0 mg Cd·kg^{-1}		
	Ri	Bu	Ri-Bu	Ri	Bu	Ri-Bu	Ri	Bu	Ri-Bu	Ri	Bu	Ri-Bu
	Bioavailable Cd (mg·kg^{-1})											
CK	2.07	2.12	0.05	3.99	4.11	0.12	1.75	1.79	0.04	2.82	2.95	0.13
P1	2.06	2.19	0.13	3.91	4.10	0.19	1.74	1.83	0.09	2.78	2.98	0.20
P2	2.07	2.24	0.17	3.91	4.19	0.28	1.74	1.89	0.15	2.79	3.05	0.26
P3	2.17	2.29	0.12	3.99	4.24	0.25	1.82	1.92	0.10	2.85	3.08	0.23

Ri and Bu represent the rhizosphere and bulk soils ,respectively. CK, P1, P2 and P3 stand for 0, 2.5 ,5.0 and 10.0 g peat·kg^{-1} soil , respectively

difference of bioavailable Cd concentrations between the rhizosphere and bulk soil in the treatment of 5 g peat·kg^{-1} soil appeared to be higher than other peat treatments.

The percentage of the amounts of Cd absorbed by plants based on the total amount of DTPA- extracted Cd was 2.47%~4.38% in the control without the application of natural acid peat, whereas that in the treatment with 5.0 g peat·kg^{-1} soil was 6.70%~8.58%. Further increase of the peat treatment to 10.0 g peat·kg^{-1} soil decrease the percentage of the amounts of Cd absorbed by plants. This is partially attributable to the adsorption of Cd by the high amount of the peat applied in the soils.

Discussion

The Cd contamination levels substantially influenced the Cd concentrations in the shoots and the amount s of Cd accumulated in the shoots (Fig. 2 and Fig. 3).

The addition of natural acid peat to the soil increased the Cd uptake of *Brassica campestris ssp. Chinesis L* plant from the contaminated soils (Fig. 2 and Fig. 3). However, although natural acid peat revealed a positive effect on phytoextraction, the bioavail-ability of Cd in the rhizosphere soil based on DTPA extraction was relatively little affected by the peat application (Table 2). The bioavailability of heavy metals in soil is influenced by many factors, such as the organic matter content (Li and Shuman, 1996), the cation exchange capacity (Alloway and Ayres, 1997), and, especially, the pH which is partially influenced by organic acids exudated by plants. Cieslinski *et al*. (1998) and Nigam *et al*. (2001) reported that organic acids had a positive effect on the metal extraction by plants.

During the last decade, there has been much success in making phytoremediation a promising environmental technology. Nevertheless, there is still a great lack of knowledge concerning the plant mech-anisms which are responsible for metal extraction, and the factors which influence the bioavailability of pollutants in soil. Furthermore, according to Brown *et al*. (1995), hyperaccumulator species are those plants whose leaves may contain >100 mg Cd·kg^{-1}. Robinson *et al*. (2000) suggested that a plant used for phy-tore-mediation should be fast growing, deep-rooted,easily propagated and accumulating the target metal. According to RÖmkens *et al*. (2002) it should also have a high biomass production. However, most hyperaccumulators grow slowly and have a small biomass.

The findings in the present study indicate that applications of the natural acid peat affected Cd positively on itse mobility in soil, resulting in the large amount of bioavailable Cd extracted by the roots and translocated to the shoots. The advantage of the application of the natural acid peat is that a larger amount of Cd can be extracted in a shorter period of time. Thus a combination of using natural chelators such as acid peat along with selection of plant species with a high biomass and sufficient metal tolerance and development of innovative farming practices would enhance significantly the efficiency of phytoextraction.

Conclusions

Application of natural acid peat promotes plant uptake of Cd and, thus accelerates the phytoextraction efficiency. Moreover, it dose not have the negative effects of synthetic chelators such as EDTA which severely decreases the plant growth. Due to the low cost in obtaining natural acid peat in sufficient amounts for phytoextration, the use of natural acid peat in remediation of Cd–contaminated soils would be economically feasible. Future research on the application of natural chelators such as the acid peat along with selection of plant species and the develop-ment of innovative strategies of land management merits attention in restoration of metal contaminated soils.

Acknowledgments

This research was sponsored by the National Basic Research Program of China (2005CB121104), Science and Technology Project of Hangzhou City (20061123B10), the Y. C. Tang Disciplinary Development Fund of Zhejiang University, and the Program of Introducing Talents of Discipline to University (B06014).

References

Adriano DC (2001) Cadmium. In: Adriano DC (ed.),

Trace Elements in Terrestrial Environments: Biogeochemistry, Bio-availability, and Risks of Metals. Springer-Verlag, New York, pp. 264-314

Alloway BJ, Ayres DC (1997) Chemical Principles of Environmental Pollution, second ed. Blackie Academic & Professional, London

Autumn S, Wang (2006) Changes in soil biological activities under reduced soil pH during Thlaspi caerulescens phytoextraction. Soil Biol. & Biochem. 38: 1451-1461

Barona A, Aranguiz I, Elias A (2001) Metal associateions in soils before and after EDTA extractive decontamination: implications for the effectiveness of further clean-up procedures. Environ. Pollut. 113: 79-85

Begonia MT, Begonia GB, Bulter A, Griffin U, Young C (2003) Chemically-enhanced phytoextraction of cadmium contaminated soils using wheat (Triticum aestivum L.). B. Environ. Contam. Tox. 71: 648-654

Brown SL, Chaney RL, Angle JS, Baker AJM (1995) Zinc and cadmium uptake by hyperaccumulator Thlaspi caerulescens grown in nutrient solution. Soil Sci. Soc. Am. J.59: 125-133

Chaney RL，Malik M, Li YM (1997) Phytoremediation of soil metal. In: Kosaikaikan, Proceedings international seminar on use plants for environmental remedia-tion, Tokyo, pp.49-65

Chen H, Cutright T (2001) EDTA and HEDTA effects on cadmium, Cr, and Ni uptake by Helianthus annuus. Chemosphere 45: 21-28

Cieslinski G, Van Rees KCJ, Szmigielska AM, Krishnamurti GSR, Huang PM (1998) Low-molecular-weight organic acids in rhizosphere soils of durum wheat and their effect on cadmium bioaccumulation. Plant Soil 203: 109-117

Ebbs SD, Lasat MM, Brady DJ, Cornish J, Gordon R, Kochian LV (1997) Phytoextraction of cadmium and zinc from a contaminated soil. J. Environ. Qual. 26: 1424-1430

Glass DJ (1999) Economic potential of phytoremediation. In: Raskin I, Ensley BD (eds.), Phytoremediation of Toxic Metals: Using Plants to Clean up the Environment. John Wiley & Sons, New York, pp. 15-31

Grcman H, Velikonja-Bolta S, Vodnik D, Kos B, Lestan D (2001) EDTA enhanced heavy metal phytoextraction: metal accumulation, leaching and toxicity. Plant Soil 235: 105-114

Hatori Hiroyuki (2006) Effect of chloride application and low soil pH on cadmium uptake from soil by plants. Soil Sci. Plant Nutri. 52: 89-94

Kayser A, Wenger K, Keller A (2000) Enhancement of phytoextraction of Zn, Cd, and Cu from calcareous soil: the use of NTA and sulfur amendments. Environ. Sci. Technol. 34: 1778-1783

Li Z, Shuman LM (1996) Heavy metal movement in metal contaminated soil profiles. Soil Sci. 161: 656-666

Lombi E, Zhao FJ, Dunham SJ, McGrath SP (2001) Phytoremediation of heavy metal-contaminated soils: Natural hyperaccumulation versus chemically enhanced phytoextraction. J. Environ. Qual. 30: 1919-1926

McGrath SP (1998) Phytoextraction for soil remediation. In: Brooks RR (ed.), Plants that Hyperaccumulate Heavy Metals: Their Role in Phytoremediation, Microbiology, Archaelogy, Mineral Exploration and Phytomining, CAB International, Walling-ford, pp. 261-287

Nigam R, Srivastava S, Prakash S, Srivastava MM (2001) Cadmium mobilisation and plant availaility−the impact of organic acids commonly exuded from roots. Plant Soil 230: 107-113

Raskin I, Smith RD, Salt DE (1997) Phytoremediation of metals: using plants to remove pollutants from the environment. Curr. Opin. Biotech. 8: 221-226

Risser JA, Baker DE (1990) Testing soils for toxic metals. In: Westermann RL (ed.), Soil Testing and Plant Analysis, third ed. Soil Science Society of America. Book Series, No. 3. Soil Sci. Soc. Am. J. Madison, WI, pp. 275-298

Robinson BH, Millis TM, Petit D, Fung LE, Green SR, Clothier BE (2000) Natural and induced cadmium accumulation in poplar and willow: implications for phytoremediation. Plant Soil 227: 301-306

RÖmkens P, Bouwman L, Japenga J, Draaisma C (2002) Potentials and drawbacks of chelate-enhanced phytoremediation of soils. Environ. Pollut. 116: 109-121

Salt DE, Smith RD, Raskin I (1998) Phytoremeiation.Annu. Rev. Plant Physiol. Plant Mol. Biol. 49: 643-668

Sun G , Zhu Z (2005) Efects of difrerent cadmium levels on the growth and nutrient elements in pakchoi. J. Agro-Environ. Sci. 24(4): 658-661

Wasay SA, Barrington SF, Tokunaga S (1998) Reme-

diation of soils polluted by heavy metals using salts of organic acids and chelating agents. Environ. Sci. Technol. 19: 369-379

Wei FS (1992) Modern Analytical Methods of Soil Elements. Chinese Environ. Sci. Press, Beijing

Yamane I (1981) Features of heavy metal pollution in Japan. In: Kitagishi K, Yamane I (eds.), Heavy Metal Pollution in Soils of Japan. Japan Scientific Societies Press, Tokyo, pp. 3-15

Session 3

Anthropogenic Organics, Crop Protection and Ecotoxicology

Interaction of Anthropogenic Organic Chemicals with Organic Matter in Natural Particles

Joseph J. Pignatello[a,b,*]

[a] Connecticut Agricultural Experiment Station, 123 Huntington St., New Haven, Connecticut, USA;
[b] Environmental Engineering Program, Yale University, New Haven, Connecticut, USA.
[*]Corresponding author. E-mail: joseph.pignatello@ct.gov.

This lecture will review sorption to organic substances in soils and sediments including natural organic matter (NOM) and black carbon (BC) materials. In it I will discuss molecular-level interactions separately from the point of view of the sorbing molecule and the sorbent matrix.

The driving forces for sorption will be described and methods for quantifying their relative importance will be discussed. Typically, the predominant driving force for sorption from water to organic substances is the "hydrophobic effect." This driving force has nothing at all to do with the sorbent, but arises from disruption of the cohesive energy of water due to the greater ordering and stronger H-bonding of water in the hydration shell of the hydrophobic entity than in bulk water itself. The relative importance of the major weak intermolecular interactions—dispersion, dipolar, and H-bonding forces—to sorption free energy has been difficult to quantify. Modest advancements in this topic will be described. Evidence will be presented for the importance of π-π electron-donor acceptor interactions for certain aromatic and pseudo-aromatic systems that possess strong π-donor or strong π-acceptor capability (for example, PAHs and nitroaromatics, respectively). Steric effects play an important role in adsorption to BC due to a molecular sieving effect at pore throats. Sorption of organic ions is complicated by the participation of other weak interactions besides coulombic attraction and by the simultaneous sorption of ion pairs.

When constructed in sufficient detail and over wide enough range in solute concentration, sorption isoth-erms on natural solids and NOM and BC reference materials are often found to be nonlinear in solute concentration and competitive with other solutes. This behavior is due to sorption site or sorption domain heterogeneity. For NOM, several postulates have been offered to explain this heterogeneity: domain-based pre-ferential sorption; functional-group based preferential sorption; and the nature of the physical state of the matrix. The glassy polymer model of NOM will be introduced and used to rationalize nonlinearity and competitive effects. The nonlinearity of sorption and competitive effects on BC are due to a combination of surface site heterogeneity and pore size heterogeneity. Sorption by BC is affected by surface polarity and pore size distribution. Furthermore, sorption to BC may be attenuated by the presence of incompletely pyrolyzed materials (uncharred biomass, unburned fuel), and the condensation of natural substances during weather-ing, such as humic substances and mineral precipitates, which may compete with contaminants or block access to pores. Hysteresis is a commonly observed phenol-menon in sorption research having major implications for environmental fate and bioavailability of con-taminants. The lecture will discuss both artificial and true causes of hysteresis in the context of the nature of NOM and BC materials. Finally, the lecture will discuss the phenomenon of strong desorption resist-ance and its potential causes.

Decontamination of Soils through Immobilization of Anthropogenic Organics by Biotic and Abiotic Catalysts

Jean-Marc Bollag*

Laboratory of Soil Biochemistry,The Pennsylvania State University,University Park, PA. 16802. USA.
*Corresponding author. Tel. No. 814 - 237 9888; E-mail: jmbollag@psu.edu.

Processes that cause immobilization of contaminants in soil are of great environmental importance because they may lead to a considerable reduction in the bioavailability of contaminants and may restrict their leaching into groundwater. Previous investigations demonstrated that pollutants can be bound to soil constituents by either physical or chemical interactions (Calderbank, 1989). From an environmental point of view, chemical interactions are preferred, because they frequently lead to the formation of strong covalent bonds that are difficult to disrupt by microbial activity or chemical treatments. Humic substances resulting from lignin decomposition appear to be the major binding ligands involved in the incorporation of contaminants into the soil matrix through stable chemical linkages (Bollag *et al.*, 1997; Gevao *et al.*, 2000).

Binding to humus constitutes one of the major reactions by which anthropogenic compounds are transformed in nature. Pollutants interact with soil colloids through several mechanisms. Adsorption occurs primarily as a consequence of the attraction between the solid surface of the soil and the soluble or vapor phase of the pollutant. The nature and strength of adsorption depend largely on the chemical structure of the molecule.

The most persistent complexes result from the covalent binding of xenobiotics to humic material. Microorganisms and their enzymes may, in fact, be indispensable in bound residue formation. Chemical bonds may be formed through oxidative coupling reactions catalyzed either biologically or abiotically by certain clays and metal oxides. These naturally occurring processes are believed to result in the detoxification of contaminants. While indigenous enzymes are usually not likely to provide satisfactory decontamination of polluted sites, amending soil with enzymes derived from specific microbial cultures or plant materials may enhance incorporation processes (Bollag, 1992).

Oxidative coupling is mediated by a number of biological and abiotic catalysts, including microbial or plant enzymes, inorganic chemicals (e.g., ferric chloride, cupric hydroxide) and clay minerals. Coupling reactions can also occur spontaneously in the presence of oxygen at neutral and alkaline pH values. Spontaneous reactions frequently lead to the incorporation of nonphenolic compounds into humic polymers.

Many soil microorganisms produce extracellular oxidoreductases capable of catalyzing the coupling of aromatic compounds. These enzymes are classified as either peroxidases or polyphenol oxidases. The polyphenol oxidases are divided into two groups: laccases and tyrosinases, which require bimolecular oxygen, but no coenzyme, for activity. However, the enzymes differ in the mechanism by which they oxidize phenols. Laccases oxidize phenolic compounds by forming their corresponding anionic free radicals, whereas tyrosinases form o-diphenols and subsequently release oxidized o-quinones. In an alkaline environment, the quinone products slowly polymerize through autooxidative processes. The laccases may prove to be the more useful of the phenoloxidases because, like the peroxidases, they produce highly reactive radicals, but unlike the latter, they do not require the presence of hydrogen peroxide.

The catalytic effect of enzymes was evaluated by determining the extent of contaminants binding to humic material, and whenever possible by structural analyses of the resulting complexes. In model studies

using ^{14}C-labeled contaminants and radiocounting, we demonstrated the formation of covalent bonds between single naturally occurring humus constituents and xenobiotic compounds in the presence of enzymes or biotic catalysts. When humus derivatives were incubated together with phenols or other reactive contaminants and a catalyst, the formation of numerous cross-coupling products was observed. The characterization of the hybrid products was based primarily on mass spectrometric analyses. An important indicator in this analysis was the appearance of a cluster of peaks typical for the isotopic pattern of a certain number of chlorine atoms. Thus, it should be emphasized that the structures are mostly hypothetical, as mass spectrometric analysis does not allow the determination of the sequence of phenol units or the position (ortho-ortho, ortho-para, etc.) or type (carbon-carbon, carbon-oxygen) of coupling.

Subsequently several studies demonstrated that the evaluation of binding can be better achieved by applying ^{13}C-, ^{15}N- or ^{19}F-labeled xenobiotics in combination with ^{13}C-, ^{15}N- or ^{19}F-NMR spectroscopy (Strynar *et al.*, 2004). The rationale behind the NMR approach was that any binding-related modification in the initial arrangement of the labeled atoms automatically induces changes in the position of the corresponding signals in the NMR spectra. The delocalization of the signals exhibits a high degree of specificity, indicating whether or not covalent binding has occurred and, if so, what type of covalent bond has been formed.

Our ^{13}C-NMR studies were carried out using two ^{13}C-labeled pollutants: 2,4-dichlorophenol, a degradation product of the herbicide 2,4-D (Hatcher *et al.*, 1993), and cyprodinil, a new phenyl-pyrimidine amine fungicide manufactured by Ciba-Geigy (Dec *et al.*, 1997). 2,4-Dichlorophenol, labeled either in the C-1 or in the C-2 and C-6 position, was incubated for 2 hours with dissolved humic acid in the presence of a peroxidase. The NMR signals generated by the ^{13}C label demonstrated bonding between the two components through carbon-carbon, ester and phenolic ether linkages.

To investigate the formation of covalent bonds under more natural conditions, cyprodinil, which was labeled either in the phenyl or pyrimidyl ring, was incubated with fresh soil for several months (Dec *et al.*, 1997). After exhaustive washing with methanol, humic acid was isolated by extraction with 0.5 mol·L^{-1} NaOH. Humic acid was then purified by dialysis and/or silylated by treatment with trimethylchlorosilane to facilitate the ^{13}C-NMR analysis. The NMR signals generated by both the dialyzed and silylated samples indicated cleavage of the cyprodinil molecule between the aromatic rings and covalent binding of the phenyl and pyrimidyl moieties to humic acid.

The results obtained confirmed that binding of contaminants to soil organic matter has important environmental consequences. In particular, now it is more evident than ever that as a result of covalent binding to humus, (a) the amount of contaminants available to interact with the biota is reduced; (b) the complexed products are less toxic than their parent compounds; and (c) groundwater pollution is reduced because of restricted contaminant mobility.

References

Bollag JM (1992) Decontaminating soil with enzymes. Environ. Sci. Technol. 26: 1876-1881

Bollag JM,Dec J, Huang PM (1997) Formation mechanisms of complex organic structures in soil habitats. Adv. Agron. 63: 237-266

Calderbank A (1989) The occurrence and significance of bound residues in soil. Rev. Environ. Contam. Toxicol. 108: 71-103

Dec J, Bollag JM (1997) Determination of covalent and non-covalent binding interactions between xenobiotic chemicals and soil. Soil Sci. 162: 858-874

Dec J, Haider K, Schäffer A, Fernandes E, Bollag JM (1997) Use of a silylation procedure and ^{13}C-NMR spectroscopy to characterize bound and sequestered residues of cyprodinil in soil. Environ. Sci. Technol. 31: 2991-2997

Gevao B, Semple KT, Jones KC (2000) Bound pesticide residues in soils: a review. Environ. Pollut. 108: 3-14

Hatcher PG, Bortiatynsky JM, Minard RD, Dec J, Bollag JM (1993) Use of high resolution ^{13}C NMR to examine the enzymatic covalent binding of ^{13}C-labeled 2,4-dichlorophenol with humic substances. Environ. Sci. Technol. 27: 2098-2103

Strynar M, Dec J, Benesi A, Jones AD, Fry RA, Bollag JM (2004) Using ^{19}F NMR spectroscopy to determine trifluralin binding to soil. Environ. Sci. Technol. 38: 6645-6655

Effects of "Aging" on Bioreactive Chemical Retention, Transformation, and Transport in Soil

Hwei Hsien Cheng[a, *], William C. Koskinen[b]

[a]Department of Soil, Water, & Climate, University of Minnesota, St. Paul MN 55108 USA;
[b]USDA-Agricultural Research Service, St. Paul, MN 55108 USA.
[*]Corresponding author. E-mail: hcheng@umn.edu.

Keywords: Sorption; Desorption; Aged residues; Bioavailability

The fate of a bio-reactive organic chemical, such as a pesticide, in the soil environment is governed by the retention, transformation, and transport processes, and the interaction of these processes. Retention is the consequence of interaction between the chemical and the soil particle surface or soil components thereon. The retention processes, frequently described as adsorption or simply sorption, may be reversible or irreversible. Understanding the sorption process for a pesticide is important as it can retard or prevent pesticide movement, and affect availability of the pesticide for plant or microbial uptake or for biotic or abiotic transformation. While sorption is affected by the physical and chemical properties of both the pesticide and the soil particle resulting in a variety of retention mechanisms, increased contact time (i.e. aging) may also result in the formation of a stronger bond or a change in the binding mechanism between pesticide and soil, matrix deformation, diffusion of pesticide into remote sorption/binding sites (i.e. microsites in soil micropores), physical entrapment or sequestration of the pesticide in soil organic matter or clays, or a combination of these processes, all of which may affect the retention or sorption/desorption of the chemical in soil and in turn affect the processes of its transformation and transport (Cheng, 1990; Cheng *et al.*, 1994; Cheng and Koskinen, 2002).

Increased sorption with aging has been observed for many pesticide classes using a variety of methods for sorption characterization. We have observed increases in the sorption coefficient K_d with incubation time for diverse pesticides such as triazines, acetanilides, pyridine carboxylic acids, substituted ureas, nitrogua-nidines, imidazolinones, and sulfonylaminocarbony-ltriazolinones. The mecha-nisms by which these compounds become sorbed, or sequestered in soils as they age are not well understood, but can be physical or chemical processes. Slow diffusion within small pores of soil aggregates, hydrophobic partitioning into solid humic materials, entrapment into the hydrophobic surface nanopores, and sorption into non-desorbable sites of soil organic matter have all been proposed as possible mechanisms involved in the aging process. In addition, for protonatable pesticides such as triazines, imizolidones, the cationic species may be irreversibly sorbed removing it from the equilibrating solution. As more cationic species are formed, they are continually sorbed. Also, chelate formation has been shown to affect sorption-desorption equilbria. For instance, desorption isotherms indicated that sorption of the biologically active diketonitrile degradate of isoxaflutole on some organoclays was irreversible (Carrizosa *et al.*, 2004). Infrared studies showed that DKN enters the interlamellar space of the organoclay and dissociates into the anion, which then forms a very stable chelate complex with the clay's residual cations and/or partially-coordinated structural cations. The strong binding results in the irreversibility of the sorptive process.

The irreversibility of pesticide sorption-desorption by soil observed in batch equilibration experiments

has been characterized using an isotopic exchange technique (Celis and Koskinen, 1999). Quantitative estimation of the irreversible and reversible components of sorption, experimentally derived from isotopic exchange experiments, indicated increased irreversibility with increased preequilibration time and at lower pesticide concentration. The isotopic exchange of pesticides and metabolites in soil can be described by a two compartment model in which the fraction of strongly bound pesticide increases with time and is accompanied by an equal and opposite decrease in the magnitude of the reversibly bound fraction. This model closely predicted the hysteresis observed in the desorption isotherms from batch experiments.

Transport models use sorption coefficients (K_d and K_{oc} values) to describe pesticide retention by soil for prediction of offsite movement though leaching and runoff. The accuracy of the sorption estimates can be more important than the choice of transport model in correctly simulating pesticide leaching, emphasiz-ing the need to understand the sorption-desorption process and the effects of soil and environmental factors on the process. For instance, a generic screening model characterizes pesticides with Koc values of 0~50 as “very high mobility”, those with Koc 50~150 as “high mobility”, and those with Koc 150~500 as “medium mobility”. Increasing Koc by a factor of 3 would change the mobility classification to a significantly less mobile chemical. We have shown that during aging in soils, numerous types of pesticides, and some of their metabolites, sorption coefficients increased by a factor > 3. For instance, Kd values for flucarbazone and propoxycarbazone and their benzensulfonamide and triazolinone metabolites increased by a factor of 3.5~6.8 within 2 wks after application to clay loam and loamy sand soils (Koskinen *et al.*, 2002). Kd of imidacloprid and two metabolites increased by a factor of 2~3 within 2 wks of application to 3 different soils and nicosulfuron. K_d increased by a factor of 2 to 3 in Mollisols from the United States and by a factor of 5 to 9 in Oxisols from Hawaii and Brazil after 41 d as compared to freshly treated soils. Increases in sorption may have been due to rates of degradation in solution and on labile sites being faster than rates of desorption from the soil particles, diffusion to less accessible or stronger binding sites with time, or a combination of the two processes.

Regardless of the mechanisms involved in aging, these results are further evidence that increases in sorption during pesticide aging should be taken into account during characterization of the sorption process for mathematical models of pesticide degradation and transport. These data show the importance of characterization of sorption-desorption in aged herbicide residues in soil, particularly in the case of prediction of herbicide transport in soil. In this case, potential transport of the pesticide would be over predicted if freshly treated soil K_d values were used to predict transport

Several studies have suggested that only pesticide in solution, or that is readily desorbable from soil, is available for degradation. Pesticides that persist in soils often become increasingly less bioavailable, as indicated by markedly declining rates of biodegradat-ion with aging. In some instances, the sorbed fraction of the pesticide is totally resistant to microbial attack, whereas in others sorption only reduces its release rate, but does not eliminate biodegradation. A variety of models have been developed to describe biodegradation of pesticides including those coupling diffusion-limited sorption-desorption and biodegradation A parameter sensitivity analysis of a two-site nonequilibrium sorption model coupled with two first-order degradation terms for the dissolved and sorbed pesticide, indicated that nonequilibrium sorption will initially favor degradation. However, over the long term degradation will decrease when desorption kinetics becomes the limiting factor in the degradation process. Regardless of the details of the models of biodegradation, they must account for pesticide bioa-vailability, particularly in aged samples.

Recently there has been renewed interest in predicting bioavailability pesticides in aged soils. However, pesticide bioavailability in aged soils has been characterized by a variety of methods with limited success, due in part to methodological limitat-ions. The amount of a bioavailable pesticide in soil has been commonly estimated by the determination of aqueous $CaCl_2$ solution extractable pesticide, and in some instances, bioavailability may be predicted from soil properties or by a mild solvent extraction, but not with vigorous more harsh solvent extraction. However, there are conflicting results on the efficacy of using mild organic solvent extractants to estimate the amount of bioavailable pesticide in soil.

In recent studies, we have found that the bacterium *Pseudomonas* sp. strain ADP, which is capable of rapidly mineralizing triazines (atrazine, simazine) could be used to characterize the

bioavailability of aged triazine residues, without the contribution of triazine desorption from soil (Barriuso *et al.*, 2004). We have found that although triazine sorption to soil increased with aging, the amounts of triazine in aged soils extracted by 0.01 $mol \cdot L^{-1}$ $CaCl_2$ and aqueous methanol were highly correlated to amounts of triazine mineralized by *Pseudomonas* sp. strain ADP. Consequently, 0.01 $mol \cdot L^{-1}$ $CaCl_2$/methanol extractable triazine in soils can be used to estimate bioavailable residues, even in aged soils.

The interaction of processes affecting pesticides can complicate the characterization of the pesticide's fate and behavior in aged soils. For instance, if there is degradation during retention characterization, there could be two possible consequences: if degradation is known and the sorption is concentration dependent, i.e. Freundlich slope ($1/n$) <1, there would be greater sorption as amount of pesticide decreased; and if degradation occurred but was not known, sorption would overpredicted and observed hysteresis during desorption would have been an experimental artifact. Numerous studies have shown that aged pesticide residues are more difficult to extract from soil for subsequent analysis. Inefficient extraction techniques would over predict transformation and under prediction transport of the pesticides.

References

Barriuso E, Koskinen WC, Sadowsky MJ (2004) Solvent extraction characterization of bioavailability of atrazine residues in soil. J. Agric. Food Chem. 52: 552-6556

Carrizosa MJ, Rice PJ, Koskinen WC, Carrizosa I, Hermosin MC (2004) Sorption of isoxaflutole and DKN on organoclays. Clay Clay Min. 52: 341-349

Celis R, Koskinen WC (1999) An isotopic exchange method for the characterization of the irreversibility of pesticide sorption-desorption in soil. J. Agric. Food Chem. 47: 782-790

Cheng HH (1990) Pesticides in the soil environment – An overview. In: Cheng HH (ed.) Pesticides in the Soil Environment. Soil Sci. Soc. Am. J., Madison, WI. pp. 1-5

Cheng HH, Koskinen WC (2002) Interactions of minerals-organic matter-living organisms on the fate of allelochemicals and xenobiotics in soil: A methodological evaluation. In: Huang PM, Bollag JM and Gianfreda L. (eds.) Soil Mineral-Organic Matter-Microorganism Interactions and Ecosystem Health: Ecological Significance of the Interactions Among Clay Minerals, Organic Matter and Soil Biota. Developments in Soil Science, Vol. 28B. A. Violante. Elsevier, Amsterdam, The Netherlands. pp. 135-145

Cheng HH, Koskinen WC, Molina JAE (1994) Effects of soil interactions on the bioreactivity of organic chemicals in soils. In: Interactions of Soil Components, Agricultural Ecosystems and Health Issues. Transact. XV. Intern. Congr. Soil Sci., Symp. Vol. 3. ID20. Acapulco, Mexico. pp. 638-655

Koskinen WC, Rice PJ, Anhalt JA, Sakaliene O, Moorman TB, Arthur EL (2002) Sorption-desorption of "aged" sulfonylaminocarbonyl-triazolinone herbicides in soil. J. Agric. Food Chem. 50: 5368-5372

Interaction of Bttoxin with Organo-mineral Surfaces and Consequences for Its Fate in the Environment

Nordine Helassa[a], Sylvie Noinville[b], Philippe Déjardin[c], Jean-Marc Jano[c], Hervé Quiquampoix[a], Siobhán Staunton[a,*]

[a] UMR 1222 Eco&Sols, INRA, place Viala, 34060 Montpellier, France;
[b] UMR 7075 - LADIR, CNRS, 2 rue Henri Dunant, 94320 Thiais, France;
[c] UMR 5635 IEM, CNRS, 2 Place Eugène Bataillon, 34095 Montpellier, France.
[*]Corresponding author. Tel. No. + 33 461 2331; E-mail: staunton@montpellier.inra.fr.

Abstract: About 40% of genetically modified crops contain the insecticidal trait engineered from the soil bacterium *Bacillus thuringiensis*. Plants produce an insectidal protein and it is important to understand how the interactions of this protein with soil influence its persistence and its biological properties. We have used various techniques to monitor the interactions of one such toxin, Cry1Aa with soils and minerals. We have investigated the persistence of the toxin as a function of soil properties and microbial activity and conclude that microbial decay is not the determinant factor in the observed decline of toxin in soil.

Keywords: Adsorption; Cry protein; Genetically modified plants; Persistence; Protein secondary structure; Soil

Introduction

Genetically modified (GM) crops were first comer-cialised in 1996 and since then their cultivation has expanded to exceed 100 Mha in 2008. About 40% of commercial GM crops contain the Bt trait. They have been engineered to produce one or more insecticidal proteins obtained from the soil bacterium, *Bacillus thuringiensis*. Advocates of GM crops point to the improved crop yield and quality obtained with Bt plants since insecticides give poor protection against boring insects and infested plants are prone to fungal infection that may lead to unacceptably high levels of mycotoxins. Furthermore, it is argued that the strong similarity between the proteins produced by GM plants and by the bacterium, used in agricultural pest control for decades, should mitigate against any adverse effects to the environment. However, there are important differences between the proteins produced by GM plants and bacteria, therefore in light of the very rapid increase of this class of crops, caution and detailed study of their impact is required. *B. thuringiensis* produces a protoxin that requires solubilisation and enzymatic cleavage to produce the activated, toxic protein. This stage contributes to the high species specificity of the toxins. In contrast, GM plants produce truncated, active proteins thereby raising the fear that some degree of species specificity might be lost. Another concern is that the current generation of GM plants produce the protein in all plant organs, and the protein is released to soil continuously as root exudates and during the decomposition of plant residues.

It is therefore important to elucidate the processes that determine the fate of Bt toxin in the environment. One of the key processes in soil is adsorption. Adsorpt-ion of proteins limits mobility, may protect against microbial attack, often leads to conformational change that may modify the biological properties.

We have studied the adsorption of a Bt toxin, Cry1Aa on soils and model mineral surfaces. Various techniques have been used to assess the extent of adsorption and the ease of desorption, the mobility in the adsorbed state, the conformational changes following adsorption and the persistence of the toxin in the adsorbed state.

Materials and Methods

Cry1Aa was obtained by growing a genetically modified strain of *B. thuringiensis* subsp. *kurstaki* HD-1 in a fermentor, the crystalline protein was then activated and purified as previously described (Helassa *et al.*, 2009). Concentrated solutions were maintained at high salt concentration and high pH to avoid polymerisation of the protein.

Reference clay minerals, montmorillonite and kaolinite, were size fractionated (<2 μm) by sedimentation, made homoionic with sodium and washed until salt free. Mica was freshly cleaved. Glass was acid-washed and, when required, made hydrophobic by silanisation. Four soils with contrasting texture and organic matter content were selected for incubation experiments. When necessary the protein was labelled with a fluorescent probe (Alexa or fluorescein isothiocyanate (FITC)). Adsorption isotherms were measured in clay suspension as a function of pH (Helassa *et al.*, 2009) and in flow cells with fluorescence detection, as described by Balme *et al.* (2006). Changes in secondary structure and self-association after adsorption on montmorillonite or silica were monitored using Fourier Transform InfraRed spectroscopy in a D_2O background, as described by Revault *et al.* (2005). Mobility of FITC-labelled protein adsorbed on montmorillonite was measured using FRAP (Fluorescence Recovery After Photobleaching) which has not hitherto been reported for proteins adsorbed on mineral surfaces. Soils were incubated with trace amounts of Cry1Aa under controlled conditions of temperature and moisture content. Various chemical and physical treatments varied the microbiological activity. Toxin was extracted and analysed using an ELISA test.

Results and Discussion

Fig. 1 shows the adsorption isotherms of Cry1Aa on montmorillonite and kaolinite as a function of pH. For both minerals, adsorption followed a low affinity isotherm and the maximum of adsorption decreased markedly as pH was increased above the isoelectric point. Adsorption was about 40 times greater on montmorillonite than on kaolinite, in line with the difference in their specific surface area. Desorption in water or alkaline buffer was small, but was very efficient when non-ionic or zwetterionic detergents were added.

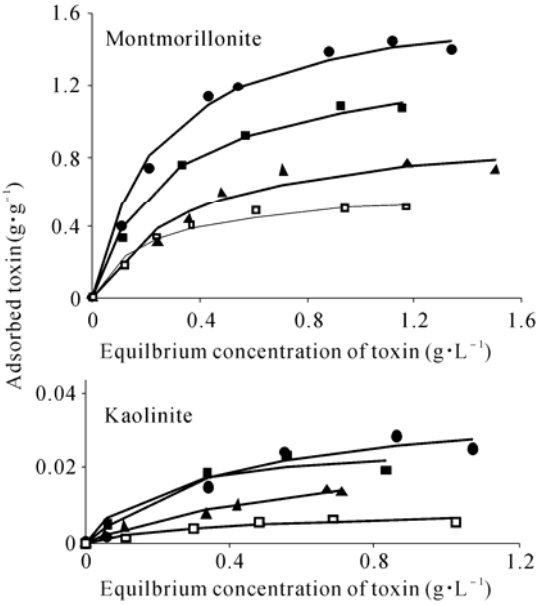

Fig. 1 The adsorption isotherms of Cry1Aa on montmorillonite and kaolinite as a function of pH

Adsorption on silica and on mica showed the same pH-dependence. The much greater adsorption on hydrophobic surfaces than hydrophilic (data not shown), implies a strong contribution of hydrophobic interactions to the adsorption process.

Fig. 2 illustrates the small change in secondary structure following adsorption on montmorillonite. In contrast, on hydrophobic silica, the protein was found

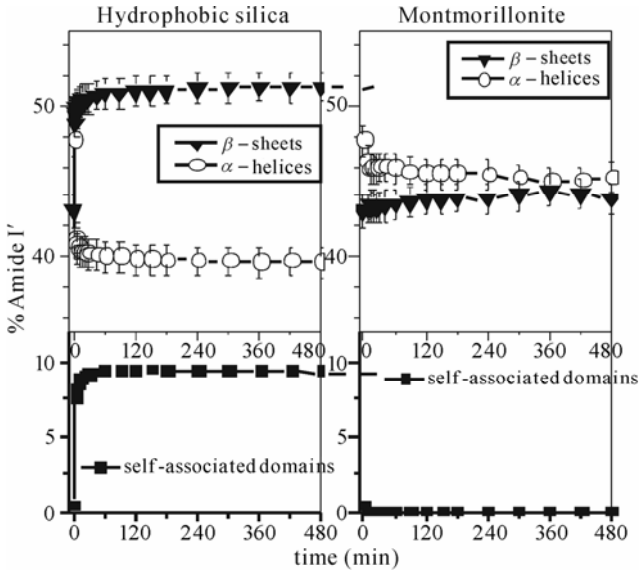

Fig. 2 The small change in secondary structure following adsorption on montmorillonite and hydrophobic silica

to self-associate and there were marked structural changes as-helices declined rapidly at the expense of-sheets.

Fig. 3 shows the decline of extractable immunoreactive toxin as a function of incubation time in the presence of each of the four soils. Toxin declined over the 3-month incubation, but could still be detected in most soils. The decline was more rapid for the two sandy soils, but little effect of organic matter content was evident.

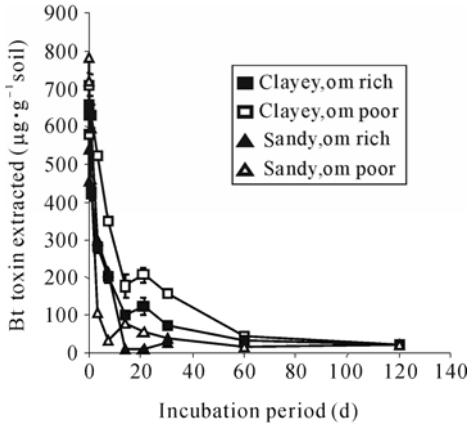

Fig. 3 The decline of extractable immunoreactive toxin as a function of incubation time in the presence of each of the four soils

Fig. 4 shows that there was no significant protection of the toxin when microbial activity was decreased by sterilisation or autoclaving the soils. Neither was there any increase in the rate of disappearance of the protein when microbial activity was stimulated by adding glucose or amino-acids. However the toxin persisted longer at lower temperature (4°C). Since other data pointed to a limited effect of microbial activity, this temperature effect probably reflects the temperature dependence of adsorption and the consequent conformational changes. The changes may lead to fixation on the surface or decrease the immuno-reactivity of the toxin. Such an effect is consistent with a large contribution of hydrophobic interactions.

In conclusion, adsorption of Bt Cry1Aa toxin on mineral surfaces depends on both electrostatic (pH-dependent) and hydrophobic interactions. Adsorption is concentration dependent, and not easily reversible. Adsorption is accompanied by conformational changes, but further study would be required to determine the relationship between secondary structure and either persistence or toxicity.

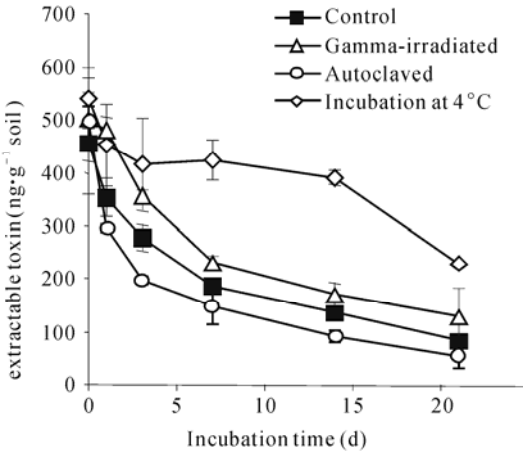

Fig. 4 No. significant protection of the toxin when microbial activity was decreased by sterilisation or autoclaving the soils

Acknowledgements

This work was financed by the French ANR and the Région Languedoc-Roussillon.

References

Balme S, Janot JM, Dejardin P, Vasina EN, Seta P (2006) Potentialities of confocal fluorescence for investigating protein adsorption on mica and in ultrafiltration membranes. J. Membrane. Sci. 284 : 198-204

Helassa N, Quiquampoix H, Noinville S, Szponarski W, Staunton S (2008) Adsorption and desorption of monomeric Bt (Bacillus thuringiensis) Cry1Aa toxin on montmorillonite and kaolinite. Soil Biol. Biochem. 41: 498-504

Revault M, Quiquampoix H, Baron MH, and Noinville S (2005) Fate of prions in soil: Trapped conformation of full-length ovine prion protein induced by adsorption on clays. Biochim. Biophys. Acta 1724: 367-374

Microbial and Abiotic Interactions between Transformation of Reducible Pollutants and Fe(II)/(III) Cycles

Fangbai Li*, Shungui Zhou*, Xiaomin Li, Chunyuan Wu, Liang Tao

Guangdong Key Laboratory of Agricultural Environment Pollution Integrated Control, Guangdong Institute of Eco-Environmental and Soil Sciences, Guangzhou, 510650, China.
*Corresponding author. E-mail: cefbli@soil.gd.cn and sgzhou@soil.gd.cn.

Abstract: This study provides fundamental information on the interactions between iron cycles and transformation of reducible pollutants transformation. We introduce 2 cases of microbial and abiotic interactions (1) Interactions between reduction of iron oxides and dechlorination of 1,1,1-trichoro-2,2-bis(*p*-chlorophenyl)-ethane (DDT) by dissimilatory Fe(III)-reducing bacterium (DIRB) S12; (2) Interactions among CY01, and reduction of iron oxides and reduction of 2,4-dichlorophenoxyacetic acid (2,4-D). We found that the transformation of DDT and 2, 4-D could be enhanced in a system of dissimilatory iron-reducing bacteria and iron oxides. This contribution demonstrated the important role of DIRB and Fe(II)/Fe(III) cycles on the transformation of pesticides under anaerobic environments, and provided scientific information for in-situ bioremediation of pesticide pollutants in Fe(III)-rich environments.

Keywords: Dissimilatory Fe(III)-reducing bacterium; Iron cycle; Dechlorination; 2,4-dichlorophenoxyacetic acid (2,4-D); 1,1,1-trichoro-2,2-bis(*p*-chlorophenyl)-ethane (DDT)

Introduction

Iron is the most abundant transition metal in soil, and very important to both biological and chemical environmental processes. It is also essential plant nutrient. Subtropical soils contain large amounts of free iron oxides, with special biogeochemistry. Therefore, the transformation of reducible pollutants may strongly depend on the biogeochemistry of iron species. In the presence of dissolved organic matters (DOM), iron oxides can be reduced. In rhizosphere soils, root exudates including various DOM can enhance the dissolution of iron oxides, resulting in the formation of various dissolved or adsorbed Fe(III)/Fe(II) species. Iron-reducing bacteria (IRB) can drive the reductive dissolution of iron oxides, and then generate Fe(II) species with lower redox potential (Lovley, 1987; 2004). The aims of the study are to (1) investigate the roles of Fe(II) species and iron-reducing bacteria (IRB) in transformation of pesticides; (2) disclose the interaction among the adsorption of iron species on minerals, chemical and biological processes of Fe(II)/Fe(III) cycles with the transformation of pesticides.

Materials and Methods

The reaction solution was injected into the serum bottles, and then purged with O_2-free N_2 gas for 1 h and sealed with Teflon-coated butyl rubber stoppers and crimp seals. Standard anaerobic techniques were used throughout all experiments. All vials were conducted in triplicate and incubated in a BACTRON Anaerobic/Environmental Chamber II (SHELLAB, Sheldon Manufacturing Inc.) at 30 ℃ in the dark. All the experiments were run in triplicate. A strict quality-assurance and quality-control program was implemented for the extraction method and analysis. We have reported the experimental procedure in detail (Li *et al.*, 2008; 2009).

Results and Discussion

Enhanced Reductive Dechlorination of DDT in a System of Dissimilatory Iron-reducing Bacteria and Goethite

This case investigated DDT transformation in a system of dissimilatory iron-reducing bacteria (DIRB) and goethite (α-FeOOH). The results showed that DDT can be degraded by DIRB and DDT removal was more effective in the system of DIRB and α-FeOOH, though α-FeOOH can not degrade DDT. The enhanced degradation of DDT was mainly attributable to biogenic Fe(II) on the surface of α-FeOOH, serving as a redox mediator for DDT reduction. The cyclic voltammetry results provided evidence of a decrease in redox potential of Fe(II) in the system, which contributed to the enhancement of Fe(II) reactivity and a subsequent increase of DDT degradation. After 9 months, DDT was only degraded to DDD by DIRB alone, while in the system of DIRB and α-FeOOH, DDT degradation followed a sequential reductive dechlorination process as DDT to DDD to DDMS to DBP, as shown in Fig. 1. This contribution demon-strated the important role of DIRB and iron oxide in DDT transformation under anaerobic environments.

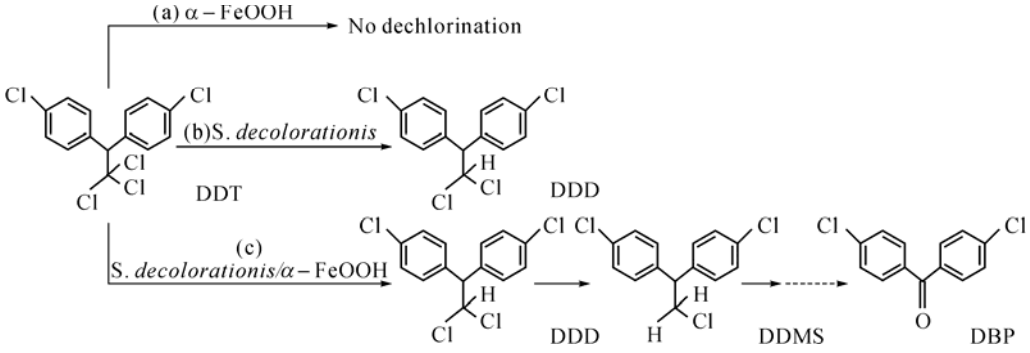

Fig. 1 The proposed pathway of DDT transformation in the three different systems. (a) goethite; (b) S. *decolorationis*; (c) S. *decolorationis* + goethite

Fe(III)-enhanced Anaerobic Degradation of 2,4-Dichlorophenoxyacetic Acid by a Dissimilatory Fe(III)-reducing Bacterium Comamonas Koreensis CY01

This case demonstrated the ability of *Comamonas koreensis* CY01 to obtain energy for microbial growth by coupling the oxidation of electron donors to dissimilatory Fe(III) reduction, and also the enhanced 2,4-dichlorophenoxyacetic acid (2,4-D) biodegrad-ation by the presence of Fe(III) oxides under anaerobic conditions. The results suggested that the anaerobic respiration of strain CY01 can utilize ferrihydrite, goethite, lepidocrocite or hematite as the terminal electron acceptor and citrate, glycerol, glucose or sucrose as the electron donor. The biodegradation pathway of 2,4-D by the strain was proposed to be 2,4-D to 4-chlorophenol (4-CP) through reductive side-chain removal and dechlorination. Under the anaerobic conditions, dissimilatory Fe(III) reduction and 2,4-D biodegradation occurred simultaneously. The presence of Fe(III) (hydr)oxides would significantly enhance 2,4-D biodegradation, probably due to that the reactive mineral-bound Fe(II) species generated from dissimilatory Fe(III) reduction can abiotically reduce 2,4-D. With the demonstrated ability of reducing both Fe(III) (hydr)oxides and 2,4-D, strain CY01 was proven to be a new bacterial strain for studying the interaction between reductive dechlorination and dissimilatory Fe(III) reduction. This study provided scientific support and information for in-situ bioremediation of chlorinated organic pollutants in Fe(III)-rich environments.

Conclusions

Iron cycle is an important physical-chemical-biological process in subtropical soils and is driven by iron-reducing bacteria. Fe(II) species are important reductants with low redox potential. DOM act as electron donor for iron-reducing bacteria and reductants for Fe(III) reduction. DIRB act as a driver of reduction of Fe(III) and pollutants. Humic acid acts as an electron mediator. We proposed a mechanism of

microbial and abiotic interaction in the reductive dechlorination of DDT and 2,4-D which can be undergone via three ways, (1) direct biotic dechlorination by iron-reducing bacteria; (2) chemical dechlorination by Fe(II) species; (3) interaction among Fe(II) species, bacteria and humic acid.

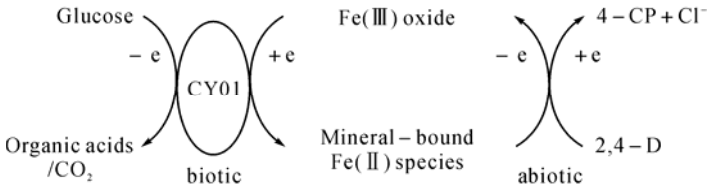

Fig. 2 The proposed mechanism of 2,4-D anaerobic transformation by *C. koreensis* CY01 in the presence of goethite

Acknowledgments

This research was supported by the National Natural Science Foundations of China (No. 40771105 and 40601043).

References

Li FB, Wang XG, Liu CS, Li YT, Zeng F, Liu L (2008) Reductive transformation of pentachlorophenol on the interface of subtropical soil colloids and water. Geoderma 148: 70-78

Li XM, Zhou SG, Li FB, Wu CY, Zhuang L, Xu W, Liu L (2009) Fe(III) oxide reduction and carbon tetrachloride dechlorination by a newly isolated Klebsiella pneumoniae strain L17. J. Appl. Microbiol. 106: 130-139

Lovley DR (1987) Organic matter mineralization with the reduction of ferric iron: A review. Geomicrobiol. J. 5: 375-399

Lovley DR (2004) Dissimilatory Fe(III) and Mn(IV) Reduction. Adv. Microbiol. Physiol. 49: 219-286

Assessment of Availability of Phenanthrene and Pyrene in Aging Soil

Wanting Ling, Yuechun Zeng, Yanzheng Gao*, Xuezhu Zhu

College of Resource and Environmental Sciences, Nanjing Agricultural University, Nanjing 210095, China.
*Corresponding author. Tel. No. +86-25 84395238; Fax No. +86-25 84395238; E-mail:gaoyanzheng@njau.edu.cn.

Abstract: The availability of polycyclic aromatic hydrocarbons (PAHs) in aging soils has not been well elucidated. In this study, sequential extraction was utilized to evaluate the availability of phenanthrene and pyrene as representative PAHs in four typical zonal Chinese soils with aging period for 16 weeks. The tested PAHs were fractionated into two groups: the extractable fractions and bound residues. The former, including desorbing and non-desorbing fractions, is the available fractions in soil that can be taken up by plants and/or soil-inhabiting animals. Both the desorbing and non-desorbing fractions were observed to generally decrease over time, primarily due to microbial biodegradation of the available residues, the desorbing fractions were more readily biodegradable (> 91.4% and > 71.2% for phenanthrene and pyrene, respectively) than the non-desorbing fractions. Attenuation of the desorbing fraction accounted for more than 92.1% and 76.8% of the observed reduction of the available residues of phenanthrene and pyrene, respectively. The observed concentrations of bound PAH residues were much lower than those of the available residues. In comparison with microbial biodegradation, the transformation of available fractions to bound residues accounted for only a negligible reduction of the available residues of the PAHs tested. These results are useful for risk assessments of PAHs related to human health and environmental contamination.

Keywords: Polycyclic aromatic hydrocarbons (PAHs); Mild-extraction; Availability; Aging; Soil; Bound residue; Form; Fractionation

Introduction

The correlations between the availabily of organic chemicals including PAHs and their forms in aging soils have yet to be elucidated. The present study was performed to characterize the temporal changes in extractability and to evaluate the availability of PAHs in several aging soils. The correlations between the availability of PAHs and their forms in aging soils were clarified. The results of this study have important applications in risk assessment of PAH-contaminated soils, as well as in the development of remedial strategies for contaminated sites.

Materials and Methods

Four typical zonal soils in China were experimented. Soils were spiked with a solution of phenanthrene and pyrene in acetone, the soil treatment process was according to literature (Gao and Ling, 2006). The forms of PAHs in soils were examined using microcosms similar to those reported previously (Macleod and Semple, 2003). The soils were sampled after aging for 0, 2, 4, 8, 12, and 16 weeks in microcosms at 25℃. The sequential extraction/ chemical mass balance approach described by Sabaté *et al.* (2006) was used to fractionate the forms of PAHs in soils. The available PAHs were separated into desorbing and non-desorbing fractions.

Results and Discussion

Available Fractions of PAHs in Soils as a Function of Aging Time

Fig. 1 shows the available fractions including desorbing and non-desorbing fractions of phenanthrene and pyrene in four tested soils as a

function of aging time. The initial soil (time 0) showed higher available fractions for phenanthrene and pyrene, and the concentrations then generally decreased with time. The data shown in Fig. 1 suggest that the aging process significantly affects the availability of the examined PAHs in soils. These PAHs were more readily available at the start of aging, and their availability decreased rapidly with increasing soil–PAH contact time.

Significant losses of tested PAHs were observed in soil 1, soil 2, soil 3, and soil 4 after 16 weeks of aging, and 72.3%, 90.0%, 87.6%, and 93.8% of available phenanthrene and 11.6%, 44.6%, 64.0%, and 85.2% of available pyrene disappeared in these soils, respectively. In the same soil samples, the available phenanthrene was more readily degradable and the dissipation ratio of the available phenanthrene was clearly higher than those of pyrene, indicating that PAHs with higher molecular weight and more benzene rings were more recalcitrant in soils.

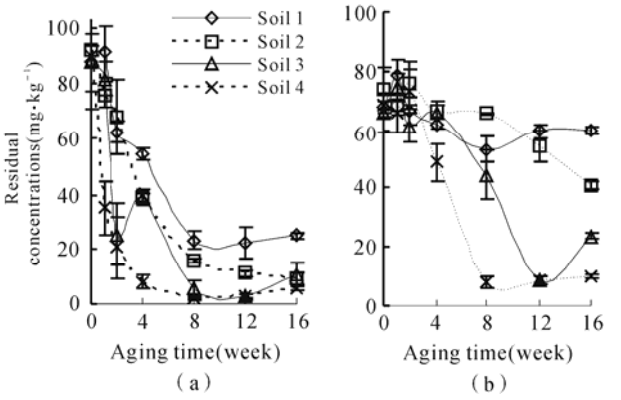

Fig. 1 Concentrations of available fraction of phenanthrene (a) and pyrene (b) in tested soils as a function of aging time

Fractionation of Available PAH Fractions in Soils

The available residues of PAHs in soil include desorbing and non-desorbing fractions, and the former has been shown to be the most bioavailable portion. In this study, we utilized water in combination with HPCD to extract the desorbing fractions of the PAHs tested (Reid *et al.*, 2000). The concentrations of desorbing PAH fractions in soils generally decreased with time (Fig. 2).

After 16 weeks, the levels of degradation of the desorbing fraction of phenanthrene and pyrene relative to their initial amounts were 73.6%, 90.5%, 88.2%, and 94.3%, and 19.5%, 54.5%, 69.1%, and 89.4% in soils 1~4, respectively. For all PAHs, the concentrations of non-desorbing fractions of phenanthrene and pyrene in soils generally showed slight decreases. The desorbing fraction was the predominant portion of the available fractions of the PAHs tested, accounting for 91.4% and 71.2% of the available fractions of phenanthrene and pyrene in soils at the beginning of aging, respectively. However, all the desorbing PAH to available fraction ratios in the tested soils was reduced after 16 weeks of aging. In contrast, the ratios of non-desorbing fractions of PAHs relative to their available fractions increased over this duration of aging.

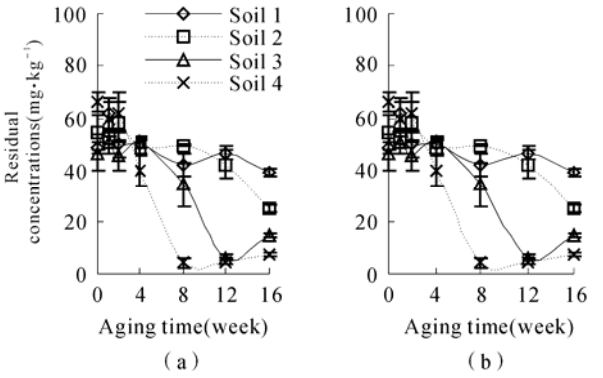

Fig. 2 Concentrations of the desorbing fraction of phenanthrene (a) and pyrene (b) in tested soils as a function of aging time

Microbial Degradation of Available Fractions of PAHs in Soils

Decreases in the available PAH fractions accessible for microbial degradation commensurate with increasing aging time were observed in the tested soils (Fig. 1). Here, the availability of phenanthrene in soils decreased rapidly even at the beginning of aging, suggesting the rapid establishment of a potent phenanthrene degrading microbial consortium in soils. However, due to the higher molecular weight and larger number of benzene rings, pyrene was more recalcitrant, and it may take longer (≥ 4 weeks) for the establishment of its microbial consortium in soils.

The desorbing fraction of PAHs in soils was more readily biodegradable than the non-desorbing fractions. The dissipation of available PAH fractions from the non-inhibited soils were primarily due to intrinsic microbial degradation. In comparison with the microbial inhibited soils, the overwhelmingly larger dissipation of extractable residues in non-inhibited soils indicated that microbial degradation was the dominant factor responsible for dissipation of

the available fractions of PAHs in soil.

Table 1 Concentrations of bound residues of phenanthrene and pyrene in soil 1

Time (week)	Phenanthrene ($mg \cdot kg^{-1}$)	Pyrene ($mg \cdot kg^{-1}$)
0	0.097±0.13	0.21±0.098
1	0.14±0.59	0.38±0.11
2	0.39±0.16	0.58±0.28
4	0.60±0.23	1.47±1.11
8	0.20±0.17	0.42±0.31
12	0.34±0.15	0.53±0.40
16	0.078±0	0.63±0

Transformation of Available Fraction of PAHs to Bound Residue in Soils

The forms of HOCs in the soil environment have been reported previously (Lesan and Bhandari, 2004), and the formation of bound residues would theoretically reduce the availability of HOCs in soils. The bound residual PAH concentrations tended to first increase and then decrease over the 16-week aging period. However, in comparison with the available PAH residues, the concentrations of bound PAH residues were always very low with maximum values of 0.60 and 1.47 $mg \cdot kg^{-1}$ for phenanthrene and pyrene in soil 1, respectively (Table 1). The results of the present study confirmed that the contribution of the transfer to bound residue to the dissipation of available fractions of PAHs in soils was negligible.

References

Gao YZ, Ling WT (2006) Comparison for plant uptake of phenanthrene and pyrene from soil and water. Biol. Fert. Soils. 42: 387-394

Lesan HM, Bhandari A (2004) Contact-time-dependent atrazine residue formation in surface soils. Water Res. 38: 4435-4445

Macleod CJA, Semple KT (2003) Sequential extraction of low concentrations of pyrene and formation of non-extractable residues in sterile and non-sterile soils. Soil Biol. Biochem. 35: 1443-1450

Reid BJ, Stokes JD, Jones KC, Semple KT (2000) Nonexhaustive cyclodextrin-based extraction techni-que for the evaluation of PAH bioavailability. Environ. Sci. Technol. 34: 3174-3179

Sabaté J, Vinas M, Solanas AM (2006) Bioavai-lability assessment and environmental fate of polycyclic aromatic hydrocarbons in biostimulated creosote-contaminated soil. Chemosphere 63: 1648-1659

Levels, Distributions and Profiles of Polychlorinated Biphenyls in Paddy Fields from Two Towns in a Typical Electronic Waste Recycling Area of Eastern China

Xianjin Tang[a], Chaofeng Shen[a], Wenli Liu[b], Congkai Zhang[a], Yingxu Chen[a,*]

[a] Department of Environmental Engineering, College of Environmental and Resource Sciences, Zhejiang University, Hangzhou 310029, China;
[b] School of Life Science, Taizhou University, Linhai, Zhejiang, 317000, China.
[*]Corresponding author. Tel. No. +86-571 8697 1159; Fax No. +86-571 8697 1898; E-mail: yxchen@zju.edu.cn.

Abstract: Surface soil (0~10 cm) samples from Zeguo and Wenqiao, two towns in a typical electronic waste (E-waste) recycling area of eastern China, were collected and analyzed for polychlorinated biphenyls (PCBs). The mean concentration of total 58 PCBs congeners in Zeguo and Wenqiao were 62.8 and 144.8 $\mu g \cdot kg^{-1}$ (dry weight), respectively, with a range from 13.3 to 242.2, and 27.1 to 526.3 $\mu g \cdot kg^{-1}$, respectively. The concentrations of total PCBs decreased in the order of paddy fields near E-waste recycling workshops (NEW) > paddy fields near E-waste recycling plants (NEP) > paddy fields in open burning villages (OBV) > paddy fields in other villages (OV). The difference of PCBs composition in OBV or OV areas between Zeguo and Wenqiao indicated that the PCBs concentration in paddy fields were affected significantly by atmospheric transportation and direct discharge. Furthermore, the composition of PCBs in Zeguo and Wenqiao was different, Zeguo soils near the E-waste recycling working plants and workshops contained more high chlorinated PCB congeners and less low chlorinated PCBs compared with Wenqiao soil, possibly indicating the difference of PCBs major source were different. The results of present study suggested that the soil in Zeguo and Wenqiao towns was heavily polluted by PCBs because of E-waste recycling activities. Compared with the large scale E-waste recycling plants, the small simple household workshops have been contributing more PCBs pollution to the soil environment. However, due to the lack of data about the human exposure in this area, it is unconvincing that the analysis of soil samples collected from the crude and inappropriate E-waste recycling area would pose significant threat to human. It is expected to learn much more about the extent and long-term effects of these particular E-waste activities on environmental and human health.

Keywords: Electronic waste (E-waste); Polychlorinated biphenyls (PCBs); Paddy fields; Distributions

Introduction

The imported electronic waste (E-waste) to Asian countries is creating an increasingly large environmental problem. Polychlorinated biphenyls (PCBs) have been used worldwide in electrical applications such as capacitors and transformers, in ship painting, and in carbon-free copy papers. During the crude and primitive recycling procedures of E-waste, various high toxic pollutants like PCBs in capacitors/transformers can be emitted or formed (Wong *et al*., 2007). WenTai area, located in Zhejiang province, East China has been involved in E-waste recycling for nearly 25 years. It is one of the best known E-waste processing centers of China (Shen *et al*., 2008; 2009). However, until now, almost all of the researches about WenTai area focused on the center city, Luqiao. There is no systematic study about pollution in Wenling, another major city of Taizhou, where the same materials have been recycled. The main objective of this study was to determine the levels, distributions and profiles of the PCBs in soils affected by E-waste recycling in Zeguo and Wenqiao towns of Wenling.

Materials and Methods

Zeguo and Wenqiao towns are located in Wenling, Taizhou city of Zhejiang province, China. Many families in these two towns are engaged in individual recycling workshops, with more and more migrant laborers employed. There are at least nine large-scale E-waste recycling plants and many simple household E-waste recycling workshops distributed in the paddy fields and along riversides, which are still in operation daily. A total of 80 soil samples (0~10 cm soil layer) were collected from different locations throughout the Zeguo and Wenqiao areas in August and September, 2008. According to the location, the samples were divided into four groups: paddy fields near E-waste recycling workshops (NEW), paddy fields near E-waste recycling plants (NEP), paddy fields in open burning villages (OBV) and paddy fields in other villages (OV). A global positioning system was employed to identify the precise location of each station. At each sampling site, five sub-samples were collected from a 100 × 100 m^2 plot (located on the crossing diagonals, four in the corners and one in the crossing point). Samples were homogenized to obtain about 1000 g representative samples in pre-cleaned aluminum containers. Pebbles and twigs were removed and samples were then air-dried at room temperature, sieved through a 2 mm sieve and stored at 4 ℃ before analysis.

Samples (5 g) were extracted for 24 h with hexane and acetone (v:v 1:1, 200 mL) in a Soxhlet apparatus. The extracted solutions were concentrated to about 1~2 mL in a rotary evaporator and dissolved in 10 ml hexane. The resulted extracts were then passed through the column packed with layers of Florisil column and anhydrous sodium sulphate, and eluted with 100 mL hexane. The eluate was evaporated to 1 ml prior to analysis (Shen *et al.*, 2009). The concentrations of 58 PCB congeners, which included six indicator PCBs (PCB-28, -52, -101, -118, -153, -138), were measured on Agilent 6890 GC system equipped with ^{63}Ni electron capture detector and a 30m × 0.25 mm × 0.25μm DB-5 capillary column (J & W Scientific Co. Ltd., USA).

Results and Discussion

The levels of PCBs (total 58 PCBs) in surface paddy field were analyzed. The mean concentration of total PCBs among the 50 sites in Zeguo town and 30 sites in Wenqiao town were 62.8 and 144.8 μg·kg^{-1} (dry weight), respectively, with a range from 13.3 to 242.2 μg·kg^{-1}, and 27.1 to 526.3 μg·kg^{-1} (dry weight), for Zeguo and Wenqiao towns, respectively. The concentrations of the six PCB indicators varied from n.d to 86.7 with mean value of 13.1 μg·kg^{-1} for Zeguo area, and from n.d. to 125.1 with mean value of 33.6 μg·kg^{-1} for Wenqiao area. The concentrations of these six PCB indicators were well correlated with total PCB concentrations (R^2=0.985, 0.942 for Zeguo and Wenqiao, respectively), accounting for 12.5% (Zeguo) and 20.1% (Wenqiao) of the total PCB concentrations.

Table 1 The average concentrations of soil PCBs in different sampling areas (μg·kg^{-1})

Sampling areas		NEW	NEP	OBV	OV
Zeguo	Total PCBs	124.1±78.3 a	88.4±40.6 a	35.5±20.7 b	24.1±7.3 b
	Indicative PCBs	33.8±31.2 a	22.2±20.0 a	3.1±5.1 b	0.4±0.8 b
	Sample No.	6	18	15	11
Wenqiao	Total PCBs	284.2±185.0 a	243.7±200.1 a	135.7±90.6 b	74.9±39.7 b
	Indicative PCBs	69.7±48.4 a	67.2±63.1 a	27.7±26.6 b	17.1±12.9 b
	Sample No.	6	3	9	12

NEW, paddy fields near small E-waste recycling workshops; NEP, paddy fields near large scale E-waste recycling plants; OBV, paddy fields in open burning villages; OV, paddy fields in other villages. Values are averages with standard deviations. Values in the same row followed by the same small letter are not significantly ($p < 0.05$) different

PCBs levels in Zeguo were less than those observed in Wenqiao soil, and it was found that there were large scale E-waste recycling plants with relatively better E-waste recycling industry management in Zeguo, while in Wenqiao town, E-waste could be found anywhere. Otherwise, the difference of PCBs concentrations might come from different types of E-waste, Wenqiao had more electric power capacitor, transformer and electromotor, which contained more PCBs, however, the difference of PCBs concentrations between two towns should be further studied.

PCB levels in Zeguo and Wenqiao were compared with those in other regions for the evaluation of pollution degree of soils. In general, the soil concentration levels of PCBs in Zeguo and Wenqiao were comparable to those found in farmland soils from Luqiao, the famous E-waste recycling centre in WenTai area. Compared with Guiyu, another E-waste centre, the levels were higher than those found at rice field or area near the open-burning site, and at the same level as the open-burning site in Guiyu (Wong *et al*., 2007).

Table 1 presents the concentrations of PCBs in the four sampling areas. Total concentrations increased in the order of OV < OBV < NEP<NEW. Mean PCB concentrations were significantly lower in OBV and OV areas than those in other two sampling areas close to E-waste recycling activities. The PCB congeners exhibited a rather uniform distribution of concentrations with less than one order of magnitude of variation for each of the sampling area. The lowest PCB concentrations are OV areas without E-waste recycling activities, showing 24.1 and 74.9 $\mu g \cdot kg^{-1}$ for Zeguo and Wenqiao areas, respectively. The relatively higher PCBs concentrations in OV areas indicated that PCBs in the OBV or OV areas may be transported from areas closed to E-waste recycling areas through the long distance transfer. For the NEW and NEP areas, PCBs in the soil samples collected in the NEW areas were higher, followed by the NEP sites, but the differences were not significant.

The pattern of PCB profiles varied widely in different areas. The composition of PCBs in soil was different between the two towns. Generally, Zeguo soil contained more high chlorinated congeners and less low chlorinated ones when compared to the composition in Wenqiao soil, especially for the soil taken from the NEW and NEP areas. In the NEW and NEP sampling areas in Zeguo, compositions of low chlorinated congeners (tri-, tetra- and petan-PCBs) were 74.9% and 63.0% of the total PCBs, respectively, while the relative values in Wenqiao soil were 88.4% and 93.3%, respectively. The difference was more significant when each chlorinated PCBs in each sampling areas in Zeguo and Wenqiao towns were compared. The main reason might be the PCBs sources were different. Generally, in the simple small house workshops in Wenqiao town, PCBs 1242 and 1254 had been found from E-waste recycling workshops dealing with the disposal of electric power capacitors or transformers. This might be the reason for high contents of low chlorinated congeners in soil samples of house workshops in Wenqiao. Previous studies also reported the presence of less low chlorinated PCB congeners in soils collected from the vicinity of an illegal trading and dismantling site for PCB-containing equipment in Taizhou area. While in Zeguo, these electric power capacitors or transformers were relatively less. It was also interesting when the differences of PCBs composition in OBV and OV of the two towns were compared. In Zeguo soil, higher composition of low chlorinated PCBs was observed when comparing the NEW or NEP sampling areas, while the composition of low chlorinated PCBs were less than those observed in relative NEW or NEP sampling areas in Wenqiao. It was found the total PCBs in OV and OBV from Zeguo ranged 24.1 $\mu g \cdot kg^{-1}$ to 35.5 $\mu g \cdot kg^{-1}$, respectively, while 74.9 $\mu g \cdot kg^{-1}$ and 135.7 $\mu g \cdot kg^{-1}$ were observed in OV and OBV from Wenqiao, respectively. Therefore, it was speculated that the major source of soil PCBs in Zeguo might be atmospheric transportation and deposition of less chlorinated PCBs, while OV or OBV areas in Wenqiao might be affected by some PCBs sources directly. PCBs were also suspected of being discharged from the incineration of electric wires and printed circuit boards. A study carried out in Wanli, China, a former E-waste disposal center, also found that combustion of waste electric wires and magnetic cards could result in soil PCB contamination.

References

Shen CF, Chen YX, Huang SB, Wang ZJ, Yu CN, Qiao M, Xu M, Setty K, Zhang JY, Lin Q (2009) Dioxin-like compounds in agricultural soils near E-waste recycling sites from Taizhou area, China:

Chemical and bioanalytical characterization. Environ. Int. 35: 50-55

Shen CF, Huang SB, Wang ZJ, Qiao M, Tang XJ, Yu CN, Shi DZ, Zhu YF, Shi JY, Chen XC, Setty K, Chen YX (2008) Identification of Ah receptor agonists in soil of E-waste recycling sites from Taizhou area in China. Environ. Sci. Technol. 42: 49-55

Wang DG, Yang M, Jia HL, Zhou L, Li YF (2008) Levels, distributions and profiles of polychlorinated biphenyls in surface soils of Dalian, China, Chemosphere. 73: 38-42

Wong MH, Wu SC, Deng WJ, Yu XZ, Luo Q, Leung A, Wong CSC, Luksemburg WJ, Wong AS (2007) Export of toxic chemicals - a review of the case of uncontrolled electronic-waste recycling. Environ. Pollut. 149: 131-140

Phytoremediation of Contaminated Soils with Polycyclic Aromatic Hydrocarbons and Its Ecologically Enhanced Techniques

Shiqiang Wei [a,b,*]

[a] College of Resources and Environment, Department of Environment Science and Engineering, Southwest University, Chongqing, China;
[b] Chongqing Key Laboratory of Agricultural Resources and Environment, Chongqing, China.
[*]Corresponding author. E-mail: sqwei@swu.edu.cn.

Abstract: In this paper, a series of research results with respect to the phytoremediation of PAH-contaminated soil were introduced, including the remediation potential of plant species, the utilization of earthworm, the interaction techniques of plants, earthworm and aboriginal microbe, etc.. The results derived from this study may offer an improved knowledge for the scientific evaluation of phytoremediation of PAHs polluted soil.

Keywords: Phytoremediation; Polycyclic aromatic hydrocarbons (PAHs); Soil; Earthworm; Ecological remediation

Polycyclic aromatic hydrocarbons (PAHs) are important pollutants that decrease the environmental quality and harm human health (Manoli and Samara, 1999; Tao *et al.*, 2004; Li and Ma *et al.*, 2006; Fismes *et al.*, 2002). Among all treatments regarding the removal of PAHs from soil, phytoremediation is a promising alternative approach due to its convenience, cost-effectiveness and environmental acceptability (Parrish *et al.*, 2005; Xu *et al.*, 2006). Plants can enhance the remediation of PAH-polluted soil by various processes, such as the modification of microbial community structure and functional diversity (Jennifer *et al.*, 2005; Nichol, 1997; Jodahl *et al.*, 1997), the improvement of soil physico-chemical conditions as affected by the root exudation (Schwab and Banks, 1998; Ryan *et al.*, 1988; Zhang *et al.*, 2001), and the enhancement of oxygen diffusion by their roots through providing channels for air flow. However, the impact of each process and the involved mechanisms are up-to-date far from clear. The efficacy of each process may vary greatly among plant species and is closely related to properties of contaminants and environmental characteristics. In this paper, the remediation potential of twelve plant species on the removal of phenanthrene (Phe) or pyrene (Pyr) in soil were investigated by pot experiments in a greenhouse, and the mechanisms and efficiencies of PAHs removal from soils through different planting pattern were also compared. The effects of earthworm activity, and the interaction phytoremediation system that was composed of plants, earthworm and aboriginal microbe was developed. The main original conclusions are as follows.

Screening of Twelve Plants Species for Phytore Mediation of Phenanthrene or Pyrene in Soils

Twelve plant species, which include *Ophiopogon japnicus, Sorghum vulgare, Pogonatherum paniceum, Lolium multiform, Medicago sativa, Zea may, Iris japonica Thunb, Trifolium repens, Brassica campestris, Lactuca sativa, Brassica oleracea* and *Festuca arundinacea*, were screened for their potential of PAH removal at a series of concentrations from 20 to 322 $mg \cdot kg^{-1}$ using pot experiments in a greenhouse. The results indicated that plants could decrease effectively the concentration of Phe and Pyr at different degrees.

Among twelve plants investigated, *Ophiopogon japnicus, Sorghum vulgare, Pogonatherum paniceum, Lolium multiform* and *Festuca arundinacea* caused more significant decreases in the planted soil than that in the unplanted, and would be effective in the phytoremediation of PAH-polluted soils. At the end of the experiment (55d), the remaining concentrations of Phe and Pyr in spiked vegetated soils, with initial Phe of 161.44 $mg \cdot kg^{-1}$ and Pyr of 161.44 $mg \cdot kg^{-1}$, were 16.33~122.39 $mg \cdot kg^{-1}$ and 45.73~124.82 $mg \cdot kg^{-1}$, respectively, and were lower than those in the non-vegetated soils. The removal rates of Phe and Pyr in the vegetated soils were 24.18%~77.49% and 22.29%~71.53%, respectively. It thus suggested a feasibility of the establishment of phytoremediation for soil PAHs contamination.

Removal and Remediation of PAHs in Soil by *Pogonatherum Paniceum*

Pot experiments were carried out to investigate the accumulation and removal mechanisms of PAHs by rock plant *P.paniceum.* The results showed *P. paniceum* significantly removed Phe or Pyr from soil. About 50.97%~86.77% of Phe and 46.45%~76.7% Pyr were removed from soils, respectively. Meanwhile, compared with two different soils with or without NaN_3, it's evident to know the important role of bioconcentration factors (BCFs) for PAHs tended to decrease with increasing concentrations in soils.

Effect of Multispecies Phytoremediation on the Fate of Phenanthrene or Pyrene in Soil

The potentials of three plant species, rape, alfalfa and white clover, separately or jointly on the degradation of PAHs in soil were estimated by pots experiments in a greenhouse. The results showed that the presence of vegetation apparently enhanced the dissipation of PAHs in soils at their initial concentrations ranging from 20.05 to 322.06 $mg \cdot kg^{-1}$, but the efficacy varied greatly among plant species and cropping patterns. Results suggested a feasibility of the establishment of multispecies remediation for the improvement of remediation efficiencies of PAHs, which may also decrease the accumulations of PAHs in plants and thus reduce their risks to humans.

Dynamic Changes of PAH Removal Factors and Soil Enzyme Activities in the Phytoremediation Process

In this study, the dynamic changes of PAH biotic and abiotic removal factors in soil-plant (S.vulgare) system with initial Phe of 81.05 $mg \cdot kg^{-1}$ or Pyr of 79.86 $mg \cdot kg^{-1}$, and soil enzyme (polyphenoloxidase, dehydrogenase and urease) activities were monitored every 12 d in pot experiments. The results showed that the contribution rates of PAH removal factors and soil enzyme activities varied greatly at different monitoring stage during the 72 d experiment. At early monitoring time (0~36 d), the predominant pathway responsible for the degradation of PAHs was the microbial degradation among all pathways, but at late monitoring time (36~72 d), the plant-microbial interactions was the main mechanisms for the remediation of PAH polluted soil. From the above results, it suggested that in soil-plant system, plant-microbial interactions may facilitate the degradation of PAHs in soils by means of reactivating or activating soil enzyme activities.

Earthworm's Tolerance and Its Ecological Effects on PAH-contaminated Soils

The earthworm's ability to tolerate PAHs in soils and its influence on physicochemical properties of the PAHs spiked soils were elucidated. The results showed that earthworms were able to survive in medium spiked soils with initial Phe of 20.05~322.06 $mg \cdot kg^{-1}$ or Pyr 20.24~321.42 $mg \cdot kg^{-1}$, but the growth of earthworms was inhibited significantly at heavily spiked conditions where the initial concentrations of Phe and Pyr were at 502.82 $mg \cdot kg^{-1}$and 509.33 $mg \cdot kg^{-1}$, respectively. The study indicated that earthworms were able to survive in medium spiked soils and their activities were also beneficial to the improvements of soil properties.

Enhanced Dissipation of PAHs in Planted Soils by Earthworm Activities

The potential of *Sorghum vulgare*, with or without inoculating earthworm (*Pheretima sp.*), on the

dissipation of PAHs in soils were estimated in the greenhouse pot experiments. Results showed that plantation of vegetation apparently enhanced the dissipation of PAHs in soils at their initial concentrations ranging from 20.05 to 322.06 $mg \cdot kg^{-1}$. It thus suggested a feasible way for the establishment of high efficiency phytoremediation of PAHs with inoculating earthworms, which might be especially beneficial for promoting dissipation of PAHs compounds containing more benzene rings.

Plant-earthworm-aboriginal Microbe Interactive System for Removal of PAHs in Soils

The orthogonal design with L16 (45) in pot-test was used to investigate the effect of three kinds of environmental factors (soil moisture, humus content and earthworms activity) on the removal of PAHs in soils with their initial concentrations ranging 20.05 to 322.06 $mg \cdot kg^{-1}$. The results indicated that growth status of plant root system played an important role in the phytoremediation process, and the removal rate of PAHs was significantly and positively correlated to root weight per plant. In addition to imposing a direct impact on soil properties, environmental conditions (moisture content, humus content, earthworm activity) also further promoted the extent of removal of PAHs by improving the growth status of plant root system in soil. Among all the environmental factors monitored, the moisture content was tested as the dominant factor influencing the dissipation of PAHs in soils. The following was the utilization of earthworm, while the humus content did a relatively small contribution. Results from this study suggested that in an appropriate environmental conditions, the utilization of the interactive system, composed of plant, earthworm and indigenous microbe, is feasible to achieve the ecological remediation of PAH-contaminated environments.

References

Fismes J, Perrin-Ganier C, Empereur-Bissoneet P (2002) Soil-to-root transfer and translocation of polycyclic aromatic hydrocarbons by vegetables grown on industrial contaminated soil. J. Environ. Qual. 32: 1649-1656

Jennifer LK, John NK, Huang L, *et al.* (2005) The effect of perennial ryegrass and alfalfa on microbial abundance and diversity in pertroleum contaminated soil. Environ Pollut. 133: 455-465

Jodahl JL, Foster L, Schnoor JL (1997) Effect of hybrid trees on microbial populations important to hazardous waste bioremediation. Environ. Toxicol. Chem. 16:1318-1321

Li XH, Ma LL, Liu XF, *et al.* (2006) c in urban soil from Beijing, China. J. Environ. Sci. 18(5): 944-950

Manoli E, Samara C (1999) Polycyclic aromatic hydrocarbons in natural waters: sources, occurrence and analysis. Trac-Trends Anal. Chem. 18(6): 417-428

Nichol TD (1997) Rhizosphere microbial populations in contaminated soils. Water Air Soil Pollut. 95:165-176

Parrish ZD, Banks MK, Schwab AP (2005) Assessment of contaminant liability during phytoremediation of polycyclic aromatic hydrocarbons impacted soil. Environ. Pollut. 137: 187-197

Ryan JA, Bell RM, Davidson JM, *et al.* (1988) Plant uptake of nonionic organic chemical from soils. Chemosphere 17: 2299-2323

Schwab AP, Banks MK (1998) Adsorption of naphtha alene onto plant roots. J Environ Qual 27:220-224

Tao S, Cui YH, Xu FL, *et al.* (2004) Polycyclic aromatic hydrocarbons (PHAs) in agricultural soil and vegetable from Tianjin. Environ. Sci. Technol. 320:11-24

Xu SY, Chen YX, Wu WX, *et al.* (2006) Enhanced dissipation of phenanthrene and pyrene in spiked soils by combined plants cultivation. Sci. Total. Environ. 363: 206-215

Zhang QZ, Davis LC, Erikson LE (2001) Transport of methyl tert-butyl ether through alfalfa plants. Environ Sci. Technol. 35:725-731

The Contribution of Rhizosphere to Remediation of Polycyclic Aromatic Hydrocarbons (PAHs) and Their Toxicity in Soil: Evaluating with Sequential Extraction and Toxicity Risk

Bin Ma, Huaihai Chen, Yan He*, Jianming Xu*

Zhejiang Provincial Key Laboratory of Subtropical Soil and Plant Nutrition,
College of Environmental and Natural Resource Sciences, Zhejiang University, Hangzhou 310029, China.
*Corresponding author. Tel. No. +86-571 8697 1955; Fax No. +86-571 8697 1955;
E-mail: yhe2006@zju.edu.cn and jmxu@zju.edu.cn.

Abstract: To investigate the effects of rhizosphere process on PAHs bioavailability, a sequential solvent extraction experiment was implemented to identify extractable and non-extractable PAHs in rhizosphere and bulk soils of horsebean. The results showed that the primary fraction was methylene chloride (DCM)-extracted and crude-humin-bound PAHs among extractable and non-extractable fractions, respectively. The proportions of sum toxicity concentrations of DCM-extracted fraction decreased sharply in rhizosphere. The partial least square regression model indicated that the partition tendency of PAHs to plant tissues was similar with that to organic C-enriched humin. The contribution of absorption of plant to PAHs remediation, however, can be neglected comparing with that of soil. In conclusion, rhizosphere poses a vital contribution to PAHs remediation in soil, especially when evaluating with toxicity risk.

Keywords: Non-extractable PAHs; Rhizoremediation; Sequential solvent extraction; Toxicity equivalence factors (TEFs)

Introduction

The sorption of polycyclic aromatic hydrocarbons (PAHs) to soil is an important process controlling their bioavailability and toxicity. PAHs that persist in soil would exhibit declining extractability and bioavailability to organisms with increasing contact time (Northcott and Jones, 2001). Phytoremediation is now considered as the most promising remediation way for PAHs in soil. Rhizosphere process, therefore, dominates the phytoremediation through interactions with microorganisms and absorption of root directly (Mackova *et al.*, 2006). The fate of PAHs in rhizosphere is expected distinct with bulk soil as the bioavailability of PAHs would be significantly different. Up to date, however, the discrepancy has been masked by the exhaustible extraction procedures which used single organic solvent as extractant when studying phytoreme-diation as in most previous studies (Oleszczuk, 2009).

In the present study, we sequentially extracted PAHs in soils using various organic solvents with contrasting extraction capacity. Then the non-extractable PAHs bound to humic acid, crude humin, and organic C-enriched humin were extracted. Toxicity equivalence factors (TEFs) were used to convert PAHs concentrations into toxicity concentrations. A unique feature of this study is the simultaneous application of sequentially extractable and non-extractable fractions of PAHs in soil for determining the contribution of rhizosphere to PAHs phytoremediation.

Materials and Methods

Sampling of Rhizosphere Soils

Soil samples were collected from areas closed to a forge workshop which would generate PAHs pollution to the surrounding due to coal combustion. A plot

was chosen with horsebean growing. Rhizosphere samples were collected by removing the soil adhering to the plant roots. The soils collected by shaking were treated as bulk soils. Soils and plants tissues were freeze-dried and passed through a 2-mm sieve.

Sequential Solvent Extraction of PAHs from Soils

The 2 g (dry weight) of soil was extracted with methanol/ water mixture (1:1, V:V) in 50-mL centrifuge tubes. The supernatant was carefully removed and purified with silicar gel SPE cartridge (0.5 g, 6 mL, Alllabware, China). The PAHs were eluted from the sorbent with 8 mL of methylene chloride (DCM), and dried under N_2. The resulting PAHs were re-dissolved by n-hexane, and then identified by GC-MS. The centrifuged soil pellet was sequentially shaken with n-butanol for 24 h and then centrifuged. The supernatant was carefully removed, and the following extracting procedures were implemented as described above. The soils remaining in the centrifuge tubes were continuously ultrasonic extracted for 0.5 h twice using DCM. The seperation, purification and identification of these PAHs fractions were implemented as the same procedures described above.

Investigation into Solvent Non-extractable PAHs Residues

Humic-acid-bound PAHs were extracted with NaOH for 12 h. The supernatant was acidified to pH 1 using HCl. The suspension was extracted for 3~4 times with DCM. The collected DCM was purified with the silicar gel SPE cartridge. Crude-humin-bound PAHs was extracted with methanol, methanol/DCM mixture (1:1, V:V),and DCM twice step by step in an ultrasonic bath. All extractions were combined and distilled water was added. The organic solvent phase of DCM was collected and purified with SPE cartridge as the above procedures. PAHs bound within organic-C-enriched humin were extracted as below. The crude humin was treated with HCl and HF:HCl (1:1) successively, followed by the rinse in HCl. After treatment by HCl and HF, the sample was defined as organic-C-enriched humin. The organic-C-enriched humin was then ultrasonic extracted twice using 100 mL methanol. Acid extracting solutions and organic solvent extracting solution were combined and extracted with DCM three times. The resulting liquids were purified with the SPE cartridge as described above.

Extraction of PAHs from Plant Tissues

Plant tissues were dried at 105 ℃ overnight. They were grinded and extracted with 50 mL of toluene for 2 h in an ultrasonic bath. The toluene was evaporated in a rotary evaporator at 60 ℃. The residue was then treated with 50 mL of 1 $mol \cdot L^{-1}$ KOH in 1:4 methanol–water mixtures (V:V) for 60 min at ca. 60 ℃. The 50 mL saponified solutions were deposited onto the SPE cartridge, and then washed by 10 mL of water to remove interferences. The remaining water in the cartridges was removed by vacuum aspiration. The PAHs were eluted from the sorbent with 8 mL of methylene chloride, and the extracts were dried with anhydrous Na_2SO_4.

Results and Discussion

The profiles of sequential extraction fractions were different between rhizosphere and bulk soils (Fig.1(a)). Although the primary fraction was DCM extracted and crude-humin-bound PAHs among extractable and non-extractable PAHs in both soils, respectively, the concentrations and proportions of these two fractions in rhizosphere soil were significantly lower than those in bulk soils (p<0.05). Additionally, the sum concen-trations of ten PAHs in rhizosphere were significantly lower than those in bulk soils. However, the sum concentrations of 10 PAHs in either root or shoot were extremely low, accounting for only about 5% of the total PAHs in soil. These results emphasized the vital contribution of rhizosphere to PAHs remediation in soil. The relative invariability of both methanol and n-butanol extracted fractions indicated that desorption of PAHs from DCM extraction fraction in rhizosphere maintained at stable concentrations of these two fractions. The unchangeability of non-extractable PAHs residues between rhizosphere and bulk soils, however, demonstrated low bioavailability of these fractions. The results also revealed the less contribution of plant absorption to PAHs remediation in soil.

In order to evaluate the toxicity risk of soils polluted by PAHs, toxicity equivalence factors (TEFs) were employed to convert the PAHs concentrations to toxicity concentrations based on the relative carcinogenic potential of other PAHs to Benzo[a]pyrene (B[a]P) (Nisbet and LaGoy, 1992).

Interestingly, the profiles of sequential extraction fractions in rhizosphere were remarkable changed contrasted to the profiles in bulk soils (Fig.1(b)). The proportions of sum toxicity concentrations of crude-humin-bound PAHs were significantly lower in both rhizosphere and bulk soils compared with the sum concentrations of PAHs. The proportions of sum toxicity concentra-tions of DCM-extracted fraction were, however, just sharply decreased in rhizosphere.

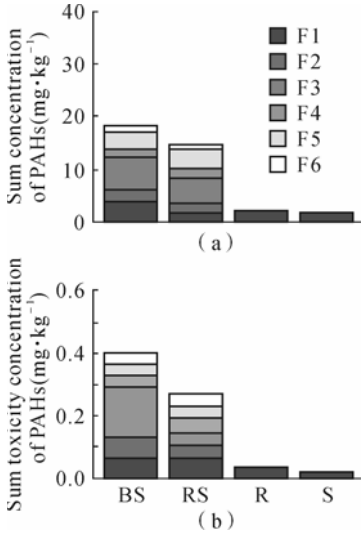

Fig. 1 Sum concentrations and B[a]P equivalent concentrations of 10 PAHs in soils and plant tissues. BS-bulk soil; RS-rhizosphere soil; R-root; S-shoot. The bar fragments from below to above indicate the sequential extraction fractions; F1, methanol/water extracted fraction; F2, n-butanol exracted fraction; F3, DCM-extracted fraction; F4, humic-acid-bound PAHs; F5, crude-humin-bound PAHs; F6, organic-C-enriched-humin-bound PAHs

Among ten PAHs, the TEFs of B[a]A, anthracene and chrysene were 0.1, 0.01 and 0.01, respectively. The TEFs of other seven PAHs were all 0.001. The decreased proportions of toxicity concentrations compared with the sum concentrations of corresponding PAHs fractions indicated that the proportions of B[a]A, anthracene and chrysene in DCM-extracted fraction in rhizosphere were significantly lower than those in bulk soils. This revealed a new benefit in soil rhizo-remediation that the toxicity of PAHs in soil could decrease even faster than the concentrations of PAHs. This might be caused by the differences in physical, chemical, and biological characteristics between bulk soil and rhizosphere, and the differences in soil organic matter compositions, which could affect the partition pattern of PAHs. Additionally, the proportions of B[a]A, anthracene and chrysene were lower in crude-humin-bound PAHs pool than those in other non-extractable PAHs residues in both rhizosphere and bulk soils.

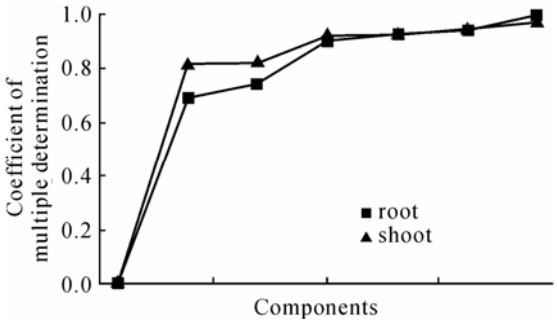

Fig. 2 The coefficient of multiple determination of partial least square regression

Partial least square regression showed that ten PAHs either in root or shoot were dramatically related with component one in all models (Fig. 2). The loading matrices of all four models (data not shown) indicated that the PAHs bound within organic-C-enriched humin contributed to the component one. This indicates the similar partition characteristics of PAHs to plant tissues and organic-C-enriched humin.

In conclusion, horsebean rhizosphere poses a vital contribution to PAHs remediation in soil, especially when evaluating with toxicity risk. The contribution of plant absorption is relatively low. PAHs may pose similar partition coefficient to plant tissues and organic-C- enriched humin.

Acknowledgements

This work was jointly supported by the National High Technology Research and Development Program of China (863 Program, 2007AA061101), the National Natural Science Foundation of China (20707020, 40671092), and the Key Science and Technology Projects of Zhejiang Province (2008C13024-3).

Reference

Mackova M, Dowling DN, Macek T (2006) Phytoremediation and Rhizoremediation. Springer, Dordrecht

Nisbet C, LaGoy P (1992) Toxic equivalency factors

(TEFs) for polycyclic aromatic hydrocarbons (PAHs). Regul. Toxicol. Pharm. 16: 290-300

Northcott G, Jones K (2001) Partitioning, extractability, and formation of nonextractable PAH residues in soils. 1. Compound differences in aging and sequestration. Environ. Sci. Technol. 35: 1103-1110

Oleszczuk P (2009) Application of three methods used for the evalution of polycyclic aromatic hydrocarbons (PAHs) bioaccessibility for sewage sludge composting. Bioresource Technol. 100: 413-420

Spectral Studies of the Toxin of *Bt* Adsorbed by Minerals

Qingling Fu[a], Hongqing Hu[a], Shouwen Chen[a], Li Huang[a], Qiaoyun Huang[a,*], Tongmin Sa[b]

[a] Key Laboratory of Subtropical Agricultural Resources and Environment, Ministry of Agriculture, Huazhong Agricultural University, Wuhan, 430070, China;
[b] Department of Agricultural Chemistry, College of Agriculture, Chungbuk National University, Cheongju, 361-763, R.O. Korea.
[*]Corresponding author. Tel. No. 86 27 62058679; Fax No. 86 27 87288618; E-mail: hqhu@mail.hzau.edu.cn.

Abstract: The persistence of the toxin of *Bacillus thuringiensis* (*Bt*) may constitute risk to the soil ecosystem, and toxin structure in soils could affect their persistence, insecticidal activity, and decomposition. The structural changes of *Bt* toxin during adsorption and desorption on montmorillonite, kaolinite, goethite and silicon dioxide were investigated by infrared spectroscopy (IR) and fluorescence spectroscopy. A comparison between the IR spectra of native toxin and toxin-mineral complexes indicated no obvious structural changes appeared, and the C-N radicel played a key role on the adsorption of the toxin by minerals. Fluorescence spectroscopy showed that two fluorescence peaks of the *Bt* toxin were at 338 nm and 314.5 nm by the excitation at 282 nm, which attributed to tryptophan and tyrosine residues, respectively. The maximum fluorescence emission (λ_{em}, 338 nm) of *Bt* toxin desorbed from kaolinite and montmorillonite were red-shifted 5 nm and 9.5 nm, respectively, while λ_{em} of *Bt* toxin desorbed from goethite and silicon dioxide did not shift obviously. This investigation may help evaluate the behavior and fate of *Bt* toxins in the soil ecosystem.

Keywords: Adsorption; *Bt* toxin; Fluorescence spectroscopy; Infrared spectroscopy; Minerals

Introduction

The *Bacillus thuringiensis* (*Bt*) toxin can be introduced into soil from the pollen, plant biomass and root exudates of *Bt*-transformed crops. The toxin can be adsorbed rapidly to clay minerals, soil humic acids, and organo-mineral complexes (Stotzky, 2000). The adsorption or desorption of *Bt* toxin to minerals usually produces a change in physicochemical properties, which could be strongly influenced by changes in toxin structure (Norde and Giacomelli, 2000). The objective of this work was to investigate the structural changes of *Bt* toxin adsorbed on montmorillonite (Mont), kaolinite (Kaol), goethite (Goet) and silicon dioxide (SiO_2) by infrared spectroscopy (IR), and changes induced by desorption process using fluorescence spectroscopy.

Materials and Methods

The *Bt* toxin and minerals were prepared as described by Fu *et al.* (2007). The toxin and the stock mineral suspensions were dissolved in Na_2HPO_4-NaH_2PO_4 buffer (pH 7.0). Stoppered polyethylene test tubes, containing mixtures of minerals and toxins, were shaken end-over-end (using a rocking device) at 200 $r \cdot min^{-1}$ and 25±1 ℃ for 2 h, and centrifuged at 16,000 g for 15 min. The toxin-mineral complexes in the sediment were collected for spectroscopy studies. Control experiments were performed with the minerals, but without the toxin. Toxin adsorption on the walls of the test tubes was negligible as assessed by control tubes containing the toxin, but without the minerals.

A portion of the toxin-mineral complexes and native toxins were lyophilized and examined by IR

spectroscopy. Other samples of the toxin-mineral com-lexes were desorbed using 2 mL 0.01 mol·L^{-1} Na_2HPO_4-NaH_2PO_4 (pH 7.0) buffer. The concentrations of desorbed toxin were measured by the Lowery method and the solution was measured by fluorescence spectroscopy.

A Jasco FP-6500 spectrofluorometer (Jasco, Tokyo, Japan) was used to collect fluorescence spectra from 300 to 450 nm using an exciting wavelength of 282 nm and a slit width of 5 nm. An Avatar-330 spectrometer (Thermo Nicolet Corp., Madison, USA) with a resolution of 2 cm^{-1} was used to collect IR scans from 400 to 4000 cm^{-1} for samples of adsorbed *Bt* toxin. The KBr pellets were prepared by well blending KBr with dried *Bt* toxin, minerals or toxin-mineral com-lexes. All spectra were subtracted from background scans of an empty cell in order to eliminate the influences of water vapor and carbon dioxide in the air.

Results and Discussion

The IR spectra of the native *Bt* toxin based on the deconvolution were identified at 669, 1055, 1240, 1402, 1456, 1543, 1653, 2362, 2926, 2962 and 3672 cm^{-1} (Fig. 1(a)). The 1653 cm^{-1} and 1543 cm^{-1} components were ascribed to the COO^- or C-O stretching in the Amide Ⅰ and Amide Ⅱ of the *Bt* toxin, respectively, and the 1456 cm^{-1} component was attributed to the COO^- and C-N motion. The 1402 cm^{-1} and 1240 cm^{-1} components were assigned to bending vibration of the N-H chains and stretching vibration of C-N chains in the amide IV and the amide V of the *Bt* toxin, respectively. The 669, 2926, and 2963 cm^{-1} components were due to the stretching vibration of C-H, the 1055 cm^{-1} component was the result of the C-O or C-N motion, and the stretching vibration of C≡N and O-H induced the 2362 cm^{-1} and 3672 cm^{-1} components, respectively.

IR Spectroscopy of Bt Toxin

Comparing the IR spectra of Mont and Bt toxin-Mont complex, several special bands of the complexes appeared at 1402, 1541, 1653, 2362 and 2960 cm^{-1} (Fig. 1(b)). Although the 1653 cm^{-1} band was very close to the water 1639 cm^{-1} band in the untreated Mont sample, the unobvious shifted amide bands (less than 2 cm^{-1}) of *Bt* toxin suggested that the toxin bonded to Mont without obvious structure changes. Several infrared bands of the complexes disappeared comparison to the native toxin, such as 1055, 1240, and 1456 cm^{-1}, which were all attributed to the C-N motion, suggesting that the C-N radicel played a key role on the adsorption of *Bt* toxin by Mont.

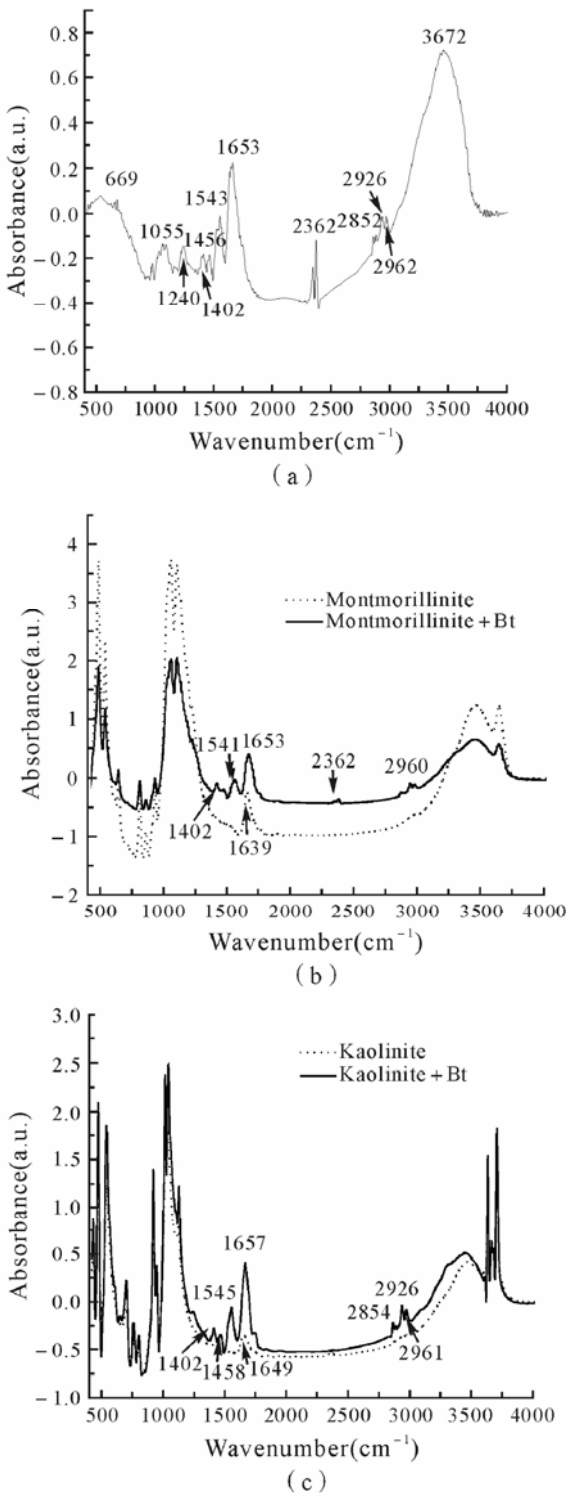

Fig. 1 IR spectra of *Bt* toxin and *Bt*-mineral complex based on deconvolution

The 1458, 1545, and 1657 cm^{-1} bands of the toxin-Kaol complexes were red-shifted less than 4 cm^{-1} comparison to the native toxin, and the 1055, 1240, and 2362 cm^{-1} bands gone after the toxin adsorbed on Kaol (Fig. 1(c)), the changes in the infrared spectra showed the same conclusions as that from Mont. To the other two tested minerals (Goet and SiO_2), expect more infrared bands of the toxin-Goet complexes disappearance, the same results could be achieved by a comparison between the IR spectra of native toxin and toxin-mineral complexes (data not shown).

The Fluorescence Spectra of Bt Toxin

The 338 nm maximum fluorescence emission peak of the native *Bt* toxin in phosphate buffer was tryptophan residues' peak. Additionally, the *Bt* toxin emission spectrum had another emission peak at 314.5 nm of the tyrosine residues (Fig. 2).

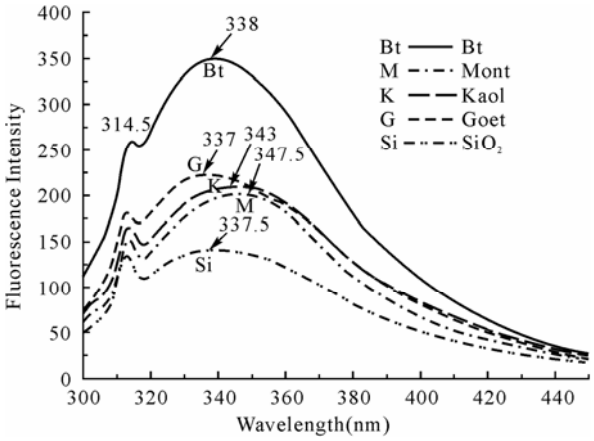

Fig. 2 The fluorescence spectra of *Bt* toxin

The maximum fluorescence emission peaks of *Bt* toxin desorbed from Kaol and Mont were at 343 nm and 347.5 nm, respectively, which were red-shifted 5 nm and 9.5 nm in comparison to the native toxin. However, their tyrosine peak remained at 314.5 nm without shift (Fig. 2). The tryptophan peak was at 337 nm and 337.5 nm, respectively, for *Bt* toxin desorbed from Goet and SiO_2 and the tyrosine peak was at 313 nm for both minerals (Fig. 2). The small fluorescence peak blue-shift for *Bt* toxin desorbed from Goet and SiO_2 suggest little changes appeared in toxin microenviro-ment. However, the desorption of *Bt* toxin from Mont and Kaol induced a greater polarity of the microenvironment (Mallick *et al.*, 2003) and the enhancement by Mont was greater than that Kaol.

Conclusions

The polarity of the *Bt* toxin microenvironment after desorption from Kaol and Mont increased, but no obvious changes in polarity was observed for *Bt* toxin adsorbed and desorbed from Goet and SiO_2. However, the IR spectra indicated no obvious difference in the structure between the native toxin and the toxin in toxin-minerals complexes.

References

Fu QL, Dong YJ, Hu HQ, Huang QY (2007) Dsorption of the insecticidal protein of Bacillus thuringiensis subsp. kurstaki by soil minerals: Effects of organic acid ligands, Appl. Clay Sci. 37: 201-206

Mallick A, Maity S, Haldar B, Purkayastha P, Chattopadhyay N (2003) Photophysics of 3-acetyl-4-oxo-6,7-dihydro-12H indolo-[2,3-a] quinolozine: emission from two states, Chem. Phys. Lett. 371: 688-693

Norde W, Giacomelli CE (2000) BSA structural changes during homomolecular exchange between the adsorbed and the dissolved states, J. Biotechnol. 79: 259-268

Stotzky G (2000) Persistence and biological activity in soil of insecticidal proteins from Bacillus thuringiensis and of bacterial DNA bound on clays and humic acids, J. Environ. Qual. 29: 691-705

Genotypic Differences in Responses of Wheat (*Triticum durum*) Roots to Oxytetracycline

Zhaojun Li[a], Xiaoyu Xie[a], Alin Song[a], Ruihuan Qi[a], Fenliang Fan[a], Yongchao Liang[a,b,*]

[a] Ministry of Agriculture Key Laboratory of Crop Nutrition and Fertilization, Institute of Agricultural Resources and Regional Planning, Chinese Academy of Agricultural Sciences, Beijing 100081, China;
[b] Key Laboratory of Oasis Eco-Agriculture and College of Agriculture, Shihezi University, Shihezi 832003, China.
[*]Corresponding author. Tel. No. +86-10 8210 8657; Fax No. +86-10 8210 8657; E-mail: ycliang@caas.ac.cn.

Abstract: A pair of oxytetracycline (OTC)-sensitive (cv. Heyou 1) and OTC-tolerant (cv.Yannong 21) wheat (*Triticum durum* L.) was grown hydroponically to investigate the effects of OTC on morphologic characteristics and loss of membrane integrity of roots. The number, total length, total surface area, and total volume of roots of both tested wheat cultivars were significantly decreased by OTC. The number of roots was more sensitive to OTC than other indicators such as total length, total surface area, and total volume of roots. The inhibitory effect of OTC on root growth was larger in the sensitive cultivar than in the tolerant. The number and the total surface areas of roots were decreased by 89.6% and 75.9% respectively for sensitive cultivar, and only 87.5% and 68.7% respectively for tolerant cultivar. The cell membrane of Yannong 21 roots was more integrative, and was less oxidative damage than Heyou 1 under the stress of OTC. These results suggested that OTC is toxic to wheat, being similar to other organic pollutants such as herbicides. The root number could be taken as the indicator to predict the risk of OTC to plants at the early stage. The risks of OTC to agriculture would be alleviated through planting the OTC-tolerant wheat cultivars in the OTC-contaminated soils.

Keywords: Oxytetracycline (OTC); Wheat; Root morphologic characters; Loss of membrane integrity

Introduction

Oxytetracycline is one of the tetracyclines (TCs), a group of structurally-related antibiotics used to treat bacterial infectious and accounting for about 66% of the total consumption of antibiotics in recent years (Chopra and Roberts, 2001). Residues of TCs have already been discovered in soil environments (Simon, 2005). More and more scientists postulated that TCs have a strong potential ecological risk based on the hazard quotients (HQs) of TCs (Park and Choi, 2008). The objective of the present paper was to investigate the different effects of oxytetracycline on wheat root growth including morphologic characters and loss of membrane integrity of wheat root in the early period.

Materials and Methods

Plants were grown in 3-liter PVC pots under environmentally-controlled conditions with a photoperiod of 14h, a light intensity of 400 $\mu mol \cdot m^{-2} \cdot s^{-1}$ and temperatures of 25 ℃ /20 ℃ (day/night). Two contrasting wheat (*Triticum durum* L.) cultivars were used in the present study, cv. Heyou 1, a sensitive cultivar and cv. Yannong 21, a tolerant cultivar. Wheat seeds were surface sterilized in 1% (v/v) NaOCl for 15 min, rinsed, and soaked in distilled water for 24 h at 33 ℃ in dark, and then sown in plastic trays containing acid-washed and sterilized quartz sand. After 1 week, uniform-sized seedlings were transplanted into a 3-liter-plastic-container filled with 1/2-strength Hoagland nutrient solution. After one week, OTC was fed to plants by

amending the full-strength nutrient solution with 0.00 (control), 0.01, 0.02, 0.04, and 0.08 mmol·L^{-1}. The control plants were continuously fed with the full-strength Hoagland nutrient solution. The solution was renewed daily to protect OTC from degradation during the entire period of experiment. At the seedling stage of wheat (14 days after OTC application), dry weight, morphological characteristics of root, and loss of membrane integrity were investigated. Morphological characteristics of wheat root like root number, total length, total surface area, and total volume of roots were scanned by root scanner after wheat roots were rinsed carefully with tap water. The root pictures got from scanner were analyzed with WinRHIZO Reg 2002c software. Histochemical detection of loss of plasma membrane integrity in roots was performed by Evans blue (Wang and Yang, 2005). Histochemical detection of lipid peroxidation was performed as described by Pompella *et al.* (1987). All of the roots that stained with the specific reagents as indicated above were washed three times with sufficient volume of distilled water, observed under a light microscope (model: SZX12, Olympus in Japan) and photographed.

Results and Discussion

Effects of OTC on Morphological Characteristics of Wheat Roots

The number, total surface area, total length, and total volume of both wheat roots decreased with increasing concentrations of OTC (Fig. 1). Effects of OTC on the number of roots were higher than those on other tested indicators. For example, the decreased percentages of the root number ranged from 44.9% to 89.6% at the tested levels of OTC, however, the corresponding data were only 26.8% to 80.6% for the total length, 23.9% to 75.9% for total surface area, and 21.1% to 68.8% for total volume, respectively. It was also found that effects of OTC on Heyou 1 were much stronger than that on Yannong 21. For example, effects of OTC decreased the number and the total surface areas of roots by 89.6% and 75.9% respectively for Heyou 1, but only 87.5% and 68.7% respectively for Yannong 21. It indicated that OTC

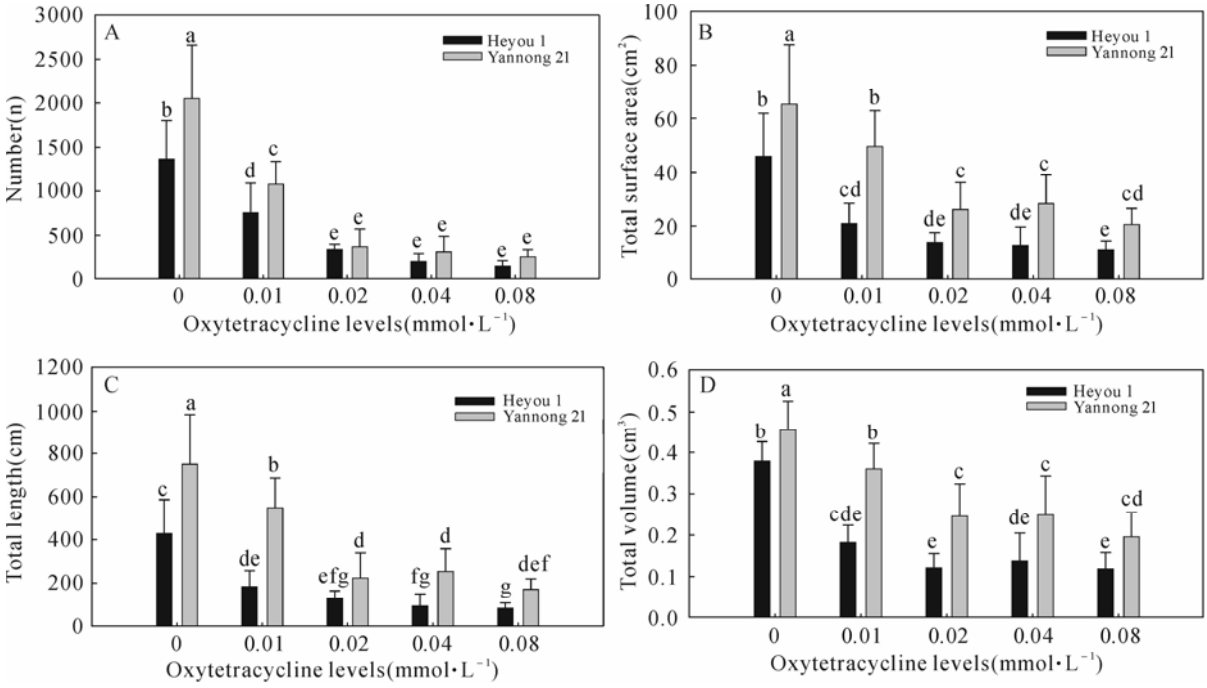

Fig. 1 Effects of OTC on wheat root growth. Roots were scanned with root scanner on 28 days after oxytetracycline application. A, B, C, D, and E indicate the number, total surface area, total length, and total volume of roots of Heyou 1, and Yannong 21 stressed by OTC at levels of 0, 0.01, 0.02, 0.04, 0.08 mmol·L^{-1}, respectively. Bars are the standard error of means of three replications; lowercase letters indicate significant difference at the level of 5%

was toxic to wheat, a non-target organism for OTC, which was similar to other organic pollutants such as herbicides (Li *et al.*, 2005). The number of wheat roots was more sensitive than other tested root indicators and thus could be taken as the senstive indicator to predicate the risk of OTC pollution at early stage of wheat growth.

Oxidative Damage in Wheat Roots Stressed by OTC

To investigate oxidative damage of OTC to wheat roots, the experiment was performed with histochemical staining with Evans blue and Schiff's reagent (Fig. 2 A, B, C, and D). The Evans blue was applied to determine the loss of plasma membrane integrity and the Schiff's reagent was applied to determine the degree of peroxidation of membrane lipids (Wang and Yang, 2005). For both wheat cultivars, the roots treated with five levels of OTC were stained to different extents, and under the higher OTC treatment (from 0.02 mmol·L^{-1} to 0.08 mmol·L^{-1}) the roots were stained extensively. At the same level of OTC, the roots of Yannong 21 were less strained than those of Heyou 1. For example, when the level of OTC was 0.02 mmol·L^{-1}, the root of Heyou 1 was stained significantly heavier than Yannong 21 (Fig. 2, C and D). This phenomena was also observed in Evans blue staining result (Fig. 2, A and B). It indicated that the cell membrane of Yannong 21 roots was more integrative, and was less oxidative damage than Heyou 1 under the stress of OTC at the same level. This maybe contribute to the more tolerance of Yannong 21 to OTC as compared with Heyou 1.

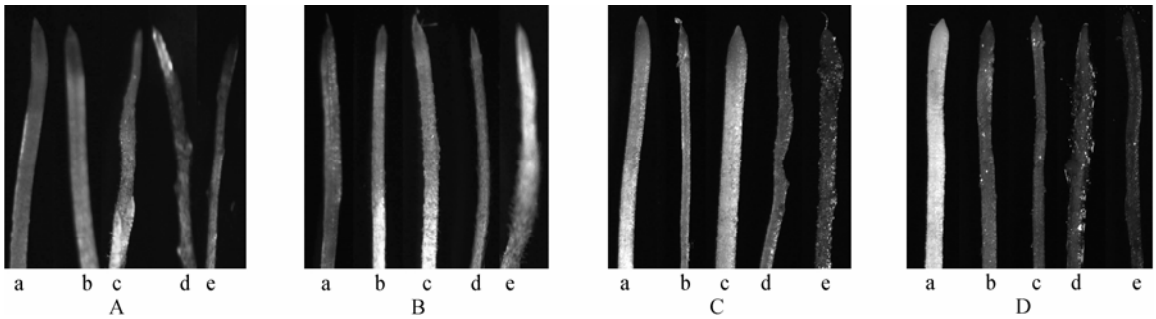

Fig. 2 Effect of the OTC on loss of plasma membrane integrity (A (Heyou 1), B (Yannong 21)) and lipid peroxidation (C (Heyou 1), D (Yannong 21)) in the root tips of wheat. Seedlings were treated with OTC for 14 days. Afterwards, the roots were rinsed with 0.5 mmol·L^{-1} $CaCl_2$ (pH 4.5) solution and were stained with Evans blue (A, B) or Schiff's reagent (C, D), and immediately photographed under a light microscope. The scale bar in the graph indicates 0.5 cm. a, b, c, d, and e indicate wheat plants treated with OTC at levels of 0, 0.01, 0.02, 0.04 and 0.08 mmol·L^{-1}, respectively

References

Chopra I, Roberts M (2001) Tetracycline antibiotics: mode of action, applications, molecular biology, and epidemiology of bacterial resistance. Microbiol. Mol. Biol. Rev. 65: 232-260

Li ZJ, Xu JM, Muhammad A, Ma GR (2005) Effect of bound residues of metsulfuron-methyl in soil on rice growth. Chemosphere 58: 1177-1183

Park S, Choi K (2008) Hazard assessment of commonly used agricultural antibiotics on aquatic ecosystems. Ecotoxicology 17: 526-538

Pompella A, Maellaro E, Casini AF, Comporti M (1987) Histochemical detection of lipid peroxidation in the liver of bromobenzene-poisoned mice. Am. J. Pathol. 129: 295-301

Simon NS (2005) Loosely bound oxytetracycline in riverine sediments from two tributaries of the Chesapeake Bay. Environ. Sci. Technol. 39: 3480-3487

Wang YS, Yang ZM (2005) Nitric oxide reduces aluminum toxicity by preventing oxidative stress in the roots of *Cassia tora* L. Plant Cell Physiol. 46: 1915-1923

Dynamics of Dissolved Organic Carbon in the Rhizosphere of Ryegrass (*Lolium multiflorum* L.) Induced by PCBs Pollution

Na Ding, Malik Tahir Hayat, Yan He, Haizhen Wang, Jianming Xu*

Zhejiang Provincial Key Laboratory of Subtropical Soil and Plant Nutrition,
College of Environmental and Natural Resource Sciences, Zhejiang University, Hangzhou 310029, China.
*Corresponding author. Tel. No. +86-571 8697 1955; Fax No. +86-571 8697 1955; E-mail: jmxu@zju.edu.cn.

Abstract: The objective of this study was to examine ryegrass for phytoremediation of polychlorinated biphenyls (PCBs)-contaminated soils. A rhizobox was designed to allow the harvest of an intact layer of rhizosphere soil from plant root without the removal of the root material itself. Ryegrass was grown under controlled conditions in rhizobox for 45, 90 and 135 days. Results indicated that dissipation of PCBs in the rhizosphere were much higher at various layers compared to the no-plant control soils. The DOC concentrations suggested a trend over time. Dissolved organic carbon (DOC) concentrations at 45 days occurred as high as 11.63 $mg \cdot L^{-1}$ in the rhizosphere, then decrease rapidly to 7.86 $mg \cdot L^{-1}$ at 90 days after sowing. Finally, there was no significant change from 90 days to 135 days in DOC concentration. Moreover, dissipation rates of PCBs correlated positively with DOC concentrations at 45 days and 90 days after sowing. In this study, an average 6.8% loss of PCBs occurred due to the biotic activity without ryegrass planted.

Keywords: Polychlorinated biphenyls (PCBs); Degradation; Dissolved organic carbon (DOC); Rhizosphere

Introduction

The rhizosphere is a unique zone around a root characterized by complex biological interactions. Influences of the plant roots that define the rhizosphere are numerous but perhaps chief among these is the input of organic carbon compounds to the soil through exudation by active roots or root senescence and sloughing; the process of rhizodeposition (Villacieros *et al.*, 2003). Plants are able to directly extract and remove many persistent organic pollutants from soil but also produce root exudates (amino acids, simple sugars, flavonones, phenolic compounds, enzymes and other organic materials), which enhance microbial and biochemical activities in the immediate vicinity of the roots (rhizosphere) causing favorable environment for more intensive metabolism of contaminants than in the surrounding bulk soil. More rapid degradation of several xenobiotics in the rhizosphere of plant species/varieties related to the bulk soil was revealed (Liste and Alexander, 2000, Chekol *et al.*, 2004). However, the fate of PCBs in rhizosphere and how they affect the biochemical activities, especially the dissolved organic matter (DOM) which is involved in many soil processes, have not much been studied so far. Special chambers-rhizoboxes proposed by He *et al.* (2005) allow to separate rhizosphere soil compartment from adjacent plant roots and to slice it into thin layers successfully. Our objectives were (1) to investigate degradation process of PCBs in the immediate vicinity of the roots over time depending on the novel design of a rhizobox system and (2) to determine dissolved organic matter (DOM) dynamics in the rhizosphere of ryegrass induced by PCBs pollution.

Materials and Methods

The soil was obtained from the surface layer

(0~20 cm) of cultivated soils in Longyou town of Zhejiang Province, China. The soil was classified as a sandy loam and was identified to be free of Aroclor 1242. Soil pH (1:1 water), total organic C, total N were 4.46, 1.48 g·kg^{-1}, and 0.33 g·kg^{-1}, respectively. The rhizobox used in this experiment was designed in a similar way to those of Wang *et al.* (2002) and He *et al.* (2005). The dimension of the rhizobox was 120 × 110 × 180 (length × width × height in mm). The rhizobox was divided into three sections: a root compartment (RC), or the central zone (20 mm in width), left and right soil compartments, or rhizosphere zones (60 mm in length). 2.5 kg of air-dried soil was mixed thoroughly with Aroclor 1242 and then used to fill the central and rhizosphere compartments. The target concentration of Aroclor 1242 was 16.0 mg·kg^{-1}. The spiked soils were equilibrated in the greenhouse for 10 days at field capacity before seeding with ryegrass. There were three replicates with ryegrass and three unplanted controls, and sampling was conducted at a 45-day intervals. The experiment ran for 135 days. The concentration of PCBs in soils was determined by GC/MS analysis after ultrasonic extraction and subsequent solid phase enrichment. Water-soluble organic carbon was extracted with deionized water from fresh soils using a solid: water ratio of 1:2.5 by shaking 180 r·min^{-1} for 24 h at 20 ℃. The suspensions were centrifuged for 30 min at 10000 × g and filtered through a 0.45-μm cellulose acetate filter. A total organic carbon (TOC) analyzer was used for analyzing the content of water-soluble organic carbon (Ling *et al.*, 2005).

Results and Discussion

Changes in Reduction of Aroclor 1242 Over Time

By Day 45, there was a slight reduction of Aroclor 1242 at various layers with ryegrass planted as compared with the unplanted treatments (Fig. 1). There were no significant differences in Aroclor 1242 depletion among various layers. In the unplanted treatment, there was almost no reduction at each layer. By Day 90, of the two treatments, the planted treatment showed that much higher depletion relative to the unplanted treatment. At 2 mm and 3 mm layers, total removal rates of Aroclor 1242 were higher than in other layers, which were up to 9.86% and 10.67%, respectively. However, in the unplanted soils, the average removal rates at various layers were only 4.0%. Furthermore, there was no significant difference among the layers in the control soils. It seemed that both biodegradation and abiotic process played a role in the dissipation of PCBs during this period. In general, abiotic processes include leachates with irrigation, evaporation, direct plant-uptake and adsorp-tion by soil or organic matter. However, in this study leachates were not a factor in these results since the rhizosphere were maintained at constant moisture, preventing leaching from the bottom. In other words, the growth of young roots might contribute to a reduction of Aroclor 1242. Our results reconciled other reports of plant-enhanced degradation of organic contaminants. The reasons might be that the rhizosphere was a zone of intense microbial activity, which was caused by root exudates containing

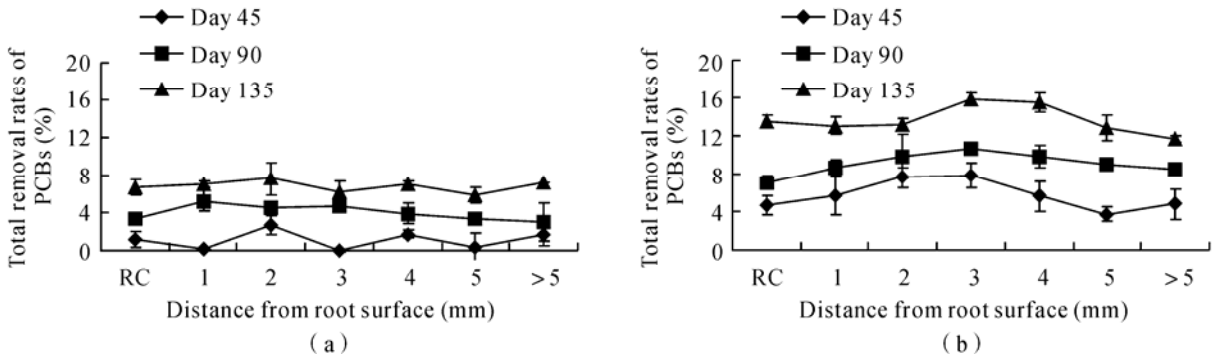

Fig. 1 Total removal rates (%) of Aroclor 1242 in various sampling zones as a function of proximity to ryegrass roots grown in the soil treated with 16.0 mg Aroclor 1242 kg^{-1}. Bars are the standard error of means of three replicates. "RC" indicates the root compartment. (a) Aroclor 1242 total removal rates (%) in the unplanted treatment; (b) Aroclor 1242 total removal rates (%) in the planted treatment

carbohydrates, amino acids and organic acids (Yu *et al.*, 2003, Singh *et al.*, 2004). From Days 90 to 135, removal rates continued to increase at various layers. Reduction at 2 mm and 3 mm layers remained higher than other layers. And the average of total removal rates was up to 13.64%, much higher than dissipation rate (9.07%) which was obtained at day 90. The results are supported by He *et al.* (2005) which noted that the 3 mm layer from the root zone in the rhizobox was the optimumal biodegradation location for pentachloro-phenol. Possibly, root exudates provide substrates for microbial growth to accelerate PCBs degradation. Conversely, root exudates provide a more energy-rich non-PCB source of available carbon and hence are likely to be more favored by the microbial biomass as a substrate than PCBs. Thus the greatest decrease in Aroclor 1242 concentration could be achieved here because 3 mm zone represents balance between microbial activities and availability of root exudates.

Changes in Dissolved Organic Carbon (DOC) Concentrations Over Time

Fig. 2 shows that the mean concentration of DOC in various layers of the planted treatments was 11.63 $mg \cdot kg^{-1}$ at 45 days after sowing. Concentrations of DOC in near-rhizosphere (2, 3, 4 and 5 mm) were higher than at the root compartment (RC, 1 mm) and far-rhizosphere (>5 mm). At 90 days after sowing, DOC concentrations at various layers had significantly decreased to 7.91 $mg \cdot kg^{-1}$ (mean value). From 90 to 135 days after sowing, DOC concentrations hardly changed at corresponding layers (mean value of 7.48 $mg \cdot kg^{-1}$). Whereas DOC concentrations at each layer in the unplanted treatment were significantly lower than at the corresponding layers in the planted treatment after 45 days. Then after 90 and 135 days of sowing, there was no marked change in DOC concentrations compared to those in the first 45 days. Furthermore, there were no remarkable changing trends in DOC concentrations over time in the unplanted treatment.

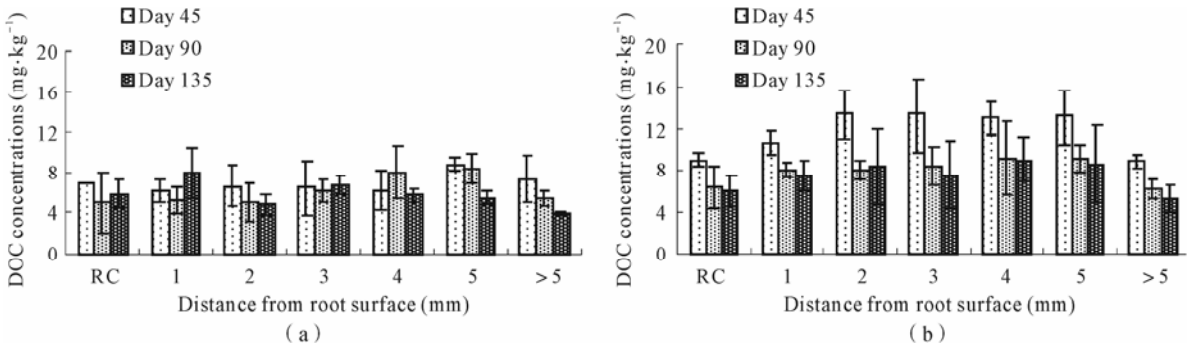

Fig. 2 Concentrations of dissolved organic C (DOC) in various sampling zones as a function of proximity to ryegrass roots grown in the soil treated with 16.0 mg Aroclor 1242 kg^{-1}. Bars are the standard error of means of three replicates. "RC" indicates the root compartment. (a) DOC concentrations in the unplanted treatment; (b) DOC concentrations in the planted treatment

It is likely that plant roots increase the organic carbon content of the soil through exudation of soluble organic matter, and have the potential to increase contaminant absorption and decrease contaminant bioavailability (Banks *et al.*, 2003). Root growth also opens deeper soil to better water infiltration and oxygen diffusion (Singer *et al.*, 2003). According to Banks *et al.* (2003), the fine roots of aggressive plants can disrupt soil aggregates, increase exposed surface area, and enhance biodegradation of entrapped hydro-phobic contaminants. Furthermore, the correlations between DOC and reduction of PCBs were analyzed. The results showed that DOC concentrations at each layer (except the 5-mm layer) had a significant positive correlation with PCBs dissipation at 45 and 90 days after sowing. Whereas there was no significant correlation between DOC concentrations and PCBs dissipation at 135 days after sowing (Fig. 3). It is therefore assumed that dissipation of PCBs in the planted soil is stimulated by the plant roots. In our study, the final reduction of PCBs at 135 days after sowing in the unplanted treatment was 6.80% (mean value). This percentage loss occurred due to biotic activity. However, this loss is relatively small when compared with the planted treatment.

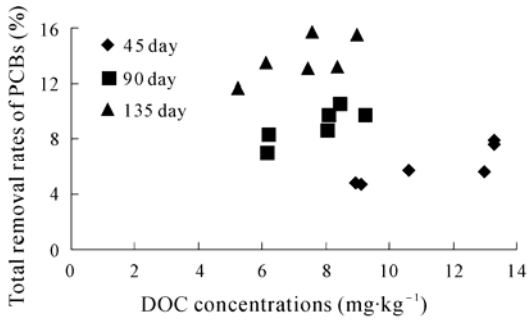

Fig. 3 Relationship between the total removal rates of PCBs and concentrations of DOC in the planted treatment during the 135-day experiment

Acknowledgements

This work was jointly supported by the National Natural Science Foundation of China (40671092), the National Nature Science Foundation for Distinguished Young Scholars of China (40425007), and the Science and Techology Projects of Zhejiang Province (2009C33119).

References

Banks MK, Kulakow P, Schwab AP, Chen Z, Rathbone K (2003) Degradation of crude oil in the rhizosphere of Sorghum bicolor. Int. J. Phytorem. 5: 225-234

Banks MK, Schwab P, Liu B, Kulakow PA, Smith JS, Kim R (2003) The effect of plants on the degradation and toxicity of petroleum contaminants in soil: a field assessment. Adv. Biochem. Eng. Biotechnol. 78: 75-96

Chekol T, Vough LR, Chaney RL (2004) Phytoremediation of polychlorinated biphenyl-contaminated soils: the rhizosphere effect. Environ. Int. 30: 799-804

He Y, Xu JM, Tang CX, Wu YP (2005) Facilitation of pentachlorophenol degradation in the rhizosphere of ryegrass (Lolium perenne L.). Soil Biol. Biochem. 37: 2017-2024

Ling WT, Wang HZ, Xu JM, Gao YZ (2005) Sorption of dissolved organic matter and its effects on the atrazine sorption on soils. J. Environ. Sci. (China) 17: 478-482

Liste HH, Alexander M (2000) Accumulation of phenanthrene and pyrene in rhizosphere soil. Chemosphere 40: 11-14

Singer AC, Smith D, Jury WA, Hathuc K, Crowley DE (2003) Impact of the plant rhizosphere and augmentation on remediation of polychlorinated biphenyl contaminated soil. Environ. Toxicol. Chem. 22: 1998-2004

Singh N, Megharaj M, Kookana RS, Naidu R, Sethunathan N (2004) Atrazine and simazine degradation in Pennisetum rhizosphere. Chemosphere 56: 257-263

Villacieros M, Power B, Sanchez-Contreras M, Lloret J, Oruezabal RI, Martin M, Fernandez-Pinas F, Bonilla I, Whelan C, Dowling DN, Rivilla R (2003) Colonization behaviour of Pseudomonas fluorescens and Sinorhizobium meliloti in the alfalfa (Medicago sativa) rhizosphere. Plant Soil 251: 47-54

Wang ZW, Shan XQ, Zhang SZ (2002) Comparison between fractionation and bioavailability of trace elements in rhizosphere and bulk soils. Chemosphere 46: 1163-1171

Yu YL, Chen YX, Luo YM, Pan XD, He YF, Wong MH (2003) Rapid degradation of butachlor in wheat rhizosphere soil. Chemosphere 50: 771-774

Dynamic Behavior of Persistent Organic Pollutants in Soil and Their Interaction with Organic Matter

Malik Tahir Hayat[a], Jianming Xu[a,*], Na Ding[a], Tariq Mahmood[b]

[a] Zhejiang Provincial Key Laboratory of Subtropical Soil and Plant Nutrition, College of Environmental and Natural Resource Sciences, Zhejiang University, Hangzhou 310029, China;
[b] Department of Environmental Sciences, PMAS-Arid Agriculture University, Rawalpindi Pakistan.
[*]Corresponding author. Tel. No. +86-571 8697 1955; Fax No. +86-571 8697 1955; E-mail: jmxu@zju.edu.cn.

Abstract: Persistent organic pollutants (POPs) pose threat to environment because of their potential for long-range atmospheric transport, bioaccumulation and toxicity. The POPs behave dynamically in the environment according to their nature of action like volatilization, sorption, desorptin and transportation from their source of production to some where. These POPs migrate on air currents from warmer regions of the globe towards the colder Polar Regions. Once they reach colder temperatures they condense, precipitate out, and are deposited again on the earth's surface. Environmental variables like temperature, soil pH, moisture have serious effects on the POPs behavior in the soil. Inorganic minerals also have good interaction with the xenobiotics and play an important role in the transformation of xenobiotics. The manganese and iron oxides and clay minerals (e.g. smectites containing Fe(III)) have well-documented properties to promote the oxidation of a number of organic pollutants. Organic matter is considered the most important factor limiting availability and mobility of POPs in soil and a substantial percentage of the total amount of an organic contaminant applied to a soil may become associated with the humic fraction of that soil. Organic pollutants strongly adsorb to carbonaceous sorbents such as black carbon. In particular, activated charcoal (AC) is known for a strong adsorptive capacity due to its high specific surface area. Adsorption to activated charcoal can render hazardous organic pollutants in soils and sediments less available to organisms and hinder their dispersal into unaffected environments. Some studies also show that some sorbents from natural organic materials, such as peat, soybean stalk and pine needle under superheated temperature/ pressure conditions, for sorption of polycyclic aromatic hydrocarbons (PAHs) in contaminated soils. Natural materials significantly decrease the extractability and bioavailability of PAHs from contaminated soils. Main objective of this review article is to compile some valuable information regarding the existence, dynamic behavior, effect of environmental variables on POPs and their interactions with organic matter.

Keywords: Persistent organic pollutants; Polychlorinated biphenyls; Polycyclic aromatic hydrocarbons; Sorption desorption; Mechanochemical reaction; Organic material

Introduction

Persistent organic pollutants (POPs) are chemical substances that persist in the environment, bioaccumulate through the food web, and pose a risk of causing adverse effects to human health and the environment. The POPs can be divided into three main categories: 1) Pesticides e.g. DDT, 2) Industrial Chemicals e.g. polychlorinated biphenyls (PCBs) & polycyclic aromatic hydrocarbons (PAHs), and 3) Unintentional by products e.g. dioxins, furans. While the risk level varies from POP to POP, by definition all of these chemicals share four properties: 1) they are highly toxic; 2) they are persistent, lasting for years or even decades before degrading into less dangerous forms; and 3) they evaporate and travel long distances through the air and through water, and, 4) They accumulate in fatty tissue.

Three properties of POPs such as persistence, toxicity and bioaccumulativity make POPs highly dangerous. They are, arguably, the most problematic chemicals that natural systems can be exposed to.

For many POPs, the level in fat increases as one animal eats another, so that the highest levels are found in predator animals at the top of food webs. In the arctic food chain this includes predators such as polar bears, seals, toothed whales, birds of prey and humans. Research from numerous countries throughout the world has demonstrated that measurable quantities of POPs are present in human adipose tissue, blood and breast milk, because they are soluble in fats and are not easily broken down in the body.

POPs are of environmental concern because of their potential for long-range atmospheric transport, bioaccumulation and toxicity (Klecka *et al.*, 2000). Encompassing the polychlorinated biphenyls (PCBs) and polycyclic aromatic hydrocarbons (PAHs), POPs display high affinities for soils where they can persist over protracted time frames (years to decades). Persistence of organic pollutants in soils has been attributed to sequestration mechanisms including intra organic matter and intraparticle diffusion of the parent compound and transformation products; contaminant humification to soil organic matter (SOM); low aqueous solubility; and/or microbial recalcitrance (Northcott and Jones, 2000).

There are quite number of organic pollutants exist in the environment and these are gigantic source of pollution difficult to study all these at the same time in this review article we mostly emphasize on some organic pollutants and their effects on the environment shoddily and entery in the environment through industries or unintentional by products such as PCBs and PAHs. This article reviews existence of POPs dynamic behavior in soil, and environmental factor affecting POPs persistence and their interactions with organic matter.

Dynamic Behavior of POPs

POPs behave dynamically in the environment according to their nature of action as they volatilize in the air and cause pollution. Their sorption and desorption strength is very important to study their toxicity levels, some are highly mobile, the transport from their source of production to far away; these are easily distributed in different areas so difficult to control their hazardous effect.

In recent decades, vast numbers of POPs have been produced and used worldwide. Many are still in production and used in everyday products. These chemicals have become widespread environmental pollutants. POPs contaminate local areas close to sites where they are released into the environment from industry and agriculture. However, volatile and semi-volatile POPs also contaminate regions remote from their source, because they can be transported for thousands of kilometers via air currents. These POPs migrate on air currents from warmer regions of the globe towards the colder polar regions. Once they reach colder temperatures they condense, precipitate out, and are deposited again on the earth's surface. POPs may also be transported for long distances by rivers, ocean currents and as contaminants in wildlife.

Sorption is a phase distribution process that accumulates solutes at surfaces and interphases (i.e., adsorption) or from one phase to another (i.e., partitioning). This process is known to affect the transport and reduce chemical and biological reactivity of relatively hydrophobic organic chemicals (HOCs) such as PAHs and chlorinated aliphatic and aromatic compounds in surface aquatic and groundwater systems (Weilin *et al.*, 2003).

It has been widely recognized that the ecotoxicity or biodegradability of POPs like PAHs and PCBs in soils is controlled by the rate and extent of desorption from the solid phase. The sorption strength decreases with increasing residence time of the compounds in soil (Alexander, 2000; Reid *et al.*, 2000) and depends on the nature and quality of the SOM. This is reflected by the wide variation of organic carbon (SOC)–water partition coefficient (KOC) ranging up to three orders of magnitude among different soils (Chiou *et al.*, 1998; Krauss and Wilcke, 2001).

Environmental Factors Affecting POPs Activity in Soil

The application of bioremediation for site decontamination may be further limited by a number of environmental parameters, such as temperature, pH, presence of oxygen, nutrients, moisture and salinity. Soil and groundwater temperatures vary regionally and seasonally. Optimizing these variables in-situ would enhance and maintain remediation of POPs,

most biodegradation studies have been performed at temperatures between 20 ℃ and 30 ℃. Only a limited number of studies have illustrated the biodegradation of PAHs at low temperatures and they generally agree that PAH biodegradation rates and efficiencies are lower at lower temperatures (Eriksson *et al.*, 1999; Phillips *et al.*, 2000; Yuan *et al.*, 2000). Although some studies have shown that a decrease in temperature does not affect PAH biodegradation (Whyte *et al.*, 1997; Mohammed *et al.*, 1998).

Temperature has a significant effect on the growth and physiological activity including uptake and enzymatic dehalogenation of PCB congeners. The influence of temperature is multifaceted. Effects include changes in the adsorption and desorption kinetics of PCB from soil particles, like temperature, pH affects the equilibrium between PCBs that are dissolved and those that are adsorbed to organic matter and thus influences the bioavailability of PCBs in soil (Jota and Hassett, 1991). Moisture levels determine the oxygen content, redox potential, and type of microflora for a soil. The amount of water in soil then has a profound effect on the interactions of humus and xenobiotics. When soils are flooded and, therefore, reduced, dinitroanilines and nitrobenzenes are changed to anilines, which can react with humus (Moza *et al.*, 1979).

Inorganic minerals also have good interactions with the xenobiotics and play an important role in the transformation of xenobiotics. The manganese and iron oxides and some clay minerals have been found to promote the oxidation of a number of organic pollutants (Mortland and Halloran, 1976; Pizzigallo *et al.*, 1995).

The potential capacity of soil abiotic components (oxides, clay minerals, humic substances) to promote the transformation of aromatic molecules, is unexplored for xenobiotics characterised by a very low water solubility like PCBs. Taking into account that the adsorption process represents the first fundamental step of the oxidation reaction, the interaction between the inorganic catalyst and the xenobiotic could be studied by mixing and grinding the two reactants in solid phase. This method called ‘‘mechanochemical’’ and is well known in environmental field and has recently attracted attention in degradation of organo-chlorinated molecules (Loiselle *et al.*, 1997; Nasser *et al.*, 2000; Mio *et al.*, 2002). The treatment provokes a solid-state transformation at the mineral surface without any deformation of the structure. The solid contact of the modified surface with the xenobiotic seems to induce the production of radicals, which are very active in subsequent oxidative coupling reactions. Thus, the ‘‘mechanochemical’’ procedure could furnish a tool to start the reaction between the xenobiotic and the minerals without any interference of organic solvents that should be used in batch experiments to solubilise non-polar compounds. Mechanochemical treatments of soils contaminated with organochlorine molecules were conducted by grinding using a ball mill with different dechlorinating reagents (Loiselle *et al.*, 1997; Aresta and Pastore, 2001; Mio *et al.*, 2002). Few authors provided the information on the mechanochemical technique applied to oxidative reactions. Some researchers (Nasser *et al.*, 2000; Shin *et al.*, 2000) successfully tested the degradation of herbicides such as 2,4-D and atrazine using very gentle grinding of the organic molecules and manganese oxide. The authors advocated that the grinding of a reactive mineral in the presence of adsorbed organic molecules can operate a 1486 Pizzigallo *et al.* (1995) surface alteration of the mineral structure producing structural defects. These defects might produce a chemical activation, which promotes the break-up of chemical bonds and consequently the degradation of chlorinated compounds. Therefore, mechano-chemical treatments provide a way to initiate a reaction between organic compounds and minerals.

This technique could represent an important alternative to more drastic oxidative processes in removing recalcitrant organochlorine compounds from heavily contaminated soils.

POPs Activity in the Presence of Organic Matter

Organic matter is considered as a very important factor that can limit availability and mobility of POPs in soil (Northcott and Jones, 2000), and a substantial percentage of the total amount of an organic contaminant applied to a soil may become associated with the humic fraction of that soil (ranging as much as 20%~90% (Xie *et al.*, 1997; Burauel and Fuhr, 2000). Humic material has been traditionally divided into three operationally defined fractions: 1) fulvic acid 2) humic acid (HA); and 3) humin which is defined as that fraction that is insoluble in an aqueous solution at any pH (Kohl and Rice, 1998). According

to Fabio and Alessandro (2001), the microcosome that received Humic substance (HS) at the 1.5% rate showed a higher persistence of the specialize bacteria and yields of PCB biodegradation and dechlorination about 150% and 100%, respectively, larger than those found for the HS-free microcosms. So it showed that humic substance as well as other humic like product can be of great interest as enhancing agent of PCB bioavailability and biodegradation for soil bioremediation. Kastner and Mahro (1996) also reported that the presence of the solid organic matrix of the compost seemed to be essential for the enhanced degradation PAHs in the soil.

Work showed that PCB bind to humus in the soil environment. The adsorption of PCB has been related to organic matter content and the toxicity of the PCB herbicide Aroclor 1254 decreases in the presence of organic matter (Strek and Weber, 1982a). Moza *et al.* (1979) speculate that PCB's in soil are metabolized to phenols which polymerize to form bound residues. However, it is more commonly accepted that these xenobiotics are bound to humic material noncovalently through charge-transfer complexing, electrostatic attractions, and hydrophobic bonding (Strek and Weber, 1982b). Adsorption increases as the number of chlorine atoms in the PCB molecule increases and is influenced by the position of the chlorine substituent on the biphenyl ring. The 2,4-monochloro isomers and 3,4-dichlorobiphenyl were more likely to bind to organic matter than other biphenyls (Bollag and Loll, 1983) .

Organic pollutants strongly adsorb to carbonaceous sorbents such as black carbon (Bucheli and Gustafsson, 2000; Cornelissen *et al.*, 2006; Koelmans *et al.*, 2006; Ghosh, 2007). In particular, activated charcoal is known for a strong adsorptive capacity due to its high specific surface area (Cornelissen *et al.*, 2005). Adsorption to activated charcoal can render hazardous organic pollutants in soils and sediments less available to organisms (Burgess *et al.*, 2009) and hinder their dispersal into unaffected environments. Tomaszewski *et al.* (2007) added 3.2% of carbon or reactivated carbon to a contaminated sediment (containing up to 252 mg DDT·kg^{-1}) and thereby reduced aqueous equilibrium concentrations up to 83%. In a study by Vasilyeva *et al.* (2001), the addition of 1% of activated carbon to a TNT-contaminated soil reduced the concentrations of extractable TNT (2000 mg·kg^{-1}) and its metabolites by 89% within 120 days. The accelerated removal was attributed to reduced toxicity of the contaminants leading to enhanced microbial degradation.

In situ remediation method to reduce bioavailability of organic pollutants by repartitioning of organic contaminants to carbonaceous sorbents that were mixed with soil to enhance the natural process of contaminant stabilization was proposed by Weber *et al.* (2006). They developed engineered sorbents from natural organic materials, such as peat, soybean stalk and pine needle under superheated temperature/ pressure conditions, for sorption of PAHs in contaminated soils. Both natural and engineered natural materials significantly decreased the extractability and bioavailability of PAHs from contaminated soils (Tang and Weber, 2006; Weber *et al.*, 2006; Tang *et al.*, 2007). Addition of active carbon to sediments affected desorption of PCBs and PAHs (Zimmerman *et al.*, 2004). The bioavailability and bioaccumulation of PCBs were reduced remarkably by activated carbon amendment in both laboratory (Millward *et al.*, 2005) and field (Cho *et al.*, 2007) tests. These works demonstrated clearly the effectiveness of amendments for immobilization of hydrophobic organic contaminants in soil/sediment.

Acknowledgements

This work was jointly supported by the National Natural Science Foundation of China (40671092, 20707020, 40701075), the Key Science and Technology Projects of Zhejiang Province (2008C13024-3), and the Science and Technology Projects of Zhejiang Province (2009C33119).

Reference

Alexander M (2000) Aging bioavailability and overestimation of risk from environmental pollutants. Environ. Sci. Technol. 34: 4259-4265

Aresta M, Pastore T (2001) Abs II European meeting on Environmental Chemistry Digion, 12-15 December, pp. 85

Bollag JM, Loll MJ (1983) Incorporation of xenobiotics into soil humus. Experientia 39: 1221-1231

Bucheli TD, Gustafsson O (2000) Quantification of the soot-water distribution coefficient of PAHs provides mechanistic basis for enhanced sorption

bservations. Environ. Sci. Technol. 34: 5144-5151

Burauel P, Fuhr F (2000) Formation and long-term fate of nonextractable residues in outdoor lysimeter studies. Environ. Pollut.108: 45-52

Burgess RM, Perron MM, Friedman CL, Suuberg EM, Pennell KG, Cantwell MG, Pelletier MC, Ho KT, Serbst JR, Ryba SA (2009) Evaluation of the effects of coal fly ash amendments on the toxicity of a contaminated marine sediment. Environ. Toxicol. Chem. 28: 26-35

Chiou CT, McGroddy SE, Kile DE (1998) Partition characteristics of polycyclic aromatic hydrocarbons on soils and sediments. Environ Sci. Technol. 32: 264-269

Cho YM, Smithenry DW, Ghosh U, Kennedy AJ, Millward RN, Bridges TS, Luthy RG (2007) Field methods for amending marine sediment with activated carbon and assessing treatment effectiveness. Marine Environ. Res. 64: 541-555

Cornelissen G, Breedveld GD, Kalaitzidis S, Christanis K, Kibsgaard A, Oen AMP (2006) Strong sorption of native PAHs to pyrogenic and unburned carbonaceous geosorbents in sediments. Environ. Sci. Technol. 40: 1197-1203

Cornelissen G, Gustafsson O, Bucheli TD, Jonker MTO, Koelmans AA, Van Noort PCM (2005) Extensive sorption of organic compounds to black carbon, coal, and kerogen in sediments and soils: mechanisms and consequences for distribution, bioaccumulation, and biodegradation. Environ. Sci. Technol. 39: 6881-6895

Eriksson M, Dalhammar G, Borg-Karlson AK (1999) Aerobic degradation of a hydrocarbon mixture in a natural uncontaminated potting soil by indigenous microorganisms at 20 ℃ and 6 ℃. Appl. Microbiol. Biot. 51: 532-535

Fabio F, Alessandro P (2001) Effect of Humic Substance on the Bioavailability and aerobic biodegradation of polychlorinaeed biphenyls in a model soil. Biotechnol. Bioeng. 77: 204-221

Ghosh U (2007) The role of black carbon in influencing availability of PAHs in sediments. Human Ecol. Risk Assess. 13: 276-285

Jota MAT, Hassett JP (1991) effect of environmental variable on binding of PCB Congener by dissolved humic substances. Environ. Toxicol. Chem. 10: 483-491

Khstner M, Mahro B (1996) Microbial degradation of polycyclic aromatic hydrocarbonsin soils affected by the organic matrix of compost. Appl Microbiol Biot. 44: 668-675

Klecka G, Boethling B, Franklin J, Graham G, Grady L, Howard P, Kannan K, Larson R, Mackay D, Muir D, van der Meent K (2000) Evaluation of persistence and long-range transport of organic chemicals in the environment. SETAC Special Publication Series: Pensacola, FL

Krauss M, Wilcke W (2001) Predicting soil-water partitioning of polycyclic aromatic hydrocarbons (PAHs) and polychlorinated biphenyls (PCBs) by desorption with methanol-water mixtures at different temperatures. Environ. Sci. Technol. 35: 2319-2325

Koelmans AA, Jonker MTO, Cornelissen G, Bucheli TD, Van Noort PCM, Gustafsson O (2006) Black carbon: the reverse of its dark side. Chemo-sphere 63: 365-377

Kohl SD, Rice JA (1998) The binding of contaminants to humin:a mass balance. Chemosphere 36: 251-261

Loiselle S, Branca M, Mulas G, Cocco G (1997) Selective mechanochemical dehalogenation of chlorobenzenes over calcium hydride. Environ. Sci. Technol. 31: 261-265

Millward RN, Bridges TS, Ghosh U, Zimmerman JR, Luthy RG (2005) Addition of activated carbon to sediments to reduce PCB bioaccumulation by a polychaete (Neanthes arenaceodentata) and an amphipod (Leptocheirus plumulosus). Environ. Sci. Technol. 39: 2880-2887

Mio H, Saeki S, Kano J, Saito F (2002) Estimation of mechanochemical dechlorinated rate of poly (vinyl chloride). Environ. Sci. Technol. 36: 1344-1348

Mohammed S, Sorensen DL, Sims RC, Sims JL (1998) Pentachlorophenol and phenanthrene biodegradation in creosote contaminated aquifer material. Chemosphere 37: 103-111

Mortland MM, Halloran LJ (1976) Polymeri-zation of aromatic molecules on smectite. Soil Sci. Am. J. 40: 367-370

Moza P, Schneunert I, Klein W, Korte F (1979) Studies with 2,4',5-trichlorobiphenyl-14C and 2,2',4,4',6-pentachlorobiphenyl-14C in carrots, sugar beets, and soil. J. Agric. Food Chem. 27: 1120-1124

Nasser A, Sposito G, Cheney MA (2000) Me-chanochemical degradation of 2,4-D adsorbed on synthetic birnessite. Colloids Surf. A 163: 117-123

Northcott GL, Jones KC (2000) Experimental approaches and analytical techniques for determining organic compound residues in soils and sediment. Environ. Pollut 108: 19-43

Reid BJ, Jones KC, Semple KT (2000) Bioavailability of persistent organic pollutants in soils and sediments—a perspective on mechanisms, consequences and assessment. Environ. Pollut. 108: 103-112

Phillips TM, Seech AG, Liu D, Lee H, Trevors JT (2000) Monitor ing biodegradation of creosote in soils using radiolabels, toxicity tests, and chemical analysis. Environ. Toxicol. 15: 99-106

Pizzigallo MDR, Ruggiero P, Crecchio C, Mininni R (1995) Manganese and iron oxides as reactants for oxidation of chlorophenols. Soil Sci. Soc. Am. J. 59: 444-452

Shin JY, Buzgo CM, Cheney MA (2000) Mechanochemical degradation of atrazine adsorbed on four synthetic manganese oxides. Colloids Surf. A 172: 113-123

Strek HJ, Weber JB (1982) Adsorption and reduction in bioactivity of polychlorinated biphenyl (Aroclor 1254) to redroot pigweed by soil organic matter and montmorillonite clay. Soil Sci. Soc. Am. J. 46: 318-322.

Strek HJ, Weber JB (1982) Behavior of polychlorinated biphenyls (PCBs) in soils and plants. Environ. Pollut. A 28: 291-312

Tang J, Petersen EJ, Huang Q, Weber Jr WJ (2007) Development of engineered natural organic sorbents for environmental applications: 3. Reducing PAH mobility and bioavailability in contaminated soil and sediment systems. Environ. Sci. Technol. 41: 2901-2907

Tang J, Weber WJ (2006) Development of engineered natural organic sorbents for environmental applications. 2. Sorption characteristics and capacities with respect to phenanthrene. Environ. Sci. Technol. 40: 1657-1663

Tomaszewski JE, Werner D, Luthy RG (2007) Activated carbon amendment as a treatment for residual DDT in sediment froma superfund site in San Francisco Bay, Richmond, California, USA. Environ. Toxicol. Chem. 26: 2143-2150

Vasilyeva GK, Kreslavski VD, Oh BT, Shea PJ (2001) Potential of activated carbon to decrease 2,4,6-trinitrotoluene toxicity and accelerate soil decontamination. Environ. Toxicol. Chem. 20: 965-971

Weber WJ, Tang J, Huang Q (2006) Development of engineered natural organic sorbents for environmental applications. 1. Materials, approaches, and characterizations. Environ. Sci. Technol. 40: 1650-1656

Weilin H, Ping'an P, Zhiqiang Y, Jiamo F (2003) Effects of organic matter heterogeneity on sorption and desorption of organic contaminants by soils and sediments. Appl. Geochem. 18: 955-972

Whyte LG, Bourbonniere L, Greer CG (1997) Biodegradation of petroleum hydrocarbons by psychrotrophic Pseudomonas strains possessing both alkane (alk) and naphthalene (nah) catabolic pathways.Appl. Environ. Microbiol. 63: 3719-3723

Xie H, Guetzloff TF, Rice JA (1997) Fractionation of pesticideresidues bound to humin. Soil Sci. 162: 421-429

Yuan SY, Wei SH, Chang BV (2000) Biodegra-dation of polycyclic aromatic hydrocarbons by a mixed culture. Chemosphere 41: 1463-1468

Zimmerman JR, Ghosh U, Millward, RN, Bridges TS, Luthy RG (2004) Addition of carbon sorbents to reduce PCB and PAH bioavailability in marine sediments: physicochemical tests. Environ. Sci. Technol. 39 (4): 1199-1200

Effect of Crude Water Extract of *Fructus Gleditsiae Sinensis* on the Removal of Phenanthrene and Pyrene from Contaminated Soils

Ran Wei, Jun Wang, Hongyu Yang, Yi Chen, Peifen Liu, Jinzhi Ni*

Key Laboratory of Subtropical Resources and Environments of Fujian Province, School of Geographical Sciences, Fujian Normal University, Fuzhou 350007, China.
*Corresponding author. E-mail: nijz@fjnu.edu.cn.

Abstract: Polycyclic aromatic hydrocarbons (PAHs) in soils can be mobilized by surfactants and other mobilizing agents such as dissolved organic matter (DOM). DOM from *Fructus Gleditsia sinensis* contains a large amount of natural non-ionic surfactant triterpenoid saponins and thus can be considered as a natural complex of general DOM and natural non-ionic surfactants. In this study we use crude water extract of *Fructus Gleditsiae Sinensis* Lam. (CWE-FGS) as a removal agent with no purification procedure to investigate the possibility of developing a more green and more cost effective remediation agent that may compete for the chemically synthesized "man-made" surfactants or purified or partially purified natural biosurfactants. Results showed that the removal rates of phenanthrene and pyrene from contaminated soils by 5% of CWE-FGS were 59% and 52%, respectively. The removal capacities of Tween 80 and rhamnolipids for PAHs from contaminated soils were also studied for comparison. The removal capacity of CWE-FGS for PAHs from contaminated soils was lower than that of Tween 80, but higher than that of rhamnolipids. Thus, it can be safely conclude that CWE-FGS can be a potential natural remediation agent for PAHs from contaminated soils.

Keywords: Polycyclic aromatic hydrocarbons (PAHs); Surfactant; Dissolved organic matter (DOM); *Fructus Gleditsiae Sinensis*; Remediation agent

Introduction

Polycyclic aromatic hydrocarbons (PAHs) are environmentally important because some of them are considered to be possible or probable human carcinogens and may be toxic to the environment (Menzie *et al.*, 1992; Brown and Steinert, 2003). They tend to accumulate in soils for many years because of their high hydrophobicity and low desorption rate (Northcott and Jones, 2001). Accordingly, the bioavailability of PAHs in soils is often limited by their low solubility and the strong sorption by soil.

More and more evidences have shown that PAHs in soils can be mobilized by surfactants and other mobilizing agents. In Particular, nonionic surfactants are often used to enhance the remediation of PAHs in contaminated soils (Paria, 2008, review). Considering that synthetic surfactants per se are chemical engineering products and may be toxic to environment, biosurfactants are considered to be relative safe remediation agents due to their lower toxicity and higher biodegradability. Saponins belong to glycoside family which is a class of biosurfactant widely distributed in plants. Saponins are structurally composed of one or more hydrophilic sugar moieties combined with a hydrophobic aglycone (sapogenin) moiety and can be classified as a natural nonionic surfactant. Thus this class of biosurfactant has received much attention for the remediation of contaminated soil as a substitute of chemically synthesized nonionic surfactant.

Dissolved organic matter (DOM) is the dissolved or water soluble part of natural organic matter in terrestrial and aquatic ecosystems which include soil organic matter, water organic matter, plant organic matter, etc. It is a complex mixture of compounds

varied largely in molecular size and solubility. DOM also has surface activity because it contains both hydrophilic and hydrophobic components just as chemically synthesized surfactant and biosurfactant. It's well documented that soil DOM can bind to non-ionic organic contaminants such as PAHs and act as a transport carrier and thus increase the solubility and desorption rate of them from soil (Conte *et al.*, 2005). And the contact between PAHs and soil microbes is thus increased which result in elevated bioavailability and degradation rate of these hydrophobic organic contaminants. Non-soil DOM such as DOM derived from pig manure, green manure and sludge were also investigated for its enhancement ability of remediation of soil organic contaminants in recent years (Raber, 1997; Cheng *et al.*, 2006). Evidence shows that DOM acts synergetically with non-ionic surfactant on the remediation of soil organic contaminants (Cho *et al.*, 2002; Cheng *et al.*, 2006).

Fructus Gleditsiae Sinensis is the dried fruit of *Gleditsia sinensis* Lam., a deciduous tree in the family Fabaceae, subfamily Caesalpinioideae. *Gleditsia sinensis* Lam. is widely distributed in China and can be found in most provinces. *Gleditsia sinensis* Lam. contains a large amount of triterpenoid saponins in its fruit or pod. It has been estimated that triterpenoid saponins contributes approximately 15%~30% of dry weight of the pod. Thus the DOM from *Fructus Gleditsia sinensis* can be considered as a natural complex of general DOM from general plant litter and natural non-ionic surfactant triterpenoid saponins. In this study we used crude water extract of *Fructus Gleditsiae Sinensis* Lam. (CWE-FGS), which is widely distributed and thus very inexpensive in China, as a removal agent with no purification procedure and no organic agent included in extraction procedures to investigate the possibility of developing a more green and more cost effective remediation agent compared to chemically synthesized "man-made" surfactants or purified or partially purified natural biosurfactants.

Materials and Methods

The organic C content in the soil used in this study, which was collected from a paddy field, was 3.13% and the pH of the soil is 5.76. The extractable phenanthrene and pyrene in the spiked soils were 47.12 $mg \cdot kg^{-1}$ and 51.3 $mg \cdot kg^{-1}$ respectively. CWE-FGS was extracted from *Fructus Gleditsiae Sinensis* with distilled water and freeze-dried followed by passing a 0.45 μm filter. For kinetics analysis, 1.0 g of spiked soil was combined with 10 mL of 1% CWE-FGS solution and then shaken with a rotatory shaker under 25 ℃. Samples were taken at regular time intervals and then centrifuged. The PAHs in the supernatant were extracted with hexane and determined by HPLC with fluorescence detector. During experiments for maximum PAH extraction, 1 g of PAH-spiked soil was combined with 10 mL of CWE-FGS, rhamnolipids and Tween 80 of different initial concentrations (0%, 1%, 3% and 5%), respectively. After 6 h of shaking, the samples were centrifuged, and the PAH concentrations in the supernatants were analyzed.

Results and Discussion

Kinetics of PAH Extraction by CWE-FGS

The time course for Phe and Pyr extraction was conducted for 48 h with 1% CWE-FGS solution. The results indicated that the maximum removals of Phe and Pyr were about 24% and 20% at 6 h, respectively. The removal rate of Phe and Pyr increased during the first six hours with time and then decreased gradually to an equilibrium value after 12 hours which was around 70% of the peak value.

Maximum Extraction of PAHs at Different CWE-FGS Concentrations

According to the kinetics experiments, we chose 6 h as the extraction time to study the extraction capacity of CWE-FGS. Gradient concentrations, which were 0%, 1%, 3% and 5%, of CWE-FGS were used for PAH extraction. Results showed that the relationships between the removal rates of PAHs from contaminated soils and the concentrations of CWE-FGS conformed to the exponential functions y=79.9-77.1×0.77^x (R^2=0.9992) and y=84.1-83.6×0.83^x (R^2=0.9994) for Phe and Pyr, respectively. The removal rates of phenanthrene and pyrene from contaminated soils by 5% of CWE-FGS were 59% and 52%, respectively. Theoretically, according to the exponential curve, the removal rates would continue to rise if the concentration of CWE-FGS increased. Considering that some ingredients of CWE-FGS of *Fructus Gleditsiae Sinensis* can not dissolve easily, we did not investigate the removal rates of

phenanthrene and pyrene by CWE-FGS of concentrations greater than 5%.

Comparisons of PAH Removal Capacity of CWE-FGS, Rhamnolipids and Tween 80

Rhamnolipids, a well-known biosurfactant, and Tween 80, a widely used chemically synthesized nonionic surfactant, were also investigated for the removal capacities for phenanthrene and pyrene from spiked soils. The results showed that the maximum removal rates for phenanthrene and pyrene by rhamnolipids were 52% and 45% respectively, which were obtained by 3% of the concentration. The removal rates for phenanthrene and pyrene decreased when the concentration of rhamnolipids was greater than 3%. The removal rates of phenanthrene and pyrene by Tween 80 conformed to the exponential functions y=93.6-91.1×0.18^x (R^2=0.9991) and y=83.2-80.9×0.18^x (R^2=0.9988) respectively. The removal rates reached a plateau when the concentration of Tween 80 was greater than 3%.

From the data above, the removal capacity of CWE-FGS for PAHs from contaminated soils was lower than that of Tween 80, but higher than that of rhamnolipids. Thus, it can be safely conclude that CWE-FGS, which is DOM from plant source according to its preparation procedure, can be a potential natural remediation agent for PAHs from contaminated soils.

Acknowledgements

This research was funded by the Natural Science Foundation of Fujian Province (No. D0710008).

References

Brown JS, Steinert SA (2003) DNA damage and biliary PAH metabolites in flatfish from Southern California bays and harbors, and the Channel Islands. Ecol. Indic. 3: 263-274

Cheng KY, Wong JWC (2006) Combined effect of nonionic surfactant Tween 80 and DOM on the behaviors of PAHs in soil–water system. Chemosphere 62(11): 1907-1916

Cho HH, Choi J Goltz MN, Park JW (2002) Combined Effect of Natural Organic Matter and Surfactants on the Apparent Solubility of Polycyclic Aromatic Hydrocarbons. J. Environ. Qual. 31(1): 275-280

Menzie CA, Potocki BB, Santodonato J (1992) Exposure to carcinogenic PAHs in the environment. Environ. Sci. Technol. 26: 1278-1284

Northcott G, Jones K (2001) Partitioning, Extractability, and Formation of Nonextractable PAH Residues in Soil. 2. Effects on Compound Dissolution Behavior. Environ. Sci. Technol. 35: 1111-1117

Paria S (2008) Surfactant-enhanced remediation of organic contaminated soil and water. Adv. Colloid. Interfac. 138: 24-58

Raber B, Kögel-Knabner I (1997) Influence of origin and properties of dissolved organic matter on the partition of PAH. Eur. J. Soil Sci.48: 443-455

Distribution Pattern, Sources and Potential Risks of Polycyclic Aromatic Hydrocarbons in Urban Soils of Fuzhou City, China

Jinzhi Ni*, Xiaoyan Li, Juan Guo, Jun Wang, Hongyu Yang, Ran Wei

Key Laboratory of Subtropical Resources and Environments of Fujian Province, School of Geographical Sciences, Fujian Normal University, Fuzhou 350007, China.
*Corresponding author. E-mail: nijz@fjnu.edu.cn.

Abstract: Polycyclic aromatic hydrocarbons (PAHs) were analyzed in 64 surface soil (0~5 cm depth) samples collected from Fuzhou city, China. The sampling sites were randomly selected from various functional zones including parks, colleges and universities, residential areas, agricultural fields, industrial areas, and gas stations. Total PAHs (∑PAHs) concentrations ranged from 14.0 to 5442.9 μg·kg^{-1} with a mean of 578.1 μg kg^{-1}. The mean concentration of ∑PAHs in soil samples from different functional zones decreased in the order of gas stations (1140.9 μg·kg^{-1}) > industrial areas (1131.6 μg·kg^{-1}) > agricultural fields (514.3 μg·kg^{-1}) > residential areas (393.3 μg·kg^{-1}) > colleges and universities (245.8 μg·kg^{-1}) > parks (222.0 μg·kg^{-1}). The calculated PAH isomer ratios indicated that pyrogenic origins such as motor vehicle exhaust, industrial activities and coal burning were the dominant sources. The total carcinogenic potency for each sampling site was calculated using toxicity equivalency factors (TEFs) to convert concentration of individual PAH to an equivalent concentration of benzo[a]pyrene (BaP_{eq}). Comparing with the reference total carcinogenic potency calculated as a sum of Dutch target value for unpolluted soil with appropriate BaP_{eq}, above 42% soil sampling sites in this study, especially for the sampling sites of gas stations, had certain potential ecological risks to human health.

Keywords: PAH concentration; Soil; PAH isomer ratio; Ecological risks

Introduction

Polycyclic aromatic hydrocarbons (PAHs) are ubiquitous environmental contaminants derived from natural sources that include forest fires and/or anthropogenic processes such as urban and industrial activities. This class of organic contaminants is environmentally important because of their carcinogenic and mutagenic activities in animals and/or humans. PAH compounds are likely to accumulate in soils for many years because of their persistence and hydrophobicity (Harrad *et al*., 1994; Ockenden *et al*., 2003).

Fuzhou, the capital city of Fujian province, is located in the southeast coastal area of China, between 25°16′ and 26°39′ north latitude and between 118°23′ and 120°31′ east longitude. Climate is subtropical marine monsoon climate, mild weather, and rich rainfall with an annual average temperature of 19.7 ℃. Fuzhou is separated from Taiwan only by a narrow strait, namely Taiwan Strait. Thus under the slogan of "Construction of the Economic Zone on the Western Coast of the Taiwan Straits", Fuzhou has benefited from cross strait investment and is today a major commercial and manufacturing center. With the development of economy, more and more attention was paid to the environmental pollution. However, up to now, little information is available on the PAHs contamination in urban soils of Fuzhou city. In this study, the concentrations of 15 United States Environmental Protection Agency (USEPA) priority PAHs in topsoil of Fuzhou city were therefore determined, and their sources and ecological risks were also analyzed. This study will (may) serve as

essential reference information for the government to prepare city development strategies of Fuzhou.

Concentrations and Distributions of PAHs in Soils

The total concentrations of PAHs (∑PAHs) ranged over 2 orders of magnitude from 14.0 to 5442.9 $\mu g \cdot kg^{-1}$ with an overall mean of 578.1 $\mu g \cdot kg^{-1}$ in 64 topsoil samples. High molecular weight PAHs with 4–6-rings, especially 4-ring PAHs were the major fractions of most soil samples. The mean values of ∑PAHs in different functional zones decreased in the order of gas stations > industrial areas > agricultural fields > residential areas > colleges and universities > parks. However, there were no significant differences of ∑PAHs among different functional zones. According to the soil target value of 1000 $\mu g \cdot kg^{-1}$ for 10 PAHs (Nap, Phe, Ant, FluA, BaA, Chry, BkF, BaP, BghiP, IP) concentration set by the Netherlands, about 7.8% of the collected soils in Fuzhou city would be considered contaminated with PAHs, indicating their potential risks to human health.

Sources of PAHs

Most PAH contaminants in the terrestrial environment are anthropogenic including petrogenic, which is primary associated with crude oil and natural oil seeps, and pyrogenic, which is formed in high heat or combustion processes. The fingerprints of PAHs from pyrogenic or petrogenic origin may be used to differentiate these origins by using molecular indices based on ratios of selected PAH concentrations (Colombo *et al*., 1989). A FluA/(FluA + Pyr) ratio <0.4 indicates petroleum input, a ratio between 0.4 and 0.5 indicates liquid fossil fuel (vehicle and crude oil) combustion and a ratio >0.5 indicates grass, wood or coal combustion. Similarly, a IP/(IP+BghiP) ratio <0.2 likely implies petroleum, between 0.2 and 0.5 liquid fossil fuel (vehicle and crude oil) combustion and a ratio >0.5 implies grass, wood and coal combustion (Yunker *et al*., 2002). On the basis of the ratios of FluA/(FluA + Pyr) and IP/(IP+BghiP), it would appear that the pyrogenic origins such as motor vehicle exhaust, heavy industry emissions and coal combustion are the dominant sources of PAH in topsoils of Fuzhou city.

Risk Assessment of PAHs in Topsoil of Fuzhou City

PAHs have received much attention due to their toxicity, carcinogenicity and mutagenicity. USEPA recommends that a toxicity equivalency factor (TEF) be used to convert concentrations of carcinogenic polycyclic aromatic hydrocarbons to an equivalent concentration of benzo[a]pyrene (BaP_{eq}) when assessing the risks posed by these substances (USEPA/600/R-93/089, July 1993). The TEF is based on the potency of each compound relative to that of BaP. TEFs for individual PAH used by Tsai *et al*. (2004) was adopted in this study. Comparing the carcinogenic potencies associated with the total PAHs at the contaminated sites, the sum of each individual BaP_{eq} (i.e., total BaP_{eq}) was used as a surrogate indicator. The toxicity and carcinogenity of the investigated sites was estimated by comparing the reference total carcinogenic potency which was calculated as a sum of Dutch target value for unpolluted soil with appropriate BaP_{eq} (VROM, 1994).

The results indicated that total BaP_{eq} in 42.2% of soil samples in this study exceeded the reference total carcinogenity potency value (32.96 $\mu g \cdot kg^{-1}$), and most of which were due to the high concentration of BaP in soils. The percentages of soil samples with total BaP_{eq} exceeding the reference value were 23.1% for parks, 28.6% for colleges and universities, 33.3% for residential areas, 50% for agricultural fields, 28.6% for industrial areas and 81.8% for gas stations. We can infer, therefore, that above 42% of soil sampling sites in this study, especially for the sampling sites of gas stations, had certain potential ecological risks to human health.

Acknowledgements

This research was funded by the Natural Science Foundation of Fujian Province (No. D0710008).

References

Colombo JC, Pelletier E, Brochu C, Khalil M, Cataggio JA (1989) Determination of hydrocarbon

sources using n-alkanes and polyaromatic hydrocarbon distribution indices. Case study: Rio de la Plata estuary, Argentina. Environ. Sci. Technol. 23:888-894

Harrad SJ, Sewart AP, Alcock RE, Boumphrey R, Burnett V, Duarte-Davidson R, *et al*. (1994) Polychlorinated biphenyls (PCBs) in the British environment, sinks, sources and temporal trends. Environ. Pollut. 85:131-146

Ockenden WA, Breivik K, Meijer SN, Steinnes E, Sweetman AJ, Jones KC (2003) The global recycling of persistent organic pollutants is strongly retarded by soils. Environ. Pollut. 121:75-80

Tsai PJ, Shieh HY, Chen HL, Lee WJ, Lai CH, Liou SH (2004) Assessing and predicting the exposures of polycyclic aromatic hydrocarbons (PAHs) and their carcinogenic potencies from vehicle engine exhausts to highway toll station workers. Atmos. Environ. 38:333-343

US EPA (1993) Provisional guidance for quantitative risk assessment of polycyclic aromatic hydrocarbons. EPA/600/R-93/089

VROM (1994) Environmental quality objectives in the Netherlands. Ministry of Housing, Spatial Planning and Environment

Yunker MB, Macdonald RW, Vingarzan R, Mitchell RH, Goyette D, Sylvestre S (2002) PAHs in the Fraser river basin: a critical appraisal of PAH ratios as indicators of PAH sources and composition. Org. Geochem. 33:489-515

Thermal Degradation of Chloroteracycline in Animal Manure and Soil

Mingkui Zhang*, Huimin Zhang

Zhejiang Provincial Key Laboratory of Subtropic Soil and Plant Nutrition,
College of Environmental and Resource Sciences, Zhejiang University, Hangzhou 310029, China.
*Corresponding author. E-mail: mkzhang@zju.edu.cn.

Abstract: Veterinary antibiotics used in livestock and poultry production may be present in manure and slurry as the parent compound and/or metabolites. The environment may therefore be exposed to these antibiotics due to the application of animal manure to agricultural land. In order to reduce the amount of veterinary antibiotics ultimately released into the environments, it is necessary to treat properly animal manure before its application in agricultural land. In this paper, the effect of temperature on degradation of chlortetracycline (CTC) in animal manure and soil was investigated under laboratory conditions. Degradation of the CTC in both animal manure and soil under different temperature conditions followed first-order kinetics. Increasing temperature greatly accelerated CTC degradation, and thermal degradation became significant at high temperature (>30 ℃). The degradation rate of the CTC was faster in animal manure than manure-amended soil and soil, suggesting that CTC may become persistent in the environment once it was released from manure into soil.

Keywords: Chlortetracycline; Degradation; Manure; Soil; Temperature

Introduction

Veterinary antibiotics are used in agriculture to prevent disease in livestock and treat illness. Following administration, quantities of these drugs may be excreted as the parent compound and /or metabolites and enter the environment due to the spreading of manure and slurry on agricultural land, or due to direct deposition by grazing livestock (Halling-Sorensen *et al.*, 1998). Antibiotics are biologically active compounds designed to kill microbes or reduce their growth. As a result, questions have been raised over the potential impacts of antibiotics in the environment on human and animal health, such as adverse effect on soil micro-organisms, the promotion of the spread of antibiotic resistance and the triggering of adverse immunological reactions (Chee-Sanford *et al.*, 2001). Therefore, the disposal of antibiotic-contaminated manure is necessary before the manure is applied to agricultural land. Determination of degradation rate of antibiotics in the disposal is crucial in defining the environmental impact of antibiotics. Chlortetracycline (CTC) is a major member of tetracyclines, which are widely used in animal husbandry to treat and prevent bacterial diseases in China. The effect of various environmental factors on the degradation of CTC in manure has not yet been well documented. Thermophilic composting is an important way to treat the manure. Therefore, the effect of temperature on antibiotics degradation will control the impact of antibiotics residuals in the environment. The objective of this study is to determine the effect of temperature on decomposition of CTC in manure and soil.

Materials and Methods

Manure and Soil

Fresh pig manure in the study was collected from a household animal houses, and air-dried in the laboratory for ten days at 25 ℃, and then sieved to 5 mm. The soil used in this study was loamy mixed active thermic aeric humaquepts, which was sampled

from the agricultural experiment farm, Huajiachi Campus of Zhejiang University, Hangzhou, China. The soil samples were air-dried in the laboratory at 25 ℃, and then sieved to 2 mm. The manure and soil samples were analyzed, and no CTC residues were detected.

Degradation Experiment

500 g samples of manure, manure-amended soil (manure/soil = 2:98 by dry weight), and non-amended soil were weighed into three plastic zip bags. Each of the sample was spiked with CTC at rate of 5 $mg \cdot kg^{-1}$, the moisture of the samples was controlled at 75% of maximum water-holding capacity. Each of the samples was thoroughly mixed and weighed into seven 250 mL glass bottles at approximately 70 g (dry weight) per bottle. After the weight of each bottle was recorded, the bottles were loosely covered with plastic membrane and incubated under different temperature. The incubation temperature was controlled at 18 ℃ (constant-temperature room), 35 ℃ (incubator), and 50 ℃ (oven). Every other day, each bottle was weighed, and water was added to compensate any moisture loss. At day 2, 5, 10, 20, 30, 40, and 50, one bottle from each temperature set was taken out, and immediately transferred into a plastic zip bag, and stored in a freezer at -15 ℃ until analysis.

Analysis of CTC

The manure/soil sample in each bag was thawed at room temperature. Residual CTC in the sample was extracted with EDTA-McIlvaine buffer solution. The concentration of CTC in the extracts was measured by high performance liquid chromatography (Liu *et al.*, 2007). As the extraction recoveries of the method used in this study were above 82%, all obtained CTC concentrations in manure and soil were presented without recovery adjustments.

Results

Degradation experimental data of CTC in manure and soil under different temperature is shown in Fig. 1. The simple first-order kinetic model [$C_t = C_0 e^{-kt}$, where C_0 and C_t were the CTC concentrations at times 0 and t (day)] was used to fit the experimental data. The regression coefficients, r, of the model ranged from 0.9677 to 0.9962 ($p<0.05$). CTC degradation in manure at different temperatures exhibited different kinetics. When the temperature was increased from 18 ℃ to 50 ℃, CTC degradation was enhanced, and k markedly increased from 0.030 to 0.1413 for manure. This result implied that the increasing temperature accelerated the degradation process of CTC in the manure.

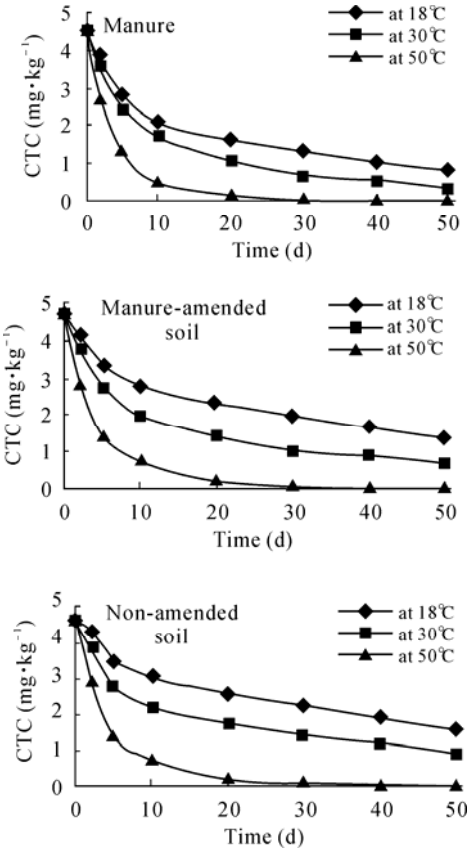

Fig.1 CTC degradation in manure and soil under different temperatures

CTC degradation in manure happened much faster at 50 ℃ than at 18 ℃. At 50 ℃, the CTC decrease became almost linear after 10 days of incubation. The rapid degradation of CTC at high temperatures might be a useful clue to manure treatment designs. The contamination of CTC in animal manure may be greatly diminished if manure is kept at a high temperature for a certain period of time.

The degradation kinetics of CTC in both non-amended and manure-amended soil also obeyed the simple first-order kinetic model. CTC degradation in non-amended and manure-amended soil appeared much slower than that in manure. As indicated by the faster degradation of CTC in manure-amended soil than that in non-amended soil at the same temperature,

the much faster degradation of CTC in manure than that in soil may mainly result from the riched degradation microorganisms in manure. This result implies that CTC may become much more persistent in the environment once it was released from contaminated manure into soil. High temperatures during manure storage and composting treatment might be critical.

Table 1 Half-life of CTC degradation in manure and soil under different temperature (d)

Temperature	Manure	Manure-amended soil	Non-amended soil
18℃	23.1	31.9	37.3
30℃	14.6	20.4	26.4
50℃	4.9	5.2	5.6

Conclusions

Degradation of the CTC in both animal manure and soil under different temperature conditions followed first-order kinetics. Increasing temperature greatly accelerated CTC degradation. The degradation rate of the CTC was faster in animal manure than manure-amended soil and soil. High temperatures during manure storage and composting treatment might be critical.

Acknowledgements

This work was financially supported by the research foundation of the doctorial programs of the Education Ministry (20060335018).

References

Chee-Sanford JC, Ainov R I, Krapac IJ, *et al.* (2001) Occurrence and diversity of tetracycline resistance genes in lagoons and groundwater underlying two swine production facilities. Appl. Environ. Microbiol. 67(4): 1494-1502

Halling-Sorensen B, Nielsen SN, Lansky PF, *et al.* (1998) Occurrence, fate, and effects of pharmaceu-ticals in the environment—A review. Chemosphere 36: 357-365

Liu H, Zhang GP, Liu CQ (2007) Determination of chloramphenical and three tetracyclines by solid phase extraction and high performance liquid chromatography-ultraviolet detection. Chinese J. Anal. Chem. 35(3): 315-319

Enhancement of Atrazine Degradation in Paddy Soils by Organic Amendments

Chaolan Zhang[a], Jianming Xu[b,*], Bin Yao[c]

[a] College of Agriculture, Guangxi University, Nanning 530005, China;
[b] Zhejiang Provincial Key Laboratory of Subtropic Soil and Plant Nutrition, College of Environmental and Resource Sciences, Zhejiang University, Hangzhou 310029, China;
[c] Key Laboratory of Forest Ecology and Environment, CAF, Beijing 100091, China.
[*]Corresponding author. Tel. No. +86-571 8697 1955; Fax No. +86-571 8697 1955; E-mail: jmxu@zju.edu.cn.

Abstract: The effect of three organic amendments, e.g. decomposed pig manure, rice straw and Chinese clover, on soil microbial biomass carbon content (SMBC) and the degradation of atrazine in three paddy soils spiked with atrazine at a rate of 10 $mg \cdot kg^{-1}$ soil were studied. The results showed that SMBC significantly ($P<0.01$) increased with the application of organic amendments in all three soils. The largest increment of SMBC was observed in the treatment of decomposed pig manure, followed by addition of Chinese clover, and the smallest increase occurred in the application of rice straw. The dissipation of extractable atrazine was significantly enhanced by the organic amendments. Compared with the unamended treatment, the average half-life of atrazine in soil was reduced by 2, 1.6, and 1.4-fold in the treatments with decomposed pig manure, Chinese clover and rice straw, respectively. These results suggest that application of organic fertilizers in paddy fields may significantly alter soil microbial communities and affect the fate of agrochemicals such as atrazine. As the use of organic wastes is an important practice in rice production in many regions in Asia, such interactions should be considered when evaluating the fate and risk of pesticides in the environment.

Keywords: Atrazine; Enhanced degradation; Biodegradation; Organic amendment; Soil microbial biomass

Introduction

Microbial degradation is the principal mechanism for the dissipation of atrazine [2-chloro-4-(ethylamino)-6-(isopropylamino)-s-triazine] in the environment (Kaufman and Kearney, 1970; Esser *et al.*, 1975). Complete and rapid mineralization of the triazine ring by microorganisms has been shown to occur in soil (Mandelbaum *et al.*, 1993; Assaf and Turco, 1994; Mandelbaum *et al.*, 1995; Radosevich *et al.*, 1995) and the possible adaptation of soil microflora to atrazine degradation after repeated field applications has also been demonstrated (Barriuso and Houot, 1996; Vander-heyden *et al.*, 1997). Microbial growth has been observed with atrazine as the sole carbon source (Behki and khan, 1986; Yanze-Kontchou and Gschwind, 1994; Stucki *et al.*, 1995). Rapid triazine ring mineralization also suggests the development of microorganisms using triazine nitrogen as a nitrogen source (Mandelbaum *et al.*, 1995; Radosevich *et al.*, 1995; Cook and Hütte, 1981).

The addition of organic materials in paddy fields is a popular and conventional practice in China and many other rice production regions. Introduction of organic amendments into the soil can potentially modify the degradation rate and pathways of a pesticide and thus its environmental risk. For instance, it is known that hydrophobic pesticides are readily adsorbed to soil organic matter. Therefore, organic amendments may promote sorption of pesticides, reduce their bioavailability and slow down their biodegradation in soils (Barriuso and Houot, 1996). On the other hand, organic amendments may accelerate pesticide degradation through a general

stimulation of soil microbial activity (Hance, 1973). Interest in the effect of herbicides on soil microbial biomass is also driven by the importance of soil microorganisms in controlling C, N, P and S flows in soils (Sarathchandra *et al.*, 1988). Exposure to some xenobiotic compounds may force the soil microbial biomass to direct a large part of its energy budget into reducing mineralization activity (Anderson and Domsch, 1990). This interaction may have long-lasting negative effects on soil health and fertility. In addition, some modern agricultural management practices may reduce soil organic matter content, causing an impoverishment of the physical, chemical and microbiological properties of soils (Haider, 1992; Kirchner *et al.*, 1993). Studies show that the amount of microbial biomass is closely related to the soil C concentration (Witter and Kannal, 1998). Nitrogen availability also influences atrazine behavior in soils and the effect varies with the form and amount of N present. For instance, high concentrations of mineral N greatly decreased atrazine mineralization in soil when added alone or with organic amendments (Entry, 1993; Alvey and Crowley, 1995). On the other hand, dairy manure with abundant organic N stimulated atrazine mineralization (Topp *et al.*, 1996).

The purpose of the present study was to understand the dynamic response of microbial biomass to organic amendments in paddy soils and the subsequent effect on atrazine dissipation kinetics. In particular, this study focused on the effect of organic amendments with different ratios of C/N on SMBC and atrazine degradation to better understand the relationship between microbial biomass, atrazine degradation and organic amendment in paddy soils.

Materials and Methods

Soils and Organic Amendments

Three paddy soils used in this study were collected from the surface layer (0~20 cm) of paddy fields on a desalting muddy polder near Yuanpu (PMP), a blue clayey paddy soil near Pinghu (BCP) and a paddy soil on quaternary red clay near Longyou (PRC). All sampling locations are in Zhejiang Province located on the east coast of China.

Three organic amendments, rice straw, decomposed pig manure and Chinese clover (Astragalus Sinicus Linn), were used (Table 1). The rice straw and the decomposed pig manure came from the farm of Guangxi University, Guangxi, China. The Chinese clover was collected from Pinghu, Zhejiang Province. All organic amendments were air-dried and ground in a plant-blender to a 1 mm maximum particle size.

Table 1 Characteristics of paddy soils and organic materials used in this study

SSoil or organic amendment	Total P ($g \cdot kg^{-1}$)	Organic matter ($g \cdot kg^{-1}$)	Total N ($g \cdot kg^{-1}$)	C/N	CEC ($mmol \cdot kg^{-1}$)	pH (1:2.5)	Clay ($g \cdot kg^{-1}$)	Silt ($g \cdot kg^{-1}$)	Sand ($g \cdot kg^{-1}$)
PMP[a]	0.7	20.4	1.9	11.3	98.8	7.4	290	627	83
BCP	0.9	23.1	2.4	9.6	182.5	6.1	464	421	115
PRC	0.3	7.9	0.8	10.0	84.3	4.9	260	495	245
Rice straw	2.0	174.4	4.8	36.3					
Chinese clover	8.1	144.4	13.6	10.6					
Decomposted pig manure	14.5	394.6	30.8	12.8					

PMP[a], Paddy field on desalting muddy polder; BCP, Blue clayey paddy soil; PRC, Paddy field on quaternary red clay

Reagents

Analytical standard of atrazine (purity 98.4%) was purchased from the Center for Examination of Pesticides of China (Nanjing, Jiangsu Province, China). HPLC-grade methanol was purchased from Siyou, Tianjin, China. HPLC-grade water was

obtained by purifying distilled water with a Milli-Q® water purification system (Millipore, Bedford, MA). All other chemicals used were products of analytical-reagent purity, and methanol and dichloromethane were redistilled prior to use.

Incubation Experiments

Spiked soil samples were prepared by adding 0.8 mL of methanol solution containing 1000 $mg \cdot kg^{-1}$ atrazine to 80 g (oven dry weight basis) of fresh soil. After complete removal of methanol by evaporation at room temperature for 24 h, the treated soil was thoroughly mixed with additional fresh soil to obtain an initial atrazine concentration of 10 $mg \cdot kg^{-1}$. The organic amendments were individually added to the herbicide-spiked soil samples in a series of jars at a rate of 10 $g \cdot kg^{-1}$. Five treatments were prepared: control (CK), unamended atrazine soil (10 $mg \cdot kg^{-1}$ soil) (A), A + 10 $g \cdot kg^{-1}$ decomposed pig manure (AM), A + 10 $g \cdot kg^{-1}$ rice straw (AS), and A + 10 $g \cdot kg^{-1}$ Chinese Clover (AC). The soil moisture was adjusted to 50% of the soil water-holding capacity with deionized water. The amended soil jars were then incubated at 25 ± 1 ℃. The loss of water from each jar was compensated daily with deionized water. All treatments were prepared in three replicates. During incubation, SMBC and concentrations of solvent-extractable atrazine in the soil samples were determined at 0, 7, 14, 28, 42, 56, 70 and 98 d after treatment.

Microbial Biomass Measurement

The biomass C was determined using the chloroform fumigation and extraction method (Brookes *et al.*, 1982; Vance *et al.*, 1987). Briefly, soil samples were fumigated with chloroform and then extracted with 0.5 $mol \cdot L^{-1}$ K_2SO_4 at 1:5 soil-to-solution ratios by shaking for 2 h on an end-over-end shaker. The dissolved organic carbon content in the supernatant was measured on a Shimadzu TOC-500 automated Total Organic Carbon Analyzer (Shimadzu, Kyoto, Japan). The content of microbial biomass carbon was calculated from the difference between fumigated and nonfumigated samples (Wu *et al.*, 1990).

Analysis of Methanol-extractable Atrazine Residues

A 10-g aliquot of the incubated soil sample (oven dry weight equivalent) was extracted by ultrasonic agitation in 50 mL methanol for 15 min (40 kHz, 25 ℃). After centrifugation at 4,000 rpm for 15 min, the supernatant was collected. The soil residues were extracted with fresh methanol four times, and the extracts were combined. The methanol extract was extracted with 25 mL dichloromethane three times, and the dichloromethane phase was collected in a flask after dehydration using anhydrous sodium sulfate. The solvent phase was then evaporated to dryness under vacuum on a Rotavapor (RE-52A, Shanghai, China). The residues were recovered in 5 mL methanol and filtered through a 0.2 μm membrane (Anpel, Shanghai, China). The filtrate was stored at 4 ℃ until analysis by HPLC.

The extractable atrazine was analyzed on HPLC using a Symmetry ® C_{18} column (5 μm, 3.9 × 150 mm; Waters, Milford, MA). The HPLC system (Waters Alliance 2698, Milford, MA) consisted of a Waters 2695 multisolvent delivery system, a Waters 717 autosampler, and a Waters 2487 dual-λ absorbance UV detector operating at 228 nm. The mobile phase was a mixture of methanol and water (Milli-Q water) at 60:40 (v/v) and the flow rate was maintained at 0.7 $mL \cdot min^{-1}$ .The injection volume was 10 μL. Recoveries of atrazine added in soils ranged between 81.8% and 98.0%.

Results and Discussion

Soil Microbial Biomass (SMCB) Dynamics

The SMBC level was noticeably different among the three soils without organic amendment (Fig. 1). In PMP and BCP, the mean SMBC level was significantly higher ($p<0.01$) than that in PRC. The average values of SMBC were 351.2, 345.8 and 181.0 $mg \cdot kg^{-1}$ in PMP, BCP and PRC at 98d, respectively, This might be a result of differences in factors such as long-term organic C input (McGill, 1986; Jenkinson, 1981), soil texture (Hassink, 1994a; 1994b) and crop rotation history (Anderson and Domsch, 1989). Soil SMBC levels were significantly ($p<0.01$) educed in all treatments regardless of the soil type during the initial 7-d incubation period when compared to the initial values, even in CK. The SMBC levels in soils treated with atrazine were consistently lower than those in the other treatments throughout the entire incubation period. Compared to the pesticide-free

control, the mean SMBC with addition of atrazine decreased by 13.5% in PMP, 6.3% in BCP, and 7.3% in PRC at day 7. This might be caused by the addition of atrazine at a relatively high rate, which affected the activity of indigenous soil microor-ganisms. However, SMBC in all soils consistently increased after addition of the organic materials, regardless of the soil type. The addition of decom-posed pig manure enhanced the mean SMBC by 99.5% in PMP, 50.6% in BCP, and 70.5% in PRC. When Chinese clover was added, the mean SMBC increased by 57.6% in PMP, 35.0% in BCP, and 39.0% in PRC. The smallest increases of SMBC were observed in the treatments with rice straw, which were 30.1% in PMP, 29.7% in BCP, and 27.0% in PRC. The differences might be partly attributed to the rapid metabolism of soluble organic matter by soil microbes after organic amendments were added to the soils. The organic substrates in decomposed pig manure and Chinese clover might be more readily available than in rice straw to soil microorganisms. It is also likely that the introduction of organic matter into the soil increased atrazine sorption by soil, thus decreasing the microbial toxicity by the herbicide. Shen *et al.* (1993) reported that the growth of microorganisms was closely dependent on the content of available organic carbon in soil. Previous studies consistently showed that the soil microbial biomass increased after application of straw (Shen *et al.*, 1993; Chilima *et al.*, 2002; Shinjiro *et al.*, 1988). Entry and Emmingham (Entry *et al.*, 1995) demonstrated that the addition of readily decomposable organic matter and crop residues stimulated soil microbial activity. The microbial biomass C and N, organic matter, total N, available P, respiration rate and cellulose-decomposing capacity in soil were all enhanced when the application rate of refuse compost was increased (Xu and Gu, 1995).

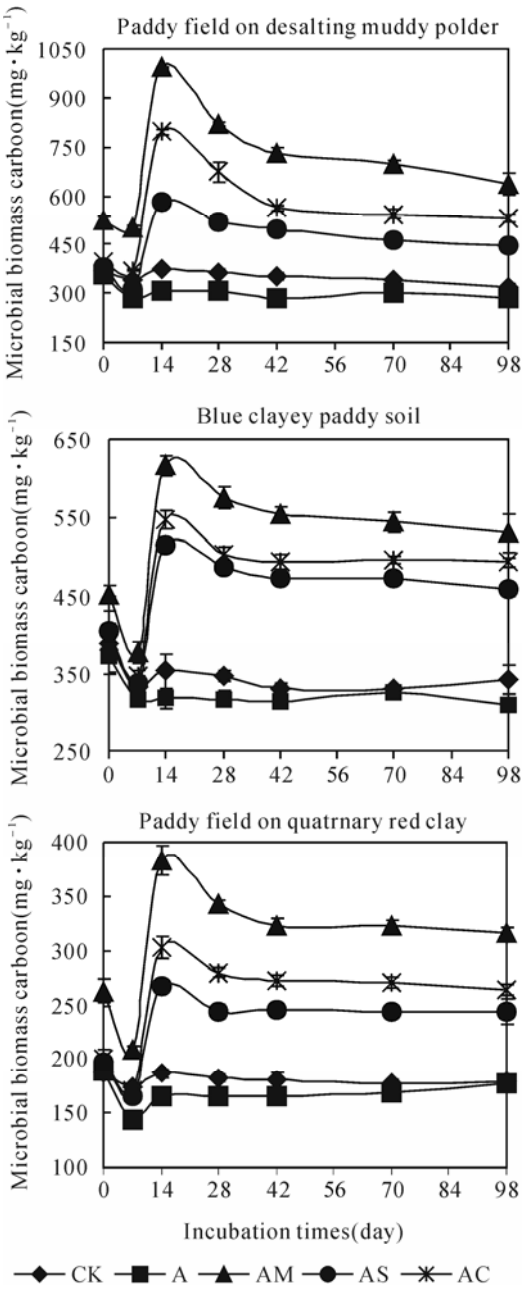

Fig. 1 Dynamics of microbial biomass carbon with incubation time in three soils treated with different organic amendments. For abbreviations see Table 2

The dynamic responses of SMBC over the incubation time were similar for different soils and different treatments, although the relative levels of SMBC were different. The levels of SMBC decreased during the first 7 d of incubation, but the reduction in SMBC was less in all amendment treatments. Following the initial decrease, the SMBC level consistently increased between 7 and 14 d, and then often decreased again between 14 and 28 d. After 28 d of incubation, SMBC levels generally reached a plateau, but remained significantly higher in amended treatments than unamended treatments or control treatments. This observation likely reflected the progress of organic matter decomposition by soil microbes and the dynamic change of the soil microbial communities. During the initial 7 d, addition of atrazine might have greatly affected the composition and activity of soil microorganisms. From 7 to 14 d, it was likely that the readily decomposable organic matter was quickly utilized by soil microbes, resulting in increases of SMBC. After 14 or 28 d, the amount of readily decomposable organic matter became depleted and the overall decomposition rate of the added organic materials

declined, resulting in smaller populations of microorganisms in the soil.

Atrazine Dissipation

Soil pH had been shown to be one of the key factors that control the degradation of atrazine in soils (Howard, 1991). In alkaline soils, microbial metabolism is the main pathway for the dissipation of atrazine. In acidic soils, atrazine degrades mainly through chemical hydrolysis. The half-life of atrazine in acidic soils was 63 d (pH 4.9), shorter than that in weakly acidic soil (pH 6.1) (84 d) (Howard, 1991). The half-life of atrazine was even shorter in alkaline soils (51 d) (Qiao *et al.*, 1995). However, our results were inconsistent with above findings. The rate of dissipation of extractable atrazine was significantly different in the three tested soils without organic amendment (Fig. 2). At the end of incubation, 77.5% of initially added extractable atrazine dissipated in PRC, while 89.4% disappeared in BCP and 84.4% in PMP. Therefore, the shortest atrazine persistence was found in BCP (pH 6.1), followed by PMP (pH 7.4), and PRC (pH 4.9) (Table 2). The inconsistency might be caused by factors such as previous history of atrazine application and soil texture. The background level of atrazine was found to be about 0.05 mg·kg^{-1} in PRC, but none in PMP and BCP. The presence of trace residues of atrazine in PRC suggests a more extensive use history. Accelerated atrazine mineralization was observed after repeated applications to a soil (Rahima *et al.*, 2000). In soils receiving repeated applications of atrazine, the microbial community was able to mineralize the triazine ring of atrazine, while such community was not present in untreated soils (Barriuso and Houot, 1996).

Results in Fig. 2 also showed that the dissipation of extractable atrazine was significantly accelerated when soils were incubated with decomposed pig manure, rice straw or Chinese clover compared to the unamended treatments. At the end of incubation, 95.2%, 91.2%, and 87.8% of the initially added atrazine disappeared in PRC with amendment of decomposed pig manure, Chinese clover and rice straw, respectively. The corresponding dissipation rates were 99.2%, 97.9% and 96.4% for BCP, and 97.7%, 86.9% and 93.7% for PMP. Consequently, the half-life of atrazine was significantly shortened in all amended treatments. In general, the shortest half-life of atrazine was observed in treatments with decomposed pig manure, followed with the addition of Chinese clover, and the longest persistence was found in treatments of rice straw (Table 2 and Fig. 2). Compared with the unamended control the average half-life of atrazine was 2, 1.6, and 1.4–fold shorter in, treatments amended with decomposed pig manure, Chinese clover and rice straw, respectively. The enhanced herbicide degradation coincided with increases in SMBC levels in the amended soils. As the highest SMBC and the most rapid loss of atrazine were found in the same treatments (AM), it was likely that a wide range of microflora were involved in the degradation of atrazine. These results suggested that

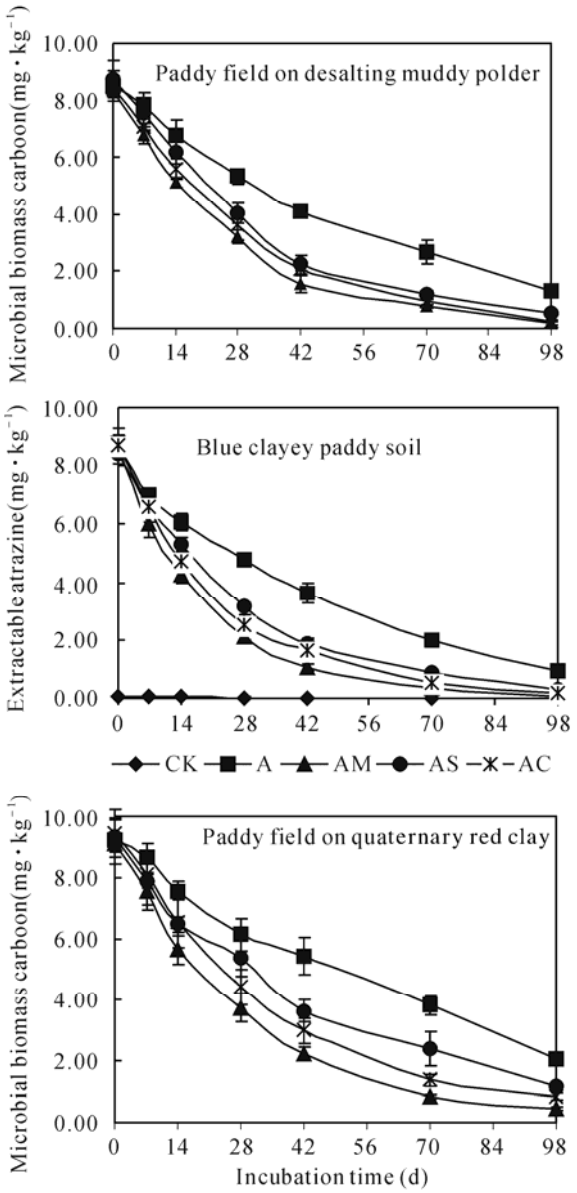

Fig. 2 Changes of extractable atrazine residues with incubation time in three soils treated with different organic amendments. For abbreviations see Table 2

the microor-ganisms in the organic amendments played a significant role in the biodegradation of atrazine. It seemed that a large number of microorganisms and a large amount of nutrients (nitrates and phosphates) were introduced into the soils with the application of decomposed pig manure, which contributed to the enhancement of microbial activity and biodegradation of atrazine. Organic matter has been found to increase pesticide degradation by stimulating microbial activity in several earlier studies (Topp *et al.*, 1996; Entry *et al.*, 1995). For instance, poultry litter contained a large number of microorganisms and large amounts of nutrients that contributed to enhanced bioremediation of soil organic contaminants (Gupta and John, 1996). In addition, the application of organic amendments might decrease the soil concentration of extractable atrazine by increasing atrazine sorption in soil and the subsequent formation of bound or non-extractable residues (Sabine *et al.*, 1998; Gian and John, 1996). It was likely that atrazine was adsorbed to a greater extent in soils amended with decomposed pig manure than with straw residues, as found in a previous study (Abdelhafid *et al.*, 2000). Sorption of pesticides by organic matter from sludge was shown to affect their bioavailability and spatial and temporal distribution patterns (Scow, 1996).

Table 2 Kinetic equations and half-lives ($T_{1/2}$) for atrazine degradation in paddy soils amended with different organic materials

Soil[a]	Treatment[b]	Kinetic equation of degradation[c]	r [d]	variance explained (%)	$T_{1/2}$ (d)[e]
PMP	A	$Y=9.4995e^{-0.0146x}$	-0.9721**	94.5	36.6aA
	AM	$Y=8.9537e^{-0.0329x}$	-0.9803**	96.1	17.9cC
	AS	$Y=9.1717e^{-0.0207x}$	-0.9654**	93.2	24.5bB
	AC	$Y=9.2517e^{-0.0257x}$	-0.9690**	93.9	19.4cC
BCP	A	$Y=8.6416e^{-0.0221x}$	-0.9726**	94.6	30.2aA
	AM	$Y=8.4758e^{-0.0484x}$	-0.9920**	98.4	14.0dD
	AS	$Y=8.375e^{-0.0338x}$	-0.9929**	98.6	20.3bB
	AC	$Y=8.3485e^{-0.034x}$	-0.9935**	98.7	17.6cC
PRC	A	$Y=8.8523e^{-0.0185x}$	-0.9628**	92.7	45.7aA
	AM	$Y=8.6887e^{-0.0377x}$	-0.9545**	91.1	22.3dD
	AS	$Y=8.8541e^{-0.0289x}$	-0.9803**	96.1	32.3bB
	AC	$Y=9.1379e^{-0.0351x}$	-0.9701**	94.1	27.9cBC

[a] PMP, Paddy field on desalting muddy polder; BCP, Blue clayey paddy soil; PRC: Paddy field on quaternary red clay.

[b] A, 10 mg atrazine·kg^{-1} soil; AM, 10 mg atrazine·kg^{-1} soil + 10 g decomposed pig manure·kg^{-1} soil; AS, 10 mg atrazine·kg^{-1} soil + 10 g rice straw·kg^{-1} soil; AC, 10 mg atrazine·kg^{-1} soil + 10 g Chinese Clover·kg^{-1} soil.

[c] Y, the content of methanol-extractable atrazine residues in soils (mg·kg^{-1}); x: incubation times.

[d] ** Correlation is significant at 0.01 probability level.

[e] Different letters A, B, C and D indicate significant difference at 0.01 probability level, and a, b, c, and d. at 0.05 probability level.

The rate of atrazine dissipation was always faster at the early stages of incubation, and variations were found among soil types. In BCP, atrazine loss occurred sooner and the rate of dissipation was greater than that in PMP and PRC, and the most rapid degradation of atrazine was found at 7 d after incubation, reaching 37.9%, 29.7% and 24.8% in the treatments of decomposed pig manure, Chinese clover and rice straw, respectively. In comparison, the rapid degradation of atrazine was reached after 14 d incubation in PMP and PRC, and the corresponding losses were 23.6%, 19.7%, and 21.4% for PMP, and

27.3%, 20.2% and 22.3% for PRC, respectively. No apparent lag was noticeable during the course of atrazine dissipation from any of the treated BCP soils, indicating that atrazine biodegradation in the amended BCP soils was relatively fast and commenced immediately. However, a lag phase was found in amended PMP and PRC soils, and the highest atrazine loss was around 14 d after the treatment. Any lag period after the commence-ment of incubation was followed by an increase in the atrazine dissipation rate, indicating the development of a microflora adapted to the mineralization of the atriazine ring structure. This further suggested that the size of microbes responsible for degradation of atrazine was substantially larger in BCP than in PMP or PRC.

Conclusions

The application of organic materials evidently increased soil microbial biomass in the tested soils and accelerated the degradation of atrazine regardless of the soil type. The measured SMBC level was closely related to the physicochemical characteristics of the soils and the type of organic amendment. The effect of organic amendment on the rate and dynamics of atrazine degradation in the soils varied in relation to the type of organic amendments, soil texture, and pH. The findings of this study provide implications for understanding the fate and risks of pesticides such as atrazine in paddy soils because application of organic materials in agricultural fields is a traditional practice in many regions of China and is gaining popularity in other production regions. On the other hand, treatment of pesticides such as atrazine might affect nutrient cycling and soil microbial ecology in amended soils, which might influence the overall chemical and biological quality of soil.

Acknowledgments

This work was jointly supported by the National Key Technologies R&D Program of China (2006 BAD17B06), the National Natural Science Foundation for Distinguished Young Scholars of China (Grant No. 40425007), and the Science and Technology Projects of Zhejiang Province (2009C33119).

Rerefences

Abdelhafid R, Houot S, Barriuso E (2000) Dependence of atrazine degradation on C and N availability in adapted and non-adapted soils. Soil Biol. Biochem. 32: 389-401

Alvey S, Crowley DE (1995) Influence of organic amendments on biodegradation of atrazine as a nitrogen source. J. Environ. Qual. 24: 1156-1162

Anderson TH, Domsch KH (1989) Ratio of microbial biomass carbon to total organic carbon in arable soils. Soil Biol. Biochem. 21: 471-479

Anderson TH, Domsch KH (1990) Application of eco-physiological quotients (qCO2) and qD) on microbial biomass from soils of different cropping histories. Soil Biol. Biochem. 22: 251-255

Assaf NA, Turco RF (1994) Accelerated biodegradation of atrazine by a microbial consortium is possible in culture and soil. Biodegradation 5: 29-35

Barriuso E, Houot S (1996) Rapid mineralization of the s-triazine ring of atrazine in soils in relation to soil management. Soil Biol. Biochem. 28: 1341-1348

Behki RM, Khan SU (1986) Degradation of atrazine by Pseudomonas: N-dealkylation and dehalogenation of atrazine and its metabolites. J. Agr. Food Chem. 34: 746-749

Brookes PC, Powlson DS, Jenkinson DS (1982) Measurement of microbial biomass phosphorus in soil. Soil Biol. Biochem. 14: 319-329

Chilima J, Huang CY, Wu CF (2002) Microbial biomass carbon trends in black and red soils under single straw application: effect of straw placement, mineral N addition and tillage. Pedosphere 12: 59-72

Cook AM, Hütter R (1981) s-Triazines as nitrogen sources for bacteria. J. Agr. Food Chem. 29: 1135-1143

Entry JA, Emmingham WH (1995) The influence of dairy manure on atrazine and 2, 4-dichlorphenoxy acetic acid mineralization in pasture soils. Can. J. Soil Sci. 75: 379-383

Entry JA, Mattson KG, Emmingham WH (1993) The influence of nitrogen on atrazine and 2, 4-dichlorophenoxyacetic acid mineralization in grassland soils. Biol. Fert. soils 16: 179-182

Esser HO, Dupuis G, Ebert E, Marco GJ (1975) s-Triazines. In Kearney, P. C. (eds.), Herbicides, Chemistry, Degradation and Mode of Action, Vol. 1. Marcel Dekker, New York pp. 129-208

Gian G, John B (1996) Biodegradation of atrazine in soil using poultry litter. J. Hazard. Mater. 45: 185-192

Gupta G, John B (1996) Biodegradation of atrazine in soil using poultry litter. J. Hazard. Mater. 45: 185-192

Haider K (1992) Problems related to the humiliation processes in soils in temperate climates. Soil Biol. Biochem. 7: 55-94

Hance RJ (1973) The effect of nutrients on the decomposition of the herbicides atrazine and linuron incubated with soil. Pesticide Science 4: 817-822

Hassink J (1994a) Effects of soil texture and grassland management on soil organic C and N and rate of C and N mineralization. Soil Biol. Biochem. 26: 1221-1231

Hassink J (1994b) Effect of soil texture on the size of the microbial biomass and on the amount of C and N mineralization per unit of microbial biomass in Dutch grassland soils. Soil Biol. Biochem. 26: 1577-1581

Howard PH (1991) Handbook of environmental fate and exposure data: Organic Chemicals, Vol. III, Lewis Publishers, Chelsea, MI, pp. 31

Jenkinson DS, Ladd JN (1981) Microbial biomass in soils: measurement and turnover. In: Paul EA, Ladd JN (eds.), Soil Biochemistry, Marcel Dekker, New York pp. 415-471

Kaufman DD, Kearney PC (1970) Microbial degradation of s-triazine herbicides. Residue Reviews 32: 235-265

Kirchner MJ, Wollum AG, King LD (1993) Soil microbial populations and activities unreduced chemical input agro-ecosystems. Soil Sci. Soc. Am. J. 57: 1007-1012

Mandelbaum RT, Allan DA, Wackett LP (1995) Isolation and characterization of a Pseudomonas sp. that mineralizes the s-triazine herbicide atrazine. Appl. Environ. Microb. 61: 1451-1457

Mandelbaum RT, Wackett LP, Allan DL (1993) Mineralization of the s-triazine ring of atrazine by stable bacterial mixed cultures. Appl. Environ. Microb. 59: 1695-1701

McGill WB, Cannon KR, Robertson JA (1986) Dynamics of soil microbial biomass and soluble carbon in Breton L after 50 years cropping to two rotations. Can. J. Soil Sci. 66: 1-19

Qiao XW, Ma LP, Hummel HE (1995) Pathways of atrazine degradation in soils and effects on the persistence of atrazine. Rural Eco-Environment 11: 5-8 (in Chinese)

Radosevich M, Traina SJ, Hao YL (1995) Degradation and mineralization of atrazine by the white rot fungus Phanerochaete Chrysosporium. Appl. Environ. Microb. 60: 705-708

Rahima A, Sabine S, Enrique B (2000) Dependence of atrazine degradation on C and N availability in adapted and non-adapted soils. Soil Biol. Biochem. 32: 389-401

Sabine H, Enrique B, Valerie B (1998) Modifica-tions to atrazine degradation pathways in a loamy soil after addition of organic amendments. Soil Biol. Biochem. 30: 2147-2157

Sarathchandra SU, Perrot KW, Boase MR, Waller JE (1988) Seasonal change and the effects of fertilizers on some chemical, biochemical and microbiological characteristics of high-producing pastoral soil. Biol. Fert. soils 6: 328-335

Scow KM (1996) Effect of sorption-desorption and diffusion processes on the kinetics of biodegra-dation of organic chemicals in soil. Soil Sci. Soc. Am. J. 32: 73-114

Shen QR, Xu SM, Shi RH (1993) Effect of incorporation of wheat straw and urea into soil on biomass nitrogen and nitrogen supplying characteristic of paddy soil. Pedosphere 3: 205-205

Shinjiro K, Susumu A, Yasuo T (1988) Effect of fertilizer and manure application on microbial number, biomass, and enzyme activities in volcanic ash soils. I. Microbial numbers and biomass soils. Soil Sci. Plant Nutr. 34: 429-439

Stucki G, Yu CH, Baumgartner T, Gonzalez-Valero JF (1995) Microbial atrazine minera-lization under carbon limited and denitrifying conditions. Water Res. 29: 291-296

Topp E, Tessier L, Gregorich EG (1996) Dairy manure incorporation stimulates rapid atrazine mineralization in an agricultural soil. Can. J. Soil Sci. 76: 403-409

Vance ED, Brookes PC, Penkinson DS (1987) An extraction method for measuring soil microbial biomass C. Soil Biol. Biochem. 19: 703-707

Vanderheyden V, Debongnie P, Pussemier L (1997) Accelerated degradation and mineralization of

atrazine in surface and subsurface soil materials. J. Pestic. Sci. 49: 237-242

Witter A, Kannal A (1998) Characteristics of the soil microbial biomass in soils from a long-term field experiment with different levels of C input. Appl. Soil Ecol. 10: 37-49

Wu J, Joergensen RG, Pommerening B, Brookes PC (1990) Measurement of soil microbial biomass C by fumigation extraction —an automated procedure. Soil Biol. Biochem. 22: 1167-1169

Xu YR, Gu XX (1995) Effect of refuse compost on soil microbes. Chinese Journal of Applied Environmental Biology 1: 308-402 (in Chinese)

Yanze-Kontchou C, Gschwind N (1994) Mineralization of the herbicide atrazine as a carbon source by a Pseudomonas strain. Appl. Environ. Microb. 60: 4297-4302

Session 4

Environmental Nanoparticles: Distribution, Formation,Transformation, Structural and Surface Chemistry,and Biogeochemical and Ecological Impacts

Soil Science at the Nanoscale: A New View of Structure, Stability, and Reactivity

Patricia A. Maurice*

Dept. of Civil Engineering & Geological Sciences, University of Notre Dame, Notre Dame, IN 46556, USA.
*Corresponding author. Tel. No. (574)-210-0244; E-mail: pmaurice@nd.edu.

Abstract: A revolution is occurring in science and technology as new methods and approaches allow scientists and engineers to investigate materials and processes at the nanoscale and to engineer new nanomaterials. Materials from ~1 to 100 nm in size, where 1 nanometer = 10^{-9} m, or 10Å, are generally considered to be nanomaterials. Nanomaterials are uquitous in near-Earth-surface environments, and often have properties that are distinct from those of single, small molecules or of larger, bulk materials. Many of the key components of soils, such as humic substances; iron, aluminum, and manganese oxides; and aluminosilicate clays may occur as nanoparticles or with nano-scale components or domains.This presentation will define terminology in the field of nanoscience and nanotechnology as applied to soil science, and will describe some of the special properties and behaviors of nanomaterials in soils, drawing primarily from examples of Fe (hydr)oxides. The presentation will emphasize the importance of nanoscience as a new frontier in soil science, along with how the unique experience of soil scientists can benefit broader nano-scale research.

Keywords: Nanoparticle; Hematite; Stability; Sorption

A Brief Introduction to Nanoscience

Nanoscience is a new interdisciplinary field that has evolved as scientists have come to understand that within the range of 1 to ~ 100 billionths of a meter, known as the nanoscale, materials may display properties and behaviors that are unique with respect to individual (small) molecules and bulk systems. Application of a variety of approaches such as transmission electron microscopy (TEM), scanning probe microscopy (SPM) and spectroscopy, X-ray absorption spectroscopy (XAS) and various types of modeling coupled with systematic study of the effects of size on structure and reactivity is allowing us to begin to understand nanomaterials.

One common definition of a *nanoparticle* is any ultrafine particle that is between 1 and 100 nanometers in size; this size limit is sometimes applied to just 2 dimensions. Banfield and Zhang (2001) suggested that the upper limit to the size of a *nanoparticle* might be defined based on the size at which fundamental properties differ from those of the corresponding bulk material. According to Hochella *et al.* (2008), the size range in which particles of Earth materials behave differently is often between 1 and at most several tens of nanometers.

Hochella *et al.* (2008) defined *nanominerals* as minerals such as ferrihydrite that only exist in the nanoparticle size range, or clays that only exist with at least one nanoscale dimension. They defined *mineral nanoparticles* as minerals that are in the nano-size range, but that also exist at larger sizes.

Many of the key components of soils, such as humic substances; iron, aluminum, and manganese oxides; and aluminosilicate clays may occur as nanoparticles or with nano-scale components or domains (e.g., Maurice and Hochella, 2008). Viruses generally are nanoparticles, and other microorganisms such as bacteria may have nano-scale features such as flagella (nanometer scale in thickness but potentially micron-scale in length) and may precipitate nanominerals or mineral nanoparticles. The nanotechnology industry is

releasing an enormous number of new nanomaterials into a vast array of products. These nanomaterials are making their way into the environment; yet, we do not yet know their environmental consequences.

Nanoparticle Surface Area and Surface Free Energy

Nanoparticles have high specific surface areas and a significant proportion of atoms associated with nanoparticles thus occur at or near surfaces. The high specific surface area means that surface free energy is a significant component of the overall free energy of a nanoparticle. For small nanoparticles with high specific surface area, anything that affects surface free energy, such as the pH of a suspension or the presence and concentration of adsorbed molecules or ions, can affect overall nanoparticle stability.

Nanoparticle Size and Stability

Classical mineral nucleation theory suggests that nanoparticles in aqueous environments should be highly unstable and should evolve into larger, more stable crystals. Yet, many nanoparticles can remain stable for long periods of time, even in suspension. Particle size and stability can be related in a complex manner at the nanoscale, and these observations need to be fit into a new theoretical framework.

Navrotsky and her colleagues (e.g., Navrotsky, 2001; Navrotsky, 2003; Navrotsky *et al.*, 2008) are demonstrating that both kinetics and thermodynamics can play a role in nanoparticle longevity. As Navrotsky (2008, pers. commun.) has argued, in order to determine the controls on mineral nanoparticle stability as a function of size, one would ideally like to be able to grow nanoparticles of a given mineral phase in which the size alone changes, independent of the structure or composition. However, for many phases, it is impossible to change size without simultaneously changing structure and/or hydration (e.g., Navrotsky *et al.*, 2008). Nanoparticles in the 1 to ~10 nm size range have a high proportion of total atoms at or very near the surface, and these atoms experience different bonding environments than atoms of the same mineral in the bulk of a larger crystal. For very small mineral nanoparticles, the high proportion of surface and near-surface atoms can make it virtually impossible to change size independently of structure and/or composition.

Particle size and hydration can play a key role in determining the relative stabilities of hematite and goethite of different nanoparticle sizes (Navrotsky *et al.*, 2008). Surface enthalpy and free energy are generally much higher for anhydrous oxides such as hematite than for oxyhydroxides such as goethite. The lower surface enthalpy/energy for goethite allows this mineral to be stabilized relative to hematite at particle size < ~60 nm. Although micron-scale hematite particles in water tend to be more stable than goethite, the nanoparticles of goethite tend to be more stable than hematite nanoparticles. These equilibrium relationships are sensitive to temperature, the activity of water, Al substitution, and likely many other factors, as well.

Reactivity: Adsorption, Dissolution, and Redox Phenomena

Because the surface properties of nanoparticles change with particle size, we can expect the behaviors of nanoparticles with respect to sorption and dissolution to vary with size.

Ha *et al.* (2009) showed that (surface) precipitates of Zn occurred on nanoparticulate hematite but not on micron-scale hematite particles under otherwise identical conditions. Barton *et al.* (in prep.) showed that sorption of Pb to hematite nanoparticles varied with nanoparticle size and shape and that dissolution rate of hematite nanoparticles < 10 nm in diameter was considerably faster than that of larger particles, when normalized to surface area.

When studying the size, structure, and reactivity of mineral nanoparticles, it is important to consider shape factors because mineral nanoparticles of different shapes may present different crystallographic surfaces, proportionately, to solution. Surface topography can also be important, but is often difficult to characterize for nanoparticles.

Size quantization of the electron structure, coupled with changes to surface structure and surface defect site density of nanoparticles, may lead to different rates of electron transfer in redox reactions. Madden and Hochella (2005) showed that the rate of heterogeneous manganese oxidation by hematite nanoparticles was up to 1½ orders of magnitude greater for 7.3 nm average diameter particles than for

37 nm particles. Their investigation took into account differences in surface area in the rate calculations.

Summary and Conclusions

Although surface scientists have long understood that very small particles have unique properties and require specialized techniques of investigating, it is only within the last few decades that nanoscience has advanced to the point where we can study soil nanomaterials in a systematic fashion. These new studies are helping us to understand apparent discrepancies in previous data sets and forming the framework for new theoretical understandings. It is important that soil scientists take a leadership role in understanding the structures and reactivities of both natural and man-made nanoparticles as well as the complex behaviors of nanoparticles in the environment.

Acknowledgments

P. Maurice thanks the NSF-funded (grant EAR02-21966) Environmental Molecular Science Institute at the University of Notre Dame for funding her group's nano-scale environmental research. She thanks Andrew Quicksall, Tom Kosel, Lauren Barton, and Erin Hunter at the University of Notre Dame for collaborative research and discussion on nanoparticles in the environment.

References

Banfield JF, Zhang H (2001) Nanoparticles in the Environment. Chapter 1, In: Banfield JF, Navrotsky A (eds.) Nanoparticles and the Environment. Mineralogical Society of America, Washington, DC. pp. 1-58

Barton L, Quicksall A, Kosel T, Maurice PA (in prep.) Effects of nanoparticle size on sorption and dissolution

Ha JY, Trainor TP, Farges F, Brown GE (2009) Interaction of Aqueous Zn(II) with Hematite Nanoparticles and Microparticles. Part 1. EXAFS Study of Zn(II) Adsorption and Precipitation. Langmuir 25: 5574-5585

Hochella MF, Jr., Lower SK, Maurice PA, Penn RL, Sahai N, Sparks DL, Twining BS (2008) Nanominerals, mineral nanoparticles, and Earth chemistry. Science 21: 1631-1635

Madden AS, Hochella MF, Jr. (2005) A test of geochemical reactivity as a function of mineral size: Manganese oxidation promoted by hematite nanoparticles. Geochim. Cosmochim. Acta 69: 389-398

Maurice PA, Hochella MF, Jr. (2008) Nanoscale particles and processes: A new dimension in soil science. 100th Anniversary edition, Adv. Agron. 100: 123-153

Navrotsky A (2001) Thermochemistry of Nanomaterials. Chapter 3, In: Banfield JF and Navrotsky A (eds.) Nanoparticles and the Environment. Reviews in Mineralogy and Geochemistry 44. Mineralogical Society of America and Geochemical Society, Washington, D.C. pp.73-103

Navrotsky A (2003) Energetics of nanoparticle oxides: interplay between surface energy and polymer-phism. Geochem. Transact. 4: 34-37

Navrotsky A, Mazeina L, Majzslan J (2008) Size-driven structural and thermodynamic complexity in iron oxides. Science 319: 1635

Environmental and Colloidal Behavior of Engineered Nanoparticles

Baoshan Xing*

Department of Plant, Soil and Insect Sciences, University of Massachusetts, Amherst MA 01003, USA.
*Corresponding author. Tel. No. 1-413-545-5212; Fax No. 1-413-545-3958; E-mail: bx@pssci.umasss.edu.

Abstract: Engineered nanoparticles (ENPs) are increasingly used in various industries and can be readily found in the products surrounding our everyday life. They are increasingly attracting attention from scientists, government regulators, and the public due to the concern over their potential toxicity and harms. Because of the widespread use of ENPs, they are most likely to release into the environment; however, scientific understanding on their environmental fate and behavior is very limited. Therefore, environmental and colloidal behaviors of carbon nanotubes (CNTs), fullerene, and oxide nanoparticles were examined using various spectroscopic and microscopic techniques. CNTs could greatly adsorb organic contaminants including PAHs and endocrine disrupting compounds, which may affect the toxicity and fate of both CNTs and organic contaminants in the environment. Adsorption mechanisms are also discussed. Dissolved organic matter (DOM) is able to adsorb on both CNTs and oxide ENPs, thus could increase their dispersion and suspension stability. Preliminary data demonstrate that oxide ENPs are more toxic than their bulk counterparts to nematode (*C. elegans*) and three bacteria species. Also, ZnO ENPs could inhibit plant growth and may be taken up by plant. This work highlights the importance of a better understanding of environmental impact of ENPs and calls for safe design, development, and use of nanoparticles.

Keywords: Nanoparticle; Adsorption; Contaminant; Toxicity; Colloidal stability; Organic matter

Introduction

Nanotechnology is to control, understand and use matter at a scale of 1 to 100 nm in any dimension. This technology is one of the most promising ones in this century along with biotechnology. With rapid development and wide application of nanotechnology, engineered nanoparticles (ENPs) can be seen in the products of our daily life such as socks, paints, lotion, shampoo (to just list a few) and in other industry uses (e.g., biomedical and catalytic). Therefore, ENPs will likely be introduced to the environment through production, use, and disposal (Klaine *et al.*, 2008). As a matter of fact, nano-TiO_2 particles were detected in the receiving water from the house facades where nano-TiO_2 containing paint was used (Kaegi *et al.*, 2008). From toxicological studies, many ENPs can be toxic and harmful (Kagan *et al.*, 2005; Medina *et al.*, 2007; Roberts *et al.*, 2007; Nowack and Bucheli, 2007). However, available data on ENPs in the environment are scarce. Therefore, in this paper, environmental and colloidal behavior of ENPs are examined and reported.

Materials and Methods

Carbon-based ENPs, multi-walled carbon nanotubes (MWCNT), single-walled carbon nanotubes (SWCNT) and fullerene (C_{60}), and oxide ENPs (Al_2O_3, ZnO, TiO_2) were used. Several humic acids (HA) were extracted and used to coat and suspend ENPs. Polyaromatic hydrocarbons (PAHs, naphthalene, phenanthrene, pyrene) and endocrine disrupting compounds (e.g., 17α-ethinyl estradiol and bisphenol A) were used as adsorbates (Yang and Xing, 2009; Pan *et al.*, 2008). In addition, plants, bacteria and nematodes were selected for ENPs toxicity tests (Lin and Xing, 2008a; Wang *et al.*, 2009; Jiang *et al.*, 2009). Adsorption isotherms were obtained by a batch

equilibration technique. Colloidal stability, particle size, and zeta potentials of ENPs suspensions were examined with a Zetasizer. Colloidal stability was also investigated as affected by pH and the presence of cation and dissolved organic matter (Ghosh *et al.*, 2008). TEM, AFM, and XPS were used to characterize ENPs. NMR and FTIR were used to characterize HA and HA-coated ENPs (Yang and Xing, 2009). Detailed characterization, measurement procedures, and the properties of selected ENPs can be in the references cited above.

Results and Discussion

All sorption isotherms (phenanthrene, naphthalene, pyrene, 17α-ethinyl estradiol) on carbon nanotubes (CNTs) were nonlinear and fit well by Polanyi-Manes model. Sorption capacity of organic chemicals by CNTs was very high and generally increased with decreasing diameter of CNTs. SWCNT had higher sorption capacity than MWCNT while fullerene had the lowest capacity. Adsorption of PAHs by the CNTs used in this study did not have any significant hysteresis, which along large sorption capacities may pose high health and environmental risk once PAH-laden CNTs are inhaled and ingested. However, 17α-ethinyl estradiol and bisphenol A showed strong hysteresis due possibly to enhanced π-π interaction and re-organization of CNT aggregates, indicating that CNTs may be potentially used for water treatment (Pan *et al.*, 2008).

ZnO nanoparticles (NPs) significantly inhibited root growth of ryegrass and reduced the biomass relative to the control, thus were toxic to ryegrass and perhaps other plants, too. In addition, ZnO NPs appear to be taken up by the plant root and internalized in the root cells as shown in the TEM images (Lin and Xing, 2008). For the nematode experiments, Al_2O_3 and TiO_2 NPs were clearly more toxic than their bulk particle counterparts (Wang *et al.* 2009). Similarly, Al_2O_3 and ZnO NPs demonstrated higher toxicity to several bacteria species than the bulk counterparts even with the same chemical composition (Jiang *et al.*, 2009).

CNTs have hydrophobic surfaces, and strongly aggregate and settle down in water. However, dissolved organic matter (DOM) could adsorb on CNTs and promote the dispersion of CNTs and their aqueous stability. We clearly observed that tannic acid used as a surrogate of DOM substantially increased the suspendability and stability of CNTs in water (Lin and Xing, 2008b). In addition, surface oxidation of CNTs increased the polar functional group content and possibly shortened the tube length, as a result, greatly increased the suspension stability. DOM- and oxidation-facilitated suspension of CNTs will potentially increase their mobility and exposure of CNTs in aquatic systems.

We extensively studied how pH and DOM affect colloidal behavior of Al_2O_3 NPs. The surface charge of the NPs decreased with increasing pH and reached the point of zero charge (ZPC) at pH 8. Surface charge of the NPs also decreased with the addition of HA. The NPs aggregated at pH around the ZPC, but were stable at pH being far away from the ZPC. Colloidal stability was strongly enhanced in the presence of HA (DOM) at the pH of ZPC or above it, but in acidic conditions NPs showed strong aggregation in the presence of HA due to charge neutralization (Ghosh *et al.*, 2008). HA-coated Al_2O_3 NPs were much stable in water than the pure NPs. Aggregation of a few Al_2O_3 NPs can be seen on the Ca^{2+}-saturated mica surface while HA-coated Al_2O_3 NPs were well dispersed (Fig. 1). Later extracted HA-coated NPs required much higher Ca^{2+} concentration to flocculate than the first extracted HA-coated NPs, strongly suggesting that physico-chemical characteristics of DOM affect colloidal stability of ENPs, and thus, potentially their mobility, bioavailability and toxicity in the environment.

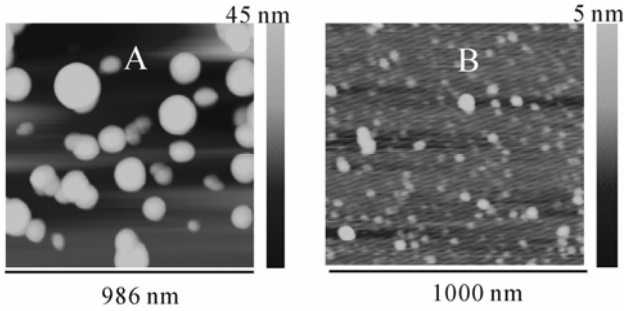

Fig. 1 AFM height images of pure (A) and HA-coated (B) Al_2O_3 NPs on Ca^{2+}-saturated mica surface. HA coating decreased the size and increased the colloidal stability of the NPs

Acknowledgement

I very much thank all the talented students, postdoctoral research fellows, and visiting scientists in

the lab for their contribution to this nanoparticle research.

References

Ghosh S, Mashayekhi H, Pan B, Bhowmik P, Xing B (2008) Colloidal behavior of aluminum oxide nanoparticles as affected by pH and natural organic matter. Langmuir 24(21): 12385-12391

Jiang W, Mashayekhi H, Xing B (2009) Bacterial toxicity comparison between nano- and micro-scaled oxide particles. Environ. Pollut. 157: 1619-1625

Kaegi R, Ulrich A, Sinnet B, Vonbank R, Wichser A, Zuleeg S, Simmler H, Brunner S, Vonmont H, Burkhardt M, Boller M (2008) Synthetic TIO_2 nanoparticle emission from exterior facades into the aquatic environment. Environ. Pollut. 156: 233-239

Kagan VE, Bayir H, Anna A, Shvedova AA (2005) Nanomedicine and nanotoxicology: two sides of the same coin. Nanomedicine: Nanotechnology, Biology, and Medicine 1: 313-316

Klaine SJ, Alvarez PJJ, Batley GE, Fernades TF, Handy RD, Lyon DY, Mahendra S, McLaughlin MJ, Lean JR (2008) Nanomaterials in the environment: behavior, fate, bioavailability and effects. Environ. Toxicol. Chem. 27: 1825-1851

Lin DH, Xing B (2008a) Root uptake and phytotoxicity of ZnO nanoparticles. Environ. Sci. Technol. 42(15): 5580-5585

Lin DH, Xing B (2008) Tannic acid adsorption and its role for stabilizing carbon nanotube suspensions. Environ. Sci. Technol. 42(15): 5917-5923

Medina C, Santos-Martinez MJ, Radomski A, Corrigan OI, Radomski MW (2007) Nanoparticles: pharmacological and toxicological significance. Br. J. Pharmacol. 150: 552-558

Nowack B, Bucheli TD (2007) Occurrence, behavior and effects of nanoparticles in the environment. Environ. Pollut. 150: 5-22

Pan B, Lin DH, Mashayekhi H, Xing B (2008) Adsorption and hysteresis of bisphenol A and 17α-ethinyl estradiol on carbon nanomaterials. Environ. Sci. Technol. 42(15): 5480-5485

Roberts AP, Mount AS, Seda B, Souther J, Qiao R, Lin SJ, Ke PC, Rao AM, Klaine SJ (2007) In vivo biomodification of lipid coated carbon nanotube by Daphnia magna. Environ. Sci. Technol. 41: 3025-3029

Yang K, Xing B (2009) Sorption of phenanthrene by humic acid-coated nanosized TiO_2 and ZnO. Environ. Sci. Technol. 43(6): 1845-1851

Wang HH, Wick RL, Xing B (2009) Toxicity of nanoparticulate and bulk ZnO, Al_2O_3 and TiO_2 to the nematode *Caenorhabditis elegans*. Environ. Pollut. 157: 1171-1177

Humic Substances as Natural Nanoparticles Ubiquitous in the Environment

Nicola Senesi*

Department of Agroforestal and Environmental Biology and Chemistry, University of Bari,
Via Amendola, 165/A, 70126-Bari, Italy.
*Corresponding author. E-mail: senesi@agr.uniba.it.

Humic substances (HS) are recognized to be the most widespread and ubiquitous components of natural nonliving organic matter (NOM) in the global environment. The estimated level of soil organic carbon (SOC) on the earth surface occurring as HS is 30×10^{14} Kg. In particular, approximately 60%~70% of the total SOC has been estimated to occur in HS. These substances consist of a physically and chemically heterogeneous mixture of relatively high-molecular weight, yellow to black organic compounds of mixed aliphatic and aromatic nature, formed by secondary synthesis reactions (humification) of products of the microbial and chemical decay and transformations of biomolecules released from organisms into the surrounding environment both during life and after death. The HS are universally recognized as the most relevant and chemically, biologically and physically active components of NOM thanks to their typical composition, macromolecular structure, polyfun-tionality, surface properties, presence of multiple reactive sites, variable sizes and shapes, and intrinsic porosity. Further, several studies have demonstrated that HS are able to interact efficiently with various organic pollutants (OPs) in soil through various mechanisms and processes, among which the most important is adsorption, and that this action is increased markedly upon addition to soil of organic amendments rich in HS, such as composts. Nowadays, engineered (or synthetic) nanoscale materials (nanoparticles, NP) are increasingly used, or proposed to be used, for soil decontamination by adsorption/ rapping of various OPs. This, thanks to their appropriate average dimensions (ranging from 1 to 100 nm), high porosity and hydrophobic surfaces. However, the ascertained toxicity to organisms of these engineered NPs is posing increasing serious concerns for human and environmental exposure. Based on the intrinsic chemical and physical properties of HS, including the average size (from about 1 nm to 1000 nm) and the typical cross-linked spatial networks containing highly-branched polymer chains exhibiting fractal features, HS can be qualified as natural NPs in the environment. In the first part of this presentation specific properties of HS which support their NP nature will be highlighted. In the second part, some preliminary comparative results will be discussed on the adsorption efficiency for a selected OP of various types of soils added with either a compost rich in HS or with a selected NP. Three different soils with various content of SOC (2.9%, 1.1%, and 0.4%) and different chemical properties have been considered, and adsorption of the polycyclic aromatic hydrocarbon pyrene, a very common OP, has been measured comparatively on each original soil, and on the soil added with either 1% of a compost rich in HS or 5% of the NP fullerene. Preliminary results show that: 1) in any case, the adsorption data for pyrene best fit into a Langmuir-type isotherm, which means that a maximum of adsorption, i.e., saturation, is reached by filling all available vacant sites; 2) as expected, the adsorption capacity for pyrene of the three soils, either in the absence or the presence of compost or fullerene, is a function of their original content in SOC; 3) for any soil, the values of adsorption distribution coefficients for pyrene, which are an indication of the adsorption capacity of the substrate for the OP, increase in the order: original soil<soil+fullerene soil+compost. These results indicate that the content of native SOC is the most important factor influencing the adsorption capacity of soil for pyrene, even if additional powerful sorbents,

such as compost or fullerene, are added. However, the addition of either a source of HS, such as compost, or an engineered NP, such as fullerene, is able to enhance at various extent the adsorption capacity of soil for pyrene. More important, the HS-rich compost appears more efficient than fullerene in enhancing the adsorption capacity of soil for pyrene. Thus, the compost amendment practice could be preferred to the application of engineered NPs to soil for OP decontamination purposes.

References

Senesi N, Miano TM (1994) Humic Substances in the Global Environment and Implications on Human Health. Elsevier, Amsterdam, pp. 1368

Loffredo E, Senesi N (2008) The role of natural organic matter (humic substances) on adsorption of pesticides possessing endocrine disruptor acitivity. In: Mehmetli E, Koumanova B (eds.), The Fate of Persistent Organic Pollutants in the Environment. NATO Sciences for Peace and Security Series-C: Environmental Security, Springer, pp. 369-383

Senesi N, Boddy L (2002) A fractal approach for interactions between soil particles and Microorganisms. In: Huang PM, Bollag JM, Senesi N (eds.), Interactions of Soil Particles and Microorganisms and their Impact on the Terrestrial Environment, IUPAC Series on Analytical and Physical Chemistry of Environmental Systems, Wiley, New York 8: 41-83

Senesi N, Loffredo E, D'Orazio V, Brunetti G, Miano TM, La Cava P (2001) Adsorption of pesticides by humic acids from organic amendments and soils. In: Humic Substances and Chemical Contaminants (Clapp CE, Hayes MHB, Senesi N, Bloom PR, Jardine PM, Eds.), Soil Science Soc. of America, Inc., Madison, WI, 129-153

Senesi N (1999) Aggregation patterns and macroolecular morphology of humic substances: a fractal approach. Soil Sci. 164: 841-856

Senesi N, Loffredo E (1999) The Chemistry of Soil Organic Matter. In: Sparks DL (ed.), Soil Physical Chemistry, 2nd Edit, CRC Press, Boca Raton, 239-370

Okuda I, Senesi N (1998) Fractal principles and methods applied to the chemistry of sorption onto environmental particles. In: Huang PM, Senesi N, Buffle J (eds.), Structure and Surface Reactions of Soil Particles, IUPAC Series on Anal. Phys. Chem. Environ. Systems, Wiley, New York, 77-105

Senesi N, Rizzi FR, Dellino P, Acquafredda P (1997) Fractal humic acids in aqueous suspensions at various concentration, ionic strength, and pH. Colloids Surfac. A 127: 57-68

Senesi N, Rizzi FR, Dellino P, Acquafredda P (1996) The fractal dimension of humic acids in aqueous suspension as a function of pH and time. Soil Sci. Soc. Am. J. 60: 1773-1780

Senesi N (1996) Fractals in general soil science and in soil biology and biochemistry. In: Stotzky G, Bollag JM (eds.), Soil Biochemistry M. Dekker, New York 9: 415-472

Senesi N, Miano TM (1995) The role of abiotic interactions with humic substances on the environmental impact of organic pollutants. In: Huang PM, Berthelin J, Bollag JM, McGill WB, Page AL (eds.), Environmental Impact of Soil Component Interactions. Natural and Anthropogenic Organics, CRC-Lewis, Boca Raton, I: 311-335

Senesi N (1993) Nature of interactions between organic chemicals and dissolved humic substances and the influence of environmental factors. In: Beck AJ, Jones KC, Hayes MHB, Mingelgrin U (eds.), Organic Substances in Soil and Water: Natural Constituents and their Influence on Contaminant Behaviour, Royal Society of Chemistry, Publ., London, 73-101

Senesi N (1993) Organic pollutant migration in soils as affected by soil organic matter. Molecular and mechanistic aspects. In: Petruzzelli D, Helfferich FG (eds.), Migration and Fate of Pollutants in Soils and Subsoils. NATO-ASI Series, Springer-Verlag, Berlin, G32: 47-74

Degradation of Organochlorine Compounds Using Zero Valent Iron (ZVI) Nano Particles Impregnated in Hydrophobic Modified Bentonite

Sandro Froehner*, M. Maceno, E.C. Da Luz, K.S. Machado, F. Falcão

Department of Environmental Engineering, Federal University of Parana, Curitiba-PR, 81531-980, Brazil.
*Corresponding author. Tel. No. +55 41 3361 3146; Fax No. +55 41 3361 3224; E-mail: froehner@ufpr.br.

Abstract: The degradation of perchloroethylene (PCE) adsorbed on hydrophobic modified bentonite was investigated. The degradation occurred via reduction of iron particles with zero valence (ZVI) incorporated in hydrophobic surface of bentonite. We compared two different systems, one containing ZVI and another without ZVI. The degradation of PCE was accompanied by decreasing concentrations of PCE and the increase of resulting compounds such as trichloroethylene (TCE), 1,2-dichloroethylene, trans and cis forms, (1,2-cis-DCE and 1,2-trans-DCE). The results show that the PCE is rapidly adsorbed and in contact with ZVI particles is degraded to less toxic compounds, while in the systems without ZVI no significant decrease of PCE was observed, clearly demonstrating that the degradation process occurs through the reduction with ZVI. The rate constant for the system containing ZVI was 0.215 h^{-1}, while for the system without ZVI it was only 0.031 h^{-1}. The results agree with other research, however the reaction was conducted in columns and the clay was zeolite. It can be concluded that the system impregnated with ZVI is extremely interesting as an alternative application for removal of organic compounds containing chlorine due to their persistence and toxic effect on the microorganisms. The system can also be applied as barrier content.

Keywords: Organochlorine compounds; Degradation; Nano particles; Iron oxidation; Barriers content; Bioavailability

Introduction

Organochlorine compounds are considered as persi-stent in the environment. Generally these organochlorine compounds are toxic to microorganisms and have low solubility. These characteristics contribute to high retention in the environment. However, such compounds as, for instance, perchloroethylene (PCE) can be decomposed by reduction with zero valent iron (ZVI) (Fig.1). However, organocompounds with chlrorine in their chemical structures can be accommodating in hydrophobic environments, for instance on the surface of hydrophobic modified clays. The hydro-phobic modified clays can be obtained thorough the replacement of mono valent cations, naturally present on clay surfaces by hydrophobic cations such as hexadeciltrymethylammonium (HDTMA). Although, the hydrophobic modified clay can adsorb hydro-phobic compounds, the degradation will take a long time. Recently, the degradation of organochlorine compounds has been investigated by reducing with ZVI. ZVI is an effective and low cost way to degrade such compounds. The process seems very efficient, however, it is still difficult to find and bring together such reagents in the same environment. Nevertheless, hydrophobic modified clays have the ability to retain little water-soluble compounds. In this work we attempt to use hydrophobically modified bentonite (HDTMA-BT) impregnated with ZVI nano particles. In this way hydrophobic environment can accommodate both the chlorine compounds and ZVI. Thus, bentonite was used in hydrophobic form impregnated with ZVI to degrade PCE. The intention was to construct a model for degradation of other toxic and persistent organochlorine compounds commonly found in the environment, which cause problems for the industry.

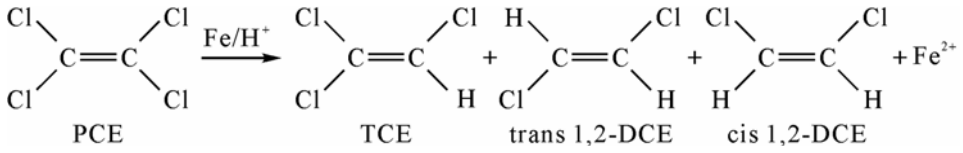

Fig.1 PCE reduction products by ZVI particles

Materials and Methods

All chemical reagents used in experiments were 99% pure and purchased from Sigma-Aldrich. The standards for chromatography (PCE, TCE, cis-DCE and trans-DCE) determination were purchased from AccuSatandards. The clay used in the experiments was bentonite kindly provided by local mining companies with the following chemical composition (given by the supplier): SiO_2 66%; Al_2O_3 23%; Fe_2O_3 0.99%; CaO 0.20%; MgO 0.62%; Na_2O 0.13%; K_2O 1.60%. The ZVI was prepared according to the procedures described by Sung *et al.* (2006). The ZVI was obtained through the reduction of Fe^{3+} by BH_4^-.

Bentonite Modification

The hydrophobic modified bentonite was synthesized by cation exchange with 10 mmol·L^{-1} hexadecyltrimethylammonium chloride (HDTMA) solution with thorough stirring; the detailed procedures are described in Froehner *et al.* (2009) and Li *et al.* (2006). The preparation consist in mixing clay and HDTMA (equally) with ZVI. The mixture was stirred for 8 h and then centrifuged. The other steps were similar for the preparation of modified bentonite, but absent of ZVI particles. The impregnation of ZVI was confir-med by scan electronic microscopy (MEV).

Batch Kinetics Studies

To accompany the degradation of PCE ten vials containing 0.5 g of HDTMA-BT with ZVI were set up to follow PCE degradation. In each vial 20 mL of a saturated solution of PCE were added. The bottles were closed. Each bottle corresponds to a kinetic point. For comparison and also control purposes a similar series was prepared, but without the reduction agent (ZVI).

Chemical Analysis

PCE, trichloroethylene (TCE), cis-1,2-Dichloroethylene (cis-1,2-DCE), and trans-1,2-Dichloroethylene (trans-1,2-DCE) concentrations were determined using an Schimadzu LC20A HPLC equipped with a 4.6- by 150-mm Thermo ODS column and a UV-Vis detector at 195 nm. The mobile phase was 70% acetonitrile/30% water. The detection limit was 0.05 mg·L^{-1} and the linear response range was up to 40 mg·L^{-1} for both PCE and TCE. Calibrations were also made in the concentration ranges of 0.044~3.5 mg·L^{-1} for cis-1,2-DCE, and 0.040~0.236 mg·L^{-1} for trans-1,2-DCE. All calibration curves using four to six standards had linear regression coefficients greater than 0.99. Accuracy and precision were determined by six to eight replicate analyses of a standard for each compound. Typical retention times for PCE, TCE, trans 1,2-DCE, and cis 1,2-DCE were 6.0, 3.8, 2.8, and 2.5 min, respectively. Other possible reduction products were analyzed, such as Cl^-. The chlorine and Fe^{2+} concentrations were determined by liquid chromatography Dionex DX-120 equipped with ionic conductivity detector.

Results and Discussion

The results of the PCE batch kinetics experiments are shown in Fig. 2. It is clear that the reduction in the presence of HDTMA-BT with ZVI was much more efficient than the reduction in the presence of HDTMA-BT alone. However, in the predominant process in the reduction by ZVI, according to the scheme in Fig. 1, some sorption may have occurred, with much intensity in process conducted in absence of ZVI (Froehner *et al.*, 2009b). HDTMA-BT impregnated with ZVI can rapidly decrease PCE concentration after contact between reagents. The PCE reduction followed a pseudo-first-order reaction confirmed by Fig. 2(b). It was also observed that the concentration of TCE was not significant, although it is one of the products formed. Along with the decrease of the PCE concen-tration and increased concentrations of other products formed, there was an

increase in the concentration of Fe^{2+} and Cl^- (not shown). The increased concentration of these products takes place concurrently with the decrease of PCE. The rate constant for PCE degrada-tion was 0.215 h^{-1} for the system containing ZVI and 0.031 h^{-1} for the system without ZVI. Bowman *et al.* (2005) found 0.136 h^{-1}. The literature has shown that the reduction rate of TCE was several times faster than that of PCE (Arnold and Roberts, 2000). The same behavior was also observed in experiments conducted in columns filled with modified clay and ZVI pellets (Li *et al.*, 2005). Wang and Farrell (2003) showed that the TCE reduction rate was controlled by its concentration and available atomic hydrogen, while the PCE reduction rate was controlled by electron transfer to chemisorbed PCE. For PCE reduction to occur, the first step is to form a p-bonded surface species (Arnold and Roberts, 2000). In this sorption step, the alkenes serve as the Lewis base and partially or fully oxidized metal ions represent the Lewis acid (Arnold and Roberts, 2000). On the SM-ZVI surface, the main group of sorbed HDTMA may serve as the Lewis acid, thus promoting the interaction. The sorbed PCE, after formation of a di-σ-bonded intermediate, may undergo either reductive β-elimina-tion producing dichloroacetylene, or hydrogenolysis resulting in TCE formation (Arnold and Roberts, 2000). The lack of significant TCE accumulation during PCE reduction has been attributed to predo-minantly β-elimination during PCE reduction (Arnold and Roberts, 2000). However, the lack of significant TCE accumulation in PCE reduction could also be interpreted as a faster TCE reduction rate compared to PCE.

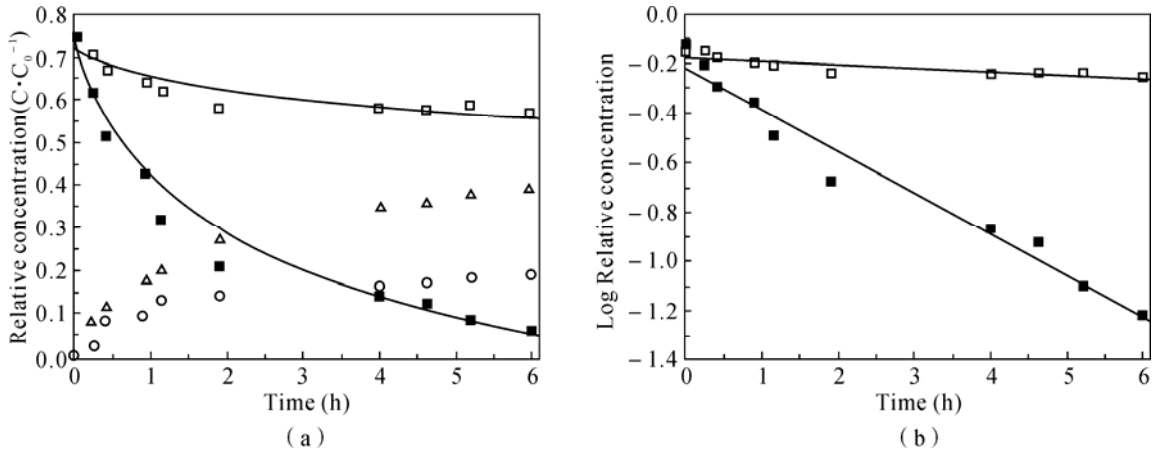

Fig. 2 (a) Decrease of PCE in the presence of ZVI (■) and without ZVI (□), increase of TCE (○) and cis and trans 1,2-DCE (△). (b) Decrease of PCE for systems with ZVI (■) and without ZVI (□) in semilog scale

Clearly, the results show that ZVI can degrade chlorine organic compounds adsorbed on hydrophobic surfaces such as hydrophobic modified clay. Thus, these clays are shown in promising environmental applications whose purpose is decontamination of the impacted areas with persistent organic compounds. It is also able to form a reactive barrier in decon-tamination or degradation of toxic organic compounds in products less toxic and more prone to microbial degradation or chemical reactions. Finally, the results indicate sorption of PCE onto hydrophobic surface and reduction by ZVI impregnated on HDTMA-BT. The sorption was almost instantaneous and readily suffered reduction into less toxic compounds.

References

Arnold WA, Roberts AL (2000) Pathways and kinetics of chlorinated ethylene and chlorinated acetylene reaction with Fe(0) particles. Environ. Sci. Technol. 34: 1794-1805

Froehner S, Furukawa W, Martins RF, Errera MR (2009) Water remediation by adsorption of phenol onto hydrophobic modified clay. Water Air Soil Poll. 199: 107-113

Froehner S, Machado KS, Falcão F (2009) Exploring

the adsorption of dibenzothiophene by vermiculite in hydrophobic form, impregnated with copper ions and in natural form. Water Air Soil Pollution. Submitted

Li Z, Willms C, Alley J, Zhang P, Bowman RS (2006) A shift in pathway of iron-mediated perchloroethylene reduction in the presence of sorbed surfactant—A column study. Water Research 40: 3811-3819

Sung HJ, Feitz AJ, Waite TD (2004) Oxidative degradation of the carbothioate herbicide, molinate, using nanoscale zero-valent iron. Environ. Sci. Technol. 38: 2242-2247

Wang J, Farrell J (2003) Investigating the role of atomic hydrogen on chloroethene reactions with iron using Tafel analysis and electrochemical impedance spectroscopy. Environ. Sci. Technol. 37: 3891-3896

Effect of Electrolyte on Adsorption/Desorption of Cu^{2+} on Nano-particle Mn Oxide

Wenfeng Tan[a,b,*], YuanPeng Wang[b], Fan Liu[b], Xionghan Feng[b]

[a] State Key Laboratory of Soil Erosion and Dryland Farming on the Loess Plateau, Institute of Soil and Water Conservation, CAS and MWR, Yangling, 712100, China;
[b] Key Laboratory of Subtropical Agriculture and Environment, Ministry of Agriculture, Huazhong Agricultural University, Wuhan, 430070, China.
[*]Corresponding author. E-mail: wenfeng.tan@hotmail.com.

Abstract: Oxides are the active and important component in soils and sediments. They are generally in fine particles and attached to surface of soil clay as a cutan or coating. Therefore, they play an important role in controlling chemical reactions of soil interface, and thus affect bioavailability and transformation of heavy metals in soils and sediments. At the common pH range of the natural environment, Fe and Al oxides possess positive charge. The adsorption amounts of heavy metals on Fe and Al oxides increased and their desorption percentage decreased with increasing ionic strength. However, Mn oxide has a low point of zero charge (PZC) and thus displays negative charges in the natural environment. It is unclear how electrolyte affects adsorption-desorption by Mn oxides. This paper studied the influences of electrolytes (KNO_3, KCl) on Cu^{2+} adsorption and desorption on synthetic birnessite. The PZC and specific surface area (SSA) of birnessite was 2.5 and 75 $m^2 \cdot g^{-1}$, respectively. The birnessite consisted of clusters or ball-like aggregates with a size of 50~100 nm. The pH of birnessite in suspension increased slightly with increasing electrolyte concentration, but the effect of KCl solution was higher than in the effect of KNO_3 at a given concentration. The amount of Cu^{2+} absorbed on birnessite decreased gradually with increasing ionic strength. However, the desorption percentage of Cu^{2+} absorbed on birnessite surface increased with increasing electrolyte concentration. Furthermore, the desorption percentage of Cu^{2+} was higher in KCl solution than in KNO_3 solution. These results are different from the adsorption/desorption of Fe and Al oxides.

Keywords: Adsorption/desorption; Oxide; Electrolyte; Birnessite

Introduction

Manganese oxide minerals are widely present in soils and sediments. Although their content is less than 1% in soils, Mn oxide plays an important role in the chemical reactions of soil interface due to the finer particles and coating onto the surface of soil clay as a cutan. In particular, Mn oxide exhibits a lower point of zero charge (PZC), larger specific surface area, more negative charges, and higher capacity of absorbing and fixing heavy metals. These characteristics will affect concentrations, forms, chemical activity, and biotoxicity of heavy metals in soils and sediments.

The adsorption characteristics of heavy metals on oxides are generally affected by electrolytes. At the common ranges of soil pH, the adsorption of heavy metals on Fe and Al oxides, which were positively charged, increased while the desorption declined with increasing electrolyte concentration (Zou *et al.*, 1996a; 1996b) However, manganese minerals were negatively charged at a natural pH. The effect of electrolyte on sorption/desorption of Mn oxides is unknown. Therefore, the influence of the electrolytical types and concentrations on adsorption/desorption of Cu^{2+} by birnessite was studied. Birnessite is the most common manganese mineral in soils and sediments, and made up of a layer MnO_6 octahedron and a layer H_2O molecule.

Materials and Methods

The birnessite was synthesized according to McKenzie (1989). The pH value of birnessite was 4.5 in water (the ratio of birnessite to water is 1:5), and the PZC of 2.5 and a specific surface area of 75 $m^2 \cdot g^{-1}$ (BET method) were determined.

Isotherm adsorption 10 ml of 0.01~6 $mmol \cdot L^{-1}$ $Cu(NO_3)_2$ solutions were added to ten centrifugal tubes with 0.05 g brinessite. Their ionic strength of 0.01 was controlled by KNO_3, and the pH was adjusted to 4.5. After shaking for 2 h at 25±1 ℃ and equilibrium for 22 h, the suspensions were centrifuged.

Influence of the electrolyte A series of 10 mL $Cu(NO_3)_2$ solutions with 0, 0.001, 0.01, 0.1, 0.5, 1 $mol \cdot L^{-1}$ KNO_3 or KCl solutions at pH 4.5 were added to each plastic centrifugal tubes with containing 0.05 g brinessite, respectively. Then, the suspensions were shaken for 2h, equilibrium for 22 h at 25±1 ℃, and centrifuged.

The amounts of Cu^{2+} and Mn^{2+} in the supernatant were measured by an atomic absorption spectrometer (Varian AAS240FS). The pH of the aqueous solutions was measured using a pH meter (model 410) with a glass-mercury electrode (model 9165BN). The experiments above were repeated twice.

Results and Discussion

As shown in Fig. 1, by using the Langmuir equation, the maximum amount of Cu^{2+} absorbed on birnessite was 280 $mmol \cdot kg^{-1}$, and the correlation coefficient was 0.997 (n=8, α=0.01, r=0.798).

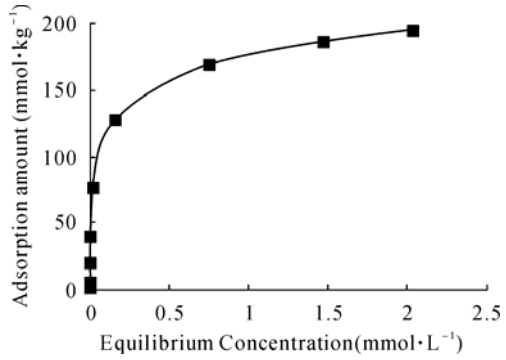

Fig. 1 Isotherm curves for Cu^{2+} absorbed on birnessite

Fig. 2 showed that the amount of Cu^{2+} adsorbed on birnessite decreased with increasing ionic strength (KNO_3 and KCl solution). However, the effects of different concentrations of KNO_3 and KCl solutions on adsorption amount were different.

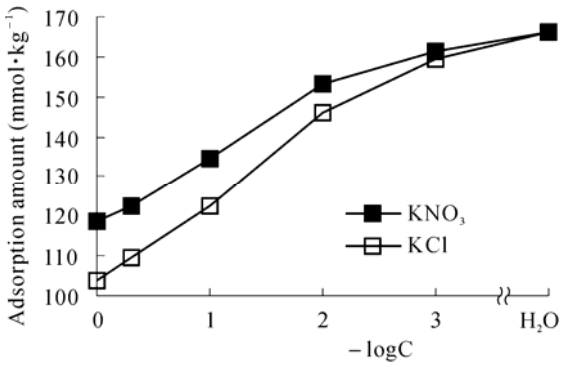

Fig. 2 The amounts of Cu^{2+} adsorption on birnessite *vs.* the negative logarithm of the electrolyte oncentrations

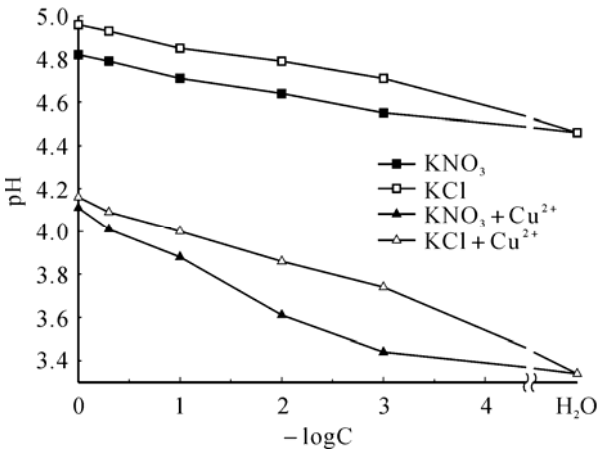

Fig. 3 pH value *vs.* the negative logarithm of the electrolyte concentrations

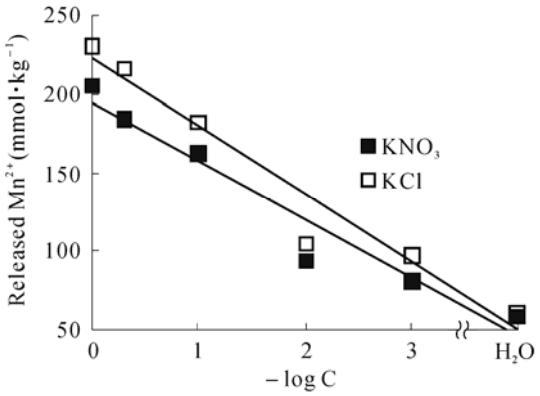

Fig. 4 Released Mn^{2+} *vs.* the negative logarithm of the electrolyte concentrations

The electrolyte types and concentrations affected the characteristics of adsorption/desorption of Cu^{2+} on manganese minerals (Fig. 3, Fig. 4, Fig. 5). With increasing electrolyte concen-rations, the amounts of Cu^{2+} absorbed on birnessite reduced, but the desorption percentage increased. The influence of KNO_3 on the amounts of Cu^{2+} adsorption was greater than that of KCl. However, the amounts of Cu^{2+} desorption by KNO_3 was lower than that by KCl. The difference might be related with ligand exchange and chelated capacity.

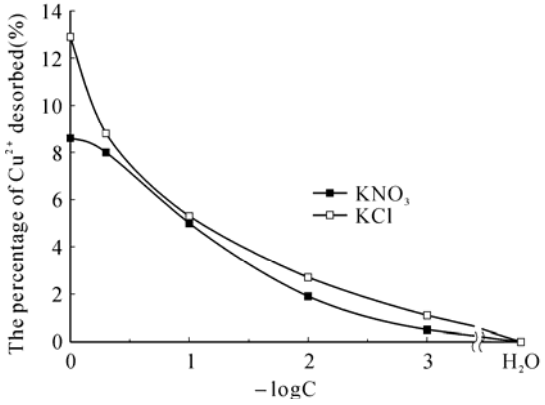

Fig. 5 Desorption percentage of Cu^{2+} adsorbed on birnessite *vs.* the negative logarithm of the electrolyte concentrations

Therefore, the influence of electrolytes on adsorption desorption by Mn oxide is different from that of iron or aluminum oxides. Accordingly, it is essential to pay attention to these discrepancies resulting from the different types of surface charges when the forms, chemical behaviours and bioavailibility of the heavy metals are investigated using different types of oxides.

References

McKenzie RM (1989) Manganese oxides and hydroxides. In: Dixon J, and Weed SB (eds.) Minerals in Soil Environments. Madson WI: SSSA, pp. 439-465

Zou DH, Li XY, Xu FL (1996a) Influences of electrolyte concentration on heavy metal ions desorption on surfaces of Fe and Al oxides. Chinese Sci. Bull. 41: 421-425

Zou DH, Xu FL, Dong YY, Li XY (1996b) Some problems relating to characterizing specific adsorption of heavy-metal ions on surface of oxide. Chinese Sci. Bull. 41: 1483-1487

Sorption of Selected Organic Compounds in Two Black Carbon Particles

Yang-hsin Shih[a,*], Po-Hsin Su[b]

[a] Department of Soil and Environmental Sciences and Center of Nanoscience and Nanotechnology, National Chung Hsing University, Taichung 402, Taiwan, China;
[b] Kaohsiung District Agricultural Research and Extension Station, Council of Agriculture, Executive Yuan, Taiwan, China.
[*]Corresponding author. Tel. No. 886-4-22854152; Fax No. 886-4-22854152; E-mail: yhs@nchu.edu.tw.

Abstract: Black carbons (BCs) have been reported to exhibit an extremely strong sorption of organic compounds in the environment. The basic physicochemical properties of two selected black carbons characterized and showed mainly non-polar. The polarity of BC1 was slightly higher than BC2. Sorption coefficients of selected organic compounds on two BCs were investigated by a reversed-phase liquid chromatography (RP-LC) method. Sorption coefficients of organic chemicals on BC1 were larger than those on BC2 because BC1 had more surface area. Normalized surface area sorption coefficients of BC2 were larger than those of BC1, indicating that not only surface area but surface heterogeneity is also responsible for the resulting sorption capacity. By the regression of the sorption coefficients of organic compounds on these black carbons with the properties of organic compounds, two linear solvation energy relationship (LSER) equations were obtained. The main interactions involved in the adsorption process are generally London dispersion forces and π- and n- pair electron interactions. These LSERs can facilitate to predict the adsorption coefficients and evaluate the sorption mechanism of organic contaminants on black carbons through the molecular properties of sorbates and sorbents.

Keywords: Black carbon; Organic contaminants; Sorption coefficient; Linear solvation energy relationship

Introduction

Sorption of organic contaminants in soil and sediments plays a key role in the fate and remediation of them in the environment. Shih and Wu (2002, 2004) have proposed the intrinsic sorption kinetics and equilibrium of volatile organic chemicals in humic substances and clays not contribute the slow sorption desorption process. Shih (2007) also presented similar behaviors for chlorinated compounds and even proposed the molecular dynamic simulation methodology to predict the sorption kinetics of organic chemicals in humic acid. Recently, black carbons (BCs), environmental pyrogenic carbon particles such as soot and char, are significantly better sorbents than total particulate organic matters for organic contaminants in the environment (Cornelissen *et al*., 2005). Linear solvation energy relationships (LSERs) have been used to study and predict the sorption interactions of organic chemicals on activated carbon (Shih and Gschwend, 2009). Sorption coefficients of selected organic compounds on two black carbons were investigated to explore potential sorption interactions through molecular view by using LSER. With the results of the characterizations and sorption coefficients of black carbon, the sorption mechanisms of these two black carbons were elucidated. Better black carbon-inclusive sorption modeling of selected compounds can be achieved.

Materials and Methods

Sorbents and Sorbates

The two sorbents included a standard reference

black carbon (BC1) and an environmental black carbon (BC2). BC1 (SRM2975) is a soot standard from the National Institute of Standards and Technology (NIST). BC2 is the diesel soot obtained from the diesel engine combusted in a diesel truck. The selected sorbates and their molecular properties were shown in Table 1.

Table 1 LSER parameters of selected organic compounds

chemicals	V	E	S	A	B
acetone	0.55	0.18	0.70	0.04	0.49
acetonitrile	0.24	0.90	0.07	0.32	0.40
ethyl acetate	0.75	0.11	0.62	0.00	0.45
dichloroethylene	0.59	0.36	0.34	0.00	0.05
trichloroethylene	0.72	0.52	0.53	0.12	0.03
tetrachloroethylene	0.84	0.64	0.42	0.00	0.00
phenol	0.78	0.75	0.89	0.60	0.20
4-chlorophenol	0.90	0.92	1.08	0.67	0.20
3,4-dichlorophenol	1.02	1.02	1.14	0.85	0.03
benzene	0.72	0.60	0.52	0.00	0.14
toluene	0.85	0.60	0.52	0.00	0.14
ethyl benzene	1.00	0.61	0.51	0.00	0.15
chlorobenzene	0.72	0.65	0.00	0.07	0.84
diphenyl ether	1.38	1.22	1.08	0.00	0.19
naphthalene	1.09	1.34	0.92	0.00	0.20

Characteristic of Black Carbon

The morphologies and chemical composition of two black carbons were analyzed by a Field-emission scanning electron microscope (FE-SEM), and the chemical composition was studied with an elemental analyzer (EA). Surface analysis was conducted using the X-ray photoelectron spectroscopy (XPS) (data not shown).

Linear Solvation Energy Relationships

The reversed-phase liquid chromatography (RP-LC) method was used to obtain the black carbon sorption coefficients of a diverse of organic compounds on black carbon particles. The collected data were used to treat by the LSER approach:

$$\log K_d = vV + eE + sS + aA + bB + c \quad (1)$$

where K_d is sorption coefficient, V is the McGowan volume, E is a calculated excess molar refraction parameter that provides a quantitative indication of polarizable n and π electrons, S the capability of a molecule to stabilize a neighboring charge or dipole, A and B are the measure effective hydrogen-bond acidity and basicity, respectively (Abraham *et al.*, 1999). Five regression coefficients (v, r, s, a, and b) can be obtained from the equations via a multiple linear regression analysis.

Results and Discussion

Sorbent Morphology

These two black carbons from commercially soot and environmental soot have not been well characterized before. The physical and chemical characteristics of these two pyrogenic carbonaceous materials were required to correlate their properties with the sorption behaviors and mechanisms of organic compounds. Particles of BC1 are composed of clustered nanometer- ized globules and look like “bunches of grapes”. Particle size of BC2 was larger than that of BC1 and in the range of tens and hundreds of nanometers. The agglomerated structure of BC2 was more obviously due to the impurity of BC2, which was obtained from local trunk without any pretreatments. Gustafsson and Gschwend (1997) have also observed that traffic soot originated from combustion of fluid fuels contained some impurities such as oil and inorganic matters.

Elemental Analysis

The elemental analysis of BC1 indicated that the carbon, hydrogen, oxygen, and nitrogen contents of BC1 were 88.1%, 2.20%, 5.74% and 2.08%, respectively. The carbon, hydrogen, oxygen, and nitrogen contents of BC2 were 44.6%, 2.50%, 26.3% and 1.69%, respectively. NIST soot (BC1) has higher carbon content than BC2. BC2 contained more impurities and more measured O content. The NIST soot (BC1) and environmental soot (BC2) seem non-polar adsorbents via their H/C atomic ratio. Comparing to their (O+N)/C atomic ratio, this polar index indicated that BC2 has a higher hydrophilic ability for sorbates than BC1.

Surface Area and Pore Distribution

The surface properties of BCs were controlled by their production conditions and also depend on their starting material. According to the classification from

International Union of Pure and Applied to Chemistry (IUPAC), these average pore size of these two BCs is mesopore. There is a large difference between these two investigated BCs. The BET surface area of BC1 (87.0 $m^2 \cdot g^{-1}$) is larger than that of BC2 (3.62 $m^2 \cdot g^{-1}$). The major part of BET surface area provided from mesopores and macropores. The micropore volume values of two black carbons were closed to zero.

Sorption Behavior

Because the surface area of BC1 is more than BC2, the sorption coefficients of organic chemicals on BC1 are larger than those on BC2 (Table 2). Due to most non-polar surface on these two black carbons, it can be mainly occurred van der Waals and dipolar/ olarizable interactions through non-polar sorbates and non-polar sorbents. The sorption coefficients of diphenyl ether with the highest octanol-water partition coefficient in this study are the largest for these two black carbons. The high contents of double bonds via XPS analysis show lots of π electrons on the two black carbons. The other mechanism of the π-π interaction between the diphenyl ether and the black carbons may also contribute to the sorption process.

Effect of sorption behaviors on black carbons also depends on surface functional groups, so we normalized sorption coefficients with surface area to banish the effect of surface area. The sorption coefficients of organic compounds with more functional groups on BC2 were larger than those on BC1 with less functional groups (data not shown).

Sorption coefficients of chloroethylenes and phenols on BCs became larger with more chloro atoms on the molecular structures of chloroethylenes and chloro-henols due to more contribution of hydrophobic interactions for more highly chlorinated compounds on pyrogenic carbonaceous materials. By the regression of the average of triple observed sorption coefficients of organic compounds on these BCs with their LSER parameters, two linear solvation energy relationship (LSER) equations were obtained:

For BC1

$$\log K_{BC1} = (0.89 \pm 23)\, E + (0.05 \pm 0.32)\, S + (-0.49 \pm 0.30)\, A + (0.05 \pm 0.29)\, B + (0.98 \pm 0.43)\, V + (2.48 \pm 0.24)$$

For BC2

$$\log K_{BC2} = (0.65 \pm 0.26)\, E + (-0.09 \pm 0.37)\, S + (-0.60 \pm 0.34)\, A + (0.09 \pm 0.33)\, B + (1.10 \pm 0.48)\, V + (2.08 \pm 0.27)$$

Table 2 Sorption coefficients of organic compounds on BCs

chemicals	log K_{BC1} ($\mu g \cdot kg^{-1}$)	logK_{BC2} ($mg \cdot L^{-1}$)
acetone	3.37	2.93
acetonitrile	3.38	2.96
ethyl acetate	3.40	2.92
dichloroethylene	3.51	3.00
trichloroethylene	3.65	3.19
tetrachloroethylene	3.97	3.56
phenol	3.60	2.94
4-chlorophenol	4.00	3.04
3,4-dichlorophenol	4.41	3.33
benzene	3.55	2.98
toluene	3.70	3.15
ethyl benzene	3.97	3.45
chlorobenzene	3.80	3.27
diphenyl ether	4.93	3.77
naphthalene	4.92	4.75

Under aqueous conditions at low sorbate concentrations, the main interactions involved in the adsorption process are generally London dispersion forces and π- and n- pairs interactions between black carbons and organic compounds. BC1 and BC2 materials are able to give negative contribution of hydrogen acceptor for hydrogen bond interactions. The interactions of the dipolarity/polarisability and the hydrogen bond donors were not significant. The LSER equation was developed to facilitate the prediction of different organic compounds on black carbons.

References

Cornelissen G, Gustafsson O, Bucheli TD, Jonker MTO, Koelmans AA, van Noort PCM (2005) Extensive sorption of organic compounds to black carbon, coal, and kerogen in sediments and soils: mechanisms and consequences for distribution, bioaccumulation, and biodegradation. Environ. Sci. Technol. 39: 6881-6895

Shih Y (2007) Sorption of trichloroethylene in humic acid studied by experimental investigations and

molecular dynamics simulations. Soil Sci. Soc. Am. J. 71: 1813-1821

Shih Y, Wu S (2002) Sorption kinetics of toluene in humin under two different levels of relative humidity. J. Environ. Qual. 31: 970-978

Shih Y, Wu S (2004) Kinetics of toluene sorption and desorption in Ca- and Cu- montmorillonites investigated with FTIR spectroscopy under two different levels of humidity. Environ. Toxicol. Chem. 23: 2061-2067

Shih Y, Gschwend PM (2009) Evaluating activated carbon-water sorption coefficients of organic compounds using linear solvation energy relationship approach and sorbate chemical activities. Environ. Sci. Technol. 43: 851-857

Adsorption and Inhibition of Butyrylcholinesterase by Different Nanoparticles

Zhenyu Wang[a,*], Kai Zhang[a], Jian Zhao[a], Fengmin Li[a], Dongmei Gao[a], Baoshan Xing[b]

[a]College of Environmental Science and Engineering, Ocean University of China, Qingdao 266100, China;
[b]Department of Plant, Soil and Insect Sciences, University of Massachusetts, Amherst MA 01003, USA.
[*]Corresponding author. Tel. No. +86-532 6678 2092; Fax No. +86-532 6678 2092; E-mail: wang0628@ouc.edu.cn.

Abstract: Nanoparticles may have potential neurotoxicity. This study used 5 nanoparticles including 2 metal nanoparticles and 3 oxide nanoparticles to test their adsorption and inhibition on BChE. We used a modified Ellman method to measure BChE activity. At 800 mg·L^{-1}, the adsorption and inhibition of BChE by Cu were the highest, 54% and 86%, respectively. While Al nanoparticles showed the lowest adsorption (6.8%) and inhibition rates (3.3%). Inhibition was caused mainly by the adsorption of BChE on tested nanoparticles and partly by ions released in nanoparticle suspensions. Inhibition of BChE by Cu^{2+} ions was higher than 39%. Other ions had slight or little effect on BChE activity. The contribution of ions to nanoparticle inhibition followed a decreasing sequence of Al (66%) > Cu (46%) > Al_2O_3 (44%) > SiO_2 (4%). Our results indicate that these nanoparticles may have neurotoxicity.

Keywords: Copper; Enzyme; Neurotoxicity; Metal ion; Biomarker

Introduction

Nanoparticles (NPs) could gain access to the body including central nervous system (CNS) by passing blood-brain barrier, or through olfactory bulb (Kashiwada, 2006; Wang *et al.*, 2008). They could have significant neurotoxicity. Butyrylcholinesterase (BChE) is abundant in serum and in the CNS (Mack and Robitzki, 2000). Inhibition of BChE results in the accumulation of acetylcholine in neural synapses, which can disrupt normal functions of the nervous system (Remor *et al.*, 2009). NPs in the animal body may influence BChE activity and function, consequently disrupt the normal functioning of the CNS, and finally show neurotoxicity. The aim of our study was to provide information on 1) adsorption and inhibition of BChE by NPs, 2) inhibition of BChE by ions released and 3) possible clues to neurotoxic mechanisms of NPs.

Materials and methods

In this study, 5 NPs including Cu, Al, Al_2O_3, TiO_2 (rutile) and SiO_2 were used to test their adsorption and inhibition on human serum BChE. NPs suspensions were prepared by adding dry NPs into phosphate buffer solution (PBS, 0.1 mol·L^{-1}, pH 8.0), treating by ultrasonic (100 W, 40 kHz) for 1 h, and vibrating for 6 h at 200 rpm in a shaking incubator to increase the dispersion of NPs in PBS. Concentrations of ions released from NPs suspensions were determined by inductively coupled plasma optical emission spectrometer (ICP-OES) after NPs suspensions (800 mg·L^{-1}) were centrifuged (4000 rpm, 20 min) and filtrated twice using a 0.45-μm membrane. Ion solutions were prepared by dissolving their salt forms in PBS at equivalent concentrations according to the result of ICP-OES. $Na_2SiO_3·9H_2O$, $Al_2(SO_4)_3·18H_2O$ and $CuSO_4·5H_2O$ were used to supply ion Si, Al and Cu, respectively. NPs suspension filtrates were obtained by centrifuging NPs suspensions (800 mg·L^{-1}) at 4000 rpm for 20 min and filtrating twice of the supernatants using a 0.45-μm membrane. NPs can adsorb any reactant, intermediate or product in enzymatic reactions, thus causing lower photometric measurements. Therefore, BChE activity was determined by the modified Ellman assay and the

adsorption and inhibition rates were calculated (Ellman *et al.*, 1961).

Results and discussion

The adsorption and inhibition of BChE by 5 NPs were tested at 800 mg·L^{-1}. Inhibitions of BChE by ion solutions and NPs suspension filtrates were measured to evaluate the effect of ions existed in metal-based NPs suspensions. NPs could adsorb the yellowish product in the enzymatic reaction. It lowered the absorbance difference, thus lowering photometric quantification. Therefore, we modified the Ellman method for our experiment based on our preliminary study.

Adsorption and inhibition of BChE by defferent NPs at 800 mg·L^{-1} are shown in Fig. 1. Cu had the most obvious effect on BChE, and its inhibition on BChE was about 86% (Fig. 1). NPs such as TiO_2, Al_2O_3 and SiO_2 showed trivial effects on BChE (Fig. 1). Al NPs showed the lowest adsorption (6.8%) and inhibition rates (3.3%) (Fig. 1). Overall, the results showed that these NPs had different adsorption and inhibition on BChE. This may due to the difference in NPs size, surface area and structure. The inhibition of BChE may mainly result from the adsorption of NPs. Studies showed that proteins adsorbed onto NPs changed their structure and function, consequently lost their activity (Lynch and Dawson, 2008; Vertegel *et al.*, 2004). NPs properties such as dimension, surface area and structure have a strong influence on the adsorption, structure and function of proteins.

Ions were present in all tested NPs suspensions except TiO_2. The concentrations of ions released from SiO_2, Cu, Al and Al_2O_3 NPs suspensions were 48.41±0.38, 1.20±0.09, 0.61±0.02 and 0.50±0.07 mg·L^{-1}, respectively. However, Ti ion was not detected in TiO_2 NPs suspensions. Fig. 2 showed the inhibition of BChE by ions made from their salts, NPs suspensions and their filtrates. Cu^{2+} ions released in Cu NPs suspensions inhibited BChE obviously, with a degree of 39% (Fig. 2). Other ions had a slight or little influence on BChE activity (Fig. 2). The contribution of dissolved ions to NPs inhibition followed a declining of Al (66%) > Cu (46%) > Al_2O_3 (44%) > SiO_2 (4%). There was no significant difference between the inhibition of BChE by NPs suspension filtrates and metal ion solutions (Fig. 2). While NPs suspensions inhibited BChE activity much greater than ion solutions, especially Cu NPs (Fig. 2). The inhibition of BChE may partly result from ions dissolution from NPs. BChE has allosteric property, the conformation of the substrate binding site and the catalytic site must be changed after metal ions bound to the negatively charged groups in the peripheral anionic sites (PAS) or catalytic triad. Al^{3+} may interact with the γ-peripheral anionic sites of BChE and change ligand binding at the catalytic site (Sarkarati *et al.*, 1999). Therefore, released ions are one of the important factors that should be considered when assessing toxicity of NPs. After NPs (e.g. Cu) gain access to the animal body and distribute in blood, nervous system and brain that have BChE, ions resulting from dissolution of NPs may inhibit the activity of BChE, and contribute to neurotoxicity of NPs.

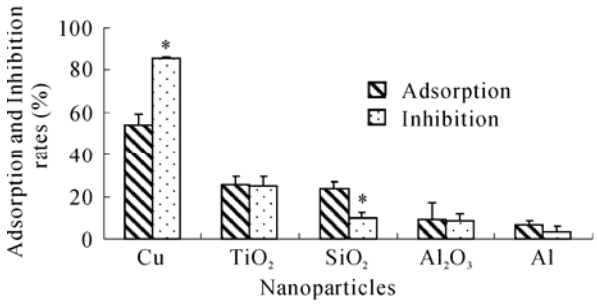

Fig. 1 Adsorption and inhibition rates of BChE by different nanoparticles at the concentration of 800 mg·L^{-1}. Asterisks indicate statistically significant difference from adsorption by nanoparticles (p<0.05). Data present as mean ± SD (n =3~4)

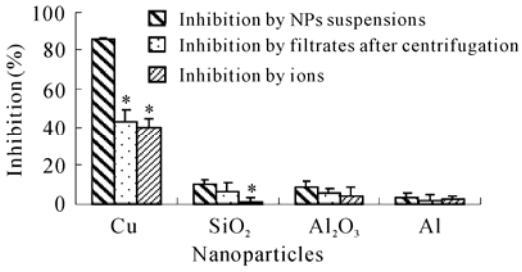

Fig. 2 Inhibition of BChE by ion solutions, nanoparticle suspensions (800 mg·L^{-1}) and their filtrates after centrifugation. Asterisks indicate statistically significant difference from inhibition by nanoparticles (p<0.05). Data present as mean ± SD (n =3~4)

References

Ellman GL, Courtney KD, Andres V, Feather-stone

RM (1961) A new and rapid colorimetric determination of acetylcholinesterase activity. Biochem. Pharmacol. 7: 88-95

Kashiwada S (2006) Distribution of nanoparticles in the see-through medaka (Oryzias latipes). Environ. Health Perspect. 14: 1697-1702

Lynch I, Dawson KA (2008) Protein-nanoparticle interactions. Nano Today 3: 40-47

Mack A, Robitzki A (2000) The key role of butyrycholinesterase during neurogenesis and neural disrders: an antisense-5'butyrylcholinesterase-DNA study. Prog. Neurobiol. 60: 607-628

Remor AP, Totti CC, Moreira DA, Dutra GP, Heuser VD, Boeira JM (2009) Occupational exposure of farm workers to pesticides: Biochemical paraeters and evaluation of genotoxicity. Environ. Int. 35: 273-278

Sarkarati B, Çokuğraş AN, Tezcan EF (1999) Inhibition kinetics of human serum butyrylcholinesterase by Cd^{2+}, Zn^{2+} and Al^{3+}: comparison of the effects of metal ions on cholinesterases. Comp. Biochem. Physiol. Part C 122: 181-190

Vertegel AA, Siegel RW, Dordick JS (2004) Silica nanoparticle size influences the structure and enzymatic activity of adsorbed lysozyme. Langmuir 20: 6800-6807

Wang JX, Liu Y, Jiao F, Lao F, Li W, Gu YQ, Li YF, Ge CC, Zhou GQ, Li B, Zhao YL, Chai ZF, Chen CY (2008b) Time-dependent translocation and potential impairment on central nervous system by intranasally instilled TiO_2 nanoparticles. Toxicology 254: 82-90

Characterization of Soil Clay Minerals Using Mid-infrared Spectroscopy

Changwen Du*, Guiqin Zhou, Jing Deng, Jianmin Zhou

State Key Laboratory of Soil and Agricultural Sustainability,
Institute of Soil Science Chinese Academy of Sciences,Nanjing 210008, China.
*Corresponding author. Tel. No. +86-25 8688 1565; Fax No. +86-25 8688 1000; E-mail: chwdu@issas.ac.cn.

Abstract: Clay mineral is one of the most important components in soil, and the characterization of soil clay is very useful to study the interactions between soil clay and soil organic materials. Chemical analysis of soil clay is time-consuming, while the infrared spectroscopic method seems promising. In this research, the characterization of three source clay minerals, i. e. illite, kaolin and montmorillonite, were analyzed using three mid-infrared spectroscopic techniques (attenuated total reflectance (FTIR-ATR), transmittance spectroscopy, and photoacoustic spectroscopy (FTIR-PAS)). For the FTIR transmittance spectra of the three source clays, there were three main absorption regions: 2600~3800 cm^{-1}, 1300~1800 cm^{-1}, and 500~1200 cm^{-1}, and sharp differences could be found in each region; for the FTIR-ATR spectra of the three source clays, there were absorptions with minor difference in the region of 800~1200 cm^{-1}; for the FTIR-PAS spectra of the three source clays, there were also three similar absorption regions as FTIR transmittance spectra, but more absorptions were found in the FTIR-PAS spectra comparing with FTIR transmittance absorptions. Comprehensively, FTIR-PAS spectroscopy showed more merits in the characterization of soil clays among the three infrared spectroscopic techniques. The FTIR-PAS was applied to charactrize three soil types, and the interactions between soil clay and soil organic materials could be studied using the step-scaning function of FTIR-PAS.

Keywords: Infrared spectroscopy; Kaolin; Montmorillonite; Illite; Photoacouctic spectroscopy

Introduction

The interactions between soil clay and soil organic materials play key roles in the soil chemistry, which will influence soil quality and soil fertility. Chemical analysis of soil clay and soil organic materials is time consuming, further more, chemical analysis is difficult to be used in situ monitoring, and soil extraction may destroy soil structure, and therefore, some real information can not be disclosed (Du and Zhou, 2009). Infrared spectroscopy is an alternative technique for qualifying the interactive effect of soil clay and soil organic materials, and is thus widely used in soil analysis (McCarty & Reeves, 2006). Recenly, the infrared photoacoustic spectroscopy (FTIR-PAS) is applied in soil science, which shows great potential in the soil analysis (Du *et al.*, 2007; 2008; 2009). In this study, three source clays were characterized using different infrared spectroscopic techniques, and the initial application of FTIR-PAS in soil chemistry was explored.

Materials and Methods

Three kinds of clays (illite, kaolin and montmorillonite) were purchased from International clay society (Patricial, 2001). Four soils (0~20 cm) in different location, i. e. black soil from Hailun Ecological experimental station, red soil from Yingtan Ecological experimental station, and Fluvo-aquic soil from Fengqiu Ecological experimental, were collected, air-dried and passed through 2 mm sieve for use.

The soil infrared spectra were recorded for all soil samples using a Nicolet 380 spectrophotometer (Thomalelemental, USA). Tansmittance spectra were recorded by KBr pellet. Attenuated total reflectance (ATR) were obtained using accessary of Smart SpeculATR, in order to have a good touch between soil sample and ATR crystal. Soil paste was developed by adding 2 mL water into 3 g air dried soil, and so it was easily spread onto the ATR crystal (Linker *et al.*, 2005). Photoacoustic spectra were tested using a photoacoustic cell (Model 300, MTEC, USA). After placing the sample (about 200 mg) in the cell holding cup (diameter 5 mm, height 3 mm) purging the cell with dry helium (10 mL·min^{-1}) for 30 s to minimize interferences due to water vapor and impurities. The scans were conducted in the wavenumber region of 1150~850 cm^{-1} for FTIR-ATR, 4000-500 cm^{-1} for FTIR-PAS and transmittance spectra. The resolution was 4 cm^{-1} with 32 successive scans. For the recording of FTIR-PAS spectra, a moving mirror velocity of 0.31 cm·s^{-1} was used.

Infrared spectra were pre-processed with a smoothing filter. The Savitzky-Golay filter method essentially performs a local polynomial regression to determine the smoothed value for each data point. This method is superior to adjacent averaging because it tends to preserve features of the data such as peak height and width, which are usually 'washed out' by adjacent averaging, and the detail of the smoothing filter was given by Savitzky and Golay (1964). The software of Matlab 7.0 was used to treat the spectral data.

Results and Discussion

There are three main absorption regions for the transmittance spectra of three source clays: 500~1200 cm^{-1}, 1300~1800 cm^{-1}, and 2600~3800 cm^{-1} (Fig. 1 a). Significant differences were observed in the above absorptions. 1:1 layer kaolin showed a narrow absorption in 3600 cm^{-1}, while 2:1 layer illite and montmorillonite showed wide absoption in the region of 2600~3650 cm^{-1} with a shoulder peak. For the FTIR-ATR spectra, the valuable absorptions were only showed in the region of 850~1150 cm^{-1} due to water interference, and useful information was very limit (Fig. 1 b). For the FTIR-PAS spectra, the absorptions were more abundant than transmittance spectra and FTIR-ATR spectra (Fig. 1 c), and the spectra differences of three clay minerals were more prominent, which would be more useful and valuable in the characterization of soil clay minerals.

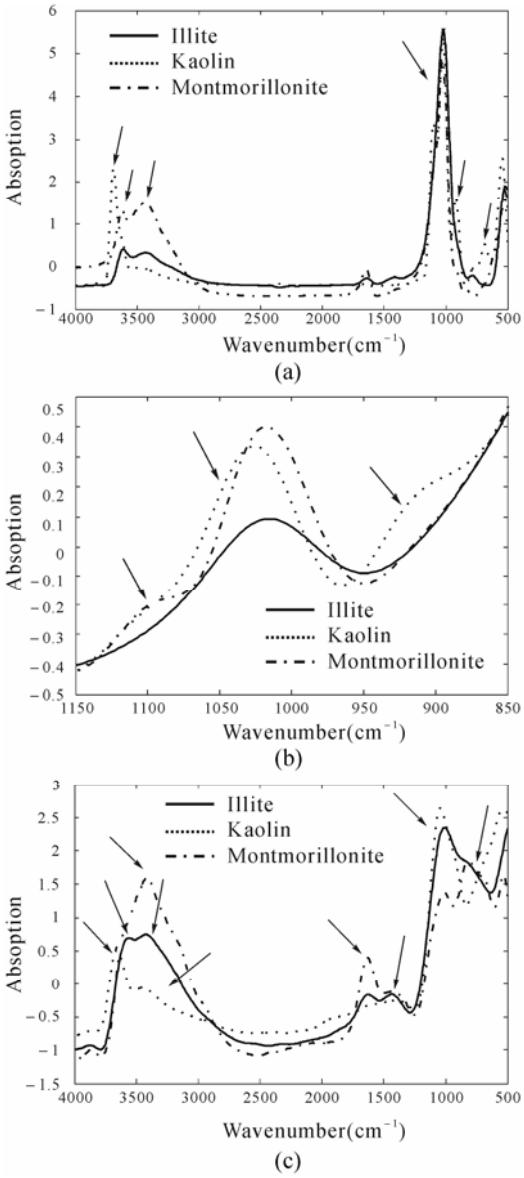

Fig. 1 Mid-infrared spectra of three source clays (a, Transmittance spectra; b, FTIR-ATR spectra; c, FTIR-PAS spectra)

The kaolin mineral structure is a layer of a single tetrahedral sheet and a single octahedral sheet, and the structural formula is $Al_4Si_4O_{10}(OH)_8$; more hydroxyls in the octahedral sheet are exposed, and the O-H vibration is relative weak since this OH is one of the group in the octahedral structure, which results in a narrow absorption in 3600 cm^{-1}. Montmorillonite are composed of two silica tetrahedral sheets with a central octahedral sheet, and the theoretical formula is $(OH)_4Si_8Al_4O_{20}\cdot nH_2O$; most of O-H vibration is from

water attached in the surface of silica tetrahedral sheet , which was verified by the stronger absorption in 1600 cm^{-1} (Fig. 1 c) (Du *et al.*, 2007); this O-H vibration was relative stronger, thus there was a wide absorption in the region of 2600~3650 cm^{-1}. The fingerprint absorptions were mainly contributed by Si-O, Al-O and O-H vibration, which were difficult to interpret, but were valuable in the clay structure characterization.

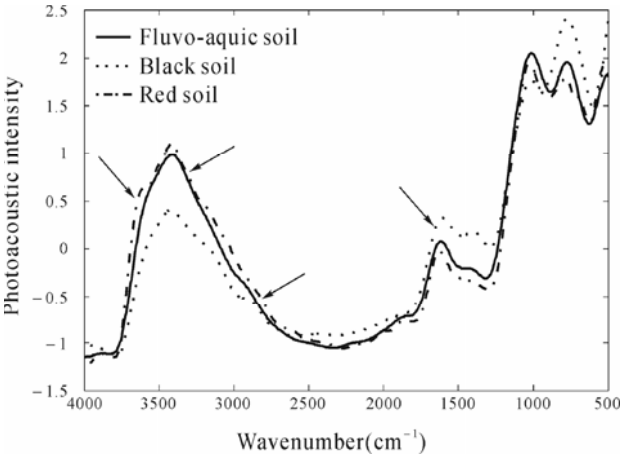

Fig. 2 FTIR-PAS spectra of different soils

The FTIR-PAS spectra of different soils are showed in Fig. 2. Black soil from Hailun soil was characterized as montmorillonite type soil, Fluvo-aquic soil from Fengqiu was characterized as montmorillonite/illite type soil and red soil from Yingtan was characterized as kaolin type soil. Actually, not only the clay structure but also the organic matter structure information were indicated in the soil FTIR-PAS spectra such as absorption in 2900 cm^{-1}, which was assigned as aliphatic C-H stretching (He *et al.*, 2006). Therefore, it would be very useful to separate the information of soil clays and the soil organic materials in the FTIR-PAS spectra. Fortunately, the step-scanning function of PAS technique made the direct separation possible.

The surface information from the depth of 0~100 um can be explored by changing the modulate frequency or changing the rate of moving mirror in the PAS technique (Du and Zhou, 2009). Higher rate of moving mirror resulted in information of surface layer, and lower rate of moving mirror resulted in information of sub-surface layer. Soil organic material usually exists in the soil surface layer, while soil clay exists in sub-surface layer. In the higher rate of moving mirror, more absorptions were observed (Fig. 3), such as the absorption in 2900 cm^{-1}, it was more prominent comparing with the result in lower rate of moving mirror, which were assigned as the aliphatic C-H stretching.

The step-scanning function of PAS technique made it possible to study the properties of surface layer in different depth, which would be a great promising to uncover the interaction between soil clays and soil organic materials in molecular level.

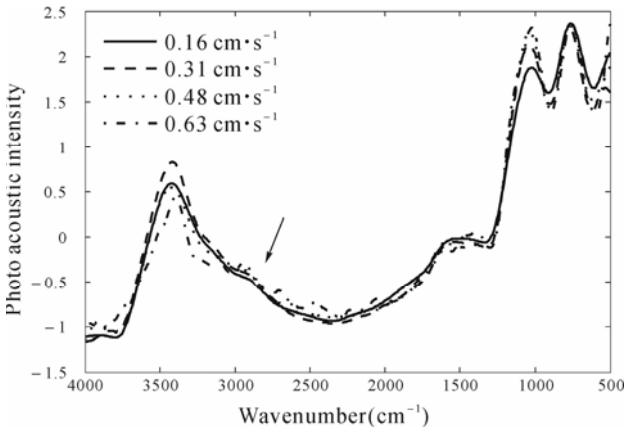

Fig. 3 FTIR-PAS spectra of Fluvo-aquic soil under different rate of moving mirror

References

Du CW, Zhou JM (2009) Evaluation of soil fertility using infrared spectroscopy: a review. Environ. Chem. Lett. 7: 97-113

Du CW, Raphael L, Shaviv A (2007) Characterization of soils using photoacoustic mid-infrared spectroscopy. Appl. Spectrosc. 61: 1063-1067

Du CW, Raphael L, Shaviv A (2008) Identification of agricultural Mediterranean soils using mid-infrared photoacoustic spectroscopy. Geoderma 143: 85-90

Du CW, Zhou JM,Wang HY *et al.* (2009) Determination of soil properties using Fourier transform mid-infrared photoacoustic spectroscopy. Vib. Spectrosc. 49: 32-37

He ZQ, Ohno T, Cade-Menum BJ *et al.* (2006) Spectral and chemical characterization of phosphatesassiciated with humic substances. Soil Sci. Soc. Am. J. 70: 1741-1751

McCarty GW, Reeves JB (2006) Comparison of near infrared and mid infrared diffuse reflectance

spectroscopy for field-scale measurement of soil fertility parameters. Soil Sci. 171: 94-102

Linker R, Shmulevich I, Kenny A *et al.* (2005) Soil identification and chemometrics for direct determination of nitrate in soils using FTIR-ATR mid-infrared spectroscopy. Chemosphere 61: 652-658

Nanni MR, Demattе JAW (2006) Spectral reflectance methodology in comparison to traditional soil analysis. Soil Sci. Soc. Am. J. 70: 393-407

Patricial MC (2001) Baseline studies of the clay minerals society source clay: introduction. Clay Clay Miner. 49: 372-373

Savitzky A, Golay MJE (1964) Smoothing and differentiation of data by simplified least-squares procedures. Anal. Chem. 36: 1627-1639

Investigation Mechanism of MTBE on Wall of Carbon Nanotube (CNT) to Other Products from Air-groundwater (in Environment): MNDO

Leila Mahdavian[a,*], Mahmoud Raouf[b]

[a] Department of Chemistry, Islamic Azad University Doroud Branch, P.O. Box: 133, Doroud. Iran;
[b] Department of Physical Education, Islamic Azad University Doroud Branch, P.O. Box: 133,. Doroud. Iran.
[*]Corresponding author. Tel. No. 0098-9166682145; Fax No. 0098-6654232626; E-mail: Leila_mahdavian@yahoo.com.

Abstract: Gasoline and heating oil travel through pipelines and are also distributed by truck to above ground and underground storage tanks. Through its extensive use as a fuel oxygenate, methyl tert-butyl ether (MTBE) is found nearly ubiquitously throughout the environment. MTBE, a widely used gasoline additive, is recently being scrutinized for potential environmental damage in groundwater and in the atmosphere. The calculations have quantum mechanical detail and are based on a semi-empirical (MNDO method), which is applied to the evaluation of both the electronic structure and of the conductance. We study the structural, total energy, thermodynamic and conductive properties of absorption MTBE on CNT, which convert to CO and H_2O.There are four situations for MTBE near by SWNT that we have investigated adsorption it on CNT and is converted to other products. The properties thermodynamic are calculated for them.

Keyword: MTBE (methyl tert-butyl ether); CNT (carbon nantube); Pollution environment; MNDO method; Gas sensor

Introduction

MTBE (methyl t-butyl ether) is a chemical added to gasoline to increase octane. Its use began in the 1970's to replace lead in gasoline. After 1995, many metropolitan areas of the country with smog problems also added MTBE to gasoline because it helps to reduce harmful emissions from automobile exhaust. Adding MTBE to gas has been one way to meet EPA's oxygenate mandate.

The major concern about MTBE (and other oxygenate compounds) is focused on their occurrence in groundwater and drinking water supplies. In MTBE, the use of oxygenates as octane enhancers, principally in replacement of alkyl-lead compounds.

Many processes will govern exchange of MTBE between surface waters and the atmosphere. As a major process in removing MTBE from aquatic systems, atmospheric behavior and fates of the compound are clearly important (Guitart *et al.*, 2004).

Air–water exchange appears to be the major process in the removal of MTBE from the estuarine and coastal waters. CNT, however, is likely to contribute to removal (albeit to a lesser extent) (Star *et al.*, 2004).

Single wall carbon nanotubes (SWNTs) have attracted great interest due to their unique electronic properties and nanometer size. Because of these unique properties, they are great potential candidates in many important applications such as nanoscale electronic devices, chemical sensors and field emitters. The effect of gas adsorption on the electrical resistance of a CNT has received great attraction because of fast response, good sensitivity of chemical environment gases and low operating temperature (Doo Lee *et al.*, 2006). Theoretical studies have confirmed the remarkable change in electronic properties of CNT due to the detection and removed of gas molecules (Jiang *et al.*, 2007; Sinha *et al.*, 2006). Most molecules are known to be an electron-acceptor such as O_2 or an electron donor such as MTBE and H_2O displaying relatively small charge

transfer between adsorbed molecules weakly on the CNT wall. SWNT re used for investigation for detection and removed MTBE in air-water.

Interaction between MTBE molecules and SWNT is investigated using MNDO method by semi-empirical methods. We study the structural, total energy, thermodynamic properties of passing MTBE and SWNT in room temperature. All the geometry optimization structures were carried out using Gaussian program package. Density Functional Theory (DFT) optimized intermediates and transient states of them. The results show a sensitivity enhancement in resistance and capacitance when MTBE is passing across SWNT.

The computational methods

The geometry optimizations were performed using an all-electron linear combination of atomic orbital density functional theory (DFT) calculations using the Gaussian program package.

Another advantage is that for specific and well-parameterized molecular systems, these methods can calculate values that are closer to experiment than lower level ab initio techniques. The accuracy of a molecular mechanics or semi-empirical quantum mechanics method depends on the database used to parameterize the method. Configuration Interaction (or electron correlation) improves energy calculations using CNDO, INDO, MINDO/3, MNDO, AM1, PM3, ZINDO/1 and ZINDO/S for these electron configure-tions.

The mechanism conversion ethanol to other produces on nano-crystal SnO_2 (110) are investigated with MNDO methods, because MNDO calculated heats of formation, molecular geometries, dipole moments, ionization energies, electron affinities, and other properties for them (Dewar *et al.*, 1977; Dewar *et al.*, 1977). The other methods in DFT can not calculate these parameters for SnO_2 with 24 Sn atoms and theirs calculation are most heavy.

The adsorption, electric, binding nuclear energy, RMS gradient, heat of formation and Gibbs free energy are calculated by MNDO methods in semi empirical quantum in DFT. The electric resistance for them is following as:

$$E_{\text{elec}}=RI \tag{1}$$

where E_{elec} is electric energy (V), R (Ω) is electric resistance and I (A) is electric intensity that is $I=q/t$ and q(C) is electric charge and t is time interaction, in experimental data, it is so:

$$R=\frac{E_{\text{elec}}t}{nF} \tag{2}$$

where n, F and t are electron number of conversion, faraday constant and time (h) respectively.

Results

MTBE moves quickly through soil, dissolves easily in water, and takes longer to break down than some other chemicals. Drinking water with MTBE levels of 20 to 40 "parts per billion" (acceptable taste and odor) would probably not pose health risks. MTBE at 20 μ g·kg^{-1} in water is about the same as one drop in 500 gallons of water. Therefore, farm and residential releases, car accidents, spills, boats, and storm water run off also release gasoline into the environment. MTBE moves quickly through soil, dissolves easily in water, and takes longer to break down than some other chemicals. Drinking water with MTBE levels of 20 to 40 "parts per billion" (acceptable taste and odor) would probably not pose health risks. MTBE at 20 μ g·kg^{-1} in water is about the same as one drop in 500 gallons of water. We have used Single-Walled Carbon Nanotube (SWNT) for removed MTBE in environment.

Therefore, SWNTs have been used utilizing as the sensing material in pressure (Dharap *et al.*, 2004; Dag *et al.*, 2005), field emission effect (Lee *et al.*, 2006), thermal (Smart *et al.*, 2006), gas (Kong *et al.*, 2000), optical (Modi *et al.*, 2003), mass (Jiang *et al.*, 2007), position (Silva *et al.*, 2004), stress (Fu *et al.*, 2005), strain (Wang *et al.*, 2003), chemical (Li *et al.*, 2003), and biological sensors (Qi *et al.*, 2003; Sinha *et al.*, 2006) that is showed in Fig. 1.

Upon exposure to gaseous molecules such as MTBE, the electrical resistance of a semi-conducting SWNT is found to dramatically increase or decrease.

The main reaction product for MTBE-CNT in this interaction is: methanol and t-Butyl alcohol that secondary product: CO and H_2O in air- water.

To understand the effects MTBE in SWNT, the properties thermodynamic calculated by MNDO

methods in semi-empirical quantum with Gaussian program package.

This type of interaction is more known as an acid-base interaction, where the H atom of the acid (in this case MTBE) interacts with carbons in end SWNT (the base). Simultaneously, the carbon site (acting as Lewis acid) interacts with the O (2p) orbital of the oxygen of the adsorbed MTBE molecule.

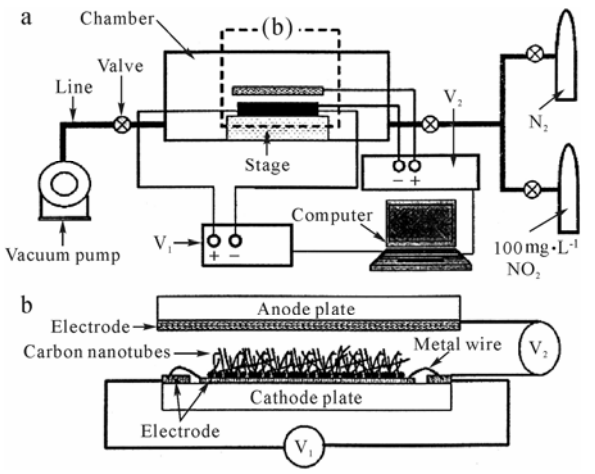

Fig.1 Single-Walled Carbon Nanotube based gas sensors for MTBE in environment

oxidative dehydrogenation of MTBE and H_2O depends critically upon the reaction step that requires the oxide surface to acquire a negative charge. It is well accepted that upon adsorption, the C–O–C bond of the ether dissociates heterolytically to yield a methoxid and a proton. Ball-and-stick models of the SWNT and MTBE are showed in Fig. 2.

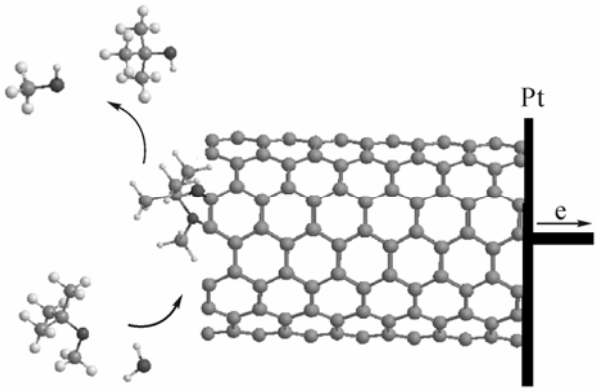

Fig.2 The MTBE in air-water converted to methanol and t-Butyl alcohol on SWNT gas sensor

Formation of methanol and t-Butyl alcohol by the

Table 1 The properties thermodynamic of interaction MTBE – SWNT to alcohols in air-water at 298K

Distance (Å)	E_{total} (MJ·mol^{-1})	Dipole Moment (D)	RMS (Kcal·mol^{-1}·Å^{-1})	E_{ele} (V)
6.11	12191.02	1.61×10^4	4555	-103.24
3.63	9619.70	1.30×10^4	3891	-109.86
2.76	12356.18	1.56×10^4	4708	-104.36
1.96	12253.32	1.51×10^4	4726	-104.68
3.58	12100.67	1.64×10^4	4741	-105.72
6.56	11817.75	1.70×10^4	4634	-104.68
Distance (Å)	E_{bin} (MJ·mol^{-1})	H (MJ·mol^{-1})	G_{ele} (MJ·mol^{-1})	E_{nuc} (MJ·mol^{-1})
6.11	14418.17	14569.13	-41838	54558
3.63	11846.86	11983.95	-44520	54516
2.76	14583.33	14720.42	-42292	54558
1.96	14480.47	14617.57	-42420	54852
3.58	14360.91	14498.69	-42840	55020
6.56	14078.00	14215.78	-42420	54180

In this work, the first situation is investigated for MTBE. The effects of MTBE on based SWNT-gas sensor was shown at Table 1.

In this mechanism is transition electron between MTBE and SWNT-H_2O, which those steps are transient state converted MTBE to alcohols. Adsorption of MTBE and H_2O-reduced on nano-surface has also been studied in air-water.

The total energy (12356.18 MJ·mol^{-1}) and binding energy (14583.33 MJ·mol^{-1}) for this adsorption has maximum amount in 2.76 Å to SWNT, which the heat of formation energy of them is the most quantity in this distance (14720.42 MJ·mol^{-1}).

The enthalpy difference (ΔH) and Gibbs free difference (ΔG) energy for this reaction are -353.35 and -582 MJ·mol^{-1}, respectively which is interaction exothermic and spontaneous and MTBE is separated from air- water. The dipole moment is 1.7×10^4 D when MTBE converted to alcohols in 6.54 Å. RMS gradient (Kcal·mol^{-1}·Å^{-1}) is different for conversion of MTBE on SWNT in 298K.

The CO and H_2O represent the second most important reaction product in our calculations. This sort of products formation from oxidation has been reported on the surfaces. In Fig. 3, ball-and-stick models of conversion methanol to CO and H_2O in air have showed. Alcohols oxidation resulted in the peeling of the outer graphite layers from the nanotubes.

Table 2 show properties thermodynamic those at 298 K obtained this way for the pure oxides.

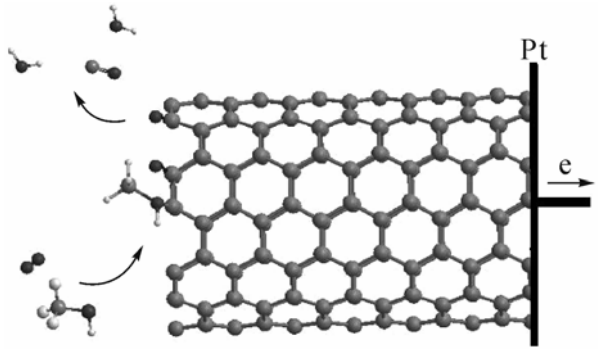

Fig. 3 The methanol in air-water converted to CO and H_2O on SWNT gas sensor

Table 2 The properties thermodynamic of interaction methanol and t-Butyl alcohol– SWNT to CO and H_2O

Distance (Å)	E_{total} (MJ·mol^{-1})	Dipole Moment D	RMS (Kcal·mol^{-1}·Å^{-1})	E_{ele} (V)
6.56	11817.75	1.70×10^4	4634	-104.68
3.58	12100.67	1.64×10^4	4741	-105.72
2.49	12792.40	1.57×10^4	4591	-105.72
1.98	12183.20	1.57×10^4	4501	-106.31
3.69	12100.67	1.64×10^4	4741	-105.72
5.54	11290.05	1.23×10^4	3792	-129.55
Distance (Å)	E_{bin} (MJ·mol^{-1})	H (MJ·mol^{-1})	G_{ele} (MJ·mol^{-1})	E_{nuc} (MJ·mol^{-1})
6.56	14078.00	14215.78	-42420	54200
3.58	14360.91	14498.69	-42840	55000
2.49	15052.65	15190.43	-42840	55904
1.98	14443.45	14581.23	-43079	55400
3.69	14360.91	14498.69	-42840	54900
5.54	13979.02	14119.86	-52500	63700

In Table 2, the total energy different for this conver-sionis negative (-527.70 MJ·mol^{-1}), which this inter-action is exothermic. In table.2, their binding energy (E_{bin}) and heat of formation energy increased until 2.49 Å so it decreased for this conversion on surface because electrons are translated between surface and alcohols molecule in transient state. In Table 2, Gibbs free energy is enhanced for

intermediates and transient state and then it is reduced for product. That nuclear energy is too. The dipole moment is 1.23×10^4 D when alcohols converted to CO and H_2O in 5.54 Å.

The goal of this work is to improve the detection of surface species of SWNTs gas sensors under their working conditions using computer calculation, and to correlate the sensor signals with the relative changes of the electric resistance (Ω). When uniform alcohol pressure was applied on the membranes, a change in electric resistance of the SWNTs was observed Fig.4. In the interaction, correlate the sensor signals with the relative changes of the electric resistance (Ω) so we have to convert calculation data (E_{ele} (V)) to the electric resistance (Ω) (Eq.(2)) that showed in Fig. 4.

A current versus voltage curve recorded with a SWNT sample after time exposure to MTBE showed down-fold conductance depletion. Exposure to MTBE molecules increased the conductance of the SWNT sample.

The SWNT is a down hole-doped semiconductor, as can be gleaned from the current versus gate voltage curve shown in Fig. 4 (middle curve), where the resistance of the SWNT is observed to decrease.

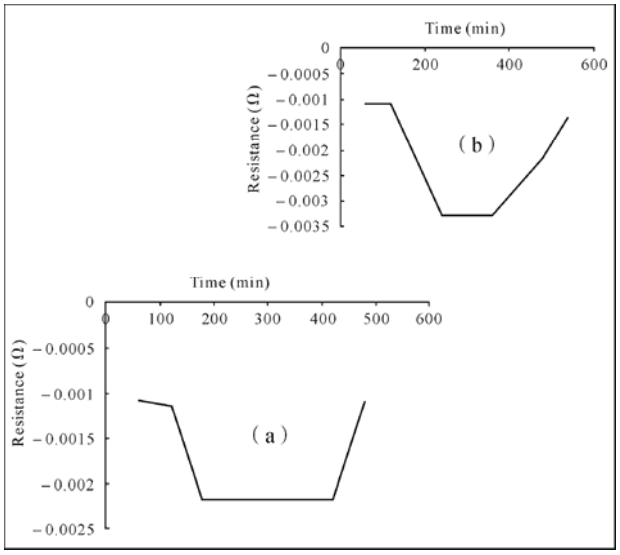

Fig.4 The electric resistance: (a) MTBE converted to methanol and t-Butyl alcohol, (b) methanol and t-butyl alcohol converted to CO and H_2O

The conductance of the SWNT with alcohols to CO and H_2O (Fig. 4(b)) is more than MTBE to alcohols (Fig. 4(a)).

The MTBE-air is injected into the nano-reactor containing either pure SWNT compound a large fraction of MTBE that was found to be transformation to CH_3OH and $(CH_3)_3COH$. It then be adsorbed in the form of CO and H_2O producing an adsorbed oxygen atom. At about, this transformed to formaldehyde (CH_3O) forming an adsorbed hydrogen atom for methanol.

$$CH_3OH_{(g)} \rightarrow CH_3O_{ads} + H_{ads}$$
$$CH_3O_{ads} + O_{ads} \rightarrow CO + OH_{ads} + H_{ads}$$
$$OH_{ads} + H_{ads} \rightarrow H_2O$$

There are same results for t-butyl alcohol too, that can use to this method for remove or reduce MTBE in environment.

Conclusion

We effort to use SWNT for decrease MTBE in air-water, because the SWNT is snared or adsorption it on wall and impossible it is converted to CO and H_2O. The results in Table.2 are confirming this topic.

The prominent peak is corresponding to increasing distances (Å) adsorption of MTBE on SWNT at 298K that is affected to electric properties SWNT.

The sensitivity could be measured when the detecting gas) was mixed homogeneously with the air. The sensitivity depends on MTBE concentration at each work temperature. The sensitivity increases with increasing the MTBE gas concentration. The response and sensitivity of the MTBE-treated sensor was found to be very high when compared to the air-treated sensor.

References

Dag S, Ozturk Y, Ciraci S, Yildirim T (2005) Adsorption and dissociation of hydrogen molecules on bare and functionalized carbon nanotubes. Phys. Rev. B. 72: 155404-1-8

Dewar MJS, McKee ML (1977) Ground states of molecules. 41. MNDO results for molecules containing boron. J. Am. Chem. Soc. 99: 5231-5241

Dewar MJS, Thiel W (1977) Ground states of molecules. 38. The MNDO method. Approximations and parameters. J. Am. Chem. Soc. 99: 4899-4907

Dharap P, Li P, Nagarajaiah S, Barrera EV (2004) Nanotube film based on nanotubes for strain sensing. Nanotechnology. 15: 379-382

Doo Lee Y, Cho WS, Moon SI, Lee YH, Kim JK, Nahm S, Ju BK (2006) Gas sensing properties of printed multiwalled carbon nanotubes using the field emission effect. Chem. Phys. Lett. 433: 105-109

Fu Q, Liu J (2005) Integrated Single-Walled Carbon Nanotube/Microfluidic Devices for the Study of the Sensing Mechanism of Nanotube Sensors. J. Phys. Chem. B. 109: 13406-13408

Guitart C, Bayona JM, Readman JW (2004) Sources, distribution and behaviour of methyl *tert*-butyl ether (MTBE) in the Tamar Estuary, UK. Chemoshere. 57 (6): 429-437

Jiang L, Colmenares L, Jusys Z, Sun GQ, Behm RJ (2007) Ethanol electrooxidation on novel carbon supported Pt/SnO*x*/C catalysts with varied Pt:Sn ratio. Electrochimica Acta. 53: 377-389

Kong J, Franklin NR, Zhou C, Chapline MG, Peng S, Cho K, Dai H (2000) Nanotube molecular wires as chemical sensors. Science. 287: 622-625

Lee YD, Cho WS, Moon SI, Lee YH, Kim JK, Nahm S, Ju BK (2006) Gas sensing properties of printed multi walled carbon nanotubes using the field emission effect. Chem. Phys. Lett. 433: 105-109

Li J, Lu Y, Ye Q, Cinke M, Han J, Meyappan M (2003) Carbon Nanotube Sensors for Gas and Organic Vapor Detection. Nano Lett. 3: 929-933

Modi A, Koratkar N, Lass E, Wei B, Ajayan PM (2003) Miniaturized Gas Ionization Sensors using Carbon Nanotubes. Nature 424: 171-174

Qi P, Vermesh O, Grecu M, Javey A, Wang Q, Dai H, Peng S, Cho KJ (2003) Toward Large Arrays of Multiplex Functionalized Carbon Nanotube Sensors for Highly Sensitive and Selective Molecular Detection. Nano Lett. 3: 347-351

Silva LB, Fagan SB, Mota R (2004) Ab Initio Study of Deformed Carbon Nanotube Sensors for Carbon Monoxide Molecules. Nano Lett. 4: 65-67

Sinha N, Ma J, Yeow JTW (2006) Carbon Nanotube-Based Sensors. J. Nanosci. Nanotechnol. 6 (3): 573-590

Smart SK, Cassady AI, Lu GQ, Martin DJ (2006) The biocompatibility of carbon nanotubes. Carbon 44: 1034-1047

Star A, Bradley K, Gabriel JChP, Grüner G (2004) Carbon Nanotube Nanoelectronic Devices for Chemical Detection in Liquid Hydrocarbons. Prepr. Pap.-Am. Chem. Soc., Div. Fuel Chem. 49 (2): 888-889

Wang J, Musameh M, Lin Y (2003) Solubilizat-ion of Carbon Nanotubes by Nafion toward the Preparation of Amperometric Biosensors. J. Am. Chem. Soc. 125: 2408-2409

Extraction of Nanoparticles from Argosols and Ferrosols

Wenyan Li[a], Jianming Xu[a,*], Pan Ming Huang[b] †

[a] Zhejiang Provincial Key Laboratory of Subtropical Soil and Plant Nutrition, Zhejiang University, Hangzhou 310029, China;
[b] Department of Soil Science, University of Saskatchewan, Saskatoon, SK Canada.
[*]Corresponding author. Tel. No. +86-571 8697 1955; Fax No. +86-571 8697 1955; E-mail: jmxu@zju.edu.cn.

Abstract: Soil nanoparticles are ubiquitous and play an important role in migration and transformation of pollutants in nature. The present study was aimed to obtain soil nanoparticles from Argosols and Ferrosols, which are two typically zonal soils distributing in the north and south China, respectively. Ultrasonic-centrifugal method was used to disperse the soil and extract soil nanoparticles. The nitrogen adsorption-desorption method was employed to determine the specific surface area of soil nanoparticles. More soil nanoparticles were obtained from Argosols than from Ferrosols. The soil nanoparticles from Argosols could not, however, keep stable in water even at 4 ℃. To preserve in solid, it should be freezing dried immediately. Furthermore, the nanoparticles from the two soils were different in the physical characteristics including fractions and morphology. After ultrasonic extraction, the specific surface area of two soils had increased nearly four times.

Keywords: Soil nanoparticles; Dispersion; Stability; Zeta potentials; The specific surface area

Introduction

Nanoparticles are one kind of emerging materials with quiet abroad applications in scientific and technolo-gical research, and nowadays most nanoparticles for use in remediation of contaminated soils are anthro-pogenic materials. The special characteristics of anthro-pogenic nanoparticles will not only bring the advantages of the new technology, but also introduce problems. To nature, anthropogenic nanoparticles are also an exogenous additive, however, for its special characteristics. It would even be difficult to remove from the environment. Best on, the application of natural nanoparticles has been proposed.

A wide range of natural nanoparticles should be existed in nature (Banfield and Navrotsky, 2001), but few studies have elucidated its quantity, distribution and morphology, and how they migrate and transfer in the environment. There are various types of soils posing a wide range in properties in China. The aim of this study was to extract soil nanoparticles from Argosols and Ferrosols, and elucidate their characteristics.

Materials and Methods

The soils used (Table 1) were different in pH, carbonate content, texture and cation exchange capacity (CEC). The Argosols soil was collected from Shandong, with organic materials being the dominant stabilizing agents, while the Ferrosols soil from Guangxi had oxides as dominant stabilizing agents. Both soils were collected from 0~15 cm. All soil samples were air-dried and sieved through 2 mm. The determination of pH, TOC, texture, carbonate content, CEC and Fe were all followed the protocols of the National Standards of China (Table 1).

The instrument used for ultrasonic dispersion of soils was Ultrasonic Cell Crusher SCIENTZ-IID (a probe–type ultrasonic vibrator) fitted with a solid probe (tip diameter, 5 mm). For dispersing soil, this instrument was operated with a stable power output (power rating of 300 W) and the tip of the probe was fixed 1 cm below the surface of the soil suspension. Dispersion was performed by vibrating 3 g of soil in 25 mL water for 15 min in a 50-mL glass beaker fitted with a cooling tank. The cooling tank was filled with ice in order to keep the temperature of the vibrated

suspension below 20 ℃. After dispersion, the suspension was passed through a 50-μm sieve.

The fraction (<100 nm) was obtained using the Stoke's law. The suspension was placed into a 50-mL centrifuge tube and centrifuged at 3000 $r \cdot min^{-1}$ for 6 min. The dispersion and stability of soil nanoparticles in water were studied by the method of Zeta potential (Zetasizer nano ZS 90). The size of soil nanoparticles was characterized by transmission electron microscopy (TEM) and the specific surface area was characterized using the Brunauer-Emmett-Teller (BET) by Tristar 3020 Surface Area and Porosimetry Analyzer.

Table 1 Basic properties of two tested soils

Soil				pH	TOC ($g \cdot kg^{-1}$)	Clay (%)	Silt (%)	Sand (%)	$CaCO_3$ (%)	CEC ($cmol \cdot kg^{-1}$)	Fe_o ($g \cdot kg^{-1}$)	Fe_d ($g \cdot kg^{-1}$)
No.	Series	Order	Source									
1	Zhongrang	Argosols	Shandong	6.26	8.96	27.3	37.6	35.0	0.18	14.3	3.9	11.7
2	Hongrang	Ferrosols	Guangxi	4.23	10.73	37.0	28.7	34.2	0.48	9.8	2.1	24.9

Results and Discussion

Two soils were ultrasonically dispersed, filtered, and centrifuged to seen whether soil nanoparticles existed and how much they could be extracted. Fig. 1 showed that soil nanoparticles could be obtained from both soils, but percentage of soil nanoparticle in Argosols was significantly higher than that in Ferrosols.

The soil nanoparticles from Argosols are relatively small in size, according to Table 2. The size distribution of nanoparticles from Argosols ranged from 6.5 nm to 43.8 nm, and 65.9% was about 10 nm. The distribution of size fractions of nanoparticles from Ferrosols ranged from 11.7 nm to 58.8 nm, in which 64% were about 15 nm. The average size of soil nanoparticles from Ferrosols was greater than those from Argosols.

Zeta potential is an indicator for the stability of nanoparticles in water suspension. After centrifugation, zeta potential was tested to elucidate that whether soil nanopartiles-water mixture could be stable in 4 ℃.

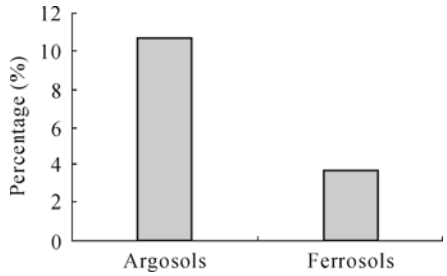

Fig. 1 Percentage of soil nanoparticle values after vibration of soils

Table 2 Distribution of particle size fractions of the nanoparticles extracted from the two soils

Mean %	Particle size (nm)							
	6.5	7.53	8.72	10.1	11.7	13.5	15.7	18.2
Argosols	1.9	12.1	25.2	25.2	15.5	8.2	4.6	2.9
Ferrosols	0	0	0	0	5.1	17.1	24.6	21.9
Mean %	Particle size (nm)							
	21	24.4	28.2	32.7	37.8	43.8	50.7	58.8
Argosols	1.9	1.2	0.7	0.3	0.2	0.1	0	0
Ferrosols	14.9	8.5	4.3	2	0.8	0.4	0.2	0.1

Table 3 Zeta potential of the nanoparticles extracted from the two soils at the 16th day

Soils	Zeta potential (mV)							
	1	2	3	4	5	6	7	8
Argosols	-21.4	-13.7	-14.4	-13.8	-12.1	-12.7	-12.6	-12.7
Ferrosols	-18.2	-17.2	-17.0	-16.4	-17.4	-17.1	-16.4	-17.4
Soils	Zeta Potential (mV)							
	9	10	11	12	13	14	15	16
Argosols	-13.5	-12.2	-12.0	-11.6	-8.89	-10.3	-14.0	-12.5
Ferrosols	-17.9	-17.4	-17.9	-17.7	-18.1	-16.5	-17.2	-18.7

Zeta potential of soil nanoparticles from Ferrosols remained constant at the initial value over 16 days, but the absolute value of zeta potential of Argosols dramatically reduced 36% after one day (Fig. 2). The results indicated that after ultrasonic dispersion, soil nanoparticles from Argosols could not be maintained its stability.

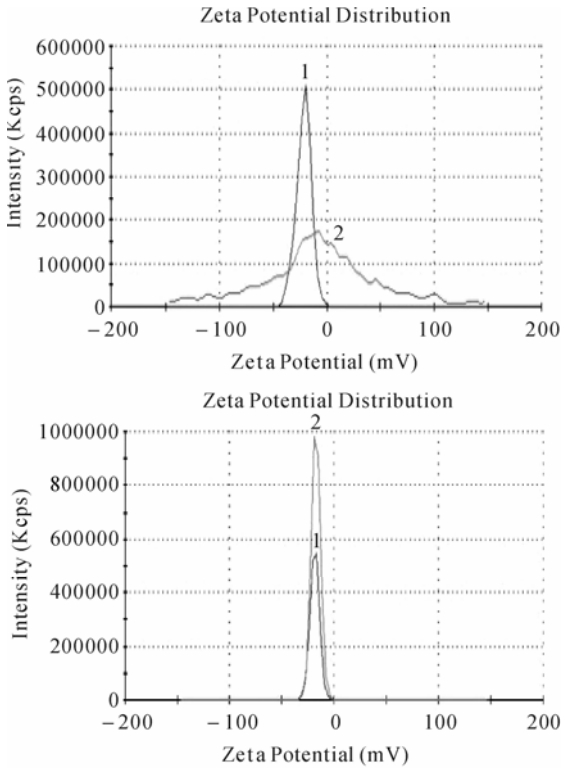

Fig. 2 Zeta potentials of the nanoparticles extracted from the Argosols (top) and Ferrosols (bottom). Line 1 was the zeta potential of soil nanoparticles just after extraction. Line 2 on top was the zeta potential of soil nanoparticles from Argosols at the second day. Line 2 on bottom was the zeta potential of soil nanoparticles from Ferrosols at the 16th day

Some researchers claimed that there were two mechanisms of soil dispersion (Oades and Waters, 1991). One is that soil aggregates are broken down in steps. For example, the Argosols had larger aggregates in which organic materials are the dominant stabilizing agents. When ultrasonically dispersed, aggregates with size of 20~2000 μm is disaggregated and formed sub-complexes (2~20 μm), which were subsequently dispersed into discrete clay particles (<2 μm). The other mechanism is liberation, as in Ferrosols in which oxides is dominant stabilizing agents. The discrete clay particles are directly released through the ultrasonic dispersion. Due to different dominant stabilizing agents, aggregate hierarchy could only be observed in soil nanoparticles from Argosols. The change in the zeta potential of soil nanoparticles from Argosols indicated the soil nanoparticles re-aggregated in the water suspension. This study proved that preservation of nanoparticles in water was not suitable to all soils. Alternatively, nanoparticles can be dried at low temperature immediately after the extraction.

The morphology of soil nanoparticles is showed in Fig. 3, It appears that soil nanoparticles were easily aggregated in water. The size of soil nanoparticles from Ferrosols was consistent with the data in Table 3 which was tested by Zetasizer nano. and the Fig. 3(a) had a slight distinct from the date, Table 2 showed that particle size of soil nanopartiles from Argosols was about 10 nm, but in Fig. 3 particle size was about 50 nm, it indicated that agglomeration had happened in Argosols, and it also could explain the great reduction in absolute value of zeta potential of Argosols.

BET surface area is an indicator for nanoparticles characteristics. Table 4 showed that BET surface area had a significant increase after dispersion into discrete nanoparticles. The BET surface area of soil nanoparticles from Ferrosols was smaller than that of Argosols. Compared with the original value of the soils, the BET surface of the soil nanoparticles increased nearly four times.

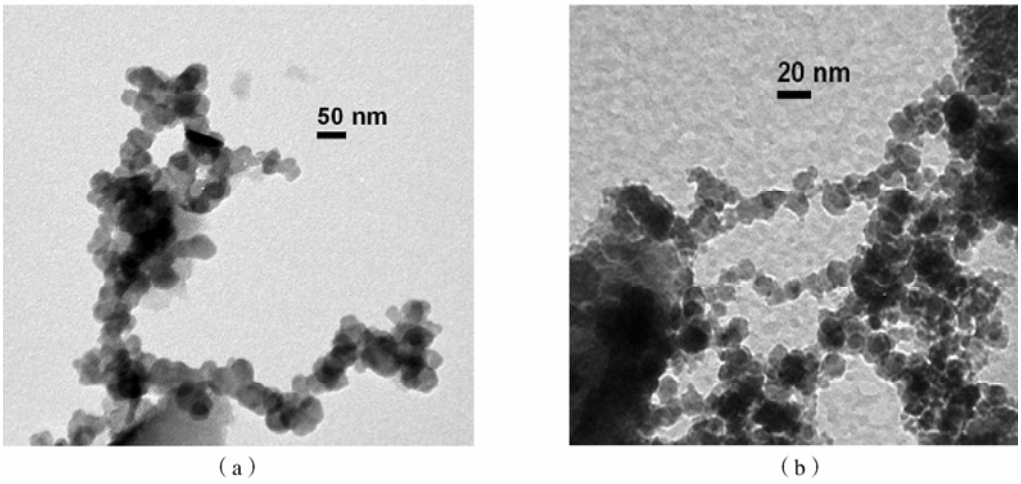

Fig. 3 Transmission electron micrographs of soils nanoparicles from Argosols and Ferrosols

Table 4 Comparasion in specific surface areas of original soils and soil nanoparticles

	BET surface area ($m^2 \cdot g^{-1}$)	
	Argosols	Ferrosols
Soils	24.0	14.0
Nanoparticles	112.0	55.6

Conclusion

This study extracted soil nanoparticles from Argosols and Ferrosols soils, the percentage of soil nanoparticle in Argosols was significantly higher than that in Ferrosols. Compared to Ferrosols, soil nanoparticles from Argosols were stable in water suspension, but for preservation, the nanoparticles can be dried at low temperature immediately after the extraction. The micrographes indicated that soil nanoparticles from both soils were easily aggregated in water, but agglomeration happened in soil nanoparticles from Argosols. The BET surface area of soil nanoparticles extracted from both soils dramatically increased compared with the original soils.

Acknowledgements

This work was jointly supported by the Y.C. Tang Disciplinary Development Fund of Zhejiang University, and the Program of Introducing Talents of Discipline to University (B06014).

References

Banfield J, Navrotsky A (2001) Nanoparticles and the Environment, Geochemistry Society of America and American Mineralogical Society. Washington DC, USA

Oades JM, Waters AG (1991) Aggregate hierarchy in soils. Aust. J. Soil Res. 29: 815-828

Surface and Adsorption Characteristics of Black Carbon from Different Sources

Mingkui Zhang*, Zhaoyun Liu

Zhejiang Provincial Key Laboratory of Subtropic Soil and Plant Nutrition,
College of Environmental and Resource Sciences, Zhejiang University, Hangzhou 310029, China.
*Corresponding author. E-mail: mkzhang@zju.edu.cn.

Abstract: Two black carbon (BC) samples, new BC and soil BC isolated from the burning residues and soil repectively, were characterized for their surface areas, surface acidity, zero point of charge, and adsorption capacity for metal (Cu) and organic pollutant (oxytetracycline). Compared with new BC, soil BC had a low surface area but a high surface acidity and thus a low isoelectric point. Soil BC had a stronger capacity for adsorbing Cu(II), but less for oxytetracycline. This study demonstrated that BC may be an important adsorbent of heavy metals and organic pollutants in soil, and the adsorption capacity of BC may be significantly influenced by soil environmental conditions where BC was formed.

Keywords: Black carbon; Surface characteristics; Adsorption; Heavy metals; Antibiotics; Soil

Introduction

Black carbon is the residues of incomplete combustion of biomass or fossil fuel. Black carbon is regarded as a chemically and biologically very stable carbon pool and can persist in nature for long periods of time (Goldberg, 1985). Black carbon may significantly affect nutrient retention and play a key role in a wide range of biogeochemical processes in soils, especially for nutrient cycling and pollutant adsorption (Liang *et al.*, 2006). However, the long-term persistence of black carbon does not mean that the properties of black carbon remain unchanged after its deposition. Cheng *et al.* (2006) have reported that properties of black carbon in soil environment could be altered through the formation of oxygen-containing functional groups. Therefore, properties of black carbon found in different environments could vary greatly. That also changes the ability of black carbon for acting as a filter to retain both organic and inorganic pollutants. The aim of this work was to compare differences in surface and adsorption characteristics of black carbon collected from the burning residues and soil.

Materials and Methods

Two different sources of BC samples were collected. One sample was wood burning residues, collected directly from farmyard. Another sample was taken from soil near the historical charcoal blast furnace. The BC found in the soil near the furnace site was deposited about 40 years ago. More than 100 large fragments of BC with a size 5~10 mm were carefully picked from the soil, pooled and used for this research. The collected BC samples were treated three times using 1 $mol \cdot L^{-1}$ HCl for demineralization and HCl-HF (1 $mol \cdot L^{-1}$-1 $mol \cdot L^{-1}$) for Si removal, subsequently. Following a thorough rinsing with distilled water four times until the electric conductivity was close to the background of distilled water, the residues were then oven-dried at 65 ℃ for 24 h for further analyses. Carbon, H, and N concentrations of BC samples were measured using an elemental analyzer. Ash content was analyzed by the loss of weight via combusting the BC samples at 550 ℃ for 2 h. Oxygen (O) concentrations were etermined by difference. Elemental composition of C, N, H, and O of BC samples were presented on a dry ash-free basis. Cation exchange capacity of BC was

measured by 1 mol·L^{-1} NH_4OAc (pH 7) exchange method. The spectra of FTIR absorbance were recorded between 400 and 4000 cm^{-1} with a FTIR Spectrometer. Potassium bromide (KBr) pellets containing 0.3% of finely ground black carbon powder were prepared and scanned. The surface charge of black carbon samples was assessed by the ion adsorption method (Uehara and Gillman, 1981). A KCl electrolyte (0.01 mol·L^{-1}) was used in the present study, in which both K and Cl ions were assumed to be bound by non-specific adsorption. Briefly, the method comprised three main steps: 1) preparation of a KCl saturated black carbon paste; 2) adjustment of the pH of black carbon to a range of pH values under the same ionic strength; 3) displacement of adsorbed K and Cl by 1 mol·L^{-1} ammonium nitrate. Surface positive charge was defined as the adsorption of anions (Cl^-), and surface negative charge was the adsorption of cations (K^+). Point of zero net charge (PZNC) was defined as the pH that had an equal amount of surface positive and negative charge. Surface areas of BC samples were measured using N_2 adsorption method. Surface acidity/basicity of BC samples was assessed by the selective acid/base neutralization method (Boehm, 1994).

The Cu (II) adsorption on BC samples at pH 5.0 values was measured by batch equilibration technique. Various amounts of the Cu (II) stock solution were introduced into a series of 50-mL plastic bottles containing 0.100 g of BC sample. Appropriate volumes of 0.01 mol·L^{-1} $NaNO_3$ solution were added to bring the final volumes in all bottles to 25 mL and make the initial concentrations of Cu (II) in bottles of 0, 6, 12, 18, 24, and 30 mg·L^{-1}. The background ionic strength was 0.01. The pH of the solution was then adjusted to desired value with 0.1 mol·L^{-1} HCl or 0.1 mol·L^{-1} NaOH. The bottles were capped and agitated at 25 ℃ on a shaker at 150 r·min^{-1} for 24. The amounts adsorbed were calculated from the difference between the initial and equilibrium concentrations.

The sorption experiment of oxytetracycline was performed as followings. For pre-equilibration, 0.1 g of air-dried, radiated black carbon sample was mixed with 20 mL 0.01 mol·L^{-1} $CaCl_2$ in 50 mL polypropylene test tubes and agitated in a rotary shaker for 24 h. In a preliminary test, 24 h was found to be a sufficient equilibration time. Five different concentrations of oxytetracycline, 1.25, 2.5, 5.0, 12.5, and 25.0 mg·L^{-1}, respectively, were made in 0.01 mol·L^{-1} $CaCl_2$. 20 mL of $CaCl_2$ solution and 5 mL of antibiotic solution were made for each soil at each concentration to reach a final volume of 25 mL with antibiotic concentrations of 0.25, 0.5, 1.0, 2.5, and 5.0 mg·L^{-1}, respectively in the test tubes. A blank for each soil and a control for each concentration were made. Blanks contained 25 mL of $CaCl_2$ solution and 0.1 g of each black carbon sample, and the control contained 20 mL of $CaCl_2$ solution and 5 mL antibiotic solution in a test tube without black carbon sample. All samples were agitated for 24 h in the rotary shaker. After centrifugation at 3000 g for 15 min samples of the supernatants were transferred to amber glass vials and subsequently analyzed by liquid chromatography combined with mass spectrometry (LC-MS).

Results

Carbon concentration in new BC was 85.1%, higher than in soil BC (71.8%). However, Oxygen, H, and N concentrations in new BC were much lower than in soil BC. The O, H, and N concentrations were 10.3%, 2.1%, and 2.5% for new BC, and 19.9%, 4.1%, and 4.2% for soil BC. The FTIR spectra of new BC showed a "flat" pattern and no bands were observed. However, the spectrum of soil BC showed discernable bands at wavenumbers of 3400 cm^{-1}, 1600, 1585, 1380, and 1260 cm^{-1}. The band at 3400 cm^{-1} was assigned to OH bonds, 1700 cm^{-1} to carboxylic acid groups, 1600 cm^{-1} to molecular vibration of ring stretching in C=C, 1585 and 1380 cm^{-1} to carboxylate, and 1260 cm^{-1} to phenolic acid functional (C-O) and COOH groups. The results suggested that soil BC possessed more oxygen-containing surface functional groups. This was manifested by the Boehm titration that soil BC had higher contents of carboxyl, lactonic, and phenolic groups than new BC. It was thus apparent that soil BC had much higher surface acidities than new BC (Table 1). Compared with new BC, soil BC had much smaller basicities.

Compared with new BC, soil BC exhibited a much lower surface area of 59 $m^2 \cdot g^{-1}$, being about 60% of that of new BC (98 $m^2 \cdot g^{-1}$). However, CEC of soil BC (27.77 cmol·kg^{-1}) was much higher than new BC (1.37 cmol·kg^{-1}). New BC had much lower CEC than soil BC. New BC had high amounts of surface positive charge, but very low amounts of surface negative charge (Fig. 1). In contrast to new BC, soil BC showed substantial amounts of surface negative

charge and had an average surface negative charge. The PZNC of new BC was at pH 5.5. The soil BC showed acidic PZNC value of around pH 3.4.

Table 1 Surface acidity and basicity of new BC and soil BC samples (cmol·kg^{-1})

Acidity/basicity	New BC	Soil BC
Carboxyl	17	45
Lactonic	14	28
Phenolic	12	23
Total acid	43	96
Base	16	5

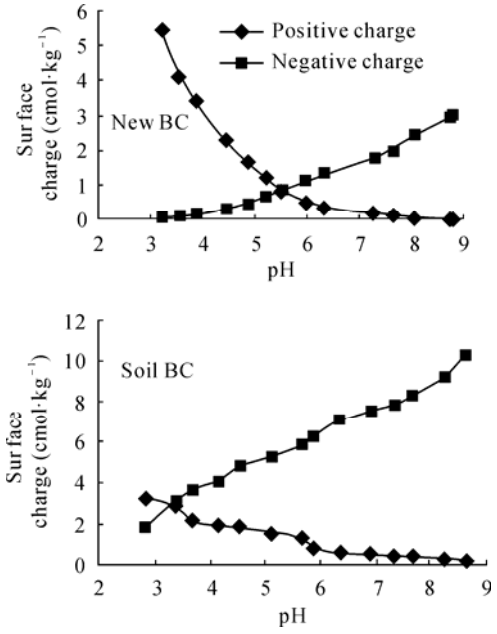

Fig.1 Values of surface positive charge and surface negative charge versus pH of black carbon samples

The adsorption isotherms of Cu (II) on new and soil BC from solution at pH 5.0 are conventionally plotted as the amount adsorbed (mg·kg^{-1}) vs. the equilibrium concentration (mg·L^{-1}). These isotherms were fit to the Langmuir equation with high correlation coefficients (*r*=0.9994~0.9996, *n*=5). In general, soil BC exhibited higher Cu (II) adsorption than new BC. The maximum adsorption capacity (Q_m) of Cu(II) for soil BC, calculated from the Langmuir equation was 3662 mg·kg^{-1}, higher than new BC (3163 mg·kg^{-1}). This result is consistent with the surface properties of the BC that soil BC had higher surface acidity than new BC.

The adsorption distribution coefficient of oxytetracycline, Kd, is defined as the ratio between the concentration of oxytetracycline bound to the soil (C_{soil}) and the concentration in solution after equilibration (C_{aq}). More than 99% of the added oxytetracycline was adsorbed, resulting in the extremely high Kd values. Generally, oxytetracycline had higher Kd values in the new BC (3773±836 L·kg^{-1}) than in soil BC (3331±788 L·kg^{-1}), suggesting that new BC had stronger capacity for adsorbing oxytetracycline than soil BC.

References

Boehm HP (1994) Some aspects of the surface chemistry of carbon blacks and other carbons. Carbon 32: 759-769

Cheng CH, Lehmann L, Thies JE, *et al.* (2006) Oxidation of black carbon through biotic and abiotic processes.Org. Geochemi. 37: 1477-1488

Goldberg ED (1985) Black Carbon in the Environment. John Wiley, New York

Liang B, Lehman J, Solomon D, *et al.* (2006) Black carbon increase cation exchange capacity in soils. Soil Sci. Soc. Am. J. 70: 1719-1730

Uehara G, Gillman G (1981) The Mineralogy, Chemistry, and Physics of Tropical Soils with Variable Charge Clays. Westview Press, Boulder, CO

A High-resolution TEM Investigation of Nanoparticles in Soils

Rui Zhu, Shenggao Lu*

Zhejiang Provincial Key Laboratory of Subtropical Soil and Plant Nutrition,
College of Environmental and Natural Resource Sciences, Zhejiang University, Hangzhou 310029, China.
*Corresponding author. E-mail: lusg@zju.edu.cn.

Abstract: Soil nanoparticles are nanometer-sized (-1~100 nm) crystalline to amorphous solid material formed in soil environment. It is now possible to understand their very interesting structure and properties using techniques developed for nanotechnology such as transmission electron microscopy. Structures and chemical composition of nanoparticles in red soil (Ultisol) were studied by high-resolution transmission electron microscopy (HRTEM), electron diffraction and elemental analysis (EDX). Electron-dense, well crystalline iron oxide nanoparticles were identified. The iron oxide phase usually coated and/or embedded on the surface of larger size aluminosilicate phase. High-resolution studies using HRTEM and EDX of nanoparticles in soil have a great potential for understanding physical properties, chemical reactivity and environmental processes of nanoparticles in the soils.

Keywords: Soil nanoparticle; High-resolution transmission electron microscopy (HRTEM); Iron oxide; Energy-dispersive X-ray analysis (EDX)

Introduction

Nanominerals and mineral nanoparticles are common and widely distributed throughout the atmosphere, oceans, groundwater and surface waters, soils, and even in most living organisms. Well-known examples of soil nanoparticles include certain clays as well as iron and manganese (oxyhydr-) oxides. Soil nanoparticles contribute greatly to such dynamic soil processes as soil genesis, trace element cycling, contaminant transport and chemical reaction (Nowack and Bucheli, 2007; Wigginton *et al.*, 2007; Wilson *et al.*, 2008). For example, the Fe-oxide nanoparticles in soils affected a great number of environmental processes, such as metal contaminant immobilization, geocatalysis and degradation of organic contaminants (Hochella *et al.*, 2008; Laham, 2008; Waychunas *et al.*, 2005). Therefore, soil nanoscience will facilitate to understand the physical property, chemical reactivity, and soil environmental processes as are various aspects of nanotechnology applications in environmental science. High-resolution transmission electron microscopy (HRTEM) combined with its accompanying analytical techniques is one of the best tools for direct visualization on size distribution, surface area, and the chemical makeup and /or mineral phase of the nanoparticles in soils. However, these techniques that are well used for nanoanalysis in materials science are little known and used in soil sciences. In order to achieve an improved understanding of nanoparticles in soils, the HRTEM was applied for the direct observation of the crystalline structure and mineral phase of individual soil nanoparticles.

Materials and Methods

A topsoil (0~20 cm) sample of red soil (Ultisol) formed Quaternary red clay was used for this study. The sample was air dried, gently crushed and passed through a 100 mesh sieve. The mineralogical composition of soil sample was characterized using X-ray diffraction (Rigaku D/Max 2550pc) at Cu Ka radiation at 40 kV and 40 mA. The samples were scanned from 2 to 70° θ and the scanning rate was 2° θ

per min. The soils were dispersed ultrasonically and a drop of the suspension was air-dried onto carbon-coated copper grids. Transmission electron microscopy (TEM) observation of the samples was performed with a high resolution transmission electron microscopy (HRTEM, JEM-2010HR) coupled with an energy-dispersive X-ray (EDX) spectrometer (Dxford-1NCA).

Results and Discussion

X-ray diffraction analysis showed the existence of several kinds of crystalline clay mineral phases in soil samples, including kaolinite, illite and iron oxides. The TEM images of nanoparticles are shown in Fig.1. TEM observation indicated that many micro-crystalline aluminosilicate and iron (hydr) oxides minerals as well as amorphous substances occured in soils as nanoparticles (Fig. 1). They were irregular in shape and usually ranged from tens of nm to near hundred of nm in size. Very dense cluster packing by nanoparticles observed in the TEM images suggested strong bonding between mineral phases. The iron oxide nanoparticles were usually coated or embedded within the surface of larger particles of aluminosilicate. The EDX results revealed that the composition of these nanoparticles was dominated by Si, Fe, and Al. Selected area electron diffraction (SAED) of iron oxide revealed that they were well crystallized. The associated technique of X-ray energy-dispersive spectra also helped us to differentiate the iron oxide from silicate minerals. Iron oxide and hydroxide phases such as goethite, hematite and maghemite, were frequently identified in the tropical and subtropical soils. Such minerals are generally considered as potential sinks for trace elements and toxic heavy metals.

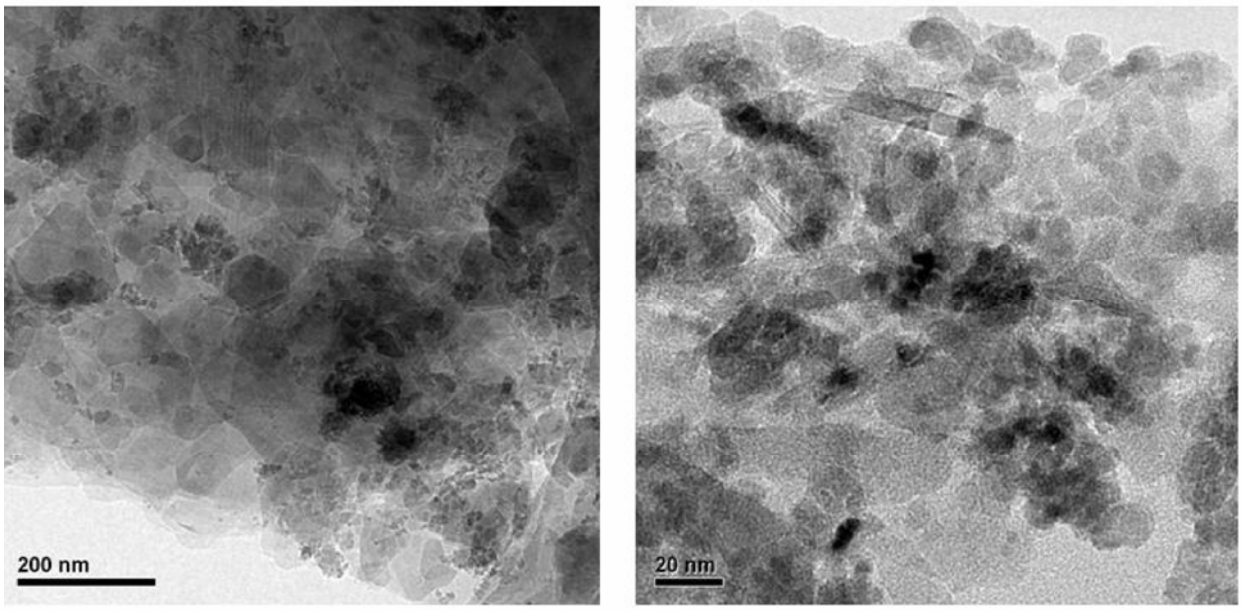

Fig. 1 TEM images of nanoparticles in the soil (Ultisol). Nano microcrystalline particles are evident from these images. Electron-dense, well crystalline particles can be identified as iron oxide nanoparticles

The HRTEM image of nanoparticles is shown in Fig. 2. The fast Fourier transformation (FFT) of lattice fringes for the selected regions of the HRTEM image of nanoparticles was shown as an inset. The lattice fringes observed in the HRTEM image indicated that the nanoparticles were well crystallized. The measured lattice fringe spacing values were 0.274 and 0.331 nm, respectively. The measured d-spacings were consistent with hematite and/or maghemite. Elemental composition of the nanoparticles was investigated with an energy dispersive X-ray analyzer (EDX). All analysed electron-dense particles exhibited an iron peak and an oxygen peak (Fig. 2). The copper peak present in the spectrum was due to the grids used for the analysers.

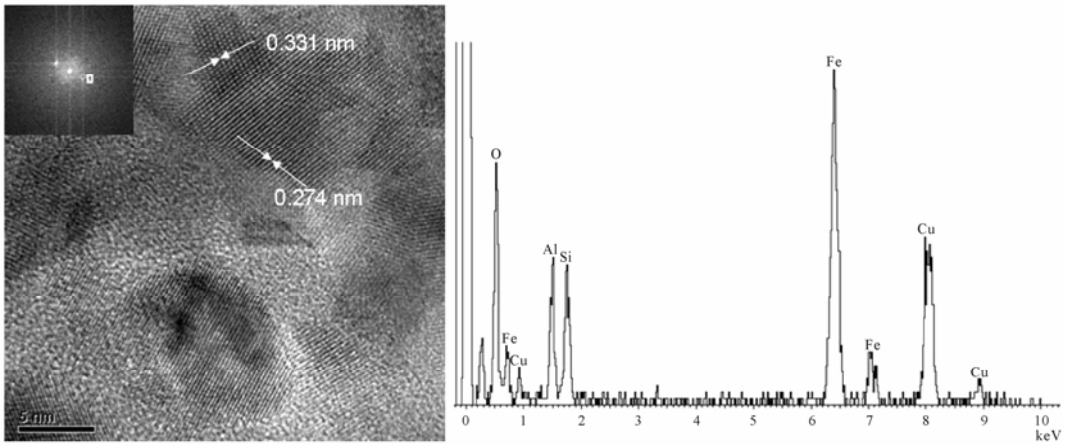

Fig. 2 High-resolution TEM image of nanoparticle in soil. The measured values of lattice fringe spacing value were indicated. Inset on the left corner shows the fast-Fourier-transform (FFT) of the HRTEM image, which indicated the direction in which the crystallite was examined and lattice planes contributing to the diffraction. The well-resolved lattice fringes indicate the crystalinity of the nanoparticles in soil

The HRTEM investigation indicated the major mineral phases that could exist as nanoparticles. These nanoparticles were very different in size, shape and chemical composition. Among them, the iron oxides were one of the most important environmental nanoparticles. These iron oxide nanoparticles are commonly formed as weathering by-product of minerals and biogenic products of microbial activity. Recent studies indicated that nanocrystalline iron oxide had significant implications for trace metal and toxic heavy metal transport (Nowack and Bucheli, 2007; Waychunas *et al.*, 2008). Iron oxides nanoparticles were found to have a high sorption capacity for heavy metals (Wigginton *et al.*, 2007; Lahann, 2008). Another considerable interest for iron oxide nanoparticles is to apply synthetic nanoparticles for the remediation of environmental contaminants (Lahann, 2008; Waychunas *et al.*, 2005).

Our HRTEM studies based on the analyses of individual iron oxide nanoparticles provided insights into how the mineral particles interacted with heavy metal ions. The HRTEM observation suggests clearly that iron oxide nanocrystalline phases are major nanomineral phases in the red soils. Therefore, TEM can be a particularly efficient method for the investigation of nanoparticles in soils. Measuring and understanding nanomineral and mineral nanoparticle origin, geographic distribution, relevant nano-chemistry, and overall influence and impact within the soil environment are the critical challenges for the future research of soil science. The TEM combined with either selected area electron diffraction (SAED) or the fast Fourier transform (FFT) of high resolution images has the great potential for characterizing the atomic structure and mineral phase of nanoparticle in soils.

References

Hochella Jr MF, Lower SK, Maurice PA, Penn RL, Sahai N, Sparks DL, Twining BS (2008) Nanominerals, mineral nanoparticles, and Earth systems. Science 319: 1631-1635

Lahann J (2008) Environmental nanotechnology: nanomaterials clean up. Nature Nanotechnol. 3: 320-321

Nowack B, Bucheli TD (2007) Occurrence, behavior and effects of nanoparticles in environment. Environ. Pollut. 150: 5-22

Waychunas GA, Kim CS, Banfield JF (2005) Nanoparticulate iron oxide minerals in soils and sediments: unique properties and contaminant scavenging mechanism. J. Nanopart. Res. 7: 409-433

Wigginton NS, Haus KL, Hochella MF, Jr (2007) Aquatic environmental nanoparticles. J. Environ. Monit. 9: 1306-2636

Wilson MA, Tran NH, Milev AS, Kamali Kannangara GS, Volk H, Max Lu GQ (2008) Nanomaterials in soils. Geoderma 146: 291-302

Adsorption and Desorption of Tylosin on the Colloidal Fractions of Black Soil

Chunhong Wang, Aifang Xue, Wei Liang, Peng Cai, Qiaoyun Huang*

State Key Laboratory of Agricultural Microbiology, Key Laboratory of Subtropical Agriculture and Environment, Huazhong Agricultural University, Wuhan 430070, China.
*Corresponding author. Tel. No. +86 27 87671033; Fax No. +86 27 87280670; E-mail: qyhuang@mail.hzau.edu.cn.

Abstract: Adsorption and desorption of tylosin on different colloidal fractions from Black soil were studied. The adsorption isotherms of tylosin conformed to the Langmuir equation. The amount of Tylosin adsorbed followed the order: fine organic clay > fine inorganic clay > coarse organic clay > coarse inorganic clay. Marked decreases in the adsorption of tylosin on soil colloids were observed in the presence of Na^+ and Ca^{2+} ions, and the influence of Ca^{2+} was stronger than that of Na^+. The sorbed tylosin on soil colloids was sequentially desorbed by 10 mmol·L^{-1} Tris, 100 mmol·L^{-1} NaCl and 100 mmol·L^{-1} phosphate solutions at pH 7.0. The percent desorption by Tris and NaCl was 79%~105%, showing that electrostatic interaction played an important role in the adsorption of tylosin by soil colloidal components.

Keywords: Adsorption; Desorption; Soil colloid; Tylosin

Introduction

Large amounts of antibiotic substances have been used for growth-promoting purpose and the increase of feed efficiency over the past years. As antibiotics are poorly adsorbed in the gut of the animals, the majority is excreted unchanged in faeces and urine (Sarmah K *et al.*, 2006). Soil environment receives animal waste containing antibiotics as a supplement to fertilizer. It is possible that antibiotics accumulate in the surface soils or enter water environments due to their higher mobility (Johannes T, 2000). Therefore, increasing attention has been paid to the behavior of antibiotics in soil and associated environments. In the present study, the adsorption and desorption of tylosin on different active particles from Black soil were investigated.

Materials and Methods

Tylosin tartrate was purchased from Sigma Company. Black soil was sampled from Jilin province. Soil colloids were obtained through siphon method after dispersion, and they were separated into coarse clays and fine clays by centrifugation. Part of fine and coarse clays was oxidized by H_2O_2 to remove organic matter. The adsorption experiments of tylosin on soil colloids were conducted at tylosin concentrations ranging from 5 mg·L^{-1} to 90 mg·L^{-1}. Tylosin in the supernatant was determined by high performance liquid chromatogramphy (HPLC). The amount of tylosin adsorbed was calculated by the difference between the amount of tylosin added and that remaining in the supernatant. A sequential extraction with Tris buffer, NaCl and phosphate solutions was performed to wash the adsorbed tylosin. The washings were repeated until no more tylosin was detected in the supernatant.

Results and Discussions

Equilibrium Adsorption of Tylosin

Tylosin adsorbed by soil colloids fitted the Langmuir equation (Table 1). The amount of tylosin adsorption on fine clays was greater than that on coarse ones. For coarse or fine clays, the amount of

tylosin adsorption on organic clay was larger than that on inorganic clays. The estimated K values were in the order of coarse inorganic clay > coarse organic clay = fine inorganic clay > fine organic clay, indicating that the affinity of tylosin on coarse clays was higher than that on fine clays and inorganic clays had a greater affinity for tylosin than organic ones.

Table 1 Langmuir parameters for adsorption of tylosin on soil colloids

Soil colloid	X_m (mg·g^{-1})	K (L·mg^{-1})	R
Coarse organic clay	17.80	0.02	0.99
Coarse inorganic clay	13.54	0.05	0.99
Fine organic clay	33.81	0.01	0.99
Fine inorganic clay	22.22	0.02	0.99

Effect of Electrolyte

Fig. 1 shows that the adsorption of tylosin on soil clays was decreased significantly in the presence of Na^+ and Ca^{2+} ions. The inhibiting effect of Ca^{2+} ions was stronger than that of Na^+ ions. These observations suggest that the binding of tylosin on examined soil components was mainly via ion exchange processes. The bivalent cations might occupy more exchange sites and compete more effectively with tylosin on the surface of soil colloidal fractions.

Desorption of Tylosin

The percent desorption of bound tylosin by Tris and NaCl from examined clays was 79%~105% (Table 2). The results conformed that the electrostatic force played a vital role in the adsorption of tylosin by the examined soil colloids. The desorption rates by three reagents were in the order of coarse organic clay > coarse inorganic clay > fine organic clay > fine inorganic clay. These data implied that the fine clays exhibit higher affinity for tylosin and some other interactions except for electrostatic force could be involved in the adsorption of the antibiotic by these soil particles.

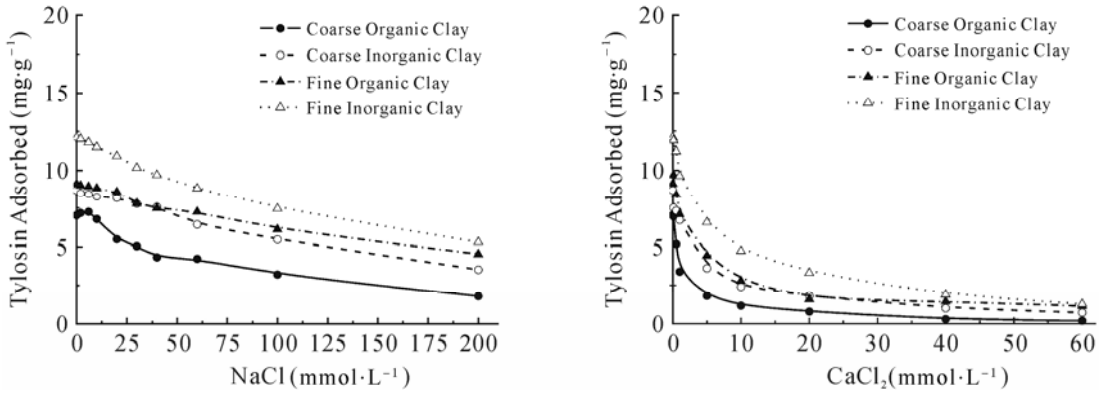

Fig. 1 Equilibrium adsorption of Tylosin on soil colloids in the presence of Na^+ and Ca^{2+}

Table 2 The percent desorption of tylosin on soil colloids by Tris, NaCl and phosphate sequentially extraction

Soil colloid	Tris-HCl (%)	NaCl (%)	Phosphate (%)	Total (%)
Coarse organic clay	90	15	0	105
Coarse inorganic clay	81	19	0	100
Fine organic clay	69	13	0	82
Fine inorganic clay	58	21	0	79

In conclusion, tylosin was adsorbed mainly by electrostatic force on the surface of Black soil colloids and was easily desorbed. Fine soil clays showed higher adsorption capacity and affinity for the antibiotics. Findings obtained in this study are helpful for the understanding of interaction mechanisms of antibiotics with soil constituents.

References

Sarmah AK, Meyer MT, Boxall ABA (2006) A global perspective on the use, sales, exposure pathways, occurrence, fate and effects of veterinary antibiotics (VAs) in the environment. Chemosphere. 65: 725-759

Johannes T (2001) Sorption of veterinary phamaceuticals in soils: a review Environ. Sci. Technol. 35: 3397-3406

Session 5

Environmental Processes and Ecosystem Health

Spatial and Temporal Dimensions of Environmental Processes in Soils— An Integrated Approach

Winfried E.H. Blum*

University of Natural Resources and Applied Life Sciences (BOKU), Vienna, Peter Jordan Str. 82, 1190 Vienna, Austria.
*Corresponding author. Tel. No. (+43-1-)47654-3101; Fax No. (+43-1)47654-3130; E-mail: winfried.blum@boku.ac.at.

Abstract: We explain the spatial and temporal dimensions of physical, chemical and biological processes in the soil pore space through an integrated approach.

Keywords: Energy forms; Process parameters; Time scale of reactions

Extended Abstract

Environmental processes in soils are governed by 4 different types of energy (Blum, 2008):

-ravitational energy (gravity);
-orogenic energy (chemical and crystallographical composition of the rock parent material);
-solar energy (radiation and organic matter);
-anthropogenic energy (mainly fossil energy).

All environmental processes in soils occur exclusively in the pore space, which is not constant in time and determines the type and the velocity of processes through its varying spatial dimensions (pore diameters) and its physical, chemical and biological conditions (Blum, 2002; 2006).

Moreover, the time scale of physico-chemical and biological-biochemical reactions in the soil pore space is quite different, because the velocity of physico-chemical surface reactions, such as adsorption, desorption, precipitation, complexation, hydrolysis, oxidation, reduction etc. is rather high (seconds, minutes, hours), whereas the velocity of biological /biochemical processes, like mineralisation and metabolisation of organic compounds is rather low (hours, days, weeks, years).

Five main soil parameters are determining these processes:

-the total inner surface of the soil (total surface of the pore walls) and its spatial distribution (pore diameters);
-the constituents of the inner soil surface (pore walls), e.g. clay minerals, oxides, organic matter, their physico-chemical structures and electric charges (positive/negative);
-the soil organisms (flora and fauna) living in the pore space;
-the pH and redox potential of the soil solution, and
-the soil temperature (energy).

The genesis of the soil pore space, its constituents and specific physical, chemical and biological characteristics are described and the interactions between biological and physico-chemical processes are discussed.

References

Blum WEH (2002) Soil pore space as communication channel between the geosphere, the atmosphere and the biosphere. 17th World Congress of Soil Science, 14-21 August 2002, Bangkok/Thailand. - CD-ROM Transactions No. 2014, Abstracts, Volume V, 1942, IUSS.

Blum WEH (2006) Chemical impacts on hydrophysical processes in porous media—Methodological and theoretical approaches to study hydro- and thermo- physical characteristics of porous media. Workshop Lublin, 12-14 February 2006, Book of Abstracts, p.6, IAP Lublin

Blum WEH (2008) Forms of energy involved in soil and sediment processes. J. Soils Sediments 8, 1-2

Emission, Fate and Exposure Risk of Polycyclic Aromatic Hydrocarbons in China

Shu Tao*, Yanxu Zhang

Laboratory for Earth Surface Processes, College of Urban and Environmental Sciences,
Peking University, Beijing 100871, China.
*Corresponding author. E-mail:taos@urban.pku.edu.cn.

Abstract: An Euler atmospheric transport model was applied to model the near ground atmospheric concentration of polycyclic aromatic hydrocarbons (PAHs) in China based on a high-resolution emission inventory. The results were used to assess inhalation exposure and lung cancer risk of Chinese population. Monte Carlo simulation was conducted to address the uncertainty and variability in exposure concentration, intake rate and cancer risk. Frequency distributions of inhalation rate and lung cancer susceptibility were used for the simulation. For the latter, the frequencies of various genotypes for genes associated with the metabolism of PAHs and DNA repair were collected and a dose-response relationship between the number of at-risk alleles and DNA adduct level was derived from the literature. The distribution of the risk-related genotypes was transformed to the distribution of DNA adduct level as an indicator for individual susceptibility. It was found that the means of the total PAH concentration and banzo[a]pyrene equivalent concentration were 200 (106~370 as interquartile range, IR) $ng \cdot m^{-3}$ and 2.43 (IR 1.29~4.50) $ng \cdot m^{-3}$, respectively. 5.8% (IR 2.0%~11%) of territory where 30% (IR 17%~43%) of population live, exceeded the national standard for PAHs. The calculated extra life-long lung cancer morbidity of Chinese population due to inhalation exposure to PAHs was 51.5×10^{-5} (IR $27.3 \times 10^{-5} \sim 95.3 \times 10^{-5}$). Due to inter-individual viabilities in inhalation rate and susceptibility, size of the populations with very low or very high lung-cancer risk increased and the size of population with PAH induced extra lung-cancer morbidity greater than 100×10^{-5} were 11% (IR 3.3%~24%) and 22% (IR 15%~32%) with or without taking the inter-individual viabilities into consideration.

How Do Microbial Extracellular Enzymes Locate and Degrade Natural and Synthetic Polymers in Soil

Richard G. Burns*

School of Land, Crop and Food Sciences, The University of Queensland, Brisbane, Queensland 4072, Australia.
*Corresponding author. Tel. No. +61 7 3365 2509; Fax No. +61 7 3365 1177; E-mail: r.burns@uq.edu.au.

Abstract: In soils, microorganisms encounter complex organic matter that is rich in the energy, carbon and nutrients that are required for cell maintenance and growth. Cellulose and lignin are two of the most abundant biopolymers. However, bacteria and fungi do not have the ability to transport these into the cytoplasm; instead they depend on the activity of enzymes that are secreted into their immediate environment. These extracellular catalysts decompose organic compounds and generate soluble chemicals that are recognized by cell wall receptors and transported into the cell. Many organic pollutants in soil are polymeric, and poorly soluble and these also require extracellular catalysis prior to uptake, metabolism and detoxification. The complexity and diversity of extracellular enzymes and the macromolecules that they degrade will be reviewed and the many locations and multiple fates of these enzymes discussed. Ways in which extracellular enzymes overcome the destructive or inhibitory properties of the soil matrix and various strategies they adopt for effective substrate detection and utilization will be described.

Keywords: Extracellular enzymes; Cellulose; Lignin; Microbial ecology; Cellulosomes; Soil-enzyme complexes

Introduction

Enzyme synthesis and externalization is an energetically expensive process and regulatory mechanisms and ecological strategies have evolved to ensure the efficient capture of the products of substrate catalysis. However, soil is an hostile environment for extracellular enzymes because, once they leave the cell, they are subject to denaturation, degradation, adsorption and dilution. The locations and functions of enzymes in soil have been researched and discussed for decades (e.g. Burns, 1978; Burns and Dick, 2002; Caldwell, 2005) but recent advances in molecular, microscopic, and analytical techniques coupled with imaginative thinking (e.g. Schimel and Weintraub 2003; Allison, 2005) have begun to provide new insights. Other stimuli are due to the recognized importance of enzyme activity to a large number of industrial, medical and environmental problems.

Substrate and Enzyme Diversity in Soils

Extracellular enzymes in soils catalyze the degradation of a huge variety of plant, animal and microbial macro-molecules primarily through hydrolytic and oxidative reactions. Cellulose and lignin require the simultaneous and/or sequential activities of a large number of enzymes produced by a diverse community of bacteria and fungi; it is likely that more than fifty different extracellular enzymes are involved in the breakdown of a plant leaf even before the low molecular mass carbon sources can enter the cell. Cellulose is a structurally complex and insoluble polymer that different microbes have developed different strategies to deal with. The rewards are great: an abundance of glucose. Basidiomycete and ascomycete fungi are major degraders of cellulose, typically employing a battery of extracellular hydrolytic enzymes including endo-1, 4-β-glucanases, cellobiohydrolases and β-glucosidases.

The best known cellulose degrader, *Trichoderma reesei*, has thirty or more glycosyl hydrolases including seven endo-glucanases, and a secretome containing greater than one hundred proteins. Lignin, with which cellulose is usually associated, is a chemically complex phenylpropanoid that is degraded by a suite of oxidative enzymes including laccases, manganese peroxidases, lignin peroxidases, cellobiose dehydro-genases and pyranose-2-oxidases (Baldrian, 2006). The involvement of Fenton chemistry in the process demands the input of enzymes generating hydrogen peroxide as well as Fe^{2+} and Mn^{2+}. Lignin degradation involves white-rot, soft-rot and brown-rot fungi and each has a different strategy (Osono, 2007). The white rot fungus *Phanero-chaete chrysosporium* has more than 100 glycosyl hydrolases, in excess of 20 "ligninases" and a secretome of almost 800 proteins. The feasibility of using *P. chrysosporium* (and other fungi) for the oxidative degradation of organic pollutants, such as PAHs and PCPs, has been much studied (Rubilar *et al*., 2008).

Regulation and Location of Extracellular Enzymes

In some cases, microbes produce small amounts of extracellular enzymes regardless of substrate availability as a speculative mechanism to detect substrate. If the substrate is present, these constitutive enzymes generate signals that induce additional enzyme synthesis. The synthesis *de novo* of many extracellular enzymes is stimulated in the presence (or sometimes absence) of a suitable substrate or other inducer. Cellulases are controlled by organic substrates and products but ligininases respond to redox potential, ionic strength, Fe^{2+}, CO_2, light, sulphide and sulfate and oxalic acid. The subsequent metabolism of complex carbon and energy sources will be governed by the growth require- ments of the microorganisms and C:N, C:P and even C:Ca, C:Mg and C:Fe ratios. Extracellular enzymes are contained within the periplasmic space (Gram-negative bacteria), associated with the outer cell wall, or released into the soil. The third group may be sorbed and inactivated or denatured and degraded although many extracellular enzymes are inherently more stable than their intracellular counterparts because they are glycosylated or have disulfide bonds. These modifications provide thermo-stability, a broad pH range for activity, and also some resistance to proteases. Once in the aqueous phase, some enzymes become stabilized through interactions with clay minerals and humic acid and retain activity (Burns, 1982; Allison, 2006). However, other enzymes may have reduced or even no *in-situ* activity (Quiquampoix and Burns, 2007). Nonetheless, stabilized soil enzymes represents a reservoir of potential enzyme activity. Indeed, it may represent the first catalytic response to changes in substrate availability in soils and may serve as the originator of signaling molecules for the microbial community.

Soil Enzyme Ecology

The multiple locations of extracellular enzymes combined with the capacity of the microbial community to detect potential substrates, suggest that there are many ways by which macromolecular organics can be transformed into soluble matter. Enzymes that are retained on the outer cell wall are likely to be configured such that their active sites are exposed and the zones that are susceptible to attack by proteases are protected. Other cell-bound extracellular enzymes include those contained within a multicellular biofilm and others that are protected by structures attached to the cell wall. These are the cellulosomes and contain cellulases (as well as hemi-cellulases and pectins) that are arranged on a scaffold that facilitates efficient cleavage of polysaccharides (Bayer *et al.*, 2008).

Once enzymes have diffused away from their parent cell they encounter a hostile environment. Even if the enzymes survive, the substrate may not be found and, even if it is, the correct combination of enzymes in the right sequence must be present for catalysis to occur. A way to overcome some of these constraints is suggested by a mechanism that involves microbes 'sensing' both the substrate and their own population numbers. In this way gene function is connected to cell density and enzymes are only synthesizing and/or secreted when cell numbers are high enough to have a major impact. This is a process known as quorum sensing and has been well-described for many phytopathogens especially *Erwinia* species (Barnard and Salmon, 2007). Quorum sensing in the rhizosphere is believed to be an important controlling process for all sorts of microbial interactions (DeAngelis *et al*., 2008).

Once in contact with their substrate many polysaccharases have a number of ways in which they not only maintain their stability but also increase their activity. One mechanism relates to the all-important substrate binding moiety (Wilson, 2008) which, in the case of cellulase, anchors the enzyme to the substrate at appropriate points for the enzyme's catalytic domain to cleave the β-1, 4-linkages. Few microorganisms secrete all the necessary enzymes and must rely on other microbes to successfully generate the soluble products. This observation reinforces the idea of a community-driven process.

The products of extracellular organic matter break-down may be intercepted by other microbes which, although not investing any resources in enzyme production, will benefit (Allison, 2005). Some microbes employ antibiotics and enzymes to reduce this 'cheating', others rely on the activities of predators to control their rivals. Of course, what might appear to us as cheating may be part of a complex and poorly understood microbial community synergy: the so-called cheaters provide some direct or indirect benefit to the cheated. Or it may be that the benefits of a successful extra-cellular depolymerization far outweigh the disadvantages derived from some of the products being high-jacked. It would be useful to produce an energy budget that compares investment to interest within the microbial community.

Conclusions

An enhanced knowledge of extracellular enzyme function will have many practical applications, including manipulating the soil for bioremediation, biocontrol, plant nutrient generation and availability, and C cycling and sequestration. There are also implications for plant and mammalian pathology, biofuel production, and the impacts of climate change on enzyme activities and the humic matter pool. One of the greatest challenges in soil biology is to link the functional and ecological aspects of microbial extracellular enzyme activities to organic matter degradation. We are equipped with the analytical (electrophoretic, chromatographic, mass spectrometric), microscopical (fluorescence, scanning probe, atomic and ultrasonic force, confocal laser, differential interference), molecular (genomics, proteomics, metabolomics, secretomics, metagenomics) and bioinformatic tools to achieve these objectives (Wallenstein and Weintraub, 2008). Are the activities of microbial enzymes in soil an example of organized chaos, ongoing selection processes or the expression of an advanced and stable community? The next few years will answer many of these questions.

References

Allison SD (2005) Cheaters, diffusion and nutrients constrain decomposition by microbial enzymes in spatially structured environments. Ecol. Lett. 8: 626-635

Allison SD (2006) Soil minerals and humic acids alter enzyme stability: implications for ecosystem processes. Biogeochemistry 81: 361-373

Baldrian P (2006) Fungal laccases, occurrence and properties. FEMS Microbiol. Rev. 30: 215-242

Barnard AML, Salmon GPC (2007) Quorum sensing in *Erwinia* specioes. Anal. Bioanal. Chem. 387: 415-423

Bayer EA, Lamed R, White BA, Flint HJ (2008) From cellulosomes to cellulosomics. Chem. Record 8: 364-377

Burns RG (1978) Soil Enzymes. Academic Press, New York

Burns RG (1982) Enzyme activity in soil-location and a possible role in microbial ecology. Soil Biol. Biochem. 14: 423-427

Burns RG, Dick RP (2002) Enzymes in the Environment: Activity, Ecology and Applications. Marcel Dekker, New York

Caldwell BA (2005) Enzyme activities as a component of soil biodiversity: A review. Pedobiologia 49: 637-644

DeAngelis KM, Lindow SE, Firestone MK (2008) Bacterial quorum sensing and nitrogen cycling in rhizosphere soil. FEMS Microbiol. Ecol. 66: 197-207

Osono T (2007) Ecology of ligninolytic fungi associated with leaf litter decomposition. Ecol. Res. 22: 955-974

Quiquampoix H, Burns RG (2007) Environmental and health consequences of protein interactions with soil mineral surfaces. Elements 3: 401-406

Rubilar O, Diez MC, Gianfreda L (2008) Transformation of chlorinated phenolic compounds by white rot fungi. Crit. Rev. Environ. Sci. Tech. 38: 227-268

Schimel JP, Weintraub MN (2003) The implications of exoenzyme activity on microbial carbon and nitrogen limitation in soil: a theoretical model. Soil Biol. Biochem. 35: 549-563

Wallenstein MD, Weintraub MN (2008) Emerging tools for measuring and modeling the in situ activity of soil extracellular enzymes. Soil Biol. Biochem. 40: 2098-2106

Wilson DB (2008) Three microbial strategies for plant cell wall degradation. Ann. NY Acad. Sci. 1125: 289-297

Influence of Solution Composition on the Exfoliation of Organic Matter from a Model Soil System

Charisma Lattao[a], Robert L. Cook[a,b,*]

[a]Department of Chemistry, Louisiana State University, Baton Rouge, LA, 70803;
[b]Department of Chemistry, Southern University, Baton Rouge, LA, 70813.
[*]Corresponding author. Tel. No. 1-225-578-2980; Fax No. 1-225-578-3458; E-mail: rlcook@lsu.edu.

Abstract: It has recently been demonstrated that small perturbation of hydrophobic interactions and hydrogen bonding via small changes in solution composition can greatly alter the conformation of dissolved organic matter. This work investigates if the same holds for in-situ soil organic matter (SOM) by exfoliating it with solvent systems (SSs) of different compositions. The effects of aqueous solutions composed of 4.6×10^{-3} mol·L^{-1} acetic acid (AA), acetonitrile (ACN), dimethyl sulfoxide (DMSO), hydrochloric acid (HCl), and methanol (MeOH) as well as 18 MΩ H_2O were investigated. Only the ACN SS showed marked difference in the amount and type of organic matter exfoliated compared to that exfoliated by H_2O only, as monitored by UV/Vis absorbance, fluorescence, attenuated total reflectance Fourier transformed infrared (ATR-FTIR), and ^{13}C cross polarization magic angle spinning (CP-MAS) spectroscopy. It was found that after 20 days the ACN exfoliation solution had turned brown while the other solutions remained yellow, and that this color change could be attributed to more of the humified materials being exfoliated. It was also found that an additional 25 days allowed for a larger amount of the less humified material to be subsequently exfoliated. Based on these findings, a solvation model is put forward along with an explanation for the differences seen for the ACN SS. Both are relevant to hydrophobic organic compound sorption, remediation, and soil wetting processes.

Keywords: Soil organic matter; Exfoliation; Synchronous fluorescence; Humification index; CP-MAS ^{13}C; Wetting

Introduction

The view of humic materials as polydispersed polymers as well as micelles is slowly being replaced by the notion of a collection of loosely associated (via hydrophobic interactions and hydrogen bonds) diverse compounds, and is largely based on studies performed on dissolved extracted fractions (Piccolo, 2001; Sutton and Sposito, 2005). Thus, it is of great interest, and an objective of this work, to see how this modern view extends to SOM in its native state, and how one views the sorption of xenobiotic compounds by soils, the remediation of polluted soils, bioremediation, and SOM dynamics and their role in the ecosystem (e.g. water retention) (Stevenson, 1994; Pignatello and Xing, 1996; Luthy *et al.*, 1997; National Research Council, 2002).

This work investigates the role played by very small amounts of completely miscible organic solvent (CMOS) in water in perturbing the association of SOM and liberating organic matter from the geomatrix (from hereon called exfoliation). These experiments can be viewed loosely as the whole soil analogs to those carried on extracted humic materials.

Materials and Methods

Materials and Reagents

The model soil used throughout the experiment is IHSS Pahokee Peat II (PP). 18 MΩ de-ionized water

was used for all sample preparations. All other reagents were sources from Acros and allsolvents were HPLC grade.

Exfoliation Procedure

4.6×10^{-3} mol·L^{-1} SSs of AA, ACN, DMSO, HCl, and MeOH were prepared. Experiments were carried out at 0.005 w/v ratio e.g. 0.1 g soil 20 mL of SS (including the 18 MΩ de-ionized H_2O) in aluminum wrapped 20 mL capped glass vials (in triplicate) or 125 mL capped glass bottles (45 day exfoliations). 1 mL aliquots were taken and diluted to 50 mL with H_2O; in addition, for the 45 day runs, 4 mL, 2 mL, and 0.5 mL aliquots were diluted to 50 mL.

Spectroscopic Analysis of the Diluted Supernatant

UV-Vis data were collected using an Agilent 8453 or a Cary spectrophotometer using a 1.0 cm quartz cell. Emission and synchronous fluorescence spectra were acquired using a Spex 3 Fluorolog Jobin Yvon spectrofluorometer utlilizing 1 scan, 0.2 s integration, 1 nm increments, and 4 nm for both emission and excitation slit widths.

Results and Discussion

SOM swelling and solvation were expected to be slow processes, as was the exfoliation process. This is supported by the fact that 280 nm absorbances after 1 hour of sitting (the time needed for particle settlement) were found to be 0.028, 0.027, 0.028, and 0.30 for the H_2O, DMSO, ACN, and MeOH SS, respectively, and are substantially lower than those reported in Table 1 for the samples exfoliated for 20 days. Fluorescence at longer wavelengths is linked to an increased number of highly substituted aromatics, conjugated unsaturated systems capable of a high degree of resonance, and/or donor acceptor complexes. All three factors are expected to become more prevalent with increased humification of the organic material. the more humified the material is. This, in turn, means that the higher the number reported in Table 1 the more humified the exfoliated material. Two major questions arise from the data presented above: 1) Why are the kinetics for less humified material slower than those for more humified materials? and 2) Why does the ACN SS exfoliate differently than any of the other SSs?

To address question 1 we must consider soil drying, during which it can be assumed that water in the outer layers (at the air interface) of the SOM is driven off before water within the middle layers can be removed.

Table 1 Summary of UV-Vis and HIX data for the 20 and 45 day exfoliations

Sample	Abs[#]	HIX[*] Method			
		HIX_{18}	HIX_{254}	HIX_{370}	HIX_{465}
20 days					
H_2O	0.051	1.11	8.40	0.77	1.19
DMSO	0.050	1.12	8.01	0.76	1.17
ACN	0.116	1.36	8.74	1.12	2.57
MeOH	0.071	1.18	8.46	0.78	1.42
45 days					
H_2O	0.072	0.84	7.04	0.71	1.16
DMSO	0.074	0.82	6.66	0.71	1.25
ACN	0.136	1.08	7.63	0.79	2.69
MeOH	0.078	0.81	6.60	0.71	1.20
AA	0.071	0.81	6.72	0.71	1.16
HCl	0.070	0.83	6.82	0.71	1.14

[#] Absorbance at 280 nm *HIXs are obtained from fluorescence intensities as indicated, e.g. HIX_{370} means that the excitation wavelength used was 370 nm and the intensity at 520 nm was divided by that at 470 nm (i.e. 520/470); HIX_{254} is (Σ (447-480)/ Σ (350-383)) and HIX_{465} is Σ(475-650)/10^7. HIX_{18} data were obtained from the synchronous data with an 18 nm offset

The initial water loss can be envisioned to induce conformational changes such that hydrophobic interactions become much more likely, creating a hydrophobic layer from which water entrapped in the inner layers cannot escape. Thus, the more hydrophilic and less humified material in the inner layers will be protected by this hydrophobic middle layer. This argument is meant to augment rather than displace the role of mineral surfaces in the protection of SOM from humification, and sets the stage for the soil wetting discussion to follow. Initially, SOM wetting involves the hydration, and subsequent exfoliation, of readily available hydrophilic SOM moieties containing such functional groups as –OH, COOH, $–NH_2$. This process of swelling can be viewed as a reopening of pores previously collapsed due to the presence of hydrogen bonding between hydrophilic groups within the SOM. It is expected that

the majority of the initially exfoliated matter will be very similar to fulvic acid. This can be viewed as penetrating the outer layer, which exposes the hydrophobic middle layer to subsequent wetting, similar to peeling an onion. This process is expected to be rather slow due to the amount and complexity of the conformational rearrangements that must take place to rebalance the interactions between hydrophobic and hydrophilic entities within the SOM in this middle shell. This explains the release of more humified materials during the 20 day exfoliation experiments for all the SSs. The subsequent wetting of the inner shell solvates the previously protected less humified materials, eventually exfoliating them into the SSs. This delay in the release of the less humified materials offers an explanation for the observations made during the 45 day exfoliation experiments in all the SSs. The FT-IR and ^{13}C NMR results on the exfoliated soil also show that a complex distribution of moieties is being exfoliated by water over the course of 45 days.

In order to answer the second question it is proposed that ACN has an easier access to inner SOM moieties as well as to a larger number of voids (pores) within the SOM assembly, due to low hydrogen bonding accepting density and size. In doing so, acetonitrile causes the greatest disruptive effect on the hydrophobic intermolecular forces within the SOM, exposing new SOM to hydration. This explanation is consistent with the observed kinetic effect as ACN requires time to penetrate the SOM.

The environmental implications of this study are many. First, the common assumption that CMOSs at low concentrations have a more or less negligible influence on the sorption of HOC to geomatrices must be approached with great caution (Scharzenbach *et al.*, 2003). Second, dissolving a sparingly soluble organic compound in an organic solvent and then diluting it with water to below 1% cosolvent volume fraction, as commonly practiced in sorption studies, may lead to artifacts even for CMOSs. Third, there is a kinetic effect in regards to how CMOSs in binary solutions can affect SOM in solid geosorbents, which must be taken into account when studying bi-solvent systems in the field of SOM sorption. Finally, the results of this study strongly suggest that slow kinetics may be expected for pollutants in hydrophobically protected domains and should be taken into account when evaluating remediation strategies.

References

National Research Council (2002) Bioavailability of contaminants in soils and sediments: processes, tools, and applications. National Academies Press, Washington DC

Piccolo A (2001) The supermolecular structure of humic substances. Soil Sci. 166: 810-832

Scharzenbach RP, Gschwend PM, Imboden DM (2003) Environmental Organic Chemistry 2nd Ed. Wiley-Interscience, Hoboken, New Jersey

Sutton R, Sposito G (2005) Molecular structure in soil humic substances: The new view. Environ. Sci. Technol. 39: 9009-9015

Transfer of Soil Nickel to Crops in Suburban Areas and Their Healthy Risk in Fujian Province, Southeast China

Dan Luo, Yanhui Chen, Guo Wang*

Department of Resources and Environment, Fujian Agriculture and Forestry University, Fuzhou 350002, China.
*Corresponding author. Tel. No. +86 591 83789361; Fax No. +86 59183776849; E-mail: gwang572003@yahoo.com.cn.

Abstract: To understand the bioavailability and soil-to-plant transfer of nickel (Ni), rice and 20 commonly consumed vegetable species with their corresponding soil samples were collected from the suburban areas of some major cities of Fujian Province. The total concentrations of Ni in soil ranged from 1.41 $mg \cdot kg^{-1}$ to 79.24 $mg \cdot kg^{-1}$ with a mean of 17.05 $mg \cdot kg^{-1}$. Both the DTPA-extractable Ni and the available Ni fractions were significantly correlated with the total Ni, pH, free Fe and clay. The Ni concentrations in the edible parts of the crops varied from not detected to 3.685 $mg \cdot kg^{-1}$ with a mean of 0.221 $mg \cdot kg^{-1}$ (fresh weight). The Ni concentrations of 5 crops showed significant correlations with total soil Ni while those of 10 corps were significantly correlated with DTPA-Ni. The transfer factors based on DTPA-Ni (TF_{DTPA}) of crops varied between 0.001 and 2.478. In general, the TF_{DTPA} of the crops decreased in the order of beans > gourds > rice > leafy vegetables. Daily consumption of rice and some Ni-rich vegetables could result in an excessive intake of Ni, according to the reference dose (RfD) of Ni recommended by USEPA.

Keywords: Nickel (Ni); Transfer; Bioavailability; Soil; Plant

Introduction

Compared with the other trace metals, the knowledge is relatively scarce about the behavior and uptake of nickel (Ni) depending on soil's chemical and physical properties and crop plants. Most of the published papers on the Ni transfer from soil to plant refer to Ni-contaminated soils or pot experiments by applying Ni in the soil (Zdenek, 1997; Parida *et al.*, 2003; Mordy, 1999). Since vegetables and rice constitute the majority of the diet for the people in the southeast of China, it is essential to study the transfer of Ni from soil to the edible parts of vegetables grown on the fields near cities for the evaluation of the health and ecological risks.

Material and Methods

This investigation was carried out in the suburban areas of Fujian Province described by Wang *et al.* (2006). A sampling block where the crop grew normally was selected in each field before sampling. The edible parts of rice and 20 commonly consumed vegetables grown on the selected sampling blocks and the corresponding soils (≤15 cm) were collected. The total number of crops sampled was 285. Vegetable samples were cleaned and oven-dried at 80~90 ℃ for 15~30 min, then at 65 ℃ for 12~24 h to constant weight. The rice grains were air-dried at room temperature. All the crop samples were ground to pass through 0.5 mm sieve. The soil samples were air dried at room temperature and crushed to pass through a 2-mm sieve for the analysis of soil physicochemical properties and soil available Ni. A small portion (about 50 g) of the 2-mm soils was ground into a fine powder (<0.15 mm) for evaluating the total concentration of Ni.

Soil total Ni was analyzed by digesting 0.5 g soil (<0.149 mm) with HNO_3-HCl-$HClO_4$-HF. The soil available Ni was obtained by extracting 5 g soil (<2 mm) with 25 ml DTPA-$CaCl_2$-TEA (pH=7.3) for 2 h

continuous shaking at room temperature. The crop samples were digested with HNO_3-$HClO_4$ for the determination of Ni. The determination concentrations of Ni was performed on ICP-AES (Perkin Elmer 2100DV) and graphite furnace atomic absorption spectrometer (Varian GTA120/AA240Z) with Zeeman background correction. Soil physicochemical properties were measured by conventional methods.

The transfer factor based on DTPA-Ni (TF_{DTPA}) and the daily intake of Ni (DIM, $mg \cdot kg_{weight}^{-1} \cdot day^{-1}$) were calculated as follows:

TF_{DTPA} = Ni in the edible parts ($mg \cdot kg^{-1}$, FW) / available Ni in soil ($mg \cdot kg^{-1}$, DW).

DIM = metal concentration ($mg \cdot kg^{-1}$, FW)×food intake ($kg \cdot d^{-1}$,FW) / average body weight (kg)

Results and Discussion

The total soil concentrations of Ni in this study ranged from 1.41 $mg \cdot kg^{-1}$ to 79.24 $mg \cdot kg^{-1}$ with an arithmetic mean of 17.86 $mg \cdot kg^{-1}$. About 2.88% of the samples were above the Ni limit for soil (40 $mg \cdot kg^{-1}$ for soil with pH<6.5, State Environmental Protection Administration of China, 1995). The available Ni (DTPA-Ni) varied between 0.05 and 11.28 $mg \cdot kg^{-1}$ with an arithmetic mean of 1.21 $mg \cdot kg^{-1}$. The available fraction of Ni (ratio of available Ni to total Ni) of vegetable soils varied from 0.2% to 28.2% with an arithmetic mean of 5.1% while that of paddy rice soils were between 3.5% and 24.5% with a mean of 8.1%.

We compared the total Ni, the available Ni and the available fraction of Ni with selected soil properties (Table 1). Soil pH had negative and significant correlation with the available fraction of Ni of both vegetable soils and paddy soils. The clay content, as well as the free Fe content, positively and significantly correlated with the DTPA-Ni of both vegetable soils and paddy soils. The DTPA-Ni of vegetable soils significantly increased as the content of silt increased. For paddy soils, the trend was inverse. The total Ni had significant correlations with the DTPA-Ni and the available fraction of Ni of both vegetable soils and paddy soils, indicating that the amount of available Ni depended largely on the soil total Ni.

The Ni concentration in the edible parts of the vegetables and rice varied from not detected to 3.685 $mg \cdot kg^{-1}$ (FW) with an arithmetic mean of 0.141 $mg \cdot kg^{-1}$ and from 0.039 to 3.610 $mg \cdot kg^{-1}$ (air-dried basis) with an arithmetic mean of 0.741 $mg \cdot kg^{-1}$, respectively. According to the interior controlling standard for Ni proposed by the committee of food hygiene standard (≤0.3 $mg \cdot kg^{-1}$ for vegetables and ≤0.4 $mg \cdot kg^{-1}$ for rice, Yang HF *et al.*, 1997), the Ni concentrations of about 11.2% of vegetable samples and 39.5% of rice grain samples surpassed the corresponding limits, suggesting that the vegetables and rice grown in this area might have been polluted in some extent. There were only 5 crops, namely, cabbage, leaf mustard, eggplant, garlic and rice grain, for which the Ni concentrations significantly correlated with the total soil Ni, with the correlation coefficients (r) being 0.698^{**}, 0.906^{**}, 0.679^{*}, 0.874^{**} and 0.600^{**}, respectively. The Ni concentrations of radish, pakchoi, cabbage, leaf mustard, lettuce, eggplant, towel gourd, cowpea, garlic and rice grain were significantly correlated with the DTPA-extractable Ni, with the correlation coefficients (r) being 0.502^{*}, 0.420^{*}, 0.957^{**}, 0.989^{**}, 0.715^{*}, 0.813^{**}, 0.669^{*}, 0.809^{**}, 0.990^{**} and 0.485^{**}, respectively.

The TF_{DTPA} values based on the DTPA-Ni of the crops varied from 0.001 to 2.478, with the median of the TF_{DTPA} values of various vegetable species decreased in the order: sweet potato (1.324) > kidney bean (0.641) > cowpea (0.427)> angular gourd (0.388) > towel gourd (0.381) > rice (0.214) > bottle gourd (0.211) > Chinese cabbage (0.200) > spinach (0.195) > garlic (0.168) > pakchoi (0.144) > lettuce (0.083) > eggplant (0.082) > cauliflower (0.078) > celery (0.069)> tomato = water spinach (0.061) > leaf mustard (0.056)> water rice stem (0.052) > cabbage (0.036) > radish (0.011). In general, bean vegetable and gourd vegetable showed stronger ability in accumulating Ni, followed by rice as moderate accumulator of Ni, and leafy vegetables as lower accumulators.

The daily intakes of Ni were estimated according to the average vegetable and rice grain consumption. The estimated $DIM_{vegetable}$ and DIM_{rice} were 0.686 $\mu g \cdot kg^{-1}$ and 2.983 $\mu g \cdot kg^{-1}$, respectively. Compared to the value of reference dose (RfD) for Ni (0.02 $mg \cdot kg_{weight}^{-1} \cdot d^{-1}$) from Integrated Risk Information System (IRIS, 2003), the daily intakes of Ni through consumption of vegetables and rice in this study were free of risks. Taking the highest Ni concentrations of rice and leafy vegetable as the calculation basis (3.610 $mg \cdot kg^{-1}$ for rice and 2.058 $mg \cdot kg^{-1}$ for leaf mustard), the daily intake of Ni is 0.015 $mg \cdot kg^{-1}$ by rice and

0.01 mg·kg^{-1} by leaf mustard. The sum of the daily intake of the total Ni from rice and vegetable is 0.025 mg·kg^{-1}, higher than the RfD. Also, there are other sources of Ni intake by consumption of meat, fish, milk, can and water. If all these sources of Ni exposure were taken into account, the daily intake for Ni would be even greater.

Table 1 Correlations of the DTPA-Ni and the available fraction of Ni with the soil properties

Soil properties	Correlation coefficient for vegetable soils (r, n = 247)		Correlation coefficient for paddy soils (r, n = 38)	
	DTPA-Ni	available fraction	DTPA-Ni	available fraction
pH (H_2O)	ns	-0.252**	-0.382*	-0.417**
OM	ns	ns	ns	ns
clay (<0.002 mm)	0.335**	ns	0.404*	ns
silt (0.02~0.002 mm)	0.199**	ns	-0.443**	ns
Free Fe (g·kg^{-1})	0.177**	ns	0.399*	0.361*
CEC	0.197**	ns	ns	ns
Total Ni	0.506**	-0.259**	0.667**	0.422**

ns: not significant; *significant at 5% level; **significant at 1% level

References

IRIS (2003) Integrated Risk Information System-database, US Environmental Protection Agency

Mordy AA (1999) Effect of nickel addition on the yield and quality of parsley leaves. Scientia Horticulturae 82: 9-24

Parida BK, Chhibba IM, Nayyar VK (2003) Influence of nickel-contaminated soils on fenugreek (Trigonella corniculata L.) growth and mineral composition. Scientia Horticulturae 98: 113-119

State Environmental Protection Administration of China (1995) Environmental quality standard for soils, GB15618-1995

Wang G, Su MY, Chen YH, *et al.* (2006) Transfer characteristics of cadmium and lead from soil to the edible parts of six vegetable species in southeastern China. Environ. Pollut. 144: 127-135

Yang HF, Li YM, Shen WZ (1997) Handbook of Physical Testing and Chemical Analysis on Food and Health. Beijing, Standards Press of China, pp.175-177

Zdenek P (1997) The danger of cumulation of nickel in cereals on contaminated soil. Agr. Ecosyst. and Environ. 63: 25-29

Transformation Dynamics and Memory Effect of Soil Amino Sugars Amended with Available Substrates

Hongbo He, Xudong Zhang*

Key Laboratory of Terrestrial Ecological Process, Institute of Applied Ecology,
Chinese Academy of Sciences Shenyang 110016, China.
*Corresponding author. Tel. No. +86-24-83970375; Fax No. +86-24-83970376; E-mail: xdzhang@iae.ac.cn.

Abstract: Combination of the isotope tracing technique and the identification of amino sugars is efficient to explore the microbial immobilization of extraneous nitrogen. In the present study, the transformation dynamics and memory effect of soil amino sugars amended with available substrates were investigated. The results showed that the compound-specific ^{15}N enrichment represented the transformation pattern of individual amino sugars and the calculated ^{15}N-labeled portion was derived from the immobilization of the extraneous NH_4^+. The ^{15}N enrichment in glucosamine was increased slowly and the unlabeled glucosamine was quite stable during the accumulation of newly-synthesized portion. The transformation of muramic acid was more rapid than glucosamine in short term, but the formation of ^{15}N-labeled muramic acid was concomitant with the decomposition of inherent portion. It was indicated that bacteria were more competitive than fungi to assimilate liable substrates initially, but fungus growth was dominant at later stage by utilizing the intact or metabolized substrates. Furthermore, bacterial cell wall residues were easily decomposed to be involved in the soil organic matter (SOM) turnover, while fungus-derived residue was mainly contributed to the stabilization of SOM.

Keywords: ^{15}N; Glucose; Amino sugar; Dynamics; Soil

Introduction

Labile substances such as glucose could shift soil microorganisms from dormancy to active form and microbial residues such as amino sugars would be rapidly formed and accumulated in soil concomitantly with the immobilization of extraneous nitrogen (Brant *et al.*, 2006). The most important significance of estimating amino sugars in soils might be the reflection of the historical population changes as well as the current community structure theoretically, and thus it was recognized as "memory effect" to integrate microbial community structure over time (Liang *et al.*, 2008). However, the dynamics of amino sugars can not be investigated clearly until the newly synthesized amino sugars were differentiated from the inherent portions in soil matrices. A gas chromatography-mass spectrometry (GC/MS) method, combing with ^{15}N-labeled NH_4^+ and glucose amendment, offered an opportunity to study the transformation processes from extraneous nitrogen to soil amino sugars (He *et al.*, 2006), which would have great advantage to soil nitrogen cycling exploration.

Materials and Methods

An incubation experiment of Mollisol was conducted with $(^{15}NH_4)_2SO_4$ or glucose and $(^{15}NH_4)_2SO_4$ amendments at 25 ℃. The amended amount of the substrate solution was 0.1 mg for N and 1.0 mg for C per gram soil once a week till the end of incubation. During the analysis of amino sugar by GC/MS, the intensity of the N-containing fragments (F) and the corresponding (F+1) was measured and the ^{15}N enrichment in each amino sugar (APE) was calculated as:

$$APE=(Re\text{-}Rc)/1[1+(Re\text{-}Rc)]\times 100$$

where $R = [A_{(F+1)}/A_{(F)}]$ and Re and Rc represented incubated and original samples, respectively. Accordingly, the content of ^{15}N-labeled amino sugars can be calculated as:

$$C_{15N} = C_{total} \times APE/100$$

where C_{total} is the total concentration of amino sugar and C_{15N} represents the content of ^{15}N-labeled portion.

Results and Discussion

The Isotope Incorporation into Soil Amino Sugars

The APE of individual amino sugars was quite low in the soil samples amended with $(^{15}NH_4)_2SO_4$, whereas a large amount of inorganic nitrogen was accumulated in the microcosms (data not shown), suggesting that the transformation from added NH_4^+ to soil amino sugars was restricted by the deficiency of available carbon. The concomitant addition of glucose with ^{15}N-NH_4^+ altered the transformation dynamics of amino sugars markedly and the ^{15}N incorporated into the three amino sugars was increased significantly (Fig. 1). The much higher isotope enrichment in muramic acid than glucosamine confirmed that the turnover of muramic acid was more rapid than the latter in short term, which has been widely recognized previously (Zhang *et al.*, 1999; Liang *et al.*, 2008). The low ^{15}N enrichment of GalN indicated sufficiently that the cycling of GalN was quite slow.

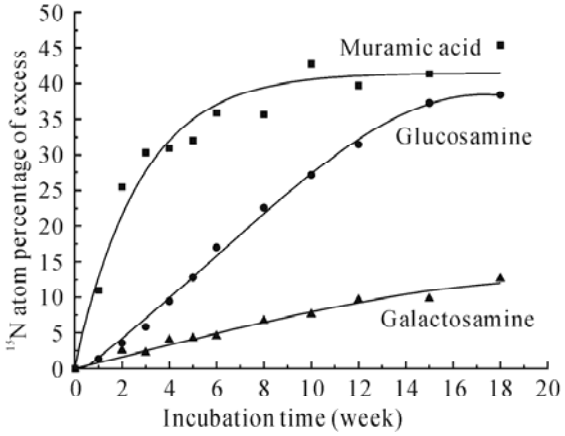

Fig. 1 ^{15}N enrichment in amino sugars during incubation with glucose and $(^{15}NH_4)_2SO_4$

The Contents of Soil Amino Sugars

The accumulation of amino sugars was enhanced significantly when amended with glucose and $(^{15}NH_4)_2SO_4$ (Fig. 2). The labeled glucosamine was formed and accumulated concomitantly with the stabilization of the original portion while the unlabeled muramic acid declined with the formation of labeled portion. Obviously, glucosamine was more stable in soil organic matter pool than muramic acid due to the multi-protection from the decomposition, thus provided a reason for the low turnover rate. Therefore, fungal cell wall residues tended to accumulate in soil matrices and dominantly contributed to the stability of the soil organic matter, while the turnover of bacterial cell walls was rapid and sensitive to the carbon and nutrient application.

Contrasted to glucosamine and muramic acid, the increment of galactosamine was mainly attributed to unlabeled portion, inferring that its transformation might be driven by the internal cycling of soil nitrogen and the effect of extraneous substrate on its accumulation was indirect.

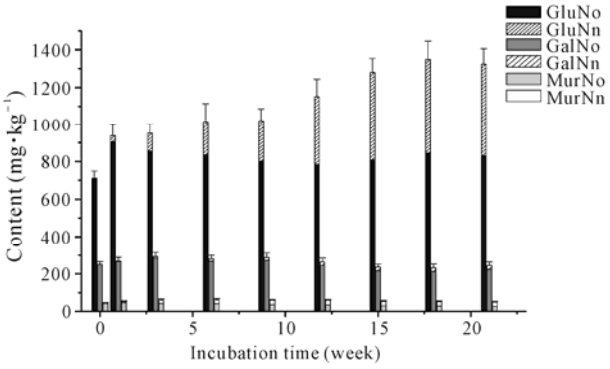

Fig. 2 Dynamics of amino sugars during incubation with glucose and $(^{15}NH_4)_2SO_4$, "No" means original and "Nn" means newly-synthesized portion

Conclusions

The transformation pattern of amino sugars after the application of the available substrates was evidently discriminative by using ^{15}N isotope tracing technique. The compound-specific dynamics of individual amino sugars was significant to distinguish the ever-active response to the substrates of different microbial communities (memory effect). The dynamics of glucosamine and muramic acid indicated

that fungus-derived residue was mainly contributed to the accumulation of soil organic matter, while bacterium-derived residue was mainly involved in the turnover of soil organic matter. Although our investigation on the dynamics of amino sugars was conducted by laboratory incubation with available carbon and nutrient application, it may be an important precursor to clarify the mechanism of soil amino sugar turnover in the natural environment.

References

Brant JB, Sulzman EW, Myrold DD (2006) Microbial community utilization of added carbon substrates in response to long-term carbon input manipulation. Soil Biol. Biochem. 38: 2219-2232

He HB, Xie HT, Zhang XD (2006) A novel GC/MS technique to assess ^{15}N and ^{13}C incorporation into soil amino sugars. Soil Biol. Biochem. 38: 1083-1091

Liang C, Fujinuma R, Balser TC (2008) Comparing PLFA and amino sugars for microbial analysis in an Upper Michigan old growth forest. Soil Biol. Biochem. 40: 2063-2065

Zhang X, Amelung W, Yuan Y, Samson-Liebig S, Brown L, Zech W (1999) Land-use effects on amino sugars in particle-size fractions of an Argiudoll. Appl. Soil Ecol. 11: 271-275

Evaluating the Maturity and Quality of Solid Waste Compost through Phospholipid Fatty Acid Biomarkers

Ghulam Jilani[a,*], Jianming Xu[b], Yuping Wu[b], Zhongzhen Liu[b]

[a]Department of Soil Science, PMAS Arid Agriculture University, Rawalpindi 46300, Pakistan;
[b]Zhejiang Provincial Key Laboratory of Subtropical Soil and Plant Nutrition, College of Environmental and Natural Resource Sciences, Zhejiang University, Hangzhou 310029, China.
[*]Corresponding author. Tel. No. +92-51-9062241; Fax No. +92-51-9290160; E-mail: jilani@uaar.edu.pk.

Abstract: Maturity and quality of compost when used as soil amendment are very important and need to be taken into consideration. Phospholipid fatty acids (PLFAS) composition has high correlation with chemical and biological parameters for compost maturity. This study was undertaken for making compost from sewage sludge and municipal refuse with some additives to enhance decomposition. The municipal solid waste(MSW) was mixed with equal weight of de-watered sewage sludge(DSS), and then treated with these additives in separate bio-reactors as: control (no amendment), zeolite, clayey soil, fly ash, lime, and effective microorganisms (EM) inoculum. Composts were analyzed for C:N ratio and microbial diversity during decomposition. Thirty nine types of PLFAs were identified, which belonged to nine major categories. Results from all the treatments depicted that straight, monounsaturated fatty acids (SMUFA) and straight, saturated fatty acids (SSATFA); SSATFA both representing for fungi were in the highest amount. These were followed by branched, saturated fatty acids (BRANCHED FAMES) that signify the presence of G +ve bacteria and actinomycetes. The straight, hydroxyl fatty acids (SOH-FAMES) specifying the anaerobic microbes were the lowest among all. A small number of aerobic G –ve bacteria was also noticed by the presence of branched, saturated, and hydroxyl fatty acids (BSHFA) and cyclopropyl fatty acids. The C:N ratio was at the lowest with EM that enhanced decomposition more than with other amendments. The EM as well as lime increased the concentration of all the PLFAs as compared with control. Therefore, both EM and lime can be the best choice amendments for rapid composting leading to early maturity and better quality of the compost product.

Keywords: Decomposition; De-watered sewage sludge (DSS); Microbial community; Municipal solid waste (MSW)

Introduction

Extensive generation and accumulation of solid wastes from municipalities have become a serious problem. Composting is an effective technique for resource recovery from such organic wastes (Kato *et al.*, 2005). They can be turned into valuable compost for raising crops on one hand (Jilani *et al.*, 2007), and get them disposed off at the other end (Ahmad *et al.*, 2007). Prior to soil application, maturity of compost must have to be ensured to avoid harmful effects to crops (Kato, *et al.*, 2005). Microbial community analysis is advocated to determine the maturity of composts (Belete *et al.*, 2001). The PLFA analysis is based on the extraction and quantification of phospholipids from microbes in the sample, and total PLFA is correlated to viable microbial biomass (Zelles *et al.*, 1995). So, it can be a good indicator of microbial communities in compost. However, research is required to establish correlation of PLFA based microbial community structure analysis with compost maturity. This study was undertaken to: find an efficient compost additive for enhancing biodegradation; and correlate the microbial

community structure with maturity and quality of compost.

Materials and Methods

Fresh MSW was collected, sun-dried, and shredded to 2~5 cm size. Then 3 kg of MSW was mixed with 3 kg DSS in the ratio of 1:1 for each treatment in composting bio-reactor (20 L). Treatments to waste mixture were: check (no additive), zeolite (5% w/w), clayey soil (5% w/w), fly-ash (5% w/w), lime (1% w/w), and EM inoculum (1% v/v in wetting water). Composting materials were mixed and maintained at 50% moisture. Air pump was installed and linked to all bio-reactors by plastic pipes. Compost samples were collected at 60 and 120 days for the estimation of microbial diversity and compost maturity.

The PLFAs were extracted from 10 g freeze-dried compost samples with 15.2 mL buffer (0.15 mol·L^{-1}, pH 4.0) of chloroform-methanol-citrate (1:2:0.8 v/v/v) in 30 mL Teflon centrifuge tubes (modified after Frostegård *et al.*, 1993). After shaking and centrifugation, decanted the supernatant to 30 mL separatory funnel. Added 7.6 mL buffer again to redistill the lipids. Put 4.8 mL citrate buffer and 6 mL chloroform, shaken and left overnight. Evaporated $CHCl_3$ layer with N_2, added 1 mL methanol, vortexed and dried with N_2. Transferred lipids to SPE cartridges with 3×0.3 mL $CHCl_3$. Added 10 mL $CHCl_3$ to elute neutral lipids, and 10 mL acetone to elute glycolipids. Added 8 mL methanol and saved this elutant. Evaporated MeOH with N_2. Put 200 μL internal standard, and dried with N_2. Added 1 mL MeOH-toluene and 1 mL methanolic KOH (Yao *et al.*, 2000). Vortexed and incubated at 35 ℃ for 15 min.

After cooling at room temperature, added 2 mL hexane-$CHCl_3$, 0.3 mL acetic acid and 2 mL Milli-Q water. Placed the tube in a rotator and gently mixed for 5 min. Centrifuged and transferred the up-layer to a new 10 mL glass tube. Added 2 mL hexane-$CHCl_3$ and transferred the up-layer to the same tube, and dried with N_2. Transferred the samples to GC vials with 3×0.15 mL hexane, and dried with N_2. Added 60 μL hexane to dissolve the fatty acids. The resulting PLFAs were determined by Gas Chromatography.

The C:N ratio of the composts was calculated after the determination of their total organic carbon contents by dry ashing, and total nitrogen contents through Kjeldahl's procedure of digestion and distillation.

Results and Discussion

Thirty nine types of PLFAs belonging to nine major categories were identified in the composts (Fig. 1). These were: branched, saturated fatty acids - BRANCHED FAMES (i 12:0, i 14:0, i 15:0, a 15:0, i 16:0, a 16:0, i 17:0, a 17:0); 10Me fatty acids - BRANCHED FAMES (10Me 16:0, 10Me 17:0, TBSA 10Me18:0, 11Me 18:1 w7c); straight, hydroxyl fatty acids - SOH-FAMES (3OH 10:0, 3OH 12:0, 3OHI 14:0); straight, saturated fatty acids - SSATFA (12:00, 14:00, 15:00, 16:00, 17:00, 18:00, 20:00); straight, monounsaturated fatty acids - SMUFA (16:1 w7c, 16:1 w5c, 17:1 w8c, 18:1 w9c, 18:1 w7c); straight, polyunsaturated fatty acids - SPUFA (18:2 w6,9c, 18:3 w6c (6,9,12), 20:1 w9c, 20:4 w6,9,12,15c); branched, saturated, and hydroxyl fatty acids - BSHFA (2-OH i 15:0, 3-OH i 15:0, 3-OH i 17:0); cyclopropyl fatty acids (17:0 cyc, 19:0 cyc w8c); alcohol (16:0 N alcohol); and a few of mixed nature (15:1 i G, 17:1 a B/i I).

In all the treatments SMUFA and SSATFA representing fungi (Frostegård *et al.*, 1993) were at the highest (Fig. 1) followed by BRANCHED FAMES indicating G +ve bacteria and actinomycetes (Fierer *et al.*, 2003). The SOH-FAMES specifying

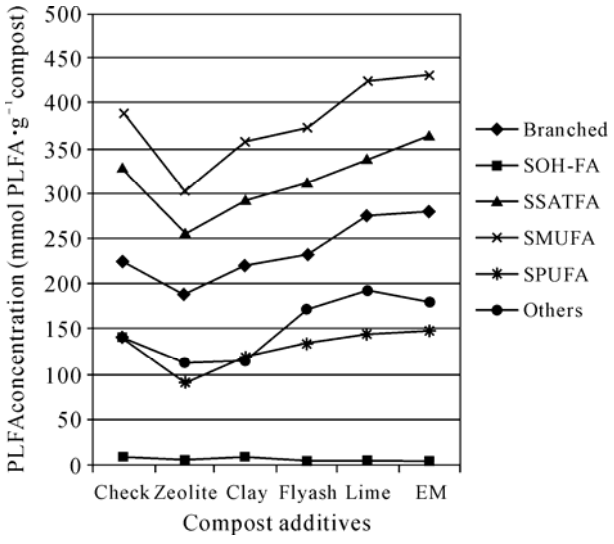

Fig. 1 Relation of additives with PLFAs

anaerobic microbes (Kato *et al.*, 2005) were at the lowest. Methane oxidizing and sulfate reducing

bacteria were indicated by SMUFA. Smaller number of aerobic G –ve bacteria was signified by BSHFA. Cyclopropyl fatty acids, the biomarkers for stress condition (Bossio and Scow, 1998) were also present. Both EM and lime increased the concentration of PLFAs over check. All PLFAs were reduced with zeolite and clayey soil. So, BRANCHED FAMES and/or SOH-FAMES can be considered for evaluating compost maturity. Proportion of BRANCHED FAMES reaching its peak, and that of SOH-FAMES going below 2 mol % coincide with maturity stage (Kato *et al.*, 2005). Fungi and G +ve bacteria known as fast decomposers were in the highest amount (Fig. 2).

As indicator of compost maturity, C:N ratio reduced over time reflecting that N contents were improved in the compost (Fig. 3). The EM inoculation to compost enhanced decomposition and lowered its C:N ratio.

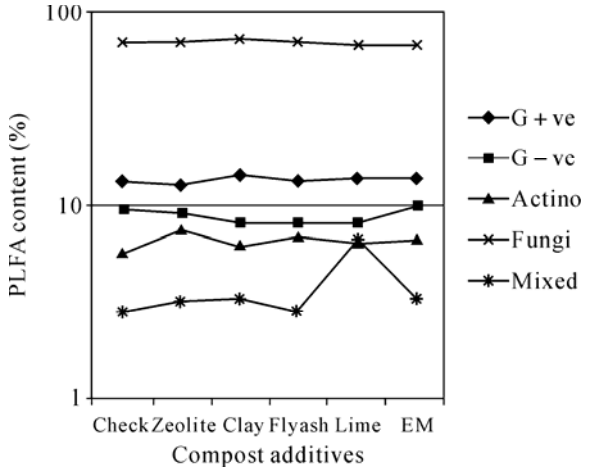

Fig. 2 Effect of additives on microbes

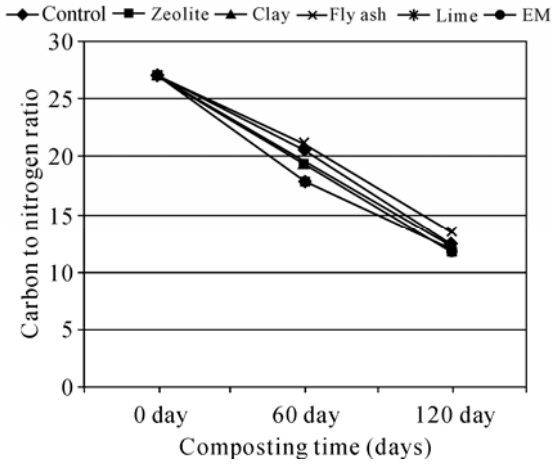

Fig. 3 Effect of additives on C:N ratio

Conclusion

For rapid composting and its maturity, microbial inoculation lime additive are useful. Sewage sludge if mixed with city refuse it can be a useful organic resource for good quality compost. The PLFA analysis and characterization gives reasonable indication for compost maturity as it relates very well to the C:N ratio.

Acknowledgements

This work was jointly supported by the National Basic Research Program of China (2005CB121104), the National Nature Science Foundation for Distinguished Young Scholars of China (40425007) and the Science and Technology Projects of Zhejiang Province (2007C22015).

References

Ahmad R, Jilani G, Arshad M, Zahir ZA, Khalid A (2007) Bio-conversion of organic wastes for their recycling in agriculture: An overview of perspective and prospects. Ann. Microbiol. 57: 471-479

Belete L, Egger W, Neunhäuserer C, Caballero B, Insam H (2001) Can community level physiological profiles be used for compost maturity testing? Compost Sci. Util. 9: 6-18

Bossio DA, Scow KM (1998) Impacts of carbon and flooding on soil microbial communities: phospholipid fatty acid profiles and substrate utilization patterns. Microbial. Ecol. 35: 265-278

Fierer N, Schimel JP, Holden PA (2003) Variations in microbial community composition through two soil depth profiles. Soil Biol. Biochem. 35: 167-176

Frostegård Å, Tunlid A, Bååth E (1993) Phospholipid fatty acid composition, biomass, and activity of microbial communities from two soil types experimentally exposed to different heavy metals. Appl. Environ. Microbiol. 59: 3605-3617

Jilani G, Akram A, Ali RM, Hafeez FY, Shamsi IH, Chaudhry AN, Chaudhry AG (2007) Enhancing crop growth, nutrients availability, economics and

beneficial rhizosphere microflora through organic and biofertilizers. Ann. Microbiol. 57: 177-183

Kato K, Miura N, Tabuchi H, Nioh I (2005) Evaluation of maturity of poultry manure compost by PLFA analysis. Biol. Fertil. Soils 41: 399-410

Yao H, He Z, Wilson MJ, Campbell CD (2000) Microbial biomass and community structure in a sequence of soils with increasing fertility and changing land use. Microbial Ecol. 40: 223-237

Zelles L, Bai QY, Rackwitz R, Chadwick D, Besse F (1995) Determination of phospholipid and lipopolysaccharide-derived fatty acids as an estimate of microbial biomass and community structures in soils. Biol. Fertil. Soils 19: 115-123

Effects of Depleted Uranium on Soil Microbial Activity: A Bioassay Approach Using ^{14}C-labeled Glucose

Rizwan Ahmad[a,*], David L. Jones[b]

[a] Institute of Natural Resource and Environmental Sciences,
National Agriculture Research Centre, Islamabad 54400, Pakistan;
[b] School of the Environment and Natural Resource, University of Wales, Bangor, Gwynedd, LL 57 2UW, UK.
[*]Corresponding author. Tel. No. +44-1248 382579; Fax No. +44-1248 1354997; E-mail: rizwan_narc@yahoo.co.in

Abstract: The short and long term influence of depleted uranium (DU) on soil microbial populations remains largely understudied. To understand short term effect of DU on soil microbial activity, an incubation study was conducted using ^{14}C-labeled glucose. Two soils of contrasting texture (Eurtic cambisol and Haplic podzol) were amended with increasing concentrations (0.5 mmol·L^{-1} to 10 mmol·L^{-1}) of either potassium nitrate (KNO_3) or DU as uranyl nitrate $UO_2(NO_3)_2$. Following addition, ^{14}C-labeled glucose was then added to the soil and $^{14}CO_2$ production from the mineralization of glucose measured at different time intervals (1 h to 14 d) to assess microbial activity. Glucose mineralization by the microbial community showed non-significant effect by different concentrations of DU on both soils. Fitting a double first order kinetic equation revealed that 87%~92% of the added glucose was retained in the microbial biomass prior to mineralization. However, comparison of the kinetic values for different concentrations of KNO_3 and DU also showed non-significant difference in both soils. The results imply that there is no significant deleterious effect of DU on soil microbial activity in the short (<24 h) or longer term (<30 d).

Keywords: Depleted Uranium (DU); Mineralization; Microbiological activity; ^{14}C-labeled glucose; Microbial community

Introduction

Depleted Uranium (DU) is the uranium that primarily composed of the isotope uranium-238 (238 U). DU is a new and emerging pollutant. It's of increasing concern due to the increased use of DU in weapons deployed in different regions of the world such as Bosnia, Afghanistan and Iraq. DU present in the soil can migrate to surface and groundwater and potentially contaminate drinking water supplies. Plants also possess the potential to take up DU present in soil and associated water bodies (Neves *et al.*, 2008). Preserving microbial community activity in soil is vital for preserving ecosystem functioning. However, the short and long-term influence of DU on soil microbial populations remains largely understudied. The objective of this work was to study the short-term effect of DU on microbial activity.

Materials and Methods

Five gram of two soils with contrasting physic-chemical characteristics (Eurtic cambisol and Haplic podzol) was weighed out in 50 mL polypropylene tubes with 12 treatments and three repeats (i.e. 36 tubes for each soil). Increasing concentrations (0.5, 1, 2.5, 5 and 10 mmol·L^{-1}) of KNO_3 and DU as $UO_2(NO_3)_2$ were made and 2.5 mL of each concentration of was mixed with 0.01 mL of normal glucose (250 mmol·L^{-1}) and 0.19 mL of ^{14}C-labeled glucose (1 μ Ci·mL^{-1}) solutions. Following mixing, the soils taken in the vials were amended with 500 μL of increasing concentrations of KNO_3 and DU and

mixed gently by shaking. A volume of 100 µL each of above solutions was also taken in 5 mL vials to measure background ^{14}C content.

Sodium hydroxide (NaOH) traps containing I mL NaOH, were gently lowered onto the soil surface and tubes were sealed by a rubber bung. The traps were removed and replaced after 1, 3, 6, 24, 48, 72 h; and 7 and 14 d. To each NaOH trap 4 mL scintillation fluid was added and mixed well on vertex mixture. The value of $^{14}CO_2$ given off at different time intervals was measured on liquid scintillation counter (Wallace 1409: Turku, Finland). The data obtained by scintillation counter was statistically analyzed and graphs were plotted in Sigma Plot 8. The results were fitted to kinetic models to determine rates of substrate utilization and kinetic values of lower and higher values of KNO_3 and DU were compared by applying T-test.

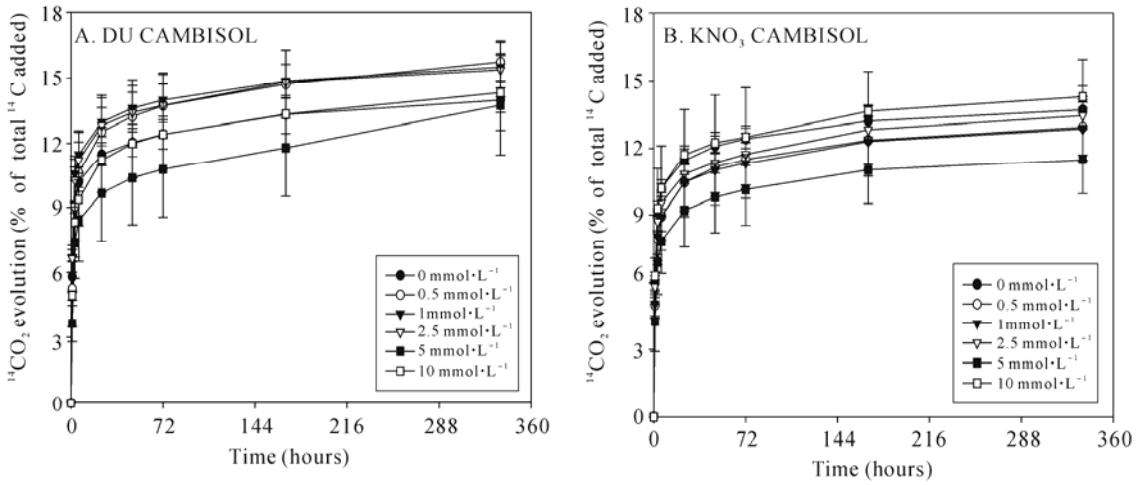

Fig. 1 Effect of different concentration of DU or KNO_3 on CO_2 evolution for cambisol soil

Results and Discussion

Effect of different concentrations of DU or KNO_3 on $^{14}CO_2$ evolution for cambisol soil is presented in Fig. 1. Both graphs show that there was non-significant difference between different concentration of DU and KNO_3 at various intervals of time ranging from 1 h to 14 days. Similar trend was also observed in case of podzol soil (data not shown).

The data was fit to kinetic model and it was found to fit double exponential decay curve with 4 parameters; $S = [a_1 \exp(-k_1 t)] + [a_2 \exp(-k_2 t)]$. The k_1 and k_2 kinetic values for different concentrations of DU and KNO_3 were calculated. The k_1 and k_2 values revealed that podzol soil retained 92% of the added glucose compared to 87% by cambisol soil. This might be due to physic-chemical characteristics of the soils, showing more microbial activity in cambisol soil than podzol soil.

The kinetic values for 1 mmol·L^{-1} and 10 mmol·L^{-1} concentration of DU and KNO_3 applied to cambisol and podzol soils were compared by applying T-test. The T-test values for different comparisons are shown in Table 1a to 2b. The results revealed no significant difference when DU and KNO_3 were compared with each other at 1 mmol·L^{-1} and 10 mmol·L^{-1} concentrations. The similar results were also obtained when 1 mmol·L^{-1} and 10 mmol·L^{-1} concentrations were compared with each other for DU as well as KNO_3.

Under appropriate conditions, microorganisms can affect the stability and mobility of U in soil by altering the chemical speciation, solubility and sorption properties and thus could increase or decrease the concentrations of U in solution and the bioavailability (Francis, 2008). So the study implies that further investigations with higher concentrations of U on microbial activity and subsequently its bioavailability will be helpful for plant growth.

Table 1a Comparison of kinetic values for cambisol soil

	1 mmol·L^{-1}		10 mmol·L^{-1}	
	k_1	k_2	k_1	k_2
DU	12.3±0.6	87.5±0.3	10.8±0.8	88.9±0.4
KNO_3	10.0±0.8	89.6±0.4	11.1±0.8	88.7±0.4
T-test	0.13	0.15	0.84	0.85

Table 1b Comparison of kinetic values for cambisol soil

	DU		KNO_3	
	k_1	k_2	k_1	k_2
1 mmol·L^{-1}	12.3± 0.6	87.5±0.3	10.0±0.8	89.6±0.4
10 mmol·L^{-1}	10.8±0.8	88.9±0.4	11.1±0.8	88.7±0.4
T-test	0.55	0.59	0.24	0.25

Table 2a Comparison of kinetic for values podzol soil

	1 mmol·L^{-1}		10 mmol·L^{-1}	
	k_1	k_2	k_1	k_2
DU	9.9±0.5	90.3±0.3	8.3±0.3	91.7±0.2
KNO_3	9.1±0.4	91.1±0.2	7.2±8.7	92.4±8.7
T-test	0.08	0.15	0.50	0.62

Table 2b Comparison of kinetic values for podzol soil

	DU		KNO_3	
	k_1	k_2	k_1	k_2
1 mmol·L^{-1}	9.9±0.52	90.3±0.31	9.1±0.4	91.1±0.25
10 mmol·L^{-1}	8.3±0.30	91.7±0.18	7.2±8.7	92.4±8.7
T-test	0.28	0.26	0.39	0.50

Conclusion

Results of the study conclude that DU appears to have no significant deleterious effect on the soil microbial activity in the short (<24 h) or longer term (<30 d). There was also no significant difference between lower and higher concentrations of DU on the soil microbial activity in the short term (<24 h) and longer term (<30 d).

References

Francis AJ (2008) Microbial transformations of uranium in wastes and implication on its mobility. Int. Conf. U Min. Hydr. Germany

Neves O, Abreu MM, Vicente EM (2008) Uptake of uranium by lettuce (Lactuca sativa L.) in natural uranium contaminated soils in order to assess chemical risk for consumers. Water Air Soil Pollut. 195: 73-84

Is the Alkalinity within Agricultural Residues Soluble

Clayton R Butterly[a], Jeffrey A Baldock[b], Jianming Xu[c], Caixian Tang[a,*]

[a] Department of Agricultural Sciences, LaTrobe University, Melbourne 3086, Australia;
[b] CSIRO Land and Water, PMB 2, Glen Osmond 5064, Australia;
[c] Zhejiang Provincial Key Laboratory of Subtropical Soil and Plant Nutrition, College of Environmental and Natural Resource Sciences, Zhejiang University, Hangzhou 310029, China.
[*]Corresponding author. Tel. No. +61 3 9479 2184; Fax No. +61 3 9471 0224; E-mail: C.Tang@latrobe.edu.au.

Abstract: A laboratory experiment was carried out to determine the contribution of whole residues of canola, chickpea and wheat and their fractions (insoluble/soluble) to soil pH changes during a 14-day incubation. Residues were added (1% w/w) to Frankston and Shepparton soils of initial pH of 4.45 and 6.20, respectively. Increases in pH were greatest for chickpea, less for canola and the least for wheat. The experiment confirmed that the soluble fraction of residues is important for the alkalinity release within initial stages of decomposition and also the source of components responsible for pH decreases in subsequent incubation. However, the relative differences of whole residues and the fractions were influenced by the initial soil pH.

Keywords: pH; Soluble alkalinity; Agricultural residues

Introduction

Soil acidification is a widespread problem with approximately 40% of the world's arable land area consisting of acid soils (pH <5.5) (Kochian *et al.*, 2004). Plant residues can have a liming effect when added to soil in the absence of plants and leaching (Sakala *et al.*, 2004; Tang *et al.*, 1999; Yan *et al.*, 1996; Xu *et al.*, 2006). It is commonly recommended that residues be retained within Agricultural production systems. However, the mechanisms by which residues alter pH after incorporation to soil remain unclear. The potential alkalinity of residues is thought to be related to the excess cation content of the ashed material, which indicates their organic anion content. It is the decomposition of these organic anions via decarboxylation that consumes H^+ and gives rise to the pH increase (Yan *et al.*, 1996). The net effect of residue addition on soil pH will also be determined by association/dissociation reactions between organic materials and soil surfaces and acidifying processes that occur during N mineralisation. We established a field experiment in 2008 to determine the influence of residue characteristics (particularly C:N and ash alkalinity) on pH after incorporation into soil. Increases in pH were related to ash alkalinity of the residues. However, some of the alkalinity released during the first 2 months moved down the soil profile (unpublished data). Previous studies have shown that a large proportion (up to 70%) of the alkalinity within plant materials is potentially soluble (Sakala *et al.*, 2004; Yan and Schubert, 2000), but this is not known for agricultural residues. The laboratory incubation study described here was established to determine the contribution of the soluble and insoluble residue fractions to soil pH. We hypothesized that the initial change in soil pH would be related to the alkalinity contained within the soluble fraction.

Materials and Methods

Soil was collected from Frankston (38°14'S 145°22'E) and Shepparton (36°28'S 145°36'E) and had initial soil pH of 4.45 and 6.20, respectively. Residues of canola, chickpea and wheat were collected from field-grown crops, dried at 70 ℃ and

finely ground. Chemical properties of the residues are outlined in Table 1. Residues were extracted (1:10) using reverse osmosis (RO) water at 70 ℃ for 1 h, followed by centrifugation at 6400 rpm (3700 g) for 15 min. The supernatant was filtered through Whatman #1 and kept on ice until the end of the extraction period. The remaining material (including material collected on filter paper) was resuspended in RO water and extracted a further time. Filtered solutions from both extractions, termed the "soluble fraction" were combined and evaporated at 70 ℃ overnight. The remaining "insoluble fraction" was immediately dried in an oven at 70 ℃. Fractionation was performed <48 h before the start of the incubation experiment. Soil was adjusted to 40% of field capacity (FC) and pre-incubated at 25 ℃ for 14 days. Whole plant material and insoluble fractions were added to soil at 1% w/w. Soluble fractions which were extracted from an equivalent mass of residue, were resuspended in RO water immediately prior to adding to soil. All soils were then thoroughly mixed and adjusted to 70% FC. Twenty-five grams was packed into PVC cores (bulk density 1.4 $g \cdot cm^{-3}$) with 3 replicates, transferred into individual incubation chambers (Butterly *et al.*, 2009) and incubated at 25 ℃. At 2, 7 and 14 days, soil cores were destructively sampled and immediately extracted with 0.01 $mol \cdot L^{-1}$ $CaCl_2$ (1:5) on an end-over-end shaker for 1 h followed by centrifuging at 2000 rpm (492 g) for 10 min. pH of the supernatant was determined using a Thermo Orion pH meter (Thermo Orion 720A+, USA).

Results and Discussion

Changes in pH after the addition of residues and their fractions to Frankston and Shepparton soils are shown in Fig. 1 and Fig. 2, respectively. Increases in pH were greatest for chickpea, followed by canola and the least for wheat. These results are most likely related to the differences in alkalinity of the residues (Table 1). However, further information regarding

Table 1 Chemical properties of residues

Residue	C:N	Alkalinity ($cmol \cdot kg^{-1}$)
Chickpea	21	150
Canola	40	130
Wheat	64	45

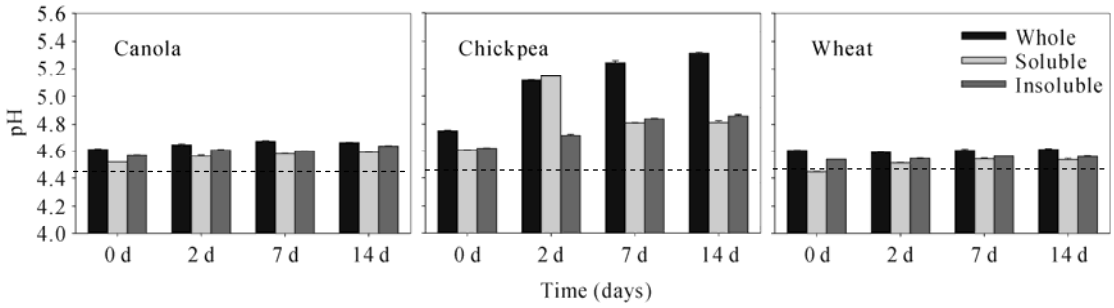

Fig. 1 pH in Frankston soil after incubation with whole, soluble and insoluble components of canola, chickpea and wheat residues. Bars indicate standard error of the mean (n=3) and dotted lines the initial soil pH

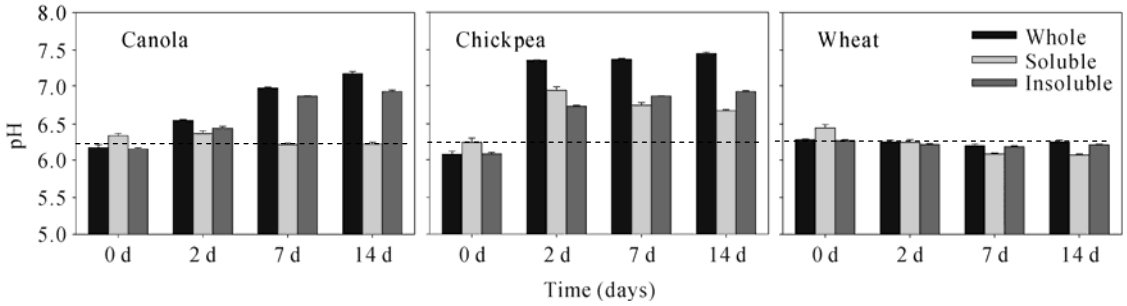

Fig. 2 pH in Shepparton soil after incubation with whole, soluble and insoluble components of canola, chickpea and wheat residues. Bars indicate standard error of the mean (n=3) and dotted lines the initial soil pH

changes in pH buffer capacity and patterns of decomposition are required. Alkalinity release from wheat and canola, which have higher C:N ratios than chickpea, may be limited by N availability. The results confirmed that the soluble fraction of residues is important in altering soil pH.

In the Shepparton soil, the soluble fraction was the source of alkalinity during the initial 2-day period. In addition, Shepparton soils that received the soluble fraction decreased in pH after 2 days, indicating that this fraction may have contained organic N which acidified the soil via nitrification. The results confirmed the importance of initial soil pH as suggested by other studies (Tang *et al.*, 1999; Xu *et al.*, 2006). In the Frankston soil, which had a lower initial pH, wheat and canola soluble fractions had less liming effect during the first 2 days compared with the Shepparton soil. In addition, acidification after 2 days in soils that received soluble fractions was not apparent in the Frankston soil, possibly explained by the inhibition of nitrification at low pH (Tang *et al.*, 1999). Alkalinity released from all canola fractions was much less at low pH. Total alkalinity and N composition of the soluble and insoluble residue fractions is yet to be determined. Further studies should quantify temporal changes in N forms and mineralisation (CO_2 production) to help elucidate the contribution of residue fractions to soil pH changes. However, the soluble fraction appeared to contribute a substantial (40%~60%) component of the alkalinity.

Acknowledgements

This work is supported by the Australian Research Council and the National Natural Science Foundation of China (40728001). The technical assistance of Bhawana Bhatta and Meredith Jay is gratefully appreciated.

References

Butterly CR, Bünemann EK, McNeill AM, Baldock JA, Marschner P (2009) Carbon pulses but not phosphorus pulses are related to decreases in microbial biomass during repeated drying and rewetting of soils. Soil Biol. Biochem. 41: 1406-1416

Kochian LV, Hoekenga OA, Pineros MA (2004) How do crop plants tolerate acid soils? Mechanisms of Aluminum tolerance and phosphorus efficiency. Ann. Rev. Plant Biol. 55: 459-493

Sakala GM, Rowell DL, Pilbeam CJ (2004) Acid-base reactions between an acidic soil and plant residues. Geoderma 123: 219-232

Tang C, Yu Q (1999) Impact of chemical composition of legume residues and initial soil pH on pH change of a soil after residue incorporation. Plant Soil 215: 29-38

Xu JM, Tang C, Chen ZL (2006) The role of plant residues in pH change of acid soils differing in initial pH. Soil Biol. Biochem. 38: 709-719

Yan F, Schubert S, Mengel K (1996) Soil pH increase due to biological decarboxylation of organic anions. Soil Biol. Biochem. 28: 617-624

Yan F, Schubert S (2000) Soil pH changes after application of plant shoot materials of faba bean and wheat. Plant Soil 220: 279-281

Soil Micro-interfaces Control the Fate of Pollutants in Soil Environment

Jizheng He*, Yuanming Zheng

Research Centre for Eco-environmental Sciences, Chinese Academy of Sciences, Beijing 100085, China.
*Corresponding author. Tel. No. +86-10 6284 9788; Fax No. +86-10 6292 3563; E-mail: jzhe@rcees.ac.cn.

Abstract: Environmental soil micro-interfaces are the collection and continuum of surfaces of soil clay minerals, oxides, organic matters, plant roots and microbes. The soil colloidal interfaces could be simply described as a diffuse electrical double-layer structure on the interface of soil particles and solutions. These heterogeneous micro-interfaces can be divided into three types based on their surface structure characterizations: siloxane, hydrous oxide and organic matter surfaces. The transport, transformation and degradation of pollutants in the soil are dynamic processes, including a series of reactions of sorption/desorption, precipitation/dissolution, complexation/chelation, and oxidation/reduction. Rhizosphere interface is the most active area in soil-plant ecosystems with intensive interactions among soil particles, organic compounds, plant roots and microorganisms. It is the channel of pollutant transporting to plants and linking with food chain. Microbial interface plays important roles not only in sorption and redox reactions of heavy metals, but also degradation and transformation of organic pollutants. As a dynamic continuum, different soil heterogeneous micro-interfaces interact with each other and control the forms, bioavailability, toxicity, transformation (degradation) and transport of pollutants in soil-plant ecosystems. Therefore, they are of significance in soil pollution control and remediation.

Keywords: Environmental micro-interface; Soil colloid; Rhizosphere; Microorganism; Pollutants; Reaction mechanism; Pollution control

Introduction

Soil is an important component of the environment, bonding the organic and the inorganic. Soil environment is an aggregate of all kinds of micro-interfaces inside. These micro-interfaces mainly are the interfaces formed between soil colloids and soil solution, which can be described as double electrical layer structure on the interface of soil particles and solutions. Soil colloids, including clay minerals, clay oxides, humus and microbial cells, are attributed with big specific surface area and charges. Therefore the micro-interfaces are the most active point position in the soil, which play a crucial role in the transportation, transformation and degradation of soil pollutants. Moreover, the micro-interface in plant rhizosphere is the most active area in soil-plant ecosystems, which has close relations with the transportation of pollutants in food chain. The study aimed at the micro-interfaces is important and significant to the soil pollution control and remediation.

Soil Colloidal Micro-interfaces

The transport and transformation of environmental pollutants in the micro-interfaces of soil colloids are dynamic processes, including a series of reactions of sorption/desorption, dissolution/precipitation, complexation/chelation, and oxidation/reduction (Fig. 1). These micro-interfaces processes determine the occurrence speciation, bioavailability and fate of the pollutants in the soil environment.

Mobility, activity and toxicity of heavy metals in the soil are determined, to some extent, by the surface characteristics of the soil components, particularly oxides of Fe, Al, and Mn. The adsorption of soil clay

particles to heavy metals is specific adsorption or strong selective adsorption. The ability of soil minerals adsorbing metal ions also changes with the characteristics of the ion types. In addition, the pH, Lewis acid and surface potential affect the affinity of metal ions to the solid surfaces of the soil.

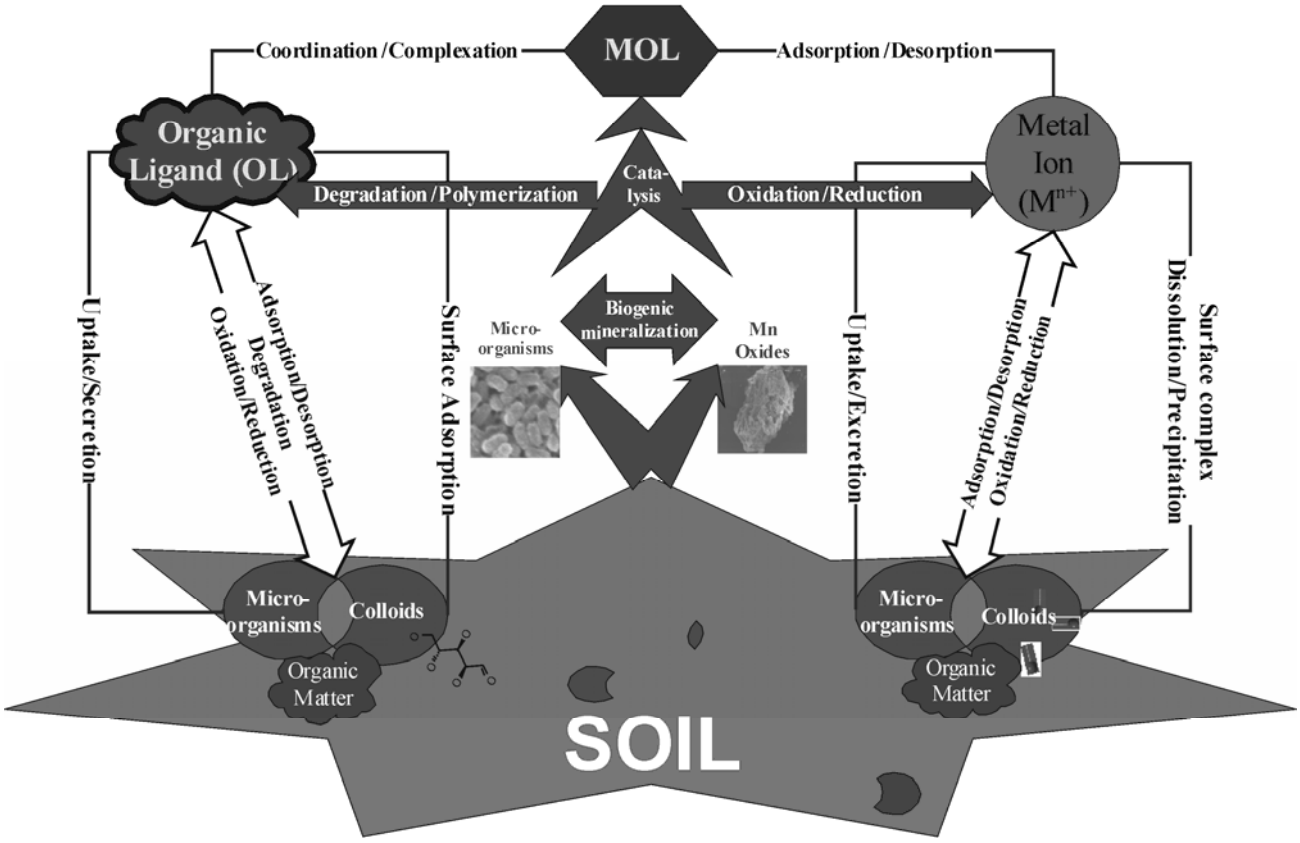

Fig. 1 Schematic processes on soil colloidal micro-interfaces

Rhizosphere Micro-interfaces

The micro-interfaces between root system of plants and soil can be described as rhizosphere micro-interfaces, or root/soil micro-interfaces, which range several micrometers or millimeters. In this mini-ecosystem, the physical, chemical and biological properties are very different from far-root area because of the dynamic processes of uptake and excretion of plants. The transport and uptake of environmental pollutants are determined by this mini-ecosystem, which play an important role in soil pollution control, especially the safety of agricultural products.

Perspectives and Conclusions

The micro-interfaces of soil environment are of a collection of soil components (minerals and organic matters), root system of plants, microorganisms, a continuum and a heterogeneous micro-interface with dynamic changes. Through the regulation to the characteristics of micro-interfaces, for example the changes of soil minerals surface properties, environmental behaviors of pollutants can be changed correspondingly. This regulation can be botanical or microbial. In fact, a joint control of plant and microorganisms is paid more and more attention in soil pollution control by now. Based on the description above, the characteristics, reaction processes and mechanisms of soil environmental micro-interfaces are becoming the focus of soil sciences. Along with the improving of research instruments and further going of research work, it is hopeful to obtain important progresses in modeling and expressing of micro-interfaces reactions, which can be used in the direction of soil pollution control and remediation.

References

He JZ, Zheng YM, Qu JH (2009) Soil environmental micro-interfaces and pollution control. Acta Scientiae Circumstantiae 29: 21-27 (in Chinese)

Li XY (2001) Soil Chemistry. Beijing: Higher Education Press pp.1-406 (in Chinese)

Meng YT, Zheng YM, Zhang LM, He JZ (2009) Biogenic Mn oxides for effective adsorption of Cd from aquatic environment. Environ. Pollu. 157: 2577-2583

Zhu YG (2003) Micro-interfacial processes in soil-plant systems and their environmental impacts. Acta Scientiae Circumstantiae 23(2): 205-210 (in Chinese)

Soil Microbial Biomass and pH as Affected by the Addition of Plant Residues

Yunfeng Wang[a], Ling Zhou[a], Jianjun Wu[a], Clayton R Butterly[b], Caixian Tang[b], Jianming Xu[a,*]

[a] Zhejiang Provincial Key Laboratory of Subtropical Soil and Plant Nutrition, College of Environmental and Natural Resource Sciences, Zhejiang University, Hangzhou 310029, China;
[b] Department of Agricultural Sciences, La Trobe University, Bundoora (Melbourne), Vic. 3086, Australia.
[*]Corresponding author. Tel. No. +86-571 8697 1955; Fax No. +86-571 8697 1955; E-mail: jmxu@zju.edu.cn.

Abstract: The soil microbial biomass is involved in the decomposition of organic materials and thus, the cycling of nutrients in soils. Reductions in the size and activity of the microbial biomass are frequently used as an early indicator of changes in soil chemical and physical properties resulting from management and environmental stresses in agricultural ecosystems. In a laboratory-incubated soil, we found a strong relationship between microbial biomass C and microbial biomass N. Irrespective of the type of plant residues added, soil pH was significantly correlated with microbial biomass C and microbial biomass N. Different C/N ratio of the residues was the main characteristic that affected soil microbial biomass C, N and soil pH. Microbes played a main role in plant residues decomposition and indirectly influenced of soil pH.

Keywords: Residue decomposition; C and N dynamics; Soil pH; Microbial biomass

Introduction

In China plant residues are usually burnt in the field after harvesting and may cause environmental problems such as air pollution. In addition, upland soils are becoming degraded due to low organic matter inputs. Incorporation of plant residues into upland soil may improve soil structure and reduce soil degradation (Zhang and Yao, 2005). Soil microbes are the most active part in terrestrial ecosystems and are responsible for the biological decay of residues, soil nutrient transformations and energy cycling via organic carbon (C) metabolism (Wang *et al.*, 1998). These processes require a soil to have a sufficiently large and diverse microbial biomass. The role of C cycling, including the microbial biomass, in soil acidification is not fully understood. The current study aimed to quantify changes in soil microbial biomass and pH as affected by the addition of plant residues.

Materials and Methods

Soil was collected from a paddy field on red sandstone soil in Long you county of Zhejiang Province. Soil was sieved (<2 mm) and thoroughly mixed for subsequent analysis and incubation experiments. The initial pH of the soil was 4.34. Three types of plant residues were selected in this study.

These were a legume residue (Chinese milk vetch), rice straw and wheat straw and had C and nitrogen (N) contents of 420.5, 399.9 and 442.8 g $C \cdot kg^{-1}$ and 25.1, 10.0 and 5.9 g $N \cdot kg^{-1}$ respectively. Air-dried soil was rewet to field capacity and pre-incubated for ten days at 25 ℃ in the dark to recover soil microbial biomass. Residues were added at a rate of 12 $g \cdot kg^{-1}$ soil. At 0, 1, 3, 7, 15, 30, and 60 days after the addition of plant residues, soil pH and microbial biomass C, N were determined. The effects of residue addition on microbial biomass C, N, soil pH and their interactions were tested using Analysis of Variance. LSD and correlation analysis were also performed.

Results and Discussion

Soil Microbial Biomass C and N Dynamics

Microbial biomass C and N were increased by the addition of plant residues, especially Chinese milk

vetch and rice straw (Fig. 1). The addition of wheat residue significantly increased microbial biomass C however; the increase in microbial biomass N was not significant. These results indicate that the high C content and low N content of wheat residue was not able to provide adequate N for the growth of microorganisms.

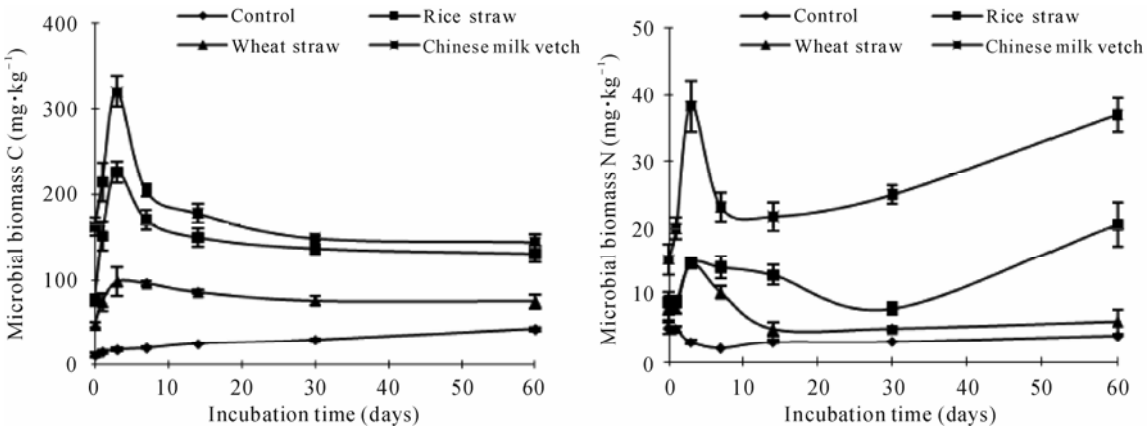

Fig. 1 Microbial biomass C and N dynamics during the 60-day incubation with plant residues. Bars indicate standard deviation of the mean

Microbial biomass C was positively correlated with microbial biomass N (r=0.71, P<0.01). These results are consistent with Jin *et al.*, (2007) who showed a significant positive correlation between microbial biomass C and microbial biomass N (r=0.864, P<0.01) for 25 calcareous surface soils with differing fertility from a Loess Plateau. The changes in soil microbial biomass N differed depending on the organic materials added. Similar to the findings of the current study, Aoyama and Nozawa (1993) showed that the addition of rice straw increased microbial biomass N content. The influence of adding different type's organic material on the microbial biomass would include comprehensive mineralization and immobilization reactions (Zhou *et al.*, 2001). In our study, the changes in the size of the microbial biomass are likely to result from the decomposition of both the added residues and native soil organic matter via priming. The higher availability of energy and nutrients from fresh organic matter addition results in an overall increase in soil microbial activity, which can have a priming effect on native soil organic matter decomposition (Bingeman *et al.*, 1953).

Soil pH Dynamics

In the control soil pH was between 4.32 and 4.43 and was relatively constant during the incubation period (Table 1). With increased time of incubation, the pH of the control markedly increased in the first week and generally reached the maximum at day 60. All plant residues significantly increased soil pH when added to soil. The increase was greatly affected by the type of residue with the largest increase for Chinese milk vetch (0.6 pH units), followed by rice (0.4 pH units) and the least for wheat (0.3 pH units).

Table 1 Soil pH changes during the 60-day incubation

Incubation time	Control	Rice straw	Wheat straw	Chinese milk vetch
Day 0	4.33	4.48	4.40	4.63
Day 1	4.43	4.63	4.59	4.77
Day 3	4.32	4.62	4.53	4.90
Day 7	4.34	4.62	4.59	4.90
Day 14	4.33	4.69	4.60	4.92
Day 30	4.36	4.68	4.62	4.98
Day 60	4.34	4.75	4.65	5.04

In our study, the C/N ratio of the plant residues appeared to be related to the change in soil pH, with larger increases in pH with lower C/N ratios. However, the neutralising capacity of the residues may be related to the excess cation content. Pocknee and Sumner (1997) concluded that the basic cations were the major cause of soil pH increase. In contrast, other studies suggest that the excess cations only indicate the organic anion content and it is the decarboxylation of these organic anions that consumes H^+ and neutralizes acidity. However, the degree of

decomposition of the plant residue, the pattern of release of anions and cations, and immobilization by microbes will also influence soil pH change.

Acknowledgements

This work was jointly supported by the National Natural Science Foundation of China (40728001) and the Science and Technology Projects of Zhejiang Province (2007C22015).

References

Aoyama M, Nozawa T (1993) Microbial biomass nitrogen and mineralization immobilization processes of nitrogen in soils incubated with various organic materials. Soil Sci. Plant Nutr. 39(1): 23-32

Bingeman CW, Varner JE, Martin WP (1953) The effect of the addition of organic materials on the decomposition of an organic soil. Soil Sci. Soc. Am. Proc. 29: 692-696

Jin FH, Li SQ, Lu HL, Li S (2007) Relationships of microbial biomass carbon and nitrogen with particle composition and nitrogen mineralization potential in calcareous soil, Chin. J. Appl. Ecol. 18(12): 2739-2746 (in Chinese)

Pocknee S, Sumner ME (1997) Cation and nitrogen contents of organic matter determine its soil liming potential. Soil Sci. Soc. Am. J. 61: 86-92

Wang XF, Li SY, Bai KJ, Kuang TY (1998) Influence of doubled CO_2 on plant growth and soil microbial biomass C and N, Acta Bot. Sin. 40 (12): 1169-1172 (in Chinese)

Zhang B, Yao S (2005) Soil wettibility during straw incubation as affected by numbers and intensities of wetting and drying. Geophys. Res. Abstr. 7, 09867

Zhou JB, Chen ZJ, Li SX (2001) Contents of soil microbial biomass nitrogen and its mineralized characteristics and relationships with nitrogen supplying ability of soils, Acta Ecol. Sin. 21(10): 1718-1724 (in Chinese)

Changes of Soil Enzyme Activities in the Process of Karst Forest Degradation in Southwest China

Fang Liu[a,b], Shijie Wang[b,*], Xiuming Liu[b], Yuansheng Liu[a], Jian Long[a]

[a] Institute of Environment and Resources, Guizhou University, Guiyang 550025, China;
[b] Key Laboratory of Environment Geochemistry , Institute of Geochemistry,
Chinese Academy of Sciences , Guiyang 550002, China.
[*]Corresponding author. Tel. No. +86-851-5891338; Fax No. +86-851-5891609; E-mail: wangshijie@vip.skleg.cn.

Abstract: Sample plots (15 m × 20 m) were set up in the karst areas in Guizhou Province with an attempt to reveal the changes of soil enzyme activities under karst forest degradation. The results showed that the extent of degradation of plant communities was enhanced leading to the clayification of soil, the drastic decrease in SOM contents, and the reduction of soil nutrients available for plants. The urease activities, peroxidase activities and alkaline phosphatase activities of the soils had also decreased significantly.

Keywords: Karst forest degradation; Soil nutrients; Soil enzyme activities

Introduction

In the karst mountainous areas of Southwest China, which cover about 42.6×10^4 km^2, largely in Guizhou Province (11×10^4 km^2), no sufficient attention has been paid to the problem of karst rocky desertification caused by irrational and intensive land use on a fragile karst geo-ecological environment (Wang *et al.*, 2002). Guizhou, which is located in the center of the karst region of Southwest China, was taken as the study region (Wang *et al.*, 2004b) to explore soil changes in the process of karst forest degradation, so as to establish suitable soil indices to evaluate the impact of karst forest degradation on ecological environment and provide the scientific basis for the restoration of vegetation and rational utilization of soil resources in karst areas.

Materials and Methods

Three regions were investigated, i.e., the Huajiang canyon karst region, the Qingzhen peak forest karst region and the Huaxi peak cluster karst region. Under the condition of relative consistency in landform, geomorphology, slope and lithology, the authors set up sample plots (15 m × 20 m) on the slopes under different vegetation conditions and conduct investigations into the vegetation and soil during February-May 2008. The surface layer of each soil sample (0~15 cm) was obtained by mixing 5~8 sub-samples respectively collected from 5~8 locations in each quadrat.

Results and Discussion

Due to the evolution of plant communities, changes occured in the physicochemical properties of soil. Significant differences appeared in the contents of clay particles in karst soils lying beneath the different plant communities. The contents of <0.01 mm-sized clay particles varied over the range of 43.6%~80.7%, and those of <0.001 mm-sized clay particles, 22.3%~64.2%. It could be seen clearly that soil tended to develop toward clayification following the order of degradation-evolution sequence of plant communities: broad-leaved forest → broad-leaved woodland → shrub forest → open shrub woodland → shrub grassland. The variation of plant communities

had also changed the contents of organic matter, which varied from 18.4~198.8 $g \cdot kg^{-1}$. Changes had also taken place in contents of main nutrients in soils with the variation of plant community. The contents of total nitrogen (TN) and total phosphorus (TP) in soil varied over the ranges of 1.82~10.3 $g \cdot kg^{-1}$ and 0.35~1.71 $g \cdot kg^{-1}$, respectively; acid-soluble potassium in soil, 190~412 $mg \cdot kg^{-1}$; available N, P and K in soil, 64~508 $g \cdot kg^{-1}$, 1.4~12.8 $g \cdot kg^{-1}$ and 60~185 $g \cdot kg^{-1}$, respectively. It was evident that following the order of degradation-evolution sequence of plant communities, the contents of main nutrients in soil decreased.

With the precise degradation-evolution sequence of plant communities as described above, the urease activities, peroxidase activities and also alkalin phosphatase activities of the soils had decreased significantly. Compared with the soil in broad-leaved forest, the urease activities decreased by 60%, the peroxidase activities decreased by 38%, and the alkalin phosphatase activities decreased by 43% for the soil of shrub grassland. During the degradation process of karst forest from broad-leaved forest → broad-leaved woodland → shrub forest → open shrub woodland → shrub grassland, the soil respiration was gradually decreased.

The results of correlation analysis (Table 1) indicated that the contents of organic matter, nitrogen, phosphorus and potassium in soils showed obvious positive correlations with the soil enzyme activities. The contents of organic matter, nitrogen, phosphorus and potassium had obvious positive correlations with the soil respiration. It could be seen that the reduction of vegetation coverage and the variation of plant community were the prerequisites for the changes of soil enzyme activities, and karst forest degradation was necessarily a decisive factor.

Table 1 Correlation coefficients between enzyme activities and soil nutrient contents in the study plots

Enzyme activities	Soil nutrient contents						
	SOM	TN	TP	AK	N	P	K
urease	0.571**	0.546**	0.620**	0.540**	0.613**	0.551**	0.590**
peroxidase	0.560**	0.610**	0.644**	0.680**	0.612**	0.474**	0.542**
phosphatase	0.794**	0.772**	0.745**	0.632**	0.830**	0.720**	0.732**
proteinase	0.370**	0.345**	0.322*	0.205	0.457**	0.365**	0.335*
invertase	0.455**	0.450**	0.505**	0.503**	0.466**	0.308*	0.427**
soil respiration	0.631**	0.674**	0.601**	0.491**	0.620**	0.659**	0.677**

Note: * $P < 0.05$; ** $P < 0.01$; n-1=59. soil organic matter (SOM), total nitrogen (TN), total phosphorus (TP), acid-soluble potassium(AK)

Reference

Lu RK (2000) The analytical methods for soil and agrochemistry. China Agricultural Science and Technology Press, Beijing (in Chinese)

Taylor JP, Wilson B, Mills MS, *et al.* (2002) Comparison of numbers and enzymatic activities in surface soils and subsoil using various techniques. Soil Biol. Biochem. 34: 387-401

Wang SJ, Li RL, Sun CX, Zhang, DF, Li FQ, Zhou DQ, Xiong KN, Zhou ZF (2004) How types of carbonate Rock Assemblages constrain the distribution of Karst Rocky Desertified land in Guizhou Province, PR China, Phenomena and Mechanisms. Land Degrad. Dev. 15: 123-131

Wang SJ, Liu QM, Zhang DF (2004) Karst Rocky Desertification in southwestern China: Geomorphology, landuse, impact and rehabilitation. Land Degrad. Dev. 15: 115-121

Effect of *cry1Ab* Gene Transformation on the Microbial Mediated Decomposition of Rice Residues under Intensive Rice Cropping System

Haohao Lu[a,b], Weixiang Wu [a,*], Yingxu Chen[a]

[a] College of Environmental and Natural Resource Sciences, Zhejiang University, Hangzhou 310029, China;
[b] College of Life Sciences, Zhejiang University, Hangzhou 310029, China.
[*]Corresponding author. Tel. No. +86-571 8160 4036; Fax No. +86-571 8160 4036; E-mail: weixiang@zju.edu.cn.

Abstract: Although genetically modified (GM) plants can offer many benefits, the planting of transgenic crops has raised a number of concerns, including the ecological impact of these plant residues on soil ecosystems. In this study, the effects of rice expressing the *Bacillus thuringiensis* Cry1Ab protein (*Bt* rice) on the residue decomposition processes were assessed in comparison with parental rice variety (non-Bt rice) under rapeseed-rice cropping system and surface or incorporated placement conditions. Bacterial and fungal communities associated with residue decomposition were studied by terminal restriction fragment length polymorphism (T-RFLP) method and additive main effects multiplicative interaction (AMMI) analysis model. After 276 days and residue decomposition in the field condition, bacterial and fungal communities associated with decomposition were strongly affected by the temporal factor which represented the grouping of T-RFLP fingerprint according to the time factor alone IPC 1. The placement effect on soil bacterial and fungal communities was also detected which represented the grouping of T-RFLP fingerprint alone IPC 2. Although some differences were found between Bt and non-Bt rice varieties in some special stages and placements, the impact of *cry1Ab* gene transformation on microbial mediated decomposition was lower than temporal and placement factors.

Keywords: *Bt* transgenic rice; Microbial community; T-RFLP; AMMI

Introduction

In 2008, genetically modified (GM) crops have been adopted in 25 countries covering an area of more than 125 million hectares with an annual growth rate of 9.4% (James, 2008). Nevertheless, the ecological effects of GM crops remain poorly understood. Randomly integrating a foreign gene into the plant genome may cause changes in the amount and composition of crop residues and may also affect organic matter decomposition, nutrient cycling and biodiversity in soil. Hence, the objective of this study was to assess if *cry1Ab* gene transformation into rice would affect microbial community associated with litter decaying process under intensive rice cropping system in the field.

Materials and Methods

The trial was conducted in Zhejiang University's experimental farm, Zhejiang Province, China (30°50′N, 120°40′E). Field soil is classified as a Fluvio marine blue-purple clay soil. It contained 2.01% total organic C, 2.53 $g \cdot kg^{-1}$ total N, with a pH 7.01 (H_2O). Two rice varieties, Bt transgenic rice line KMD (Bt) derived from a commercial Chinese japonica rice variety Xiushui 11 by the Agrobacterium method and non-Bt parental rice Xiushui 11 (Ck), were grown to obtain the residue for this study. The straw of the two rice cultivars for the current study was collected after harvest in 2005. Straw and roots were both dried at 60 ℃ to constant weight and cut into small pieces (about 5 cm) for the decomposition experiment. The decomposition experiment was set up

as a completely randomized design for two types of rice residues, Bts and Cks with three replicates. Litterbag method was used for the experiment. Briefly, two grams of Bt and non-Bt rice roots or 5 g of rice straw were sealed in a 10 cm × 15 cm nylon mesh litterbag (0.5-mm mesh for roots and 1-mm mesh for straws). The 60 straw and root samples each was prepared and randomly removed on day 31, 68, 137, 207, 276 for T-RFLP analysis after placement in the field. Sampled litterbags for T-RFLP analysis were immediately transported to laboratory. Samples were ground using liquid nitrogen and DNA extraction was conducted using bead beating method (FastDNA^{TM} SPIN Kit for Soil, Bio101 Inc., USA). DNA extracts were then quantified using image analysis (Quantity One 4.5.2, Gel Doc XR, Bio-Rad, USA) and stored at -20 ℃ for future research. DNA extracts diluted with nuclease-free water to approximately 10 ng·μL^{-1}. DNA was then amplified by polymerase chain reaction (PCR) using the fluorescently labeled forward primer D4-27f and the unlabeled reverse primer 1492r (Invitrogen Biotechnology Co., Ltd, USA) which target the bacterial 16S rRNA gene (Moeseneder *et al.*, 1999). The 50 μL reaction volume of each sample was amplified. All amplification products were electrophoresed in 1 % (w/v) agarose gels stained with SYBR green I (Invitrogen Biotechnology Co., Ltd, USA) and visualized under UV light. Samples after PCR reaction were quantified described above. The amplicons were purified with AxyPrep kit (Axygen, USA) and were resuspended in nuclease-free water to a concentration of approximately 10 ng·μL^{-1}. The restriction enzymes *Msp I* (Fermentas, USA) was used to digest amplified sample DNA. The digested samples were purified with AxyPrep kit (Axygen, USA) and mixed with an internal lane standard (Beckman, USA). Terminal fragment-size analysis was performed using a CEQ8000 electrophoretic capillary sequencer (Beckman, USA). T-RFLP analyses were also applied to characterize fungal communities of samples as described above for bacteria, with the following changes. The fluorescently labeled forward primer D4-ITS1f and the unlabeled reverse primer ITS4r (Invitrogen Biotechnology Co., Ltd, USA) which targeting the fungal internal transcribed spacer (ITS) region were used for fungal community DNA amplification (White *et al.*, 1990). The restriction enzymes *Hha I* (Fermentas, USA) was used to digest amplified sample DNA. Analyses of T-RFLP data were performed on binary variables of peak presence (presence/absence) and analyzed by Additive Main Effects Multiplicative Interaction (AMMI) model using MATMODELTM software (Microcomputer Power, Ithaca, NY) (Culman *et al.*, 2006).

Results and Discussion

The AMMI analysis of two bacterial T-RFLP data sets revealed a relationship between soil microbial community and decomposition time. The bacterial T-RFLP fingerprints from straw and root decomposition grouped together according to the time factor which reflected by first increasing then decreasing in values along the first IPC (IPC 1) (Fig. 1(a) and Fig. 1(c)). Similarly, the AMMI analysis of fungal T-RFLP fingerprints from both straw and root also revealed a relationship between soil fungal community and decomposition time (Fig. 1(b) and Fig. 1(d)). However, the trends were complicated. The fungal T-RFLP fingerprints from root decomposition represented an increase value along the IPC 1. Whereas in straw experiment, the fungal T-RFLP fingerprints represented an increase along IPC 2 on days 31 and 68, and then decreased along IPC 2. The placement effect on soil microbial community was detected by AMMI analysis (Fig. 1). The T-RFLP bacterial fingerprints from both straw and root decomposition all grouped by placement along the IPC 2. Although we found there was some genotype effect on fungal mediated decomposition on days 31 and 68 under incorporated placement (data not shown), the effect of rice genotype factor on the soil bacterial and fungal community was lower than temporal and placement factors both in straw and root trials.

Our results showed that the microbial community associated with rice residues was affected by temporal and placement stronger than Bt gene transformation using T-RFLP and AMMI analysis. Similarly, Lawhorn *et al.* (2009) found no adverse effects on microbial community composition in field condition using extracellular enzyme assays. The present results were consistent also with our previous research (Wu *et al.*, 2004) which indicated that decomposing transgenic Bt rice straw (Cry1Ab protein) had no significant effect on the to culturable bacteria, actinomycetes and fungi in a flooded paddy soil under laboratory conditions despite some transient effects on the populations of anaerobic fermentative bacteria, denitrifying bacteria, hydrogen-producing bacteria,

and methanogenic bacteria.

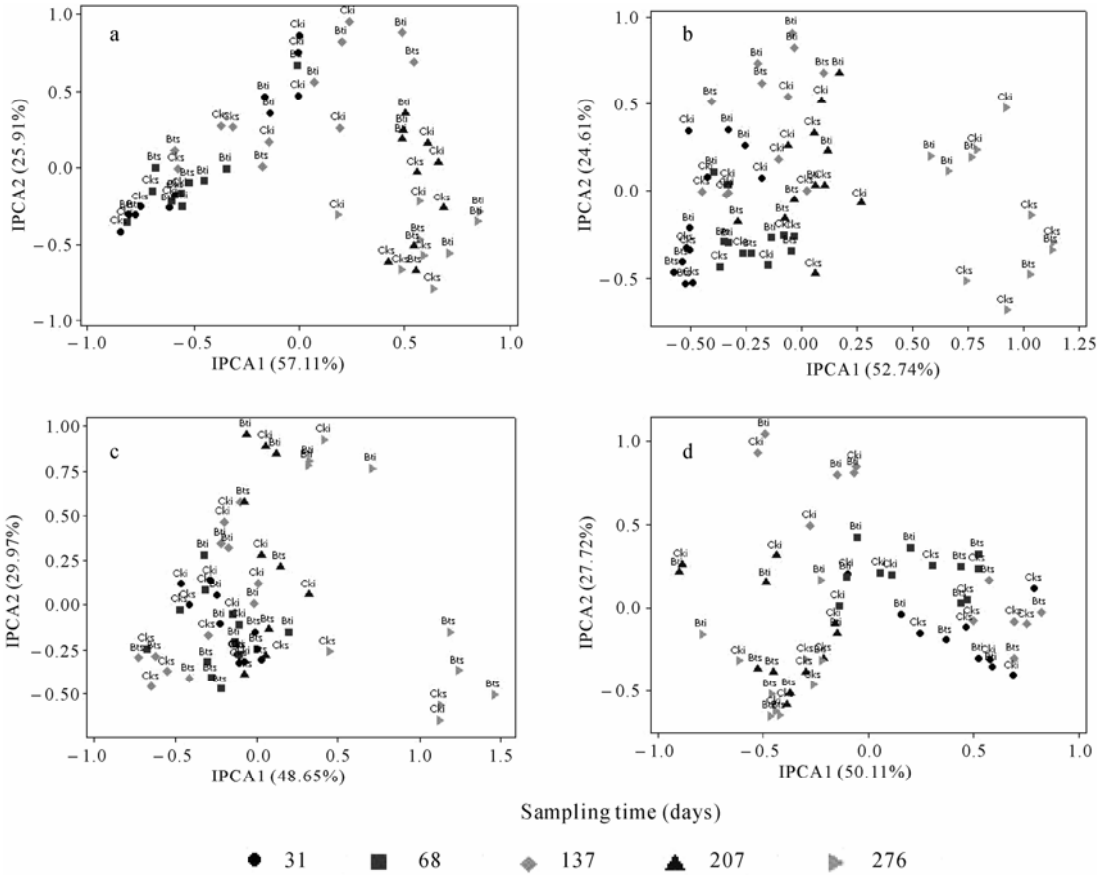

Fig. 1 AMMI analysis of bacterial (a and c) and fungal (b and d) T-RFLP profile during the rice root (a and b) and straw (c and d) decomposition. Graphs generated from T-RFs of PCR amplicons digested with Msp I for bacterial 16S rDNA gene and Hha I restriction endonuclease for Fungi ITS region. Bts: Transgenic Bt variety placed at the surface; Cks: Non-Bt variety placed at the surface; Bti: Transgenic Bt variety placed at 10cm depth in soil;Cki: Non-Bt variety placed at 10cm depth in soil

References

Culman SW, Duxbury JM, Lauren JG, Thies JE (2006) Microbial community response to soil solarization in Nepal's rice-wheat cropping system. Soil Biol. Biochem. 38: 3359-3371

James C (2008) Executive Summary Global Status of Commercialized Biotech/GM Crops: 2008. International Service for Acquisition of Agri-biotech Applications, Ithaca, NY

Lawhorn CN, Neher DA, Dively GP (2009) Impact of coleopteran targeting toxin (Cry3Bb1) of Bt corn on microbially mediated decomposition. Appl. Soil Ecol. 41: 364-368

Moeseneder MM, Arrieta JM, Muyzer G, Winter C, Herndl GJ (1999) Optimization of terminal-restriction fragment length polymorphism analysis for complex marine bacterioplankton communities and comparison with denaturing gradient gel electrophoresis. Appl. Environ. Microbiol. 65: 3518-3525

White TJ, Bruns TD, Lee S, Taylor J (1990) Analysis of phylogenetic relationships by amplification and direct sequencing of ribosomal RNA genes. (Innis MA, Gelfand DH, Sninsky JJ & White TJ, eds.), pp. 315-322. Academic Press, New York

Wu WX, Ye QF, Min H, Duan X, Jin W (2004) Bt-transgenic rice straw affects the culturable microbiota and dehydrogenase and phosphatase activities in a flooded paddy soil. Soil Biol. Biochem. 36: 289-295

Characterization of Microbial Community and Phosphorus-releasing Bacteria in the Sediments of a Eutrophic Shallow Lake, Eastern China

Yichao Qian[a,b], Yingxu Chen[a,b,*], Jiyan Shi[c], Liping Lou[a]

[a] Zhejiang Province Key Laboratory for Water Pollution Control and Environmental Safety, Hangzhou 310029, China;
[b] Institute of Environmental Science and Technology, Zhejiang University, Hangzhou 310029, China;
[c] Ministry of Agriculture Key Laboratory of Non-point Source Pollution Control, Hangzhou 310029, China.
[*]Corresponding author. Tel. No. +86-571 8697 1392; Fax No. +86-571 8697 1411; E-mail: yxchen@zju.edu.cn.

Abstract: To understand the interactions between phosphorus (P) and microbial community and characterize some P-releasing bacteria, ten representative sediment samples were collected in a small eutrophic lake and a clean wetland. Total P concentration in wetland sediment was much lower than that in the lake, while NaOH-extractable P was relatively high in wetland which indicated high releasable risk. According to Standards Measurements and Testing Program of the European Commission (SMT protocol), P in lake rooted in agricultural runoff and P in wetland was mainly of anthropogenic origin, and the microbial communities were significantly different between these two kinds of sediment. Enumeration of inorganic P-releasing bacteria (IPB) and organic P-releasing bacteria (OPB) showed these groups were not very rich in the ecosystem. Molecular identification indicated there were various kinds of bacteria involved in the P transition cycle, but the P release abilities of different bacteria were dissimilar.

Keywords: Phosphorus (P); Sediment; Distribution; P-releasing bacteria; 16s rDNA

Introduction

Phosphorus (P), one of the key limiting factors for bacterial activity and for primary production of the aquatic system, distributes in several forms in sediments. Although the effects of eutrophication are well known, the process mechanisms of P release are poorly understood (Wang *et al.*, 2003). To clarify the process, much of the emphasis has been focused on the physical and chemical field. However, previous studies have seldom considered the significance of the biological field, especially on microbial community and bacteria with the abilities to transform inorganic P and/or organic P. The objective of this work was to investigate the distribution and origins of different P forms and microbial compositions in two shallow wetlands with different eutrophic levels. Moreover, we studied the abundance and characteristics of P-releasing bacteria (PRB) in order to make the biological transformation process of P more clearly expounded.

Materials and Methods

Representative ten sites in West Lake and Xixi Wetland were selected for this study. At each site, three sediment cores were taken with a gravity core sampler and a self-made tube. The P fractions were determined using an analytical protocol developed by the Standards Measurements and Testing Program of the European Commission (SMT protocol). SRP concentrations were analyzed using the molybdate blue method. Sediment DNA was extracted from 0.5 g soil using a bead beating method. For bacteria DGGE analysis, the V3 region of 16S rDNA was amplified with the primers 357F-GC clamp and 518R. A touchdown thermal cycle program was used to

prevent non-specific amplification, amplified DNA was verified by running the PCR product on a 1% agarose gel stained with SYBRTM Green I (Sigma, USA) and visualized with the Fluor-S Multimager (Bio-Rad, USA). The DGGE was performed using a Dcode^{TM} Universal Detection System instrument according to the manufacturer's instructions (Bio-Rad, USA). A polyacrylamide gel was prepared with a denaturing gradient of 30%~55%. The 30 mL PCR products were mixed with loading dye and 30% glycerol (v/v)) and transferred to the bottom of the wells and electrophoresed in 1×TAE buffer at 60 ℃ for 5~6 h at a constant voltage of 160 V. After electrophoresis, the gels were stained with SYBRTM Green I (Sigma, USA) for 30 min and photographed under UV light with the Fluor-S MultiImager (Bio-Rad, USA) and digitized with Quantity One Software (Bio-Rad, USA). To enumerate IPB and OPB, aqueous extracts of 1g fresh sediment samples were serially diluted and smeared onto IP agar with calcium phosphate as sole P source and OP agar. P release ability was quantitatively estimated by inoculating the isolated bacterium to IP and OP liquid medium. EZ Spin Column Bacteria Genomic DNA Isolation Kit and PCR technique were employed to characterize predominant PRB. The resulting products were analyzed by electrophoresis in 1% agarose gel and sequences were determined at Invitrogen Corporation, Shanghai.

Results and Discussion

The average concentration of the total P in the sediment of lake was about 0.75 mg·g^{-1} while it was 0.45 mg·g^{-1} in wetland. Lacking of organic P (OP) was the main factor of this phenomenon (Fig.1). However, high content of NaOH-P showed the release potential was very high in the surface sediment of wetland. According to the different concentration ratio of NaOH-P and OP, P in lake rooted in agricultural runoff and P in wetland was mainly of anthropogenic origin, such as daily life waste (Ruban *et al.*, 1999).

The average of OPB was 27.35±2.56×10^4 CFU·g^{-1}, and IPB was 6.94±1.28×10^4 CFU·g^{-1} in lake, while the numbers were 2.91±0.38×10^4 CFU·g^{-1} and 1.28±0.25×104 CFU·g^{-1} in wetland, respectively. OPB enriched in the middle (20 cm) and bottom (40 cm) of sediment, and IPB enriched in the middle section. Abundance of two bacteria was the lowest in surface of the sediment. Microbial community was evidently different in surface sediment of two sampling areas according to the DGGE result. Microbial diversity seemed to be more complex in lake, while some distinct species existed in cleaner regions (Fig.2).

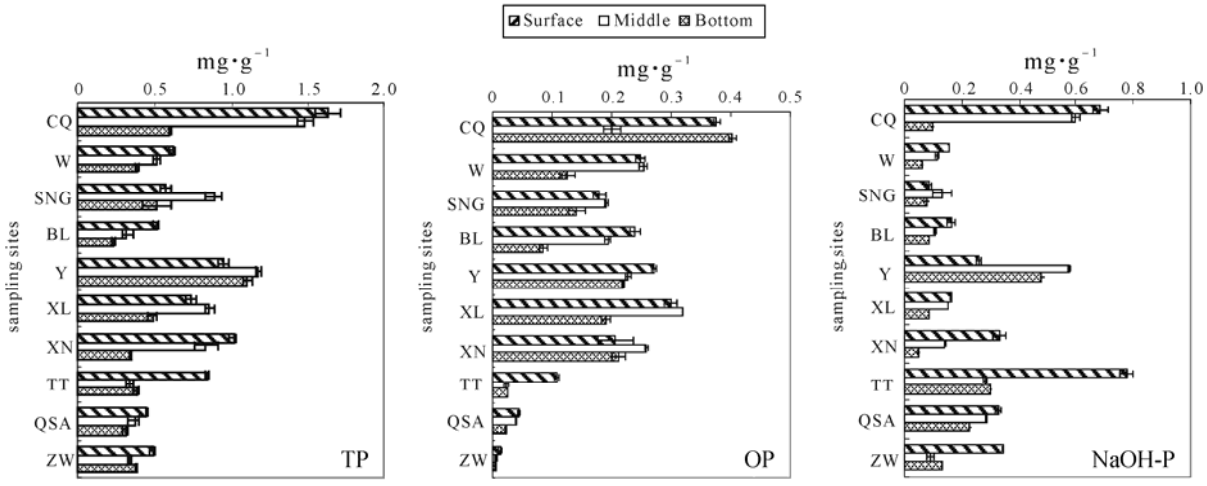

Fig. 1 The concentrations of various phosphorus fractions at the central sediment of different sampling sites of the West Lake and Xixi Wetland (CQ: Changqiaoxi; W: Wai Lake; SNG: Shaoniangong; BL:Beili Lake; Y:Yue Lake; XL: XiLi Lake; XN: Xiaonan Lake; TT: Tantu; QSA: Qiushuian; ZW: Zhiwu)

6 IPB and 8 OPB were isolated from the fresh sediment. Laboratory tests on P release abilities showed IPB could release more orthophosphate than OPB. IPBs were closely related to *Enterobacter*, and different OPBs, closely matching *Citrobacter,*

Cupriavidus, Pseudomonas, Acinetobacter, Burkholderia, some of them had already been reported to have organic phosphate solubilizing abilities (Wu *et al.*, 2005).

Table 1 Identification of predominant OPB and IPB strains by alignment with 16SrDNA sequences of organisms in the EMBL database

Bacteria	numbers	Closet match	Identity(%)
IP1	1238	*Enterobacter sp.* (DQ923747)	97.7
IP12	752	*Enterobacter sp.* (AY488028) *Pantoea agglomerans* (AY691544) *Gamma protenbacterium* (AB210969)	98.7
IP15	686	*Pantoea agglomerans* (AY691544) *Gamma protenbacterium* (AB210969)	98.8
IP53	696	*Pantoea agglomeransn* (EU275357)	98.1
IP54	625	*Pantoea agglomeransn* (AM184212) *Citrobacter freundii* (DQ133536)	99.1
IP59	668	*Enterobacter cloacae* (Eu647232)	98.0
OP32	790	*Citrobacter freundii* (DQ010114)	97.9
OP48	708	*Pseudomonas sp.* (AY464946)	100.0
OP49	1300	*Cupriavidus basilensis* (AY047217)	88.4
OP51	750	*Cupriavidus basilensis* (AY047217)	98.8
OP57	736	*Citrobacter freundii* (AB244300) *Citrobacter freundii* (AB244451)	97.6
OP59	706	*Citrobacter freundii* (DQ010114)	100.0
OP72	1285	*Acinetobacter sp.* (EU000453)	98.3
OP98	686	*Burkholderia pyrrocinia(T)* (U96930) *Burkholderia cepacia* (EF095217)	96.8

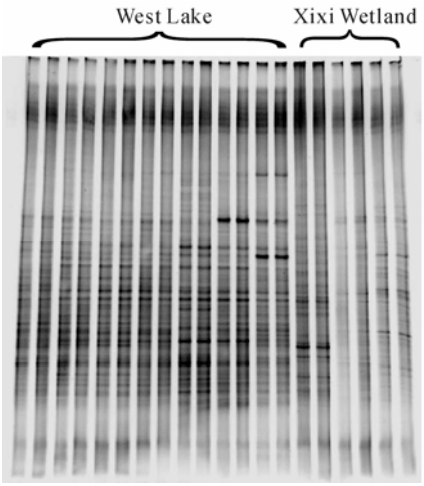

Fig. 2 DGGE patterns of DNA from the surface sediments of different sampling sites

References

Ruban V, Brigault S, Demare D, Philippe AM (1999) An investigation of the origin and mobility of phosphorus in freshwater sediments from Bort-Les-Orgues Reservoir, France. J. Environ. Monitor. 1: 403-407

Wang H, Appan A, Gulliver JS (2003) Modeling of phosphorus dynamics in aquatic sediments: II-examination of model performance. Water Res. 37: 3939-3953

Wu GF, Zhou XP (2005) Characterization of phosphorus-releasing bacteria in a small eutrophic shallow lake, Eastern China. Water Res. 39: 4623-4632

Carbon Compounds Differ in Their Effects on Soil pH and Microbial Respiration

Fatima Rukshana[a], Clayton R Butterly[a], Jianming Xu[c], Jeffrey A Baldock[b], Caixian Tang [a,*]

[a] Department of Agricultural Sciences. LaTrobe University, Melbourne 3086, Australia;
[b] CSIRO Land and Water, PMB 2, Glen Osmond 5064, Australia;
[c] Zhejiang Provincial Key Laboratory of Subtropical Soil and Plant Nutrition,
College of Environmental and Natural Resource Sciences, Zhejiang University, Hangzhou 310029, China.
[*]Corresponding author. Tel. No. +61 3 9479 2184; Fax No. +61 3 9471 0224; E-mail: C.Tang@latrobe.edu.au.

Abstract: The mechanisms of soil pH change after the addition of organic matter to soil are not fully understood. The aim of this study was to investigate changes in pH after addition of carbon compounds over a 60-d incubation period. Seven organic compounds commonly found in plant residues (acetic acid, malic acid, citric acid, benzoic acid, ferulic acid, glucosamine hydrochloride and glucose) were selected based on the number and type of functional groups, and added at 0.5 mg $C \cdot g^{-1}$ soil to two soils differing in initial pH. Addition of organic acids (R-COOH) immediately decreased pH. The magnitude of the pH decrease depended on dissociation constant of the acid and the initial soil pH. In subsequent incubation, pH was slowly returned to original levels as organic anions were mineralized, consuming H^+ ions. Glucose which contains hydroxyl (R-OH) group did not alter soil pH. However, carboxyl (R-COOH) and amine ($R\text{-}NH_2$) groups changed pH significantly. Soil respiration was also increased by the addition of C compounds. Cumulative respiration was higher in soil with malic acid, citric acid, ferulic acid and glucose than with other compounds. The addition of glucose, citric acid and malic acid resulted in priming as cumulative respiration was greater than the actual amount of C added.

Keywords: Carbon compounds; Initial soil pH; Priming; C mineralization

Introduction

Carbon compounds in plant residues may have a substantial effect on soil pH. After addition of organic matter to soil, association/dissociation of protons from organic compounds is one of the major processes resulting in soil pH change (Xu *et al.*, 2006). The change depends on the rate of H^+ release or consumption by the added organic matter. Organic compounds in plant residues contain functional groups which are one source of H^+ after dissociation (Brady and Weil, 2002). The dissociation/association of functional groups of organic matter depends on mean pKa values of the organic matter and initial pH (Ritchie and Dolling, 1985; Tang and Yu, 1999; Tang, 2004; Xu *et al.*, 2006). Furthermore, chemical reactions during decomposition of organic matter are related to the quantities and types of organic functional groups and structural components present in organic compounds (Essington, 2004). However, most of the published studies have examined pH changes associated with the whole plant residues, and there is a need to understand soil pH changes associated with the specific compounds. We hypothesized that the initial change in soil pH after addition of compounds would be related to the strength of the acid and therefore, neutral functional groups (glucose) or less labile compounds (phenolics) would not significantly affect pH in the short-term.

Materials and Methods

Two soils differing in pH were collected from Frankston (38°14'S 145°22'E) and Shepparton

(36°28'S 145°36'E) Victoria, Australia. Soils were thoroughly mixed and sieved (<2 mm) for subsequent analysis and the incubation study. The Frankston soil had an initial pH of 4.34 and contained 95% sand, 0.2% silt, 5% clay. The Shepparton soil had an initial pH of 6.11 and contained 88% sand, 4% silt, 8% clay. Seven organic compounds (acetic acid, malic acid, citric acid, benzoic acid, ferulic acid, glucosamine hydrochloride and glucose,) were selected and they represent compounds commonly found in plant residues.

These compounds differ in the type and number of functional groups.

Eighty grams of air-dried soil was pre-incubated at 60% field capacity in the dark at 25 ℃ for 10 d. At the end of the pre-incubation period, stock solution of acetic acid (62.5 $g \cdot L^{-1}$) (Rhone-Poulenc), malic acid (69.77 $g \cdot L^{-1}$) (Sigma-Aldrich), citric acid (72.9 $g \cdot L^{-1}$) (BDH Chemicals), ferulic acid (40.42 $g \cdot L^{-1}$) (MP Biomedicals, Inc), glucosamine hydrochloride (74.8 $g \cdot L^{-1}$) (Sigma-Aldrich) and glucose (62.5 $g \cdot L^{-1}$) (Ajax chemical) were added to each soil at 0.5 mg $C \cdot g^{-1}$ soil. Benzoic acid (Ajax Finechem) was added in powder form as it is not soluble in water. Soils were mixed thoroughly and 3 replicates of twenty five grams soil was packed into individual plastic cores (3.7 cm diameter and 5 cm length) with a bulk density of 1.4 $g \cdot cm^{-3}$. Cores were placed into glass incubation chambers as described by Butterly *et al.* (2009) and incubated for 60 days at 25 ℃. Cores were maintained 80% of field capacity throughout the incubation experiment.

At Days 0, 3 and 60 a set of cores was destructively sampled for analysis. Soil pH was determined using a pH meter (Thermo Orion 720A+, USA) after extraction in 0.01 $mol \cdot L^{-1}$ $CaCl_2$ (1:5 soil: solution) by shaking end-over-end for 1 h following centrifugation at 3500 $r \cdot min^{-1}$ for 10 min. Particle-size distribution was analyzed using the hydrometer method. CO_2 released was measured using an infra-red gas analyzer (IRGA).

Results and Discussion

Addition of organic acid (acetic, malic, citric, benzoic and ferulic acid) to soil instantly decreased pH due to H^+ dissociation (Fig. 1). The magnitude of pH decrease depended on dissociation degree of the acids and the initial soil pH. In subsequent incubation, pH was slowly restored to original levels as organic anions were mineralized, consuming H^+ ions. Glucosamine hydrochloride did not change pH when added to soil, however pH decreased in subsequent incubation possibly due to nitrification. Glucose did not significantly change pH as it is neutral compound. This study also showed that the magnitude of the pH change was greater in the Shepparton soil which is related to its lower pH buffer capacity (0.53 $cmol \cdot pH^{-1} \cdot kg^{-1}$) compared to the Frankston soil (0.69 $cmol \cdot pH^{-1} \cdot kg^{-1}$).

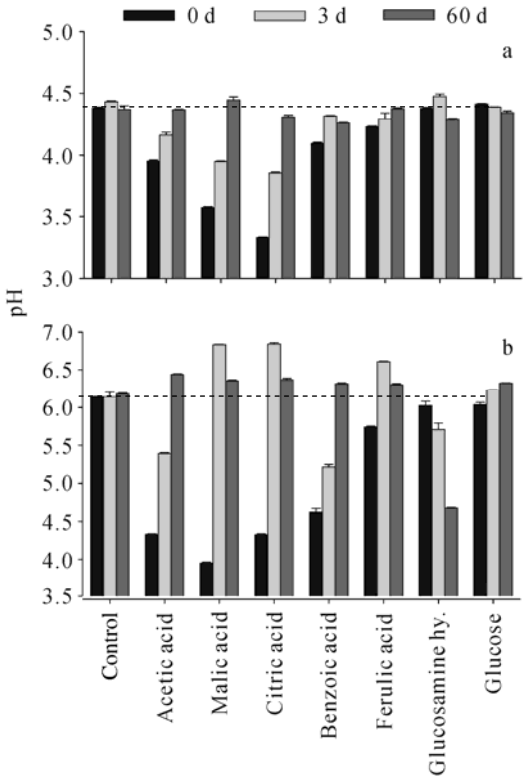

Fig. 1 Soil pH changes after the addition of model carbon compounds at 0.5 mg $C \cdot g^{-1}$ soil to a) Frankston soil and b) Shepparton soil. Bars represent standard error of the mean, (n = 3). Dotted lines indicate the initial pH of the soil. Note the different scales of pH on the Y axis

The addition of C compounds increased cumulative respiration in both soils (Table 1). Malic acid, citric acid and glucose treatments had much greater levels of respiration than other C compounds during the 60-d incubation. Moreover, total respired C after addition of malic acid, citric acid, ferulic acid and glucose was higher than the amount of C added, even when counting for background respiration of the controls. Therefore, some of the C that was mineralized did not originate from added C, indicating that priming occurred. The

largest priming response occurred after the addition of malic acid. Addition of C compounds resulted in higher cumulative respiration in the Shepparton soil than the Frankston soil, even in the control treatment. The higher respiration activity in the Shepparton soil might be due to a higher size or activity of microbial biomass or greater amounts of labile material. Soil pH was not changed over time with the addition of glucose but cumulative respiration was more than 4-fold greater in the Frankston and 2-fold in the Shepparton soil than the control. As simple sugars (glucose) are readily available to microorganisms and are converted to CO_2 or other carbohydrates, or incorporated into other microbial products, such as amino acids or lipids (Essington, 2004). Interestingly, pH changes occurred in some treatments even though very little mineralization had occurred (e.g. acetic acid treatment in the Frankston soil), indicating that these changes are physiochemical rather than microbial. Further studies will examine the role of mineralization and N cycling in more details.

Table 1 Effect of carbon compounds on cumulative respiration in Frankston and Shepparton soils during a 60-d incubation. Means with different letters indicate significant differences (P<0.05) between soils and treatments using the post-hoc Tukey test

Compounds	Cumulative respiration (μg CO_2-C·g^{-1} soil)	
	Frankston	Shepparton
Control	331[a]	724[b]
Acetic acid	337[a]	917[cd]
Malic acid	1461[f]	1745[g]
Citric acid	1443[f]	1684[g]
Benzoic acid	397[a]	1407[f]
Ferulic acid	927[d]	1432[f]
Glucosamine hydrochloride	832[c]	1297[e]
Glucose	1459[f]	1703[g]

Acknowledgements

This work is supported by the Australian Research Council and the National Natural Science Foundation of China (40728001).

References

Brady NC, Weil RR (2002) The Nature and Properties of Soils. New Jersey, Prentice Hall

Butterly CR, Bunemann EK (2009) Carbon pulses but not phosphorus pulses are related to decreases in microbial biomass. Soil Biol. Biochem. 41: 1406-1416

Essington ME (2004) Soil and Water Chemistry: An Integrative Approaches. Florida, CRC press LLC.

Ritchie GSP, Dolling PJ (1985) The role of organic matter in soil acidification. Aust. J. Soil Res. 23: 569 - 576

Tang C (2004) Causes and management of subsoil acidity. 3rd Australian New Zealand Soils Conference. University of Sydney, Australia, www.regional.org.au/au/assi/

Tang C, Yu Q (1999) Impact of chemical composition of legume residues and initial soil pH on pH change of a soil after residue incorporation. Plant Soil 215: 29-38

Xu JM, Tang C, *et al.* (2006) The role of plant residues in pH change of acid soils differing in initial pH. Soil Biol. Biochem. 38: 709-719

Effects of Soil Water Content on Soil Microbial Biomass and Community Structure Based on Phospholipid Fatty Acid Analysis

Yuping Wu, Yan He, Haizhen Wang, Jianming Xu*

Zhejiang Provincial Key Laboratory of Subtropical Soil and Plant Nutrition,
College of Environmental and Natural Resource Sciences, Zhejiang University, Hangzhou 310029, China.
*Corresponding author. Tel. No. +86-571 8697 1955; Fax No. +86-571 8697 1955; E-mail: jmxu@zju.edu.cn.

Abstract: Three different kinds of soils collected from Heilongjiang, Jiangsu and Guangxi province of China were used to test the effects of different water contents on soil microbial biomass and community structure. Soils were moistened to 40%, 60% and 80% of water holding capacity (WHC) first. Then the moist soils were incubated in the dark room at 25 ℃ for 56 days. Phospholipd fatty acid (PLFA) analysis were carried on days 0, 3, 7, 14, 28 and 56 to track the changes of soil microbial organisms. The results showed that soil microbial biomass and community structure based on PLFA analysis did not response to the different soil water contents. Soil microbial organisms might get used to a wide range of soil water contents.

Keywords: Water content; Soil microbial biomass; Soil microbial community; Phospholipid fatty acid (PLFA)

Introduction

Soil moisture can influence a number of soil physic-chemical properties, such as redox potential, pH, O_2 and CO_2 levels (Barros *et al.*, 1995) and the concentrations of mineral nutrients in soil solutions (Misra and Tyler, 1999), which in turn influence the microbial population and its activity. There are some researches about the effects of soil water contents on soil microbial organisms. However, most of them were about soil microbial organisms respond to extreme environment conditions, like flooding (Bossio and Scow, 1995; Bossio and Scow, 1998) and drying and rewetting (Gordon *et al.*, 2008; Xiang *et al.*, 2008). There are no reports about how soil microbial biomass and communities respond to natural gentle soil moistures. The aim of this study was to compare the differences of soil microbial biomass and community structure under three different gentle water content regimes. This was accomplished by moistening three different kinds of soils to 40%, 60% and 80% of water holding capacity (WHC) and incubated at 25 ℃ for 56 days. PLFA analyses were conducted intervals to investigate the changes of soil microbial organisms.

Materials and Methods

Three different kinds of soils collected from Heilongjiang, Jiangsu and Guangxi province of China were used in this study (Wu *et al.*, 2009b). The fresh soils were taken to the laboratory in cool boxes with ice bags in, sieved (2 mm) and stored at 4 ºC before use. Heilongjiang soil is an argiustoll in U.S. taxonomy with a pH of 5.38, organic C content of 32.1 $g \cdot kg^{-1}$ and clay content of 36.4%. Jiangsu soil is a Typudalf. The pH, organic C and clay content were 5.12, 15.5 $g \cdot kg^{-1}$ and 25.2% respectively. Guangxi soil is a Plinthudult with a pH of 4.23, organic C content of 10.7 $g \cdot kg^{-1}$ and clay content of 37.0%. Before the main incubation, moist soils were pre-incubated at 25 ℃ for a week to activate soil microbial organisms. The soils were then adjusted to three different moisture levels (40%, 60% and 80% of WHC) and incubated at 25 ℃ for 56 days. At days 0, 3, 7, 14, 28 and 56, 5 g soil samples were collected respectively for the PLFA analysis. PLFAs were extracted and identified according to Wu *et al.* (2009a).

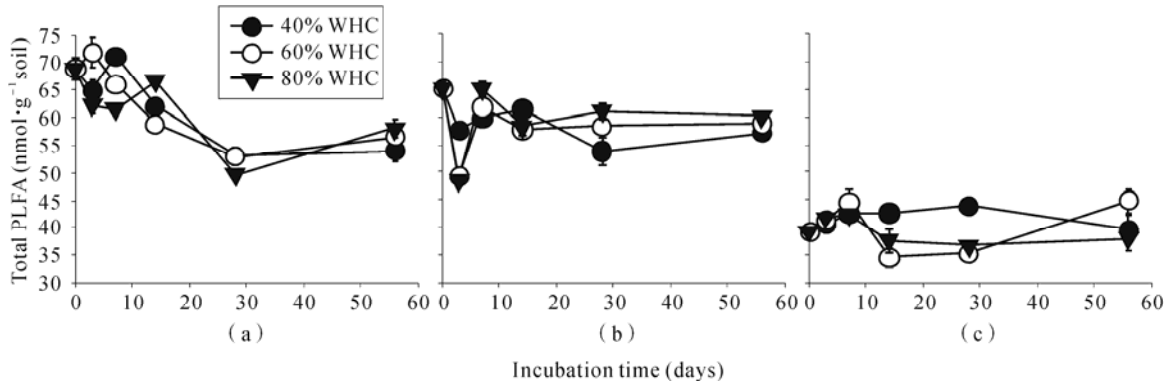

Fig. 1 Total PLFA concentrations during incubation at 40%, 60% and 80% Water Holding Capacity (WHC) of soils collected from Heilongjiang (a), Jiangsu (b) and Guangxi (c) provinces

Results and Discussion

Soil microbial biomass indexed by total phospholipid fatty acid concentration (total PLFAs) was not significantly different in the different soil moisture regimes in all the three soils (Fig. 1). Total PLFAs in the Heilongjiang soils were decreased with the incubation time in all the three soil water contents (Fig. 1(a)). The reason for this may be that the temperature of 25 ℃ caused thermal stress to soil microbial organisms inhabited in Heilongjiang soils. Heilongjiang soil was collected in the coldest region of China with a mean annual temperature of 1.2 ℃. Raising the incubation to 25 ℃ can increase the mortality of Heilongjiang soil microbes by thermal denaturation (Wu *et al.*, 2009b). For the Jiangsu and Guangxi soils, after some initial fluctuations, soil microbial biomass was kept consistent till the end of incubation (Fig. 1(b) and 1(c)).

Principle component analysis (PCA) was carried to check the dynamic changes of soil microbial community under different soil moisture regimes. PLFA profiles did not change regularly when increasing soil moistures from 40% WHC to 80% WHC in all the three kinds of soils for the whole 56 days' incubation (Fig. 2).

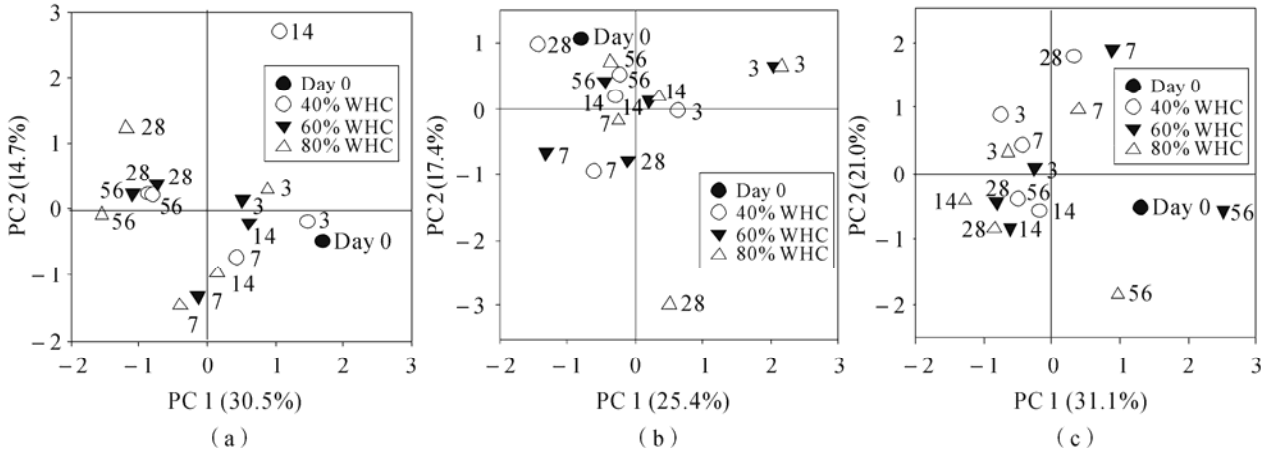

Fig. 2 Principal component analyses (PCA) of phospholipid fatty acid (PLFA) profiles in Heilongjiang (a), Jiangsu (b), and Guangxi (c) soils incubated at different water content (40%, 60% and 80% WHC) for up to 56 days

Theoretically, increasing soil moisture will reduce the aeration of soil pores and increase the utilization of nutrients, thus influence the growth of soil microbes. In this study, we did not find any significant differences when increasing soil moistures from 40% WHC to 80% WHC. This is consistent with Gordon *et*

al. (2008) and Bossio and Scow (1995). The reason why increasing soil moistures did not affect soil microbial biomass and community structures might be that the moisture range in the present study was not bigger enough to change microbial available oxygen, substrates and water in the soil pore space. The size of soil microbes (including bacteria and fungi) is about 0.3~20 μm (Cao, 2007), which is almost three times smaller than their habitat space the soil pore space (Young and Ritz, 2000). Soil pore space is a very complicated network with surprisingly structures and tortuosities. Over the past decade, research has moved from highly qualitative descriptors of pore shape to more quantitative measures of pore connectivity and tortuosity. However, it is progressing slowly. Till now, we do not know where and how soil microbes living in the soil pores (Young and Crawford, 2004).

Acknowledgements

This work was jointly supported by the National Natural Science Foundation of China (20707020, 40671092), and the National Basic Research Program of China (2005CB121104).

References

Barros N, Gomez-Orellana I, Feijoo S, Balsa R (1995) The effect of soil moisture on soil microbial activity studied by microcalorimetry. Thermochim. Acta. 249: 161-168

Bossio DA, Scow KM (1995) Impact of carbon and flooding on the metabolic diversity of microbial communities in soils. Appl. Environ. Microbiol. 61: 4043-4050

Bossio DA, Scow KM (1998) Impacts of carbon and flooding on soil microbial communities: Phospholipid fatty acid profiles and substrate utilization patterns. Microb. Ecol. 35: 265-278

Cao Z (2007) Soil ecology (Eds. Cao Z). Beijing: Chemical Industry Press. pp. 41

Gordon H, Haygarth PM, Bardgett RD (2008) Drying and rewetting effects on soil microbial community composition and nutrient leaching. Soil Biol. Biochem. 40: 302-311

Misra A, Tyler G (1999) Influence of soil moisture on soil solution chemistry and concentrations of minerals in the calcicoles Phleum phleoides and Veronica spicata grown on a limestone soil. Ann. Bot. 84: 401-410

Wu Y, Ding Na, Wang G, Xu J, Wu J, Brookes PC (2009a) Effects of different soil weights, storage times and extraction methods on soil phospholipid fatty acid analyses. Geoderma 150: 171-178

Wu Y, Yu X, Wang, H, Ding, N, Xu, J (2009b) Does history matter? Temperature effects on soil microbial biomass and community structure based on the phospholipid fatty acid (PLFA) analysis. J. soil. sediment. DOI 10.1007/s11368-009-0118-5

Xiang SR, Doyle A, Holden PA, Schimel JP (2008) Drying and rewetting effects on C and N mineralization and microbial activity in surface and subsurface California grassland soils. Soil Biol. Biochem. 40: 2281-2289

Young IM, Crawford JW (2004) Interactions and self-organization in the soil-microbe complex. Science 304: 1634-1637

Yong IM, Ritz K (2000) Tillage, habitat space and function of soil microbes. Soil Tillage Res. 53: 201-213

Effects of Cadmium and Mercury alone and in Combination on the Soil Microbial Community Structural Diversity

Min Liao*, Haijun Zhang, Shouna Yu, Chengli Chen, Changyong Huang

Zhejiang Provincial Key Laboratory of Subtropical Soil and Plant Nutrition, College of Environmental and Natural Resource Sciences, Zhejiang University, Hangzhou 310029, China.
*Corresponding author. Tel. No. +86-571 8697 1955; Fax No. +86-571 8697 1955; E-mail: liaomin@zju.edu.cn.

Abstract: To assess effects of cadmium (Cd) and mercury (Hg) alone and in combination on soil microbial community structural diversity, an incubation experiment was conducted, employing two soils, namely, the marine sediment silty loam soil and the yellowish red soil, in which five levels of Cd, Hg or Cd and Hg in combination were added. After incubated 56 days, phospholipid fatty acids (PLFAs) were tested. The results showed that the composition of the microbial communities changed significantly after different levels of metals application. The principal component analysis (PCA) of PLFAs indicated the structure of the microbial community was also significantly influenced by the pollution of metals, with the increases in PLFAs biomarkers for fungi and actinomycetes, and the increases in the ratio of Gram-positive to Gram-negative bacteria. By comparing the effects of Cd, Hg alone and in combination, the results revealed that the combined pollution of Cd and Hg had higher toxicity to soil microbial community structural diversity than that of Cd or Hg applied alone.

Keywords: Soil microbial community structural diversity; Cadmium; Mercury

Introduction

Heavy metal pollution is a serious environmental problem. Heavy metals have an obvious effect on or are potentially harmful to biota, including cadmium (Cd) and mercury (Hg) (Hu *et al*.,2007; Kamala *et al*., 2006). Microorganisms play a unique role in the soil ecosystem, because of their contributions to maintain soil productivity. An increasing body of evidence suggests that microorganisms are far more sensitive to heavy metal stress than soil animals or plants growing on the same soils (Zhong *et al*., 2007). More recently, an increasing awareness has emerged concerning the importance of microbial diversity in terrestrial ecosystems and soil microbial community structure has also been considered as a biological indicator of heavy metal stress (Liao *et al*., 2005). The microbial community structure is characterized as one of the important parameters of soil ecosystem community structure and stability (Cai *et al*., 2006). Cd, Hg contamination in agricultural soils not only aroused the changes of soil microorganism and its activities, but also resulted in soil fertility deterioration, Thus, in our present study, a incubation experiment was conducted, employing two soils, in which five levels of metals were added, including the controlled (CK), Cd8(8 $mg \cdot kg^{-1}$ Cd), Hg8(8 $mg \cdot kg^{-1}$ Hg), Cd8Hg30 (8 $mg \cdot kg^{-1}$ Cd and 30 $mg \cdot kg^{-1}$ Hg) and Hg8Cd30 (8 $mg \cdot kg^{-1}$ Hg and 30 $mg \cdot kg^{-1}$ Cd). And the PLFA profiles and sole carbon source utilization pattern were examined. The objectives of this study were to assess the effects of Cd and Hg alone and in combination on soil microbial community diversity and microbial functional diversity.

Materials and Methods

Two soils with contrasting physico-chemical characteristics were used (S1 and S2), collected from surface layer (0～20 cm), air-dried, ground, sieved through 2 mm mesh and some basic physico-chemical

properties were measured. For the laboratory incubation study, the homogenized moist soil in portions equivalent to 250 g oven-dry weight that were first adjusted to 40% of soil water-holding capacity (WHC) by deionized water was transferred into 500 ml plastic beakers, enveloped with permeable film and then putted into incubator at 25 ℃ for three weeks (conditioning period).The sieved soil samples were added with Cd and Hg using $CdCl_2$ and $HgCl_2$ solutions. The samples were then thoroughly homogenized and filled into plastic beakers. The soil was incubated for 56 days at 25 ℃. During the incubation period, the soil moisture contents were monitored by weighing and adjusted to 60% water holding capacity by deionized water. Samples from each pot were collected at 56 days for the date analysis of soil microbial community structure diversity.

Some soil basic physical and chemical properties were measured using the routine analytical methods (ACSSSC, 1983), listed in Table 1. The soil microbial community structure was determined by analyzing the ester-linked phospholipid fatty acids (PLFAs) composition of the soil, using the modified Bligh and Dyer method (Bligh and Dyer, 1959; Frostegård *et al*., 1993). The fatty acids i15:0, a15:0, 15:0, i16:0, 17:0, cy17:0 and cy19:0 were chosen to represent bacterial PLFAs (Frostegård *et al*., 1993). The polyenoic, unsaturated PLFA 18:3ω6c was used as an indicator of fungal biomass (Federle, 1986). The ratio of Gram-positive (G^+) to Gram-negative (G^-) bacteria was calculated by taking the sum of the predominant Gram-positive PLFAs 10Me16:0, 10Me17:0, 10Me18:0, i15:0, a15:0, i16:0, i17:0 and a17:0 (O'Leary and Wilkinson, 1988) divided by the sum of the predominant Gram-negative bacterial PLFAs cy17:0 and cy19:0 (Zogg *et al*., 1997).

For all experimental data, the regression and multivariate analysis were performed using Genstat 5.3 (NAG Ltd., Oxford, UK).

Table1 Basic physical and chemical properties of soil samples tested

Soil	pH (H_2O)	Organic C ($g \cdot kg^{-1}$)	CEC [c] ($cmol \cdot kg^{-1}$)	Avail.		Total.		Size composition (%)		
				Hg ($mg \cdot kg^{-1}$)	Cd ($mg \cdot kg^{-1}$)	Hg ($mg \cdot kg^{-1}$)	Cd ($mg \cdot kg^{-1}$)	2~0.02 (mm)	0.02~0.002 (mm)	<0.002 (mm)
S1[a]	5.97	11.55	14.59	0.003	0.106	0.0455	0.743	65	28.8	6.2
S2[b]	5.12	29.69	12.47	0.004	0.036	0.0617	0.72	22.5	57	20.5

[a] S1: marine sediment silty loam; [b] S2: yellowish red soil. [c]CEC : the cation exchange capacity.

Results and Discussions

The PLFA profiles of two soils under CK, Cd8, Hg8, Cd8Hg30 and Hg8Cd30 treatments were analyzed. Twenty PLFAs from C_{12} to C_{20} were identified and varied significantly in their relative abundance between soils (Fig.1). The soil microbial communities of contaminated soils were different from the control soil and PCA of the PLFA profiles indicated a similar separation of the data sets. PLFA analyses revealed an increase in several iso- and anteiso-branched PLFAs with elevating the single or combined levels of Cd and Hg, such as i15:0, a15:0, i16:0, i17:0, all commonly found in Gram-positive bacteria, in the single or combined Cd and Hg contaminated soils. This indicates a predominance of Gram-positive over Gram-negative bacteria in single or combined Cd and Hg contaminated soils. A further indication that such a shift had occurred in two soils was indicated by the decrease in cy19:0, which is considered to be typical for Gram-negative bacteria (Zogg *et al*., 1997), due to the elevated single or combined levels of Cd and Hg.

Correspondingly, the ratio of Gram-positive to Gram-negative bacteria increased with the elevating levels of single or combined Cd and Hg in soils. The highest ratio appeared in the Cd and Hg combined contaminated soil (Hg30Cd8), and showed an order: CK < Cd8 < Hg8 < Cd30Hg8 < Cd8Hg30 (Fig. 2). The fungal PLFAs, mostly 18:2ω6,9c 18:3ω6c, (Federle, 1986), was not found in controlled soils, whereas the significant higher values were observed in soils containing relatively higher Cd or Hg level, indicating that the fungi tend to be more resistant to heavy metal than bacteria (Turpeinen *et al*., 2004). The relative abundance of several PLFAs, including the methyl-branched 10Me16:0, 10Me17:0 and

10Me18:0, varied in response to metal contamination. The PLFAs 10Me16:0, 10Me17:0 and 10Me18:0 are found almost exclusively in actinomycetes (Frostegård *et al*., 1993). In the contaminated soils, no significant difference was found in the relative amount of the actinomycetic PLFAs 10Me16:0, 10Me17:0 and 10Me18:0. While, there was an increase in the fatty acids of 10Me18:0 and 10Me17:0, and the change of relative amount of the fatty acids 10Me16:0 was not significant (Fig.1). Other results in the literature also indicate that different actinomycetes can respond differently to the elevated heavy metal concentrations (Frostegård *et al*., 1993; Turpeinen *et al*., 2004). Therefore, it may be explained by the different responses of different actinomycete population to the elevated Cd, Hg concentrations.

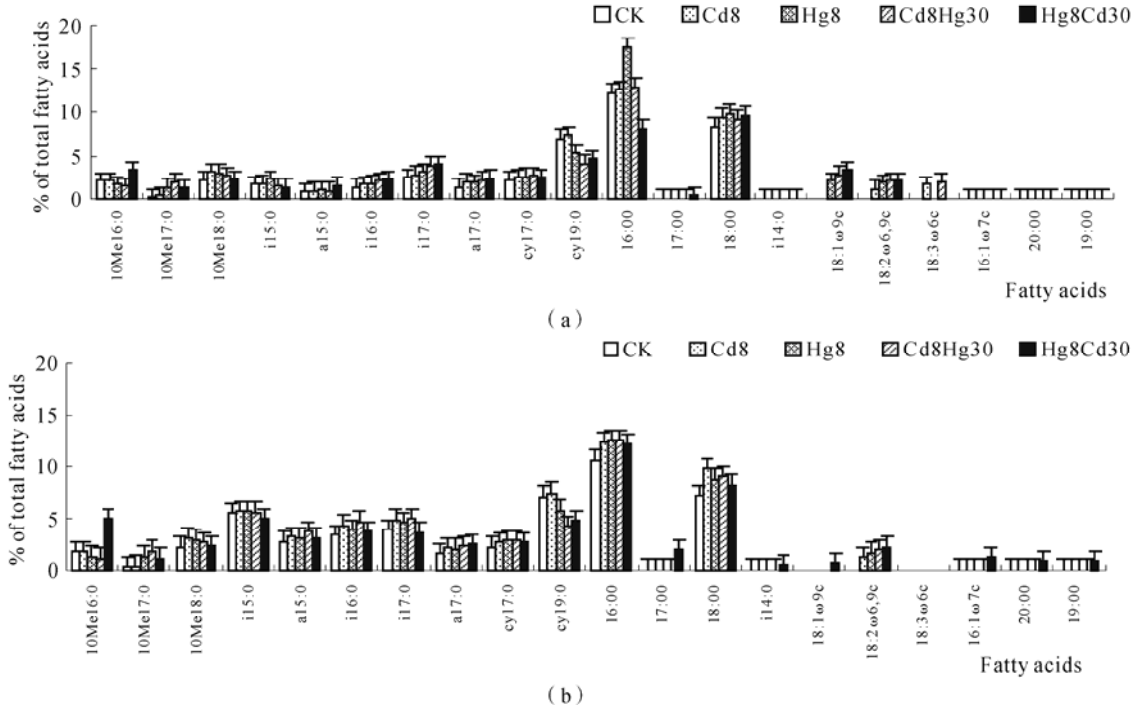

Fig.1 Abundance of total PLFAs (nmol%) in two soil under different heavy metal treatment. (a): the marine sediment silty loam soil; (b): the yellowish red soil; Cd8: 8 mg·kg^{-1} Cd; Hg: 8 mg·kg^{-1} Hg; Cd8Hg30: 8 mg·kg^{-1} Cd and 30 mg·kg^{-1} Hg; Hg8Cd30: 8 mg·kg^{-1} Hg and 30 mg·kg^{-1} Cd; Total amount of PLFA in nmol·g^{-1} dry wt; The different letters indicate significant difference at 5% lever according to LSD test.

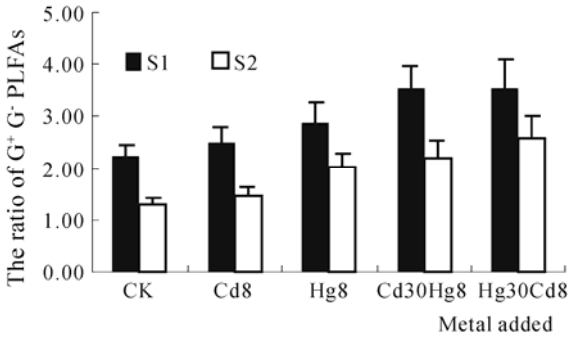

Fig.2 Ratios of Gram-positive to Gram-negative PLFAs in two soils (values are means±S.D.); S1: the marine sediment silty loam soil; S2: the yellowish red soil; Cd8: 8 mg·kg^{-1} Cd; Hg: 8 mg·kg^{-1} Hg; Cd8Hg30: 8 mg·kg^{-1} Cd and 30 mg·kg^{-1} Hg; Hg8Cd30: 8 mg·kg^{-1} Hg and 30 mg·kg^{-1} Cd

Similar to the PLFA profiles, the PCA results were also proved to be a very powerful way for the analysis of PLFA composition (as lg mol% values). From the treated soil samples of CK,Cd8, Hg8, Cd8Hg30 and Hg8Cd30, the PLFA data indicated that differences in microbial community structure for the different treatments were evident with respect to PC1 (Fig. 3). In Fig. 3 (a), the first principal component (PC1) accounted for 74.76% of the variation in PLFA patterns, and the second principal component (PC2) accounted for 18.39% of the variation. Specifically in PLFA patterns, the PC loading plots showed that non metal amended soils had higher scores on both PC1 and PC2 than Cd, Hg alone or combined amended soils, the fatty acids with negative correlation

coefficients for PC1 included 18:3ω6c、18:2ω6, 9c and 10Me17:0, whereas, another fatty acids, cy19:0 and 17:0, had a positive coefficient which showed those fatty acids had significantly lower relative amounts in the combined contaminated soils. These correlation coefficients combined with the PCA graph indicated that the combined contaminated soils had higher relative amounts of 18:3ω6c,18:2ω6,9c and 10Me17:0. In Fig. 3(b), The PC1 accounted for 58.31% of the variation in PLFA patterns, and the PC2 accounted for 37.87% of the variation in PLFA patterns, the PC loading plots showed that there were lower scores on both PC1 and PC2 in non metal amended soils than in contaminated soils, especially lower that in Cd and Hg combined contaminated soils, and the fatty acids with a positive correlation coefficient for PC1 included 18:2ω6,9c and 10Me17:0, which correlation coefficients combined with the PCA graph indicated that there were relative amounts of 18:2ω6,9c and 10Me17:0 in Cd and Hg combined contaminated soils. Whereas, another fatty acids, cy19:0 and i14:0 had a negative coefficient which showed those fatty acids had relatively lower relative amounts in Cd and Hg combined contaminated soils. In a word, the result showed the microbial community structure had a significant change in the Cd and Hg combined contaminated soils.

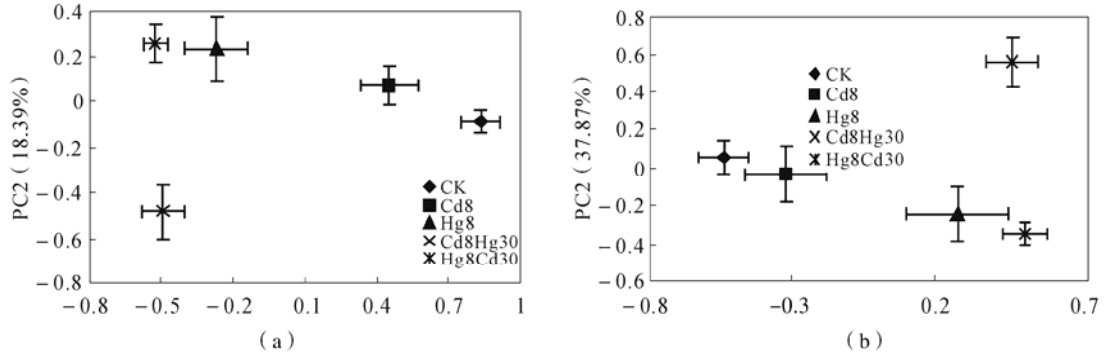

Fig.3 Principal components analysis (PCA) of the PLFA composition (as lg mol% values) in two soils: (a) the marine sediment silty loam soil; (b) the yellowish red soil, Cd8: 8 mg·kg^{-1} Cd, Hg: 8 mg·kg^{-1} Hg, Cd8Hg30: 8 mg·kg^{-1} Cd and 30 mg·kg^{-1} Hg, Hg8Cd30: 8 mg·kg^{-1} Hg and 30 mg·kg^{-1} Cd

Refereces

Agrochemistry Commission, Soil Science Society of China (ACSSSC) (ed.) (1983) Routine Methods for Soil and Agrochemical Analysis. Science Press, Beijing

Bligh EG, Dyer WJ (1959) A rapid method of total lipid extraction and purification. Can. J. Biochem. Phys. 37: 911-917

Cai XD, Qiu RL, Chen GZ, Zeng XW, Fang XH (2006) Response of microbial communities to phytoremediation of nickel contaminated soil. Acta Pedol. Sin. 43(6): 919-925

Federle TW (1986) Microbial distribution in soil-new techniques. In: Megusar F, Gantar M (eds.), Perspective in Microbial Ecology. Slovene Society for Microbiology, Ljubljana, pp. 493-498

Frostegård A, Tunlid A, Bååth E (1993) Phospholipid fatty acid composition, biomass, and activity of microbial communities from two soil types experimentally exposed to different heavy metals. Appl. Environ. Microbiol. 59: 3605-3617

Hu Q, Qi HY, Zeng JH, Zhang HX (2007) Bacterial diversity in soils around a lead and zinc mine. J. Environ. Sci. 19: 74-79

Kamala SK, Krishnamoorthy R (2006) Isolation of mercury resistant bacteria and influence of abiotic factors on bioavailability of mercury-A case study in Pulicat Lake North of Chennai, South East India. Sci. Total Environ. 367: 341-353

Liao M, Chen CL, Huang CY (2005) Effect of heavy metals on soil microbial activity and diversity in a reclaimed mining wasteland of red soil area. J. Environ. Sci.-Chin. 17(5): 832-837

Turpeinen R, Kairesalo T, Haggblom MM (2004) Microbial community structure and activity in arsenic-, chromium-, and copper- contaminated soils. FEMS Microbiol. Ecol. 47: 39-50

Zhong WH, Cai ZC (2007) Long-term effects of inorganic fertilizers on microbial biomass and community functional diversity in a paddy soil derived from quaternary red clay. Appl. soil Ecol. 36: 84-91

Zogg GP, Zak DR, Ringleberg DB, MaPbonald NW, Pregitzer KS, White DC (1997) Compositional and functional shifts in microbial communities due to soilwarming. Soil Sci. Soc. Am. J. 61: 475-481

Author Index

H

I

J

K

L

M

N

P

Q

R

S

T

W

X

Y

Z